

OF
ELECTRICAL APPARATUS

BY

JOHN H. KUHLMANN

*Associate Professor of Electrical Design, University of Minnesota
Minneapolis, Minnesota; Member American Institute of
Electrical Engineers; Society for the Promotion
of Engineering Education*

NEW YORK

JOHN WILEY & SONS, INC.

LONDON: CHAPMAN & HALL, LIMITED

1930

52 10 10 10
10 10
COPYRIGHT, 1930,
BY
JOHN H. KUHLMANN

3354

9/32

Printed in U. S. A.

PRESS OF
BRAUNWORTH & CO., INC.,
BOOK MANUFACTURERS
BROOKLYN, NEW YORK

CONTENTS

SECTION I—DIRECT-CURRENT MACHINES

CHAPTER I CONSTRUCTION

	PAGE
SPIDER	3
ARMATURE	3
COMMUTATOR	5
FIELD POLES	9
FIELD YOKE	11
BEARINGS	12
BRUSH HOLDER AND BRUSH YOKE	12
BASE	13
MOTOR AND GENERATOR ASSEMBLY	13

CHAPTER II VOLTAGE FORMULA AND OUTPUT EQUATION

VOLTAGE FORMULA	14
OUTPUT EQUATION	14
ARMATURE PERIPHERAL SPEED	18
ARMATURE DIAMETER AND LENGTH	19
NUMBER OF POLES	20
DESIGN OF POLE SHOE	21
CONSTRUCTION OF NO-LOAD FIELD FORM	22
AIR GAP FLUX DISTRIBUTION FACTOR	26
SAMPLE DESIGN (DIAMETER AND LENGTH)	27

CHAPTER III ARMATURE WINDINGS AND INSULATION

SIMPLEX LAP WINDINGS	30
SIMPLEX WAVE WINDINGS	34
EQUALIZER CONNECTIONS	40
FROGLEG WINDINGS	42
NUMBER OF ARMATURE SLOTS	42
ARMATURE COIL CONSTRUCTION AND INSULATION	44
CHOICE OF ARMATURE WINDING	50
ARMATURE CONDUCTOR SECTION	52
SIZE OF ARMATURE SLOTS	53
MEAN-TURN RESISTANCE AND WEIGHT OF ARMATURE WINDING	55
SAMPLE DESIGN (DESIGN OF ARMATURE WINDING)	56

CHAPTER IV

THE MAGNETIC CIRCUIT

	PAGE
AMPERE-TURNS FOR THE AIR GAP	61
AMPERE-TURNS FOR THE ARMATURE TEETH	63
AMPERE-TURNS FOR THE ARMATURE YOKE	65
AMPERE-TURNS FOR THE POLE	66
AMPERE-TURNS FOR THE FIELD YOKE	66
THE FIELD LEAKAGE FACTOR	67
THE OPEN-CIRCUIT SATURATION CURVE	69
SAMPLE DESIGN (DESIGN OF MAGNETIC CIRCUIT)	70

CHAPTER V

ARMATURE REACTION AND FIELD WINDING DESIGN

ARMATURE DEMAGNETIZING AMPERE-TURNS	76
ARMATURE CROSS-MAGNETIZING AMPERE-TURNS :	77
SHUNT AND SERIES FIELD AMPERE-TURNS	80
DESIGN OF FIELD WINDINGS	81
DESIGN OF SHUNT FIELD RHEOSTAT	86
SAMPLE DESIGN (DESIGN OF SHUNT AND SERIES FIELD WINDING)	89

CHAPTER VI

COMMUTATION AND COMMUTATING POLE DESIGN

WIDTH OF COMMUTATING ZONE	96
REACTANCE VOLTAGE	98
DESIGN OF COMMUTATING POLE	101
COMMUTATING POLE AMPERE-TURNS	104
DESIGN OF COMMUTATOR AND BRUSHES	106
SAMPLE DESIGN (DESIGN OF COMMUTATOR AND COMMUTATING POLES)	110

CHAPTER VII

LOSSES, EFFICIENCY AND TEMPERATURE RISE

ARMATURE COPPER LOSSES	115
COMMUTATING FIELD COPPER LOSS	116
SERIES FIELD COPPER LOSS	116
SHUNT FIELD COPPER LOSS	116
BRUSH CONTACT LOSSES	116
CORE LOSS	117
BRUSH FRICTION LOSS	118
FRICTION AND WINDAGE LOSS	118
EFFICIENCY	120
TEMPERATURE RISE	121
SAMPLE DESIGN (LOSSES, EFFICIENCY AND TEMPERATURE RISE)	125

CHAPTER VIII

SAMPLE DESIGN

	PAGE
DESIGN OF CONSTANT-SPEED, DIRECT-CURRENT MOTOR	131

SECTION II—SYNCHRONOUS MACHINES

CHAPTER IX

CONSTRUCTION

ARMATURE	154
ARMATURE FRAME	158
FIELD	159
SPIDER	164

CHAPTER X

VOLTAGE FORMULA AND OUTPUT EQUATION

VOLTAGE FORMULA	166
OUTPUT EQUATION	167
ARMATURE DIAMETER AND LENGTH	170
DESIGN OF POLE SHOE	171
CONSTRUCTION OF NO-LOAD FIELD FORM	171
FLUX DISTRIBUTION FACTOR AND FORM FACTOR	172
SAMPLE DESIGN (DIAMETER AND LENGTH)	177

CHAPTER XI

ARMATURE WINDING AND INSULATION

CHAIN WINDINGS	179
DOUBLE-LAYER WINDINGS	179
GRAPHIC METHOD OF LAYING-OUT ARMATURE WINDINGS	182
NUMBER OF ARMATURE SLOTS	192
ARMATURE COIL CONSTRUCTION AND INSULATION	193
CONDUCTOR SECTION AND SLOT SIZE	196
MEAN-TURN RESISTANCE AND WEIGHT OF ARMATURE WINDING	198
SAMPLE DESIGN (DESIGN OF ARMATURE WINDING)	201

CHAPTER XII

MAGNETIC CIRCUIT

AMPERE-TURNS FOR AIR GAP	206
AMPERE-TURNS FOR ARMATURE TEETH	207
AMPERE-TURNS FOR ARMATURE YOKE	208
AMPERE-TURNS FOR THE POLE	209
AMPERE-TURNS FOR THE FIELD YOKE	210
SAMPLE DESIGN (DESIGN OF MAGNETIC CIRCUIT)	211

CHAPTER XIII

ARMATURE REACTIONS IN SYNCHRONOUS MACHINES

	PAGE
ARMATURE LEAKAGE REACTANCE	216
ARMATURE REACTION	222
SHORT-CIRCUIT CHARACTERISTIC	223
EXCITATION FOR ANY LOAD AND POWER FACTOR	225
FIELD WINDING DESIGN	226
SAMPLE DESIGN (DESIGN OF FIELD WINDING)	229

CHAPTER XIV

LOSSES, EFFICIENCY AND TEMPERATURE RISE

ARMATURE COPPER LOSSES	234
FIELD COPPER LOSSES	234
CORE LOSSES	234
FRICTION AND WINDAGE LOSSES	235
STRAY LOAD-LOSSES	238
EFFICIENCY	238
TEMPERATURE RISE	239
SAMPLE DESIGN (LOSSES, EFFICIENCY AND TEMPERATURE RISE)	244

CHAPTER XV

SAMPLE DESIGN

DESIGN OF SELF-STARTING SYNCHRONOUS MOTOR	248
---	-----

SECTION III—INDUCTION MOTORS

CHAPTER XVI

CONSTRUCTION

STATOR	266
ROTOR	267

CHAPTER XVII

THE STATOR

OUTPUT CONSTANT	274
AIR GAP DENSITY	274
AMPERE CONDUCTORS	274
EFFICIENCY AND POWER FACTOR	274
DIAMETER AND LENGTH	281
WINDINGS	281
NUMBER AND SIZE OF SLOTS	283
STATOR TOOTH AND YOKE DENSITIES	286
SAMPLE DESIGN (DESIGN OF STATOR)	287

CHAPTER XVIII

THE ROTOR

	PAGE
AIR GAP LENGTH	291
ROTOR WINDINGS	291
NUMBER AND SIZE OF ROTOR SLOTS	292
ROTOR TOOTH AND YOKE DENSITIES	298
SAMPLE DESIGN (DESIGN OF SQUIRREL-CAGE ROTOR)	298

CHAPTER XIX

MOTOR CHARACTERISTICS

THE MAGNETIZING CURRENT	301
AIR GAP AMPERE-TURNS	301
AMPERE-TURNS STATOR AND ROTOR TEETH	302
AMPERE-TURNS STATOR AND ROTOR YOKE	302
NO-LOAD CURRENT	303
CORE LOSSES	303
FRICTION AND WINDAGE LOSSES	304
NO-LOAD STATOR COPPER LOSSES	304
SHORT-CIRCUIT CURRENT	306
ROTOR RESISTANCE	306
LEAKAGE REACTANCE	307
RHEOSTAT DATA	311
SAMPLE DESIGN (OPERATING CHARACTERISTICS)	311

CHAPTER XX

SAMPLE DESIGN

DESIGN OF WOUND-ROTOR INDUCTION MOTOR	320
---	-----

SECTION IV—TRANSFORMERS

CHAPTER XXI

CONSTRUCTION

CORE	336
TANK	340

CHAPTER XXII

CORE AND WINDINGS

DESIGN OF CORE	347
DESIGN OF WINDINGS	353

CHAPTER XXIII

OPERATING CHARACTERISTICS

	PAGE
RESISTANCE	365
LEAKAGE REACTANCE	365
REGULATION	368
EXCITING CURRENT	368
EFFICIENCY	369
TEMPERATURE RISE	369
DESIGN OF TANK	369

CHAPTER XXIV

SAMPLE TRANSFORMER DESIGNS

DESIGN OF SINGLE-PHASE, CORE TYPE, POWER TRANSFORMER	372
DESIGN OF THREE-PHASE, CORE TYPE, POWER TRANSFORMER	384
DESIGN OF SINGLE-PHASE, FOUR-PART DISTRIBUTED-CORE TYPE, DISTRIBUTION TRANSFORMER	396
DESIGN OF SINGLE-PHASE, SHELL TYPE, POWER TRANSFORMER	406
LIST OF SYMBOLS	433
INDEX	445

DESIGN OF ELECTRICAL APPARATUS

I—DIRECT-CURRENT MACHINES

CHAPTER I

CONSTRUCTION

DIRECT-CURRENT generators and motors may be divided into three general classes: (1) The non-commutating-pole machine, (2) the commutating-pole machine, (3) the compensated machine.

(1) The non-commutating-pole machine is practically obsolete, being used only for generators and motors for low voltages and small capacities.

(2) The commutating-pole machine is built with small poles between the main poles, which are called commutating poles and are magnetized by a winding in series with the armature. The brushes are so placed that the coils, during commutation, come under the influence of the flux from the commutating poles, which flux is of such value and direction that cutting it produces in the coils a voltage which neutralizes the voltage of self-induction. In a generator, the flux from the commutating pole must be in the same direction as the flux from the main pole preceding it, and in a motor it must be in the same direction as the flux from the main pole following it.

(3) The compensated machine may be looked upon as a modified commutating-pole machine. The commutating-pole machine has the exciting winding concentrated on the commutating pole, whereas the compensated machine has part of the exciting winding distributed in the main pole faces. By such construction, the leakage flux of the commutating pole is reduced, which increases the commutation capacity of the machine. The compensated machine has two distinct advantages over the commutating-pole machine. It has a greater commutating capacity and, since the armature cross magnetization under the main pole is neutralized, the maximum voltage between adjacent commutator segments is reduced. By taking advantage of these two points, it is possible to increase the speed of generators and to build motors for more difficult cycles of operation.

CONSTRUCTION

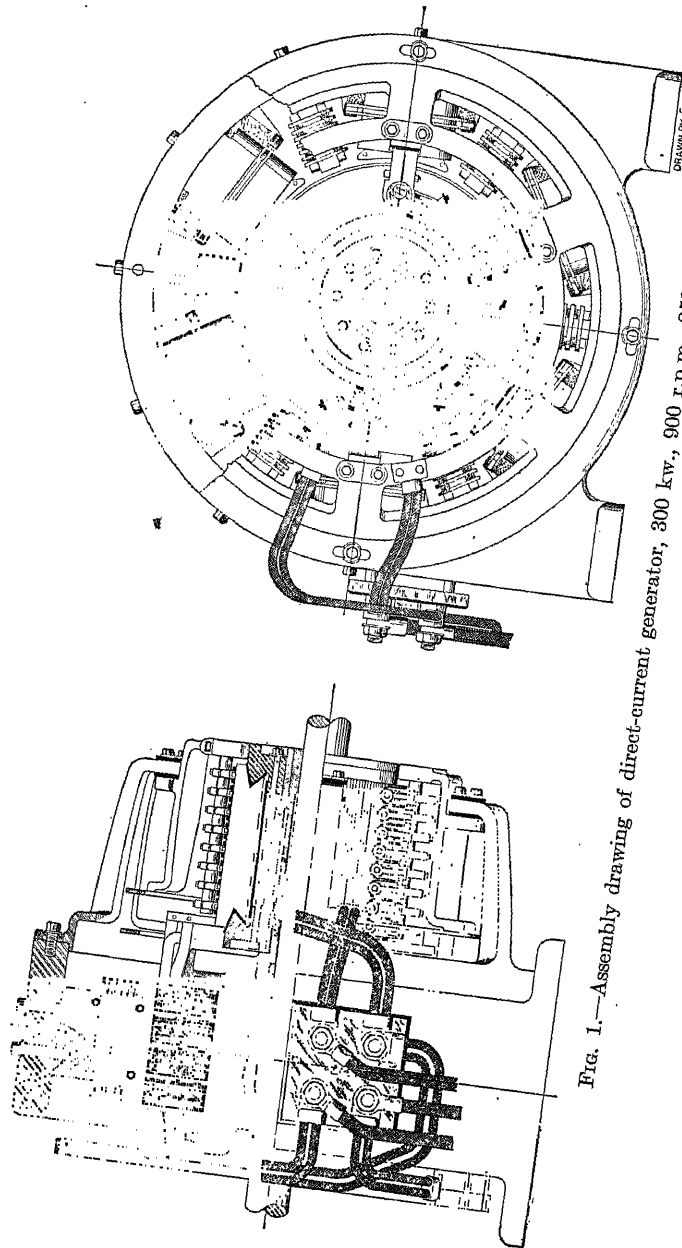


FIG. 1.—Assembly drawing of direct-current generator, 300 kw., 900 r.p.m., 250 volts.

The type of construction generally used for direct-current generators and motors is shown in Fig. 1.

Spider.—The spider of a direct-current generator or motor is the frame upon which the armature laminations are assembled. By designing the spider with large axial ventilating ducts, good ventilation of the inside of the armature is obtained and the weight of the armature is kept small. The spider for large machines is either a steel casting or is fabricated from rolled steel.¹ Figure 2 shows a cast steel spider of a large-diameter, slow-speed machine. For machines with small armature diameter, the type of construction shown in Fig. 3 is used, that is, the spider is part of the armature lamination.

Armature.—The armature of direct-current generators and motors is built up of electric sheet-steel laminations varying in thickness from 0.0141 to 0.025 in. The laminations are punched to correct size by means of dies, carefully annealed and insulated. For arma-

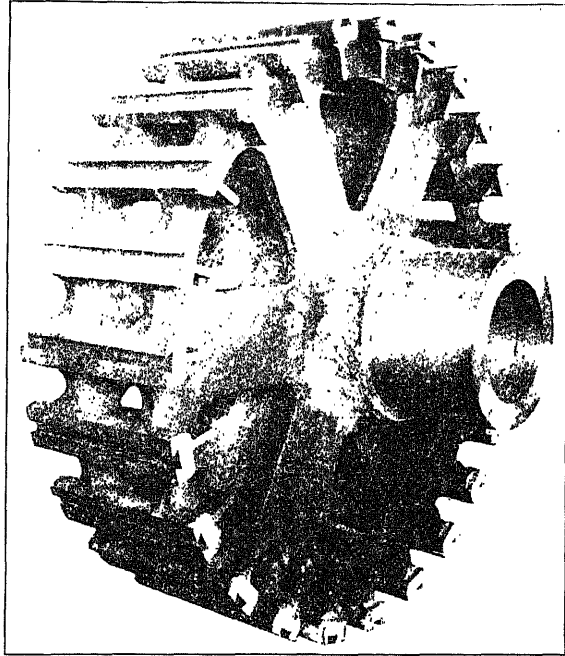


FIG. 2.—Armature spider for 1700-h.p., 90 to 205-r.p.m., 600-volt motor.

ture diameters smaller than approximately 30 in., the armature laminations are punched in one piece, whereas for larger armature diameters the circle is divided into several segments. One segment for a large-diameter, slow-speed machine is shown in Fig. 4.

The usual method of insulating the armature punchings is that of applying a thin coat of core plate varnish to each side of the punching. The insulating varnish is generally applied by passing the punchings between two rolls coated with the insulating varnish. The varnish on

¹ "Standard Line of Direct-Current Machines Fabricated by Arc Welding," *Electric Journal*, Vol. 25, p. 575, Dec., 1928.

the punchings is either air dried or artificially dried. When the artificial drying process is used, the punchings are first passed over an open flame, to burn out the volatile matter in the varnish, and then through

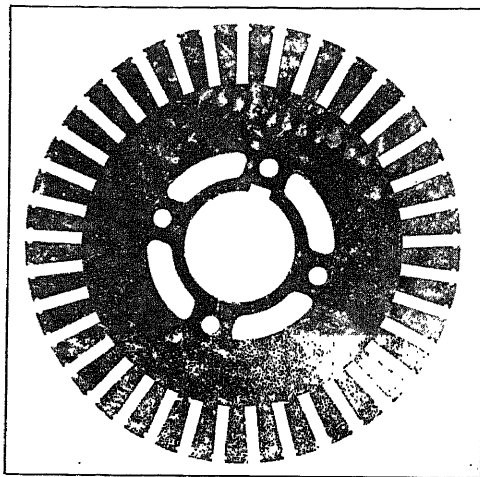


FIG. 3.—Armature punching with spider.

an oven, to bake the varnish. Paper is sometimes used to insulate the armature laminations from one another. The paper is applied to the sheet steel before it is punched out.

The insulated armature punchings are assembled on the spider between two end-plates. These are cast of the same material as the spider. The end-plate on the commutator end of the armature is often cast in one piece with the spider. The one on the opposite end, however, is always a

separate casting, and is used to press the laminations tightly together to prevent vibrations. The end-plates extend to the bottom of the armature slots and, therefore, do not support the armature

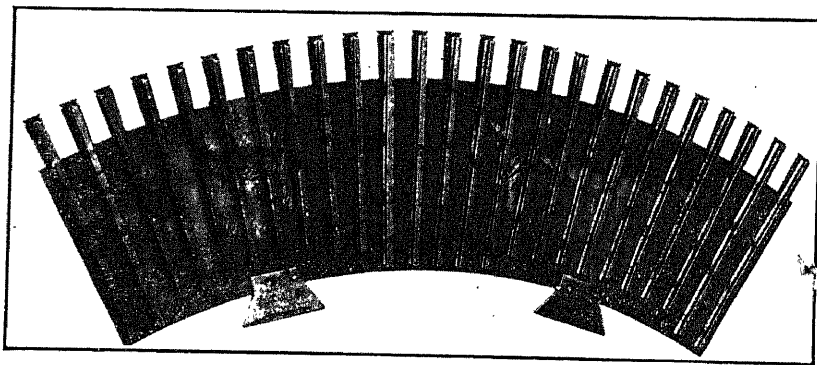


FIG. 4.—One segment for large-diameter armature with welded duct spacers.

teeth (see Fig. 1). For all except very small motors and generators, which have round or very shallow slots, the armature teeth must be supported by a tooth support.

The tooth support generally consists of a piece of rolled steel, spot-welded to the end lamination. The position of the tooth support and the shape of the section of the rolled steel piece are shown in Fig. 4.

The length of the armature iron is divided into sections, as shown in Fig. 1, by radial ventilating ducts; these are usually from $\frac{1}{4}$ to $\frac{3}{4}$ in. wide. The narrow duct is used on the small-diameter, high-speed machine, and the wide duct on the large-diameter, slow-speed machine. Except for very small machines, such as fractional horsepower motors, there is always a ventilating duct at each end of the armature laminations. When the length of the armature exceeds approximately 4 in., the armature also is divided into sections by radial ventilating ducts. Enough ducts should be used so that the length of each section will not be more than 3 in.

The ventilating duct spacer must extend from the top of each tooth to the inside of the armature lamination so that neither the teeth nor the inside edge of the armature lamination will flare and close the duct when the punchings are pressed together. Loose armature laminations will vibrate and produce a buzzing noise, because of the flux reversals in the armature core. The construction of the ventilating duct spacer is similar to that of the tooth support shown in Fig. 4.

On motors and generators with totally enclosed frame, such as street railway motors, the radial ventilating ducts are often omitted. For this type of construction, the cooling air is forced through the machine, parallel to the shaft, by a fan mounted on the shaft at the end of the armature opposite to the commutator.

The armature coils are placed into the slots with the required amount of insulation between armature iron and coils, and the slots are sealed with wedges. The type of wedge generally used is of horn fiber impregnated with paraffin. The position and thickness of the wedge are shown in Fig. 5 *a* and *b*. Bands of phosphor bronze or steel wire are used to hold the armature coil end-connections in position. The slots are not always sealed by wedges; they are sometimes left open and the coils held in place by phosphor bronze or steel band wires as Fig. 6 shows.

Commutator.—The commutator is built up of hard-drawn, copper segments, insulated from one another by mica. The thickness of the mica insulation varies from 0.02 to 0.06 in. and depends upon the diam-

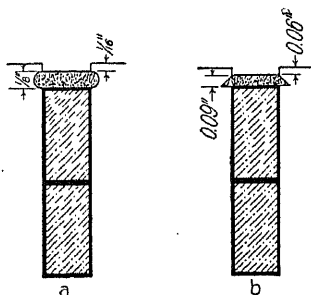


FIG. 5.

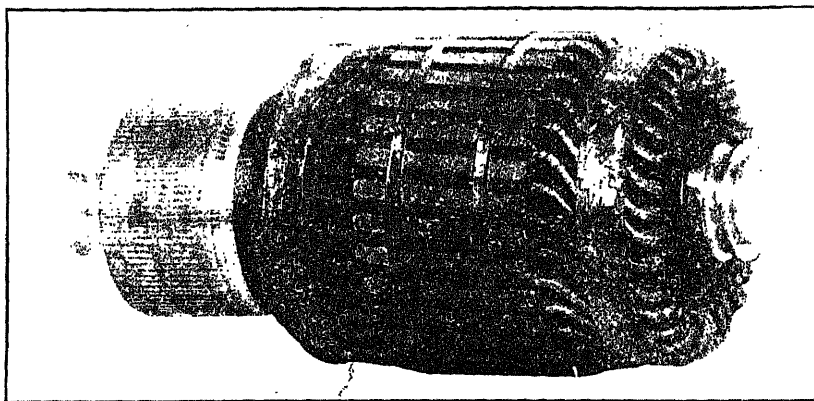


FIG. 6.—Complete armature for 7½-h.p., 1750-r.p.m., 230-volt, 4-pole, shunt-wound motor.

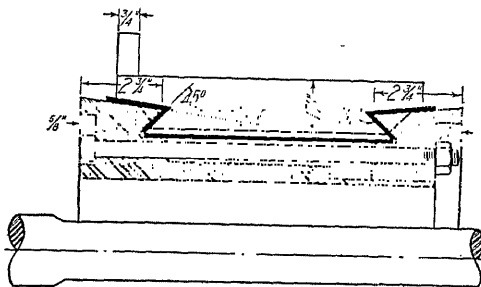


FIG. 7.—Two V-ring commutator construction.

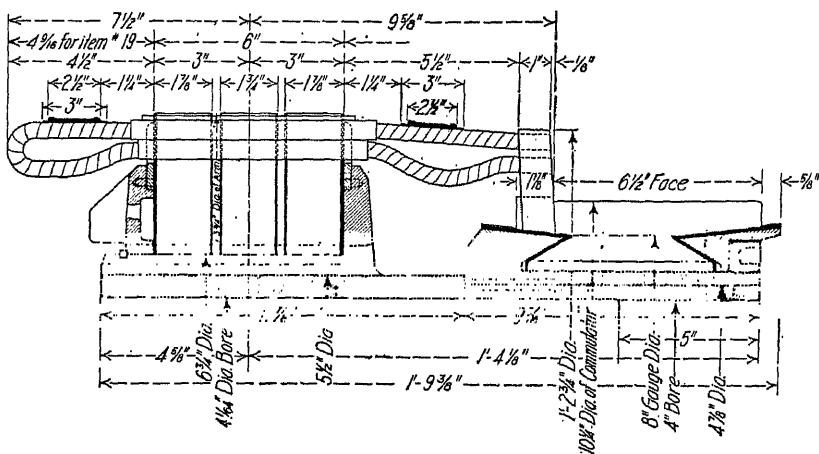


FIG. 8.—Armature and commutator assembly, 50-h.p., 850-r.p.m., 230-volt, shunt-wound motor.

eter of the commutator and the voltage between adjacent segments. The mica² used for commutator insulation must be one of the soft

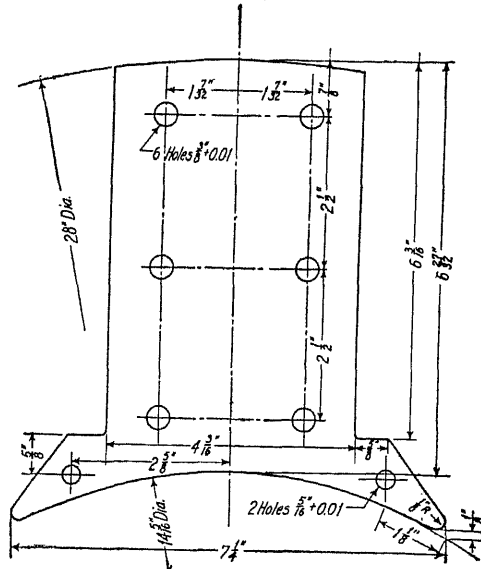


FIG. 9.—Detail drawing of pole punching, 50-kw., 1200-r.p.m. generator.

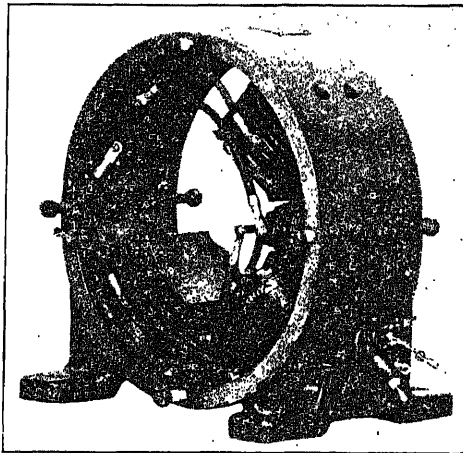


FIG. 10.—Field yoke with partially assembled field poles, 7½-h.p., 1750-r.p.m., 4-pole motor.

² See "The Manufacture of Built-Up Mica," Electric Journal, Vol. 21, p. 10, Jan., 1924; "Types of Commutator Construction," Electric Journal, Vol. 23, Nov., 1926, p. 565.

varieties so that the copper and mica will wear down at the same rate.

The mica and copper segments are clamped between V-shaped clamping rings and insulated from them by micaite, usually about $\frac{1}{16}$ in. thick. The assembled commutator is pressed on the shaft of

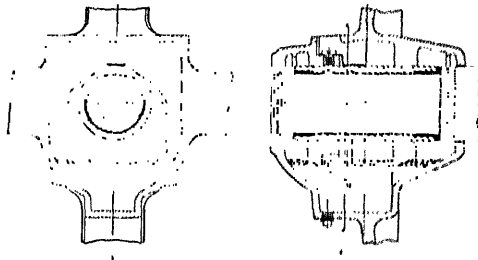


FIG. 11.—Cross-section of sleeve bearing and bearing housing.

the machine or on an extension of the armature spider. When the diameter of the commutator will permit, axial ducts are provided on the inside of the commutator for cooling purposes.

The two V-ring construction generally used is shown in Fig. 7.

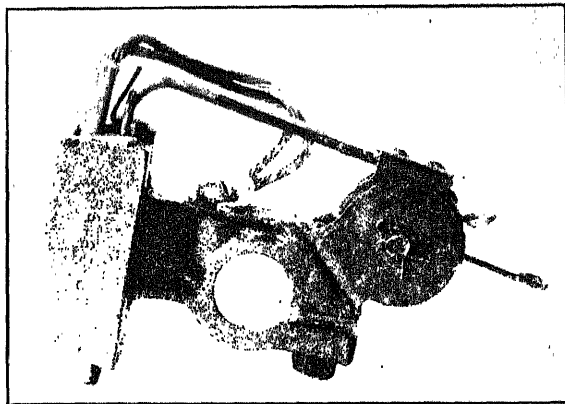


FIG. 12.—Brush holder with brush.

This method of construction can be used for high-speed commutators for peripheral speeds from 4000 to 6000 ft. per min. for lengths up to about 24 in. For longer commutators, the three V-ring construction or the shrink-ring construction is used. The armature and commutator assembly for a 50-hp. general purpose motor is shown in Fig. 8.

Field Poles.—The main poles of most modern machines are built up of sheet steel laminations, usually from 0.025 to 0.05 in. thick. The laminations are riveted together with no insulation between them. Figure 9 shows the usual shape of the laminations, with pole body and pole shoe punched in one piece. The shape of the pole body for the laminated pole construction is rectangular or square, whereas for cast steel poles with laminated pole shoes the pole body is often of circular shape, to obtain minimum length of mean-turn for the field coil.

The objection to the cast steel pole construction lies in the fact that

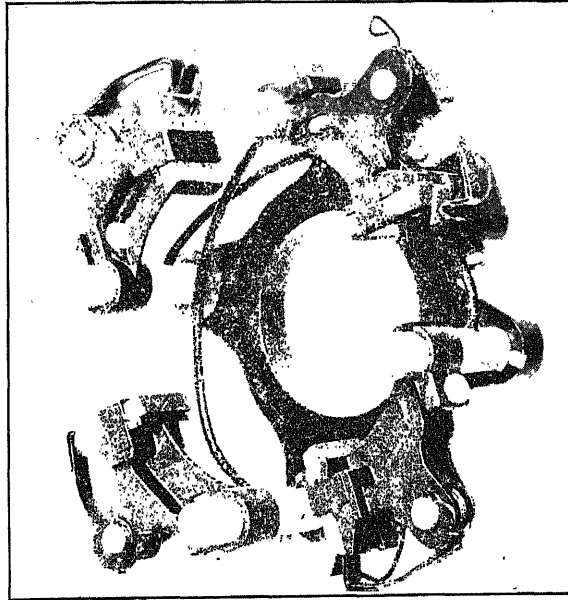


FIG. 13.—Brush yoke.

it is difficult to obtain castings of uniform material and free from defects. With open armature slots, the type generally used for direct-current motors and generators, cast steel pole shoes can not be used, because of the excessive eddy current losses in the pole face due to the air gap flux pulsations produced by the armature slots.

The field winding may be wound directly on the pole, with the necessary insulation between winding and pole, or may be wound on a form completely insulated and placed on the pole. The form-wound field coil is generally preferred because of the ease with which repairs can be made.

The commutating pole is often made of cast steel, for large high-speed machines, and for machines subjected to large load fluctuations,

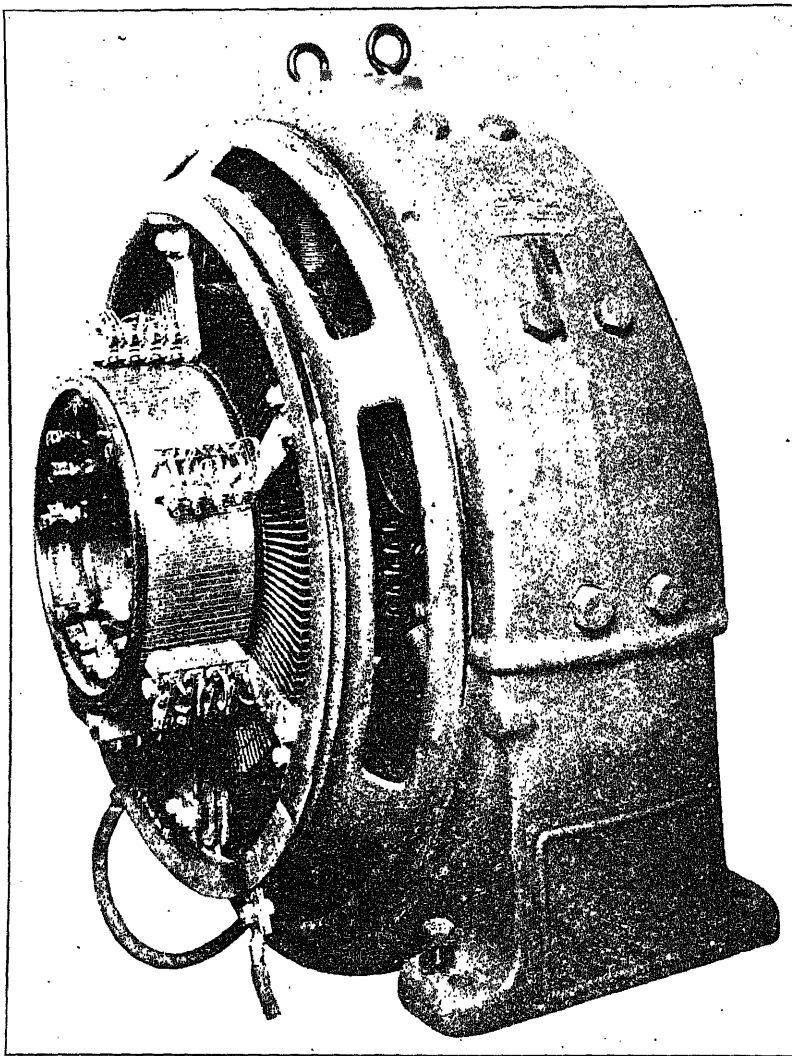


FIG. 14.—Engine-type generator.

the laminated pole is used. The commutating-pole winding is generally form-wound, insulated, and placed on the pole. The field frame, with assembled and connected field windings, is shown in Fig. 10.

Field Yoke.—The yoke is the frame to which the field poles are bolted (see Fig. 10). The section of the yoke must have the required

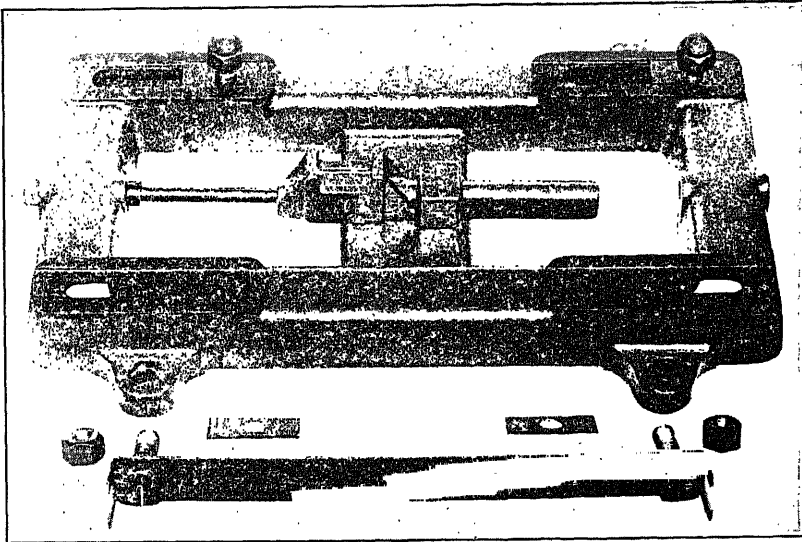


FIG. 15.—Belt tightener base.

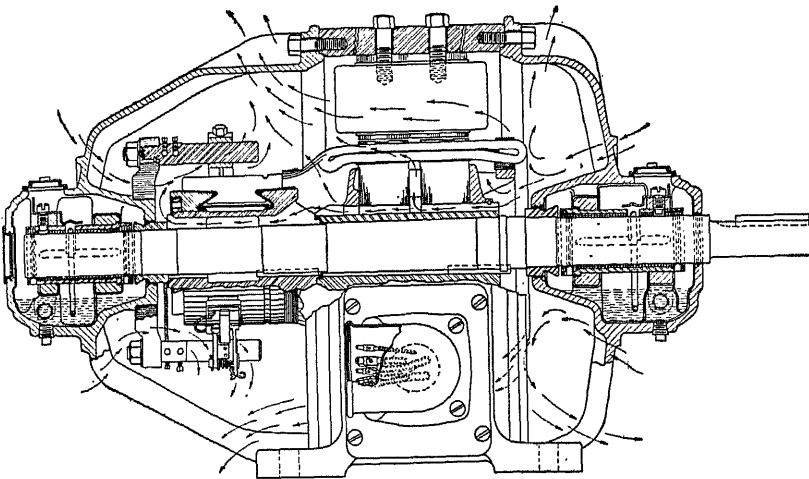


FIG. 16.—Assembly drawing of bracket type motor.

area for the flux and must also have the required mechanical strength to support the machine. Because of the difficulty of obtaining steel

castings free from internal strains, cracks, blow-holes, and the like, the yokes of large direct-current generators are being built up of $\frac{1}{4}$ -in. steel plates. On smaller diameter machines, rolled steel is being used. The feet are riveted or welded to the frame.

Bearings.—The bearings of most modern direct-current machines are of the ring oiling type. The bronze bearing is generally preferred

for small machines; for large motors and for the larger generators babbitt bearings are used. The position of the bearing in the bearing housing and the method of mounting are shown in Fig. 11.

Ball bearings and roller bearings are being used frequently for direct-current motors. Figure 18 shows the assembly drawing of a ball-bearing motor.

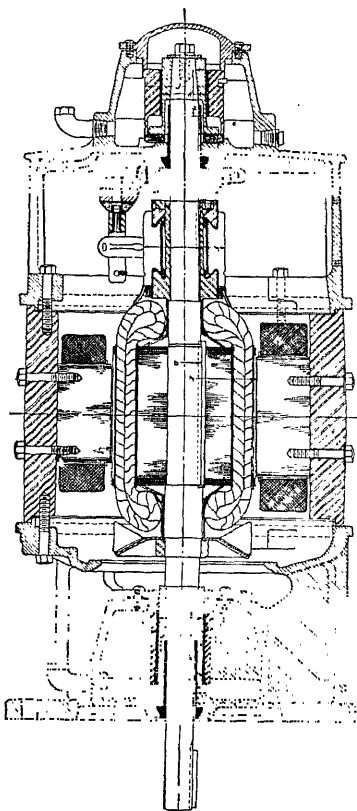


FIG. 17.—Cross-section of vertical motor.

Brush Holder and Brush Yoke.—Many different types of brush holders³ have been used for direct-current generators and motors. The type generally used on modern machines is shown in Fig. 12. The brush holders are mounted on studs or arms which are generally brass rods, from $\frac{1}{2}$ to 1 in. in diameter. The brush studs are pressed into openings properly spaced in the bearing bracket, Fig. 18, or are mounted on a brush yoke, which is supported by the bearing bracket, Fig. 16. One type of brush yoke with brush arms, brush holders, and brushes is shown in Fig. 13.

On engine type machines, for which the electrical manufacturer does not supply either the shaft or the bearings, the brush arms are supported by a brush yoke, as shown in Fig. 14. For pedestal type machines, the type of brush yoke shown in Fig. 13, or the type shown in Fig. 14, may be used.

³ See "The Development of The Direct-Current Generator in America," by B. G. Lammé, *Electric Journal*, Vol. 12, p. 164.

CHAPTER II

VOLTAGE FORMULA AND OUTPUT EQUATION

Voltage Formula.—The formula for the induced voltage in a direct-current armature is usually written in the following form,

$$E = \frac{\phi p N n}{a \times 60 \times 10^8} \text{ volts,} \quad (1)$$

where E is the voltage induced in the armature winding between adjacent brushes. When the induced voltage E is known, the flux per pole,

$$\phi = \frac{E a \times 60 \times 10^8}{N n p} \text{ lines.} \quad (2)$$

For the design of electrical machinery, it is often convenient to use a hypothetical total flux for the machine, instead of the flux per pole. To

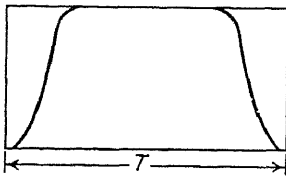


FIG. 19.

determine this hypothetical total flux, the flux density in the air gap is assumed to have maximum value over the entire pole pitch, that is, the shape of the field form is assumed to be rectangular, as shown in Fig. 19. The ratio of the area under the true field form to the area of the hypothetical rectangular field form is called the field form

distribution factor f_d . The hypothetical total flux,

$$\phi_t = \frac{\phi p}{f_d}. \quad (3)$$

Substituting for ϕ , in formula 3, the value given by formula 2,

$$\phi_t = \frac{E a p \times 60 \times 10^8}{N n p f_d} = \frac{E a \times 60 \times 10^8}{N n f_d} \text{ lines.} \quad (4)$$

Output Equation.—The capacity of a given armature diameter and length is dependent, to a large extent, upon ventilation. The best design, from an engineering standpoint, gives a maximum output at a minimum cost. A point of primary importance in accomplishing this

is to ventilate the various parts, to dissipate the maximum watts loss with the least amount of heating. Ventilation, however, can be so good as to make it impracticable to work the machine to its limit, from a heating standpoint, on account of its efficiency reaching a value below the practicable point. Rarely, if ever, assuming reasonably good ventilation, is it practicable to rate direct-current machines on a continuous temperature basis, since invariably commutation or efficiency, or both, will be the limiting factor, rather than temperature.

The armature output of a direct-current generator, expressed in kilowatts, is as follows:

$$\text{Kw}_a = EI_a \times 10^{-3}. \quad (5)$$

From formula 4,

$$E = \frac{\phi_t N n f_a}{a \times 60 \times 10^8} \text{ volts.}$$

Substituting this expression for E into equation 5 above, the output of the armature in kilowatts will be,

$$\text{Kw}_a = \frac{\phi_t N n f_a I_a}{a \times 60 \times 10^{11}}. \quad (6)$$

The total flux is equal to the product of gap area times the maximum air gap density,

$$\phi_t = \pi D l B_g \text{ lines.} \quad (7)$$

If Q equals the ampere conductors per inch of armature periphery, then,

$$Q = \frac{N I_a}{a \pi D} \quad (8)$$

and

$$\frac{N I_a}{a} = \pi D Q.$$

Substituting the expression for ϕ_t from formula 7, and the expression for $\frac{N I_a}{a}$ from formula 8, into the output equation 6,

$$\text{Kw}_a = \frac{n f_a \pi D Q \pi D B_g l}{60 \times 10^{11}} = \frac{n D^2 l f_a Q B_g \pi^2}{60 \times 10^{11}}.$$

This equation may be rearranged into the following form:

$$\frac{D^2 l n}{\text{Kw}_a} = \frac{60 \times 10^{11}}{f_a Q B_g \pi^2} = \frac{60.8 \times 10^{10}}{f_a Q B_g}. \quad (9)$$

The value of B_g , the maximum air gap density, is limited by the permissible value of B_{t2} , the maximum tooth density. The maximum tooth density exists at the root of the tooth and is calculated by the following formula:

$$B_{t2} = \frac{\phi_t}{w_{t2}k_1lS} \text{ lines per sq. in.}$$

Substituting for the total flux, the value given in equation 7, the maximum tooth density,

$$B_{t2} = \frac{B_g \pi D}{w_{t2}k_1lS} \text{ lines per sq. in.}$$

This equation shows that the tooth density is directly proportional to the air gap density. for a given number and size of slots. The m.m.f.

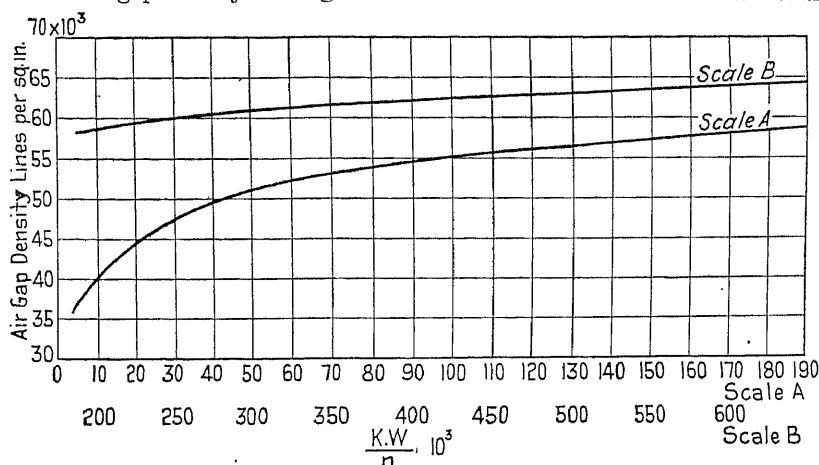


FIG. 20.—Air gap densities for direct-current generators and motors.

required to send the flux through the teeth will be large for high tooth densities, which, in turn, will require a large amount of field copper. The iron losses in the teeth will also be large for high tooth densities. The maximum tooth density, the density at the root of the tooth, should generally not exceed 150,000 lines per square inch. The air gap density must then be lower for machines with small diameters than for machines with large diameters, because of the greater tooth taper for the small diameter machines.

Air gap densities that may be used for preliminary design may be taken from the curve, Fig. 20.

The value of Q in formula 9, the ampere conductors per inch of armature circumference, is limited by commutation, efficiency, cost of construction, and armature heating. The ampere conductors per inch,

for a given rating, may be increased by increasing the number of conductors or by decreasing the armature diameter. By increasing the number of conductors, the reactance voltage will be increased, as will be shown later. If the diameter of the armature is decreased, the length of the armature must be increased in order to have enough iron to carry the flux, and the slots will have to be made deeper in order to accommodate the larger number of ampere conductors per inch of armature circumference. Both of these changes increase the reactance voltage, as may be seen from the reactance voltage formula. Commutation is therefore the limiting factor in the choice of the ampere conductors per inch of armature circumference for machines without commutating poles, whereas for machines with commutating poles, efficiency, cost of construction, and armature heating are the limiting factors. For non-commutating pole machines, Q is usually from 300 to 600. Average values of Q for commutating-pole machines are given in Fig. 21.

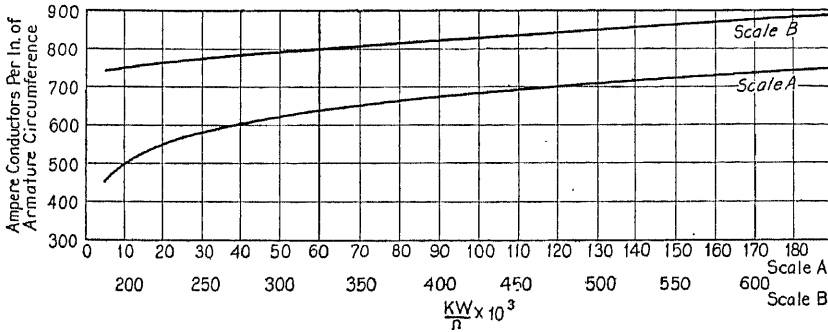


FIG. 21.—Ampere conductors per inch of armature circumference for commutating-pole, direct-current generators and motors.

The air gap flux distribution factor, f_d , depends upon the shape of the field form. The method of obtaining the field form and the field form distribution factor is shown on page 22. The value of the field form distribution factor is, for the shape of pole shoe generally used, approximately equal to the ratio of the pole arc to the pole pitch. The usual values are 0.60 to 0.75.

By substituting average values for f_d , B_a , and Q into equation 9, the right-hand member may be combined into a constant,

$$\frac{D^2 l n}{K w_a} = C \quad (10)$$

or,

$$D^2 l = \frac{K w_a C}{n} \quad (11)$$

where C is called the output constant. This constant is not the same for all machines, neither will it be the same for all machines of the same Kw rating and speed. It depends upon the value of B_a , Q , and f_a . Average values of the output constant for commutating-pole machines for 50° C. rating may be taken from the curves, Fig. 22.

Formula 11 has been developed for a generator. Kw_a in this formula is the armature kilowatt output, which is equal to $E I_a$, where E is the armature induced voltage and I_a is the armature current. This is approximately equal to the output rating in case of a generator. For a motor, the armature output is approximately equal to the motor input. For the curves for air gap density, ampere conductors per inch,

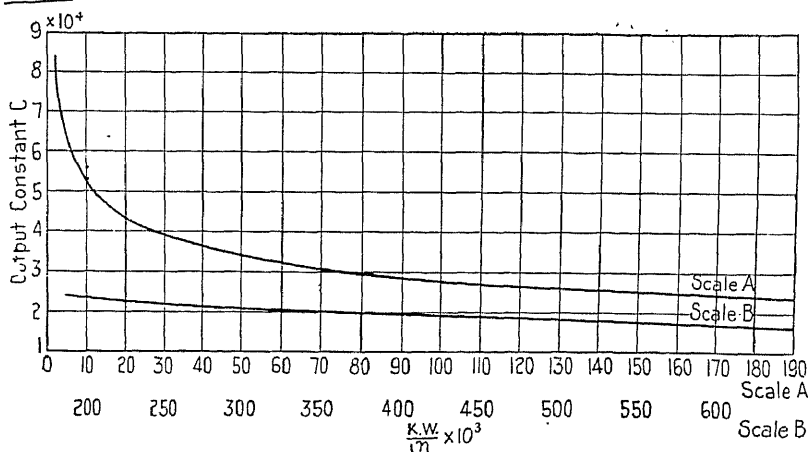


Fig. 22.—Output constants for commutating-pole, direct-current generators and motors.

and output constant, the kilowatt output may be used in case of a generator and the kilowatt input in case of a motor.

Armature Peripheral Speed.—The diameter and length of the armature should be so chosen, whenever possible, that the peripheral speed of the armature will not exceed 6000 ft. per min., as high peripheral speeds lead to expensive constructions and commutation difficulties. For generators for direct connection to steam turbines, the peripheral velocity of the armature may be 15,000 to 20,000 ft. per min. Such generators require special construction and very careful design of the commutating field. Except for turbo-generators, the peripheral velocity of direct-current generators and motors is generally from 1200 to 6000 ft. per min.

The speeds for the smaller size generators are generally chosen to

correspond to the standard 60-cycle induction motor speeds. The generators can then be directly connected to standard induction motors for motor generator sets. For the large sizes, the speeds are generally made to correspond to the standard 60-cycle synchronous motor speeds. The speeds for slow-speed engine-type generators are generally determined from the engine speeds.

✓**Armature Diameter and Length.**—When the output constant is known, the product, D^2l , is readily found. Either the diameter or the length may be assumed and the other dimension calculated. For high speed machines, the diameter is limited by the peripheral velocity.

The length of the armature must be kept within certain limits, because it is difficult to ventilate a long armature properly. If long armatures are necessary, as for turbo-generators, special means for ventilation must be provided. For small two-pole machines, the armature length is often made equal to the armature diameter.

If a value for the ratio, armature diameter to pole pitch, is assumed, then the values of D and l can be found from the product D^2l . For motors and generators with peripheral velocity below 6000 ft. per min., the ratio l/τ is generally from 0.50 to 1.0. For turbo-generators, for which long armatures are unavoidable, the ratio l/τ is sometimes larger than 1.0, whereas for slow speed engine type generators, for which large diameters are desirable, this ratio may be less than 0.50.

The pole pitch,

$$\tau = \frac{\pi D}{p} \quad (12)$$

and

$$\begin{aligned} \frac{l}{\tau} &= (0.50 \text{ to } 1.0) \\ l &= \tau(0.50 \text{ to } 1.0) \\ &= \frac{\pi D}{p}(0.50 \text{ to } 1.0). \end{aligned} \quad (13)$$

Substituting this value for l into the output equation 11,

$$D^2 \frac{\pi D}{p} (0.50 \text{ to } 1.0) = \frac{Kw_a C}{n}$$

or,

$$D = \sqrt[3]{\frac{Kw_a p C}{n \pi (0.5 \text{ to } 1.0)}} = \sqrt[3]{\frac{Kw_a C p}{n (1.5 \text{ to } 3.14)}}. \quad (14)$$

The value of l can be found by formula 11.

When designing a line of direct-current generators and motors, the armature diameters should be so chosen that as many ratings as possible can be obtained with the same armature diameter. There is no fixed rule by which the minimum and maximum length of the armature for each diameter can be determined. These limits will depend upon the operating characteristics desired and upon the cost of construction. The cost of construction will be different for different manufacturers and therefore also the limits of armature length for a given diameter. When in doubt as to the proper value of the armature diameter and length, the only satisfactory method is to make preliminary calculations for two or more machines for different diameter and length and choose the one that will give good operating characteristics for a reasonable cost of construction.

Number of Poles.—In general, the number of poles should be so chosen that good operating characteristics are obtained with minimum weight of active material, and minimum cost of construction.

The frequency of the currents in the armature conductors and of the flux reversals in the armature core is directly proportional to the number of poles and speed. The frequency,

$$f = \frac{pn}{2 \times 60} \text{ cycles per sec.} \quad (15)$$

The losses in the armature core and teeth will increase with the frequency for a given flux density. To avoid excessive iron losses with high frequencies, the flux density in the armature core and teeth must be kept low, which will require increased armature iron weight. The usual frequencies for direct-current motors and generators are from 15 to 45 cycles per second.

The pole pitch varies directly with the armature diameter and inversely with the number of poles. For a large pole pitch, the length of the armature coil end-connections will be large, and therefore also the losses and the weight of the armature copper. The ampere-turns per pole on the armature vary with the pole pitch, and, since the ratio of the field ampere-turns to the armature ampere-turns should be equal to from 1.0 to 1.25 (see p. 79, Chapter V), it follows that the ampere-turns on the field will also increase with the pole pitch. A large number of ampere-turns on the field require a heavy shunt field winding, which is difficult to ventilate and leads to high shunt field losses. Excepting for very large capacity, slow-speed machines, it is usually desirable to use a number of poles, which will give a pole pitch less than 15 in.

For large-capacity, low-voltage machines, the number of poles may be determined by the amount of current that can be collected by each

brush arm. With a brush thickness of $\frac{3}{4}$ in. and with a current density of 50 to 60 amperes per square inch of brush contact, a current of about 1000 to 1200 amperes per brush arm can be used.

To guide the beginner in selecting a number of poles, the following tables are given:

TABLE I
MEDIUM AND HIGH SPEED

Kw Output	Speed in r.p.m.	No. of Poles
Up to 10	Over 1300	2
10 to 100	Up to 1300	4
50 to 300	Up to 1000	4 or 6
200 to 600	Up to 600	6 to 10
600 to 1000	Up to 500	8 to 12

TABLE II
SLOW SPEED ENGINE TYPE

Kw Output	Speed in r.p.m.	No. of Poles
35 to 150	225 to 300	6
200 to 250	135 to 225	8
250 to 500	100 to 150	10

See also tables given by W. T. Ryan¹ in "Design of Electrical Machinery."

When in doubt as to the number of poles to use for a motor or generator of given Kw capacity and speed, it will be necessary to calculate the weight of material, losses, and cost of construction, to determine the number of poles that will give best operating characteristics at the lowest cost.

Design of the Pole Shoe.—The air gap flux distribution curve must have such shape that the best possible commutation will result. To obtain good commutation, the flux density in the air gap must decrease gradually from maximum value under the center of the pole to zero on a center line between two poles, and the flux densities near the neutral point must be low. A field form that drops off rapidly from maximum

¹ "Design of Electrical Machinery," by W. T. Ryan, Vol. I, pp. 3, 4, and 5, in Wiley & Sons, Inc., New York.

value to zero does not only lead to commutation difficulties, but may also give rise to magnetic noises in machines with slotted armatures.

The shape of the field form depends upon the shape of the pole shoe and the per cent pole embrace. The ratio of the pole arc on the armature surface to the pole pitch on the armature surface, expressed in per cent, is called the per cent pole embrace. A large per cent pole

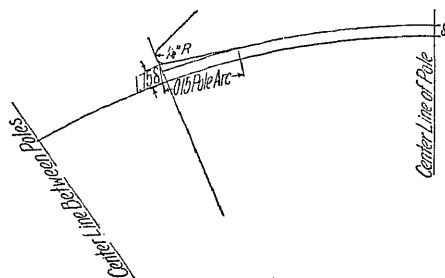


FIG. 23.

embrace is desirable, because it is possible to have a low air gap density with a large flux per pole. On the other hand, the leakage flux, the flux that passes between poles and does not cross the air gap, will be large for a large per cent pole embrace. For direct-current machines, 60 to 75 per cent pole embrace is generally satisfactory.

For commutating-pole motors and generators, the ratio of the pole arc to the pole pitch should generally not exceed 70 per cent. The lower values are necessary to avoid excessive leakage flux for main and commutating-pole. The number of slots embraced by the pole may in some cases determine the pole arc (see page 42, Chapter III).

For commutating-pole machines, 66 per cent pole embrace is generally satisfactory. A good air gap flux distribution curve is obtained with the shape of pole shoe shown in Fig. 23.

Construction of No-Load Field Form.—The useful flux per pole, in passing from the pole shoe into the armature, spreads out over the entire pole pitch. The flux will distribute itself in the air gap in such a way that the total reluctance will be a minimum. The

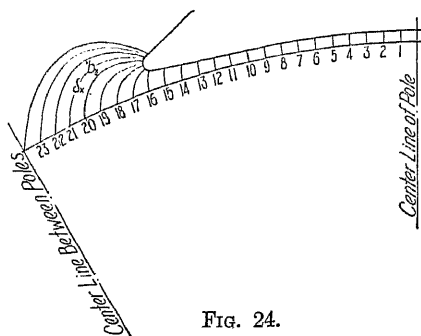


FIG. 24.

The flux path in the air gap under the pole may be assumed to be divided into tubes of force, as shown in Fig. 24, each tube being of unit length in the direction parallel to the shaft.

If b_x is the mean width of such a tube of force, and δ_x the mean length, then the permeance of the tube is proportional to $\frac{b_x}{\delta_x}$, and the flux density, B_x , for a small portion of the armature surface of width, a_x , and of unit

length, is proportional to $\frac{b_x}{a_x \delta_x}$. If B_g is the maximum air gap density at the center of the pole, where the air gap has a length δ , then B_g is proportional to $\frac{1}{\delta}$, because a_x is equal to b_x at the center of the pole.

Since the same m.m.f. acts on the tube of force at the center of the pole and at the pole tip, the air gap densities are to each other as their respective permeances, that is,

$$B_x : B_g :: \frac{b_x}{a_x \delta_x} : \frac{1}{\delta}$$

or,

$$B_x = \frac{b_x \delta}{a_x \delta_x} B_g. \quad (16)$$

To construct the air gap flux distribution curve, it will then be necessary to plot² the magnetic flux distribution in the air gap. Since

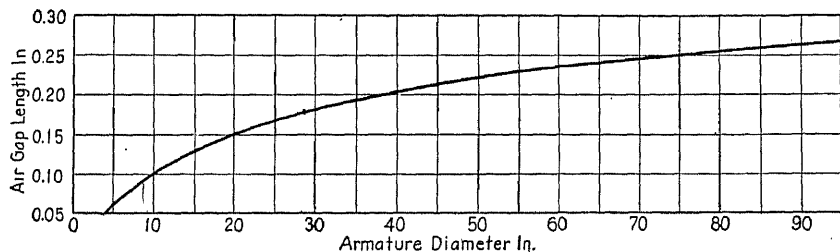


Fig. 25.—Approximate air gap lengths for direct-current generators and motors.

the pole is symmetrical about the center line, it is necessary to lay out only one-half of the pole and one-half of the pole pitch on the armature surface. For this construction the length of the air gap must be known; it may be estimated with the help of the curve Fig. 25.

In plotting magnetic fields, it is generally assumed that the iron of the pole shoe and armature have infinite permeability as compared to air. The flux lines will then leave the pole face and enter the armature at right angles.

The flux and equipotential lines must intersect at right angles and are so drawn that each tube of force is divided into a number of equal squares. From equation 16 it is apparent that the flux density at any point on the armature surface will be proportional to the ratio of

² Archiv für Elektrotechnik, Vol. 11, 1922, p. 85; Electric Journal, Vol. 23, July, 1926, p. 355; General Electric Review, Vol. 29, Nov., 1926, p. 797; A.I.E.E. Journal, Vol. 46, p. 430 and discussion, p. 614.

the length of a side of a square at the center of the pole, to the length of a side of a square at the point on the armature surface under consideration. This is true if the same number of equipotential lines is used at the center of the pole as at the pole tip. For a larger number of squares at the pole tip, the ratio of the sides of the squares must be multiplied by the ratio of the number of squares. The flux plot for a 300-kw, 900-r.p.m. direct-current generator is shown in Fig. 26.

The air gap flux distribution curve is easily obtained from the flux plot by dividing one-half of the pole pitch on the armature surface into a convenient number of equal parts. The length of the squares is

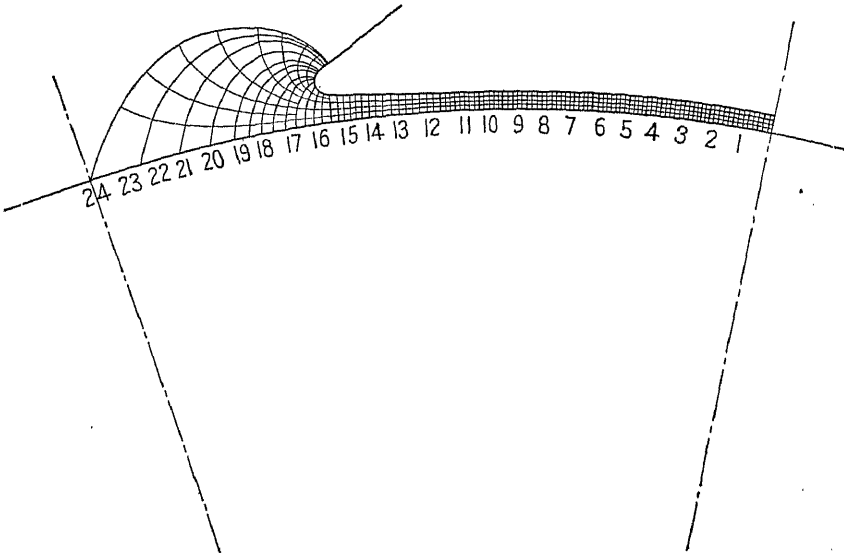


FIG. 26.—Flux plot for 300 kw. generator.

scaled from the drawing for each of the points on the armature surface, and the flux density is calculated as explained above. The density at the center of the pole is taken as 100, or 100 per cent.

By plotting the points on the armature surface as abscissas and corresponding values of flux density as ordinates, the curve, showing the flux distribution on the armature surface, is obtained. Figure 27 shows the flux distribution curve for the flux plot shown in Fig. 26. As Fig. 27 shows, the flux distribution curve does not pass through zero on the center line between poles. By superimposing a portion of the field form of the adjacent pole, which is of opposite polarity, and subtracting the corresponding ordinates, the true field form is obtained.

In Fig. 27, CF is equal to CD but is of opposite polarity. By subtracting the ordinates of CF from CB , the true flux distribution curve, BE , is obtained. The accuracy employed in making the flux plot will determine the accuracy of the flux distribution curve.

The author has used for some time in the design of electrical machinery, a very much simplified method³ to obtain the field form. It consists of dividing one-half of the pole pitch on the armature surface into a convenient number of parts, and drawing the center line of a tube of force for each point in such a way that it will leave the pole face and enter the armature surface at right angles.

If the length of the air gap at the center of the pole is taken as the unit for measuring the length of the remaining flux lines, and if the

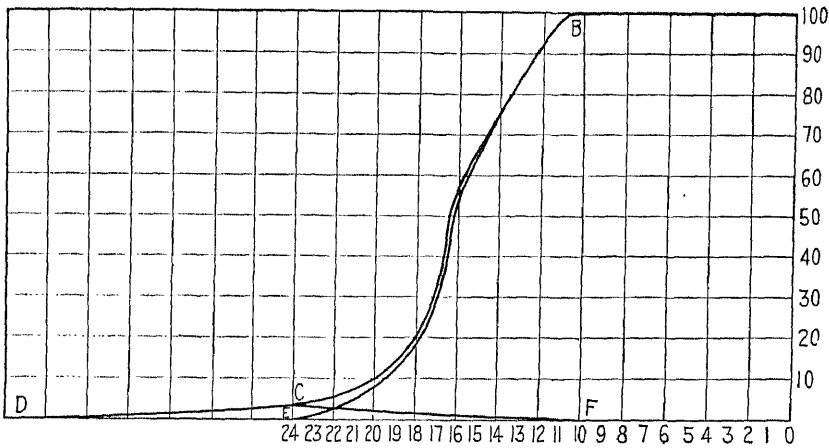


FIG. 27.—Flux distribution curve for flux plot shown in Fig. 26.

average width of the tube of force is assumed to be equal to the maximum width, then formula 16 becomes,

$$B_x = B_o \frac{1}{\delta_x} \quad (16a)$$

with δ_x measured in terms of δ , the length of the air gap at the center of the pole. The value of the flux density for each of the points on the armature surface can easily be calculated by formula 16a, and the field form curve plotted. The true field form is obtained in the same way as explained for Fig. 27. The method of drawing the flux lines is shown in Fig. 24 and is for the same pole shown in Fig. 26. The flux distribution curve is shown in Fig. 28.

³ See also *Electric Journal*, Vol. 24, May, 1927, p. 215.

This method is, obviously, only approximate and gives the density at a point approximately midway between the armature surface and pole shoe. For the purpose of determining the air gap flux distribution factor, this method is generally sufficiently accurate, because a small error in the determination of the flux distribution curve in the inter-polar space will have only a small effect upon the flux distribution constant.

The flux distribution curves shown in Figs. 27 and 28 have been constructed on the assumption that the armature core and pole tips are

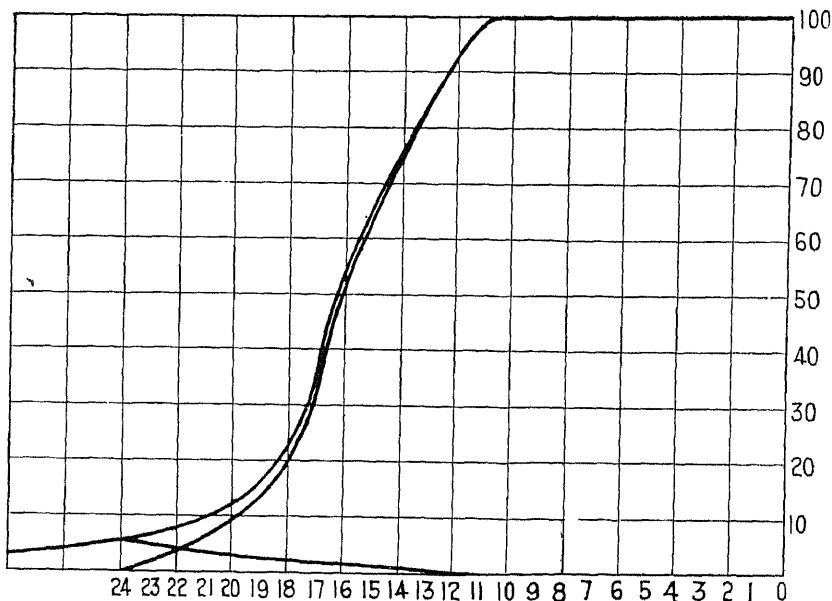


FIG. 28.—Flux distribution curve for flux plot shown in Fig. 24.

not saturated, and that the armature surface is a smooth surface with no slots. The effect of open armature slots is to produce notches in the top of the field form, as shown in Fig. 29, which is the field form of a small direct-current generator taken with an oscillograph. These notches travel along the wave during rotation so that the field forms of Figs. 27 and 28 show the average wave form.

Air Gap Flux Distribution Factor.—The definition of the air gap flux distribution factor has been given above as the ratio of the area under the flux distribution curve to the area of a rectangle having the same base and maximum ordinate. The area under the flux distribution curve can be found by the use of a planimeter; this area divided by

the area of a rectangle having the same base and maximum ordinate gives the air gap flux distribution factor.

The flux distribution curve and rectangle have the same base line. The air gap flux distribution factor can, therefore, also be defined as the ratio of the average to the maximum ordinate. The average ordinate can be found by dividing the base line into a number of equal sections, the sum of the mean ordinates of each section divided by the number of ordinates being the average ordinate. Figure 27 shows the air gap flux distribution curve and the calculations for the average ordinate and flux distribution constant for the flux plot shown in Fig. 26.

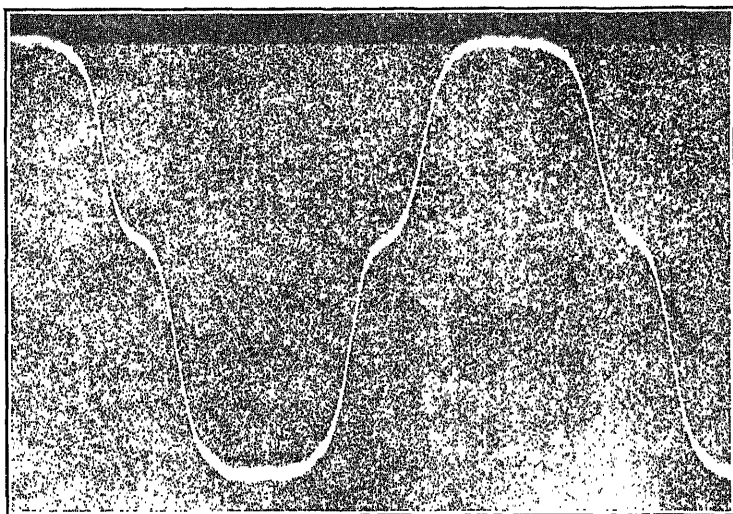


FIG. 29.—Air gap flux distribution curve of 5-kw., 1200-r.p.m., direct-current generator.

Sample Design.—A 300-Kw, 900-r.p.m., 230-volt, compound-wound, direct-current generator is to be designed. The generator is to be part of a synchronous motor generator set, to have commutating poles, and be over compounded to give a full load voltage equal to 250 volts. The efficiency of the generator should not be less than 92.0 per cent at full-load and normal voltage, and is to be calculated from the losses in accordance with the A.I.E.E. Standards. The temperature rise of no part of the generator should exceed 50° C. when operating at full load continuously.

$$\frac{Kw}{n} \times 10^3 = \frac{300}{900} \times 10^3 = 333$$

The output constant from the curve Fig. 22, is 2.04×10^4 .

Table I, page 21, shows that the best design can generally be obtained with 6 poles for a machine of this size and speed.

By formula 14, page 19,

$$D = \sqrt[3]{\frac{Kw_a C p}{n(1.5 \text{ to } 3.14)}} = \sqrt[3]{\frac{300 \times 2.04 \times 10^4 \times 6}{900(1.5 \text{ to } 3.14)}}$$

$$= 30.0 \text{ to } 23.5 \text{ in.}$$

The corresponding values for l , the length of the armature, are calculated by formula 11,

$$l = \frac{Kw_a C}{nD^2} = \frac{300 \times 2.04 \times 10^4}{900 \times (30.0^2 \text{ to } 23.5^2)}$$

$$= 7.55 \text{ to } 12.30 \text{ in.}$$

The peripheral speed for 30-in. armature diameter is:

$$v = \frac{\pi D n}{12} = \frac{3.14 \times 30 \times 900}{12}$$

$$= 7060 \text{ ft. per min.}$$

and for 23.5-in. armature diameter it is 5530 ft. per min.

In order to avoid expensive constructions, it is generally desirable to use peripheral speeds of 6000 ft. per min. or less. Therefore, an armature diameter of 25 in. is chosen for this design. The peripheral speed will then be,

$$v = \frac{\pi D n}{12} = \frac{3.14 \times 25 \times 900}{12}$$

$$= 5890 \text{ ft. per min.}$$

The length of the armature,

$$l = \frac{Kw_a C}{nD^2} = \frac{300 \times 2.04 \times 10^4}{900 \times 25^2}$$

$$= 10.9 \text{ in.; use } 11.0 \text{ in.}$$

The frequency of the flux reversals in the armature core,

$$f = \frac{pn}{2 \times 60} = \frac{6 \times 900}{2 \times 60}$$

$$= 45 \text{ cycles per sec.}$$

The pole pitch on the armature circumference,

$$\tau = \frac{\pi D}{p} = \frac{\pi \times 25}{6} = 13.10 \text{ in.}$$

Choosing 66 per cent pole embrace, the pole arc on the armature circumference,

$$B = \tau \times 0.66 = 13.10 \times 0.66 = 8.64; \text{ use } 8\frac{5}{8} \text{ in.}$$

The length of the air gap is taken equal to 0.17 in. (see curve Fig. 25). The shape of the pole shoe is made the same as shown in Fig. 23. The flux plot is shown in Fig. 26 and the flux distribution curve in Fig. 27. The air gap flux distribution factor is 0.665.

3354

621.31042 N30

IISc Lib B'lore
621.31042 N30



3354

CHAPTER III

ARMATURE WINDINGS AND INSULATION

THE following armature windings are used for modern direct-current generators and motors:

1. Lap Windings.

- (a) Simplex Lap Windings, for which $a = p$
- (b) Multiplex Lap Windings,¹ for which $a = mp$

2. Wave Windings.

- (a) Simplex Wave Windings, for which $a = 2$
- (b) Multiplex Wave Windings,¹ for which $a = 2m$

3. Frogleg Windings.

Simplex Lap Windings.—A simplex lap winding for a 4-pole machine with 24 armature slots and 2 coil sides per slot is shown in Fig. 30. The position of the coils in the slots and the connection of the coils to the commutator are apparent when tracing the coils of the armature winding. Starting with commutator segment 1, Fig. 30, and passing by front end-connection to coil side 1, in the top of slot 1, along coil side 1 to the back of the armature, along back coil end-connection to coil side 14 in the bottom of slot 7, along coil side 14 to front of armature and along front end-connection to commutator segment 2, one armature coil is traced. Continuing now from commutator segment 2 to coil side 3, across the back of the armature to coil side 16 and then along coil side 16 to commutator segment 3, two armature coils are traced. In this way, after returning to commutator segment 1, along the front end-connection of coil side 48, the entire winding will have been traced.

¹ Multiplex windings are not used much in practical machine design, and discussion of them is omitted here. The reader wishing information on these windings is referred to "Armature Winding and Motor Repair," by D. H. Braymer, pp. 1-25, McGraw-Hill Book Co., New York; "Principles of Direct Current Machines," by Alexander Langsdorf, 3rd ed., pp. 116 to 147, McGraw-Hill Book Co., New York; "Die Gleichstrommaschine," by Dr. Arnold and LaCour, pp. 28-90, Julius Springer, Berlin.

From Fig. 30 it is apparent that the coil sides are arranged in two layers and that the two coil sides connected together by the end-connection on the back of the armature are in different layers, one in the top of a slot and the other in the bottom of a slot. It is also apparent that the slots in which the two sides of each coil lie are a pole pitch apart and that the terminals of each coil connect to adjacent commutator bars.

The interval between the two coil sides connected by the end-

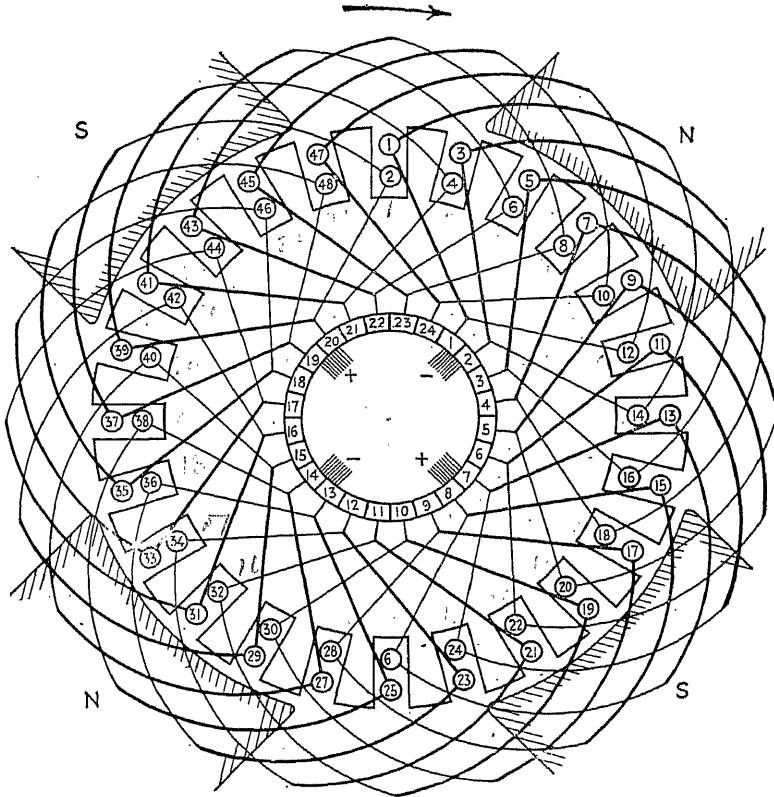


FIG. 30.—Progressive simplex lap winding, $S = 24$, $K = 24$, $p = 4$.

connection on the back of the armature is called the back pitch, Y_1 , and is expressed in terms of the number of coil sides spanned, whereas the interval between the two coil sides connected on the front of the armature is called the front pitch, Y_2 , and is also expressed in terms of the number of coil sides spanned. In tracing the armature winding, we progress in one direction at the back and in the opposite direction at the front of the armature. One pitch, usually the back pitch, is,

therefore, considered positive and the other negative. The algebraic sum of the back and front pitch is called the resultant pitch, and is always equal to 2, for simplex lap windings. The back pitch and front pitch must always be an odd integer.

The interval between the commutator segments to which the terminals of one coil are connected is called the commutator pitch, Y_c , and is expressed in terms of number of commutator segments. Figure 30 shows that the commutator pitch is always equal to one, for a simplex lap winding. The back pitch, front pitch, and commutator pitch are shown in Fig. 31, which is a developed diagram of the winding shown in Fig. 30.

The armature coils may be connected to the commutator segments

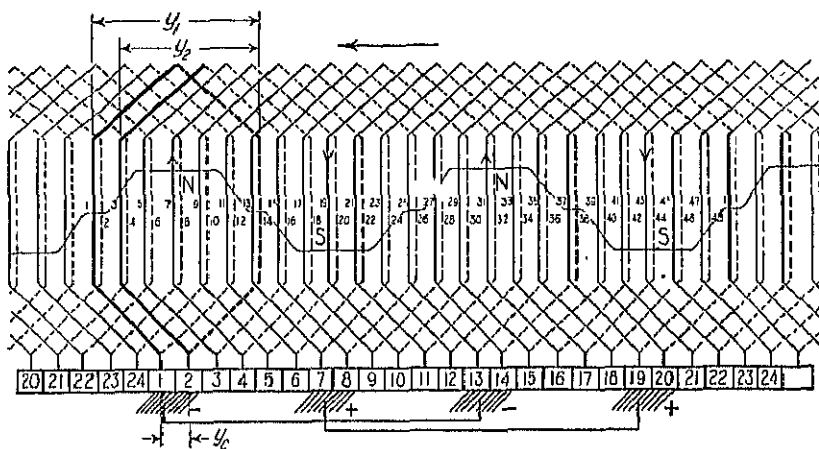


FIG. 31.—Developed progressive simplex lap winding diagram, $S = 24$, $K = 24$, $p = 4$.

as shown in Fig. 32. If we trace the winding starting with commutator segment 1 and passing along front end-connection to coil side 1, along coil side 1 to back of armature, along back end-connection to coil side 14, along coil side 14 to front of armature, we come by front end-connection to commutator segment 24 and not to commutator segment 2, as for the winding shown in Fig. 30. From commutator segment 24 we pass to commutator segment 23, etc. For the winding shown in Fig. 32, we progress around the armature in counterclockwise direction when tracing the winding, whereas for the winding shown in Fig. 30 we progress in the clockwise direction. The winding in Fig. 32 is called a retrogressive winding and that in Fig. 30 a progressive winding. For the progressive winding the back pitch is larger than the front pitch,

whereas for the retrogressive winding the front is larger than the back. The resultant pitch and the commutator pitch are positive for the progressive winding and negative for the retrogressive winding.

It is obvious from Figs. 31 and 32 that the polarity of the progressive winding is opposite to the polarity of the retrogressive winding. A motor with retrogressive armature winding will therefore run in opposite direction to a motor with progressive armature winding. The space required for connecting the armature coils to the commutator and the length of the mean-turn of the armature coil will be slightly larger for the retrogressive winding than for the progressive winding. Since the retrogressive winding offers no advantages over the progressive winding, lap windings should always be made progressive.

The back pitch expressed in terms of the number of slots embraced

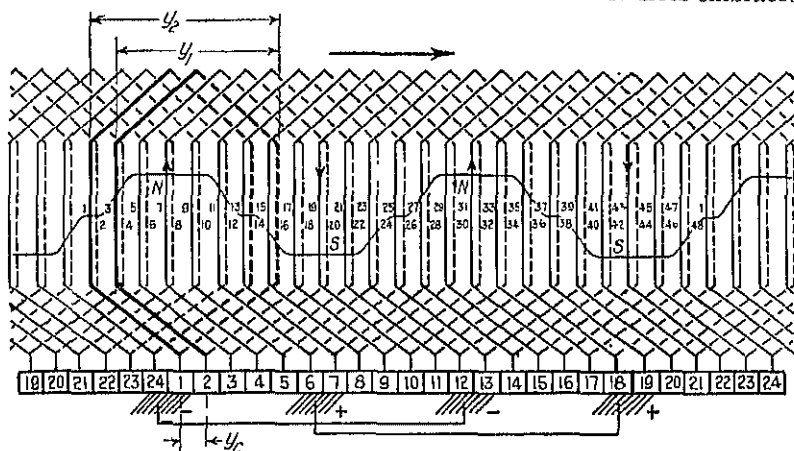


FIG. 32.—Developed retrogressive simplex lap winding diagram.

by the armature coil is called the coil pitch, Y_s ; it is always approximately equal to the number of slots per pole.

The formulas for the simplex lap winding can now be written as follows:

The coil pitch,

$$Y_s = \frac{S}{p} \quad (17)$$

the back pitch and front pitch,

$$Y_1 = C_s Y_s + 1 \quad (18)$$

and

$$Y_2 = Y_1 - 2Y_s \quad (19)$$

and one commutator pitch,

$$Y_c = \pm 1. \quad (20)$$

For the winding shown in Fig. 30,

$$Y_s = \frac{S}{p} = \frac{24}{4} = 6$$

$$Y_1 = C_s Y_s + 1 = 2 \times 6 + 1 = 13$$

$$2Y_c = Y_1 - Y_2 = 13 - Y_2$$

$$Y_2 = 13 - 2 = 11$$

and for the winding shown in Fig. 32,

$$Y_s = 6, \quad Y_1 = 13, \quad Y_2 = 13 - 2 = 11.$$

The windings thus far shown have two coil sides per slot, and the number of slots per pole is an integer. Figure 33 shows a progressive simplex lap winding for a 4-pole machine with 26 slots and 4 coil sides per slot,

$$Y_s = \frac{S}{p} = \frac{26}{4} = 6\frac{1}{2}; \text{ use } 6$$

$$Y_1 = C_s Y_s + 1 = 4 \times 6 + 1 = 25$$

$$2Y_c = Y_1 - Y_2 = 25 - Y_2$$

$$Y_2 = 25 - 2 = 23.$$

From this diagram it is obvious that the coil sides short-circuited by the brushes do not all lie in the same position in all the slots. The reason for this is the fact that the winding is chorded, that is, the coil throw is less than full pitch. Chording the armature winding has the effect of decreasing the mean-turn of the armature coil and the weight of the armature copper, but, because of its effect upon commutation, a chording of one slot pitch can ordinarily not be exceeded. For commutating-pole machines, the armature coils should in general not be chorded more than one-half slot pitch, because a wide commutating pole is required for chorded windings, in order that the coils in the commutating zone will be under the effect of the commutating pole.

Simplex Wave Windings.—A simplex wave winding for a 4-pole machine with 26 armature slots and 2 coil sides per slot is shown in Fig. 34. The development of the simplex wave winding is apparent when tracing through the armature winding. Starting with commutator segment 1, in Fig. 34, and passing along front end-connection

end-connection to coil side 14, along coil side 14 to the front of the armature, and along front end-connection to commutator segment 13, one armature coil is traced. Continuing in this way, until $p/2$ coils have been traced, the armature will have been passed around once

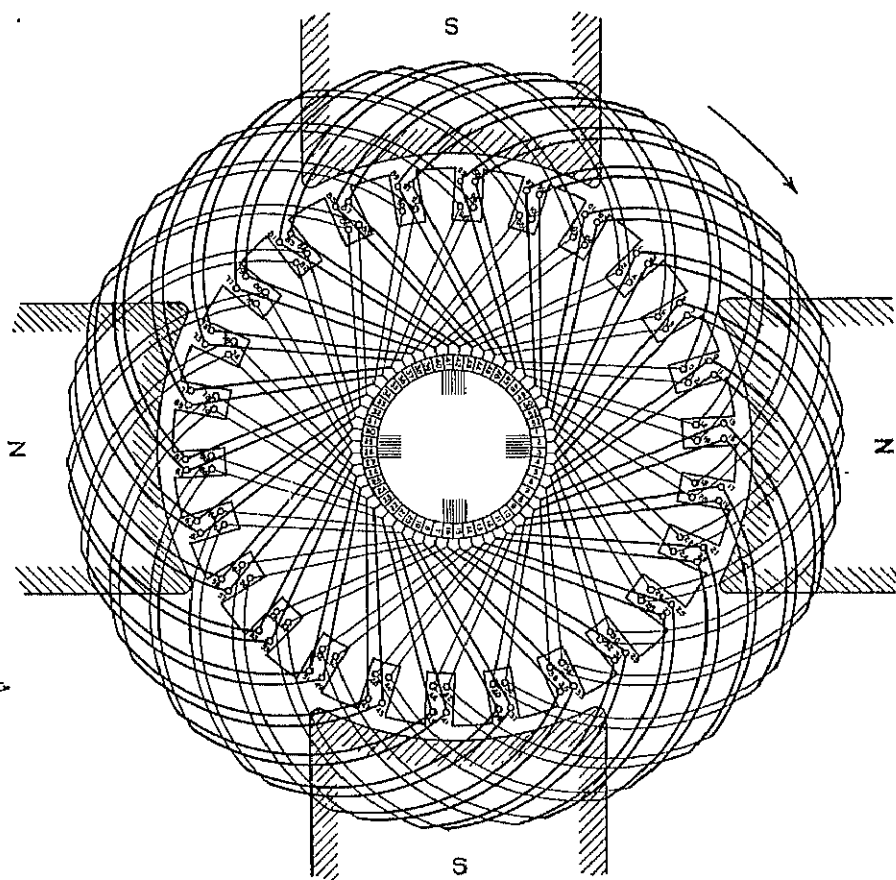


FIG. 33.—Progressive simplex lap winding, $S = 26$, $K = 52$, $p = 4$.

when commutator segment 25, adjacent to segment 1, is encountered. If the armature is passed around in this way as many times as there are commutator segments between the terminals of a coil, the winding will close on commutator segment 1.

Just as for the lap winding, the coil sides of the wave winding are arranged in two layers, with the sides of each coil lying in different

of the wave winding connect to commutator segments, which lie $\frac{2K}{p}$ segments apart.

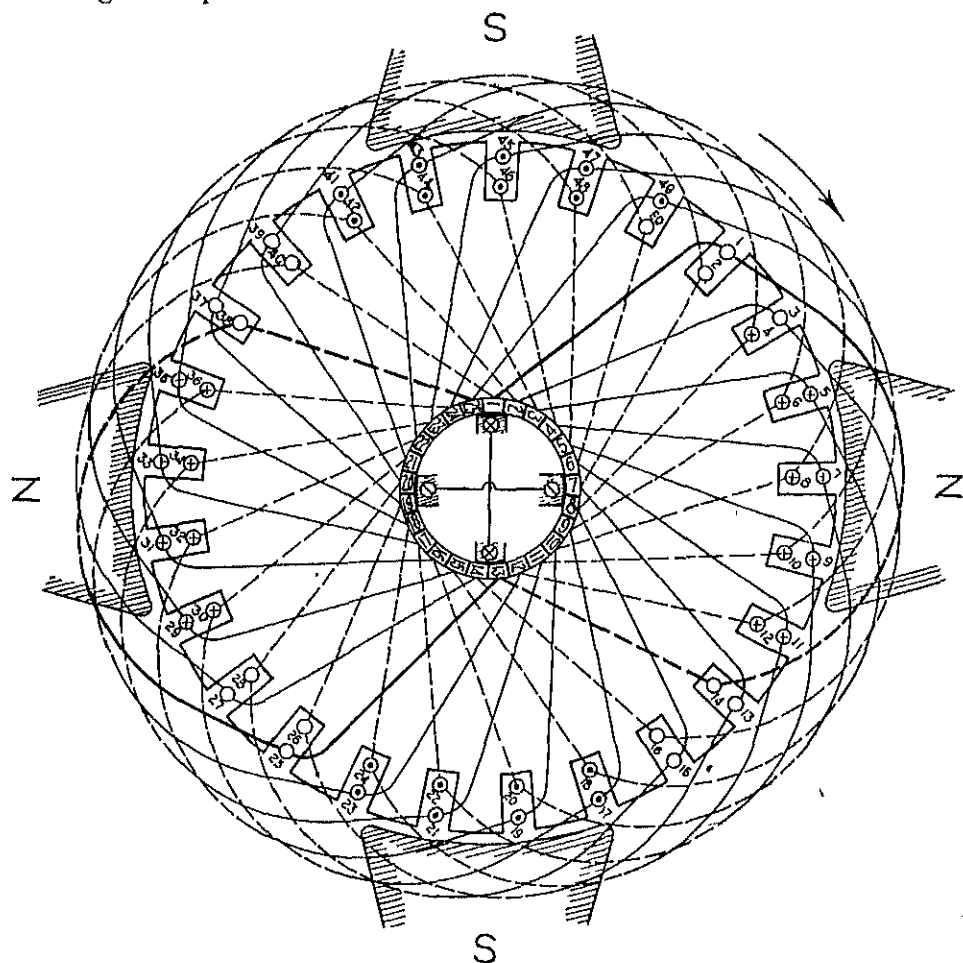


FIG. 34.—Retrogressive simplex wave winding, $S = 25$, $K = 25$, $p = 4$.

The front pitch, back pitch, resultant pitch, and commutator pitch are shown in Fig. 35, which is a developed winding diagram for the winding shown in Fig. 34. It is apparent from this diagram that the back pitch and front pitch are both measured in the same direction and that the resultant pitch is the sum of the back and front pitch.

connection is made to a commutator segment to the right of the first

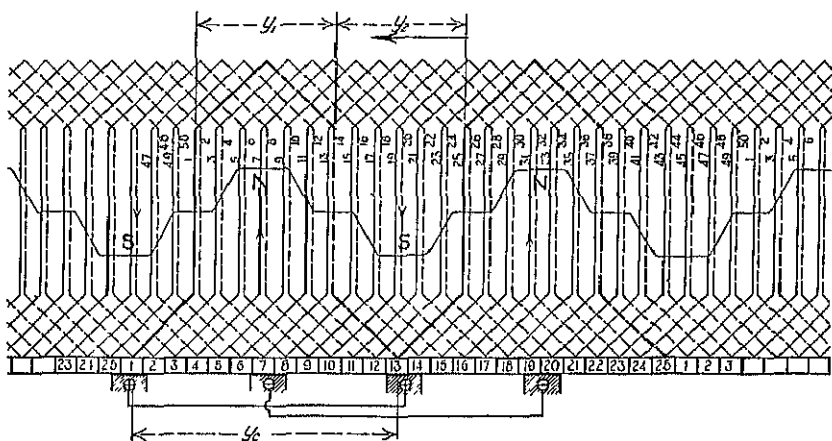


FIG. 35.—Developed retrogressive simplex wave winding diagram,
 $S = 25$, $K = 25$, $p = 4$.

segment, as shown in Fig. 36, the winding is called a progressive winding, and if connection is made to a commutator segment to the left of the first segment, as shown in Fig. 34, it is called a retrogressive

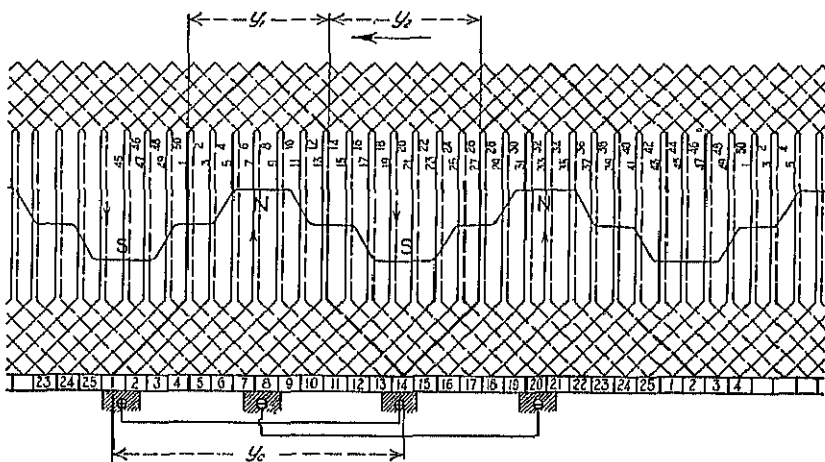


FIG. 36.—Developed progressive simplex wave winding diagram,
 $S = 25$, $K = 25$, $p = 4$.

winding. For wave windings, the retrogressive winding is used whenever possible.

ments are passed over, when passing around the armature once in tracing the winding, and that connection is made to the commutator $p/2$ times, with connection points a commutator pitch, Y_c , apart. Therefore,

$$\frac{p}{2} Y_c = K \pm 1$$

and

$$Y_c = 2 \frac{K \pm 1}{p}. \quad (21)$$

When the positive sign is used, the winding will be progressive and when the negative sign is used, it will be retrogressive. The coil pitch,

$$Y_s \cong \frac{S}{p}$$

and the back pitch and front pitch,

$$Y_1 = C_s Y_s + 1$$

$$Y_2 = 2Y_c - Y_1.$$

For the winding shown in Fig. 34:

$$Y_s \cong \frac{S}{p} = \frac{25}{4} = 6\frac{1}{4} = 6, \quad Y_1 = C_s Y_s + 1 = 2 \times 6 + 1 = 13$$

$$Y_c = \frac{K \pm 1}{p} 2 = \frac{25 - 1}{4} 2 = 12, \quad Y_2 = 2Y_c - Y_1 = 2 \times 12 - 13 = 11$$

and for the winding shown in Fig. 36:

$$Y_s = 6, \quad Y_1 = 13, \quad Y_c = 13, \quad Y_2 = 13.$$

From the developed diagram, Fig. 35, it is obvious that half of all the armature coils are connected in series, so that the number of parallel paths for a simplex wave winding is always 2, regardless of the number of poles. Figure 35 also shows that all brushes of like sign are connected by the coils lying in the neutral zone. It is then not necessary to connect brushes of like sign, and all brushes, with the exception of one positive and one negative, may be omitted. In general, wave-wound machines have as many brush arms as there are poles. In some cases, for example, in street railway motors, it is difficult to obtain access to one or more brush sets. For such cases, sets of brushes are often omitted.

The number of coil sides per slot need not be 2, as shown in Figs. 34 and 35. It can be more than 2, but must be a multiple of 2. The number of coil sides per slot that may be used for any number of poles is much more limited for a wave winding than for a lap winding. If all slots are to have the same number of coil sides and if for K , in formula 21, $\frac{C_s}{2}S$ is used, then

$$Y_c = \frac{\frac{C_s}{2}S \pm 1}{p} - 2. \quad (22)$$

If, for example, $C_s = 6$, there is no number of slots, S , for a 6-pole machine that will make the commutator pitch, Y_c , an integer. The accompanying table ² gives the number of coil sides per slot for various numbers of poles, for which a wave winding is possible with all coils connected to the commutator, that is, no dead coils.

TABLE III

No. of Poles	Coil Sides per Slot				
p	C_s				
4	2	—	6	—	
6	2	4	—	8	
8	2	—	6	—	
10	2	4	6	8	
12	2	—	—	—	
14	2	4	6	8	
16	2	—	6	—	

If it is desired to use a certain number of slots for a given number of poles and coil sides per slot, it may not always be possible to have the commutator pitch equal to an integer, with the full number of commutator segments and coils. For example, if it is desired to use 50

² "Die Gleichstrommaschine," Vol. 1, 3rd ed., p. 52, Julius Springer, Berlin.

slots on a 4-pole machine with 6 coil sides per slot, then the commutator pitch,

$$Y_c = \frac{150 \pm 1}{4} 2 = 74\frac{1}{2} \text{ or } 75\frac{1}{2}.$$

But the commutator pitch must be an integer. If one commutator bar is omitted and one coil in the armature winding is not connected, then the commutator pitch,

$$Y_c = \frac{149 \pm 1}{4} 2 = 74 \text{ or } 75.$$

The coil that is not connected is called a "dead coil." It is placed on the armature to keep the armature mechanically balanced but is not connected to the commutator. The number of armature slots will usually be an odd number, as formula 22 shows, and wave windings, therefore, will generally be chorded windings and not pitch windings. What has been stated about chording of lap windings applies also to wave windings.

Equalizer Connections.—From the developed winding diagram shown in Fig. 31 it is obvious that, for the lap winding, all the coils of one armature path lie under adjacent poles. If the flux in the air gap under the poles is not the same for all the poles, the voltage induced in the various armature paths will not be the same. In consequence of this difference in voltage of the armature paths, equalizing currents will flow through the brushes. These equalizing currents may overload the brushes³ and may cause local armature heating and sparking at the brushes.

The inequality of the flux under the poles may be caused by unequal air gap lengths under the poles, by a difference in the shape of the pole shoe, or by non-uniformity of the material of the field poles and yoke, caused by "blow-holes" and the like in cast steel poles and yoke.

If commutator bars which occupy the same position under poles of like polarity are connected, the armature current will be equalized before commutation. These connections between points of the same potential are called equalizer connections. The interval between equipotential points, expressed in number of commutator bars, is called the equalizer pitch,

$$Y_e = 2 \frac{K}{a} \quad (23)$$

The best possible equalization is obtained when all points of equal

³"History of the Development of the D.C.-Generator in America," Electric Journal, Vol. 12, p. 117.

potential are connected by equalizer connections. The number of equalizer connections shown in Fig. 37 is used only for very high-speed and large-capacity machines. An equalizer connection for every 3 or 4 commutator bars has been found to be satisfactory for normal machines.

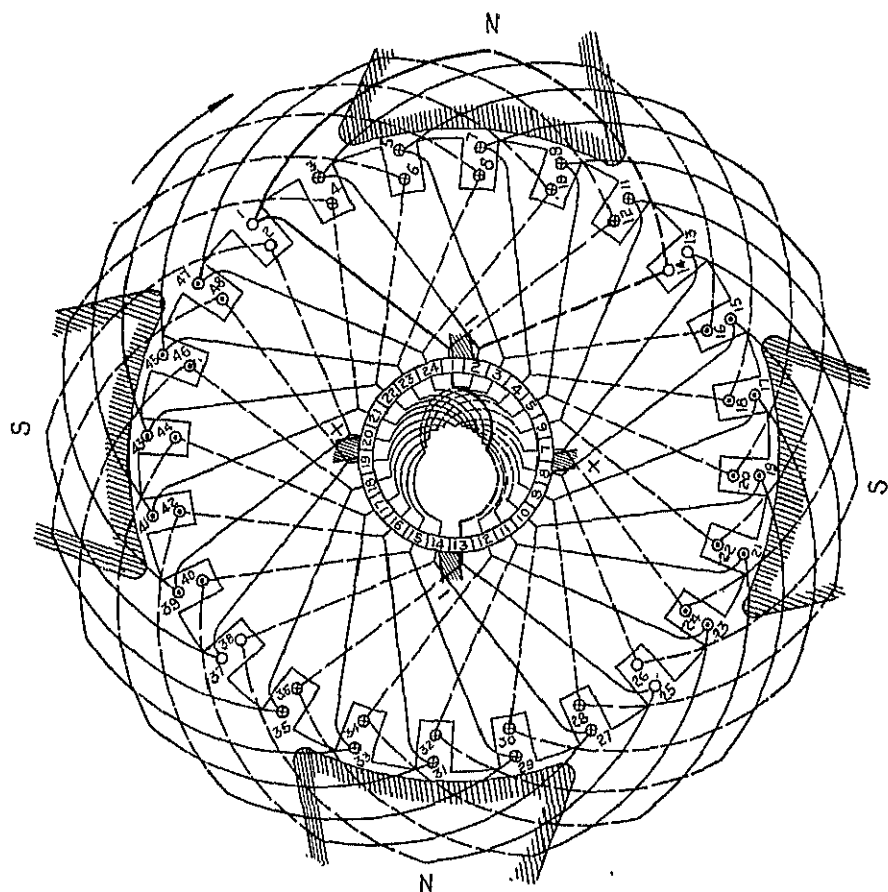


Fig. 37.—Simplex lap winding with equalizer connections.

The section area of the conductor used for equalizer connections depends upon the value of the equalizer current. This current cannot be predetermined. Practice has shown that, with the number of equalizer connections given above, a section area of the equalizer conductor equal to from 0.50 to 1.0 times the section area of the armature conductor is satisfactory for most cases.

— or wave windings, unequal flux under the various poles has no effect upon the voltage induced in each armature path, because all the coils of each path are approximately uniformly distributed under all the poles.

Frogleg Winding.—The frogleg winding consists of a lap winding and a wave winding placed on the same armature. The wave winding is connected to the commutator at the equipotential points of the lap winding. In this way, the wave winding acts as an equalizer for the lap winding at the same time that it is carrying useful current. This type of winding is described by W. H. Powell and G. M. Albrecht.⁴

Number of Armature Slots.—The total number of conductors, N , can be determined by formula 4,

$$N = \frac{Ea \times 60 \times 10^8}{\phi_{\text{infa}}}$$

The conductors per slot must be an integer, and for two-layer windings

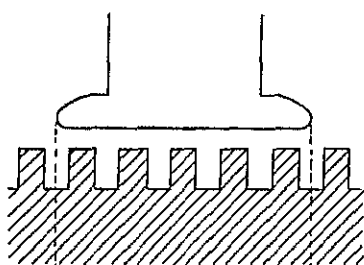


FIG. 38a.

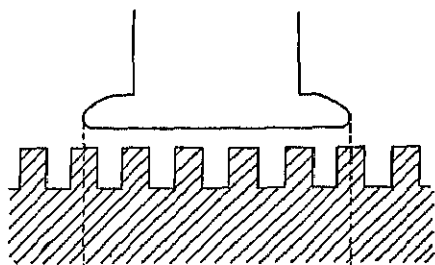


FIG. 38b.

they must be an even number. A small number of slots require a large slot, because the number of conductors per slot will then be large. A saving in insulating material is generally possible by the use of a small number of slots, but because of the effect of a small number of open slots⁵ upon the flux in the air gap, this saving can generally not be realized.

In Fig. 38a, the pole shoe covers 5 armature teeth and the flux from the pole passes through 5 teeth into the armature. In Fig. 38b, the armature is moved $\frac{1}{2}$ tooth pitch to the right, and the flux from the pole passes through 6 teeth into the armature. When the number of slots per pole is a whole number, the number of slots embraced by each pole will be the same for all positions of the armature. For the position

⁴ Iron and Steel Engineer, Vol. 2, Sept. and Nov., 1925.

⁵ "Die Gleichstrommaschine," Vol. 1, 3rd ed., p. 139, Julius Springer, Berlin

of the armature shown in Fig. 38*a*, the reluctance of the air gap is greater and the flux under the pole is smaller than for the position shown in Fig. 38*b*. When the armature rotates, the flux in the air gap will necessarily pulsate. Pulsations of the flux in the air gap produce iron losses in the pole shoes and give rise to magnetic noises.

In Fig. 39*a* and *b*, the pole shoe covers $5\frac{1}{2}$ slots. The total reluctance

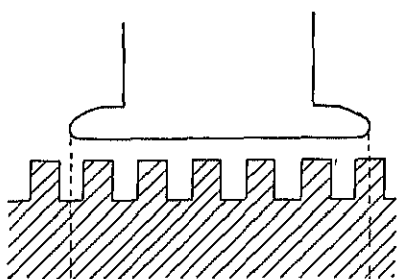


FIG. 39*a*.

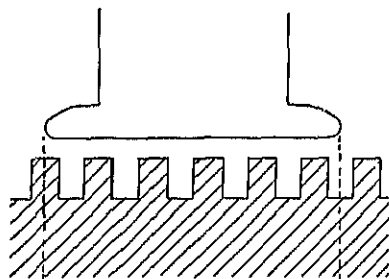


FIG. 39*b*.

tance of the flux path and the flux under the pole remain approximately the same for all positions of the armature. From Fig. 39*a* and *b* it may be seen that the reluctance and the flux under the tips of the pole are not the same for all positions of the armature, and that, when the armature rotates, the flux under the pole oscillates between the pole tips. The oscillating flux in the air gap produces ripples in the voltage induced in the conductors moving under the poles. The pulsations

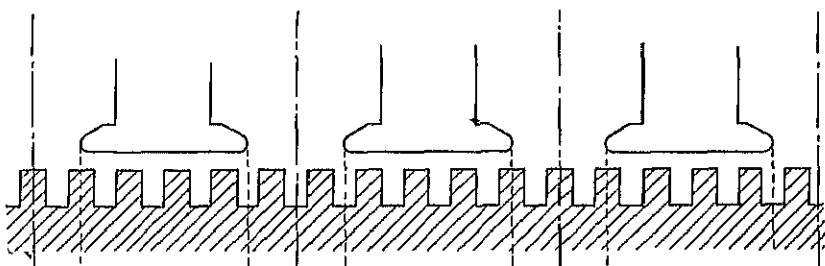


FIG. 40.

and oscillations of the flux in the air gap will be small when the pole shoes are well beveled, when the air gap is large, and when the slots are narrow in proportion to the width of the teeth.

When the number of slots per pole is equal to a whole number plus $\frac{1}{2}$ (see Fig. 40), the reluctance of the flux path per pair of

poles will be practically constant for all positions of the armature, and there will be no pulsations or oscillations of the flux in the air gap.

To avoid pulsations and oscillations of the flux in the air gap, the number of slots per pole should be equal to a whole number plus $\frac{1}{2}$. When this is not possible or advisable for other reasons, the number of slots per pole should be an integer.

Pulsations and oscillations of the flux under the commutating pole must be avoided, as they may cause sparking. A large air gap under the commutating pole and a small tooth pitch help to reduce the effect of the armature slots upon the flux under the commutating pole. In general, the number of slots between the tips of two adjacent poles should be at least 3, or

$$(1 - \psi) \frac{S}{p} \geq 3.$$

Assuming 66 per cent for ψ , the number of slots per pole,

$$\frac{S}{p} \geq \frac{3.0}{(1 - .66)} \geq 8.82.$$

For machines with small armature diameter, for which the slots per pole will be smaller than as given above, partly closed armature slots will generally be required.

Armature Coil Construction and Insulation.—Armature coils for direct-current machines are wound with insulated wire or with bare rectangular strap copper. The shape of the cross-section of the wire is round, square, or rectangular. The copper tables in the Appendix give the bare and insulated dimensions, the resistance and weight of standard round and square wire, and of some sizes of insulated rectangular wire. The dimensions, resistance, and weight of a number of sizes of strap copper are also included. Round wire is used mostly in the smaller sizes for small capacity machines and for high voltage machines. Square and rectangular wires are used whenever possible, because they give a better space factor and a mechanically stronger coil. Strap copper is used when conductors of large cross-section are required and especially for coils having only one turn.

Bare strap copper coils are formed on a mold, such as shown in Fig. 41. After the coils are formed, they are insulated, to protect them from the neighboring coils in the slot. A completely insulated full coil, comprising four coils, is shown in Fig. 42. The term "coil" refers to the element connecting two commutator bars, the term

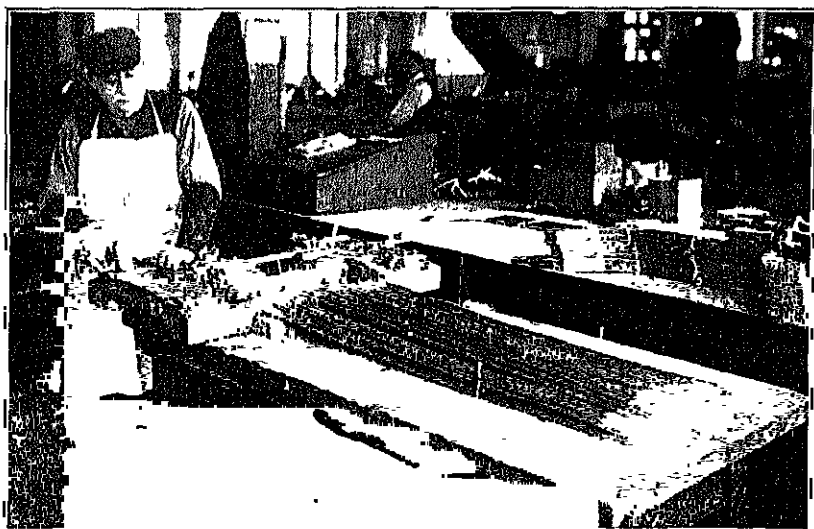


FIG. 41.—Mold for forming armature coils.

together and placed into the slot as one coil. The number of coils is equal to the number of commutator bars, and the number of full coils is equal to the number of slots.

Wire-wound coils are not always wound on a form, such as used for strap copper coils, but are often wound into the form shown in Fig. 43 and then pulled into the desired shape by a coil-pulling machine. With this method of winding wire-wound coils, all the coils comprising a full coil are wound at the same time.

Strap-wound armature coils are generally arranged in the slot as shown in Fig. 44, whereas wire-wound

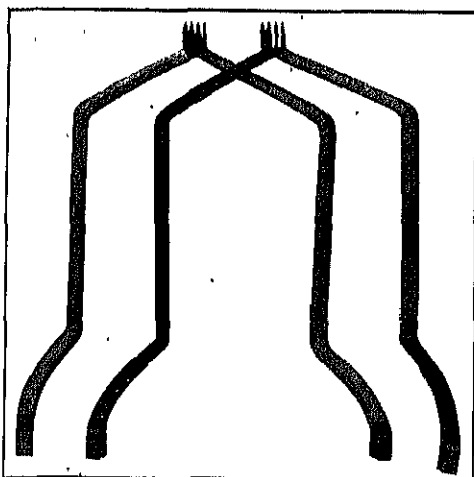


FIG. 42.—One-turn strap copper armature coils for wave winding.

coils are arranged as shown in Figs. 45

and 46. The line through the conductors indicates the conductors in parallel. The voltage between coil sides, side by side in a slot, is equal to the voltage between adjacent commutator bars, because coils, side by side, are connected to adjacent commutator bars. For coils with more than one turn, the voltage per turn is equal to the coil voltage divided by the number of turns per coil. The voltage per coil, for lap windings, is equal to the degree of multiplicity times the voltage

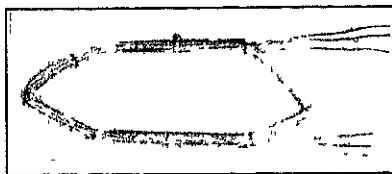


FIG. 43 — Armature coil before being pulled out.

between adjacent commutator bars, and for wave windings it is this value divided by $\frac{p}{2}$. The voltage per turn for either type of winding is,

$$e_t = \frac{a e_{sm}}{p t_a} \quad (24)$$

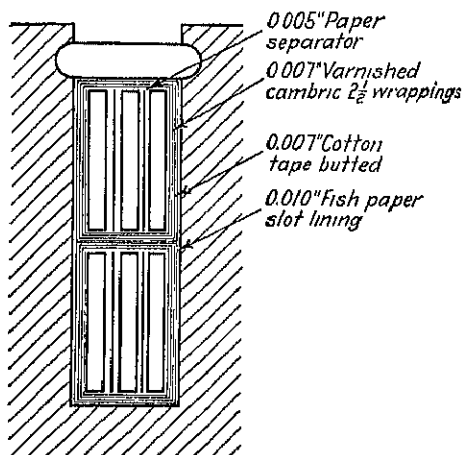


FIG. 44.

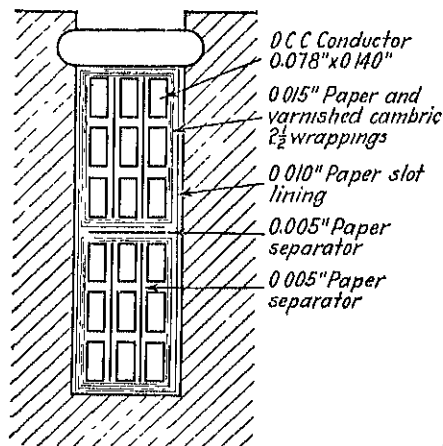


FIG. 45.

To avoid flashing, the maximum voltage between adjacent commutator bars should be less than 30 volts (see page 51).

The voltage between the coil sides in the top of the slot and those in the bottom is approximately equal to the terminal voltage, because the coil pitch is generally equal to the pole pitch.

The insulation between the winding and core is subjected to mechanical stresses and must, therefore, be heavier than is required for electrical

insulation between armature core and windings shall withstand, for one minute, a 60-cycle effective e.m.f., applied between core and winding, equal to 2 times the terminal voltage of the winding plus 1000 volts. The test voltage is to be applied to the winding after the temperature test, when the windings are at normal operating temperature.

Armature coils wound with bare strap copper are generally insulated with cotton tape. The entire coil is taped half-lapped, with linen finished cotton tape, generally 0.005 to 0.007 in. thick. The coils are then thoroughly dried in an oven, dipped in flexible baking varnish, and baked at a temperature of 100° C. for 8 or 10 hours or until dry.

For wire-wound coils, double-cotton-covered wire is generally used. For small machines, with a large number of turns of small wire per coil, single-cotton-covered enamel wire is used. After the coils are wound and pulled into the proper shape, they are dried and finished in the manner described in the preceding paragraph. The varnish treatment not only serves as a good insulator but also cements the individual conductors of the coil together and eliminates air pockets. Double-cotton-

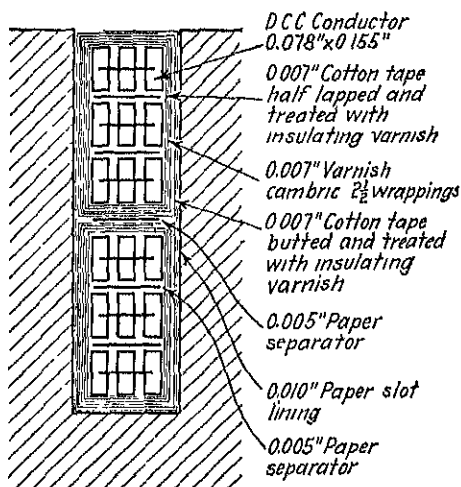


FIG. 46.

covered wire may be used for a voltage per turn as high as 25 volts. When the voltage per turn exceeds 25 volts, triple-cotton covering or some other method of insulation must be used.

A large number of insulating materials and a variety of methods⁶ are used for insulating the armature coils from the core. For open slots, which is the type of slot generally used for all except very small machines, and for formed coils, the insulation may all be placed on the coil or all in the slot, or part on the coil and part in the slot as slot lining. The first method is the one most used. For very small machines with partly closed slots, all the insulation between armature coils and core must be placed in the slot as slot lining.

⁶ "Insulation and Design of Electrical Windings," Longmans Green & Co., London.

of the coil depend upon the voltage of the winding, the size of the coil, and the mechanical stresses it will have to stand when the machine is in operation.

Figure 44 shows a method of insulating the slot portions of armature coils for 250-volt windings with strap-copper coils. The middle conductor of each layer is insulated with cotton tape, half-lapped and treated with insulating varnish. The three coils of each layer are completely insulated before they are placed into the slot. The straight part of the coil is wrapped with empire cloth in such a way that there are three thicknesses on one side and two on the other. The coil end-connections are taped with empire cloth tape, half-lapped. The entire coil is then taped with cotton tape, with the turns of the tape butted on the slot portion of the coil and half-lapped on the end-connections. The coils are then thoroughly dried in an oven, dipped in flexible baking varnish, and baked at a temperature of 100°C . for 8 or 10 hours or until dry.

The slot lining, which is generally fish paper or red-rope paper, from 0.007 to 0.010 in. thick, is used simply to afford mechanical protection to the coils when they are pushed into the slots. The slot lining extends over the top edges of the slot while the armature is being wound. It is cut off flush with the armature surface when the coils are in place and folded over the top of the coil, to protect it when the wedge is put into place. Figure 45 shows a method of insulating the slot portion of wire-wound armature coils for 250-volt windings. After the coils are wound and pulled into the proper shape, they are dipped in insulating varnish and baked. The method of insulating the coil is the same as that shown in Fig. 44, with the exception, that a wrapper of paper and varnished cambric instead of empire cloth is used on the straight part of the coil.

Figure 46 shows a method of insulating the slot portion of wire-wound armature coils for 500-volt windings. The varnish-treated coils are taped all over with cotton tape, half-lapped. The taped coils are again dried, dipped in varnish, and baked. The straight part of the coil is wrapped with empire cloth, or paper and mica, with three thicknesses on one side and two on the other. The coil is then taped all over with cotton tape, with the turns of tape butted on the slot portions and half-lapped on the end-connections. After the coils are treated with insulating varnish and baked, they are placed into the slots in the same way as described for the 250-volt strap-copper coils shown in Fig. 44.

The slot shown in Fig. 46 is not sealed by a wedge, but the coils are

to determine when band wires should be used to hold the coils in the slots or when wedges should be used. In general, band wires are used for small diameter machines, when it is necessary to keep the slot depth as small as possible.

Figure 47 shows a method of insulating direct-current armature coils for open slots, with and without wedge, for voltages including

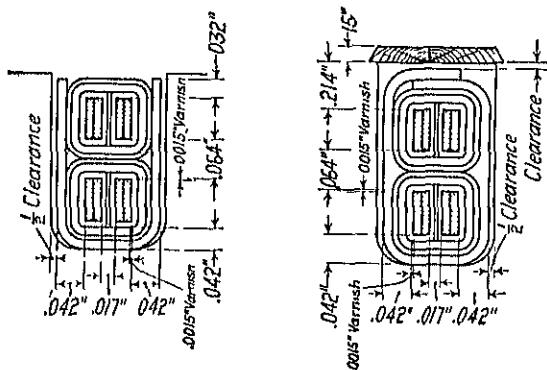


FIG. 47.

Insulation for Armature Conductors in Slot	Thickness				
	To Be Added to Depth of Con- ductors	To Be Added to Width of Conductors— Number of Conductors per Slot			
		2	4	6	8
	In.	In.	In.	In.	In.
Around conductor, 5-mil cotton tape butt— Varnish to 7 mils.	0 028	0 014	0 028	0 012	0 050
Vertical separator, 3-mil paper as shown	0 003	0 006	0 009
Around group of conductors, 10 mil—Var- nished cloth half lap	0 080	0 040	0 010	0 010	0 010
Around group, 5-mil cotton tape butt Slot armor, 10-mil horn fibre at sides and bot- tom of slot	0 020	0 010	0 010	0 010	0 010
Clearance	0 010	0 020	0 020	0 020	0 020
Total of insulation and clearance to be added to conductor to determine size of slot	0 012	0 012	0 012	0 012	0 012
<i>With Wedge</i>					
Insulation and clearance as above	0 150	0 090	0 113	0 130	0 147
Thickness of wedge	0 150				
Slot armor lapped under wedge	0 020				
Total of above insulation and clearance to be added to conductor to determine size of slot	0 320				
<i>With Depression</i> (For Binding Band)					
Insulation and clearance as above	0 150				
Depth of depression	0 060				
Total of above insulation and clearance to be added to conductors to determine size of slot	0 210				

see Table 1. The accompanying table gives the kind and thickness of insulating materials employed and the clearances used to calculate the slot size. Figure 48 shows a method of insulating the armature flanges which support the armature coil end-connections. After the armature is completely wound, it is sprayed all over with a black, high-gloss, air-drying insulating varnish.

Choice of Armature Winding.—The armature winding should generally be so chosen that the best possible space factor for the armature slot is obtained. The ratio of the area of the copper in the slot to the area of the slot under the wedge is called the space factor. The larger the number of turns per coil, the larger will be the space required for

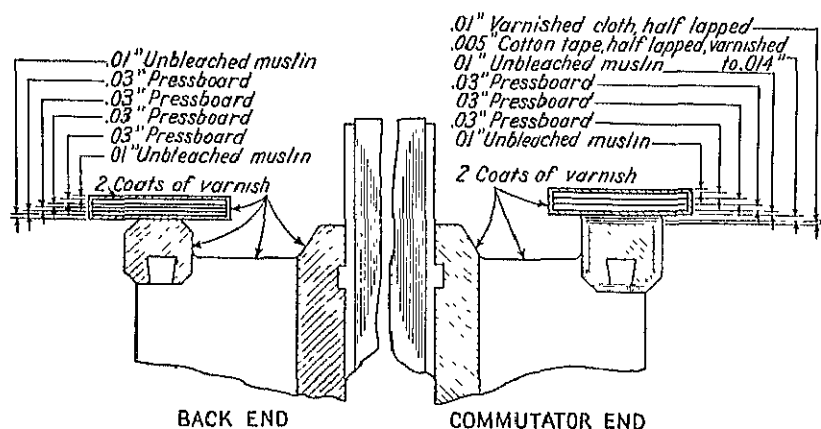


FIG. 48.—Method of insulating armature flanges.

the insulation in the slot. The best space factor is obtained when the armature coil has only one turn. The winding that gives the smallest number of turns per coil will, therefore, generally be used.

The number of conductors in series per path,

$$\frac{N}{a} = \frac{E}{n} \times \frac{1}{\phi_t f a} \times 60 \times 10^8,$$

that is, they are directly proportional to $\frac{E}{n}$ and inversely proportional

to the total flux passing through the air gap. For a given air gap density, the total flux passing through the air gap varies directly with the cylindrical surface of the armature, and the smaller the armature the larger will be the number of conductors in series per path for a given

value of $\frac{E}{n}$ and B_p . For slow-speed and high-voltage machines and for

usually have a large number of conductors in series per path, so that wave windings will usually be required.

Multiplex wave windings are used for large machines with a large number of poles, whereas multiplex lap windings are used only on very large machines, for very high speeds.

For 4-pole machines, it is desirable to choose the armature winding so that the same armature core may be used for two voltages. If, for example, the terminal voltage of a 50-Kw machine is 250 volts when the armature is simplex wave wound, then the same Kw output at one-half the voltage is obtained when the armature is simplex lap wound, with the same number and size of conductors per slot.

The armature winding must also be selected with regard to the maximum voltage between commutator bars, to prevent flashing.⁷ Large capacity machines will rarely flash when the maximum voltage between commutator bars is 28 volts. For moderate capacity machines, there is generally no flashing with 35 volts maximum between adjacent commutator bars, and for very small machines this limit may rise to 60 volts. In general, the maximum voltage between adjacent commutator bars should not exceed 30 volts.

The average voltage between adjacent commutator bars,

$$e_{av} = \frac{Ep}{K} \text{ volts.} \quad (26)$$

The maximum voltage between adjacent commutator bars for no load or for full load, for machines with compensating windings,

$$e_{em} = \frac{Ep}{Kf_d} \text{ volts.} \quad (27)$$

For non-compensated machines, the field flux is distorted by the action of the armature flux, and the maximum flux density in the air gap at full load is as much as 30 per cent larger than the maximum flux density in the air gap at no load. The maximum voltage between adjacent commutator bars for non-compensated machines,

$$e_{em} = \frac{Ep}{Kf_d} 1.3 \text{ volts.} \quad (28)$$

If 0.66 is assumed as an average value for the field form distribution factor, then the average voltage between commutator bars for com-

⁷ "Physical Limitations in D.C. Machines," by B. G. Lamme, Trans. A.I.E.E. Vol. 34, p. 1752.

20 volts, and for non-compensated machines $\frac{30 \times 0.66}{1.3}$ or approximately 15 volts.

Armature Conductor Section.—The section area of the armature conductor,

$$s_n = \frac{i_n}{A} \text{ sq. in.} \quad (29)$$

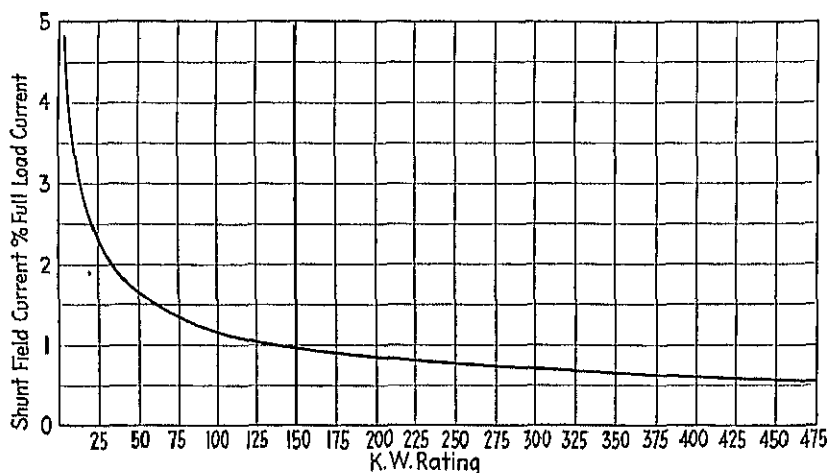


FIG. 40.—Approximate shunt field current for d.c. generators and motors.

The current per path in the armature winding for machines with shunt field windings is,

$$i_a = \frac{I \pm i_f}{a} = \frac{I_a}{a} \text{ amperes,} \quad (30)$$

where the negative sign is for motors. The shunt field current must first be estimated. This can be done by the use of the curve, Fig. 49, which gives the shunt field current in percentage of the full-load terminal current of the machine.

The current density, A , in the armature copper is limited by the permissible temperature rise of the armature winding and by the efficiency of the machine. The current density to use for the armature conductors can not be accurately predetermined, because of the many variable factors which affect the ventilation of the armature.

Assuming reasonably good ventilation, efficiency rather than temperature rise may be the limiting factor in the choice of A . For a given efficiency, the value of the armature I^2R loss may be assumed and the

should generally be chosen as high as the temperature and efficiency guaranties will permit. This not only leads to a saving in armature copper, but also enables the use of shallow armature slots, which aids commutation.

For open-type machines, of the type of construction shown in Chapter I, for continuous duty and for voltages up to 600 volts, the armature current density will be as follows:

High-speed belted or direct-connected machines,

2000 to 3500 amperes per sq. in.;

Slow-speed engine-type machines,

1200 to 2500 amperes per sq. in.

Size of Armature Slots.—The dimensions of the armature slots must be so chosen that they will accommodate the armature conductors with the necessary insulation, without producing excessive flux densities in the armature teeth. Wide-open slots produce pulsations of the flux in the air gap and increase the reluctance of the flux path in the air gap. The dimensions of the armature slots must therefore also be so chosen that the effect of the slots upon the flux in the air gap will be a minimum. For non-commutating-pole machines, the depth of the slot should generally not exceed four times the slot width, because deep slots increase the reactance voltage. For machines with commutating poles, deeper slots may be used, because the commutating pole produces a commutating field to compensate for the reactance voltage. The tooth pitch on the armature circumference,

$$t_1 = \frac{\pi D}{S} \text{ in.} \quad (31)$$

The width of the slot should generally be equal to or less than the width of the tooth on the armature circumference. The maximum tooth density, the density at the root of the tooth, should not exceed 150,000 lines per sq. in. For non-commutating poles, high tooth densities are used to minimize the effects of armature reaction, but high tooth densities, especially with high frequencies, produce high iron losses which affect the efficiency and temperature of the machine. High densities in the armature teeth also require a large number of ampere-turns on the shunt field winding, which increases the amount of shunt field copper required. When commutating poles are used, high tooth densities are not necessary, because the commutating pole prevents shifting of the neutral point and furnishes the commutating field.

the total thickness of the insulation in the width of the slot over the insulated conductors is as follows:

Varnished cambric.	$5 \times 0.007 = 0.035$ in.
Paper separator	$2 \times 0.005 = 0.010$
Cotton tape.	$2 \times 0.007 = 0.014$
Fish paper slot lining.	$2 \times 0.010 = 0.020$
	<hr/>
	0.079 in.

and in the depth of the slot,

Varnished cambric	$10 \times 0.007 = 0.070$ in.
Cotton tape	$4 \times 0.007 = 0.028$
Fish paper slot lining	$3 \times 0.010 = 0.030$
	<hr/>
	0.128 in.

From the copper tables the dimensions of the armature conductor can be found corresponding to the section area s_a , calculated by formula

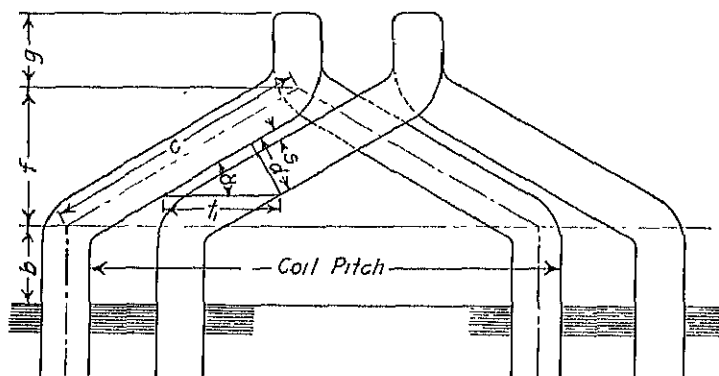


FIG. 50.—Armature coil end-connection.

29. The method of calculating the width and depth of the slot is shown by the sample designs, page 58 and Chapter VIII.

The dimensions of the armature conductor can be determined approximately by assuming a width of the armature slot equal to or less than the width of the tooth on the armature circumference. Subtracting from this value the space required for insulation plus clearance, the remainder is the space available for the insulated conductors. This space, divided by the number of conductors in the width of the slot, gives the approximate thickness of the insulated conductor. The width of the conductor can be found from the copper table for the thickness and cross-section area required.

shape of the armature coil end-connection for double-layer lap and wave windings, is shown in Fig. 50. The length of the mean-turn can be divided into two parts: the active part, embedded in the armature iron, and the end-connection, the part outside the armature iron. If d in Fig. 50 is the thickness of the coil end-connection plus the clearance between coils, then

$$\sin \alpha = \frac{d}{l_1}, \quad (32)$$

where α is the angle that the straight part of the coil end-connection makes with the edge of the armature coil, and l_1 is the tooth pitch at the armature surface. The clearance, s , between armature coil end-connections depends upon the voltage of the winding and upon the ventilation required; practical values are given in Table IV.

TABLE IV

Voltage	$2b$ in.	s in.
0 to 300	1.50	0 10
300 to 650	2.00	0 15
650 to 2000	2 25	0.18

The coil pitch is calculated on a diameter through the mean of the slot depth and

$$= \frac{\pi(D - d_s)}{p} \text{ in.} \quad (33)$$

The embedded part of the armature coil is allowed to extend beyond the edge of the armature iron a distance b , Fig. 50. Practical values for b are given in Table IV. The loop at the ends of the coils has a mean length approximately equal to the slot depth.

The complete expression for one-half the length of the mean-turn of an armature coil,

$$L_a = \frac{\pi(D - d_s)}{p \cos \alpha} + 2b + d_s + l \text{ in.} \quad (34)$$

The horizontal extension of the armature coil beyond the armature iron is equal to the sum of $b + f + g$, Fig. 50. Values for b are given in Table IV,

$$f = C \sin \alpha \text{ in.} \quad (35)$$

and g is approximately equal to the slot depth.

$$R_a = \frac{I_a N r}{a^2 s_a \times 10^6} \text{ ohms,} \quad (36)$$

where $r \times 10^{-6}$ is the resistance of copper per inch of 1 sq. in. cross-section. For 25°C , $r = 0.692$ and $r = 0.826$ for 75°C . If the armature conductor is built up of two or more wires in parallel, as is often done for large machines, the value used for s_a must be the section area of the group of parallel wires.

The resistance of the armature winding at any other temperature, T_2 , can be calculated by formula 37 when its resistance at temperature T_1 is known:

$$R_2 = \frac{234.5 + T_2}{234.5 + T_1} R_1 \text{ ohms.} \quad (37)$$

The bare weight of the armature copper,

$$G_a = L_a N s_a \times 0.321 \text{ lb.} \quad (38)$$

If the armature conductor is built up of two or more parallel wires, s_a must be the section area of the group of parallel wires.

Sample Design: Design of the Armature Winding.—From the curve, Fig. 20, Chapter II, the air gap density should be approximately 61 kilo-lines per sq. in. The total flux,

$$\begin{aligned} \phi_t &= \pi D l B_g = \pi \times 25 \times 11 \times 61 \\ &= 52,700 \text{ kilo-lines.} \end{aligned}$$

The total number of conductors required is calculated by formula 4. The induced voltage is assumed equal to 260 volts. For large machines, the voltage drop in the armature, series field, commutating field, and brush contacts can generally be assumed to be 5 volts for each 125 volts at the terminals. For small machines, this drop can generally be assumed to be equal to from 7 to 10 per cent of the terminal voltage. For a simplex lap winding, the total number of conductors,

$$\begin{aligned} N &= \frac{E_a \times 60 \times 10^8}{\phi_t n f_a} = \frac{260 \times 6 \times 60 \times 10^8}{52,700 \times 10^3 \times 900 \times 0.665} \\ &= 296 \end{aligned}$$

For a simplex wave winding, one-third of this number would be required.

The number of slots for the armature must now be so chosen that there will be at least 9 slots per pole (see page 44), and whenever possible the number of slots per pole should be equal to an integer plus one-half.

For a simplex wave winding, 99 total conductors are required. With 2 conductors per slot, only 50 slots will be necessary which, obviously, is too small a number. A simplex lap winding will therefore be used. With 4 conductors per slot, the number of slots will be 74. In order to use a whole number plus one-half slots per pole, 75 slots are required. Using 4 conductors per slot, the total number of conductors will be 300. The calculations were made for this value of conductors and it was found that the armature tooth densities were rather high. It is, therefore, necessary to decrease the total flux by increasing the total number of conductors. To do this, $13\frac{1}{2}$ slots per pole are used, giving a total of 81 armature slots.

$$\text{and } N = 4 \times 81 = 324$$

$$\phi_t = \frac{260 \times 6 \times 60 \times 10^8}{324 \times 900 \times 0.665} = 48,300 \text{ kilo-lines.}$$

One turn per coil will be used for this winding, because with two turns per coil only 81 commutator bars would be required, which would lead to a high voltage between adjacent bars. For 2, 4, 6, and in some cases, 8 conductors per slot, the number of turns per coil is 1. For larger numbers of conductors per slot, more than one turn per coil is generally required.

The sides of the coils are placed in slots 1 and 14 and the back pitch,

$$Y_1 = C_s Y_s + 1 = 4 \times 13 + 1 = 53,$$

and the front pitch,

$$Y_2 = Y_1 - 2Y_c = 53 - 2 = 51$$

$$Y_c = 1.$$

The number of commutator bars must always be equal to the number of coils in the armature winding. With 4 conductors per slot and 1 turn per coil, the number of commutator bars will be equal to 162. The average voltage between commutator segments,

$$e_{sa} = \frac{Ep}{K} = \frac{260 \times 6}{162} = 9.63 \text{ volts}$$

and the maximum voltage between bars,

$$\begin{aligned} e_{sm} &= \frac{Ep}{K f_a} \times 1.30 = \frac{260 \times 6}{162 \times 0.665} \times 1.30 \\ &= 18.8 \text{ volts.} \end{aligned}$$

The maximum voltage per turn will be equal to the maximum voltage between adjacent commutator bars (formula 24, page 46).

The terminal current at full load,

$$I = \frac{K_w \times 10^3}{E_T} = \frac{300 \times 10^3}{250} \\ = 1200 \text{ amperes.}$$

The shunt field current is taken equal to 8.4 amperes, Fig. 49, page 52.

Since the peripheral speed is rather high for this machine, 3000 amperes per sq. in. is assumed for the current density in the armature conductors, page 53. The section area of the armature conductor,

$$s_a = \frac{I + i_f}{A_a a} = \frac{1200 + 8.4}{3000 \times 6} = 0.007 \text{ sq. in.}$$

With 4 conductors per slot and one turn per coil, a bare copper strap will be the most satisfactory armature conductor. A conductor 0.125×0.625 in., section area 0.0748 sq. in., is selected from the copper table. This conductor is chosen in preference to the conductor 0.141×0.50 in., section area 0.0686 sq. in., because the latter gives slot dimensions which lead to high armature tooth densities. The conductors are arranged in the slot and insulated as shown in Fig. 47, page 49. The dimensions of the slot are,

$$w_s = (0.125 \times 2) + 0.113 = 0.363 \text{ in.}$$

$$d'_s = (0.625 \times 2) + 0.32 = 1.57 \text{ in.}$$

The tooth pitch on the armature surface,

$$t_1 = \frac{\pi D}{S} = \frac{\pi \times 25}{81} = 0.97 \text{ in.}$$

The width of the slot should, therefore, be satisfactory from the standpoint of the flux pulsations in the air gap.

The length of the one-half mean-turn of the armature coil is calculated as given on page 55,

$$\sin \alpha = \frac{d}{t_1} = \frac{0.363 + 0.10}{0.97} = 0.478$$

$$\alpha = 28^\circ 30' \text{ and } \cos \alpha = 0.879$$

$$L_a = \frac{\pi(D - d_s)}{p \cos \alpha} + 2b + d_s + l \\ = \frac{\pi(25 - 1.57)}{6 \times 0.879} + 1.5 + 1.57 + 11 \\ = 28.07 \text{ in.}$$

The resistance of the armature winding is calculated for 75° C. because the A.I.E.E. standardization rules specify that the copper losses for all loads should be calculated for a temperature of 75° C.

$$R_a = \frac{L_a N r}{a^2 s_a \times 10^6} = \frac{28.07 \times 324 \times 0.826}{6^2 \times 0.0748 \times 10^6}$$

$$= 0.00279 \text{ ohm.}$$

The voltage drop in the armature winding,

$$I_a R_a = 1208 \times 0.00279 = 3.37 \text{ volts}$$

or 1.35 per cent of the full-load terminal voltage.

The weight of the armature copper,

$$G_a = L_a N s_a \times 0.321 = 28.07 \times 324 \times 0.0748 \times 0.321$$

$$= 219 \text{ lb.}$$

Fifty-four equalizer connections are recommended for this winding, one for every 3 commutator bars (see page 40).

CHAPTER IV

THE MAGNETIC CIRCUIT

THE flux per pole that crosses the air gap and enters the armature is calculated by formula 2,

$$\phi = \frac{Ea \times 60 \times 10^8}{pNn}.$$

A definite magnetomotive force is required on each pole, to send this flux through the magnetic circuit. The fundamental law giving the relation between flux and magnetomotive force is expressed as follows:

$$\phi = \frac{0.4 \times \pi AT \mu s}{l}.$$

The ampere-turns required to send the flux ϕ through a magnetic circuit of length l and section area s are,

$$AT = \frac{l\phi}{0.4 \times \pi \mu s}.$$

The flux, ϕ , divided by the section area of the magnetic circuit is equal to the flux density, B , and the ampere-turns,

$$AT = \frac{lB}{0.4 \times \pi \mu}. \quad (39)$$

In formula 39, l is expressed in centimeters and B in lines per square centimeter. When l is expressed in inches and B in lines per square inch,

$$AT = \frac{lB}{3.2 \times \mu}. \quad (40)$$

For air, the permeability, μ , is equal to 1; for iron and steel, it is greater than 1 and is not constant but depends upon the flux density. The magnetic characteristics of magnetic materials can be determined only by test. The tests consist of determining the magnetizing force required for different flux densities. For the designer, it is more con-

venient if the magnetizing force, H , is expressed as ampere-turns per inch of flux path instead of in c.g.s. electromagnetic units. If at equals the ampere-turns per inch of flux path, then

$$at = H \times 2.03, \quad (41)$$

where H is the magnetizing force expressed in c.g.s. electromagnetic units. Standard saturation curves for cast iron, cast steel, and open hearth sheet steel, such as used for electrical apparatus, are shown in the Appendix. For a magnetic circuit through iron or steel, the ampere-turns,

$$AT = at \times l, \quad (42)$$

where at equals the ampere-turns per inch length of flux path, as found from the standard saturation curves, and l is the length.

The magnetic circuit for a multi-pole machine is illustrated in Fig. 51, which shows that the magnetic circuit per pair of poles comprises the yoke or field ring, the pole, the air gap, the armature teeth, and the armature iron below the teeth. The material is not the same for the different parts of the magnetic circuit; neither is the density the same. The ampere-turns per pole must therefore be calculated separately for each part of the magnetic circuit. The symbols used to calculate the ampere-turns per pole are as follows:

Material	Magnetic Section	Density	Ampere-turns per Inch	Length of Flux Path	Ampere-turns per Pole
Air gap	s_g	B_g	δk	AT_g
Teeth	s_t	B_t	at_t	l_t	AT_t
Armature yoke	s_{ya}	B_{ya}	at_{ya}	l_{ya}	AT_{ya}
Pole body	s_p	B_p	at_p	l_p	AT_p
Field yoke	s_{yf}	B_{yf}	at_{yf}	l_{yf}	AT_{yf}

The total ampere-turns per pole for no load and normal voltage,

$$ATP = AT_g + AT_t + AT_{ya} + AT_p + AT_{yf}. \quad (43)$$

Ampere-Turns for the Air Gap.—The maximum flux density in the air gap,

$$B_g = \frac{\phi_t}{s_g}. \quad (44)$$

The flux in the air gap distributes itself over the axial length of the armature, as shown in Fig. 52. The reluctance of the ventilating ducts is equivalent to a reduction of the armature length l , and the fringing at the ends of the core is equivalent to an increase in l . For the purpose of the designer, it is generally sufficiently accurate to assume that these two effects neutralize each other. When the axial length of the pole shoe, l_1 , is equal to the axial length of the armature, the length of

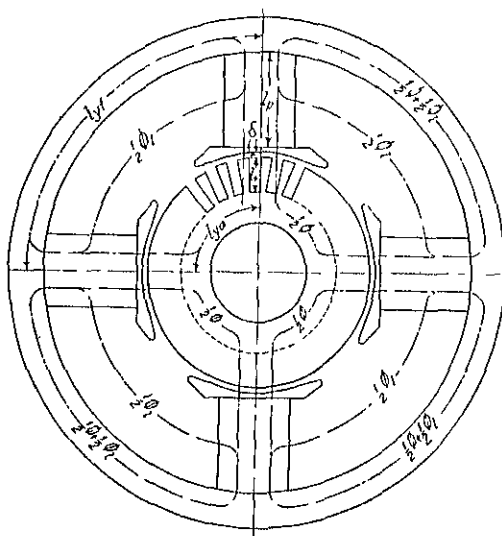


FIG. 51.—Magnetic circuit of four-pole machine without commutating poles.

the air gap section, l_g , can generally be taken equal to the armature length, and when the axial length of the pole shoe is less than the axial length of the armature,

$$l_g = \frac{1}{2}(l_1 + l).$$

The section area of the air gap,

$$s_g = \pi D l_g. \quad (15)$$

The ampere-turns per pole for the air gap for a smooth armature without slots,

$$AT_g = \frac{B \delta}{3.2}.$$

For slotted armatures, the reluctance of the air gap is increased, because of the low permeance of the slot space and the high densities in the teeth.

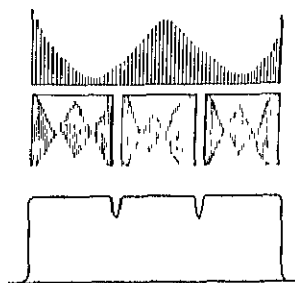


FIG. 52.

This effect is taken into account by multiplying the ampere-turns for the air gap for a smooth armature by a factor,¹

$$k = \frac{l_1}{w_{l_1} + y \delta}, \quad (46)$$

where y is taken from the curve Fig. 53.

The ampere-turns per pole for slotted armatures,

$$AT_v = \frac{B_p \ell k}{3 \ 2}. \quad (47)$$

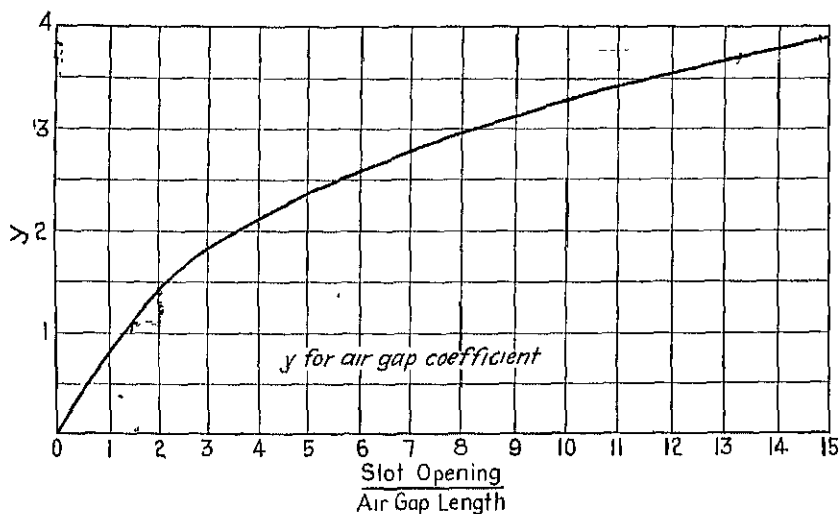


FIG. 53.

Ampere-Turns for the Armature Teeth.—When the armature slots have parallel walls, the flux density in the armature teeth is lower at the top of the tooth than at the root of the tooth. The flux density at the top of the tooth,

$$B_{t_1} = \frac{\phi_t}{s_{t_1}}. \quad (48)$$

The tooth pitch on the armature surface is given by formula 31,

$$l_1 = \frac{\pi D}{S}$$

¹"Die Gleichstrommaschine," by Arnold and La Cour, Vol. 1, p. 134, 3rd ed., Julius Springer, Berlin; Electrical World, Vol. 38, p. 884, 1901, and A.I.E.E. Journal, Vol. 46, 1927, p. 431.

and the width of the tooth at the armature surface,

$$w_{t_1} = t_1 - w_s. \quad (49)$$

The length of the armature is generally divided into sections by radial ventilating ducts, as explained on page 5, Chapter I. A sufficient number of ducts should generally be used, so that the length of each section of iron between two ventilating ducts does not exceed 3 in.

The section area of the armature teeth at the armature surface,

$$s_{t_1} = w_{t_1}(l - n_a w_s) S k_1, \quad (50)$$

where k_1 is the lamination factor and is generally equal to 0.88 to 0.93.

The section area of the teeth at the bottom of the slot,

$$s_{t_2} = w_{t_2}(l - n_a w_s) S k_1, \quad (51)$$

and the flux density at the root of the teeth,

$$B_{t_2} = \frac{\phi_t}{s_{t_2}}. \quad (52)$$

To avoid excessive iron losses in the teeth and to limit the magnetomotive force required to send the flux through the teeth, the density at the root of the teeth should generally not exceed 150,000 lines per sq. in.

In calculating the ampere-turns for the armature teeth, the fact that the flux density increases and the permeance of the iron in the teeth decreases in passing from the top to the bottom of the tooth must be taken into account. Various methods have been proposed to determine the ampere-turns required to send the flux through the armature teeth. The method which uses for the average ampere-turns per inch, the ampere-turns corresponding to a tooth density $\frac{1}{3}$ slot depth from the minimum tooth width has been found to be very satisfactory. The width of the armature tooth at a point $\frac{1}{3}$ slot depth from the minimum tooth width,

$$w_{t_3} = \frac{\pi(D - 1.33d_s)}{S} - w_s. \quad (53)$$

The density and section area of the armature teeth for this point are calculated in the same way as explained above for the density and section at the armature surface. From the standard saturation curves in the Appendix, the ampere-turns per inch for this density are obtained, and the ampere-turns per pole for the teeth,

$$AT_t = at_t l_t, \quad (54)$$

slot depth.

Ampere-Turns for the Armature Yoke.—It is apparent from Fig. 51 that each section of the armature iron below the slots carries one-half of the flux per pole. The flux per pole,

$$\phi = \frac{\phi_d f_d}{p}$$

and the flux density in the armature yoke,

$$B_{ya} = \frac{\phi}{s_{ya}} \quad (55)$$

If d_{ya} is two times the radial depth of the armature iron below the slots, then

$$s_{ya} = (l - n_d w_d) d_{ya} k_1, \quad (56)$$

where $d_{ya} = (D - 2d_s) - D_1$. The flux density in the armature yoke is first assumed and

$$d_{ya} = \frac{\phi}{(l - n_d w_d) k_1 B_{ya}} \quad (57)$$

The ampere-turns per inch for the value of B_{ya} are found from the standard saturation curve for the material used for the armature laminations. The ampere-turns per pole required to send the flux through the armature iron below the slots,

$$AT_{ya} = at_{ya} l_{ya}. \quad (58)$$

The length of the flux path, l_{ya} , may be taken equal to one-half the pole pitch on the mean circumference of the armature yoke:

$$l_{ya} = \frac{[D - (2d_s + \frac{1}{2}d_{ya})]\pi}{2p}. \quad (59)$$

When commutating poles are used, the flux in the armature iron below the slots is increased in one part and decreased in the other, because of the presence of the commutating-pole flux. The effect of the commutating-pole flux upon the ampere-turns per pole for the armature yoke may be calculated as explained by Dr. Arnold.²

² "Die Gleichstrommaschine," Vol. 1, p. 432, Julius Springer, Berlin; see also "Design of Auxiliary Poles," by A. Brunt, *Electrical Review and Western Electrician*, p. 513, Sept. 9, 1911.

The saturation curve for the commutating-pole magnetic circuit should be a straight line, so that the commutating-pole flux will increase directly with the armature current. To accomplish this, the flux densities in the armature yoke must be chosen well below the "knee" of the saturation curve. For normal designs, the flux densities in the armature core will be so low that the correction for the main pole ampere-turns for the armature yoke, because of the presence of the commutating-pole flux, will not be necessary.

For commutating-pole direct-current motors and generators, the flux density in the armature yoke is therefore generally chosen equal to from 35,000 to 75,000 lines per sq. in.

Ampere-Turns for the Pole.—The flux in the poles is not constant for all sections, but varies, being greatest near the yoke and decreasing toward the pole shoe. Figure 51 shows that the magnetic flux per pole is made up of two parts, one ϕ , which crosses the air gap and enters the armature, and the other, ϕ_l , which does not cross the air gap but passes between poles and is called the leakage flux. The ratio of $\phi + \phi_l$ to ϕ is called the leakage factor,

$$\lambda = \frac{\phi + \phi_l}{\phi} = 1 + \frac{\phi_l}{\phi}. \quad (60)$$

To calculate the flux density in the pole, it may be assumed, without appreciable error, that the flux in the pole is uniform and equal to $\phi\lambda$. The flux density in the pole,

$$B_p = \frac{\phi\lambda}{s_p}. \quad (61)$$

The section area of the pole,

$$s_p = l_1 w_p. \quad (62)$$

The flux density, B_p , should generally not exceed 100,000 lines per sq. in. for laminated poles and 80,000 lines per sq. in. for cast steel poles. From the saturation curve for the kind of material used for the pole, the ampere-turns per inch length of flux path corresponding to the pole density are found, and

$$AT_p = a l_p B_p. \quad (63)$$

The length of the flux path in the pole is taken equal to the radial height of the pole (Fig. 51).

Ampere-Turns for the Field Yoke.—The flux carried by each section of the yoke is equal to $\frac{1}{2}\phi\lambda$, as Fig. 51 shows. The density in the yoke,

$$B_{yf} = \frac{\phi\lambda}{s_{yf}}. \quad (64)$$

$$s_{yf} = l_2 d_{yf}. \quad (65)$$

For machines with bearings supported by end-brackets, the yoke should generally extend over the field winding, as shown in Figs. 16 and 18. For machines with pedestal-type bearings, the field windings often extend beyond the yoke, as shown in Fig. 1. The thickness of the yoke, d_{yf} , must be large enough to give the frame the required mechanical strength, and to give a yoke section such that the ampere-turns required to send the flux through the yoke will not be too large. The flux density, rather than the mechanical strength, is generally the determining factor in the choice of the thickness of the field yoke. The thickness of the yoke,

$$d_{yf} = \frac{\phi \lambda}{l_2 B_{yf}}. \quad (66)$$

The yoke must carry the flux of the commutating pole as well as the flux of the main poles. The effect of the presence of the commutating-pole flux in the field yoke, may be calculated in the same way as for the armature iron below the slots. For normal designs, the flux density in the yoke is generally so low that this correction is not necessary. For a cast steel yoke, B_{yf} should not exceed 65,000 lines per sq. in. and for a rolled steel yoke, B_{yf} should not exceed 80,000 lines per sq. in.

The Field Leakage Factor.—The leakage flux may be divided into four parts, as shown in Fig. 54. The leakage flux for each of the four paths is as follows:

- ϕ_{l_1} the leakage between inner pole shoe surfaces,
- ϕ_{l_2} the leakage between the pole shoe end surfaces,
- ϕ_{l_3} the leakage between inner pole body surfaces,
- ϕ_{l_4} the leakage between pole body end surfaces.

The leakage flux per pole,

$$\phi_l = \phi_{l_1} + \phi_{l_2} + \phi_{l_3} + \phi_{l_4}.$$

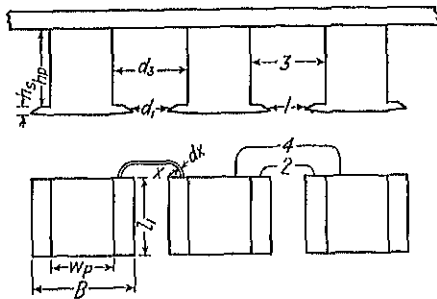


FIG. 54.—Field leakage flux paths.

When the magnetomotive force acting on each of the leakage paths and the reluctance of each path are known, the leakage flux can be calculated as follows:

$$\text{Flux} = \frac{\text{m.m.f.}}{\text{Reluctance}}.$$

The m.m.f. acting across paths 1 and 2 = $2 (AT_g + AT_i + AT_{ya}) = 2X$

Since the greatest part of the leakage flux passes through air, the reluctance of the part in the iron may be neglected. Assuming that the sides of adjacent poles are parallel, the leakage may be calculated as follows:³

The leakage flux per pole for path 1,

$$\begin{aligned}\phi_{i_1} &= 2 \times 3.2 \times 2X \frac{l_1 h_s}{d_1} \\ &= 13 X \frac{l_1 h_s}{d_1}.\end{aligned}$$

The leakage flux per pole for path 2,

$$\begin{aligned}\phi_{i_2} &= 4 \times 3.2 \times 2X \int_0^{B/2} \frac{h_s dx}{d_1 + \pi x} \\ &= 25.6 X \frac{h_s}{\pi} \log_0 \left(\frac{d_1 + \frac{\pi B}{2}}{d_1} \right) \\ &= 19 X h_s \log_{10} \left(1 + \frac{\pi B}{2d_1} \right)\end{aligned}$$

The m.m.f. across paths 3 and 4 is zero at the yoke and equal to $2X$ at the pole shoe, and the average value is equal to X . The leakage flux per pole for path 3,

$$\begin{aligned}\phi_{i_3} &= 2 \times 3.2 \times X \frac{l_1 h_p}{d_3} \\ &= 6.5 X \frac{l_1 h_p}{d_3}.\end{aligned}$$

³ "Electrical Machine Design," by Gray, p. 51, McGraw-Hill Book Co., New York.

The leakage flux per pole for path 4,

$$\begin{aligned}
 \phi_{l_4} &= 4 \times 3.2X \int_0^{B/2} \frac{h_p dx}{d_3 + \pi x} \\
 &= 4 \times 3.2X \frac{h_p}{\pi} \log_{10} \left(\frac{d_3 + \frac{\pi w_p}{2}}{d_3} \right) \\
 &= 9.5 X h_p \log_{10} \left(1 + \frac{\pi w_p}{2d_3} \right) \\
 &= \frac{\phi + \phi_l}{\phi} = 1 + \frac{\phi_l}{\phi}.
 \end{aligned}$$

The leakage factor obtained by these formulas is usually too low for 2-, 4-, and 6-pole machines, because no attempt is made to calculate the flux that passes from the pole body side and end surfaces directly to the yoke. For 2-, 4-, and 6-pole machines, the leakage factor is generally assumed. For preliminary calculations, the following values may be used:

4- and 6-pole machines	= 1.20
Multipolar machines 20 to 50 in. in diameter	= 1.20
Multipolar machines larger than 50 in. in diameter	= 1.18

The ampere-turns per pole for the field winding must be equal to or greater than the armature ampere-turns per pole (see page 79, Chapter V). The armature ampere-turns per pole,

$$ATP_a = \frac{I_a N}{2pa}.$$

If the ampere-turns per pole for the field winding,

$$ATP = AT_g + AT_l + AT_{ya} + AT_p + AT_{yf},$$

are less than the armature ampere-turns per pole, the air gap length must be increased.

The Open-Circuit Saturation Curve.—The open-circuit saturation curve gives the relation between the terminal voltage at no-load and the corresponding ampere-turns per pole. The method of calculating the ampere-turns for a given voltage has been given above. For the air gap, the permeability is constant for all values of induction. The air gap ampere-turns will therefore vary directly with the voltage. For the remainder of the magnetic circuit, the flux densities must be cal-

culated by direct proportion for the various voltages. The corresponding ampere-turns per inch are taken from the standard saturation curve and multiplied by the length of the respective flux paths to obtain the ampere-turns per pole. Table V shows the calculations for the sample design.

TABLE V

	Length	230 Volts			260 Volts			285 Volts			320 Volts		
		B	at	AT	B	at	AT	B	at	AT	B	at	AT
Air gap	0.242	19.6		3750	56.0		4240	61.4		4650	69.0		5,210
Armature teeth	1.57	111.0	190	298	125.0	525	825	137.0	955	1500	151.0	1705	2,080
Armature yoke	4.70	66.4	7	33	75.0	10	47	82.2	13.8	65	92.3	25.5	120
Pole	8.28	84.4	14	116	95.4	35	200	104.6	78.6	650	117.2	270	2,240
Field yoke	11.80	56.9	14	165	64.2	17	200	70.4	20	230	79.0	28	330
Total				4362			5602			7101			10,580

The open circuit saturation curve plotted from these values is shown in Fig. 55.

Sample Design: Magnetic Circuit.—The section area of the air gap,

$$s_g = \pi D l_g = \pi \times 25 \times 11 = 864 \text{ sq. in.}$$

The axial length of the pole shoe will be made equal in length to the armature.

The air gap density,

$$B_g = \frac{\phi_t}{s_g} = \frac{48300}{864} = 56 \text{ kilo-lines.}$$

The air gap coefficient,

$$k = \frac{l_t}{w_h + (y\delta)} = \frac{0.97}{0.607 + (1.49 \times 0.17)} \\ = 1.13,$$

and the air gap ampere-turns per pole,

$$\text{AT}_g = \frac{B_g \delta k}{3.2} = \frac{56000 \times 0.17 \times 1.13}{3.2} \\ = 3360.$$

The armature tooth pitch at the root of the armature teeth,

$$t_2 = \frac{\pi(D - 2d_s)}{S} = \frac{\pi(25 - 2 \times 1.57)}{81} = 0.847 \text{ in.}$$

The minimum tooth width,

$$w_{t_2} = t_2 - w_s = 0.847 - 0.363 = 0.484.$$

The length of the armature core must be divided into a number of sections by radial ventilating ducts. Each section of iron should not

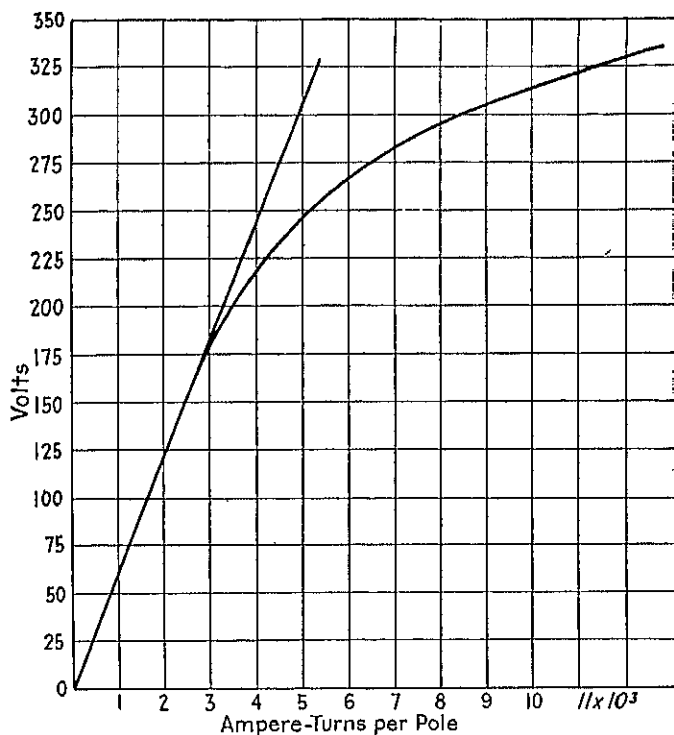


FIG. 55.—Open-circuit saturation curve, 300-kw., 250-volt, 900-r.p.m., d.c. generator.

exceed 3 in. in length. For an armature core length of 11 in., 3 ventilating ducts are required and each duct will be $\frac{3}{8}$ in. wide. The minimum section of the armature teeth,

$$\begin{aligned} s_{t_2} &= w_{t_2}(l - n_a w_a)k_1 S \\ &= 0.484 (11 - 3 \times \frac{3}{8}) 0.92 \times 81 \\ &= 356 \text{ sq. in.,} \end{aligned}$$

and the maximum tooth density,

$$B_{t_2} = \frac{\phi_t}{s_{t_2}} = \frac{48,300}{356} = 136 \text{ kilo-lines.}$$

This value must not exceed 150 kilo-lines and should preferably be less than 140 kilo-lines.

The tooth width at a point $\frac{1}{3}$ slot depth from the root of the tooth,

$$w_{t_3} = \frac{\pi(D - 1.33d_s)}{S} - w_s = \frac{\pi(25 - 1.33 \times 1.57)}{81} - 0.363 \\ = 0.525$$

and the section area of the armature teeth at this point,

$$s_{t_3} = 0.525(11 - 3 \times \frac{3}{8})0.92 \times 81 \\ = 386 \text{ sq. in.}$$

The density,

$$B_{t_3} = \frac{48,300}{386} = 125 \text{ kilo-lines.}$$

For this design, 0.014 in. open-hearth electric sheet steel will be used. From the standard saturation curve for this material, the ampere-turns per inch for the density, $B_{t_3} = 125$ kilo-lines, are found to be 525. The ampere-turns per pole for the armature teeth,

$$AT_t = at_t l_t = 525 \times 1.57 = 825.$$

The flux per pole,

$$\phi = \frac{\phi_t f_a}{p} = \frac{48,300 \times 0.665}{6} \\ = 5350 \text{ kilo-lines.}$$

For a commutating-pole machine and a frequency of 45 cycles per sec., the armature yoke density should be approximately 75 kilo-lines per sq. in. The depth of the armature yoke,

$$d_{ya} = \frac{\phi}{(l - na w_a) k_1 B_{ya}} = \frac{5350}{(11 - 3 \times \frac{3}{8})0.92 \times 75} \\ = 7.86 \text{ in.}$$

The inside diameter of the armature,

$$D_i = D - 2d_a - D_{ya} = 25 - 2 \times 1.57 - 7.86 \\ = 14.0 \text{ in.}$$

The armature yoke density is therefore 75 kilo-lines per sq. in., and the ampere-turns per inch from the standard saturation curve for open-hearth steel, $at_{ya} = 10$.

The length of the flux path in the armature yoke,

$$l_{ya} = \frac{[D - (2d_a + \frac{1}{2}d_{ya})]\pi}{2p} = \frac{[25 - (2 \times 1.57 + \frac{1}{2} \times 7.86)]\pi}{2 \times 6} \\ = 4.7 \text{ in.}$$

The ampere-turns per pole for the armature yoke,

$$AT_{ya} = at_{ya}l_{ya} = 10 \times 4.7 = 47.$$

The correction for the commutating-pole flux in the armature yoke, if necessary, must be made after the commutating pole is designed (Chapter V).

The field poles for this generator will be built up of sheet steel laminations, punched from open-hearth sheets approximately 0.023 in. thick. A flux density of 95 kilo-lines per sq. in. is selected for the pole body. For machines with half as many commutating poles as main poles, slightly lower pole densities should be used because the commutating-pole flux returns through the main poles. The leakage flux is assumed to be 20 per cent of the useful flux per pole, and the axial length of the pole is made equal to the armature length, that is,

$$l_1 = 11 \text{ in.}$$

The section area of the pole body,

$$s_p = \frac{\phi \lambda}{B_p} = \frac{5350 \times 1.20}{95} = 67.6 \text{ sq. in.}$$

The width of the pole body,

$$w_p = \frac{s_p}{l_1} = \frac{67.6}{11} = 6.15; \text{ use } 6\frac{1}{8} \text{ in.,}$$

and $B_p = 95.4$ kilo-lines.

From the standard saturation curve in the Appendix for field pole steel, the ampere-turns per inch are found to be 35.

The length of the flux path in the pole is equal to l_p , Fig. 51. The space required by the shunt field winding will determine the radial length of the pole. It can be most satisfactorily determined from the design data of previously constructed machines. When such data are not available, l_p can generally be taken as about 28 to 35 per cent of the armature diameter for diameters from 50 to 25 in. and about 35

to 66 per cent of the armature diameter for diameters less than 25 in. Choosing 33 per cent of the armature diameter,

$$l_p = 0.33 \times 25 = 8.25 \text{ in.}$$

The inside diameter of the field yoke,

$$\begin{aligned} D_{vi} &= D + 2\delta + 2l_p = 25 + 2 \times 0.17 + 2 \times 8.25 \\ &= 41.84; \text{ use } 42 \text{ in.} \end{aligned}$$

Then,

$$l_p = 8.33 \text{ in.}$$

The ampere-turns per pole for the field pole,

$$AT_p = at_p l_p = 35. \times 8.33 = 292.$$

The field yoke will be cast steel and the density 65 kilo-lines per sq. in. The section area,

$$s_{yf} = \frac{\phi \lambda}{B_{yf}} = \frac{5350 \times 1.20}{65} = 98.7 \text{ sq. in.}$$

This is the section area of the field yoke on both sides of the diameter.

The generator is to be part of a motor-generator set, and the bearings are to be mounted in pedestals bolted to the base. The extension of the yoke beyond the edge of the pole will be 2.5 in., and the axial length of the field yoke will be 16 in.

Two times the depth or thickness of the rectangular yoke section,

$$d_{yf} = \frac{s_{yf}}{l_2} = \frac{98.7}{16} = 6.17; \text{ use } 6.25 \text{ in.}$$

The flux density in the field yoke,

$$B_{yf} = \frac{\phi \lambda}{s_{yf}} = \frac{5350 \times 1.20}{6.25 \times 16} = 64.2 \text{ kilo-lines.}$$

The outside diameter,

$$D_{vo} = D_{vi} + d_{yf} = 42 + 6.25 = 48.25 \text{ in.}$$

The length of the flux path is taken on the mean diameter,

$$l_{yf} = \frac{(D_{vi} + \frac{1}{2}d_{yf})\pi}{2p} = \frac{(42 + \frac{1}{2} \times 6.25)\pi}{2 \times 6} = 11.80 \text{ in.}$$

The ampere-turns per inch of flux path taken from the standard

saturation curve for cast steel are, $at_{yf} = 17$, and the ampere-turns per pole for the field yoke,

$$AT_{yf} = at_{yf}l_{yf} = 17 \times 11.80 = 200$$

The total ampere-turns per pole for the full-load induced voltage,

$$\begin{aligned} ATP &= AT_g + AT_t + AT_{ya} + AT_p + AT_{yf} \\ &= 3360 + 825 + 47 + 292 + 200 \\ &= 4724. \end{aligned}$$

The armature ampere-turns per pole,

$$\begin{aligned} ATP_a &= \frac{I_a N}{2pa} = \frac{1208.4 \times 324}{2 \times 6 \times 6} \\ &= 5440. \end{aligned}$$

The ampere-turns per pole for the field winding are less than the armature ampere-turns per pole, which indicates that the assumed air gap length is too small. The length of the air gap is therefore increased to 0.22 in. The air gap coefficient,

$$\begin{aligned} k &= \frac{t_1}{w_1 + (y\delta)} = \frac{0.97}{0.607 + (1.25 \times 0.22)} \\ &= 1.10, \end{aligned}$$

and the air gap ampere-turns,

$$\begin{aligned} AT_g &= \frac{B_g \delta k}{3.2} = \frac{56,000 \times 0.22 \times 1.10}{3.2} \\ &= 4240. \end{aligned}$$

The ampere-turns per pole for the field winding will now be,

$$ATP = 5604,$$

and

$$\frac{ATP}{ATP_a} = \frac{5604}{5440} = 1.03$$

which is satisfactory.

The calculations for the open circuit saturation curve are shown in Table V, and the curve plotted from these values is shown in Fig. 55.

CHAPTER V

ARMATURE REACTION AND FIELD WINDING DESIGN

Armature Demagnetizing Ampere-Turns.—Figure 56 shows a four-pole generator with the brushes shifted from the no-load neutral, a distance $b_s/2$ inches of armature circumference. The armature demagnetizing ampere-turns per pole,

$$\text{ATP}_d = \frac{1}{2}b_s Q. \quad (67)$$

The ampere conductors per inch of armature circumference,

$$Q = \frac{I_a N}{a\pi D}$$

and

$$\frac{1}{2}b_s = \frac{2\beta\pi D}{360p},$$

where the angle β is expressed in electrical degrees. Making the substitutions, the demagnetizing ampere-turns per pole,

$$\begin{aligned} \text{ATP}_d &= \frac{2\beta\pi D I_a N}{360pa\pi D} \\ &= \frac{2\beta}{180} \frac{I_a N}{2pa}. \end{aligned}$$

The armature ampere-turns per pole,

$$\text{ATP}_a = \frac{I_a N}{2ap} \quad (68)$$

and the armature demagnetizing ampere-turns per pole,

$$\text{ATP}_d = \frac{2\beta}{180} \text{ATP}_a \quad (69)$$

To obtain satisfactory commutation in machines without commutating poles, the brushes are shifted from the no-load neutral, so that the coil sides short-circuited by the brushes will lie in a field strength, at no-load,

equal to from 6500 to 13,000 lines per sq. in. The angle corresponding to this brush displacement is generally approximately 18 electrical degrees.

When the machine has commutating poles, the commutating pole produces the commutating field, and the brushes remain in the no-load neutral position for all loads. For commutating-pole machines the angle of brush displacement is zero and therefore also the armature demagnetizing ampere-turns.

Armature Cross-Magnetizing Ampere-Turns.—All of the armature conductors lying outside of the double angle of brush displacement, 2β , Fig. 56, set up the armature cross-magnetizing field. The flux produced by the conductors that do not lie under the pole shoe has its path so largely in air that it may be neglected. The armature ampere-turns per pole that produce the cross-magnetizing field,

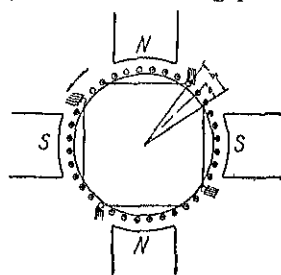


FIG. 56.—Demagnetizing and cross-magnetizing ampere-turns of a four-pole generator.

$$\begin{aligned} \text{ATP}_c &= \frac{1}{2} \tau f_a \frac{I_a N}{a \pi D} = \frac{1}{2} f_a \frac{\pi D}{p} \frac{I_a N}{a \pi D} \\ &= f_a \text{ATP}_a \end{aligned} \quad (70)$$

When the magnetic circuit becomes saturated, the reluctance of the path of the main pole flux is increased, because of the distortion of the air gap flux by the armature cross-magnetizing ampere-turns. In consequence, the ampere-turns of the field winding must be increased if the useful flux in the armature is to remain constant.

The method of determining the ampere-turns per pole required to compensate for the demagnetizing effect of the armature cross-magnetizing ampere-turns is given by Dr. Arnold and La Cour.¹ Figure, 57 shows the open-circuit saturation curve for a generator. OE is the full-load induced voltage (terminal voltage plus the voltage drop in the armature, series and commutating field windings and brush contacts) and OF is the corresponding number of ampere-turns per pole.

The m.m.f. across the leading pole tip of a generator is decreased by the armature cross-magnetizing ampere-turns per pole,

$$\text{ATP}_c = f_a \text{ATP}_a,$$

and, as a result, the flux density in the air gap and the voltage induced

¹ "Die Gleichstrommaschine," Vol. 1, 3rd ed., p. 182, Julius Springer, Berlin

in the conductors under this pole tip are also decreased. The m.m.f. across the trailing pole tip of a generator is increased by the armature cross-magnetizing ampere-turns per pole; as a result, the flux density in the air gap and the voltage induced in the conductors under this pole tip are also increased. The armature cross-magnetizing field will have no effect upon the terminal voltage of the machine when the increase in voltage at the trailing pole tip is equal to the decrease in voltage at the leading pole tip or when the area of the triangle cdG is equal to the area of the triangle abG , Fig. 57. When the area of

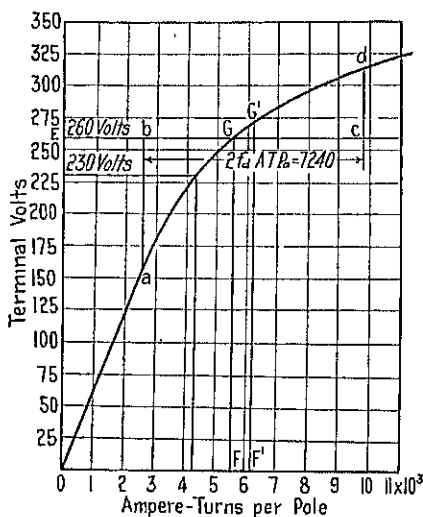


FIG. 57.

triangle cdG is equal to the area of triangle abG , the line bc will be shorter than line cd , because the open-circuit saturation curve drops off more rapidly above the line bc than below it. With a pair of dividers set equal to $bc = 2 f_a ATP_a$, the line bc may be laid off, so that the area of the triangle abG is equal to the area of the triangle cdG . The bisector of the line bc , $F'G'$, gives the voltage that must be induced in the armature winding at full-load when the brushes are in the no-load neutral, to obtain constant terminal voltage, and OF' is the corresponding number of ampere-turns per pole. The number of

ampere-turns that must be added to the main field ampere-turns, to compensate for the demagnetizing effect of the armature cross-magnetizing ampere-turns,

$$= OF' - OF, \text{ Fig. 57.}$$

The areas of the triangles, Fig. 57, can easily be found with a planimeter.

The path of the armature cross-magnetizing field comprises the armature core, the teeth and air gap under the pole tips, and the pole shoe. The saturation curve for this magnetic circuit can be found by calculating the ampere-turns required to send the flux through the teeth and air gap, the ampere-turns required to send the flux through the armature core and pole being so small that they may be neglected. This saturation curve, of the armature cross-magnetizing field, should

used to determine the demagnetizing effect of the armature cross-magnetizing field. When the open-circuit saturation curve is used, as in Fig. 57, the results will be slightly large. The error is quite small, however, and for practical purposes it is more convenient to use the open-circuit saturation curve.

The extent that the no-load field form is distorted by the armature field varies widely for different designs. The distortion will, obviously, be greater when the armature ampere-turns per pole are high in proportion to the shunt field ampere-turns per pole. The distorting effect of the armature field may be reduced by increasing the reluctance of the armature cross-magnetizing field. This can be done by using well beveled pole shoes with large air gaps under the pole tips, by using high flux densities in the armature teeth, or by building up the pole as shown in Fig. 58. With properly designed compensating windings in the pole faces, the armature cross-magnetizing field may be completely neutralized. When the latter is the case, the air gap flux distribution curve for the machine will have the same shape for full-load as for no-load. In order that the leading pole tip for a generator, the trailing pole tip for a motor, shall not become completely demagnetized, the ampere-turns per pole of the field winding for full-load generated voltage, OF , Fig. 57, must be greater than $f_a ATP_a$. The ratio of the ampere-turns per pole of the main field to the armature ampere-turns per pole is usually as follows:

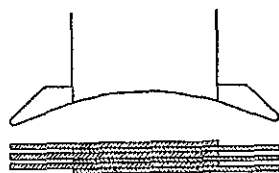


FIG. 58.

$$\frac{ATP}{ATP_a} = 1.0 \text{ to } 1.25. \quad (71)$$

Since the air gap ampere-turns per pole are generally from 65 to 85 per cent of the total ampere-turns per pole, it follows that

$$\frac{AT_g}{ATP_a} = 0.65 \text{ to } 1.0. \quad (72)$$

The air gap ampere-turns per pole formula 47,

$$AT_g = \frac{B_g \delta k}{3.2} \\ = 0.313 B_g \delta k.$$

Substituting into formula 72, the length of the air gap,

$$\delta = \frac{(0.65 \text{ to } 1.0) ATP_a}{0.313 B_g k}. \quad (73)$$

Shunt and Series Field Ampere-Turns.—Figure 59 shows the open-circuit saturation curve of a generator. OA are the ampere-turns per pole corresponding to the no-load terminal voltage, OE_t , and OB are the ampere-turns per pole corresponding to the full-load generated voltage, OE . To these ampere-turns must be added the ampere-turns per pole required to compensate for the demagnetizing effect of the armature cross-magnetizing field and the armature demagnetizing ampere-turns per pole when the brushes are shifted from the no-load neutral.

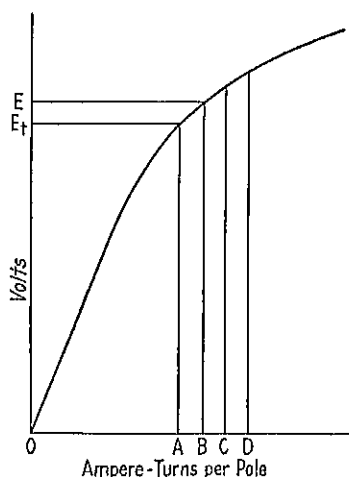


FIG. 59.—Total field ampere-turns per pole.

The total ampere-turns per pole on the field winding are then equal to OD (Fig. 59).

For a flat-compounded generator, the voltage across the shunt field winding is practically constant from no-load to full-load, and the shunt field ampere-turns per pole are the ampere-turns corresponding to no-load terminal voltage, OA , Fig. 59. The series field ampere-turns per pole are then equal to the total ampere-turns per pole minus the shunt field ampere-turns per pole = $OD - OA$, Fig. 59.

For an over-compounded generator, the voltage across the shunt field winding is higher at full-load than at no-load. Referring to Fig. 59, the shunt field ampere-turns per pole for an over-compounded generator are (assuming the long shunt connection)

$$ATP_s = \frac{\text{F.L. terminal voltage}}{\text{N.L. terminal voltage}} OA. \quad (74)$$

The series field ampere-turns per pole are equal to the difference between the total ampere-turns per pole and the shunt field ampere-turns per pole. Since the effect of the armature cross-magnetizing field cannot be accurately predetermined, it is usual to increase the series field ampere-turns per pole, determined as given above, approximately 20 per cent. The desired degree of compounding can then be obtained by the use of a series field shunt.

For a shunt-wound motor the generated voltage in the armature winding, E , is equal to the terminal voltage minus the voltage drop in the armature winding, commutating field winding, and brush contacts. The shunt field ampere-turns per pole are equal to the ampere-turns corresponding to full-load generated voltage.

Design of Pole Winding.—For the shunt field windings, single-cotton-covered, double-cotton-covered, enameled, and single-cotton-covered enameled wires are used. Asbestos-covered wire is used when high operating temperatures are required. The section area of the wire used is either round, square, or rectangular. Cotton-covered wires are sometimes treated with an insulating compound, by passing the wire through an insulating bath during winding. More often, the coils are wound with the dry cotton-covered conductor. The completely wound coils are then dried and dipped into a bath of insulating varnish or treated with an asphaltum compound by the vacuum process.² Impregnating the coils with asphaltum compound by the vacuum process is more expensive than the varnish treatment, but the asphaltum compound fills the spaces between wires better than insulating varnish and gives better heat dissipation. The coils are usually wound on a form and completely insulated before being placed on the pole.

FIG. 60.—Main pole and windings, 300-kw., 250-volt, 900-r.p.m. generator.

² See "Insulation and Design of Electrical Windings," by A. P. M. Fleming and R. Johnson, p. 68, Longmans, Green & Co., London; also *Electrical Journal*, Vol. 22, Feb., 1925, p. 95.

built up of pressboard or fuller board and is held in place by a wrapper of unbleached muslin. Figure 60 shows a ventilating duct at each end of the pole. This ventilating duct is not provided on all machines, because for some types of construction this duct will be practically closed at the yoke end of the pole. Ventilating ducts between the inside of the shunt field winding and the ends of the pole are most effective when the yoke length is small. These ventilating ducts are usually from $\frac{1}{4}$ in. to $\frac{3}{4}$ in. When heavy shunt field windings are required for large generators, a ventilated coil, as shown in Fig. 61, may be used.

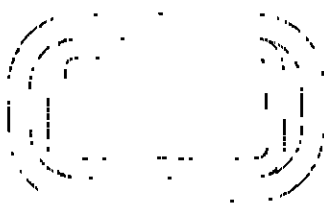


FIG. 61.—Ventilated field-coil.

The length of the mean-turn of the shunt field coil can be calculated as follows (see Fig. 60):

$$L_f = 2l_1 + 2(w_p - 2w_a) + \pi[d_f + 2(w_a + \frac{3}{8}d)] \text{ in.} \quad (75)$$

The resistance of the shunt field winding,

$$R_f = \frac{L_f \mu_f p r}{s_f 10^6} \text{ ohms,} \quad (76)$$

and

$$i_f = \frac{E_t}{R_f} \text{ amperes.} \quad (77)$$

The ampere-turns per pole on the shunt field winding,

$$i_f \mu_f = \frac{E_t s_f \times 10^6}{L_f p r}. \quad (78)$$

This equation shows that the number of ampere-turns per pole on the shunt field winding are independent of the number of turns per pole, but vary directly with the cross-section of the conductor.

For generators, the shunt field winding is generally designed for a voltage from 20 to 30 per cent less than the terminal voltage of the machine. Voltage regulation can then be obtained by means of a field rheostat. The section area of the shunt field conductor,

$$s_f = \frac{ATP_f L_f p \times 0.826}{E_t (0.70 \text{ to } 0.80) \times 10^6} \text{ sq. in.} \quad (79)$$

The size of wire having this section area is found from the copper table. When the calculated conductor section lies half way between two standard conductors, half of the shunt field winding may be wound with the

the larger conductor and the other half with the next smaller conductor. When two sizes of wire are used,

$$s_f = \frac{s_{f1}t_{f1} + s_{f2}t_{f2}}{t_{f1} + t_{f2}} \text{ sq. in.} \quad (80)$$

The current in the shunt field winding,

$$i_f = s_f A_f \text{ amperes.} \quad (81)$$

Since the losses in the shunt field winding are generally small, especially for large machines, the current density is generally chosen as high as the temperature rise will permit. The current density for the shunt field windings,

$$A_f = 900 \text{ to } 1500 \text{ amperes per sq. in.}$$

The number of turns per pole,

$$t_f = \frac{ATP_f}{i_f}. \quad (82)$$

The correct value of the current density in the shunt field copper is determined from the temperature rise of the shunt field winding. A high temperature rise indicates too high a current density, whereas a low temperature rise indicates too low a current density and an uneconomical use of shunt field copper. The method of predetermining the temperature rise of the shunt field winding is given in Chapter VII.

An approximate check of the temperature rise of the shunt field winding can be obtained from the cooling surface per watt loss. For high-speed, well-ventilated machines, with depth of field coil not over approximately 0.75 in., the cooling surface per watt loss should be greater than 2, if the temperature rise is not to exceed 50° C. For slow-speed machines, with depth of field coil not over about 1.50 in., the cooling surface per watt loss should generally be about 4, if the temperature rise is not to exceed 50° C. The cooling surface per coil is taken equal to the perimeter of the coil section times the mean-turn. The total cooling surface for the shunt field winding is,

$$S_f = 2(d_f + h_f)L_f p \text{ sq. in.,}$$

and the surface per watt loss,

$$\frac{S_f}{W_f} = \frac{2(d_f + h_f)L_f p}{i_f^2 R_f}.$$

The bare weight of the shunt field copper,

$$G_f = L_f t_f p s_f \times 0.321 \text{ lb.} \quad (83)$$

The insulated weight depends upon the kind of insulation or insulation. The copper tables give the insulated weights for wires with standard insulation.

Series Field Winding.—The series field winding is generally wound with rectangular, double-cotton-covered wire when the conductor section is 0.102 sq. in. or less. For larger conductor sections, bare strap copper is generally used, with the turns insulated from one another by paper about 0.010 in. thick or by air spaces. The series

field winding is often placed on the outside of the shunt field winding. When bare strap is used, it is wound on edge, and the separate turns are insulated from one another by air spaces. A completely insulated field coil, showing this method of winding the series field, is shown in Fig. 62. A shunt field coil with square wire series field coil wound on the outside, is shown in Fig. 63.

The series field current, I_s , is equal to the terminal current plus the shunt field current when the long shunt connection is used and is equal to the terminal current when the short shunt

winding, connection is used. The number of turns per pole on the series field

$$t_s = \frac{ATP_s}{I_s}. \quad (84)$$

The section area of the series field conductor,

$$s_s = \frac{I_s}{A_s} \text{ sq. in.} \quad (85)$$

The current density in the series field copper cannot always be chosen as high as the temperature rise will permit, because the efficiency

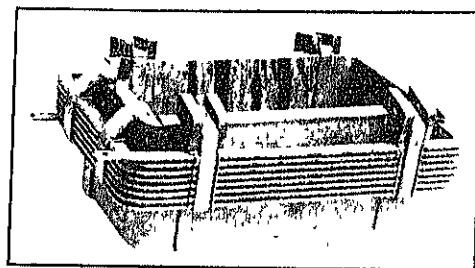
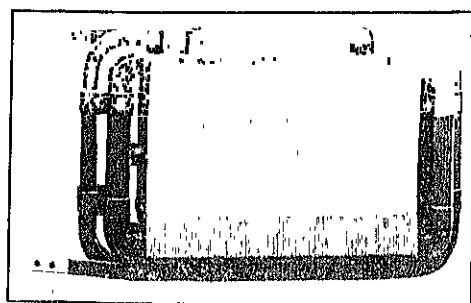


FIG. 62.—Complete field with ribbon copper series field winding outside of shunt field coil.

$$A_s = 900 \text{ to } 1800 \text{ amperes per sq. in.,}$$

and for series motors for intermittent duty,

$$A_s = 1200 \text{ to } 2000 \text{ amperes per sq. in.}$$

The mean-turn of the series field coil can be determined from a

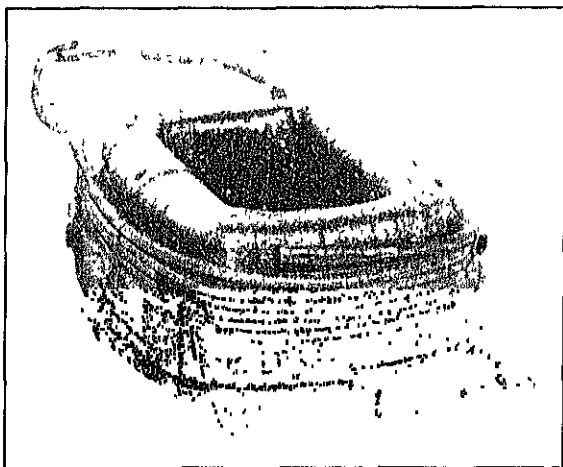


FIG. 63.—Complete field coil with wire wound series coil outside of shunt coil.

sketch of the coil by a method similar to the one used for the shunt field coil. The resistance of the series field winding,

$$R_s = \frac{L_s t_s p r}{s_s \times 10^6} \text{ ohms.} \quad (86)$$

The bare weight of the series field copper,

$$G_s = L_s t_s p s_s \times 0.321 \text{ lb.} \quad (87)$$

Commutating Field Winding.—The commutating field winding is connected in series with the armature, and the total armature current flows through the commutating field winding. As for the series field winding, rectangular, double-cotton-covered wire is generally used when the conductor section is equal to 0.102 sq. in. or less. For larger conductor sections, bare strap copper wound on edge is generally used. The turns are then insulated from one another by paper about 0.010 in. thick, cotton tape on the conductors, or by air spaces. The insulation between the winding and the pole body is generally about $\frac{1}{16}$ in. thick

mutating field coil of bare ribbon copper is shown in Fig. 61.

The number of turns per pole for the commutating field winding,

$$t_1 = \frac{ATP_1}{I_a}. \quad (88)$$

The section area of the conductor,

$$s_1 = \frac{I_a}{A_1} \text{ sq. in.} \quad (89)$$

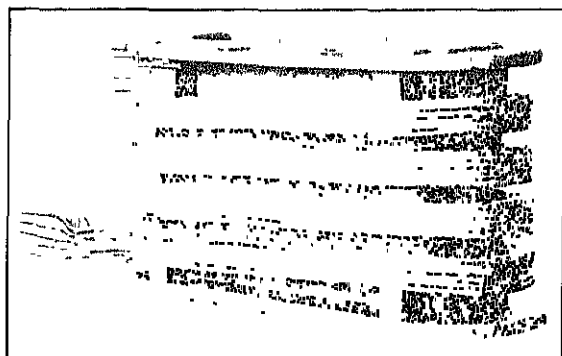


FIG. 61—Bare ribbon copper commutating field coil

The current density in the commutating field copper,

$$A_1 = 800 \text{ to } 1500 \text{ amperes per sq. in.}$$

The length of the mean-turn of the commutating field coil can easily be found from a sketch of the coil. The resistance of the commutating field winding,

$$R_1 = \frac{L_1 t_1 \rho}{s_1 \times 10^{11}} \text{ ohms.} \quad (90)$$

The bare weight of the commutating field copper,

$$G_1 = L_1 t_1 \rho s_1 \times 0.321 \text{ lb.} \quad (91)$$

Design of the Shunt Field Rheostat.—For full-load and normal voltage,

$$R_f + R_{rt} = \frac{E_f}{i_f} \text{ ohms,}$$

where r_{rt} is the shaft field rheostat resistance for full-load and normal terminal voltage. For no-load and normal terminal voltage,

$$R_f + R_{ro} = \frac{E_t}{I_{fo}} \text{ ohms}$$

$$R_{ro} = \frac{E_t}{i_{to}} - R_f \text{ ohms.}$$

To allow for variations in speed and to permit a reduction in voltage below normal,

$$R_r = 1.25 \text{ to } 2.0 \left(\frac{E_t}{i_{\text{to}}} - R_f \right) \text{ ohms.} \quad (92)$$

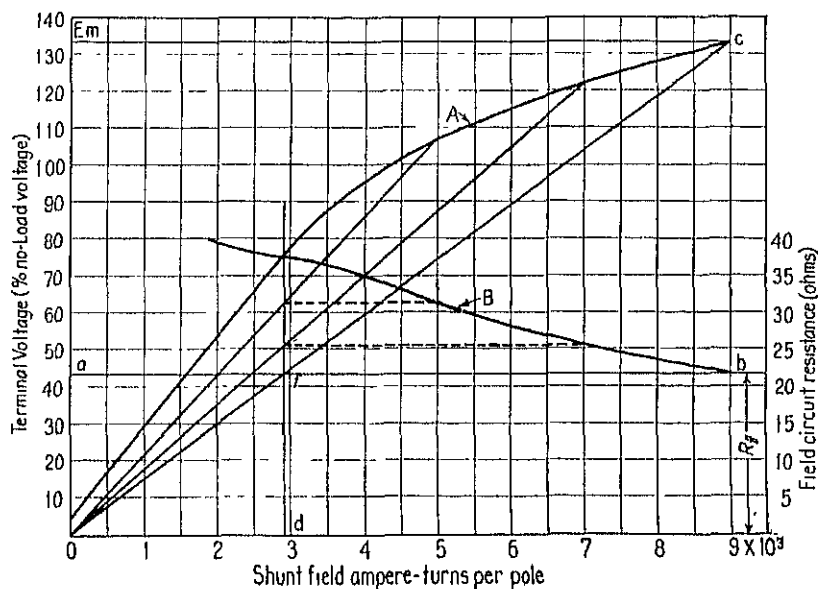


FIG. 65.—Construction of field circuit resistance curve.

The resistance steps for the rheostat can be determined by the following graphical method:³ Curve *A*, Fig. 65, is the open-circuit saturation curve for a generator, with terminal voltage plotted in percentage of normal voltage as ordinates and shunt field current as abscissas. OE_m is the maximum voltage that can be obtained when the rheostat is all cut out and the generator is self-excited. Oa is the

³ "Graphische Berechnung von Widerstandsregulatoren," by F. Tünke, *Elektrotechnische Zeitschrift*, Vol. 21, 1900, p. 801, and "Exciter Field Rheostats," by J. F. Formanok, *General Electric Review*, Vol. 28, Feb., 1925, p. 125.

ance line. The diagonal, Oc , intersects the shunt field resistance line at f , and df is the resistance in the shunt field circuit when the terminal voltage is E_m . The total resistance necessary in the shunt field circuit for other voltages can be found by drawing diagonal lines from a number of points on the open-circuit saturation curve to the origin. The intersections of these lines with df extended give the total resistance necessary in the shunt field circuit for the corresponding voltages. By plotting these values of field circuit resistance, as shown in Fig. 65, the

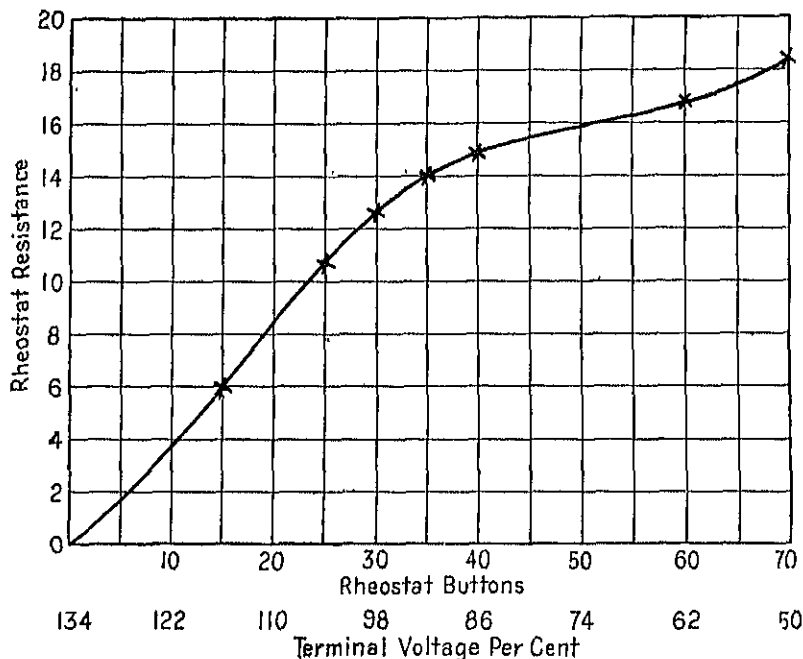


FIG. 66.—Rheostat resistance curve.

field resistance curve, B , is obtained. If the field resistance is subtracted from the values of field circuit resistance shown by Curve B , Fig. 65, the field rheostat resistance curve is obtained, as shown in Fig. 66. Field rheostats should be so designed that the same variation in voltage is obtained for all the buttons on the rheostat, regardless of the voltage at which the machine is operating. On the assumption of equal voltage increments between buttons, the voltage scale, Fig. 66, may be replaced by a scale showing rheostat buttons. Obviously, it would be impractical to make the resistance different between all

buttons of the rheostat, as shown by the curve, Fig. 66. Rheostats are generally built up of resistance units, and if a large number of these can be made alike, the construction of the rheostat will be greatly simplified. The resistance between the buttons of the rheostat can be found by subtracting the resistance for any one button from the resistance of the previous one. This would be a tedious process and would involve considerable time. For practical purposes, it is more convenient to divide the rheostat resistance curve into a number of sections, as indicated by X, Fig. 66. Straight lines drawn between these points give a broken curve which nearly coincides with the original. Each of these sections then represents a group of rheostat buttons, for which the resistance is the same. The resistance of each group can easily be

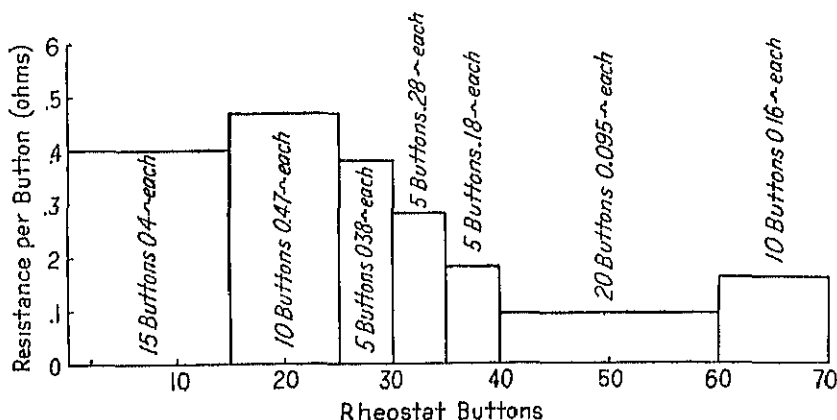


FIG. 67.—Equivalent rheostat resistance curve.

found as follows (see Fig. 66): The section of the rheostat resistance curve, for example, between 15 and 25 buttons comprises 10 buttons, and the resistance variation is from 6 to 10.7 ohms, or 4.7 ohms. Dividing this value by the number of buttons for the section, 10, gives the resistance per button equal to 0.47 ohm. Figure 67 shows the resistance between buttons for the various sections of the rheostat.

Sample Design: *Design of Shunt and Series Field Windings.*—The sample generator is to be designed with commutating poles. The brushes will therefore remain in the no-load neutral position and the armature demagnetizing ampere-turns will be equal to zero.

The demagnetizing effect of the armature cross-magnetizing ampere-turns is determined graphically as explained on page 78. The armature cross-magnetizing ampere-turns per pole = $f_a \text{ ATP}_a = 0.665 \times 5440 = 3620$. The graphic construction for the sample problem is

magnetizing field = $OF' - OF = 6200 - 5604 = 596$ ampere-turns.

At no-load, the voltage across the shunt field winding will be 230 volts, and the corresponding ampere-turns per pole are equal to 4360 (see Fig. 57). At full-load, the voltage across the shunt field winding is 250 volts. The shunt field ampere-turns per pole,

$$ATP_f = \frac{250}{230} \times 4360 = 4740 \text{ ampere-turns.}$$

The shunt field winding will be designed as shown in Fig. 60, with the series field winding on the outside of the shunt field winding. The depth of the shunt field coil must first be estimated; for this design, 0.75 in. will be used. The length of the mean-turn can easily be calculated from the sketch shown in Fig. 60, which is for the sample design.

$$\begin{aligned} L_f &= 2l_1 + 2(w_p - 2w_a) + \pi[d_f + 2(w_a + \frac{a}{2})] \text{ in.} \\ &= 2 \times 11.0 + 2(6.125 - 2 \times 0.50) + \pi[0.75 + 2(0.50 + 0.10)] \\ &= 38.38 \text{ in.} \end{aligned}$$

The section area of the shunt field conductor,

$$\begin{aligned} s_f &= \frac{ATP_f L_{fpr}}{E_t(0.70 \text{ to } 0.80)10^6} = \frac{4740 \times 38.38 \times 6 \times 0.826}{250 \times 0.75 \times 10^6} \\ &= 0.0048 \text{ sq. in.} \end{aligned}$$

A No. 12 round wire has a section area of 0.00515 sq. in. and a double-cotton-covered diameter of 0.091 in. This wire will be suitable for the shunt field winding. The shunt field current has been estimated at 8.4 amperes. For this current, the number of shunt field turns per pole,

$$t_f = \frac{ATP_f}{i_f} = \frac{4740}{8.4} = 565$$

and the current density for the shunt field copper,

$$A_f = \frac{i_f}{s_f} = \frac{8.4}{0.00515} = 1630 \text{ amperes per sq. in.}$$

From the sketch, Fig. 60, which is for the sample design, the height of the winding space for the shunt field coil, $h_f = 6.8$ in. The number of turns per layer

$$= \frac{6.8}{0.091} = 74.6; \text{ use } 73$$

The space for one turn must be allowed in passing from one layer to the next; 73 turns per layer will therefore be used. The number of layers

$$= \frac{565}{73} = 7.75; \text{ use } 8.$$

The number of shunt field turns per pole,

$$t_f = 8 \times 73 = 584;$$

the shunt field current,

$$i_f = \frac{4740}{584} = 8.12 \text{ amperes};$$

and the current density,

$$A_f = \frac{8.12}{0.00515} = 1575 \text{ amperes per sq. in.}$$

The depth of the field coil, $d_f = 0.091 \times 8 = 0.728$ in. or practically the same as first assumed. It will therefore not be necessary to recalculate the mean-turn.

The resistance at 75°C. ,

$$\begin{aligned} R_f &= \frac{L_f t_f \rho r}{s_f \times 10^6} = \frac{38.38 \times 584 \times 6 \times 0.826}{0.00515 \times 10^6} \\ &= 21.6 \text{ ohms} \end{aligned}$$

and the copper loss,

$$W_f = i_f^2 R_f = 8.12^2 \times 21.6 = 1420 \text{ watts.}$$

The cooling surface,

$$\begin{aligned} S_f &= 2(d_f + h_f)L_f p = 2(0.73 + 6.75)38.38 \times 6 \\ &= 3450 \text{ sq. in.} \end{aligned}$$

and the cooling surface per watt loss,

$$\frac{S_f}{W_f} = \frac{3450}{1420} = 2.43.$$

The weight of the shunt field copper,

$$\begin{aligned} G_f &= L_f t_f p s_f \times 0.321 \\ &= 38.38 \times 584 \times 6 \times 0.00515 \times 0.321 \\ &= 223 \text{ lb.} \end{aligned}$$

From Fig. 57, the total ampere-turns required on the field winding to generate 250 volts at the terminals of the machine at full-load are found to be 6200 ampere-turns. The shunt field ampere-turns were calculated above and are equal to 4740. The ampere-turns per pole required for the series field will be $6200 - 4740 = 1460$ ampere-turns. For the long shunt connection, the current in the series field winding will be equal to the armature current, I_a . The number of turns per pole for the series field,

$$t_s = \frac{1460}{1208} = 1.21; \text{ use } 1.5 \text{ turns.}$$

The ampere-turns per pole on the series field will then be,

$$\text{ATP}_s = 1208 \times 1.5 = 1810 \text{ ampere-turns.}$$

It is generally desirable to use a larger number of ampere-turns than the calculations show, to allow for variations in the material of the magnetic circuit, inaccuracies in the determination of armature reaction, etc.

The series field winding will be placed on the outside of the shunt field winding. For a current density of 1800 amperes per sq. in., the section area of the series field conductor,

$$s_s = \frac{I_s}{A_s} = \frac{1208}{1800} = 0.672 \text{ sq. in.}$$

A bare, strap copper conductor, wound on edge, will be most suitable for this winding. Three strap conductors, 0.219×1.00 in., in parallel, will be used, each having a section area of 0.216 sq. in. The current density is then,

$$A_s = \frac{1208}{3 \times 0.216} = 1860 \text{ amperes per sq. in.}$$

From the sketch, Fig. 60, the mean-turn of the series field winding can easily be calculated in the manner described for the shunt field winding.

$$L_s = 2 \times 11.0 + 2(6.125 - 2 \times 0.5) + \pi \times 5.15 + 6.0 = 54.45 \text{ in.,}$$

where 6 in. is added to the mean-turn of the coil to allow for the connections between poles.

The resistance of the series field winding at 75°C. ,

$$\begin{aligned} R_s &= \frac{I_s L_s \rho r}{s_s \times 10^6} = \frac{54.45 \times 1.5 \times 6 \times 0.826}{0.648 \times 10^6} \\ &= 0.000624 \text{ ohm.} \end{aligned}$$

$$I_s R_s = 1208 \times 0.000624 = 0.755 \text{ volt,}$$

or 0.302 per cent of the full-load terminal voltage.

It will not be necessary to calculate the cooling surface per watt for this type of series field winding, because experience has shown that for current densities up to about 2000 amperes per sq. in. satisfactory operating temperatures are generally obtained.

The weight of the series field copper,

$$\begin{aligned} G_s &= L_s t_s p s_s \times 0.321 \\ &= 54.45 \times 1.5 \times 6 \times 0.648 \times 0.321 = 102 \text{ lb.} \end{aligned}$$

The shunt field rheostat resistance is calculated by formula 92,

$$\begin{aligned} R_r &= 2.0 \left(\frac{E_t}{i_{fo}} - R_f \right) = 2.0 \left(\frac{230}{7.46} - 21.6 \right) \\ &= 18.4 \text{ ohms.} \end{aligned}$$

The graphic construction, to determine the value of the resistance for the various buttons on the rheostat, is shown in Figs. 65, 66, and 67.

CHAPTER VI

COMMUTATION AND COMMUTATING POLE DESIGN

WHEN the commutator segments to which the armature coils are connected pass under the brushes, the armature coils are successively transferred from one armature path, in which the current has one direction, to an adjoining armature path, in which the current is of opposite direction. During this period the coils are short-circuited by the brush, and the current must be reduced from its original value to zero and then built up again to an equal value in opposite direction.

The time variation of the current in a short-circuited coil may be represented diagrammatically as shown in Fig. 68. In this diagram, ordinates represent values of current and abscissas represent time. Before the coil under consideration enters the commutation period AB , the current in it is equal to $-i_a$, and after the completion of commutation it must be equal to $+i_a$. The curve showing the time variation of the current in the short-circuited coil is called the short-circuit current curve.

Curve 1, Fig. 68, shows the current in the short-circuited coil changing at a uniform rate from $-i_a$ to $+i_a$. This type of commutation is known as straight-line commutation. Straight-line commutation is desirable, because it gives rise to uniform current density at the brush contact surface, and the brush contact loss is a minimum.

Curve 2, Fig. 68, shows that the current has been reversed too rapidly and reaches a value greater than $+i_a$ before commutation is completed. For this case, the current may reach its final value without sparking, but it may involve local current densities at the brush contact surface of sufficient magnitude to produce glowing of the brush, which would lead to high commutator temperatures, rapid deterioration of the brushes, and excessive brush contact losses. This condition is known as over-commutation.

Curve 3, Fig. 68, shows a case of the current not being reversed with sufficient rapidity. The current builds up to a value greater than its initial value. This condition may involve excessive local current densities at the brush contact surface, which would lead to high com-

brush. This condition is known as under-commutation.

In the above, no account has been taken of the effect of the mechanical conditions of the commutator and brushes. In order to secure successful commutation, it is necessary to have the best possible contact between brushes and commutator. A most important requirement in securing such contact is that the mica between commutator bars shall not protrude. Where the current passes from the commutator to the brush, the commutator copper is eaten away but the mica remains. If good brush contact is to be maintained, the mica between bars must be worn down mechanically at the same rate that the copper is eaten away. If the copper is eaten away more rapidly than the mica is worn down, the mica will eventually stand above the copper, and the brushes will cease to make good contact, which condition will increase the burning action. To prevent the mica from protruding above the commutator bars, it is now generally under-cut, so that it is a little below the surface of the commutator.

In addition to eliminating sparking, under-cutting the mica allows the use of softer brushes. If the mica is left flush with the commutator, a brush must be used of sufficient hardness to wear down the mica as fast as the copper is eaten away. Such brushes, however, have no self-lubricating qualities and are noisy, especially on high-speed commutators. Lack of lubrication will cause the brushes to chatter and vibrate, leading to bad contact between the brushes and commutator and causing sparking. Graphite brushes or carbon brushes with considerable graphite in them are extremely good for collecting current, but because of their softness they give poor results in wearing down the mica. Because of their graphite constituents, these brushes are largely self-lubricating and thus ride on the commutator more smoothly and much more quietly than ordinary carbon brushes.

To prevent the commutator from wearing down in grooves and forming ridges between the brushes of each brush arm, it has generally been the practice to displace all the positive brushes in one direction and all the negative brushes in the other direction. But since the eating away of the copper occurs only under the brushes of one polarity, it has been found better to stagger the brushes in pairs, so that the eating away of the copper is equalized over the entire commutator.

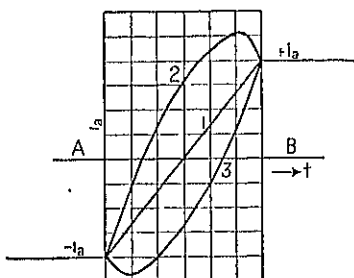


FIG. 68.—Short-circuit current curves.

between adjacent commutator bars. The thickness of the mica between adjacent commutator bars is generally about $\frac{1}{32}$ in. From this it might be presumed that a high voltage between bars is permissible. It has been found, however, that the maximum volts between adjacent commutator bars should generally not exceed approximately 30 volts¹ for large machines. For very small machines, this value may be considerably larger.

Width of Commutating Zone.—The width of the commutating zone or portion of the armature circumference where one or more armature coils are short-circuited, is of importance in calculating the reactance voltage and in determining the width of the commutating pole shoe.

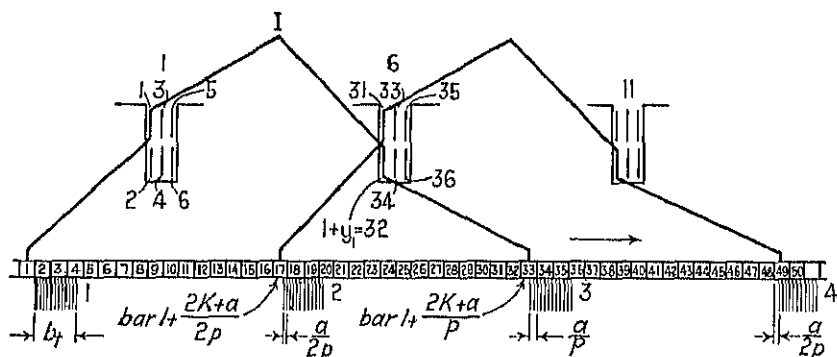


FIG. 69.—Two coils of simplex wave winding; $S=21$, $K=63$, $Y_1=31$, $Y_c=32$.

Figure 69 shows two coils of a simplex wave winding. For the position of the brushes shown, coil 1 is at the moment of beginning commutation. The width of the commutating zone of this coil is determined by the position of brushes 1 and 3 relative to the commutator bars to which the ends of this coil are connected. The distance the armature must move from the time commutator bar 1 comes in contact with brush 1 to the time when it leaves the brush again is,

$$(b + 1)\beta_r \text{ in.}, \quad (93)$$

where b is the thickness of the brush or its width along the commutator circumference, expressed in commutator bars, and β_r is the commutator bar pitch reduced to the armature diameter. Equation 93 would give the width of the commutating zone of coil 1, if its commutation

¹"Physical Limitations in D-C Commutating Machines," by B. G. Lammé, A.I.E.E., Vol. 34, p. 1752.

the commutating zone of coil 1 an amount equal to the difference between

$\frac{2K \pm a}{p}$ and $2\frac{K}{p}$. The width of the commutating zone for one coil in

inches of armature circumference is then,

$$A = \left[b + 1 \pm \left(\frac{2K}{p} - \frac{2K \pm a}{p} \right) \right] \beta_r = \left(b + 1 - \frac{a}{p} \right) \beta_r \text{ in.} \quad (94)$$

After the commutator has moved a distance equal to the width of one commutator bar, the next coil begins commutation, and the width of the commutating zone for the upper or lower part of a slot is,

$$\left(b + 1 - \frac{a}{p} + m - 1 \right) \beta_r = \left(b + m - \frac{a}{p} \right) \beta_r \text{ in.} \quad (95)$$

For a full pitch winding, the upper and lower parts of the slot commutate at the same time, and formula 95 gives the width of the commutating zone for such a winding. When chorded windings are used, the conductors in the top part of the slot do not begin commutation at the same time as those in the lower part of the slot. This condition has the effect of increasing the width of the commutating zone. If φ is the difference in phase of commutation between a conductor in the top of a slot and a corresponding conductor in the bottom of a slot, expressed in number of commutator bars, then the width of the commutating zone for either full pitch or chorded windings is,

$$w_c = \left(b + m + \varphi - \frac{a}{p} \right) \beta_r. \quad (96)$$

The difference in phase of commutation for the top and bottom of a slot is calculated as follows:²

$$\varphi = \frac{K}{p} - \frac{1}{2} (Y_1 - 1). \quad (97)$$

When $\frac{1}{2} (Y_1 - 1)$ in formula 97 is greater than K/p , or when over-chorded windings are used, the value of φ will be negative. The effect of the phase difference in commutation upon the width of the commutating zone is, however, the same, regardless of the sign of φ . The absolute value of φ with the positive sign must, therefore, always be used in the formula for w_c .

Formula 96 has been derived for the simplex wave winding. It

² "Die Gleichstrommaschine," by Dr. Arnold and La Cour, Vol. 1, 3rd ed., p. 248, Julius Springer, Berlin.

lap and wave windings.

For a wide commutating zone, the coils under commutation will come under the influence of the flux from the main pole tips and the commutating pole will be wide, which condition leads to a heavy leakage flux. Experience has shown that the width of the commutating zone should not exceed 60 per cent of the neutral zone; where the neutral zone is the portion of the armature circumference between two adjacent pole tips $= (1 - \psi)\tau$.

Reactance Voltage.—The coil undergoing commutation has induced in it an e.m.f. of self-induction due to the reversal of the current in the coil, the self-induced e.m.f. always acting to oppose the change in current. If the short-circuited coil is in inductive relation to one or more coils in the same slot undergoing commutation at the same time, there is also induced in it an e.m.f. of mutual induction. This voltage of self and mutual induction induced in a short-circuited armature coil is called the reactance voltage and is the basic cause of sparking.

The reactance voltage may be expressed by the fundamental equation:

$$e_r = (L + M)\frac{di}{dt} \quad (98)$$

where L is the coefficient of self-induction, M is the coefficient of mutual induction, and di/dt is the rate of change of current in the short-circuited coil.

It is convenient to calculate the coefficient of self and mutual induction at the same time. For this purpose L' is used as the coefficient of self and mutual induction. L' is calculated from the reluctances of the flux paths and the magnetomotive forces acting upon the flux interlinked with the short-circuited coil. It is calculated for the case for which the top and bottom of a slot, containing only two coil sides, commute at the same time, and is later corrected to take into account the actual conditions. To simplify calculations, the flux interlinked with the short-circuited coil is divided into four parts:

- (1) The flux that crosses the slot (Fig. 70).
- (2) The flux that passes through the air gap from the top of one tooth to the top of the next over the armature length $l - l_c$ (Fig. 70).
- (3) The flux that passes through the commutating pole shoe and the commutating pole air gap twice (Fig. 71).
- (4) The flux that surrounds the coil end-connections.

The coefficient of self and mutual induction for each of the four

as follows:

$$L'_1 = 4.25l \frac{l_s^2}{w_s} t_a^2$$

$$L'_2 = 9.35t_a^2(l - l_1)\log_{10} \frac{2l_1 - w_s}{w_s}$$

$$L'_3 = 2.03l t_a^2 \frac{w_1 - w_s}{\delta_1}$$

$$L'_4 = 4.06l_s t_a^2.$$

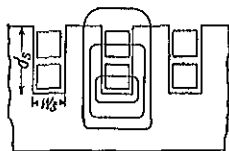


FIG. 70.—Slot and tooth tip leakage paths

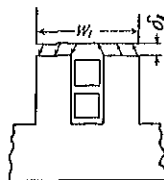


FIG. 71.—Tooth tip leakage path under commutating pole.

For the entire slot,

$$\begin{aligned} L' &= (L'_1 + L'_2 + L'_3 + L'_4)10^{-8} \text{ henrys} \\ &= \frac{t_a^2}{10^8} \left[4.25l \frac{l_s^2}{w_s} + 9.35(l - l_1)\log_{10} \frac{2l_1 - w_s}{w_s} \right. \\ &\quad \left. + 2.03l_s \frac{w_1 - w_s}{\delta_1} + 4.06l_s \right] \text{ henrys.} \end{aligned} \quad (99)$$

The rate of change of current in the short-circuited coil is assumed to be constant for the entire short-circuit period, that is, commutation is assumed to be linear. For one coil only, neglecting the effect of the other coils in the slot, the average rate of change of current,

$$\frac{di}{dt} = \frac{2i_a}{t} = \frac{2i_a}{\frac{A}{Kn_s}} = \frac{2i_a Kn_s}{A},$$

where A is the width of the short-circuited zone of one coil expressed in commutator bars $= b + 1 - \frac{a}{p}$ (see formula 94). When there are

¹ "Design of Auxiliary Poles," by A. Brunt, *Electrical Review and Western Electrician*, Vol. 59, 1911, p. 510.

more than two coil sides per slot, the number of commutator segments must pass under the brush to complete commutation for the coil sides in the top or the bottom of the slot are $A + m - 1$ and the average value of di/dt for the coil sides in the top or the bottom of the slot,

$$\frac{di}{dt} = \frac{m}{A + m - 1} K n_s 2i_a. \quad (100)$$

Equation 99 is the equation for the coefficient of self and mutual induction when there are two coil sides per slot and when the two coil sides of a slot commute at the same time. When only one part of a slot is to be considered, then the value of L' must be divided by 2. When the coil sides in the top and bottom of a slot do not commute at the same time, the mutual influence of the coil sides in the top and bottom of the slot is taken into account by multiplying $\frac{1}{2}L'$ by the factor,

$$2 - \frac{\varphi}{A + m - 1}.$$

When the coil sides per slot commute at the same time, φ is equal to zero, and the value of this factor is equal to 2. When the two parts of the slot do not influence each other, φ is equal to $A + m - 1$, and the value of this factor is equal to 1.

Taking into account the mutual influence of the two parts of the slot, the equation for the coefficient of self and mutual induction becomes,

$$L' = \frac{l_a^2}{2 \times 10^8} \left[\left(2 - \frac{\varphi}{A + m - 1} \right) \left\{ + 25l \frac{l_i}{w_s} + 9.35(l - l_i) \log_{10} \frac{2l_i - w_s}{w_s} + 2.03l_i \frac{w_i - w_s}{\delta_i} \right\} + 8.12l_s \right] = \frac{l_a^2}{2 \times 10^8} M.$$

Substituting the expression for L' and for di/dt into the fundamental equation for the reactance voltage,

$$e_r = \frac{K n_s i_a t_a^2}{10^8} \frac{m}{A + m - 1} M$$

$K t_a i_a$ = the total number of ampere-turns on the armature = $ATP_a p$, therefore,

$$e_r = \frac{ATP_a p t_a n_s}{10^8} \frac{m}{A + m - 1} M. \quad (101)$$

Formula 101 gives the reactance voltage per coil for machines

many commutating poles as main poles are used, the formula must be changed to the following form:

$$e_r = \frac{\text{ATP}_a p l_a n_s}{10^8} \frac{m}{A + m - 1} \left[\left(2 - \frac{\varphi}{A + m - 1} \right) \left\{ 4.25 l \frac{d_s}{w_s} + 4.66(2l - l_i) \log_{10} \frac{2l_1 - w_s}{w_s} + 1.02 l_i \frac{w_i - w_s}{\delta_i} \right\} + 8 \cdot 12 l_s \right]. \quad (102)$$

For the derivation of these formulas, the simplex wave winding was assumed. They apply, however, equally well to simplex lap windings and to multiplex lap and wave windings.

Design of the Commutating Pole.—The commutating pole is placed between two main poles, so that the coils undergoing commutation will cut the flux in the commutating pole air gap. They are generally made of cast steel or punched from sheet steel with no special pole shoe; that is, the length and width of the pole body are equal to the length and width of the pole shoe. For small and medium sized machines for moderate voltages, half the commutating poles are often omitted primarily for economical reasons.⁴

In order that the short-circuited coils shall come under the influence of the commutating pole, the width of the commutating-pole shoe must be equal to the width of the commutating zone; an allowance of from 1.5 to 2 times the air gap under the commutating pole may be made for the fringing of the flux at the tips of the commutating pole. The width of the commutating pole,

$$w_i = w_c - (1.5 \text{ to } 2) \delta_i. \quad (103)$$

The commutating-pole width must also be so chosen that the leakage flux will not be excessive. To avoid excessive leakage, the width of the commutating pole should generally be not greater than one-half the space between adjacent pole tips or

$$w_i \leq \frac{1 - \psi}{2} \tau. \quad (104)$$

The width of the commutating pole must further be chosen with regard to the armature tooth pitch. With narrow commutating poles,

⁴"The Number of Commutating Poles Used in Direct-Current Machines," by J. A. Elzi, *Electric Journal*, Vol. 22, March, 1925, p. 120.

the pulsations of the commutating-pole flux can be reduced by using a large number of slots, that is, by reducing the tooth pitch. A large air gap under the commutating pole will also help to reduce the flux pulsations. It is, however, not desirable to make the air gap very large, for the main pole flux will then penetrate the commutating-pole air gap. Narrow commutating poles require that the brushes be accurately located in the geometrical neutral position, to avoid the compounding effect of the commutating-pole flux. In general, the commutating-pole width should be larger than 1.5 times the tooth pitch, and if possible, should be a multiple of the tooth pitch (see Chapter III, page 44) or,

$$w, \geq 1.5 t_1. \quad (105)$$

The length of the commutating pole is generally chosen from the standpoint of economy, for the shorter the commutating pole, the shorter will be the mean-turn of the commutating-pole winding and the smaller the copper weight, losses, and leakage flux. The length must, of course, be so chosen that the flux density in the commutating pole will be below the saturation point of the material. The choice of length depends also upon the service for which the machine is intended. For machines designed for large, fluctuating loads or for variable speed motors, for which good commutation is often difficult to obtain, the commutating pole is generally made as long as the main pole. For normal motors and generators with as many commutating poles as main poles, the length,

$$l_i = (0.60 \text{ to } 0.80) l_1. \quad (106)$$

For motors and generators with half as many commutating poles as main poles, the commutating-pole length is generally equal to the main-pole length.

The commutating-pole air gap must not be so small as to produce large pulsations of the commutating-pole flux, caused by the armature slot. It must not be made too large so that the main-pole flux will not affect the commutating-pole field. In general

$$\delta_i = (1 \text{ to } 2) \delta. \quad (107)$$

For machines for which good commutation is difficult to obtain, the larger air gap will generally be found more satisfactory.

To obtain straight-line commutation, the voltage induced in the short-circuited coil by the commutating-pole flux must, for every instant of the short-circuit period, be equal and opposite to the reactance

entire short-circuit period. If straight-line commutation is assumed, the change of the current volume for either the upper or lower part of the slot can be shown as in Fig. 72a. The following data apply:

$$\beta = 0.163, K = 111, b = 2.3, a = 2, p = 4,$$

$$A = b + 1 - a/p = 2.3 + 1 - \frac{2}{4} = 2.8,$$

$$m = 3, Y_1 = 55, \varphi = 0.75,$$

$$A + m - 1 = 2.8 + 3 - 1 = 4.8.$$

The current volume of either the top or bottom part of the slot changes from $+3i_a$ to $-3i_a$. From the beginning of commutation, for the slot under consideration, to the point a , only coil 1 is in short-circuit; from a to b , coils 1 and 3 are in short-circuit; from b to c , coils 1, 3, and 5 are in short-circuit; from c to d , coils 3 and 5 and from d to e coil 5 are short-circuited. The number of commutator bars that must pass under the brush, to commutate the coils in the top or bottom of the slot, are equal to $A + m - 1 = 4.8$, as shown in Fig. 72a.

The reactance voltage in any of the three coils in the top of the slot, not taking into account the influence of the coils in the bottom of the slot, is shown in Fig. 72b, the coils being in short-circuit during the periods indicated by 1, 3, and 5. Obviously, the coils in the bottom of the slot will have the same reactance voltage as those in the top of the slot, when the influence of the two parts of the slot on each other is not taken into account. When both top and bottom of the slot are considered together, the coils in the bottom of the slot begin commutation φ commutator bars before or after those in the top of the slot. Figure 72c shows the reactance voltage for each of the three coils in the bottom of the slot, commutation beginning $\varphi = 0.75$ commutator bars after the beginning of commutation for the top of the slot. By adding the corresponding ordinates of Fig. 72b, representing the top of the slot, and Fig. 72c,

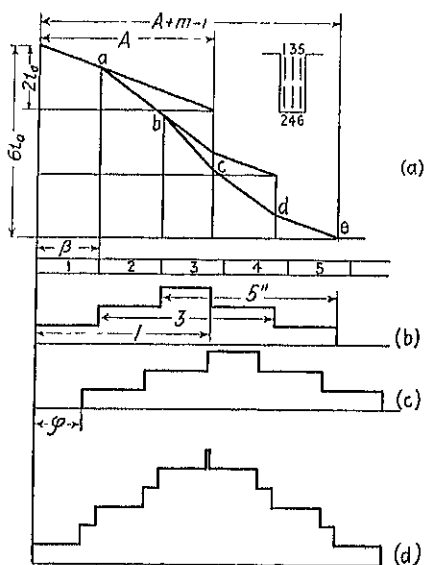


FIG. 72.

representing the bottom of the slot, the resultant reactance voltage for all the coils of the slot is obtained as shown in Fig. 72*d*. The ordinates of Fig. 72*d* represent to a certain scale the reactance voltage of the various coils of the slot.

In order to induce in the short-circuited coil a voltage equal and opposite to the reactance voltage, the flux density at each point in the commutating-pole air gap must be proportional to the reactance voltage at that point. To obtain perfect compensation of the reactance voltage, the commutating-pole shoe should have the shape of the reactance voltage curve, Fig. 72*d*, that is, the length of the commutating-pole air gap at each point of the commutating zone should be inversely proportional to the reactance voltage at that point. Obviously, the commutating-pole shoe will not be built with the shape shown by the curve, Fig. 72*d*, but will have the shape shown in Fig. 73*a* and *b*. Perfect compensation of the reactance voltage is, therefore, not always possible.

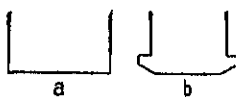


FIG. 73.—Shapes of commutating pole shoe.

It is obvious, from what has been stated above, that the curve showing the variation of the reactance voltage for the commutation period of one slot will be of rectangular shape when there are only two coil sides per slot and when they commute at the same time, that is, when $\phi = 0$. For such a case, the air gap under the commutating pole will be of the same length for all parts of the pole shoe, and the flux density for all points in the commutating-pole air gap can be made proportional to the reactance voltage. For machines for which commutation difficulties are apt to arise, it is therefore desirable to arrange the armature winding with only two coil sides per slot, with a full pitch winding (see Chapter III). Although beveled commutating-pole shoes are of great help in obtaining the best possible commutation, they should be used only in cases where difficult commutation conditions exist, because they make the machine sensitive to correct brush position. Very good results are generally obtained by using a commutating-pole shoe with a straight face.

Commutating-Pole Ampere-Turns.—Formulas 101 and 102 give the average value of the reactance voltage per coil. To induce a voltage in the short-circuited coils equal and opposite to the average value of the reactance voltage, the average value of the flux density in the commutating-pole air gap, when as many commutating poles as main poles are used, must be,

$$B_a = \frac{e_r \times 60 \times 10^8}{2l_a l_v \times 12} \text{ lines per sq. in.} \quad (108)$$

pole flux affects one side of the coil only and,

$$B_{\theta 1} = \frac{e_r \times 60 \times 10^8}{t_n l_n \times 12} \text{ lines per sq. in.} \quad (109)$$

The commutating-pole flux,

$$\phi_c = B_{\theta 1} l_n w, \text{ lines} \quad (110)$$

The flux paths of a two-pole generator, with as many commutating

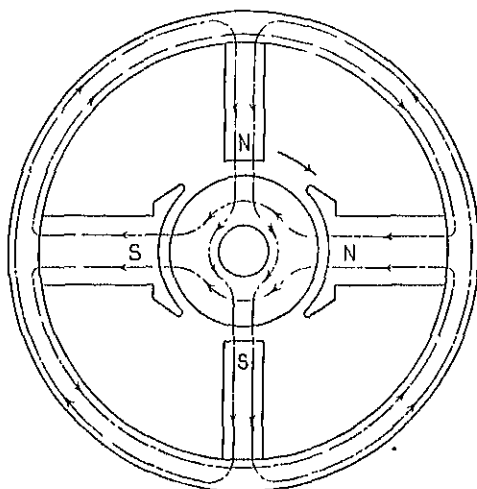


FIG. 74.—Flux paths in a two-pole d.-c. generator.

poles as main poles, are shown in Fig. 74. The ampere-turns for the commutating-pole air gap,

$$AT_{\theta 1} = \frac{B_{\theta 1} \delta_c k}{3.2}. \quad (111)$$

The ampere-turns for the remainder of the commutating-pole magnetic circuit can be calculated in the manner described for the main-pole magnetic circuit, Chapter IV.

To the ampere-turns required to send the commutating-pole flux through the magnetic circuit must be added the armature ampere-turns

acting in the interpolar space. The total ampere-turns per commutating pole are then,

$$ATP_c = ATP_a + AT_{gi} + AT_i + AT_p + AT_{ya} + AT_{yf}. \quad (112)$$

When half of the commutating poles are omitted, the commutating-pole flux returns through the main pole and main-pole air gap on each side of the commutating pole. The ampere-turns required to send the commutating-pole flux through the commutating-pole air gap, armature teeth under the commutating pole, armature yoke, and the field yoke are calculated in the same way as given above for machines with as many commutating poles as main poles. To these must be added the ampere-turns required to send the flux through the main pole, main-pole air gap, and the teeth under the main poles. (See foot note, page 65.) The sum of the ampere-turns for the various parts of the magnetic circuit plus the armature ampere-turns per pole gives the total number of ampere-turns required on each commutating pole.

In order to obtain proper compensation of the reactance voltage at all loads, the flux density in the commutating-pole air gap must vary directly with the load current, because the reactance voltage varies directly with the load current. This can only be obtained when the iron parts of the commutating-pole magnetic circuit are unsaturated. For normal machines the ampere-turns for the iron parts of the magnetic circuit are generally equal to from 0.50 to 1.0 times the air gap ampere-turns for the commutating pole. Then,

$$ATP_c = ATP_a + (0.313\delta B_g k)(1.5 \text{ to } 2.0). \quad (113)$$

Design of Commutator and Brushes.—The number of commutator bars is always known as soon as the armature winding is determined, because it is equal to the number of armature coils. The commutator diameter is generally from 60 to 80 per cent of the armature diameter. It must be chosen with regard to the peripheral speed and the thickness of the commutator bar.

The commutator peripheral speed is generally about 3000 ft. per min. Peripheral speeds of 6000 ft. per min. are used but should be avoided whenever possible. The higher commutator peripheral speeds generally lead to commutation difficulties.

The minimum thickness of the commutator bar, the thickness at the inside of the commutator, should not be less than 0.06 in., and the maximum thickness, the thickness at the commutator surface, should not be less than 0.1 in. If the thickness of the mica is $\frac{3}{32}$ in., then the

assumed, the commutator diameter,

$$D_c = \frac{K\beta}{\pi}. \quad (114)$$

The thickness of the brush or its width along the commutator circumference may be a determining factor in choosing the commutator diameter. Formula 96 shows that the thickness of the brush and the commutator bar pitch are factors which determine the width of the commutating zone. The thickness of the brush or the number of commutator bars covered by the brush determines the number of coils short-circuited at one time.

The length of the commutator depends upon the space required by the brushes and upon the surface required to dissipate the heat generated by the commutator losses. If w_b is the width of the brush or its length along the axis of the machine, and n_b is the number of brushes per brush arm, then the length of the commutator,

$$l_c = n_b(w_b + \frac{1}{8}) + c_2, \quad (115)$$

where $\frac{1}{8}$ in. is the clearance between brushes and depends upon the construction of the brush holder, and c_2 is a clearance allowed to stagger the brushes, as explained on page 95. This clearance will vary somewhat with the size of the commutator, but will generally be from 0.5 in. for small machines to approximately 1.5 in. for large machines. Formula 115 gives the minimum length of commutator, the length required for the brushes. If this length gives too small a radiating surface, so that the commutator temperature rise exceeds the permissible value, then l_c must be increased to give sufficient radiating surface, to dissipate the heat generated by the commutator losses.

The total brush contact surface (positive and negative brushes),

$$S_b = \frac{2I_a}{A_b}. \quad (116)$$

From the standpoint of commutation, the current density at the brush contact should be as high as possible, because the brush contact drop increases with increasing current density, Fig. 75. To keep the brush contact I^2R losses small, the current density must be as low as possible. The higher the current density the smaller will be the brush contact surface and also the brush friction losses. There is therefore one current density for which the total losses at the commutator will be a

minimum. The following table gives the current density in amperes

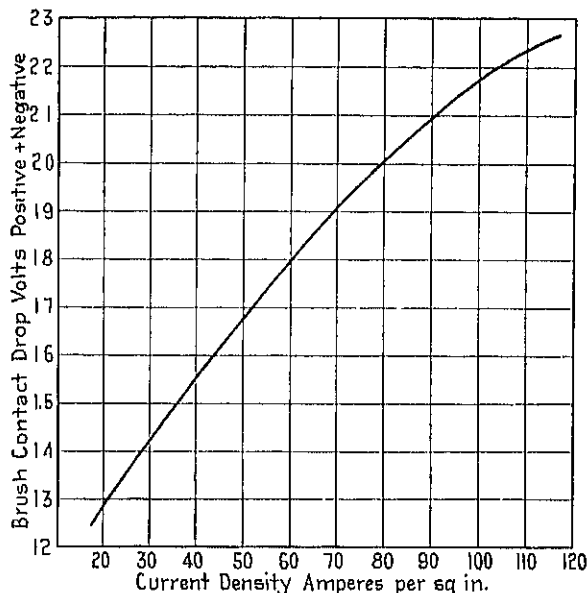


FIG. 75.—Approximate brush contact drop-carbon brushes.

per square inch for various kinds of brushes used for direct current machines:

TABLE VI

Kind of Brush	Sclero- scope Hardness	Amperes per Square Inch	Contact Drop Volts	Coefficient of Friction	Maximum Peripheral Speed
Carbon	80	35	High	High	3,500
	50	45	Medium	High	3,500
	68	45	Low	Medium	4,500
Carbon graphite	32	50	Medium	Medium	4,000
	49	55	Very high	Low	5,500
	30	45	Low	Medium	4,000
Graphite	55	50	High	Low	5,500
	40	50	High	Low	5,500
	16	65	Very high	Low	10,000
	17	65	Low	Low	6,000
Metal graphite	12	100	Very low	Very low	4,000
	11	125	Exceptionally low	Very low	4,500
	8	125	Exceptionally low	Very low	4,000

	Contact Drop	Coefficient of Friction
Very high.	2.6 and over	0.27 and over
High.	2.0 to 2.5	0.22 to 0.26
Medium	1.4 to 1.9	0.17 to 0.21
Low	1.0 to 1.3	0.12 to 0.16
Very low	0.7 to 0.9	0.07 to 0.11
Exceptionally low.	0.3 to 0.6	

The current densities given in the table are for normal load and normal operating conditions. The brush contact drops are the voltage drops at both brushes (positive and negative) at rated carrying capacity, for a brush pressure of 3 lb. per sq. in., and a peripheral speed of 3000 ft. per min. The values given for the coefficient of friction are for a brush pressure of 3 lb. per sq. in. and a peripheral speed of 3000 ft. per min.

The thickness of the brush or its width along the commutator circumference is determined from the number of bars covered by the brush. To reduce the length and cost of the commutator, it would be desirable to use a thick brush. But this is not possible, because of the effect of the brush thickness upon commutation and upon the commutating-pole width. The thickness of the brush is generally from 1 to $3\frac{1}{2}$ times the commutator bar pitch. For very low voltage machines with wide commutator bars, the thickness of the brush may be even less than the commutator bar pitch.

The total width of the brushes per brush arm,

$$n_b w_b = \frac{S_b}{n_a b_t} \quad (117)$$

A small area of contact between commutator and each brush generally gives a better contact. The contact surface for each brush is generally from 1 to 2 sq. in., and the width of each brush is generally not over 2 in. When determining the thickness and width of the brush, the standards recommended by the A.I.E.E.⁵ should be followed.

⁵ A.I.E.E. Proc., July, 1917, Vol. 36, p. 606.

FOR WIDTH OF BRUSHES AND DIAMETER OF ROUND BRUSHES

Up to $\frac{1}{4}$ in. inclusive, increase by steps of $\frac{1}{16}$ in.

Over $\frac{1}{4}$ in. to $2\frac{1}{2}$ in. inclusive, increase by steps of $\frac{1}{8}$ in.

Over $2\frac{1}{2}$ in., increase by steps of $\frac{1}{4}$ in.

Diameter of all round brushes, increase by steps of $\frac{1}{16}$ in.

NOTE.—For widths, $\frac{1}{4}$ in. steps are to be used whenever possible.

Up to $\frac{1}{4}$ in. inclusive, increase by steps of $\frac{1}{16}$ in.

Over $\frac{1}{4}$ in., increase by steps of $\frac{1}{8}$ in.

NOTE.—Whenever possible, $\frac{1}{8}$ in. steps are to be used above $\frac{1}{4}$ in. in thickness.

Sample Design: *Design of Commutator and Commutating Poles.*—The commutator diameter is generally from 60 to 80 per cent of the armature diameter. Choosing 65 per cent, in order that the peripheral speed will not be too high,

$$D_c = 0.65D = 0.65 \times 25 = 16.25 \text{ in.}; \text{ use } 16.0 \text{ in.}$$

The armature winding for this design has four conductors per slot and one turn per coil. Each conductor is, therefore, one-half of a coil and the number of armature coils and commutator bars,

$$K = 2 \times 81 = 162.$$

The commutator bar pitch,

$$\beta = \frac{\pi D_c}{K} = \frac{\pi \times 16}{162} = 0.31 \text{ in.}$$

and

$$\beta_r = 0.31 \frac{25}{16} = 0.485 \text{ in. of armature circumference.}$$

If the brush covers 2.5 commutator bars, the thickness of the brush,

$$b_t = 2.5 \times 0.31 = 0.775 \text{ in.}$$

Use a brush 0.75 in. thick, and the number of bars covered,

$$b = \frac{0.75}{0.31} = 2.42.$$

The armature winding is not a full pitch winding, therefore,

$$\begin{aligned} \varphi &= \frac{K}{p} - \frac{1}{2}(Y_1 - 1) = \frac{162}{6} - \frac{1}{2}(53 - 1) \\ &= 1.0. \end{aligned}$$

The width of the commutating zone is calculated by formula 96,

$$\begin{aligned} w_c &= \left(b + m + \varphi - \frac{a}{p} \right) \beta_r = \left(2.42 + 2 + 1 - \frac{6}{6} \right) 0.485 \\ &= 2.14 \text{ in. of armature circumference.} \end{aligned}$$

tips,

$$= (1 - \psi)\tau = (1 - 0.66)13.1 = 4.45 \text{ in.}$$

The ratio of the commutating zone to the neutral zone

$$= \frac{2.14}{4.45} = 0.481 \text{ or } 48.1 \text{ per cent.}$$

The brush thickness selected is therefore satisfactory, as it is generally desirable to keep the ratio of commutating zone to neutral zone equal to or less than 0.50.

The mica of the commutator is to be under-cut, so that a medium hard or soft brush with self-lubricating qualities will be satisfactory. Choosing a current density of 45 amperes per sq. in., the total brush contact surface,

$$S_b = \frac{2J_a}{A_b} = \frac{2 \times 1208}{45} = 53.7 \text{ sq. in.}$$

The total width of the brushes per brush arm,

$$n_b w_b = \frac{S_b}{n_a b_t} = \frac{53.7}{6 \times 0.75} = 11.95 \text{ in.}$$

With a brush width equal to 1.5 in., 8 brushes per arm are required, and the length of the commutator,

$$\begin{aligned} l_c &= n_b(w_b + \frac{1}{8}) + c_2 = 8(1.5 + \frac{1}{8}) + 1.0 \\ &= 14.0 \text{ in.} \end{aligned}$$

This commutator length will be satisfactory if the radiating surface is large enough to dissipate the heat generated by the commutator losses. The method of calculating the commutator radiating surface is given in Chapter VII.

The length of the commutating-pole air gap,

$$\begin{aligned} \delta_i &= (1 \text{ to } 2)\delta = (1 \text{ to } 2)0.22 \\ &= 0.22 \text{ to } .44; \text{ use } 0.25 \text{ in.} \end{aligned}$$

The width of the commutating pole,

$$\begin{aligned} w_i &= w_c - (1.5 \text{ to } 2)\delta_i = 2.14 - (0.375 \text{ to } 0.50) \\ &= 1.765 \text{ to } 1.64 \text{ in.} \end{aligned}$$

$$w_i \leq \frac{1 - \psi}{2}\tau = \frac{1 - 0.66}{2}13.1 = 2.23 \text{ in.}$$

$$w_i \geq 1.5t_1 = 1.5 \times 0.97 = 1.45 \text{ in.}$$

The commutating-pole shoe is therefore made 1.75 in. wide and the pole body is the same width.

Since as many commutating as main poles are used, the length of the commutating poles,

$$\begin{aligned} l_1 &= (0.60 \text{ to } 0.80)l = (0.60 \text{ to } 0.80)11.0 \\ &= 6.6 \text{ to } 8.8 \text{ in.}; \text{ use } 8.0 \text{ in.} \end{aligned}$$

The reactance voltage per coil is calculated by formula 101. The data required for this formula are:

$$\text{ATP}_a = 5440, p = 6, t_a = 1.0, n_s = 15, m = 2, b = 2.42,$$

$$A = b + 1 - \frac{a}{p} = 2.42 + 1 - \frac{6}{6} = 2.42, \quad \varphi = 1.0,$$

$$\begin{aligned} l &= 11.0, \quad d_s = 1.57, \quad w_s = 0.363, \quad l_1 = 8.0, \quad l_1 = 0.97, \\ w_1 &= 1.75, \quad \delta_1 = 0.25, \quad l_s = L_a - l = 28.07 - 11.0 = 17.07 \end{aligned}$$

$$4.25 \frac{d_s}{w_s} = 4.25 \times 11.0 \frac{1.57}{0.363} = 202$$

$$9.35(l - l_1) \log_{10} \frac{2l_1 - w_s}{w_s} = 9.35(11 - 8) \log_{10} \frac{2 \times 0.97 - 0.363}{0.363} = 18$$

$$2.03l \frac{w_1 - w_s}{\delta_1} = 2.03 \times 8 \frac{1.75 - 0.363}{0.25} = 90$$

$$8.12l_1 = 8.12 \times 17.07 = 138.5$$

$$2 - \frac{\varphi}{A + m - 1} = 2 - \frac{1.0}{2.42 + 2 - 1} = 1.708$$

$$M = 1.708(202 + 18 + 90) + 138.5 = 668.5$$

$$\begin{aligned} e_r &= \frac{\text{ATP}_a p t_a n_s}{10^8} \frac{m}{A + m - 1} M \\ &= \frac{5440 \times 6 \times 1 \times 15}{10^8} \frac{2}{2.42 + 2 - 1} 668.5 \\ &= 1.92 \text{ volts.} \end{aligned}$$

The flux density in the commutating-pole air gap,

$$\begin{aligned} B_{ai} &= \frac{e_r \times 60 \times 10^8}{2t_a l_v \times 12} = \frac{1.92 \times 60 \times 10^8}{2 \times 1 \times 8 \times 5890 \times 12} \\ &= 10,200 \text{ lines per sq. in.} \end{aligned}$$

The air gap between the main-pole and commutating-pole air gap is calculated by formula 46, in the same way as for the main-pole air gap,

$$k = \frac{t_1}{w_1 + (y\delta_1)} = \frac{0.97}{0.607 + (1.12 \times 0.25)} \\ = 1.095.$$

The ampere-turns for the commutating-pole air gap,

$$\text{AT}_g = \frac{B_{a1}\delta_1 k}{3.2} = \frac{10,200 \times 0.25 \times 1.095}{3.2} \\ = 870 \text{ ampere-turns.}$$

These are the ampere-turns required for the commutating-pole air gap, to obtain straight-line commutation at normal load. When the ampere-turns for the remainder of the magnetic circuit are neglected when calculating the commutating-pole ampere-turns, and especially for machines designed for overload capacity, practice has shown that it is desirable to increase the commutating-pole air gap ampere-turns from 1.5 to 2 times. For normal loads, slight over-commutation will then result. If the commutating field is found to be too strong, it may be reduced by increasing the commutating-pole air gap length or by means of a shunt across the commutating field winding.

The ampere-turns per pole for the commutating field winding,

$$\text{ATP}_c = \text{ATP}_a + 1.5 \text{AT}_g \\ = 5440 + 1.5 \times 870 \\ = 6750.$$

The number of turns per pole for the commutating field coil,

$$t_c = \frac{\text{ATP}_c}{I_a} = \frac{6750}{1208} = 5.58; \text{ use } 5.5.$$

The section area of the conductor, for a current density of 1300 amperes per square inch,

$$s_c = \frac{I_a}{A_c} = \frac{1208}{1300} = 0.93 \text{ sq. in.}$$

Three strap copper conductors, 0.25×1.25 in., wound in parallel, will be used. Each conductor has an area of 0.305 sq. in. The current density for the commutating field winding,

$$A_c = \frac{1208}{3 \times 0.305} = 1320 \text{ amperes per sq. in.}$$

The coil is wound, as shown in Fig. 70, and the mean length,

$$L_1 = 2 \times 8 + \pi(1.25 + 1.75 + \frac{1}{8}) + 6.0 \\ = 31.8 \text{ in.},$$

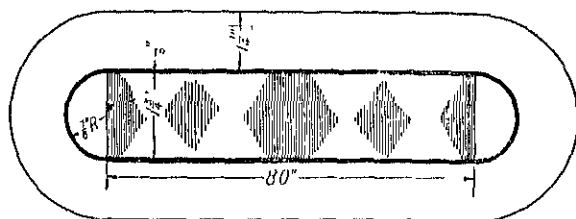


FIG. 70.

where 6.0 in. is allowed for the connection between poles.

The resistance of the commutating field winding at 75° C.,

$$R_1 = \frac{L_1 l_1 p r}{s_1 \times 10^6} = \frac{31.8 \times 5.5 \times 6 \times 0.826}{0.915 \times 10^6} \\ = 0.00095 \text{ ohm}$$

and the voltage drop,

$$I_a R_1 = 1208 \times 0.00095 = 1.15 \text{ volts}$$

or 0.46 per cent of full-load terminal voltage.

The weight of the commutating field copper,

$$G_1 = L_1 l_1 p s_1 \times 0.321 \\ = 31.8 \times 5.5 \times 6 \times 0.915 \times 0.321 \\ = 308 \text{ lb.}$$

The sketch of Fig. 77 shows the clearance between the series and commutating field windings in the interpolar space.

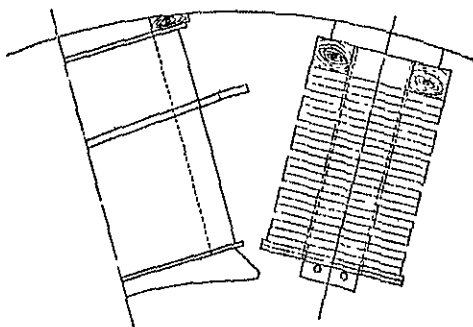


FIG. 77.

CHAPTER VII

LOSSES, EFFICIENCY, AND TEMPERATURE RISE

THE losses to be considered in direct-current motors and generators are:

- (1) Copper losses in armature and field windings.
- (2) Core or iron losses in the armature teeth and yoke.
- (3) Brush contact (I^2R) losses.
- (4) Field and armature rheostat losses (when present).
- (5) Mechanical losses—bearing friction, brush friction, and windage.

In addition to the losses given above, there are the indeterminate load losses, which may be of importance and which vary with the design of the machine. Because there is no satisfactory method available by which to determine these losses, the Standards of the A.I.E.E. recommend that they be taken equal to 1 per cent of the output for direct-current generators and motors, except for motors 200 hp, 575 r.p.m. and smaller, in which cases they shall be omitted.

In accordance with the Standards of the A.I.E.E., the copper losses for all windings are to be calculated for a temperature of 75° C. for all loads.

Armature Copper Losses.—The resistance of the armature winding has been calculated, page 59, Chapter III. The armature copper loss,

$$W_a = I_a^2 R_a. \quad (118)$$

For a generator the armature current is equal to the terminal current plus the shunt field current, and for a motor it is equal to the terminal current minus the shunt field current. For a motor the armature copper losses will then vary with the square of the load, whereas for a generator they will not do so because of the shunt field current, which does not vary directly with the load. Except for machines for which the shunt field current is a large percentage of the load current, the armature copper losses may be taken as varying with the square of the load for both generator and motor.

Commutating Field Copper Loss.—The commutating field winding and the compensating winding, when used, are connected in series with the armature winding, so that the armature current flows in the commutating field winding and compensating winding. The resistance of the commutating field winding has been calculated, page 114, Chapter VI. The copper loss in the commutating field winding,

$$W_i = I_a^2 R_i, \quad (119)$$

and varies with the square of the load.

Series Field Copper Loss.—The series field winding is connected in series with the armature winding and commutating field winding. For the long shunt connection the series field current is equal to the armature current, I_a , whereas for the short shunt connection it is equal to the line current, I . The series field resistance was calculated, page 92, Chapter V. The series field copper loss for long shunt,

$$W_s = I_a^2 R_s, \quad (120)$$

and for short shunt,

$$W_s = I^2 R_s. \quad (120a)$$

Shunt Field Copper Loss.—The shunt field resistance was calculated, page 91, Chapter V, and the shunt field copper loss,

$$W_f = i_f^2 R_f. \quad (121)$$

When a rheostat is connected in series with the shunt field winding, the rheostat losses must be included with the shunt field copper losses, when calculating the efficiency. For the long shunt connection the voltage across the shunt field is equal to the terminal voltage, but for the short shunt connection it is equal to the terminal voltage plus the drop in the series field winding. The drop in the series field winding is generally quite small and for either long or short shunt connection the shunt field copper loss plus the rheostat losses,

$$W_f + W_r = i_f E_t.$$

Brush Contact Losses.—The brush contact ($I^2 R$) losses depend upon the condition of the commutator and upon the quality of commutation obtained. It is therefore very difficult to predetermine accurately the brush contact ($I^2 R$) losses. The A.I.E.E. Standards recommend that 2 volts shall be assumed for the drop at the brush contacts, for both positive and negative brushes, for carbon and graphite brushes with pig-tails attached. A total drop of 3 volts is recommended for brushes with

Core Loss.—The iron losses in electric sheet steels consist of the hysteresis losses and the eddy current losses. In rotating electric machines, there are, in addition to the hysteresis and eddy current losses in the laminated armature core, pole face losses that are due to the flux pulsations produced by the armature slots, band losses, losses due to punching and bending strains in the laminations, losses due to imperfect insulation between the laminations (caused by burs or slot filing), and losses in the endframes due to stray fluxes. Since these additional losses cannot be easily calculated, the core loss calculations should be based upon the results obtained from tests on similar machines.

A variety of electric sheet steels are available for the armature laminations of direct-current machines. Silicon in steel increases its specific resistance and decreases the eddy current losses, but also decreases its permeability for high flux densities; it also makes it non-aging. Sheet steel, alloyed with silicon, is more expensive than open-hearth steel, and the cost increases as the thickness of the sheet decreases. More complete information on the properties and testing of electric sheet steels can be obtained from Thomas Spooner's splendid book.¹ The efficiency and cost will therefore generally determine the kind of steel to be used for the armature laminations.

Curves showing the total loss per pound per cycle, due to the fundamental frequency fluxes, are given in the Appendix for various grades of electric sheet steel. These curves are the results of tests conducted on samples in the Electrical Engineering Laboratories of the University of Minnesota. The standard method of the American Society for Testing Materials was used.

The iron loss for the armature teeth and yoke must be calculated separately, because the flux densities are not the same. For the armature yoke, the flux density is assumed to be uniformly distributed over the section area, and the flux density is calculated as shown on page 65, Chapter IV. The frequency of the flux reversals is calculated by formula 15. From the proper curve in the Appendix, the iron loss per pound per cycle can be found which, when multiplied by the weight of iron in the armature yoke and frequency, gives the core loss in the armature yoke due to the fundamental frequency flux.

The flux density is not the same for all sections of the armature teeth

¹"Properties and Testing of Magnetic Materials," McGraw-Hill Book Co., New York.

for the density, at a section $\frac{1}{3}$ slot depth from the minimum tooth width. The loss per pound per cycle, taken from the proper curve in the Appendix, multiplied by the weight of iron in the armature teeth and the frequency, gives the core loss in the armature teeth, due to the fundamental frequency fluxes. The sum of the loss in the teeth plus the loss in the yoke, calculated as just explained, is the total armature core loss, due to the fundamental frequency fluxes only and does not include the additional losses. The total armature core loss can be found by multiplying the sum of the tooth and yoke losses (due to the fundamental frequency flux) by a factor which is generally equal to from 1.5 to 3.5. This factor should be determined from tests of similar machines. When such data are not available, 2.5 may be used.

Brush Friction Loss.—The brush friction loss depends upon the brush pressure, the peripheral speed of the commutator, and the coefficient of friction between commutator and brush. It may be calculated approximately by the following formula:

$$W_{bf} = P S_c c_f v_c \times 0.0226 \text{ watt,} \quad (12)$$

where P is the brush pressure in pounds per square inch and is generally from 1.5 to 2 lb. per sq. in., and c_f is the coefficient of friction and is generally from 0.15 to 0.25 for carbon and graphite brushes. Tests on numerous machines show wide variations in brush friction loss, because the commutator and brushes do not have the smooth surfaces that come after continued operation. For this reason, the American Institute of Electrical Engineers has adopted conventional values for the brush friction loss, based upon tests of a large number of machines, which are to be used in calculating efficiencies. For carbon and graphite brushes, the brush friction loss is to be taken as 8 watts per square inch of brush contact per 1000 ft. per min. peripheral speed, and for metal graphite it is to be taken as 12 watts per square inch of brush contact per 1000 ft. per min. peripheral speed.

Friction and Windage Loss.—Like the brush friction, the bearing friction depends upon the pressure on the bearing, the peripheral speed of the shaft at the bearing, and the coefficient of friction between bearing and shaft. The bearing friction can be calculated² when the bearing dimensions are known. The windage losses cannot be calculated separately; they depend largely upon the construction of the armature.

²"Die Gleichstrommaschine," Vol. 1, p. 607, Julius Springer, Berlin, and "Electric Machine Design," by Gray, p. 97, McGraw-Hill Book Co., New York.

are determined from tests of similar machines. When such data

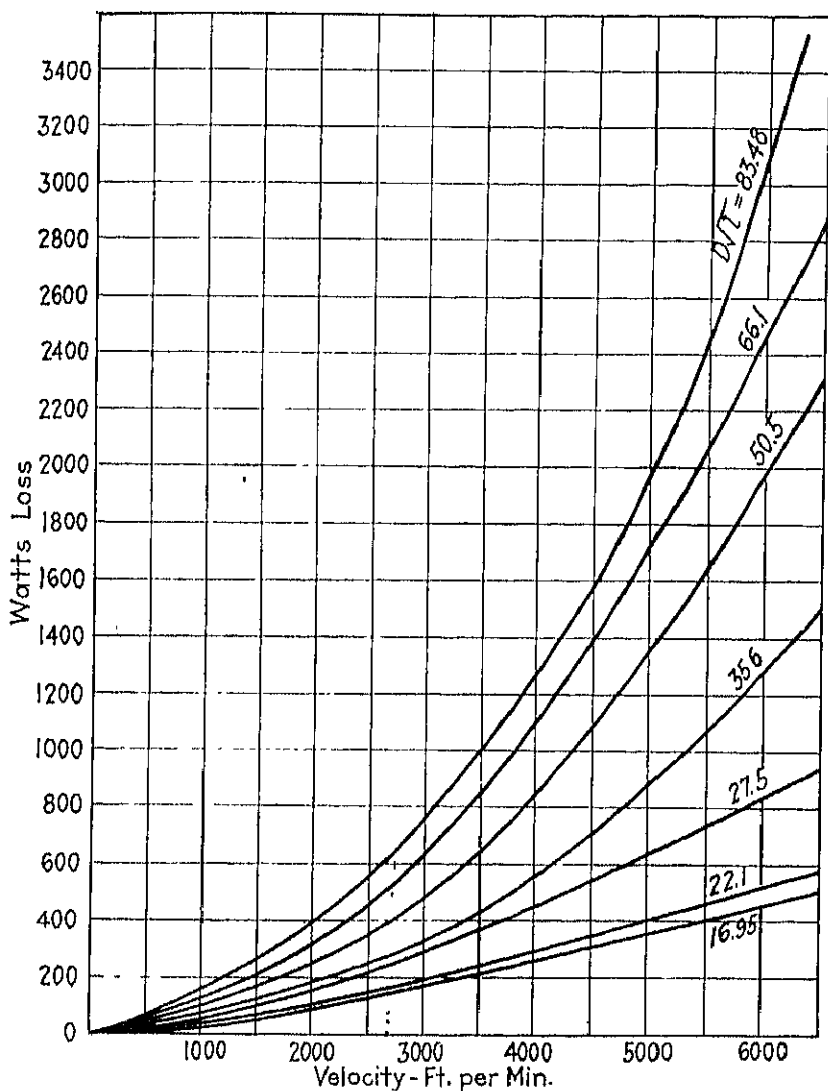


FIG. 78.—Approximate friction and windage losses for d.c. generators and motors.

are not available, they can be estimated with the help of the curves, Fig. 78.

Efficiency.—The efficiency is the ratio of the output to the output plus all the losses. It is expressed as follows:

$$\text{eff.} = \frac{\text{Output} \times 100}{\left\{ \begin{array}{l} \text{Output} + W_a + W_i + W_s + W_f + W_r \\ + W_c + W_b + W_{bf} + W_{fw} + W_o \end{array} \right\}} \text{ per cent.}$$

TABLE VII
COMMUTATING-POLE GENERATOR EFFICIENCIES

Kilowatts	Speed, Revolutions per Minute	Efficiencies		
		Full Load	$\frac{1}{2}$ Load	$\frac{1}{4}$ Load
3½	1750	80.0	79.5	78.0
3½	1150	79.5	79.0	76.0
12	1750	86.0	84.5	81.5
12	750	83.0	82.5	81.0
15	575	83.0	83.5	81.2
20	900	86.6	86.0	83.5
20	750	85.1	81.9	83.3
20	575	85.5	85.2	83.5
25	900	86.7	86.5	84.7
25	750	86.1	86.0	84.5
25	575	86.5	86.5	84.7
30	1150	88.0	87.7	85.0
30	750	87.5	87.0	85.8
30	575	87.5	87.1	85.0
50	1150	89.1	88.6	87.3
50	750	88.3	88.0	86.4
75	1150	90.2	89.6	87.6
75	725	89.6	89.2	88.0
100	1150	90.6	90.2	88.6
100	725	90.2	90.0	88.3
125	1000	91.0	90.5	88.8
125	725	90.2	90.0	88.4
150	1000	91.0	90.0	88.5
175	1000	91.2	90.3	88.5

will be a maximum for that load for which the sum of the constant losses is equal to the sum of the variable losses. Direct-current generators and motors are designed, whenever possible, to have maximum efficiency at from $\frac{3}{4}$ to full-load. Usual efficiencies for 250-volt, compound-wound, commutating-pole, direct-current generators are given in Table VII. Table VIII gives the efficiencies for 230-volt, commutating-pole, constant-speed, general purpose, direct-current motors.

TABLE VIII
CONSTANT-SPEED D.-C. MOTOR EFFICIENCIES

Rated Horsepower	Rated Full-load Speed, Revolu- tions per Minute	Efficiencies		
		$\frac{1}{4}$ Load	$\frac{1}{2}$ Load	$\frac{3}{4}$ Load
5	1750	83.0	82.0	77.0
5	1150	82.5	81.5	77.0
5	850	80.0	80.0	76.0
10	1750	84.0	83.0	78.0
10	1150	86.0	86.0	81.0
10	850	85.5	85.0	81.0
20	1750	86.5	86.0	81.0
20	1150	88.5	88.5	84.0
20	850	88.0	87.5	83.0
30	1750	88.0	88.0	85.0
30	1150	89.5	89.5	85.0
30	850	88.4	88.2	86.5
50	1750	90.0	88.0	86.0
50	1150	90.1	90.0	88.3
50	850	90.5	90.5	88.9
75	1150	91.6	91.4	89.9
75	850	91.5	91.2	89.7
100	1150	91.4	91.0	89.2

Temperature Rise.—The temperature rise³ of each of the various parts of continuous or short-time rated direct-current machines, above

³ A.I.E.E. Standards No. 5, July, 1925, p. 8.

Item		Type of Enclosure	Limiting Temperature Rise Degrees Centigrade *		
			Class O Insulation (See Par. 5-153)	Class A Insulation (See Par. 5-154)	Class B Insulation (See Par. 5-155)
1	Armature windings, wire field windings and all windings other than 2	All types except totally enclosed	35	50	70
		Totally enclosed	10	55	75
2	Single layer field windings with exposed uninsulated surfaces and bare copper windings	All types except totally enclosed	15	60	80
		Totally enclosed	45	60	80
3	Cores and mechanical parts in contact with or adjacent to insulation	All types except totally enclosed	35	50	70
		Totally enclosed	40	55	75
4	Commutators and collector rings †	All types except totally enclosed	50	65	85
		Totally enclosed	50	65	85
5	Miscellaneous parts (such as brush-holders, brushes, pole tips, etc.) other than those whose temperatures affect the temperature of the insulation material may attain such temperatures as will not be injurious.				

* The temperature limits on which the rating of general purpose motors is based are under discussion at the present time and no agreement has yet been reached. In order that work done in this connection may not be influenced or impeded, the Institute refrains from taking action at the present time towards revising its rules for this class of machinery.

† These limits for the temperature rise of commutators and collector rings apply where Class O, A or B insulation is employed in the commutator, or is adjacent thereto and its life would be affected by the heat from the commutator. It is recognized that the heating of the commutator could correspond to Class B even if the slot insulation were of Class O, on condition that the insulation of connections were not affected by the heating of the commutator.

the temperature of the cooling medium, shall not exceed the values given in Table IX.

Class O insulation consists of cotton, silk, paper, and similar organic materials when neither impregnated nor immersed in oil.

Class A insulation consists of cotton, silk, paper, and similar organic

insulation in the form of mica or asbestos, as applied to conductors.

Class B insulation consists of inorganic materials, such as mica and asbestos in built-up form, combined with binding substances. If Class A material is used in small quantities in conjunction, for structural purposes only, the combined material may be considered as Class B, provided the electrical and mechanical properties of the insulated winding are not impaired by the application of the temperature permitted for Class B materials.

It is therefore important that the designer be able to predetermine accurately the maximum temperature rise for all parts of the machine, in order that maximum output for a given amount of material may be obtained. The temperature rise, however, is not the limiting factor for the output, for all machines. For reasonably well ventilated machines, commutation or efficiency, or both, may be the limiting factor rather than temperature.

The losses in the various parts of electrical machinery are converted into heat, which produces a temperature rise above that of the surrounding air. The value of the final temperature depends upon the heat capacity of the various insulating materials used and upon the rate at which the heat is conducted through the materials to the cooling medium. The final temperature is reached when the heat is dissipated as fast as it is generated. The theory of the heat flow in electrical machinery has been given by a number of authors.⁴ The temperature rise can be determined with reasonable accuracy with the aid of test data on machines of similar construction. The general formula for the temperature rise is,

$$T = \frac{C_e}{S/W}$$

Armature Temperature Rise.—For armatures up to about 16 in. in diameter with axial ventilating ducts on the inside of the armature, the radiating surface is taken as indicated by the dotted line, Fig. 79, and for larger diameters,

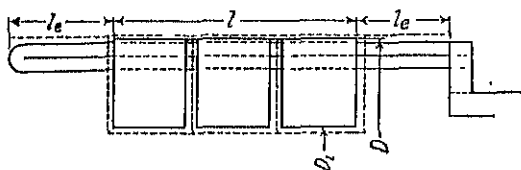


FIG. 79.

⁴ "Die Gleichstrommaschine," Vol. 1, 3rd ed., p. 606, Julius Springer, Berlin; "Electric Machine Design," by Gray, Chapter XI, McGraw-Hill Book Co., New York; "The Cooling of Electrical Machines" and bibliography, by George E. Luke, A.I.E.E. Trans., Vol. 42, 1923, p. 636; "The Thermal Time Constants of Dynamo Electric Machines," by A. E. Kennelly, A.I.E.E. Trans., Vol. 44, 1923, p. 187.

as shown in Fig. 80. The cooling surface per watt loss for Fig. 79 is,

$$\frac{S_a}{W_a} = \frac{\left[\pi D(l + 2l_e) + \pi D_l l + \frac{\pi}{4}(D^2 - D_l^2)(2 + n_d) \right]}{(1 + 0.00051\nu)} \quad (12)$$

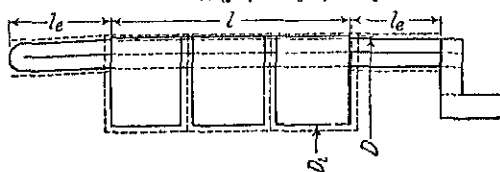


FIG. 80.

and for Fig. 80,

$$\frac{S_a}{W_a} = \frac{\left[\pi D(l + 4l_e) + \pi D_l l + \frac{\pi}{4}(D^2 - D_l^2)(2 + n_d) \right]}{(1 + 0.00051\nu)} \quad (12a)$$

The factor $(1 + 0.00051\nu)$ is given by Dr. Arnold and compensates for the increased radiating capacity of the armature, due to rotation.

The temperature rise of the armature,

$$T_a = \frac{C_{ca}}{S_a/W_a} \text{ degrees C.} \quad (12)$$

The value of C_{ca} , the cooling coefficient, can be determined only by test and will not be the same for any two machines. In the absence of accurate test data, the following values may be used:

$C_{ca} = 55$ to 65 for open type machines, Fig. 1, Chapter I

$C_{ca} = 65$ to 75 for open type machines, Fig. 16, Chapter I.

Field Winding Temperature Rise.—The radiating surface for the shunt field winding (see Fig. 60),

$$S_f = 2(d_f + h_f)L_f p$$

and the surface per watt loss,

$$\frac{S_f}{W_f} = \frac{2(d_f + h_f)L_f p}{W_f} \quad (12)$$

When ventilated field coils are used, as shown in Fig. 61, Chapter

the surface of the ducts must be included when calculating the total cooling surface.

When the series field winding is wound at either end of the shunt field coil or wound of insulated wire on top of the shunt field coil, the two windings may be treated as one winding and the combined cooling surface calculated. The losses for the calculation of the surface per watt must then be the sum of the shunt field and series field losses.

The cooling surface for the commutating field winding is calculated as explained for the shunt and series field winding.

The cooling constant for the field winding depends upon the insulation used, the thickness of the field coil, the construction of the machine, the temperature of the armature, the number of commutating poles used, etc., and can be determined only by test.

For open-type machines of the type shown in Fig. 1, Chapter I,

$$C_{cf} = 100 \text{ to } 120$$

and for the type shown in Figs. 16 and 18, Chapter I,

$$C_{cf} = 120 \text{ to } 130.$$

Commutator Temperature Rise.—The cooling surface of the commutator per watt loss,

$$\frac{S_c}{W_a} = \frac{\pi D_c l_c (1 + 0.00051 v_c)}{W_b + W_{bf}} \quad (127)$$

and the commutator temperature rise,

$$T_c = \frac{C_{cc}}{S_c/W_a}. \quad (128)$$

For commutating-pole machines with no sparking at the brushes,

$$C_{cc} = 15 \text{ to } 20.$$

When there is sparking at the brushes, it is not possible to calculate the commutator losses and the commutator temperature rise.

Sample Design: Losses, Efficiency, and Temperature Rise.—The armature copper losses for full-load,

$$\begin{aligned} W_a &= I_a^2 R_a = 1208^2 \times 0.00279 \\ &= 4070 \text{ watts} \end{aligned}$$

or 1.36 per cent of the rated output.

Chapter VI, and the commutating field copper losses for full-load,

$$\begin{aligned} W_c &= I_a^2 R_c = 1208^2 \times 0.00095 \\ &= 1380 \text{ watts} \end{aligned}$$

or 0.46 per cent of rated output.

The full-load series field copper loss,

$$\begin{aligned} W_s &= I_a^2 R_s = 1208^2 \times 0.000624 \\ &= 910 \text{ watts} \end{aligned}$$

or 0.303 per cent of rated output.

The copper loss for the shunt field,

$$\begin{aligned} W_f &= i_f^2 R_f = 8.12^2 \times 21.6 \\ &= 1420 \text{ watts} \end{aligned}$$

and the shunt field copper loss plus the rheostat loss,

$$\begin{aligned} W_f + W_r &= i_f E_t = 8.12 \times 250 \\ &= 2030 \text{ watts} \end{aligned}$$

or 0.677 per cent of rated output.

Assuming 2 volts drop for positive and negative brushes, the brush contact loss for full-load,

$$\begin{aligned} W_b &= I_a 2 = 1208 \times 2 \\ &= 2416 \text{ watts, or 0.805 per cent.} \end{aligned}$$

The maximum and minimum width of the armature tooth have been calculated (page 71, Chapter IV), and the average tooth width,

$$\begin{aligned} w_{ta} &= \frac{w_{t_1} + w_{t_2}}{2} = \frac{0.607 + 0.484}{2} \\ &= 0.545 \text{ in.} \end{aligned}$$

The weight of the iron in the armature teeth,

$$\begin{aligned} G_{at} &= w_{ta}(l - n a v_a) k_1 S d_s \times 0.278 \\ &= 0.545 (11 - 3 \times \frac{2}{3}) 0.92 \times 81 \times 1.57 \times 0.278 \\ &= 176 \text{ lb.,} \end{aligned}$$

flux density at a section $\frac{1}{3}$ slot depth from the minimum tooth width is used to calculate the iron losses in the teeth and is equal to 125 kilo-lines (page 72, Chapter IV). The loss per pound per cycle for this density is found from the loss curve for open-hearth steel in the Appendix and is 0.144 watt. The frequency of the flux reversals is 45 cycles per sec., and the loss in the armature teeth due to the fundamental frequency flux,

$$\begin{aligned} W_{at} &= 0.144 \times 45 \times 176 \\ &= 1140 \text{ watts.} \end{aligned}$$

The weight of the iron in the armature yoke,

$$\begin{aligned} G_{ay} &= \frac{\pi}{4} [(D - 2d_s)^2 - D^2] (l - n_d w_d) k_1 \times 0.278 \\ &= \frac{\pi}{4} [(25 - 2 \times 1.57)^2 - 11.0^2] (11 - 3 \times \frac{3}{8}) 0.92 \times 0.278 \\ &= 560 \text{ lb.} \end{aligned}$$

The flux density for the armature yoke is 75 kilo-lines (page 73, Chapter IV), and the loss per pound per cycle is 0.057 watt. The loss in the armature yoke due to the fundamental frequency flux,

$$\begin{aligned} W_{ay} &= 0.057 \times 45 \times 560 \\ &= 1440 \text{ watts.} \end{aligned}$$

The total core loss (see page 117),

$$\begin{aligned} W_c &= (1140 + 1440) 2.5 \\ &= 6450 \text{ watts.} \end{aligned}$$

or 2.15 per cent of rated output.

The brush friction loss will be calculated in accordance with the A.I.E.E. recommendation,

$$\begin{aligned} W_{bf} &= 8 \times 54 \times 3.77 \\ &= 1630 \text{ watts} = 0.543 \text{ per cent.} \end{aligned}$$

3000 watts = 1.0 per cent of rated output.

The stray load losses will be taken equal to 1 per cent of the output rating, which is in accordance with the A.I.E.E. Standards, page 115.

The calculations for the efficiency are shown in Table X, and the efficiency curve is shown in Fig. 81.

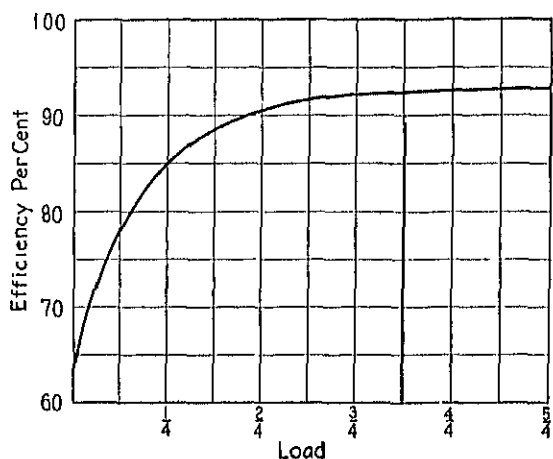


FIG. 81.—Efficiency of 300-kw., 250-volt, 900-r.p.m. generator.

TABLE X

	Load				
	$\frac{1}{4}$	$\frac{1}{2}$	$\frac{3}{4}$	1	$\frac{5}{4}$
Armature copper.....	0.25	1.02	2.29	4.07	6.35
Stray load.....	0.75	1.50	2.25	3.00	3.75
Commutating field.....	0.00	0.35	0.78	1.38	2.15
Series field.....	0.00	0.23	0.51	0.91	1.42
Brush I^2R	0.61	1.21	1.82	2.42	3.02
Shunt-field and rheostat.....	2.03	2.03	2.03	2.03	2.03
Core.....	6.45	6.45	6.45	6.45	6.45
Brush friction.....	1.63	1.63	1.63	1.63	1.63
Friction and windage.....	3.00	3.00	3.00	3.00	3.00
Output.....	75.00	150.00	225.00	300.00	375.00
Output plus losses.....	89.87	167.42	245.76	324.89	404.80
Efficiency.....	83.50	89.60	91.70	92.30	92.70

$$\begin{aligned}
 \frac{S_a}{W_a} &= \frac{\left[\pi D(l + Al_c) + \pi D_l + \frac{\pi}{4}(D^2 - D_c^2)(2 + n_d) \right] (1 + 0.00051v)}{W_a + W_c + W_s} \\
 &= \frac{\left\{ \left[\pi \times 25(11 + 4 \times 8.0) + \pi \times 14 \times 11 + \frac{\pi}{4}(25^2 - 14.0^2)(2 + 3) \right] \right\}}{(1 + 0.00051 \times 5900)} \\
 &\quad \frac{1}{4070 + 6450 + 3000} \\
 &= 1.64 \text{ sq. in. per watt}
 \end{aligned}$$

and the estimated full-load temperature rise,

$$T_a = \frac{C_{ca}}{\frac{S_a}{W_a}} = \frac{60}{1.64} = 36.6^\circ \text{ C.}$$

The surface per watt for the shunt field winding has been calculated (page 91, Chapter V), and the temperature rise,

$$T_f = \frac{C_{cf}}{\frac{S_f}{W_f}} = \frac{110}{2.43} = 45.3^\circ \text{ C.}$$

The surface per watt loss for the commutator for full-load,

$$\begin{aligned}
 \frac{S_c}{W_c} &= \frac{\pi D_c l_c (1 + 0.00051v_c)}{W_b + W_{bf}} \\
 &= \frac{\pi \times 16 \times 14 (1 + 0.00051 \times 3770)}{2420 + 1630} \\
 &= 0.507 \text{ sq. in. per watt}
 \end{aligned}$$

and the full-load temperature rise,

$$T_c = \frac{C_{cc}}{\frac{S_c}{W_c}} = \frac{20}{0.507} = 39.5^\circ \text{ C.}$$

An assembly drawing of the generator is shown in Fig. 1.

GENERATOR

Hp. Kw 300 Volts 230-250 Amps. 1200 R p m 900 Poles 6
 Watts/r.p.m. 333 Output constant 2.06×10^4 Type Compound-wound Commutating-pole

Outside diameter 26 0
 Inside diameter 11 0
 Total length 3 4
 Dents, number, also 3 4
 Length, gross 9 875 Effective, 0 008
 Number of slots 81
 Slots per pole 13 1
 Type of winding Simplex lap
 Number of coils 102
 Turns per coil 1
 Conductors total 324
 Conductors per slot 4
 Total flux 48,300 K L
 Distribution constant 0 095
 Flux per pole 5350 K L
 Conductor dimensions 0 125 \times 0 025
 Conductor section 0 0718
 Current density 2600
 Dega-con number, size, 27- 078 \times 50
 Coils in slots 1 and 1 1
 Coils in bar 1 and 2
 One-half mean turn 28 07
 Resistance, 25° C. 0 00234
 Resistance, 75° C. 0 00270
 Square inch per watt 1 04
 Cal. temperature rise 30 0
 Total ampere conductors 65,107
 Ampere conductors per inch 536
 Ampere-turns per pole 6410

COMMUTATOR AND BRUSH

Diameter 16 0
 Length 14 0
 Peripheral speed 3770
 Number of bars 182
 Bar pitch 0 31
 Thickness of mica 0 03
 Volts bar average 0 63 Max. 18 8
 Number of arms 6
 Amperes per arm 402
 Brushes per arm 5
 Size of brush 0 75 \times 1 50
 Current density 44 7
 Square inches per watt 0 507

WEIGHTS

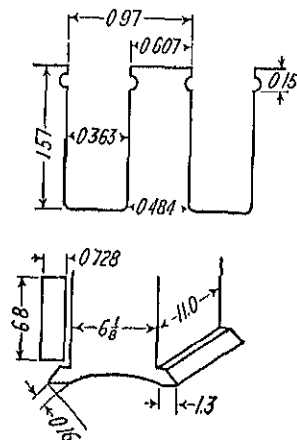
Armature copper 219 0
 Shunt field copper 223 0
 Series field copper 102 0
 Commutating field copper 308 0
 Armature teeth 176 0
 Armature yoke 500 0

FULL-LOAD LOSSES

Friction and windage 3600 0
 Brush friction 1630 0
 Core 9154 0
 Stray load 3000 0
 Armature copper 4074 0
 Shunt field copper rheo. 2030 0
 Series field copper 910 0
 Commutating field copper 134 0
 Brush contact I^2R 2110 0
 Total losses 24896 0

FULL-LOAD RESISTANCE DROP

Armature 3 37-1 35%
 Series field 0 755-0 302%
 Commutating field 1 15-0 40%
 Brushes 2 00-0 60%
 Total 7 275-2 91%
 Shunt field I^2R 176 0



POLES AND YOKE	MAIN	COMM.
Material, sheet steel	0 023	0 023
Body, length and width	11 0 \times 8 1	8 0 \times 1 75
Shoe, length and width	11 0 \times 8 1	8 0 \times 1 75
Pole pitch	13 10	6 8
Percentage of pole embrace	84	84
Pole arc	2 \times 0 22	2 \times 0 25
Total air gap length	2 \times 0 22	2 \times 0 25

Material of yoke Cast steel
 Outside diameter of yoke 18 25
 Inside diameter of yoke 42 00
 Length of yoke 10 0
 Magnetic section 0 25 \times 10 0 = 100 0

FIELD WINDING	SHUNT	SERIES	COMM.
Size of conductor	No. 12 10	3- 210 \times 1 0	3- 255 \times 1 25
Conductor section	0 00516	3 \times 0 210	3 \times 0 305
Amperes	8 12	1208	1208
Current density	1575	1806	1320
Turns per pole	581	1 6	5 6
Length of mean-turn	38 38	61 45	51 8
Resistance, 25° C.	18 1	0 000624	0 00040
Resistance, 75° C.	21 6	0 000624	0 00065
Watts loss	1420		
Square inches per watt	2 43		
Field leakage constant			120

MAGNETIC CIRCUIT

Volts, 260 R.p.m., 900

	Section	Density	Length	AT
Gap	804 0	56 0	1 1 \times 0 22	4240
Teeth	386 0	125 0	1 57	825
A. yoke	71 4	75 0	4 70	47
Pole	67 3	95 4	8 28	290
P. yoke	100 0	94 2	11 80	200
Total				5002
Shunt AT per pole full-load				4740
Series AT per pole full-load				1400
Commutating AT per pole full-load				0 0750

COMMUTATING

Bars covered by brush 2 42
 Commutating zone at armature surface 3 11
 Commutating zone, per cent neutral zone 48 1
 Reactance, volts 1 92
 Density in commutating pole air gap 10 2 K L

Remarks: 0 014—Open-heart steel

Designed by J. H. Kuhlmann

Date:

CHAPTER VIII

SAMPLE DESIGN

Sample Design 2: *Design of a Constant-Speed, Direct-Current Motor.*

—A 15-hp., 1150-r.p.m., 230-volt, constant-speed, commutating-pole, direct-current motor is to be designed. The motor is to be of the general purpose class, with 40 degrees C. continuous-duty rating. The efficiency of the motor should not be less than 87.3 per cent for rated load, voltage, and speed. (See Table VIII, page 121.)

The motor input,

$$Kw = \frac{\text{hp} \times 746}{\text{eff.}} = \frac{15 \times 746}{87.3} = 12.8 \text{ Kw}$$

$$\frac{Kw}{n} \times 10^3 = \frac{12.8}{1150} \times 10^3 = 11.1.$$

From the curve of output constants, Fig. 22, Chapter II,

$$C = 5.1 \times 10^4.$$

This motor will be designed with 4 poles, and

$$D = \sqrt[3]{\frac{Kw_a C p}{n(1.5 \text{ to } 3.14)}} = \sqrt[3]{\frac{12.8 \times 5.1 \times 10^4 \times 4}{1150(1.5 \text{ to } 3.14)}} \\ = 11.5 \text{ to } 8.96 \text{ in.}$$

Choose an armature diameter of 10 in., and

$$l = \frac{Kw_a C}{D^2 n} = \frac{12.8 \times 5.1 \times 10^4}{10^2 \times 1150} \\ = 5.67; \text{ use } 5.75 \text{ in.}$$

The peripheral speed,

$$v = \frac{\pi D n}{12} = \frac{3.14 \times 10 \times 1150}{12} \\ = 3010 \text{ ft. per min.}$$

$$f = \frac{pn}{2 \times 60} = \frac{4 \times 1150}{2 \times 60} = 38.3 \text{ cycles per sec.}$$

The pole pitch,

$$\tau = \frac{\pi D}{p} = \frac{3.14 \times 10}{4} = 7.85 \text{ in.}$$

and for 66 per cent pole embrace the pole arc,

$$B = 0.66\tau = 0.66 \times 7.85 = 5.18 \text{ in.}$$

The length of the air gap is estimated with the help of the curve Fig. 25, and the pole shoe designed as indicated in Fig. 23. The approximate method has been used for making the flux plot, which is shown in Fig. 82, and the air gap flux distribution factor,

$$f_d = 0.671.$$

From the curve, Fig. 20, the air gap density should be approximately 41 kilo-lines per sq. in. The total flux,

$$\begin{aligned}\phi_t &= \pi D l B_g = 3.14 \times 10 \times 5.75 \times 41 \\ &= 7400 \text{ kilo-lines.}\end{aligned}$$

For a motor the no-load induced voltage, which is equal to terminal voltage, is used in making the calculations for the magnetic circuit.

A simplex wave winding is selected and the total number of conductors,

$$\begin{aligned}N &= \frac{E_a \times 60 \times 10^8}{\phi_m f_d} = \frac{230 \times 2 \times 60 \times 10^8}{7400 \times 10^3 \times 1150 \times 0.671} \\ &= 483.\end{aligned}$$

Table III, page 39, Chapter III, shows that in order to avoid too many coils in the armature winding, 2 or 6 coil sides per slot must be used. The number of conductors per slot must be a multiple of 2, and if 6 coil sides per slot are to be used, a multiple of 6. With 6 conductors per slot, too many slots and commutator bars will be necessary, therefore 2 conductors per slot, with 2 turns per coil, will be used. The total number of slots,

$$S = \frac{483}{2} = 241.5, \text{ or } 242.$$

With 39 slots, or $9\frac{3}{4}$ slots per pole, it will be necessary to short chord the armature coils $\frac{3}{4}$ of a slot pitch, which is undesirable for commutating-pole machines, or to over chord $\frac{1}{4}$ of a slot pitch, which should be avoided whenever possible. Forty-one armature slots, or $10\frac{1}{4}$ slots per pole, will therefore probably be most desirable.

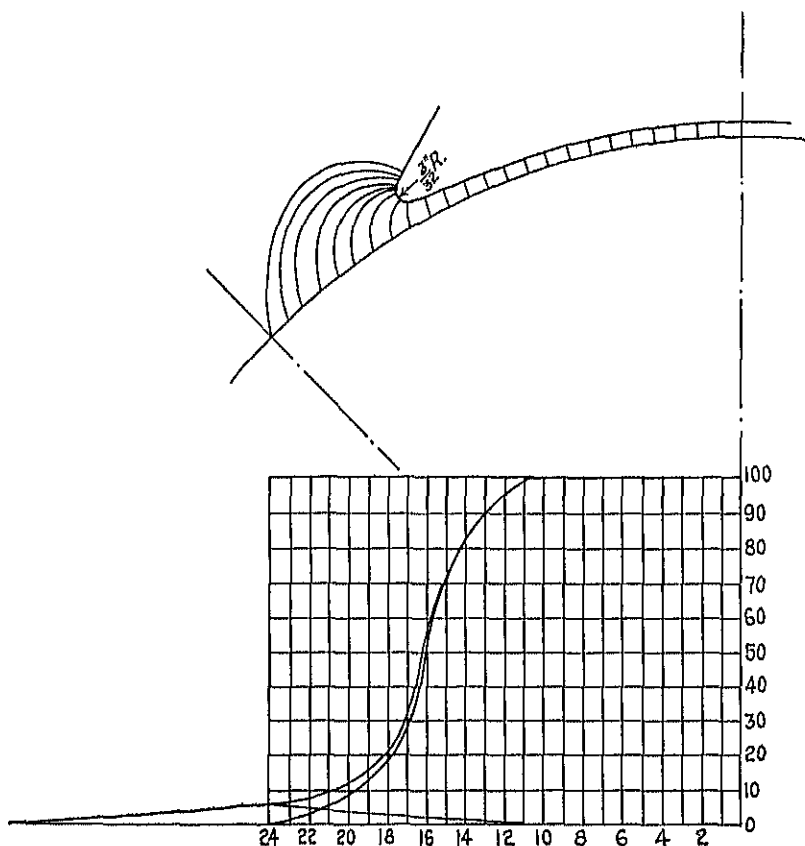


FIG. 82.

The total number of armature conductors,

$$N = 12 \times 41 = 492$$

and

$$\phi_t = \frac{230 \times 2 \times 60 \times 10^8}{492 \times 1150 \times 0.671} = 7270 \text{ kilo-lines.}$$

The armature is therefore simplex wave wound, with 12 slots, 12 conductors per slot, and 2 turns per coil.

The back pitch,

$$Y_1 = C_s Y_s + 1 = 6 \times 10 + 1 = 61.$$

The number of commutator bars,

$$K = 3 \times 41 = 123$$

and

$$Y_c = 2 \frac{K \pm 1}{p} = 2 \frac{123 \pm 1}{4} = 62.$$

The front pitch,

$$\begin{aligned} Y_2 &= 2Y_c - Y_1 = 2 \times 62 - 61 \\ &= 63. \end{aligned}$$

The average voltage between adjacent commutator bars,

$$e_{sa} = \frac{Ep}{K} = \frac{230 \times 4}{123} = 7.48 \text{ volts}$$

and the maximum voltage,

$$e_{sm} = \frac{Ep}{Kf_d} 1.30 = \frac{230 \times 4}{123 \times 0.671} 1.3 = 14.5 \text{ volts.}$$

The voltage per turn,

$$e_t = \frac{ae_{sm}}{p\ell_a} = \frac{2 \times 14.5}{4 \times 2} = 3.62 \text{ volts.}$$

The full-load terminal current,

$$\begin{aligned} I &= \frac{\text{hp} \times 746}{E_t \times \text{eff.}} = \frac{15 \times 746}{230 \times 0.872} \\ &= 55.8 \text{ amperes.} \end{aligned}$$

The shunt field current is estimated at 1.6 amperes, Fig. 49, and

$$I_a = 55.8 - 1.6 = 54.2 \text{ amperes.}$$

For a current density of 2200 amperes per sq. in., the section area of the armature conductor,

$$s_a = \frac{I_a}{A_a a} = \frac{54.2}{2200 \times 2} = 0.0123 \text{ sq. in.}$$

coils are held in the slot by binding bands. From the copper table, a d.c.c. copper ribbon is selected which has the following insulated dimensions: 0.095 in. \times 0.175 in. = 0.0126 sq. in. area. The corrected current density,

$$A_a = \frac{51.2}{2 \times 0.0126} = 2150 \text{ amperes per sq. in.}$$

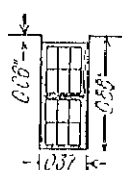


Fig. 83.

The dimensions of the slot are then,

$$w_s = (3 \times 0.095) + 0.085 = 0.370 \text{ in.}$$

$$d_s = (1 \times 0.175) + 0.182 = 0.357 \text{ in.}$$

These slot dimensions will be satisfactory if the resulting tooth densities do not exceed the limits given in Chapter IV.

The calculations for the length of one-half the mean-turn of the armature coil are (see Fig. 50):

$$\sin \alpha = \frac{d}{l_1} = \frac{0.37 + 0.10}{0.766} = 0.613$$

$$\alpha = 37^\circ 50' \text{ and } \cos \alpha = 0.79$$

$$\begin{aligned} L_a &= \frac{\pi(D - d_s)}{p \times \cos \alpha} + 2b + d_s + l \\ &= \frac{3.14(10 - 0.357)}{4 \times 0.79} + 1.5 + 0.357 + 5.75 \\ &= 17.18 \text{ in.} \end{aligned}$$

The resistance of the armature winding at 75°C. ,

$$\begin{aligned} R_a &= \frac{L_a N r}{s_a a^2 \times 10^9} = \frac{17.18 \times 492 \times 0.826}{0.0126 \times 2^2 \times 10^9} \\ &= 0.138 \text{ ohm} \end{aligned}$$

and the voltage drop,

$$I_a R_a = 51.2 \times 0.138 = 7.07 \text{ volts}$$

or 3.25 per cent of rated terminal voltage.

The weight of the armature copper,

$$\begin{aligned} G_a &= L_a N s_a \times 0.321 = 17.18 \times 492 \times 0.0126 \times 0.321 \\ &= 34.1 \text{ lb.} \end{aligned}$$

The axial length of the pole is made equal to the armature length and

$$\begin{aligned}s_g &= \pi D l_g = 3.14 \times 10 \times 5.75 \\ &= 181 \text{ sq. in.}\end{aligned}$$

The air gap density,

$$\begin{aligned}B_g &= \frac{\phi_i}{s_g} = \frac{7270}{181} \\ &= 40.2 \text{ kilo-lines.}\end{aligned}$$

The coefficient,

$$\begin{aligned}k &= \frac{t_1}{w_{t_1} + (y\delta)} = \frac{0.766}{0.396 + (2.05 \times 0.10)} \\ &= 1.275\end{aligned}$$

and the ampere-turns per pole for the air gap,

$$\begin{aligned}\text{AT}_g &= \frac{B_g \delta k}{3.2} = \frac{40200 \times 0.10 \times 1.275}{3.2} \\ &= 1600.\end{aligned}$$

The armature ampere-turns per pole,

$$\begin{aligned}\text{ATP}_a &= \frac{I_a N}{2ap} = \frac{54.2 \times 492}{2 \times 2 \times 4} \\ &= 1670.\end{aligned}$$

The air gap ampere-turns are therefore 95.8 per cent of the armature ampere-turns per pole, which is in accordance with the data given on page 79.

The minimum tooth pitch,

$$\begin{aligned}t_2 &= \frac{\pi(D - 2d_s)}{S} = \frac{3.14(10 - 2 \times 0.88)}{41} \\ &= 0.631 \text{ in.}\end{aligned}$$

and the minimum width of the armature tooth,

$$w_{t_2} = 0.631 - 0.37 = 0.261 \text{ in.}$$

One radial ventilating duct $\frac{3}{8}$ in. wide will be used in the armature core, and the tooth section,

$$\begin{aligned}s_{t_2} &= w_{t_2}(l - n_a w_d) k_1 S \\ &= 0.26(5.75 - 1 \times \frac{3}{8}) 0.92 \times 41 \\ &= 53.0 \text{ sq. in.}\end{aligned}$$

$$B_{t_2} = \frac{\phi_t}{s_{t_2}} = \frac{7270}{53.0}$$

$$= 137.0 \text{ kilo-lines per sq. in.}$$

The width of the tooth at a point $\frac{1}{8}$ slot depth from the root of the tooth,

$$w_{t_3} = \frac{\pi(D - 1.33d_s)}{S} - w_s = \frac{3.14(10 - 1.33 \times 0.88)}{41} - 0.37$$

$$= 0.307 \text{ in.}$$

and the section at this point,

$$s_{t_3} = 0.307(5.75 - 1 \times \frac{3}{8})0.92 \times 41$$

$$= 62.3 \text{ sq. in.}$$

The tooth density,

$$B_{t_3} = \frac{7270}{62.3} = 117.0 \text{ kilo-lines per sq. in.}$$

Open-hearth electric sheet steel, 0.014 in. thick, will be used for the armature laminations, and the ampere-turns per pole for the teeth,

$$AT_t = a_t l_t = 310 \times 0.88$$

$$= 273.$$

The flux per pole,

$$\phi = \frac{\phi_t f_d}{p} = \frac{7270 \times 0.671}{4}$$

$$= 1220 \text{ kilo-lines.}$$

For the flux density in the armature yoke 65 kilo-lines is assumed and

$$d_{ya} = \frac{\phi}{(l - n_a w_a) k_1 B_{ya}} = \frac{1220}{(5.75 - 1 \times \frac{3}{8})0.92 \times 65}$$

$$= 3.8 \text{ in.}$$

The inside diameter of the armature,

$$D_i = 10 - 2 \times 0.88 - 3.8$$

$$= 4.44 \text{ in.; use 4.5 in.}$$

then

$$B_{ya} = \frac{1220}{(5.75 - 1 \times \frac{3}{8})0.92 \times 3.74}$$

$$= 66.0 \text{ kilo-lines per sq. in.}$$

The length of the flux path,

$$l_{ya} = \frac{(10 - 2 \times 0.88 - 0.5 \times 3.74)\pi}{2 \times 4} = 2.5 \text{ in.}$$

and the ampere-turns per pole for the armature yoke,

$$\begin{aligned} AT_{ya} &= at_{ya} l_{ya} = 7.0 \times 2.5 \\ &= 18. \end{aligned}$$

The main poles will be built up of open-hearth sheet steel punchings. The density must not be chosen too high because the commutating pole flux passes through the main poles for machines having one-half as many commutating poles as main poles. A density of 85 kilo-lines per sq. in. is assumed and 1.20 is used for the leakage factor. If the length of the pole is equal to the armature length,

$$\begin{aligned} w_p &= \frac{\phi \lambda}{l_1 B_p} = \frac{1220 \times 1.20}{5.75 \times 85.0} \\ &= 2.99 \text{ in.; use } 3.0 \text{ in.} \end{aligned}$$

then

$$B_p = 84.8 \text{ kilo-lines per sq. in.}$$

Assuming 50 per cent of the armature diameter for the radial length of the pole, $l_p = 5.0$ in. and the inside diameter of the field yoke,

$$D_{yi} = 10 + 2 \times 0.10 + 2 \times 5.0 = 20.20 \text{ in.}$$

Use 20.25 in. and

$$l_p = 5.025 \text{ in.}$$

The ampere-turns for the pole,

$$\begin{aligned} AT_p &= at_p l_p = 14 \times 5.03 \\ &= 71. \end{aligned}$$

The field yoke will be cast steel, and a flux density of 60 kilo-lines per sq. in. is assumed.

$$\begin{aligned} s_{yf} &= \frac{\phi \lambda}{B_{yf}} = \frac{1220 \times 1.20}{60} \\ &= 24.4 \text{ sq. in.} \end{aligned}$$

This motor is to be of the bracket type shown in Figs. 16 and 18, Chapter I. The axial length of the yoke is taken equal to 10 in. and the thickness,

$$d_{yf} = \frac{24.4}{10} = 2.44.$$

$$D_{v0} = D_{v1} + d_{vf} = 20.25 + 2.5 \\ = 22.75 \text{ in.}$$

The density,

$$B_{vf} = \frac{1220 \times 1.20}{10 \times 2.5} \\ = 58.5 \text{ kilo-lines per sq. in.}$$

The length of the flux path,

$$l_{vf} = \frac{(20.25 + 1.25)\pi}{2 \times 4} = 8.45 \text{ in.}$$

and the ampere-turns,

$$\text{AT}_{vf} = a l_{vf} l_{vf} = 14.2 \times 8.45 \\ = 120.$$

The total ampere-turns per pole for the field winding,

$$\text{ATP}_f = \text{AT}_g + \text{AT}_t + \text{AT}_{va} + \text{AT}_p + \text{AT}_{vf} \\ = 1600 + 273 + 18 + 71 + 120 \\ = 2082.$$

The ratio,

$$\frac{\text{ATP}_f}{\text{ATP}_a} = \frac{2082}{1670} = 1.245$$

which shows that the assumed air gap length is satisfactory (see page 79).

The calculations for the open-circuit saturation curve are given in Table XI, and the curve plotted from these values is shown in Fig. 84.

TABLE XI

Flux Path	Length	200 Volts			230 Volts			250 Volts			275 Volts		
		B	at	AT	B	at	AT	B	at	AT	B	at	AT
Air gap	0.1275			1300	40.2		1600			1740			1911
Armature teeth . . .	0.88	101.8	65	57	117.0	310	273	127.0	585	515	110	1010	915
Armature yoke . . .	2.50	57.4	5.4	11	66.0	7	18	71.7	9.0	23	70	12	30
Pole	5.03	73.7	8.2	41	81.8	11	71	92.2	27	136	101.5	61	307
Field yoke	8.15	50.9	11.7	99	58.5	11.2	120	63.6	16.5	140	70	20	169
Total				1601			2082			2551			3332

The shunt field ampere-turns are taken from the open-circuit saturation curve, Fig. 84, for 230 volts.

$ATP_f = 2080$ ampere-turns.

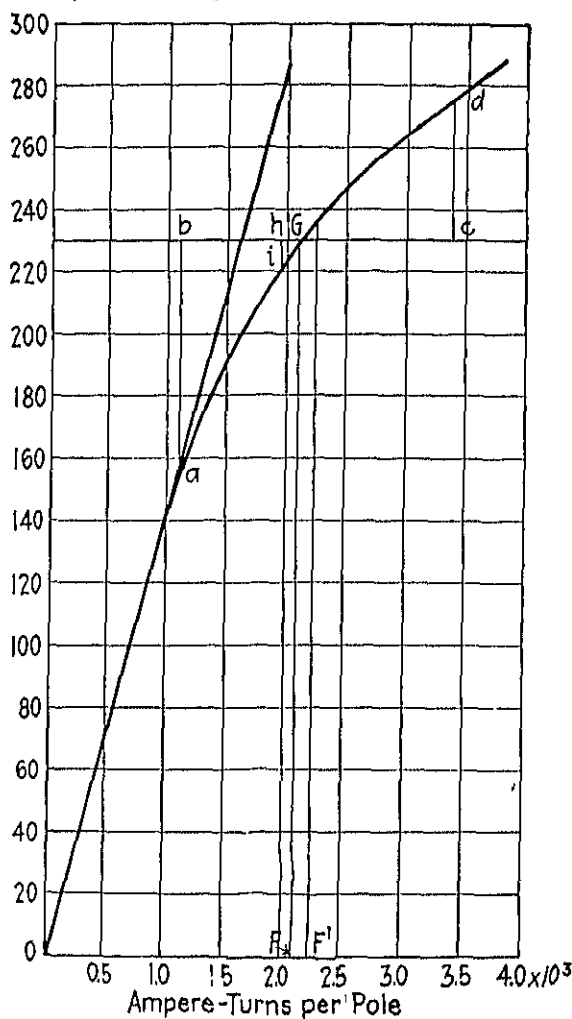


FIG. 84.—Open-circuit saturation curve.

The length of the mean-turn for the shunt field coil is calculated as explained on page 82,

$$L_f = 2 \times 5.75 + 2(3 - 2 \times 0.125) + \pi[0.75 + 2(0.125 + 0.10)] \\ = 20.8 \text{ in.}$$

$$s_f = \frac{ATP_f L_{fpr}}{E_t \times 10^6} = \frac{2080 \times 20.8 \times 4 \times 0.826}{230 \times 10^6} \\ = 0.000621 \text{ sq. in.}$$

A No. 21 B. & S. gage, s.c.c.c. copper wire, with a section area of 0.000638 sq. in., will be used for the shunt field winding.

For a current density of 1300 amperes per sq. in.,

$$i_f = s_f A_f = 0.000638 \times 1300 \\ = 0.83 \text{ ampere}$$

and the number of turns per pole,

$$t_f = \frac{ATP_f}{i_f} = \frac{2080}{0.83} = 2500.$$

From Fig. 85 the height of the winding space, $h_f = 4.25$ in. The insulated diameter of No. 21 s.c.c.c. wire is 0.0353 in., and the number of turns per layer

$$= \frac{4.25}{0.0353} = 120.$$

Using 21 layers of 119 turns each, the turns per pole,

$$t_f = 119 \times 21 = 2499.$$

The depth of the field coil,

$$d_f = 0.0353 \times 21 = 0.741.$$

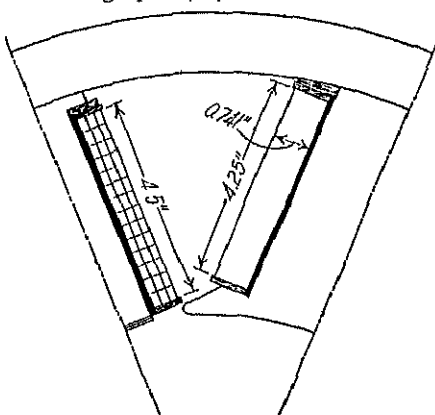


FIG. 85.

It is therefore not necessary to recalculate the mean-turn. The resistance of the shunt field winding at 75° C.,

$$R_f = \frac{L_f t_{fpr}}{s_f \times 10^6} = \frac{20.8 \times 2499 \times 4 \times 0.826}{0.000638 \times 10^6} \\ = 270 \text{ ohms.}$$

With 230 volts applied to the shunt field terminals,

$$i_f = \frac{230}{270} = 0.852 \text{ ampere}$$

and the ampere-turns,

$$ATP_f = 0.852 \times 2499 = 2130.$$

The copper loss in the shunt field winding,

$$W_f = i_f^2 R_f = 0.852^2 \times 270 \\ = 196 \text{ watts.}$$

The cooling surface,

$$S_f = 2(0.741 + 4.25)20.8 \times 4 \\ = 830 \text{ sq. in.}$$

and

$$\frac{S_f}{W_f} = \frac{830}{196} = 4.23$$

which is satisfactory (see page 83).

The weight of the copper,

$$G_f = L_f \rho_s \pi s_f \times 0.321 = 20.8 \times 2499 \times 4 \times 0.000638 \times 0.32 \\ = 42.7 \text{ lb.}$$

The commutator diameter (see page 106),

$$D_c = 7.25 \text{ in.}$$

The number of commutator bars,

$$K = 3 \times .11 = 123$$

and the bar pitch,

$$\beta = \frac{\pi D_c}{K} = \frac{3.14 \times 7.25}{123} = 0.185 \text{ in.}$$

$$\beta_r = 0.185 \frac{10}{7.25} = 0.255.$$

For a brush thickness of $\frac{3}{8}$ in.,

$$b = \frac{0.375}{0.185} = 2.03 \text{ bars.}$$

The phase difference in commutation,

$$\varphi = \frac{K}{p} - \frac{1}{2}(Y_1 - 1) = \frac{123}{4} - \frac{1}{2}(61 - 1) \\ = 0.75$$

$$w_c = \left(b + m + \varphi - \frac{a}{p} \right) \beta_r = \left(2.03 + 3 + 0.75 - \frac{2}{4} \right) 0.255 \\ = 1.35 \text{ in.}$$

The width of the neutral zone,

$$= (1 - \psi)\tau = (1 - 0.66)7.85 = 2.67 \text{ in.}$$

and the ratio of commutating zone to neutral zone

$$= \frac{1.35}{2.67} = 0.505$$

which shows that the thickness of brush selected is satisfactory (see page 98).

The mica is to be under-cut and a medium hard brush is to be used. A current density of 40 amperes per sq. in. of brush contact is assumed, and

$$S_b = \frac{2I_a}{A_b} = \frac{2 \times 55}{40} = 2.75 \text{ sq. in.}$$

The total width of all the brushes per arm,

$$n_b w_b = \frac{S_b}{n_a b_t} = \frac{2.75}{4 \times 0.375} = 1.83 \text{ in.}$$

A brush $\frac{3}{8}$ in. thick by $\frac{5}{8}$ in. wide will be used, with 3 brushes per arm. The total contact surface,

$$S_b = 0.625 \times 0.375 \times 3 \times 4 = 2.81 \text{ sq. in.}$$

The correct value of the current density at the brush contact,

$$A_b = \frac{2 \times 55}{2.81} = 39.1 \text{ amperes per sq. in.}$$

The length of the commutator,

$$l_c = n_b(w_b + 0.125) + c_2 = 3(0.625 + 0.125) + 0.75 \\ = 3.0 \text{ in.}$$

The commutating-pole air gap length is chosen equal to the length of the main-pole air gap,

$$\delta_t = 0.10 \text{ in.}$$

The width of the commutating pole,

$$w_i = w_a - (1.5 \text{ to } 2)\delta_i = 1.35 - (1.5 \text{ to } 2)0.10 \\ = 1.20 \text{ to } 1.15 \text{ in.}$$

$$w_i \approx \frac{1 - \psi}{2} \tau = \frac{1 - 0.66}{2} 7.85 = 1.34 \text{ in.}$$

$$w_i \approx 1.5t_1 = 1.5 \times 0.766 = 1.15 \text{ in.}$$

Make

$$w_i = 1.25 \text{ in.}$$

and

$$l_i = l_1 = 5.75 \text{ in.}$$

The reactance voltage per coil is calculated by formula 102.

$$\text{ATP}_a = 1690, p = 4, t_a = 2, n_s = 19.2, m = 3, b = 2.03,$$

$$A = b + 1 - \frac{a}{p} = 2.03 + 1 - \frac{2}{4} = 2.53, \varphi = 0.75,$$

$$l = 5.75, d_s = 0.88, w_s = 0.37, l_i = 5.75, l_1 = 0.766,$$

$$w_i = 1.25, \delta_i = 0.10, l_s = L_a - l = 17.18 - 5.75 = 11.43$$

$$4.25l \frac{d_s}{w_s} = 4.25 \times 5.75 \frac{0.88}{0.37} = 58.0$$

$$4.66(2l - l_i) \log_{10} \frac{2l_1 - w_s}{w_s} \\ = 4.66(2 \times 5.75 - 5.75) \log_{10} \frac{2 \times 0.766 - 0.37}{0.37} = 13.3$$

$$1.02l_i \frac{w_i - w_s}{\delta_i} = 1.02 \times 5.75 \frac{1.25 - 0.37}{0.10} = 51.6$$

$$8.12l_s = 8.12 \times 11.43 = 93.0$$

$$2 - \frac{\varphi}{A + m - 1} = 2 - \frac{0.75}{2.53 + 3 - 1} = 1.835$$

$$M = 1.835(58 + 13.3 + 51.6) + 93 = 319$$

$$e_r = \frac{\text{ATP}_a t_a p n_s}{10^8} \frac{m}{A + m - 1} M \\ = \frac{1690 \times 2 \times 4 \times 19.2}{10^8} \frac{3}{2.53 + 3 - 1} 319 \\ = 0.548 \text{ volt.}$$

$$B_{g1} = \frac{e_r \times 60 \times 10^8}{t_{al,v} \times 12} = \frac{0.548 \times 60 \times 10^8}{2 \times 5.75 \times 3010 \times 12}$$

$$= 7920 \text{ lines per sq. in.}$$

The air gap coefficient will be the same as for the main pole because the air gap length is the same.

$$k = 1.275$$

and

$$AT_{gi} = \frac{B_{g1} \delta_i k}{3.2} = \frac{7920 \times 0.10 \times 1.275}{3.2}$$

$$= 316 \text{ ampere-turns.}$$

The ampere-turns for the iron parts of the magnetic circuit will not be calculated separately, but will be taken care of by increasing the commutating-pole air gap ampere-turns (see page 106). The total ampere-turns per commutating pole,

$$ATP_i = ATP_a + 2AT_{gi}$$

$$= 1690 + 2 \times 316$$

$$= 2322.$$

The turns per pole,

$$t_i = \frac{ATP_i}{I_a} = \frac{2322}{55} = 42.2.$$

For a current density of 1200 amperes per sq. in.,

$$s_i = \frac{I_a}{A_i} = \frac{55}{1200} = 0.0458 \text{ sq. in.}$$

A rectangular d.c.c. ribbon with insulated dimensions 0.204×0.310 in. and area 0.0507 sq. in. will be used.

The current density is then,

$$A_i = \frac{55}{0.0507} = 1085 \text{ amperes per sq. in.}$$

The height of the winding space is taken from Fig. 85 and is equal to 4.5 in. The coil is wound with 3 layers of 14 turns each so that,

$$t_i = 3 \times 14 = 42 \text{ turns.}$$

The mean-turn,

$$L_t = 2 \times 5.75 + 2(1.25 - 2 \times 0.125) + \pi[0.612 + 2(0.125 + 0.10)] \\ = 16.84 \text{ in.}$$

The resistance of the commutating field winding at 75° C.,

$$R_t = \frac{L_t l_{pr}}{s_t \times 10^6} = \frac{16.84 \times 42 \times 2 \times 0.826}{0.0507 \times 10^6} \\ = 0.0231 \text{ ohm}$$

and the voltage drop,

$$I_a R_t = 55 \times 0.0231 = 1.27 \text{ volts}$$

or 0.552 per cent of the rated terminal voltage.

The copper loss,

$$I_a^2 R_t = 55^2 \times 0.0231 \\ = 70 \text{ watts}$$

and the cooling surface,

$$S_t = 2(0.612 + 4.35)16.84 \times 2 \\ = 334 \text{ sq. in.}$$

The cooling surface per watt loss is then,

$$\frac{S_t}{W_t} = \frac{334}{70} = 4.77$$

which shows that the temperature rise of the commutating field winding should not be excessive.

The weight of the commutating field copper,

$$G_t = L_t l_{ps_t} \times 0.321 \\ = 16.84 \times 42 \times 2 \times 0.0507 \times 0.321 \\ = 23.0 \text{ lb.}$$

The expression for the speed of a direct-current motor is,

$$n = \frac{Ea \times 60 \times 10^8}{\phi_t N f_d}$$

For any given motor,

$$n = \frac{E}{\phi_t} C_1 \tag{129}$$

$$C_1 = \frac{a \times 60 \times 10^8}{N f_d}$$

resistance drop in the armature, commutating field, and brush contacts. If the flux remains constant, the speed of the motor will drop in direct proportion with the induced voltage. The flux does not remain constant, however, but is decreased by armature reaction. The full-load speed of the motor will be lower than the no-load speed if the voltage drop is greater than the decrease in flux, and it will be higher than the no-load speed if the decrease in flux is greater than the voltage drop. Shunt-wound, commutating-pole motors, which have a large number of armature ampere-turns per pole, will often have a higher speed at full-load than at no-load. To keep the speed constant on such motors, a small series field winding, sometimes called a stabilizing winding, is used. To determine the effect of armature reaction, it is convenient to use, in formula 129, the voltage induced by the flux rather than the flux. Formula 129 may then be written,

$$n = \frac{E}{E_1} C_1 \quad (130)$$

with E_1 the voltage induced by the armature flux. For commutating-pole motors, the armature demagnetizing ampere-turns are equal to zero because the brushes remain in the no-load neutral position. The method of determining the ampere-turns required on the main field to compensate for the demagnetizing effect of the armature cross-magnetizing field is given on page 78, and Fig. 81 shows the construction for this design. The voltage drop, due to armature reaction, is equal to hi , Fig. 84, Ch being equal to FF' .

The voltage induced by the full-load armature flux,

$$E_1 = 221 \text{ volts.}$$

The voltage drop in armature winding, commutating field winding, and brush contacts = 10.8, with 2 volts allowed for brush contact drop and

$$E = 219.2 \text{ volts.}$$

The full-load speed of the motor,

$$\begin{aligned} n_1 &= n_0 \frac{E}{E_1} = 1150 \frac{219.2}{221} \\ &= 1140 \text{ r.p.m.} \end{aligned}$$

A series, or stabilizing, winding will then not be required.

The armature copper loss for full-load,

$$W_a = I_a^2 R_a = 55^2 \times 0.138 \\ = 414 \text{ watts}$$

or 3.70 per cent of rated output.

The full-load copper loss for the commutating field winding,

$$W_f = I_a^2 R_f = 55^2 \times 0.231 \\ = 70 \text{ watts}$$

which is 0.63 per cent of rated output.

The shunt field copper loss,

$$W_f = i_f^2 R_f = 0.85^2 \times 270 \\ = 196 \text{ watts or } 1.75 \text{ per cent.}$$

Assuming 2 volts drop for positive and negative brushes, the brush contact loss for full-load,

$$W_b = I_a 2 = 55 \times 2 \\ = 110 \text{ watts} = 0.983 \text{ per cent.}$$

The average armature tooth width,

$$w_{ta} = 0.329$$

and

$$G_{ca} = w_{ta}(l - n_a w_a) k_1 S d_s \times 0.278 \\ = 0.329(5.75 - 1 \times \frac{3}{8}) 0.92 \times 41 \times 0.88 \times 0.278 \\ = 16.4 \text{ lb.}$$

The armature tooth density at a point $\frac{1}{2}$ slot depth from the minimum tooth width = 117.0 kilo-lines per sq. in., and the loss per pound per cycle for open-hearth steel = 0.126 watt. The frequency of the flux reversals is 38.3 cycles per sec., and the loss in the armature teeth due to the fundamental frequency flux,

$$W_{ca} = 0.126 \times 16.4 \times 38.3 \\ = 79 \text{ watts.}$$

The weight of the iron in the armature yoke,

$$G_{cy} = \frac{\pi}{4} [(D - 2d_s)^2 - D_s^2] (l - n_a w_a) k_1 \times 0.278 \\ = \frac{\pi}{4} [(10 - 2 \times 0.88)^2 - 4.5^2] (5.75 - 1 \times \frac{3}{8}) 0.92 \times 0.278 \\ = 51.4 \text{ lb.}$$

per pound per cycle for open-hearth steel is 0.047 watt. The loss in the armature yoke due to the fundamental frequency flux,

$$\begin{aligned} W_{cy} &= 0.047 \times 51.4 \times 38.3 \\ &= 92.5 \text{ watts.} \end{aligned}$$

The total core loss (see page 117),

$$\begin{aligned} W_c &= (79 + 92.5) 2.5 \\ &= 426 \text{ watts} = 3.80 \text{ per cent.} \end{aligned}$$

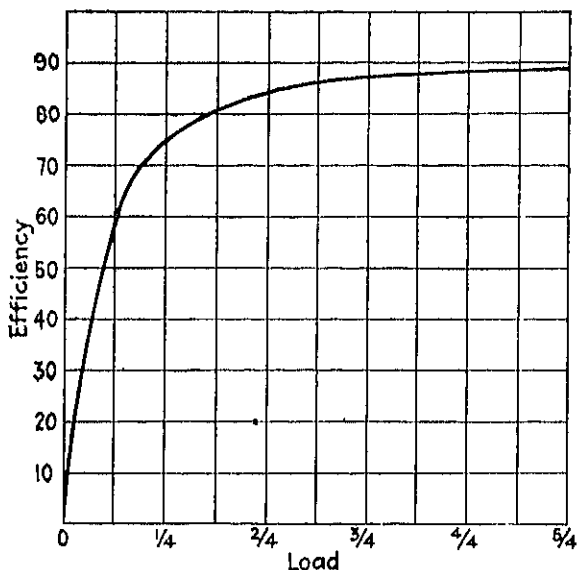


FIG. 86.—Efficiencies of 15-hp., 1150-r.p.m., 230-volt, constant speed motor.

The brush friction loss,

$$\begin{aligned} W_{bf} &= 8 \times 2.81 \times 2.18 \\ &= 49.0 \text{ watts} = 0.437 \text{ per cent.} \end{aligned}$$

From the curves of Fig. 78, the friction and windage loss,

$$W_{fw} = 240 \text{ watts} = 2.14 \text{ per cent.}$$

The stray load losses are taken equal to zero, which is in accordance with the A.I.E.E. Standards, page 115.

The calculations for the efficiency are shown in Table XII, and the efficiency curve is shown in Fig. 86.

TABLE XII

Losses	Load				
	$\frac{1}{1}$	$\frac{2}{4}$	$\frac{3}{1}$	$\frac{4}{1}$	$\frac{5}{1}$
Armature copper	25.9	104.0	233.0	414.0	649.0
Commutating field..	4.4	17.5	39.5	70.0	109.0
Brush I^2R	27.5	55.0	82.5	110.0	137.5
Shunt field..	196.0	196.0	196.0	196.0	196.0
Core	426.0	426.0	426.0	426.0	426.0
Brush friction	49.0	49.0	49.0	49.0	49.0
Friction and windage.. . . .	240.0	240.0	240.0	240.0	240.0
Output	2800.0	5600.0	8400.0	11,200.0	14,000.0
Output plus losses..	3768.8	6687.5	9666.0	12,705.0	15,806.5
Efficiency	74.20	83.80	87.20	88.40	88.50

The armature surface per watt loss,

$$\frac{S_a}{W_a} = \frac{\left[\pi D(l + 2l_c) + \pi D_c l + \frac{\pi}{4}(D^2 - D_c^2)(2 + n_d) \right] (1 + 0.00051v)}{W_a + W_c}$$

$$= \frac{\left\{ \left[3.14 \times 10(5.75 + 2 \times 4.4) + \pi 4.5 \times 5.75 + \frac{\pi}{4}(10^2 - 4.5^2)(2 + 1) \right] \right\}}{(1 + 0.00051 \times 3010)}$$

$$= \frac{\quad}{414 + 426}$$

$$= 2.18 \text{ sq. in. per watt}$$

and the full-load temperature rise,

$$T_a = \frac{C_{ca}}{\frac{S_a}{W_a}} = \frac{70}{2.18} = 32.1^\circ \text{C.}$$

The surface per watt loss for the commutating field winding (see page 146) is

$$\frac{S_i}{W_i} = 4.77 \text{ sq. in. per watt}$$

and the temperature rise,

$$T_i = \frac{C_{ci}}{\frac{S_i}{W_i}} = \frac{120}{4.77} = 25.2^\circ \text{C.}$$

$$\frac{S_f}{W_f} = 4.23 \text{ sq. in. per watt}$$

and

$$T_f = \frac{C_{ef}}{\frac{S_f}{W_f}} = \frac{125}{4.23} = 29.5^\circ \text{ C.}$$

For the commutator,

$$\begin{aligned} \frac{S_c}{W_c} &= \frac{\pi D_c L_c (1 + 0.00051 v_c)}{W_b + W_{bf}} \\ &= \frac{3.14 \times 7.25 \times 3.0 (1 + 0.00051 \times 2180)}{110 + 49.0} \\ &= 0.907 \text{ sq. in. per watt} \end{aligned}$$

$$T_c = \frac{20}{0.907} = 22.0^\circ \text{ C.}$$

A resistance must always be used in series with the armature of direct-current motors when starting. The armature current,

$$I_a = \frac{E_t - E}{R_i + R_r} \quad (131)$$

R_c is the resistance of the armature circuit, resistance of armature, commutating field, brush contacts, and series field when present, and R_r is the resistance of the starting rheostat.

The starting resistance is generally so designed that the motor will start full-load, with a starting current not to exceed approximately 150 per cent of full-load current. The resistance necessary to meet these requirements can be calculated by formula 131,

$$R_r = \frac{E_t - (E + I_a R_c)}{I_a}.$$

The starting box for the 15-hp motor is to be so designed that the starting current will not exceed 150 per cent of the full-load current. The resistance of the armature circuit, $R_c = 0.198$ ohm. At zero speed, the induced voltage, E , is zero, and the resistance that must be

connected in series with the armature to limit the current to 150 per cent of full-load value,

$$R_{r_1} = \frac{230 - (0 + 82.5 \times 0.198)}{82.5}$$

$$= 2.59 \text{ ohms.}$$

If the motor is starting full-load, the current will drop to approximately the rated value after it has accelerated its load, and the induced voltage,

$$E = E_t - I_a(R_e + R_r)$$

$$= 230 - 55(0.198 + 2.59)$$

$$= 76.5 \text{ volts.}$$

To increase further the speed of the motor, the resistance of the rheostat must be reduced to,

$$R_{r_2} = \frac{230 - (76.5 + 82.5 \times 0.198)}{82.5}$$

$$= 1.66 \text{ ohms.}$$

The induced voltage,

$$E = 230 - 55(0.198 + 1.66)$$

$$= 127.8 \text{ volts}$$

and

$$R_{r_3} = \frac{230 - (127.8 + 82.5 \times 0.198)}{82.5}$$

$$= 1.04 \text{ ohms.}$$

The calculations are carried out in this manner until the induced voltage is approximately equal to the terminal voltage. The value of the resistance for the first button of the rheostat = $R_{r_1} - R_{r_2}$, for the second button $R_{r_2} - R_{r_3}$, etc. The starting rheostat for this motor will have 7 buttons, and the resistance of each button is as follows:

Button	Resistance	Ohms
1	$R_{r_1} - R_{r_2} = 2.59 - 1.66$	= 0.93
2	$R_{r_2} - R_{r_3} = 1.66 - 1.04$	= 0.62
3	$R_{r_3} - R_{r_4} = 1.04 - 0.627$	= 0.413
4	$R_{r_4} - R_{r_5} = 0.627 - 0.353$	= 0.274
5	$R_{r_5} - R_{r_6} = 0.353 - 0.170$	= 0.183
6	$R_{r_6} - R_{r_7} = 0.170 - 0.0479$	= 0.122
7	$R_{r_7} - 0 = 0.0479 - 0$	= 0.0479

GENERATOR-MOTOR

Hp. 15 Kw Volts 230 Amps. 55.2 R.p.m. 1150 Poles 4
Watts/r.p.m. 11.1 Output constant 5.2×10^4 Type Shunt-wound-Commutating pole

Outside diameter..... 10.0
Inside diameter..... 4.5
Total length..... 5.75
Duets, number, size..... 1-1
Length, gross..... 5.1 Effective 4.05
Number of slots..... 41
Slots per pole..... 10.1
Type of winding..... Simple π wave
Number of coils..... 123
Turns per coil..... 2
Conductors total..... 492
Conductors per slot..... 12
Total flux..... 7270 K.L.
Distribution constant..... 0.071
Flux per pole..... 1220 K.L.
Conductor dimensions..... 0.095×0.175
Conductor section..... 0.0123
Current density..... 2200
Equiv.-conn. number, size..... None
Coils in slots..... 1 and 11
Coils in bar..... 1 and 63
One-half in-can-turn..... 17.18
Resistance, 25° C..... 0.116
Resistance, 75° C..... 0.138
Square inch per watt..... 2.72
Cal. temperature rise..... 26.3
Total ampere conductors..... 13,370
Ampere conductors per inch..... 426.0
Ampere-turns per pole..... 1600

COMMUTATOR AND BRUSH

Diameter..... 7.25
Length..... 3.00
Peripheral speed..... 2180
Number of bars..... 123
Bar pitch..... 0.185
Thickness of mica..... 0.03
Volts bar average..... 7.48 Max., 14.5
Number of arms..... 4.0
Amperes per arm..... 27.6
Brushes per arm..... 3
Size of brush..... 1×1
Current density..... 30.1
Square inches per watt..... 0.907

WEIGHTS

Armature copper..... 34.1
Shunt field copper..... 42.7
Series field copper..... 23.0
Commutating field copper..... 10.4
Armature teeth..... 61.4
Armature yoke..... 61.4

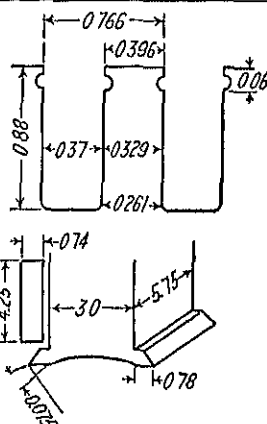
FULL LOAD LOSSES

Friction and windage..... 240.0
Brush friction..... 49.0
Core..... 426.0
Stray load..... 414.0
Armature copper..... 106.0
Shunt field copper + rheo..... 70.0
Series field copper..... 110.0
Commutating field copper..... 1605.0
Brush contact loss..... 1605.0
Total losses..... 1605.0

FULL LOAD RESISTANCE DROP

Armature..... 7.5 ~3.25%
Series field..... 1.25 ~0.545%
Commutating field..... 2.00 ~0.870%
Brushes..... 10.75 ~4.67%
Total..... 23.0
Shunt field IR..... 23.0

Remarks: 0.014—Open-hearth steel



POLES AND YOKE		MAIN	COMM.
Material		Sheet steel	Sheet steel
Body, length and width		5.75×3.0	5.75×1.25
Shoe, length and width		5.75×5.18	5.75×1.25
Pole pitch		7.85	
Percentage of pole embrace		60.0	
Pole arc		5.18	
Total air gap length		2×0.10	2×0.10
Material of yoke			Cast steel
Outside diameter of yoke			22.75
Inside diameter of yoke			20.25
Length of yoke			19.0
Magnetic section			$2 \times 12.5 = 25.0$

Square inches per watt..... 4.23 4.77
Field leakage constant..... 1.20

MAGNETIC CIRCUIT

Volts, 230

R.p.m., 1150

	Section	Length	AT
Gap	181.0	40.2	1.275×0.10
Teeth	62.3	117.0	0.88
A. yoke	18.5	60.0	2.50
Pole	17.25	81.8	6.025
P. yoke	25.00	68.5	8.45
Total			2082

Shunt AT per pole full-load..... 2082
Series AT per pole full-load..... 2302
Commutating AT per pole full-load..... 2302

COMMUTATION

Bars covered by brush..... 2.03
Commutating zone at armature surface..... 1.36
Commutating zone, per cent neutral zone..... 60.5
Reactance volts..... 0.948
Density in commutating pole air gap..... 7.02 K.L.

Designed by: J. H. Kuhlmann

Date:

II—SYNCHRONOUS MACHINES

CHAPTER IX

CONSTRUCTION

THERE are two types of synchronous machines in general use today, the salient-pole machine and the non-salient-pole machine. The salient-pole type is used for generators and motors of large and small capacities of high and very slow speeds. The non-salient-pole type is used for medium and very large capacity generators for high speeds. The latter type is generally known as the turbo-generator. Figure 87 is an assembly drawing of a non-salient-pole type of generator and shows the type of construction in general use. An assembly drawing of a small horizontal salient-pole machine is shown in Fig. 88. A vertical type salient-pole machine is shown in Fig. 89.

Armature.—Modern synchronous machines are of the revolving-field type, that is, the armature is the stationary member and the field rotates. The armature core is built up of sheet-steel laminations, generally from 0.014 to 0.0188 in. thick. The laminations are punched out and carefully annealed to remove shearing and punching strains. They are then coated with an insulating varnish in the manner described for the armature punchings of direct-current machines, page 3. The insulated punchings are next assembled in the armature frame on keys riveted to the frame or in dove-tailed grooves milled into ribs of the frame. Because the armature diameters are usually rather large for all synchronous machines, the laminations are generally punched in segments. The number of segments per circle will depend upon the number of slots, the method of punching, etc. For large-capacity machines, the number of segments per circle must be so chosen that no shaft currents will be produced.¹ One segment with spot-welded tooth supports or duct spacers is shown in Fig. 90.

¹ "Die Wechselstromtechnik," by E. Arnold and J. L. LaCour, Vol. 4, 2nd ed., p. 509, Julius Springer, Berlin; "Shaft Currents in Electrical Machines," by P. L. Alger and H. W. Samson, Trans. A. I.E.E., Vol. 43, 1924, p. 235; "Bearing Currents," by E. G. Merriek, General Electric Review, Vol. 17, Oct., 1914, p. 936; "Bearing Currents—Their Origin and Prevention," by C. T. Pearce, Electric Journal, Vol. 24, Aug., 1927, p. 374.

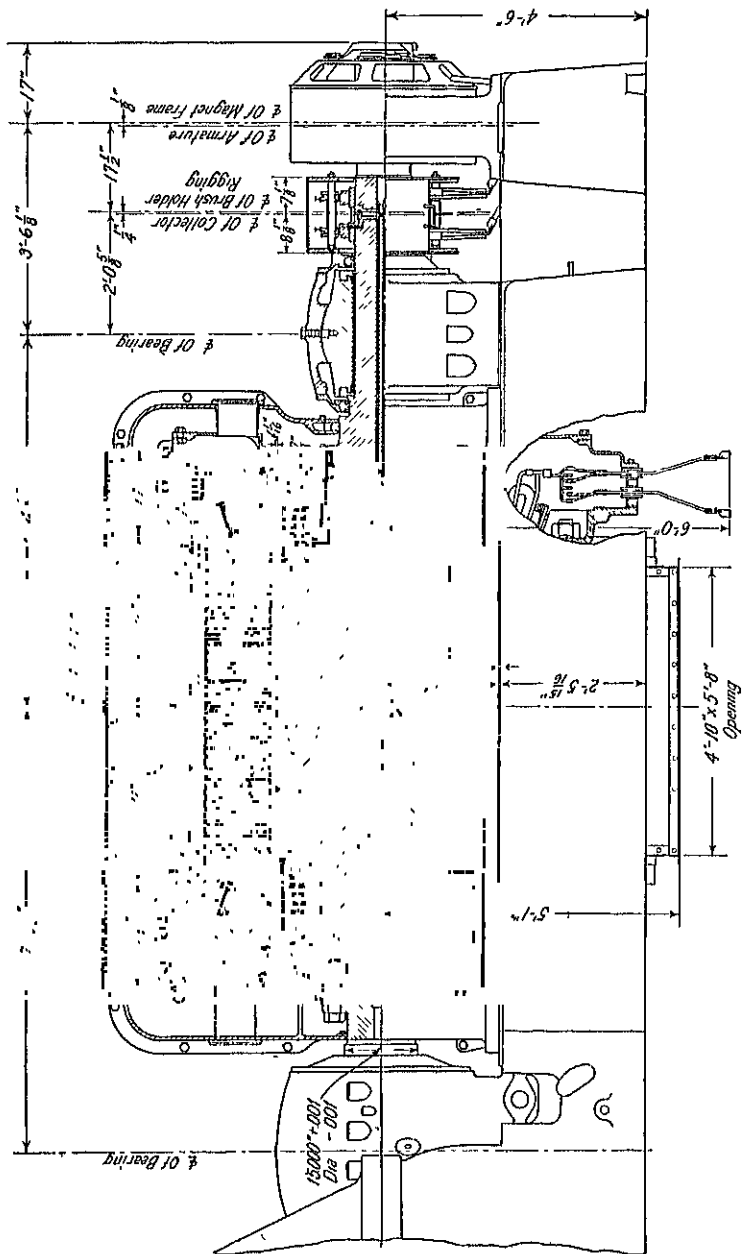


FIG. 87.—Sectional assembly of turbo-generator 12,500 kva, 1800 r.p.m., 13,200 volts

The core is clamped between two follower rings, which are held in place by a key, as shown in Fig. 88, or by long bolts passing through the frame back of the armature core, as shown in Figs. 87 and 89. The teeth are supported by a finger, or tooth support, which extends from the top of the tooth to the inside of the armature core. This tooth support is generally a piece of rolled steel, spot-welded to the last lamination (Fig. 90).

The length of the armature core must be divided into small sections

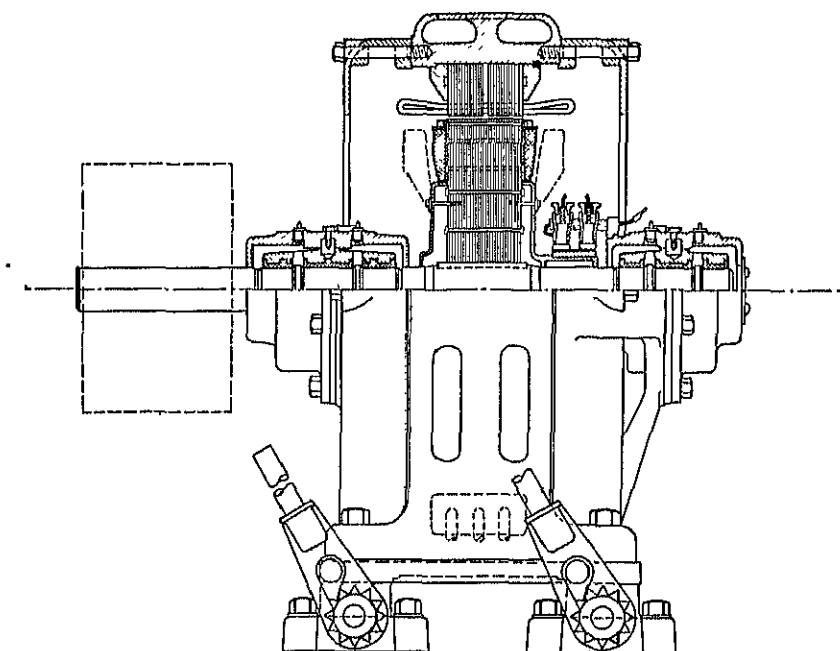


Fig. 88.—Assembly drawing of 115-hp., 1200-r.p.m., bracket-type synchronous motor.

by radial ventilating ducts, to insure proper ventilation of all parts of the armature. These ducts are usually $\frac{3}{8}$ in. wide for small and medium-size machines, and $\frac{1}{2}$ in. for large machines. The distance between centers of ducts should not exceed 3 in. The ventilating duct spacer is generally a rolled-steel piece of I-beam or T section, and like the tooth support is spot-welded to one punching (Fig. 90).

American practice favors the open type of armature slot for synchronous machines, with the two-layer type of winding. The armature coils are so formed that one side will be in the top of one slot and the

other side in the bottom of another slot, approximately a pole pitch away. The coils are completely insulated before they are placed into the slots.

The method of placing the armature coils into the slots is clearly

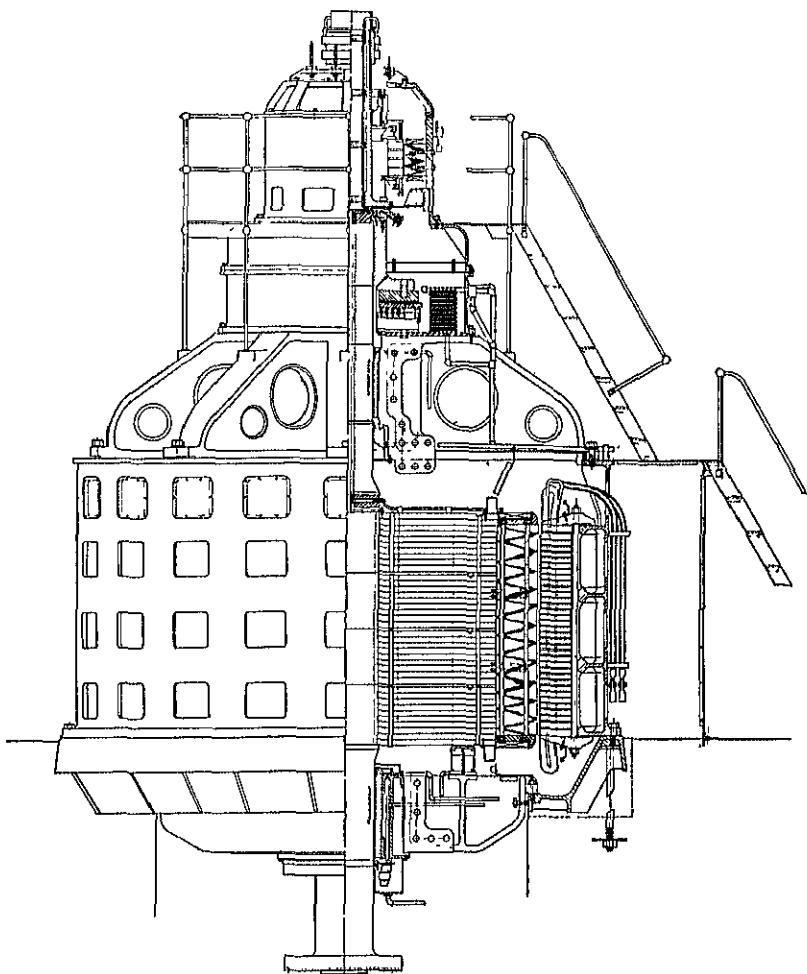


FIG. 89.—Vertical waterwheel-driven generator with direct connected exciter—
30,000 kva, 300 r.p.m., 24 poles, 11,000 volts.

shown in Fig. 91, which is a portion of a partly wound armature for a small-capacity, slow-speed machine. For turbo-generators, the armature coil end-connections are very long and the coils must be supported

to prevent distortion caused by heavy over-loads or short-circuits. Figure 92 shows a partly wound armature for a turbo-generator and

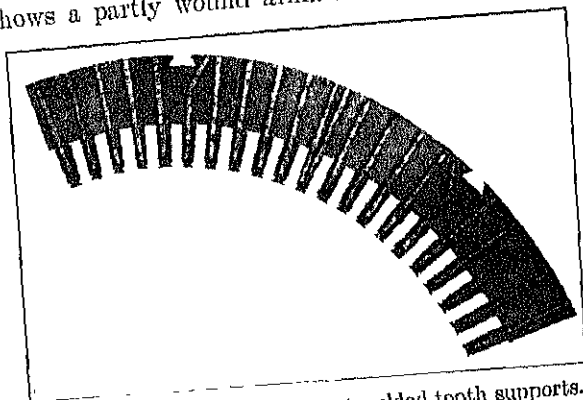


FIG. 90.—One segment with spot-welded tooth supports.

shows the method of bracing the armature coil end-connections. For large-capacity salient-pole machines, the armature coil end-connections must be supported in a similar manner.

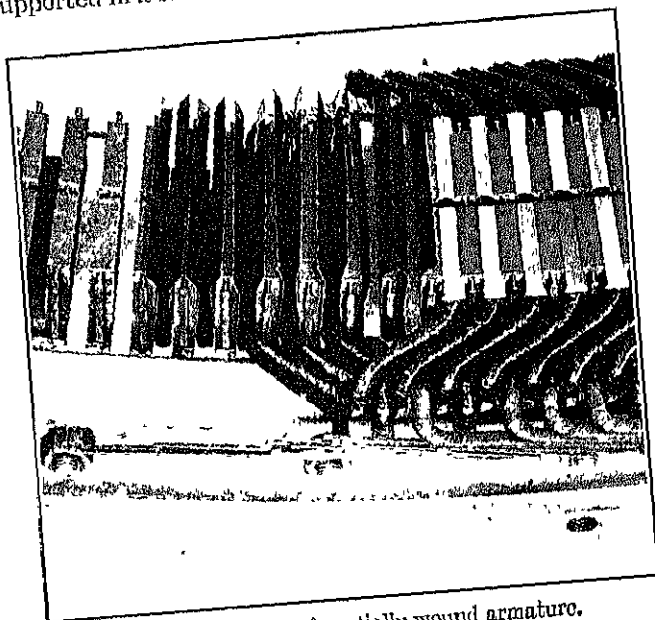


FIG. 91.—Portion of partially wound armature.

Armature Frame.—The type of construction generally employed for the armature frame of synchronous machines is shown in Fig. 93. Large

The armature frame is either of cast iron or built up of welded rolled steel.²

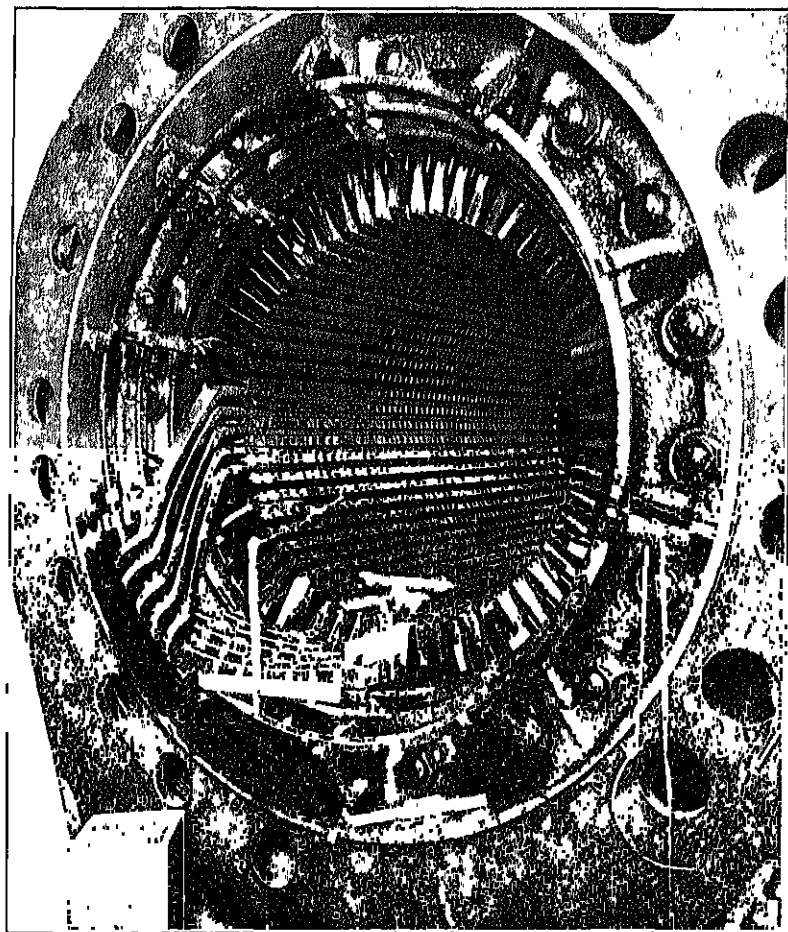


FIG. 92.—Partly wound turbo-generator armature—25,000 kva, 1800 r.p.m., 13,200 volts.

Field: *Non-Salient-Pole Machines.*—For large machines the rotor is often a solid steel forging with slots milled into it for the field winding. A completely machined, forged-steel rotor, without the field winding, for a 12,500-kva, turbine generator is shown in Fig. 94. For small machines,

² General Electric Review, July, 1927, Vol. 30, p. 330.

the rotor is often built up of sheet-steel punchings assembled on the shaft. Figure 95 shows a detail drawing of a rotor punching for a 375-kva, 2-pole turbine generator.

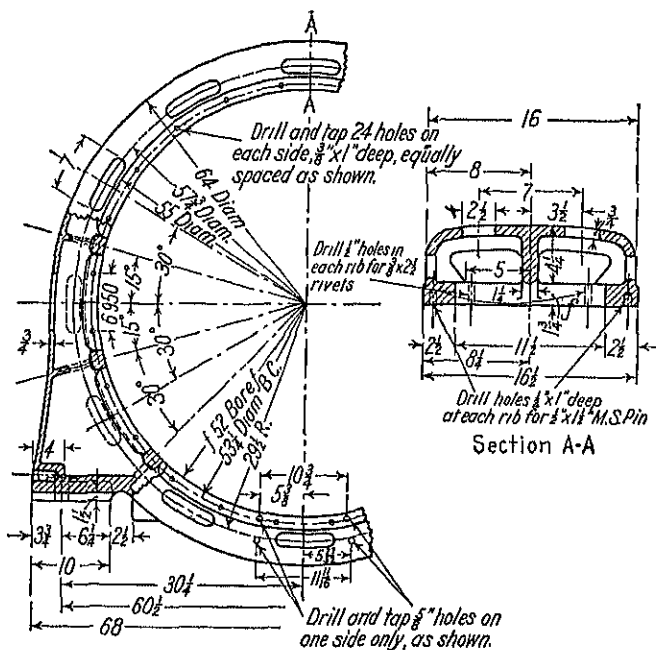


FIG. 93.—Detail drawing of armature frame.

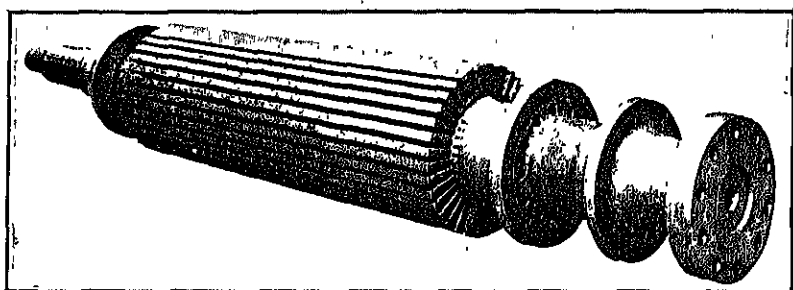


FIG. 94.—Completely machined rotor without winding for 12,500-kva turbo-generator.

The field winding is built up of bare ribbon copper, with mica insulation between turns and between field core and coils. The method of

the high peripheral speeds, heavy metal wedges are used to seal the rotor

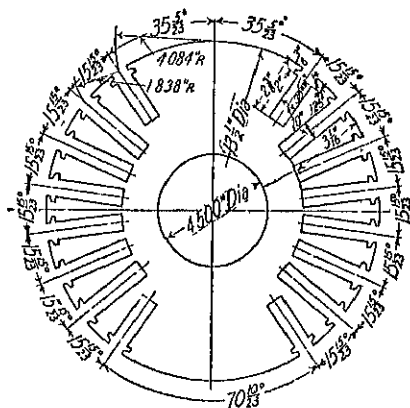


FIG. 95.—Rotor-punching, 375-kva, 3600-r.p.m. turbine generator.

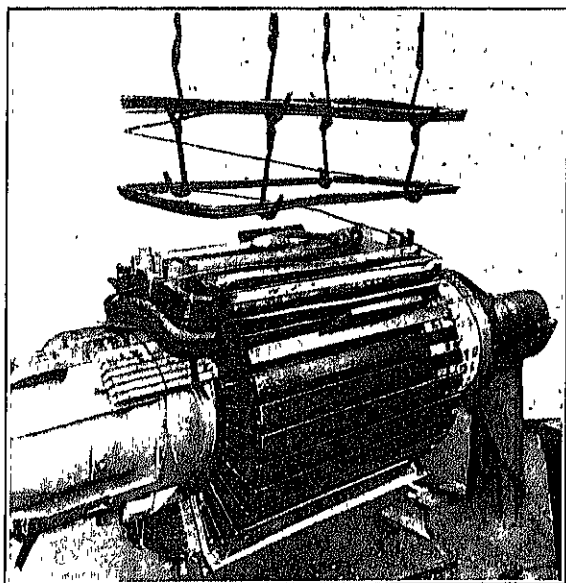


FIG. 96.—Method of placing field coils into slots of turbo-rotor.

slots. The end-connections of the field windings are insulated with mica tape and covered with aluminum saddles, as shown in Fig. 97.

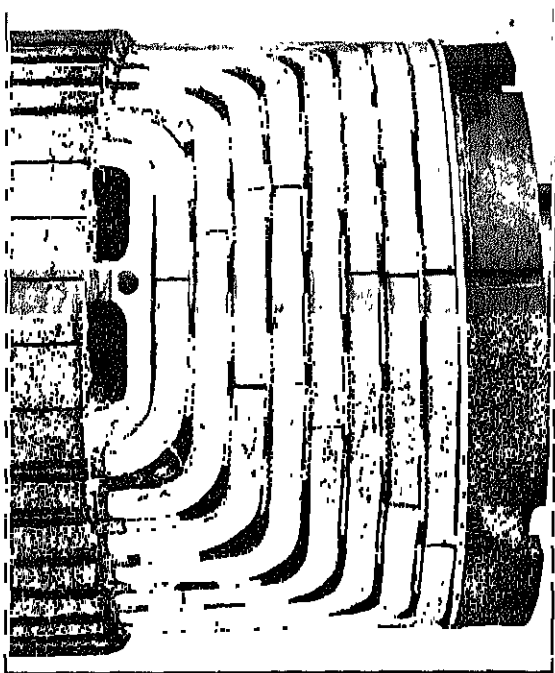


FIG. 97.—Field winding end-connections with aluminum saddles in place.

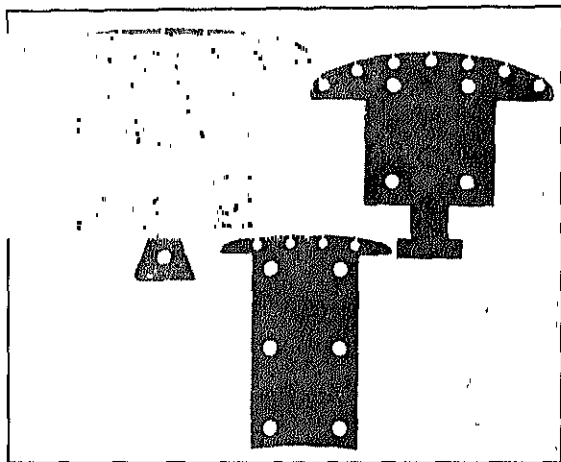


FIG. 98.—Field pole punchings.

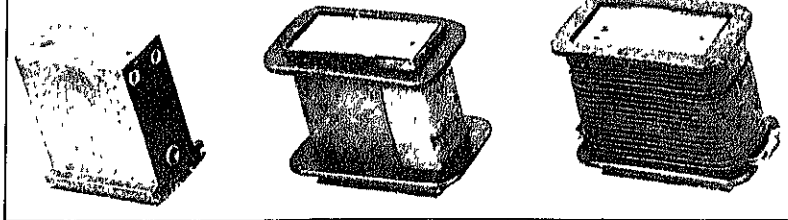


FIG. 99.—Bare pole, insulated pole, and complete wire-wound pole for a 210-kva, 48-pole generator

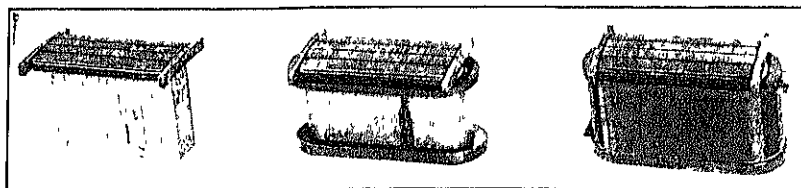


FIG. 100.—Bare pole, insulated pole, and complete ribbon-wound pole for 375 kva 36-pole generator.

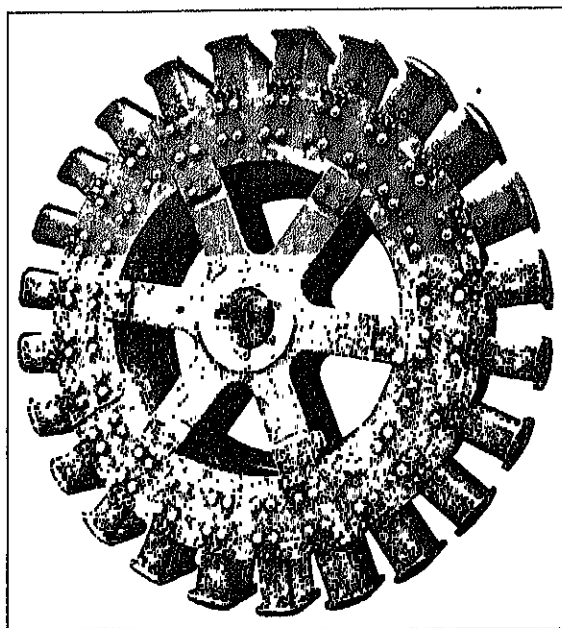


FIG. 101.—Rotor spider with laminated rim.

the aluminum-covered end-connections, as shown in Fig. 87.

Salient-Pole Machines.—The field poles of salient-pole machines are built up of sheet-steel punchings riveted together. The thickness of the sheet used is generally 0.019 to 0.050 in. The poles are either bolted or keyed to the field spider. Figure 98 shows a number of pole punchings and illustrates the methods used to fasten the field poles to the spider. The holes near the surface of the pole shoe are for the squirrel cage starting winding for synchronous motors.

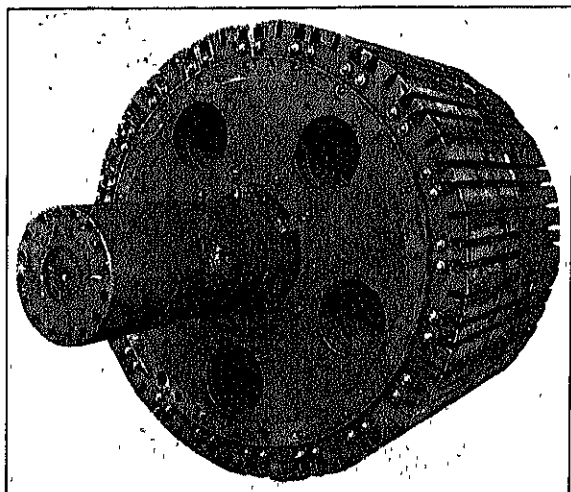


FIG. 102.—Spider built up of $\frac{1}{4}$ -in. steel plate punchings for 33,000-kva, 360-r.p.m., vertical type generator.

The field windings are wound either with d.c.c. copper wire or with bare copper strap wound on edge. A bare pole, insulated pole, and wound pole for a d.c.c. copper wire field winding are shown in Fig. 99. Figure 100 shows the same details but for a strap copper field winding.

Spider.—The spider, on which the field poles are mounted, is either of cast iron, cast steel, rolled steel, or built up of steel plates. The rim of the spider must carry the flux which passes between poles and must therefore have a high permeability besides good mechanical strength. It is, as a rule, difficult to get uniform steel castings, free from flaws, and for that reason rolled steel or built-up spider rims are preferred. A spider with cast-steel hub and arms but with rim built up of $\frac{1}{4}$ -in. steel plate is shown in Fig. 101. The complete spider for a 30,000-kva, 360-r.p.m., 20-pole generator built up of punched steel plates, is shown

with small number of poles, the spider is punched from sheet steel of the same thickness as used for the pole punching. A spider punching and

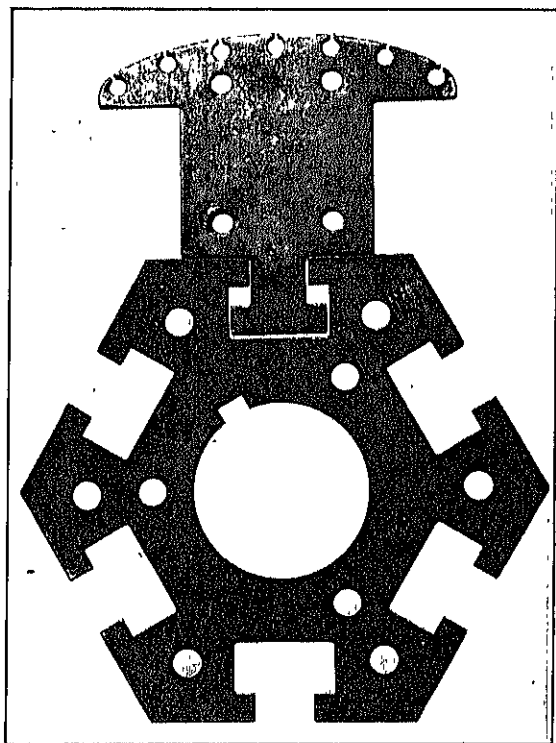


FIG. 103.—Spider punching and one-pole punching for 55 hp., 1200-r.p.m., synchronous motor.

one pole punching for a 55-hp., 6-pole, 1200-r.p.m. synchronous motor are shown in Fig. 103.

CHAPTER X

VOLTAGE FORMULA AND OUTPUT EQUATION

Voltage Formula.—The effective value of the voltage induced in each phase of a winding with one slot per pole and phase with pitch coils is given by the equation:

$$E = 4ff_b w \phi \times 10^{-8} \text{ volts.}$$

Armature windings of synchronous machines always have more than one slot per pole per phase. The voltages induced in the coils per pole and phase lying in adjacent slots are then not in phase and cannot be added algebraically but must be added vectorily. The ratio of the vector sum to the algebraic sum is called the winding distribution factor f_w . The two sides of the coils are not always placed in slots a pole pitch or 180 electrical degrees apart but are often chorded one or more slots. The voltage induced in one coil of the armature winding is proportional to the sine of the half-angle, in electrical degrees, which it subtends. The sine of the half-angle in electrical degrees embraced by a coil is called the pitch factor or chord factor, f_c .

The general formula for the effective value of the induced voltage per phase is then:

$$E = 4ff_b f_w f_c w \phi \times 10^{-8} \text{ volts.} \quad (132)$$

Just as for direct-current machines, it is often convenient to use the hypothetical total flux instead of the flux per pole (see page 14). The hypothetical total flux,

$$\phi_t = \frac{\phi p}{f_a} \text{ lines.}$$

From formula 132,

$$\phi = \frac{E \times 10^8}{4ff_b f_c f_w w}$$

and

$$\phi_t = \frac{E p \times 10^8}{4ff_b f_c f_w f_a w} \text{ lines.}$$

It is generally more convenient to use conductors in series per phase

frequency.

$$w = \frac{N}{2}$$

and

$$f = \frac{np}{2 \times 60}$$

Making these substitutions,

$$\phi_t = \frac{E \times 60 \times 10^8}{nNf_b f_w f_a}$$

The form factor f_b , winding distribution factor f_w , and flux distribution factor depend only upon the number of slots and the shape of the air gap flux distribution curve and are not affected by changes in the number of conductors per phase or the coil throw. These factors can therefore be combined into one factor, called the winding constant,

$$C_w = f_b f_w f_a \quad (133)$$

and then

$$\phi_t = \frac{E \times 60 \times 10^8}{nNf_a C_w} \text{ lines.} \quad (134)$$

Output Equation.—For alternating-current machinery, the terminal current I is equal to the armature current I_a . The armature output for a 3-phase generator expressed in kilovolt-amperes is,

$$Kva = EIm \times 10^{-3}. \quad (135)$$

From formula 134,

$$E = \frac{\phi_t n N f_a C_w}{60 \times 10^8} \text{ volts.}$$

Substituting into equation 135,

$$Kva = \frac{\phi_t n N f_a C_w Im}{60 \times 10^{11}}$$

The hypothetical total flux may be expressed in terms of the gap area times the air gap density,

$$\phi_t = \pi D l B_g.$$

If Q equals the ampere conductors per inch of armature circumference, then

$$INf_a m = \pi DQ$$

and

$$Kva = \frac{\pi D l B_g n \pi D Q C_w}{60 \times 10^{11}}$$

or

$$\frac{D^2 l n}{Kva} = \frac{6.08 \times 10^{11}}{C_w Q B_g}. \quad (136)$$

has been shown for the direct-current machine, page 16, the tooth density is directly proportional to the air gap density. For high-voltage machines, it will therefore be necessary to use a lower air gap density than for low-voltage machines, because of the greater amount of slot space required for insulation. A high air gap density will lead to high densities in the magnetic circuit and high armature tooth losses. Too low an air gap density will, of course, lead to an uneconomical use of the magnetic circuit. The density for the air gap for 60-cycle synchronous machines will generally lie between the limits:

$$B_g = 35,000 \text{ to } 55,000 \text{ lines per sq. in.}$$

When beginning a design of a motor or generator, an air gap density of 43,000 lines per sq. in. is generally a satisfactory value to assume. For frequencies below 60 cycles per sec., the above values may be increased slightly. For 25-cycle machines, the values of B_g given above may generally be increased from 10 to 15 per cent.

The ampere conductors per inch of armature circumference determine armature reaction and, for a given type of construction, they determine the armature temperature rise. A large value of Q leads to a high leakage reactance and to a large value of armature cross and demagnetizing ampere-turns. Since the voltage regulation of a generator depends upon armature reaction, it follows that low values of Q must be used when good voltage regulation is desired. Modern power systems are generally operated with some form of automatic voltage regulator and only reasonably good regulation is required. Also, generators designed for very good regulation are sensitive to rapid load changes and are difficult to operate in parallel with other machines. For well-designed synchronous generators the voltage regulation is about 20 to 25 per cent, at 100 per cent power factor. The curves, Fig. 104, give average values of Q for 60-cycle synchronous generators for voltages of 3000 volts and less. For higher voltages, lower values of Q must be used; for frequencies below 60 cycles per sec. they may be increased.

For synchronous motors, the ampere conductors per inch of armature circumference given in Fig. 104 may be increased from 10 to 15 per cent.

By substituting average values for C_w , Q , and B_g , equation 136 becomes,

$$\frac{D^2 l n}{K v a} = C^* \quad (137)$$

$$C = \frac{6.08 \times 10^{11}}{C_w Q B_g}$$

constant are given by the curves in Fig. 105 for 60-cycle, salient-pole, synchronous machines, for 3000 volts and below.

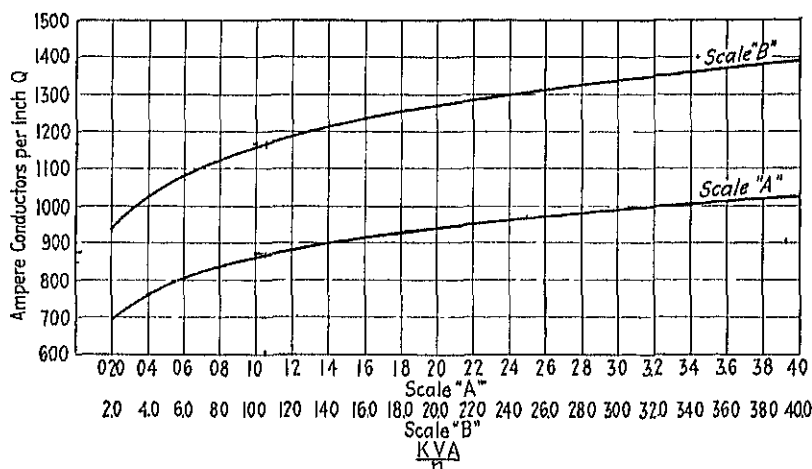


FIG. 104.—Ampere conductors per inch of armature gap circumference for 60-cycle synchronous machines for 3000 volts and below.

In formula 137, Kva is the armature kilovolt-ampere output. Since the armature resistance drop is only a very small percentage of the

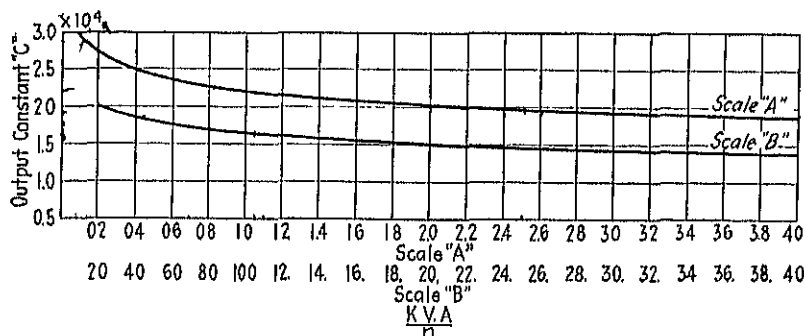


FIG. 105.—Approximate output constants 60-cycle, salient-pole, synchronous machines, 3000 volts and below

terminal voltage for synchronous machines, the rated Kva output may be used in this formula for a generator. For a synchronous motor the Kva input may be used.

Armature Diameter and Length.—With the output constant known, the product, D^2l , can be easily calculated by formula 137. Either the diameter or the length may be assumed and the other dimension calculated.

For high-speed machines, the diameter may be limited by the peripheral speed. For synchronous machines, peripheral velocities as high as safe mechanical construction will permit may be used. Peripheral speeds of 20,000 to 25,000 ft. per min. are commonly employed for turbo-generators. For salient-pole machines the peripheral speed is generally much lower, but values as high as 12,000 to 15,000 ft. per min. are possible.

The ratio of armature length to pole pitch is generally about as follows:

$$\frac{l}{\tau} = 0.80 \text{ to } 2.5.$$

The small values apply to small-capacity machines and the large values to the large capacities. For large-capacity turbo-generators larger values than given above may be required, to avoid excessive peripheral speeds.

The pole pitch,

$$\begin{aligned}\tau &= \frac{\pi D}{p} \\ \frac{l}{\tau} &= (0.80 \text{ to } 2.5) \\ l &= \frac{\pi D}{p}(0.80 \text{ to } 2.5).\end{aligned}$$

Substituting this expression for l into equation 137,

$$D^2 \frac{\pi D}{p}(0.80 \text{ to } 2.5) = \frac{Kva}{n} C$$

or

$$D = \sqrt[3]{\frac{Kva \, p \, C}{\pi(0.80 \text{ to } 2.5)n}}. \quad (138)$$

The values of the ratio armature length to pole pitch are not intended to give the limits for the armature dimensions, but are intended primarily to help the beginner to choose suitable armature dimensions. When in doubt as to the most suitable armature diameter and length for a given Kva and speed, the only satisfactory method is to make preliminary calculations for two or more machines with different dimensions and

choose the one that will give good operating characteristics for a reasonable cost of construction.

Design of Pole Shoe.—The shape of the air gap flux distribution curve depends upon the shape of the pole shoe and the per cent pole embrace. The harmonics present in the voltage wave of synchronous machines depend largely upon the flux distribution in the air gap. There are also harmonics present in the voltage wave produced by the pulsations of the air gap flux caused by the armature slots. A flux distribution curve which decreases gradually to zero on the center line between two poles can be obtained by gradually increasing the air gap from the center or near the center of the pole to the pole tips. Poles not carefully beveled at the pole tips with a large per cent pole embrace may lead to magnetic noises. This is not the only cause of noise in synchronous machines; the number of armature slots per pole or per pole arc has an important effect upon the noise, as will be discussed later.

The per cent pole embrace for synchronous machines is generally from 65 to 75. In general, 70 to 72 per cent pole embrace is most satisfactory for both generators and motors; higher values lead to excessive field leakage. For synchronous motors with heavy pole shoes to accommodate the squirrel cage starting winding, it may sometimes be necessary to use the lower value of per cent pole embrace, to avoid excessive field leakage.

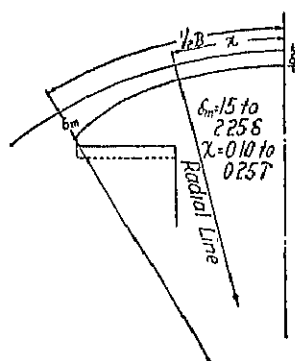


FIG. 106.

A satisfactory air gap flux distribution curve is generally obtained when the pole shoe is shaped as indicated in Fig. 106. For generators requiring no damper winding in the pole faces, the tip of the pole may be rounded off, as shown by the full line, Fig. 106. For synchronous motors and generators with damper windings, a heavier pole tip is generally required. A larger radius can then be used to round off the tip, or the tip may be shaped as indicated by the dotted line, Fig. 106.

Construction of No-load Field Form.—The flux distribution curve in the air gap of synchronous machines is derived from the flux plot in exactly the same way as described for direct-current machines (page 22). The air gap length can be estimated with the help of the curves, Fig. 107, which give average values of air-gap length for salient-pole, synchronous machines. For the flux plot, a full-scale drawing should be made of one-half of the pole shoe, with proper air gap clearance between pole and armature surface. To obtain the flux distribution on the armature sur-

face, the space between pole face and armature must be divided into approximately equal squares by flux and equipotential lines. The method of plotting magnetic fields, with practical applications to salient-pole synchronous machines, is well explained in three excellent papers presented at the winter convention of the A.I.E.E.¹

The flux plot for a 2500-kva, 225-r.p.m. sample generator design is shown in Fig. 108. From this flux plot, the air-gap flux distribution curve shown in Fig. 109 is obtained, in the manner described on page 24. For some purposes, the approximate method of mapping the magnetic field, described on page 25, is sufficiently accurate.

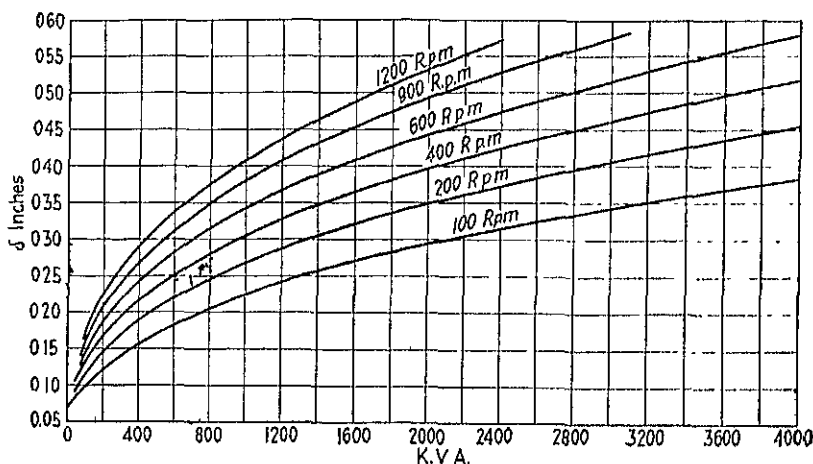


FIG. 107.—Approximate air-gap lengths for 60-cycle, salient-pole, synchronous machines.

When making the flux plot, the armature is assumed to be a smooth surface. Open armature slots produce deep notches in the top of the field form, as shown in Fig. 110, which is the no-load air gap flux distribution curve of a 55-hp, 1200-r.p.m. synchronous motor, taken with an oscillograph.

Flux Distribution Factor and Form Factor.—The ratio of the area under the flux distribution curve to the area of a rectangle with same base and maximum ordinate is called the air gap flux distribution factor. This factor can be found by either of the two methods given on page 26, or by analyzing the flux wave by the Fourier Series. The calculations for the analysis of the field form are made as shown in Table XIII, which

¹ "Graphical Determination of Magnetic Fields," presented at winter convention, A.I.E.E., New York City, Feb. 7-11, 1927.

TABLE XIII

B_x	$\sin x$	$\sin 3x$	$\sin 5x$	$\sin 7x$	$B_x \sin x$	$B_x \sin 3x$	$B_x \sin 5x$	$B_x \sin 7x$
$H_{x11} = 7.5$	0.130	0.383	0.609	0.793	0.98	2.88	4.57	5.91
$H_{x10} = 17.0$	0.250	0.707	0.966	0.996	4.50	12.15	17.00	17.00
$H_{x9} = 30.5$	0.383	0.924	0.924	0.383	11.60	28.20	28.20	11.60
$H_{x8} = 48.0$	0.500	1.000	0.500	-0.500	21.00	18.00	24.00	-21.00
$H_{x7} = 08.0$	0.000	0.024	-0.130	-0.991	41.10	62.80	-8.83	-67.40
$H_{x6} = 83.0$	0.707	0.707	-0.707	-0.707	58.70	58.70	-58.70	-58.70
$H_{x5} = 91.0$	0.703	0.383	-0.991	0.130	74.80	36.00	-93.10	12.22
$H_{x4} = 100.0$	0.866	0.000	-0.866	0.866	86.60	00.00	-86.60	86.60
$H_{x3} = 100.0$	0.924	-0.383	-0.383	0.924	92.40	-38.30	-38.30	92.40
$H_{x2} = 100.0$	0.996	-0.707	0.259	0.259	99.60	-70.70	25.90	25.90
$H_{x1} = 100.0$	0.991	-0.924	0.793	-0.609	99.10	-92.40	79.30	-60.90
$H_{x0} = 100.0$	<u>0.500</u>	<u>-0.500</u>	<u>0.500</u>	<u>-0.500</u>	<u>50.00</u>	<u>-50.00</u>	<u>50.00</u>	<u>-50.00</u>
					610.63	-2.37	-56.50	-0.25

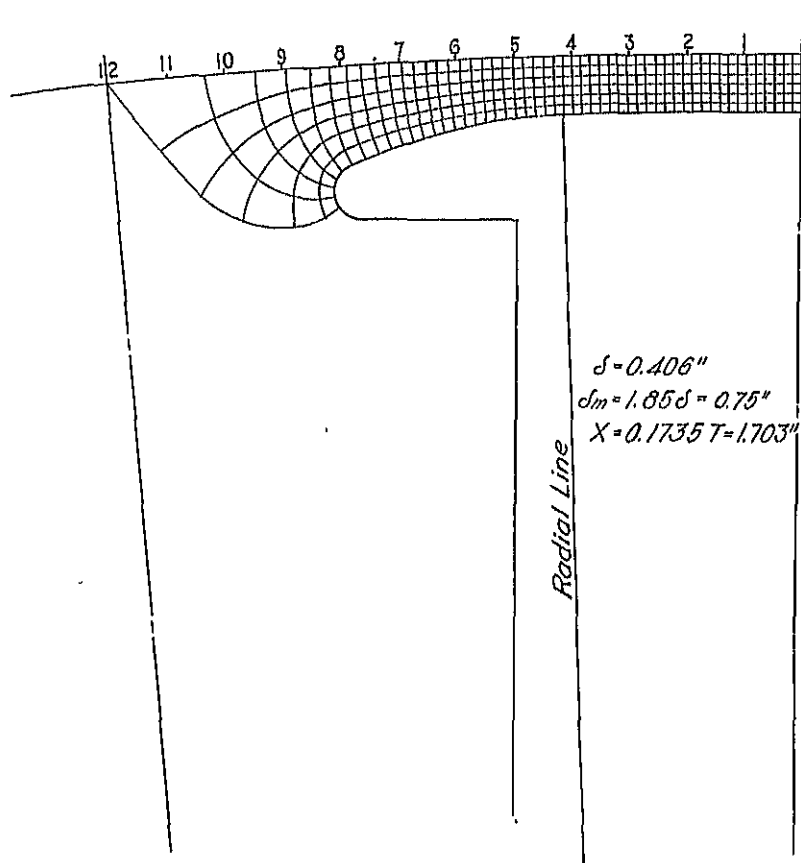


FIG. 108.—Flux plot for 2500-kva, 225-r.p.m., 32-pole generator.

are for the flux wave shown in Fig. 109. The flux distribution curve is plotted with abscissas in electrical degrees, the ordinates B_{x_1} , B_{x_2} , etc.,

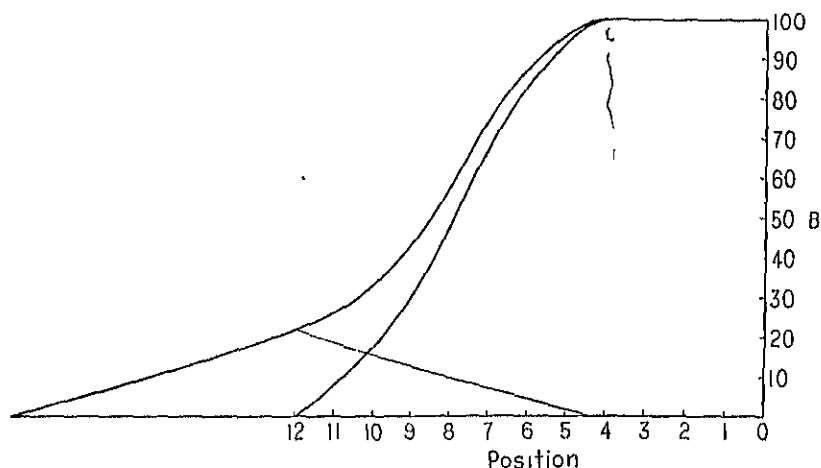


FIG. 109.—Air gap flux distribution curve for 2500-kva, 225-r.p.m., 32-pole generator.

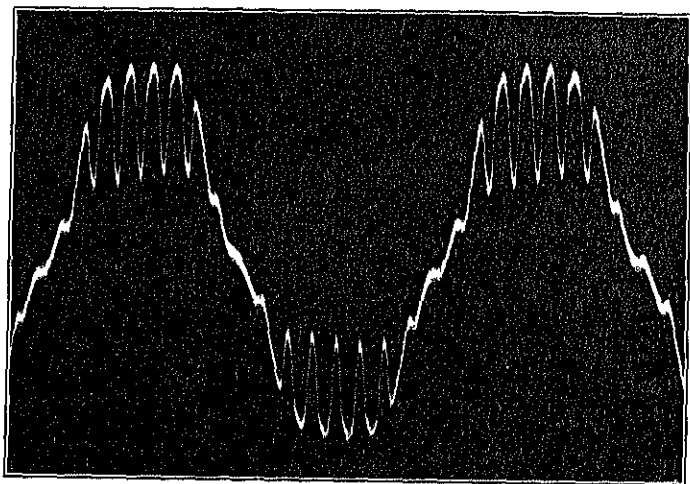


FIG. 110.—Air gap flux distribution curve of 55-hp, 1200-r.p.m., synchronous motor.

being read for every 7.5 electrical degrees. Since the flux distribution curve is symmetrical about the center line of the pole, the even har-

monies drop out. The equations for the fundamental, third, fifth, and seventh harmonics then are,

$$B_1 = \frac{1}{6}(B_{x_{11}} \sin 7.5^\circ + B_{x_{10}} \sin 15^\circ + \dots + \frac{1}{2}B_{x_0} \sin 90^\circ)$$

$$B_3 = \frac{1}{6}(B_{x_{11}} \sin 22.5^\circ + B_{x_{10}} \sin 45^\circ + \dots + \frac{1}{2}B_{x_0} \sin 3 \times 90^\circ)$$

$$B_5 = \frac{1}{6}(B_{x_{11}} \sin 37.5^\circ + B_{x_{10}} \sin 75^\circ + \dots + \frac{1}{2}B_{x_0} \sin 5 \times 90^\circ)$$

$$B_7 = \frac{1}{6}(B_{x_{11}} \sin 52.5^\circ + B_{x_{10}} \sin 105^\circ + \dots + \frac{1}{2}B_{x_0} \sin 7 \times 90^\circ)$$

$$B_1 = \frac{640.63}{6} = 106.8$$

$$B_3 = \frac{-2.37}{6} = -0.40$$

$$B_5 = \frac{-56.56}{6} = -9.41$$

$$B_7 = \frac{-9.25}{6} = -1.54$$

$$B_x = B_1 \sin x + B_3 \sin 3x + B_5 \sin 5x + B_7 \sin 7x.$$

The flux wave, fundamental, third, fifth, and seventh harmonics are shown in Fig. 111.

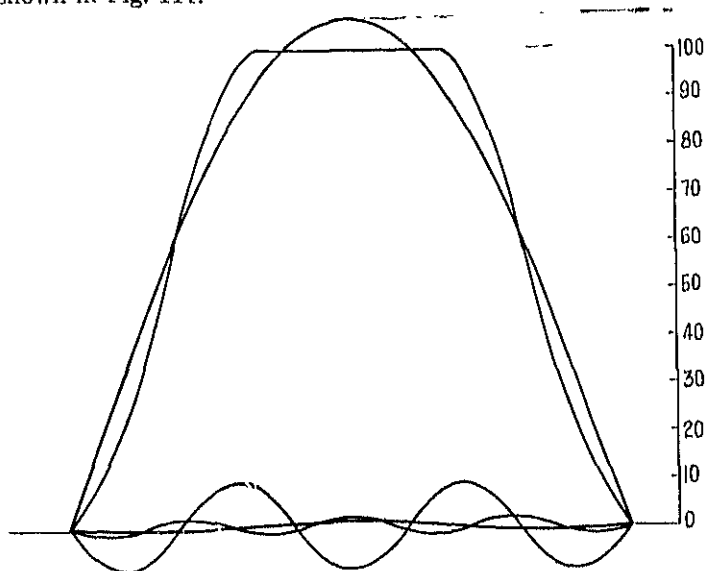


FIG. 111.—Air gap flux wave, fundamental, third, fifth and seventh harmonics for 2500-kva., 225-r.p.m. generator.

The average value, effective value, and maximum value of the flux wave are calculated from the equation for B_x as follows:

$$\begin{aligned} B_a &= \frac{1}{\pi} \int_0^\pi B_x dx = \frac{2}{\pi} (B_1 + \frac{1}{3} B_3 + \frac{1}{5} B_5 + \frac{1}{7} B_7) \\ &= \frac{2}{\pi} (106.8 - \frac{1}{3} 0.40 - \frac{1}{5} 9.41 - \frac{1}{7} 1.54) \\ &= 66.6 \end{aligned}$$

$$\begin{aligned} B_e &= \sqrt{\frac{1}{\pi} \int_0^\pi B_x^2 dx} = \sqrt{\frac{1}{2} (B_1^2 + B_3^2 + B_5^2 + B_7^2)} \\ &= \sqrt{\frac{1}{2} (106.8^2 + 0.40^2 + 9.41^2 + 1.54^2)} \\ &= 75.8 \end{aligned}$$

$$B_m = B_{x_0} = 100$$

The flux distribution factor,

$$f_d = \frac{B_a}{B_m} = \frac{66.6}{100} = 0.666.$$

The value of f_d , calculated by the method explained on page 26, is 0.667, which checks the value found by the method given above.

The form factor of the flux wave has been defined as the ratio of the effective or root-mean-square ordinate to the average ordinate. From the analysis of the flux wave, the effective and average values are calculated as shown above:

$$f_b = \frac{B_e}{B_a} = \frac{75.8}{66.6} = 1.14.$$

The root-mean-square ordinate can be calculated also from the flux distribution curve, by dividing the base line into a number of equal divisions. The square of the mean ordinate of each division divided by the number of ordinates gives the mean-square ordinate. The square root of the mean-square ordinate is the root-mean-square or effective ordinate.

By properly choosing the per cent pole embrace and the bevel of the pole tips, a flux wave with small harmonics can be obtained. Several flux plots were made for the sample design. The dimensions of the

accompanying table.

TABLE XIV

Pole Arc, Per Cent.	δ	δm	x	Maximum Funda- mental	Maximum Third	Maximum Fifth	Maximum Seventh
71.3	0.360	1.605=0.623	0.2147=2.10	112.50	+8.95	-7.17	-4.28
70.0	0.400	1.625=0.600	0.1877=1.83	110.01	+5.22	-7.25	-2.32
68.75	0.400	1.775=0.720	0.1857=1.813	108.50	+2.23	-0.53	-3.08
68.75	0.400	2.005=0.813	0.1857=1.813	101.80	-2.36	-10.02	+0.450
68.75	0.400	1.855=0.75	0.1747=1.71	106.80	-0.10	-0.41	-1.54

In the A.I.E.E. paper ² referred to above, Mr. R. W. Wieseman has given a set of curves from which the maximum value of the third harmonic in per cent of the fundamental can be found when the dimensions of the pole shoe and the per cent pole embrace are known. These curves apply to a pole shoe beveled from the center of the pole instead of from a point at a distance x from the center of the pole, as shown in Fig. 106.

Sample Design: Diameter and Length.—A 2500-Kva, 225-r.p.m., 3-phase, 60-cycle, 2400-volt, salient-pole, synchronous generator is to be designed. The generator is to be of the vertical, waterwheel type and is to have an efficiency at full-load, 100 per cent power factor, rated speed, and voltage not less than 95.6 per cent. The efficiency is to be calculated from the losses in accordance with the A.I.E.E. Standards. The temperature rise of no part of the machine shall exceed 50 degrees C. when operating continuously at rated load, voltage, and speed.

$$\frac{K_{va}}{n} = \frac{2500}{225} = 11.1$$

The output constant is taken from the curve, Fig. 105.

$$C = 1.01 \times 10^4.$$

The number of poles,

$$p = \frac{f \times 2 \times 60}{n} = \frac{60 \times 2 \times 60}{225} = 32.$$

² "Graphical Determination of Magnetic Fields—Practical Applications to Salient Pole Synchronous Machine Design." A.I.E.E. Journal, Vol. 46, May, 1927, p. 433.

as given in Table XV. The calculations for $l/\tau = 2.0$ are as follows:

$$D = \sqrt[3]{\frac{K_{vap} p C}{\pi \times 2 \times n}} = \sqrt[3]{\frac{2500 \times 32 \times 1.61 \times 10^4}{3.14 \times 2 \times 225}} \\ = 96.9 \text{ in.}$$

$$l = \frac{K_{vap} C}{n D^2} = \frac{2500 \times 1.61 \times 10^4}{225 \times 96.9^2} \\ = 19.1 \text{ in.}$$

$$\tau = \frac{\pi D}{p} = \frac{\pi \times 96.9}{32} = 9.52 \text{ in.}$$

For other values of l/τ , the dimensions are as given in the following table:

TABLE XV

l/τ	D	l	τ
1.00	122.0	12.0	12.0
1.50	100.5	16.8	10.46
1.75	101.0	17.5	9.92
2.00	96.9	19.1	9.50
2.25	93.0	20.7	9.13

For this design, the following dimensions are selected:

$$D = 100 \text{ in. and } l = 17.5 \text{ in.}$$

The pole pitch,

$$\tau = \frac{\pi D}{p} = \frac{3.14 \times 100}{32} = 9.82 \text{ in.}$$

The per cent pole embrace is made 68.75 per cent (see page 171); and the pole arc,

$$B = 0.6875 \times 9.82 = 6.75 \text{ in.}$$

The length of air gap is estimated at 0.406 in. (see curves Fig. 107). The flux plot is shown in Fig. 108 and the flux distribution curve in Fig. 109. The flux distribution factor and form factor have been calculated on page 176 and are:

$$f_a = 0.666 \text{ and } f_b = 1.14.$$

CHAPTER XI

ARMATURE WINDING AND INSULATION

THE armature windings used for modern synchronous machines are:

1. Chain windings.
2. Double-layer windings.

Chain Windings.—Chain windings have only one coil side per slot, and the number of armature coils is equal to one-half of the number of slots. The number of conductors per slot may be any integer, even or odd. The coils cannot all have the same shape because the end-connections must lie in different planes. A variety of methods are used to shape the coil end-connections. Figure 112¹ shows a two-bank, 3-phase chain winding, with 4 slots per pole per phase; Fig. 113¹ shows the same winding with the end-connections arranged in three banks. The armature coils for chain windings must be form-wound. More than one winding form is required for each machine because the coils are not all of the same shape. Large clearances can be allowed between the armature coil end-connections, which are very effective in cooling the winding. American practice has discontinued the use of chain windings; they are still used by many European manufacturers.²

Double-Layer Windings.—Each slot has two coil sides. The number of conductors per slot must therefore be a multiple of two. All coils have the same shape, and the number of coils is equal to the number of slots.

When the coils are so formed that the two sides lie a pole pitch apart, they are called pitch coils. Very often the armature coils are so constructed that the sides lie in slots less than a pole pitch apart, in which case they are called chorded coils. Chorded coils are used whenever possible for armature windings of synchronous machines.

¹ Figures 112 and 113 are reproduced from "Die Wechselstromtechnik," by E. Arnold, Vol. III, 2nd ed., pp. 65 and 66, Julius Springer, Berlin.

² For further information on chain windings see "Die Wechselstromtechnik," by E. Arnold, Vol. III, 2nd ed., Julius Springer, Berlin, and "Ankerwicklungen für Gleich- und Wechselstrommaschinen," by R. Richter, Julius Springer, Berlin.

The advantages of chorded windings are:

(1) Chording the armature coils has the effect of changing the number of conductors in the armature winding. By formula 134, page 167, the number of conductors in series per phase,

$$N = \frac{E \times 60 \times 10^8}{\phi_m C_w f_c}.$$

The conductors in series per phase are therefore inversely proportional to the chord factor, f_c . The chord factor is defined as the sine of the

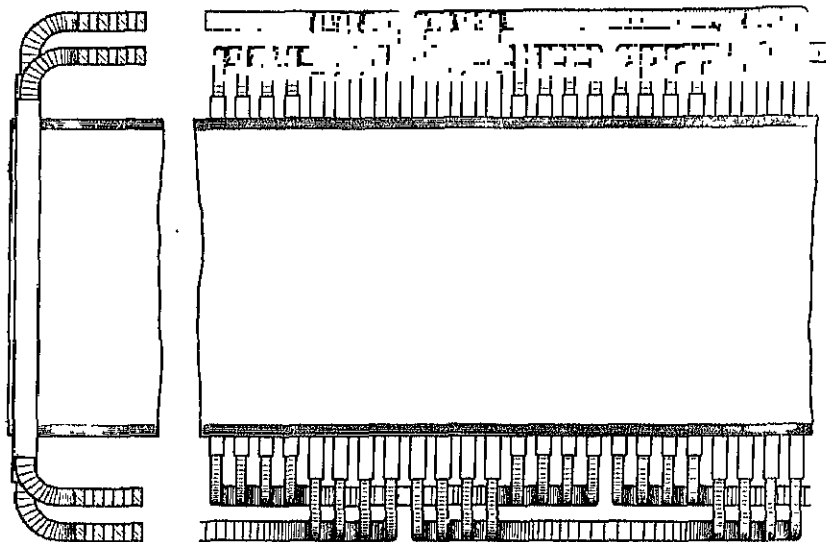


FIG. 112*.—Two-bank, three-phase chain winding with four slots per pole per phase.

* From "Die Wechselstromtechnik," by Dr. Arnold, Vol. III, p. 65, Julius Springer, Berlin.

half-angle, in electrical degrees, spanned by the coil. The pitch coil, which spans 180 electrical degrees, will therefore have as chord factor $f_c = \sin \frac{1}{2} 180^\circ = \sin 90^\circ = 1$ and will have the maximum possible voltage induced. Of the two coils shown in Fig. 114 with 9 slots per pole, the one with a coil throw from slot 1 to 10 spans 9 slots or 180 electrical degrees and $f_c = 1$. The other, with a coil throw from slot 1 to 8, spans 7 slots or $\frac{7}{9} \times 180 = 140$ electrical degrees, and $f_c = \sin \frac{1}{2} 140^\circ = \sin 70^\circ = 0.94$.

When designing the armature winding, one often finds that an odd number of conductors per slot will give the best results. But an odd

³ A.I.E.E. Trans., Vol. 26, Part 2, 1907, p. 1485-1503; also, A.I.E.E. Trans., Vol. 27, Part 2, 1908, p. 1077.

number of conductors per slot can, however, be obtained by using the next larger even number with chorded coils. For

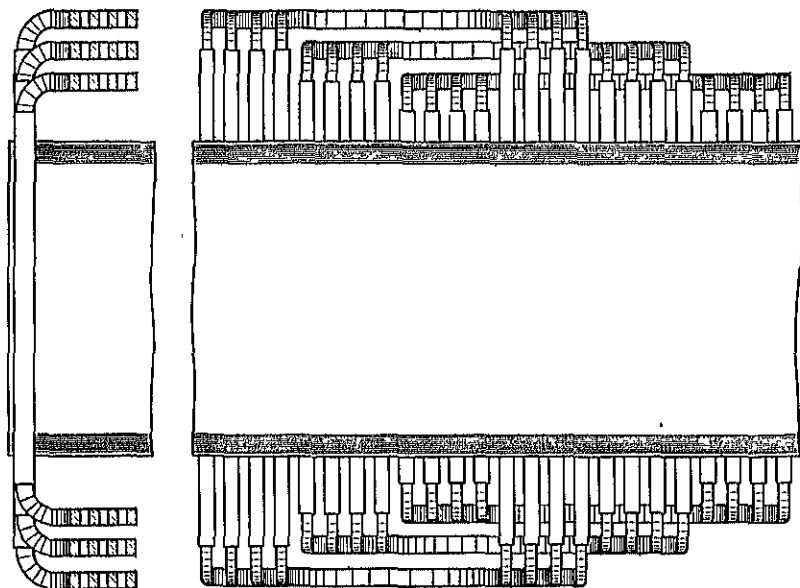


FIG. 113*.—Three-bank, three-phase chain winding with four slots per pole per phase.

*From "Die Wechselstromtechnik," by Dr. Arnold, Vol. III, p. 66, Julius Springer, Berlin.

example, the calculations for the armature winding of a 36-pole, 3-phase generator showed that 189 slots, with 13 conductors per slot, would give the best results. With 12 conductors per slot, the magnetic densities were found to be too high for best results, and with 14 too low. The desired results were obtained by using 14 conductors per slot, with the coils chorded 76.2 per cent of pitch.

(2) The length of the mean-turn and the overall length of the armature coil, parallel to the shaft, are reduced by chording. Figure 114 shows two coils for a winding, with 9 slots per pole, the one with a coil throw from slot 1 to 10 and the other with a coil throw from slot 1 to 8. It is apparent from the figure that the coil with the shorter throw has a shorter mean-turn and a smaller overall length. Reducing the mean-turn of the coils produces a direct saving in

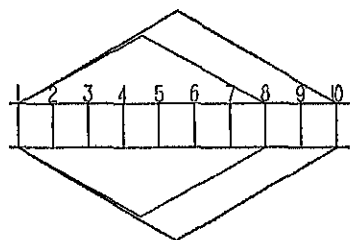


FIG. 114.

copper and reduces the armature resistance. Because of the reduced resistance, the efficiency is higher and armature heating is reduced since heating depends upon the total losses to be dissipated.

(3) For machines with a small number of poles and small diameter machine-wound, "pulled type" armature coils can be used. For 2-pole turbo-generators, for example, a pitch coil will have its sides in slots diametrically opposite. Specially constructed end-connections are required for such a design. By chording the coils, the standard "pulled type" of coil, to be described later, can be used.

(4) By chording the coils, the leakage reactance of the armature

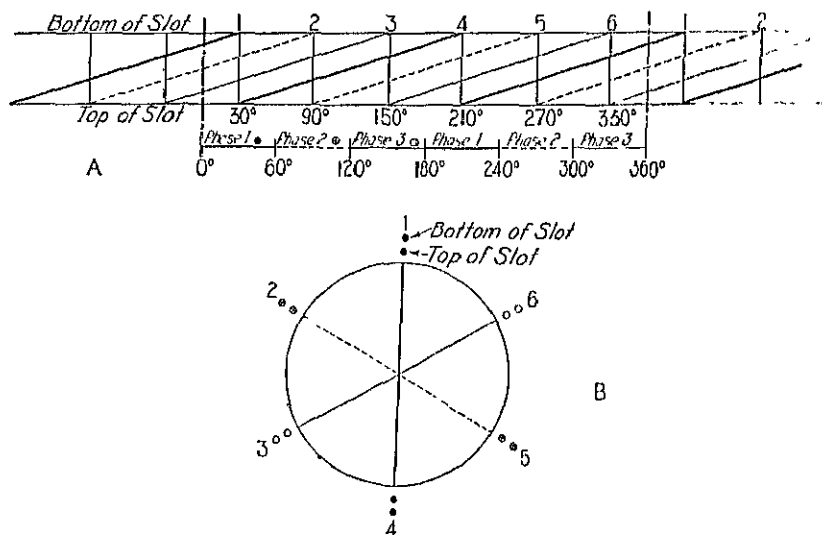


FIG. 115.—Diagram of three-phase winding—one slot per pole per phase coil throw, slot 1-4, $f_w = 1$, $f_c = 1$.

winding is reduced, as can be seen from the leakage reactance formulas, Chapter XIII.

(5) Chording the armature coils improves the generated voltage wave form of synchronous generators.

Graphic Method of Laying Out the Armature Winding.—The armature coils are placed into the slots in 60° phase belts for 3-phase machines and in 90° phase belts for 2-phase machines. The diagram to determine the sequence of the coils is made as shown in Fig. 115A, which is a developed end-view of the armature slots and coil end-connections. The two horizontal lines represent the top and bottom of the slots, and the vertical lines joining them represent the slots. The diagonal lines passing from top to bottom of slot are the coil end-connections. The

aligned at the top of the diagram and the electrical degrees for each slot. The zero or starting point for the diagrams shown is chosen on the center line between two slots. The diagram, Fig. 115, is for a 3-phase winding, with 1 slot per pole per phase or 3 slots per pole with pitch coils. The number of electrical degrees between slots is $180 \div 3 = 60$. It is apparent from the diagram that after passing through 360 electrical degrees, which corresponds to 6 slots or 2 poles, the winding repeats, that is, slot 7 is the same as slot 1. The diagram, therefore, need not be extended beyond 6 slots or 2 poles. The minimum number of poles the winding can be used for is therefore 2. For a pitch winding the coils must span 3 slots and the coil throw is from the top of slot 1 to the bottom of slot 4, etc. All slots from zero to and including 60° must have coil sides in the top belonging to phase 1, all slots from 60° to and including 120° must have coil sides in the top belonging to phase 2, and all slots from 120° to and including 180° must have coil sides in the top belonging to phase 3, and so on, as shown in the diagram. The sequence of the coil sides in the bottom of the slots is automatically taken care of by the coil throw.

From the diagram of the winding, a vector diagram of the voltages induced in the coils is made, as shown in Fig. 115*B*. The circle is drawn with any convenient radius and divided into as many equal parts as there are slots required to make the winding repeat. For the diagram in Fig. 115*A*, the circle must be divided into 6 equal parts because 6 slots are necessary to make the winding repeat. The numbers in Fig. 115*B* are slot numbers. The coil sides in top and bottom of the slots are taken from Fig. 115*A*. The length of the line joining the coil side in the top of slot 1 with the coil side in the bottom of slot 4 is proportional to the voltage induced in coil 1 to 4. Similarly, the length of the line joining the coil side in the top of slot 4 with the coil side in the bottom of slot 1 is proportional to the voltage induced in coil 4 to 1. The vectors 1 to 4 and 4 to 1, Fig. 115*B*, must pass through the center of the circle because the coils are pitch coils and have the maximum possible voltage induced. There are two vectors, both occupying the same position, one for each pole. The vectors for the three phases make an angle of 60° with each other, because the coils are placed into the slots in 60° belts.

Figure 116*A* and *B* shows the winding diagram for the same winding as shown in Fig. 115 but shows the coils chorded one slot. The coil sides in the top of the slots are the same as those in Fig. 115, but those in the bottom of the slots are not the same, because of the different coil throw. The voltage vectors do not pass through the center of the circle but are chords of the circle, which shows that the voltage induced is less than for the pitch coils. If the diameter of the circle is assumed to be 1,

then the voltage induced in each coil is less than the voltage induced in the pitch coils by the ratio of the length of the chords 1 to 3 and 4 to 6 to the diameter of the circle. The length of a chord of a circle is equal to the sine of the half angle which it subtends times the diameter. The chords 1 to 3 and 4 to 6 subtend 120° and the length of each is equal to $\sin \frac{1}{2} 120^\circ = \sin 60^\circ = 0.866$, which is equal to the chord factor $f_c = \sin \frac{2}{3} 90^\circ = 0.866$. The voltage induced in the chored winding is, therefore, 86.6 per cent of the voltage induced in the pitch winding.

For the windings shown in Figs. 115 and 116 the winding distribution

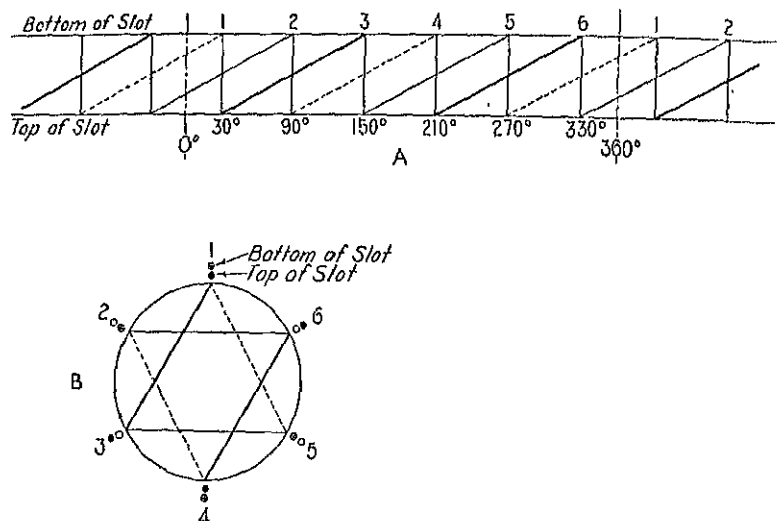


FIG. 116.—Diagram of three-phase winding—one slot per pole per phase—4 throw, slot 1-3.

factor is 1, because there is only one slot per pole and phase. Figure 1 shows the diagram for a 3-phase winding with 2 slots per pole and phase with pitch coils. This winding also repeats every two poles and can therefore be used on a 2-pole machine. There are now 4 voltage vectors for each phase in the vector diagram, one for each of the 4 coils per phase. Since this is a pitch winding, the vectors representing the voltage induced in each coil must pass through the center of the circle. The voltage induced in the two coils for each pole and phase connected in series is not equal to the arithmetical sum of the voltages induced in each of the coils, but is equal to the vector sum of the voltages induced in the two coils, because, as the diagram shows, the voltages in the two coils are

not in phase but differ by 30 electrical degrees. It is obvious from the vector diagram, Fig. 117B, that the vector sum of the voltages induced in the two coils 1 to 7 and 2 to 8 is equal to the sum of the lengths of the two chords 1 to 8 and 2 to 7. The vectors for the two coils under the second pole occupy the same position as the vectors for the first pole. The voltage induced in the 4 coils of each phase is therefore proportional to $4 \sin \frac{1}{2} 150^\circ = 4 \sin 75^\circ = 4 \times 0.966$. The arithmetical sum of the voltage induced in the 4 coils is proportional to 4. Since the chord factor is 1.0, the winding distribution factor, $f_w = \frac{4 \times 0.966}{4} =$

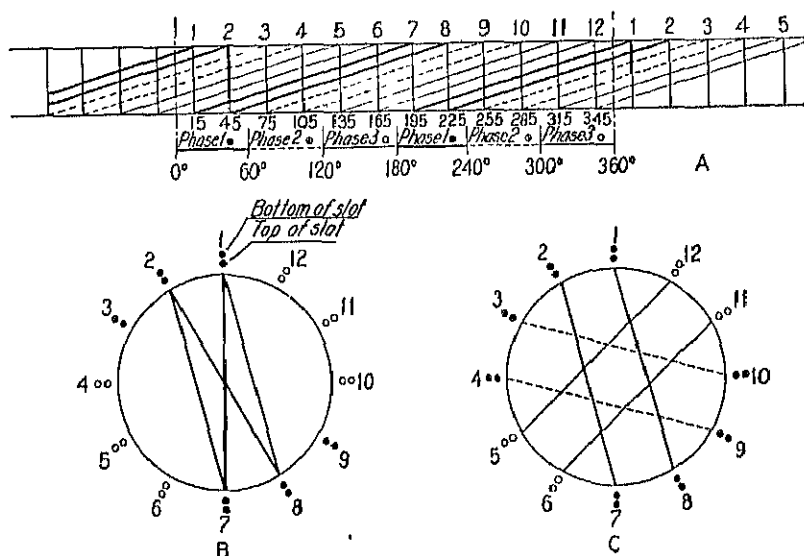


FIG. 117.—Diagram of three-phase winding—two slots per pole per phase—coil throw, slot 1-7.

0.966. The voltage vectors and chords for only one phase are shown in Fig. 117B; the complete vector diagram showing the chords for the three phases is that of Fig. 117C. The chords must always be so drawn that they connect coil sides in the top of a slot belonging to one phase with coil sides in the bottom of a slot on the opposite side of the circle belonging to the same phase. The chords for each phase must be parallel and must make an angle of 60° with the other phases.

Figure 118 shows the vector diagram for the same winding shown in Fig. 117, but with chorded coils. The coil sides in the top of the slots are the same as for the pitch winding. In the bottom of the slot they are not the same because of the shorter coil throw. For the diagram, Fig.

117, the chord factor is 1. The winding distribution factor is equal to the sum of the lengths of the chords divided by the number of chords. The voltage induced in a winding varies directly with $f_w f_c$. The ratio of the sum of the lengths of the chords to the number of the chords is therefore equal to $f_w f_c$. For Fig. 118,

$$f_w f_c = \frac{1-6 + 2-5 + 7-12 + 8-11}{4} = \frac{2 \sin 45^\circ + 2 \sin 75^\circ}{4} = 0.836.$$

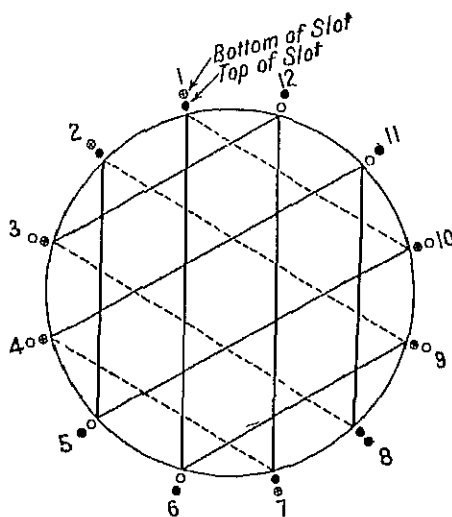


FIG. 118.—Vector diagram of three-phase winding—two slots per pole per phase—coil throw, slot 1-5.

The chord factor can easily be calculated when the coil throw is known. For a coil throw slot 1 to 5 with 6 slots per pole,

$$f_c = \sin \left(\frac{1}{3} \times 90^\circ \right) = 0.866$$

and

$$f_w = \frac{0.836}{0.866} = 0.966.$$

Figure 119 shows the layout for a 2-phase winding, with 4 slots per pole per phase and coil throw slot 1 to 7. The coils are placed in 90° phase belts and the chords for each phase are parallel and make an angle of 90° with the other phase. The chord factor,

$$f_c = \sin \left(\frac{1}{4} \times 90^\circ \right) = 0.924.$$

From Fig. 119B, the winding distribution factor is calculated as follows:

$$f_c f_w = \frac{2 \sin 33.75^\circ + 2 \sin 56.25^\circ + 4 \sin 78.75^\circ}{8} = 0.837$$

$$f_w = \frac{0.837}{0.924} = 0.906.$$

For the windings shown above, the total number of slots is a multiple of the number of poles times the number of phases, that is, the number of slots per pole per phase is an integer. The total number of slots need not

neither need the number of slots per pole per phase be an integer. It may be a mixed number, for example, $2\frac{1}{4}$, $3\frac{1}{2}$, etc.

The method of laying out a winding with a mixed number of slots per pole and phase is exactly the same as for the windings shown above. The windings for which the number of slots per pole per phase is not an integer do not always repeat every two poles. It may be necessary to lay out the winding for 4 or more poles. Figure 120 shows a 3-phase winding, with $2\frac{1}{4}$ slots per pole per phase. The number of slots per pole = $3 \times 2\frac{1}{4} = 6\frac{3}{4}$, and the electrical degrees between slots,

$$\frac{180}{6\frac{3}{4}} = 26\frac{2}{3} \text{ electrical degrees.}$$

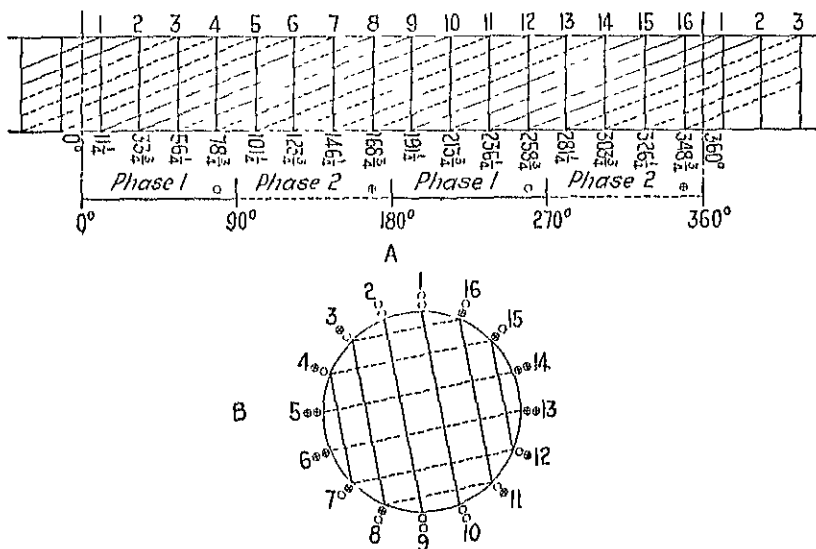


FIG. 119.—Diagram of two-phase winding—4 slots per pole per phase—coil throw, slot 1-7.

The electrical degrees are shown at the top of the slot in Fig. 120A, with the zero or starting point on the center line between two slots. The diagram shows that the winding repeats after passing over 27 slots or 4 poles, that is, slot 28 is the same as slot 1. In the vector diagram, Fig. 120B, the circle is divided into 27 equal parts because there are 27 slots necessary before the winding repeats. The calculations for the winding distribution factor are given in Fig. 120B.

A 2-phase winding with $2\frac{1}{4}$ slots per pole per phase is shown in Fig.

degrees per slot = $\frac{180}{4\frac{2}{3}} = 38\frac{1}{3}$ electrical degrees. The vector diagram and the calculations for the winding distribution factor are shown in Fig. 121B.

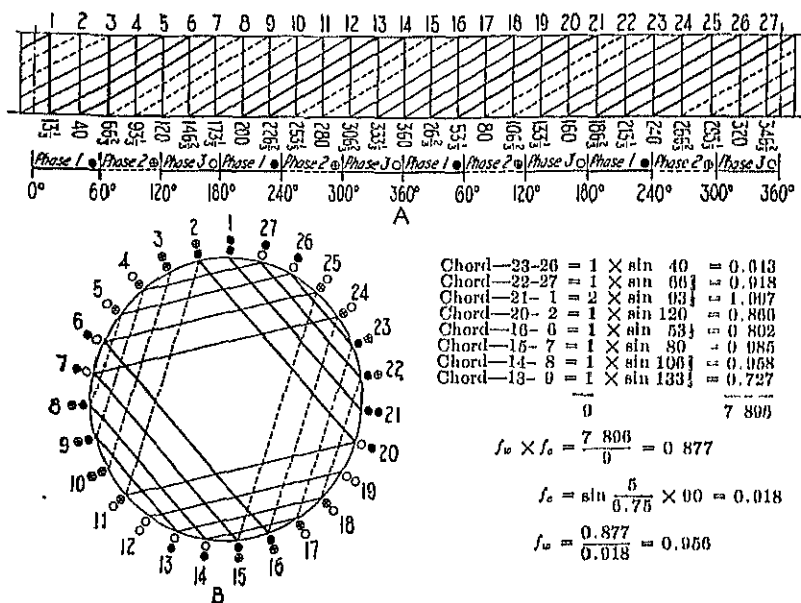


Fig. 120.—Diagram of three-phase winding— $2\frac{1}{3}$ slots per pole per phase—coil throw, slot 1-6.

Not all values of slots per pole per phase can be used for 3-phase and 2-phase windings. When the number of slots per pole and phase is a mixed number, a balanced winding can be obtained only when the denominator of the fraction is not a multiple of the number of phases. For example, $2\frac{1}{3}$ slots per pole per phase can not be used for a 2-phase winding, because 4, the denominator of the fraction, is a multiple of 2. A winding with $2\frac{2}{3}$ slots per pole per phase, for example, can be used for either 2- or 3-phase, because the denominator of the fraction is not a multiple of 2 or 3. This winding repeats every 14 poles, and the minimum number of poles for which it can be used is 14.

The curves, Fig. 122, show the winding distribution factor for 2-phase and 3-phase, double-layer windings. For windings with mixed number of slots per pole per phase, the number of slots required to make

example, the winding shown in Fig. 120 repeats every 27 slots. From

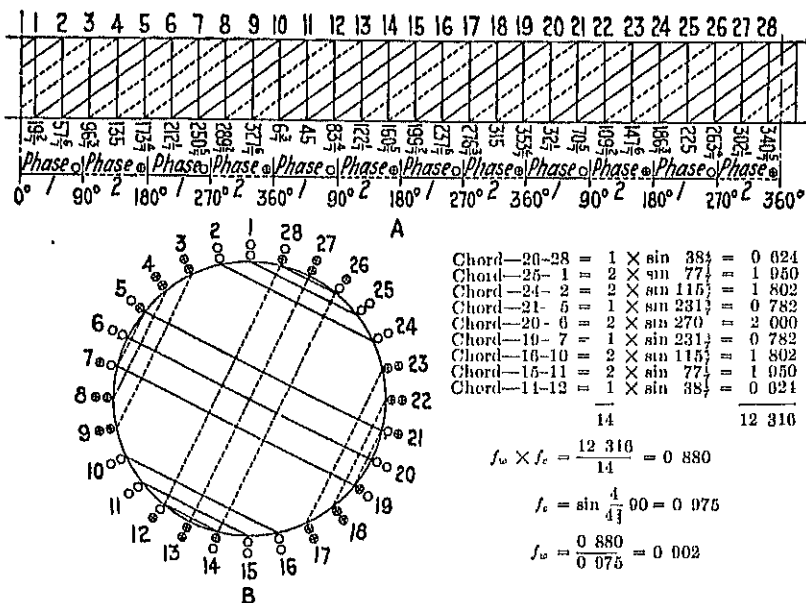


FIG. 121.—Diagram of two-phase winding— $2\frac{1}{2}$ slots per pole per phase—coil throw, slot 1-5.

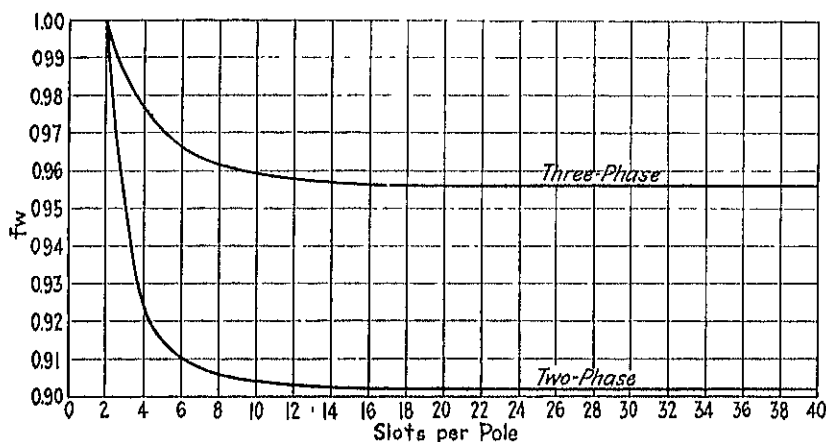


FIG. 122.—Winding distribution factors for two-phase and three-phase windings.

the curve, Fig. 122, $f_w = 0.956$, which is the same as the value given in Fig. 120B.

connected. For synchronous generators, only the star connection is used. The advantages of the star connection have been explained by T. S. Eden⁴ and are as follows: (1) Currents of triple frequency or multiples of triple frequency can not flow in star-connected windings with ungrounded neutral. (2) In general the e.m.f. wave form is nearer a true sine wave. (3) It is possible to bring out a lead from the neutral

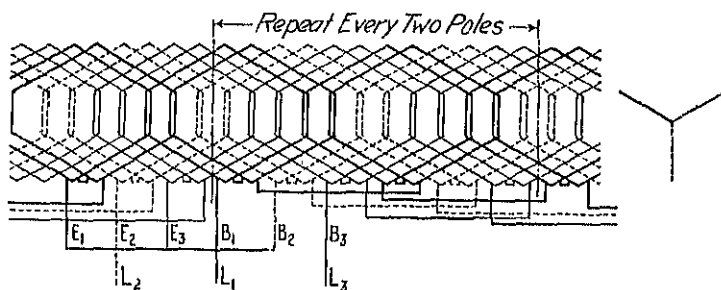


FIG. 123.—Connection diagram for three-phase winding—two slots per pole per phase—one circuit star.

point, which is useful for various purposes. (4) Grounding the neutral reduces the potential strain on the insulation of the winding, permitting reduced thickness of insulation.

The coils per phase of both 2-phase and 3-phase windings can always be connected in series, and in most cases they can also be connected in parallel, to form more than one circuit. For high voltage machines,

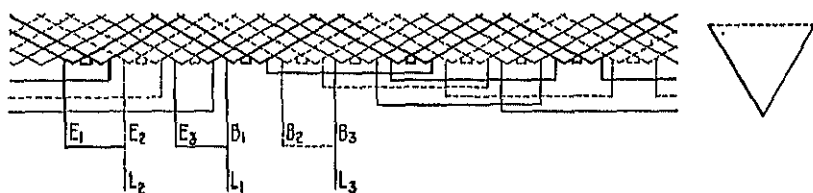


FIG. 124.—Connection diagram for three-phase winding—two slots per pole per phase—one circuit delta.

the one circuit winding, with all the coils per phase connected in series, should always be used so that the voltage per turn will not be too high. The connection diagram for the winding layed out in Fig. 117 is shown in Fig. 123, with star connection and one circuit. The ends of phases 1 and 3 and the beginning of phase 2 form the neutral. The beginning of phases 1 and 3 and the end of phase 2 are the line leads. The one cir-

⁴ A.I.E.E. Trans., Vol. 33, Part I, 1914, p. 803.

case, these connections for this same winding is shown in Fig. 124. In this diagram only the coil leads are shown. The two-circuit, star-connection is shown in Fig. 125. When more than two circuits are used, the connections are made as shown in Fig. 126, which is the connection

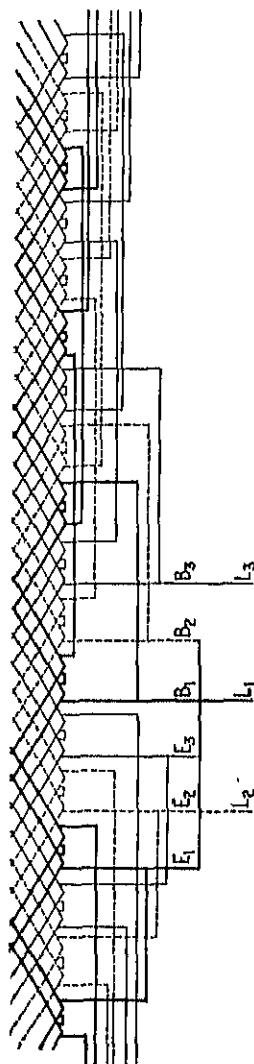


Fig. 125.—Connection diagram for three-phase winding—two slots per pole per phase—two circuit star.

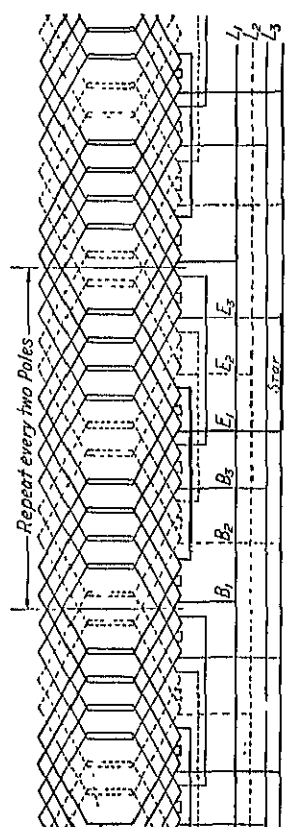


Fig. 126.—Connection diagram for three-phase winding—two slots per pole per phase—number of circuits = $p/2$.

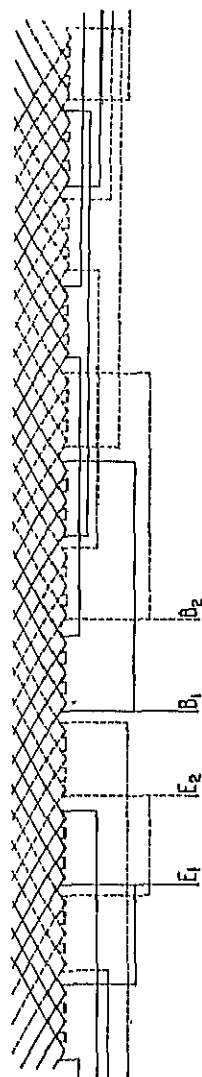


Fig. 127.—Connection diagram for two-phase winding—three slots per pole per phase—two circuits.

diagram for the two-slot per pole per phase winding laid out in Fig. 117, with as many circuits as there are pairs of poles. For windings with a mixed number of slots per pole per phase, the number of circuits possible is often very much limited. For example, a winding with $2\frac{1}{2}$ slots per

pole per phase does not repeat until 4 poles have been passed over. The minimum number of poles that this winding can be used for is therefore 4, and only one circuit is possible. On an 8-pole machine, the maximum number of parallel circuits possible with this winding is 2, etc. It is for this reason that windings for which the number of slots per pole is an integer are often chosen in preference to fractional slot windings. Small synchronous motors and induction motors are generally designed for two voltages, that is, 110 and 220 volts or 220 and 440 volts. To accomplish this, the windings must be so chosen that two circuits can be used for the low voltage and one for the high voltage. As shown above, this is not always possible with fractional slot windings.

The connection diagram for a 2-circuit, 2-phase winding with 3 slots per pole per phase is shown in Fig. 127.

Number of Armature Slots.—The number of armature slots must be an integer and must be such a number that a balanced winding can be obtained. The total number of slots will always be satisfactory for a given number of poles and phases when the numerator of the fraction $\frac{\text{slots}}{\text{poles}}$, reduced to its lowest terms, is a multiple of the number of phases. For example, with 126 slots on a 14-pole machine,

$$\frac{\text{slots}}{\text{poles}} = \frac{126}{14} = 9$$

and a balanced 3-phase winding is possible, because 9 is a multiple of the number of phases. With 120 slots on a 14-pole machine,

$$\frac{\text{slots}}{\text{poles}} = \frac{120}{14} = \frac{60}{7}$$

and a balanced 2-phase or 3-phase winding is possible, because 60 is a multiple of both 2 and 3.

With a small number of armature slots, a smaller number of coils will be required than with a larger number, but the number of turns per coil and, therefore, the slot size will be larger. A small number of slots might therefore lead to a slight saving, because there are fewer coils to wind, form, insulate, place into the slots, and connect. The armature slots affect the flux wave which the armature conductors cut.⁵ The ripples in the flux wave induce harmonics in the voltage wave of generators and produce eddy current losses in the pole faces of motors and generators. The effect of the armature slots upon

⁵ "Die Wechselstromtechnik," Vol. III, 2nd ed., p. 219, Julius Springer, Berlin; British Journal I.E.E., Vol. 37, p. 148, Vol. 39, p. 206, and Vol. 40, p. 413.

the flux wave can generally be reduced by using a large number of narrow slots.

The tooth pitch at the armature surface,

$$t_1 = \frac{\pi D}{S}.$$

It may serve as a guide when choosing the number of armature slots. The slot width is generally equal to or slightly less than the tooth width. For a small tooth pitch, the armature tooth will be narrow. This condition might lead to difficulties in construction, for the reason that it is difficult to support the armature teeth at the ventilating ducts and at the ends of the armature core without obstructing the ventilation. For synchronous motors and generators, the tooth pitch at the armature surface is generally 0.80 to 2.0 in. With a small tooth pitch, the armature coil end-connections are close together, with no space for ventilation between the coils. For high-voltage machines, which are generally built in large capacities, it is, as a rule, desirable to use a large tooth pitch. The effect of the armature slots upon the air gap flux distribution curve is generally quite small for large machines because the air gap length is large.

Armature Coil Construction and Insulation.—The armature coils for synchronous motors and generators are wound with round, square, or rectangular copper wire. For small-capacity, high-voltage machines, which require a large number of turns of small wire, round conductors are often necessary. Whenever possible, square or rectangular conductors are used because they make mechanically stronger coils with smaller air spaces between turns. For large-capacity machines requiring large conductor sections, each conductor is built up of a number of small wires in parallel. By subdividing large conductors, a more flexible coil is obtained, which can be easily formed. The eddy current losses present in large solid conductors are thereby reduced.

For some machines, form-wound coils are used. A winding form with wire-wound coil is shown in Fig. 128. The pulled type of armature coil is used for most machines. This coil is wound on a bobbin, as shown in Fig. 129, and then pulled out to the required shape on a coil pulling machine. Whenever possible, the coils should be wound in such manner that there is only one turn per layer. Fig. 130*A* shows a section of a coil wound with rectangular conductors with only one turn per layer. When the section area of the conductor exceeds approximately 0.100 sq. in. or when it is not possible to obtain satisfactory slot dimensions with one conductor, the arrangement shown in Fig. 130*B* is used. Each conductor is subdivided by using several small wires in parallel,

arranged in such manner that the conductors per layer are connected in parallel. The line through the conductor of each layer indicates the

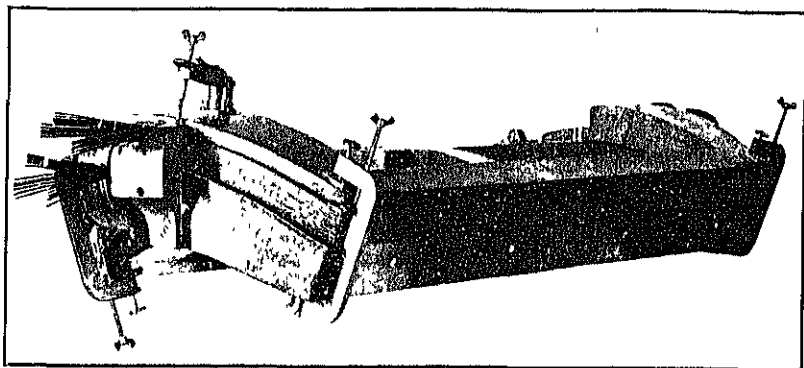


FIG. 128.—Winding form with coil.

parallel wires. Figure 131 shows a large armature coil wound with 12 wires, 0.080×0.145 in., in parallel.

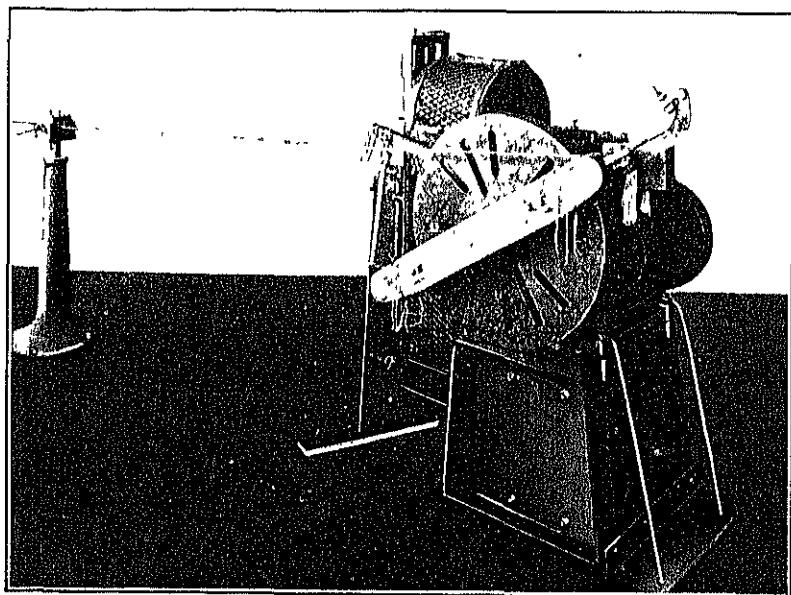


FIG. 129.—Coil winding machine.

For machines requiring a large number of turns of small wire, the arrangement of conductors shown in Fig. 130*A* and *B* cannot always be

used. For such machines the coils should be wound as shown in Fig. 132A. With this arrangement, one-half of the coil must be wound backwards, that is, in opposite direction to the other half. The two halves of the coil must be insulated from each other, because of the high voltage between the beginning and ending lead. Coils with many turns may also be wound as shown in Fig. 132B. For this method of winding the coils, the turns of each layer cross each other, and experience has shown that short circuits often occur at these cross-over points. This method should be used only with round wire and in sizes 0.0163 sq. in. area and smaller.

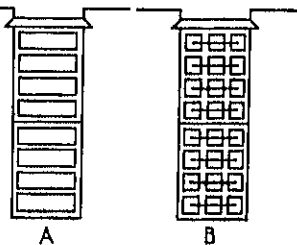


Fig. 130.

Double-cotton-covered conductors are generally used for the armature coils. For machines to operate at high temperatures or for heavy overloads for short periods, asbestos-covered

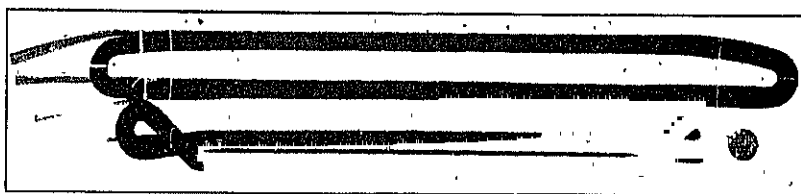


Fig. 131.—Armature coil with 12 wires, 0.08 in. \times 0.145 in. in parallel.

wire is sometimes used. The straight part of the bobbin-wound coil is molded in a steam or electrically heated mold and is then pulled out on a coil-pulling machine to the required shape. For high-voltage, large-capacity machines, the pulled-out coil is treated by the vacuum process,⁶ to fill all interstices with an insulating, moisture-resisting, heat-conducting compound. To maintain a smooth surface on the outside of the coil, it is wrapped with a sacrifice tape before it is impregnated. This tape is removed after the coil has been treated. For moderate-voltage machines, the coils are often given a varnish treatment instead of the vacuum treatment. In the varnish treatment, the coils

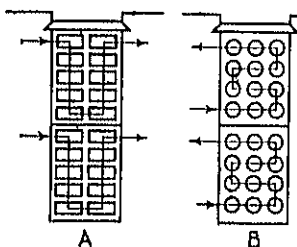


Fig. 132.

⁶ "Insulation and Design of Electrical Windings," by A. P. M. Fleming and R. Johnson, p. 68, Longmans, Green and Co., London; *Electric Journal*, Vol. 22, Feb., 1925, p. 95.

are first dried and then dipped into a bath of insulating varnish. After removal from the varnish bath they are allowed to drain and are then baked at a temperature of 100° C. until dry. This treatment is repeated two or three times, depending upon the voltage, size and type of machine.

After the varnish or impregnating treatment, the coils are ready for the insulation, which consists of wrappings or tapings of varnished cambric, mica, or combinations of both, depending upon the size of the coil and the voltage for which it is to be insulated. The standard test voltage for which the armature windings of synchronous machines must be insulated is given in the Standardization⁷ Rules of the A.I.E.E. It is

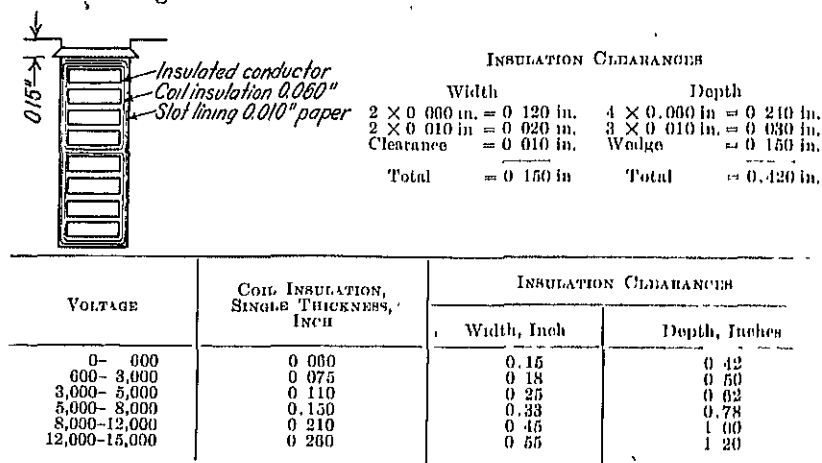


FIG. 133.—Thickness of coil insulation and insulation clearances for armature coils of synchronous machines.

twice the rated voltage of the winding, plus 1000. The high-voltage test is to be made when the windings are at operating temperature.

The insulating materials generally used are: cotton and linen tape, mica and mica tape, varnished cambric, and insulating varnishes. The insulation of the armature coils may be carried out in various ways. Figure 133 and the accompanying table give the insulation clearances required for various voltages.

Conductor Section and Slot Size.—The armature copper loss,

$$W_a = I^2 R_a \text{ watts.}$$

The current in the armature winding,

$$I = A_a s_a$$

⁷ A.I.E.E. Standards No. 7, 1925, p. 15.

and the resistance of the armature winding,

$$R_a = \frac{Lr}{s_a \times 10^6}.$$

Here L is the total length of the armature conductor.

Making the substitutions,

$$W_a = A_a^2 s_a^2 \frac{Lr}{s_a \times 10^6} = A_a^2 s_a Lr \times 10^{-6}.$$

The weight of the armature copper,

$$G_a = Ls_a \times 0.321$$

and

$$Ls_a = \frac{G_a}{0.321}.$$

For 25° C., $r = 0.692$ and

$$W_a = A_a^2 G_a \times 2.23 \times 10^{-6} \text{ watts.} \quad (139)$$

For 75° C., $r = 0.826$ and

$$W_a = A_a^2 G_a \times 2.58 \times 10^{-6} \text{ watts.} \quad (139a)$$

This equation shows that the armature copper loss varies directly with the current density squared and the weight of the copper. Since the armature copper loss is a large percentage of the total losses and since the temperature rise of the armature copper depends upon the copper losses, it follows that temperature rise or efficiency or both will generally limit the value of A_a . The number of armature conductors required for a given voltage and flux increases as the speed of the machine decreases. The copper loss for a given current density will therefore generally be higher for slow-speed machines than for high-speed machines. To obtain an economical design, the current density should be chosen as high as good operating characteristics will permit. The curves in Fig. 134, give average values for the armature current density for various capacities and speeds.

The section area of the armature conductor,

$$s_a = \frac{I}{A_a a} \text{ sq. in.} \quad (140)$$

The open type of armature slot is generally used for armatures of synchronous machines. For open type armature slots, the leakage flux is not equally distributed over the entire slot depth, and, as a result, a difference of potential is produced between the top and bottom of any

conductor in the slot. If the conductor is large, this difference of potential will set up equalizing currents in the conductor, which may lead to copper losses several times greater than that due to the normal load current alone. These eddy current losses may be reduced to a negligible value by subdividing the individual conductors. This is done by using several small wires in parallel or by using pressed cable. For large capacity machines, transposed⁸ conductors or inverted turn coils must be used in addition to subdividing the conductors. Figure 135 shows a portion of an armature coil for a 12,500 Kva turbo-generator. The coil has two turns and each turn is inverted in the end-connection. The armature conductor for synchronous machines is therefore generally built up of a number of small insulated wires in parallel.

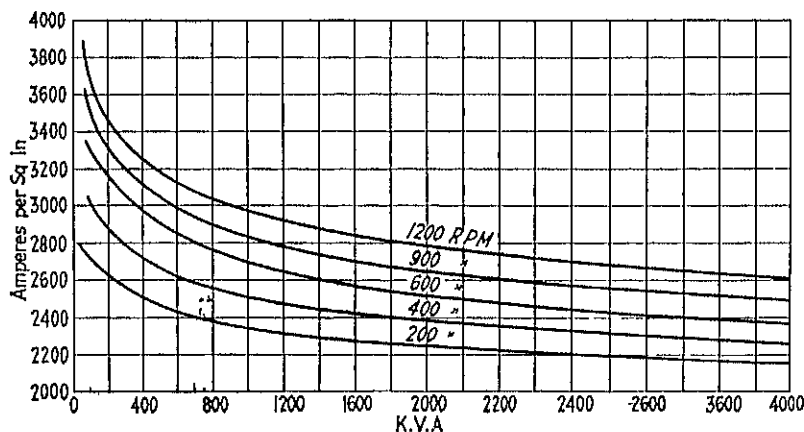


Fig. 134.—Approximate current densities for armature windings of 50° C. salient-pole synchronous machines.

The dimensions of the slot can be found by adding to the space required by the insulated conductors in the width and depth of the slot, the insulation clearance necessary. The insulation clearances for width and depth of slot are given, for various voltages, in Fig. 133.

Mean-Turn, Resistance and Weight of Armature Winding.—The shape of the armature coils for synchronous machines is approximately the same as that of the armature coils for direct-current machines. The angle α , Fig. 136, which the straight part of the end-connection

⁸ "Reduction of Armature Copper Losses," by I. H. Summers, A.I.E.E. Journal, Vol. 46, May, 1927, p. 451; "Additional Losses of Synchronous Machines," by C. M. Laffoon and J. F. Calvert, A.I.E.E. Journal, Vol. 46, June, 1927, p. 573; "Transposed Armature Coils in Alternating Current Generators," by S. L. Henderson, Electric Journal, Vol. 23; July, 1926, p. 348.

angles from the edge of the armature core can be calculated as follows:

$$\sin \alpha = \frac{d}{t_1} \quad (141)$$

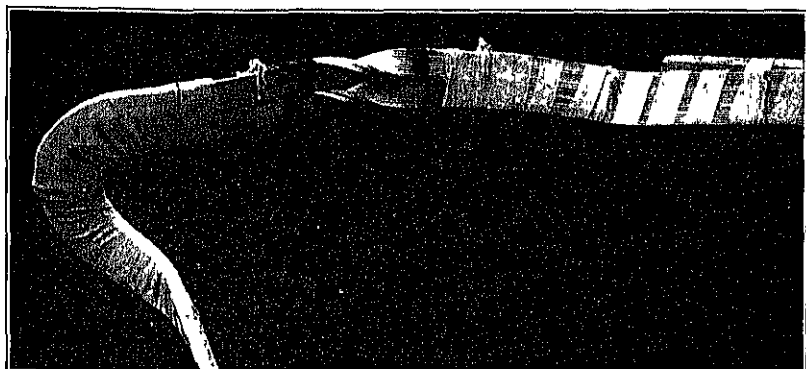


FIG. 135.—Part of turbo-generator coil showing transposition in end-connection.

Here t_1 is the tooth pitch at the armature surface and d is the thickness of one coil at the end-connections plus the clearance between adjacent end-connections. The thickness of the coil at the end-connections may be taken equal to the slot width. The clearance, s , Fig. 136, is given in Table XVI.

The coil pitch is calculated on a diameter through the mean of the slot depth. It is,

$$= \frac{\pi(D + d_s)}{p} P \text{ in.}$$

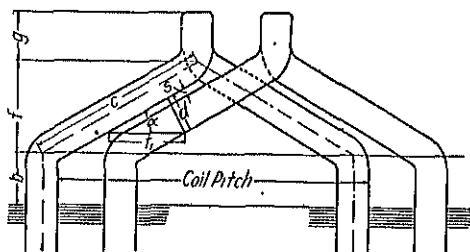
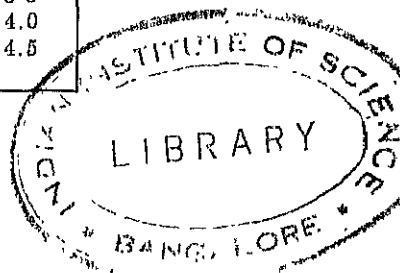


FIG. 136.—Armature coil end-connections.

TABLE XVI

Voltage	s	$2b$
0 to 600	0.15	2.0
600 to 3,000	0.18	2.5
3,000 to 6,600	0.22	3.5
6,600 to 10,000	0.25	4.0
10,000 to 15,000	0.30	4.5



r is the per cent pitch of the coil expressed as a decimal (75 per cent = 75). The length of the straight part of the end-connection for one end of the coil,

$$2C = \frac{\pi(D + d_s)}{p \cos \alpha} P \text{ in.}$$

The part of the armature coil which is embedded in the slot is allowed to extend beyond the edge of the armature core a distance b , Fig. 136. The length of this coil extension depends upon the voltage of the winding. It is given in Table XVI.

The loop at each end of the coil has a mean length approximately equal to the slot depth.

The complete expression for the length of one-half the mean-turn of an armature coil,

$$L_a = \frac{\pi(D + d_s)}{p \cos \alpha} P + 2b + d_s + l \text{ in.} \quad (142)$$

The horizontal extension of the armature coil beyond the armature core is equal to the sum of $b + f + g$, Fig. 136.

$$f = C \sin \alpha \text{ in.,}$$

and g is approximately equal to the slot depth.

The resistance per phase of the armature winding,

$$R_a = \frac{L_a N r}{as_a \times 10^6} \text{ ohms} \quad (143)$$

$r \times 10^{-6}$ is the resistance of copper per inch of 1-sq. in. section. For 25° C., $r = 0.692$ and for 75° C., $r = 0.826$. When the armature conductor is built up of several small wires in parallel, s_a in formula 143 must be the section area of the group of parallel wires. The resistance of the winding at any other temperature, T_2 , can be calculated by formula 37, page 56.

The bare weight of the armature copper,

$$G_a = L_a N a m s_a \times 0.321 \text{ lb.} \quad (144)$$

Here s_a is the section area of the group of parallel wires, when the armature conductor is built up of several small wires in parallel. The approximate insulated weight can be calculated from the data given in the copper tables.

Example 2—Design of a machine winding.—From the data given on page 168, an air gap density of 42,000 lines per sq. in. is assumed.

$$\begin{aligned}\phi_i &= \pi D l B_g = \pi \times 100 \times 17.5 \times 42,000 \\ &= 231,000 \text{ kilo-lines.}\end{aligned}$$

The design of the pole shoe is given on page 171. The air gap flux distribution curve is shown in Fig. 109. The form factor, $f_b = 1.14$, and the flux distribution factor, $f_d = 0.666$. The winding distribution factor may be taken equal to 0.956 (see curve, Fig. 122):

$$\begin{aligned}C_w &= f_b f_d f_w = 1.14 \times 0.666 \times 0.956 \\ &= 0.725.\end{aligned}$$

For a pitch winding, the number of conductors in series per phase,

$$\begin{aligned}N &= \frac{E \times 60 \times 10^8}{\phi_i n f_c C_w} = \frac{1390 \times 60 \times 10^8}{231,000 \times 10^3 \times 225 \times 1 \times 0.725} \\ &= 221.\end{aligned}$$

For a winding with one circuit per phase, the total number of conductors = $221 \times 3 = 663$.

With 3 slots per pole and phase, the total number of slots,

$$S = 3 \times 3 \times 32 = 288.$$

and the tooth pitch at the air gap surface,

$$t_1 = \frac{\pi D}{S} = \frac{3.14 \times 100}{288} = 1.09 \text{ in.}$$

The number of conductors per slot,

$$\begin{aligned}&= \frac{663}{288} = 2.3.\end{aligned}$$

As stated above, this number must be an integer and must be a multiple of 2. If a one-circuit winding is to be used, 2 conductors per slot will be required. But decreasing the number of conductors to this value will produce too large an increase in the total flux. If a 2-circuit winding is used, the conductors per slot must be doubled. With a 2-circuit winding and 4 conductors per slot, the total flux will be too small. It may be increased by using a chorded winding, but this would require a chord factor of about 0.75, which is not satisfactory for a 32-pole machine. The number of slots should therefore either be decreased, so that a 2-circuit winding with 4 conductors per slot can

be used, or increased to permit a 2-circuit winding with 4 conductors per slot.

With $3\frac{1}{2}$ slots per pole per phase, the total number of armature slots,

$$S = 3\frac{1}{2} \times 3 \times 32 = 336.$$

The tooth pitch at the air gap surface,

$$t_1 = \frac{\pi D}{S} = \frac{3.14 \times 100}{336} = 0.935 \text{ in.}$$

The armature windings for synchronous machines are generally designed with more than one turn per coil. Large-capacity turbo-generators, for which coils with transposed conductors are used, require only one turn per coil. A 2-circuit winding will therefore be used. The total number of armature conductors required $= 2 \times 663 = 1326$. The conductors per slot,

$$= \frac{1326}{336} = 3.95 \text{ or } 4.$$

For this winding, with 10.5 slots per pole, a pitch coil can not be used. A coil throw, slot 1 to 10, will be used,

$$f_c = \sin \frac{9}{10.5} 90 = 0.975.$$

The diagrams for the winding are shown in Fig. 137.

The final value of the total flux,

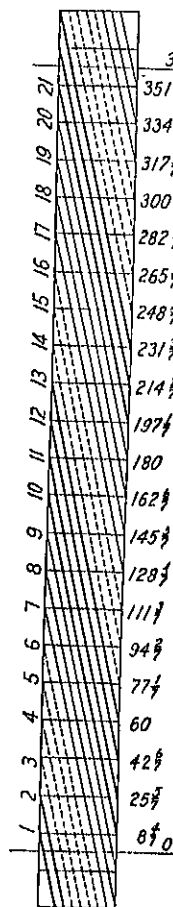
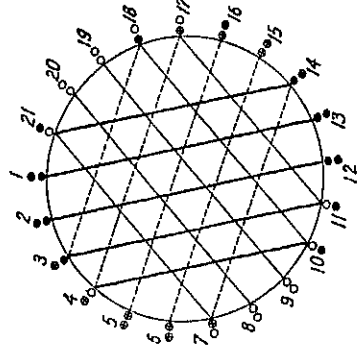
$$\begin{aligned} \phi_t &= \frac{E \times 60 \times 10^8}{NnC_w f_c} = \frac{1390 \times 60 \times 10^8}{224 \times 225 \times 0.725 \times 0.975} \\ &= 234,000 \text{ kilo-lines.} \end{aligned}$$

The armature current,

$$\begin{aligned} I &= \frac{Kva \times 10^3}{E \times 3} = \frac{2500 \times 10^3}{1390 \times 3} \\ &= 600. \end{aligned}$$

The section area of the armature conductor,

$$\begin{aligned} s_a &= \frac{I}{aA_a} = \frac{600}{2 \times 2200} \\ &= 0.136 \text{ sq. in.} \end{aligned}$$



$$f_{w} = \frac{\sin 51\frac{3}{4} + \sin 68\frac{3}{4} + 2 \sin 85\frac{3}{4} + 2 \sin 77\frac{1}{2} + \sin 60}{7 \times 0.975}$$

$$= 0.956$$

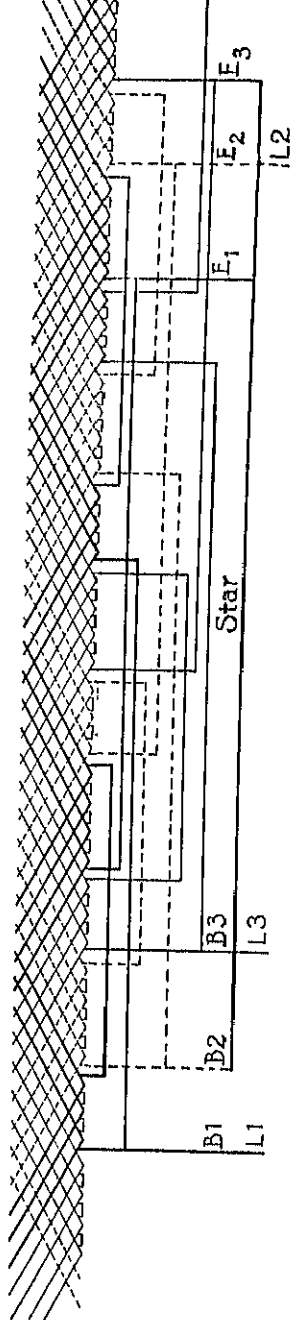


Fig. 137.—Winding lay-out and connection diagram—3½ slots per pole per phase—three-phase, two-circuit star.

The tooth pitch at the air gap surface has been calculated above, it is equal to 0.935 in. The width of the slot should not be greater than

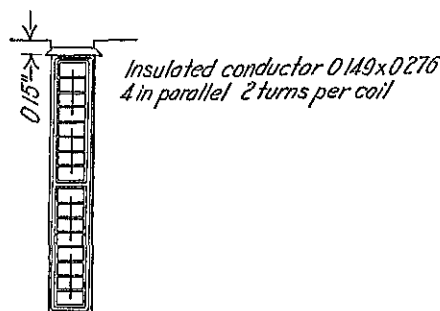


FIG. 138.

one-half of 0.935 in. or 0.4675 in. The coils will be wound with 4 d.c.c. copper ribbon conductors in parallel and arranged in the slot as shown in Fig. 138. The insulated dimensions of each conductor are (see copper tables):

Width 0.276 in., thickness 0.149 in., area 0.0325 sq. in.

The slot dimensions required are (see Fig. 133):

$$\text{Width} = 1 \times 0.276 + 0.18 = 0.456 \text{ in.}$$

$$\text{Depth} = 16 \times 0.149 + 0.50 = 2.88 \text{ in.}$$

The current density for this conductor,

$$A_a = \frac{600}{2 \times 4 \times 0.0325} = 2310 \text{ amperes per sq. in.}$$

This winding will be satisfactory, provided the densities for the various parts of the magnetic circuit do not exceed the limits given in Chapter XII.

The length of the half mean-turn of the armature coil is calculated as follows (see Fig. 136):

$$\sin \alpha = \frac{d}{t_1} = \frac{0.456 + 0.18}{0.935} = 0.680$$

$$\alpha = 42.9^\circ \text{ and } \cos \alpha = 0.733.$$

The per cent pitch,

$$P = \frac{9}{10.5} = 0.857$$

$$\begin{aligned} L_a &= \frac{\pi(D + d_s)}{p \cos \alpha} P + 2b + d_s + l \\ &= \frac{3.14(100 + 2.88)}{32 \times 0.733} 0.857 + 2.5 + 2.88 + 17.5 \\ &= 34.68 \text{ in.} \end{aligned}$$

The resistance per phase of the armature winding at 75° C.,

$$R_a = \frac{L_a N r}{as_a \times 10^6} = \frac{34.68 \times 224 \times 0.826}{2 \times 4 \times 0.0325 \times 10^6}$$

$$= 0.0247 \text{ ohm.}$$

The bare weight of the armature copper,

$$G_a = L_a N a m s_a \times 0.321$$

$$= 34.68 \times 224 \times 2 \times 3 \times 4 \times 0.0325 \times 0.321$$

$$= 1940 \text{ lb.}$$

The approximate insulated weight equals 2000 lb.

CHAPTER XII

MAGNETIC CIRCUIT

The fundamental formulas for the magnetic circuit are given on page 60, Chapter IV. The magnetic circuit for a pair of poles for a salient-pole synchronous machine with revolving field is shown in Fig. 139. The path of the magnetic flux comprises the air gap, armature teeth, armature yoke, field pole, and field yoke or spider rim. The material and flux densities are not the same for all parts of the magnetic circuit; therefore, the ampere-turns must be calculated separately for each part. The symbols used for these calculations are the same as those used for direct-current machines, page 61. The total ampere-turns per pole for no-load and normal voltage,

$$\text{ATP}_o = \text{AT}_g + \text{AT}_t + \text{AT}_{ya} + \text{AT}_p + \text{AT}_{yf}.$$

Ampere-Turns for Air Gap.—The maximum value of the flux density in the air gap,

$$B_g = \frac{\phi_t}{s_g}.$$

The section area of the air gap,

$$s_g = \pi D l_g.$$

That is, the air gap section is equal to the circumference of the armature times the length of the section l_g . For salient-pole machines which have core lengths not over from 12 to 14 in. and for which the length of the pole shoe parallel to the shaft is equal to the total armature length, l , the length of the air gap section, l_g , can be taken equal to the total length of the armature. It is assumed that the flux lost because of the ventilating ducts in the armature is equal to the flux gained because of the fringing of the flux at the pole ends. For large-capacity salient-pole machines with long armature cores and a large number of ventilating ducts, the length of the gap section,

$$l_g = l - \frac{1}{2}(n_a w_a). \quad (145)$$

The ampere-turns per pole for the air gap,

$$AT_g = \frac{B_g \delta k}{3 \cdot 2}$$

The air gap coefficient, k , is calculated by formula 46, page 63.

Ampere-Turns for Armature Teeth.—Slots with parallel sides are always used for synchronous machines. The tooth width is therefore smaller at the armature surface than at the bottom of the slot. The section area of the teeth at the armature surface,

$$s_{t_1} = w_{t_1}(l - n_{ar}a)k_1S. \quad (146)$$

The number of ventilating ducts is always so chosen that the space between ducts does not exceed 3 in. The width of the ducts is $\frac{3}{8}$ in.

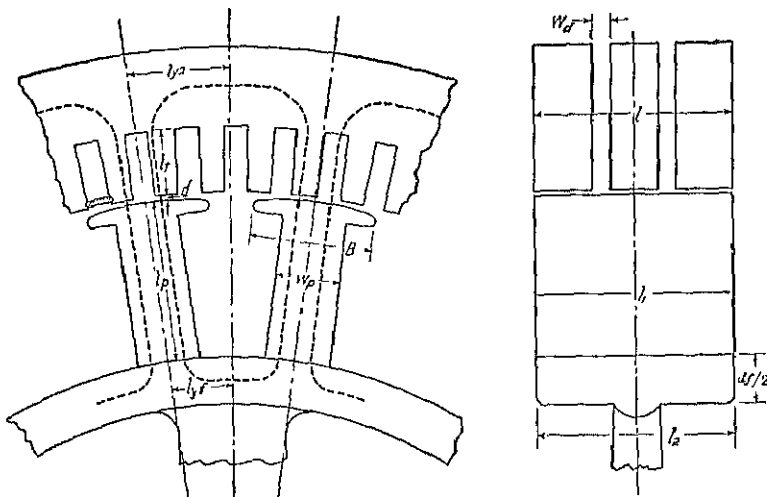


FIG. 139.—Magnetic circuit of salient-pole synchronous machine.

for small machines and $\frac{1}{2}$ in. for medium and large-capacity machines. The lamination factor, k_1 , depends upon the method of insulating the laminations and upon the kind and thickness of the sheet. For silicon sheet steel 0.014 in. thick and insulated with core plate varnish, $k_1 = 0.90$. For sheet steel 0.019 in. thick, k_1 may be taken equal to 0.93.

The maximum flux density,

$$B_{t_1} = \frac{\phi_{t_1}}{s_{t_1}}$$

The maximum flux density in the armature teeth should generally not exceed 100,000 lines per sq. in. High tooth densities produce high

iron losses and require a large number of ampere-turns on the field winding. Low tooth densities, on the other hand, result in an uneconomical use of magnetic material. The density at the armature surface will generally lie between the limits,

$$B_t = 75,000 \text{ to } 95,000 \text{ lines per sq. in.}$$

To take into account the effect of the tooth taper, the ampere-turns for the teeth are calculated for the density at a section $\frac{1}{3}$ tooth length from the minimum section.

$$s_{t_3} = w_t(l - n_a w_a)k_1 S$$

and

$$B_{t_3} = \frac{\phi_t}{s_{t_3}}.$$

The method of calculating w_t is shown in the sample design, page 212.

From the standard saturation curves for the material used in the armature laminations, the ampere-turns per inch corresponding to the density B_{t_3} are found. Then

$$AT_t = at_t l_t.$$

The length of the flux path for the armature teeth, l_t , is equal to the slot depth.

Ampere-Turns for Armature Yoke.—The flux of each pole passes through the armature teeth into the yoke and divides, one-half returning through each of the adjacent poles as shown in Fig. 139. The flux per pole,

$$\phi = \frac{\phi_t f_a}{p}.$$

The depth of the iron below the slots, d_{ya} , is calculated by formula 57 in the same way as described for direct-current machines. The flux density in the armature yoke depends upon the grade of sheet steel used for the armature laminations and upon the frequency of the flux reversals. The losses in the armature iron increase with the frequency and the density. The weight of the iron in the armature yoke is the largest part of the total iron weight; therefore low flux densities will generally be required to avoid high core losses. For 60-cycle synchronous machines, the flux densities in the armature yoke will generally lie between the limits 40,000 to 75,000 lines per sq. in. For lower frequencies, slightly higher values may be used.

The ampere-turns per pole for the armature yoke,

$$AT_{ya} = at_{ya} l_{ya}.$$

The length of the flux path for the yoke is taken equal to one-half the pole pitch on the mean diameter of the yoke.

$$l_{ya} = \frac{\pi(D + 2d_i + \frac{1}{2}d_{ya})}{2p} \quad (147)$$

Ampere-Turns for the Pole.—The flux in the poles is equal to the useful flux which crosses the air gap and enters the armature, plus the leakage flux. The pole body density,

$$B_p = \frac{\phi \lambda}{s_p}$$

The leakage flux can not be calculated until the dimensions of the pole are known. The flux density in the pole will depend upon the kind of material used. For laminated poles,

$$B_p = 85,000 \text{ to } 100,000 \text{ lines per sq. in.}$$

For cast-steel poles slightly lower values are necessary because of the non-uniformity of this material. The field leakage constant, λ , may be estimated with the help of the curves, Fig. 140. The section area of the pole body can then be calculated by the formula above. The axial length of the pole may be made slightly less than the armature length, but more often, l_1 will be equal to l .

The field leakage flux may be calculated approximately by the following formulas¹ (see Fig. 141):

$$\begin{aligned} \phi_{i_1} &= X 13 \frac{l_1 h_s}{d_i} \\ \phi_{i_2} &= X 19 h_s \log_{10} \left(1 + \frac{\pi B}{2 d_i} \right) \\ \phi_{i_3} &= X 6.5 \frac{l_1 h_p}{d_b} \\ \phi_{i_4} &= X 9.5 h_p \log_{10} \left(1 + \frac{\pi w_p}{2 d_b} \right) \\ X &= \Delta T_o + \Delta T_i + \Delta T_{ya} \\ \phi_l &= \phi_{i_1} + \phi_{i_2} + \phi_{i_3} + \phi_{i_4} \\ \lambda &= \frac{\phi + \phi_l}{\phi} = 1 + \frac{\phi_l}{\phi} \end{aligned}$$

¹The development of these formulas is given on page 68. See also, "Field Leakage in Synchronous Machines," by Theo. Schou, *Electrical Review*, Vol. 77, p. 281.

The ampere-turns per pole for the pole,

$$AT_p = at_p l_p.$$

The length of the flux path, l_p , is equal to the radial height of the pole. This value depends upon the space required by the field winding. The

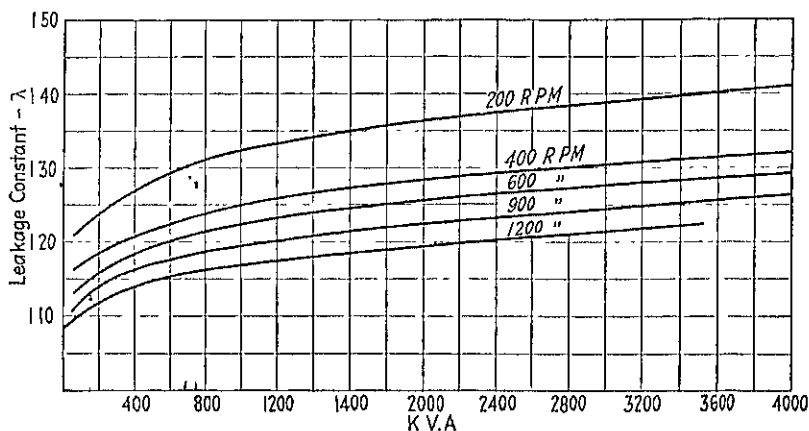


FIG. 140 — Approximate field leakage constants for salient pole synchronous machines.

ratio of the radial length of the pole to the pole pitch is generally equal to from 0.30 to 1.50. The small value is for machines with a small

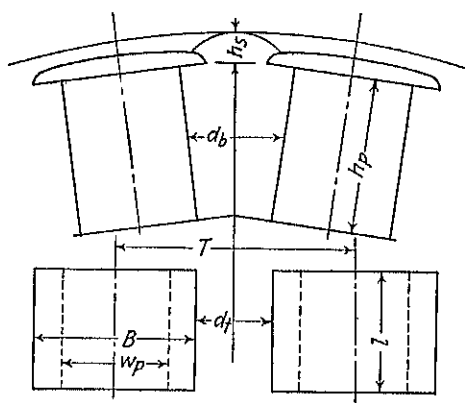


FIG. 141.

number of poles, or large pole pitch; and the large value for machines with a large number of poles, or small pole pitch.

Ampere-Turns for the Field Yoke.—The field yoke or spider rim, to which the field poles are either bolted or keyed, is either of cast iron, cast steel, rolled steel, or built up of rolled steel plate (see page 164). For cast-iron spiders, the density in the field yoke should not exceed

30,000 lines per sq. in., and for cast-steel spiders it should not exceed 60,000 lines per sq. in. With rolled steel and laminated field yoke, higher densities may be used. For large-capacity high-speed machines, the spider rim section must be checked also for mechanical strength.

Generally, however, the section that satisfies the magnetic requirements will be large enough to meet the mechanical requirements for strength. Synchronous motors and generators are often designed to have a large inherent flywheel effect. For this purpose the section area of the spider rim is larger than is necessary to meet the magnetic requirements given above.

The section area of the field yoke,

$$s_{yf} = \frac{\phi \lambda}{B_{yf}}$$

The length of the yoke section parallel to the shaft is generally equal to the length of the pole, l_1 . When extra large yoke sections are used to obtain large flywheel effect, l_2 is often made larger than l_1 .

The depth of the spider rim,

$$d_{yf} = \frac{s_{yf}}{l_2}$$

The ampere-turns for the field yoke,

$$AT_{yf} = \mu l_{yf} l_{yf}$$

The length of the flux path is shown in Fig. 139, and is taken equal to one-half of the pole pitch on the mean circumference of the spider rim.

The open-circuit saturation curve is calculated as explained on page 69. The calculations for the sample generator design are given on page 215.

Sample Design: Magnetic Circuit.—Five ventilating ducts, each $\frac{1}{2}$ in. wide, are used in the armature. The length of the air gap section,

$$l_g = l - \frac{1}{2}(naw_a) = 17.5 - \frac{1}{2}(5 \times \frac{1}{2}) = 16.25 \text{ in.}$$

The air gap density,

$$\begin{aligned} B_g &= \frac{\phi_l}{\pi D l_g} = \frac{234,000 \times 10^3}{3.14 \times 100 \times 16.25} \\ &= 45.8 \text{ kilo-lines per sq. in.} \end{aligned}$$

The length of the air gap has been estimated at 0.406 in. and the air gap coefficient,

$$\begin{aligned} k &= \frac{l_1}{w_{t1} + (\delta y)} = \frac{0.935}{0.479 + (0.406 \times 0.95)} \\ &= 1.08. \end{aligned}$$

The ampere-turns per pole for the air gap,

$$\begin{aligned} \text{AT}_g &= \frac{B_g \delta k}{32} = \frac{45,800 \times 0.406 \times 1.08}{32} \\ &= 6280 \text{ ampere-turns.} \end{aligned}$$

The maximum density in the armature teeth,

$$\begin{aligned} B_{t_1} &= \frac{\phi_t}{w_{t_1}(l - n_a w_a)k_1 S} = \frac{234,000 \times 10^3}{0.479(17.5 - 5 \times \frac{1}{2})0.93 \times 336} \\ &= 104 \text{ kilo-lines per sq. in.} \end{aligned}$$

The width of the armature tooth at a section $\frac{1}{3}$ tooth from the minimum section,

$$\begin{aligned} w_{t_3} &= \frac{\pi(D + \frac{2}{3}d_s)}{S} - w_s = \frac{\pi(100 + \frac{2}{3}2.88)}{336} - 0.456 \\ &= 0.496. \end{aligned}$$

$$\begin{aligned} B_{t_3} &= \frac{\phi_t}{w_{t_3}(l - n_a w_a)k_1 S} = \frac{234,000 \times 10^3}{0.496(17.5 - 5 \times \frac{1}{2})0.93 \times 336} \\ &= 101 \text{ kilo-lines per sq. in.} \end{aligned}$$

From the standard saturation curve for 2.5 to 3.0 per cent silicon steel, at $t_1 = 69$ ampere-turns per inch and,

$$\begin{aligned} \text{AT}_t &= at_1 l_t = 69 \times 2.88 \\ &= 199 \text{ ampere-turns.} \end{aligned}$$

The flux per pole,

$$\begin{aligned} \phi &= \frac{\phi_t f_d}{p} = \frac{234,000 \times 10^3 \times 0.666}{32} \\ &= 4870 \text{ kilo-lines.} \end{aligned}$$

The depth of the armature yoke,

$$\begin{aligned} d_{ya} &= \frac{\phi}{(l - n_a w_a)k_1 B_{ya}} = \frac{4870 \times 10^3}{(17.5 - 5 \times \frac{1}{2})0.93 \times 60,000} \\ &= 5.82 \text{ in.} \end{aligned}$$

The outside diameter of the armature core,

$$\begin{aligned} D_0 &= D + 2d_s + d_{ya} = 100 + (2 \times 2.88) + 5.82 \\ &= 111.58; \text{ make this } 112 \text{ in.,} \end{aligned}$$

and

$$\begin{aligned} d_{ya} &= D_0 - (D + 2d_s) = 112 - (100 + 2 \times 2.88) \\ &= 6.24 \text{ in.} \end{aligned}$$

$$B_{ya} = \frac{\phi}{(l - nawa)k_1 d_{ya}} = \frac{4870 \times 10^3}{(17.5 - 5 \times \frac{1}{2})0.93 \times 6.24} \\ = 56 \text{ kilo-lines per sq. in.}$$

The length of the flux path,

$$l_{ya} = \frac{\pi(D + 2d_s + \frac{1}{2}d_{ya})}{2p} = \frac{3.14(100 + 2 \times 2.88 + \frac{1}{2} \times 6.24)}{2 \times 32} \\ = 5.34 \text{ in.}$$

The ampere-turns per inch from the standard saturation curve for 2.5 to 3.0 per cent silicon steel, $at_{ya} = 2.5$ ampere-turns per in. and

$$AT_{ya} = at_{ya} l_{ya} = 2.5 \times 5.34 \\ = 14 \text{ ampere-turns.}$$

The field leakage constant is taken equal to 1.38 and the section area of the pole body,

$$s_p = \frac{\phi \lambda}{B_p} = \frac{4870 \times 10^3 \times 1.38}{95,000} \\ = 70.7 \text{ sq. in.}$$

The length of the pole parallel to the shaft is 17.5 in. and,

$$w_p = \frac{70.7}{17.5} = 4.05 \text{ in.; use 4 in.}$$

The radial height of the pole depends upon the space required by the field winding. It is estimated at 7.0 in. (see page 210).

The leakage flux is calculated by the formulas given on page 209.

$$l_1 = 17.5, \quad h_s = 1.125, \quad d_t = 3.06, \quad B = 6.75, \\ h_p = 6.25, \quad d_b = 5.0, \quad w_p = 4.0.$$

$$(1) \quad 13 \frac{l_1 h_s}{d_t} = 13 \frac{17.5 \times 1.125}{3.06} = 83.60$$

$$(2) \quad 19 h_s \log \left(1 + \frac{B\pi}{2d_t} \right) = 19 \times 1.125 \times \log \left(1 + \frac{6.75 \times \pi}{2 \times 3.06} \right) \\ = 13.90$$

$$(3) \quad 6.5 l_1 \frac{h_p}{d_b} = 6.5 \frac{17.5 \times 6.25}{5.0} = 142.00$$

$$(4) \quad 9.5h_p \log \left(1 + \frac{\pi w_p}{2d_b} \right) = 9.5 \times 6.25 \log \left(1 + \frac{\pi \times 1.0}{2 \times 5.0} \right) \quad 21.0$$

$$X = 6280 + 199 + 1.1 = 6493$$

$$\phi_l = X \times 260.50 = 6493 \times 260.50 = 1,690,000$$

$$\lambda = \frac{\phi_l}{\phi} + 1 = \frac{1,690,000}{4,870,000} + 1 = 1.347.$$

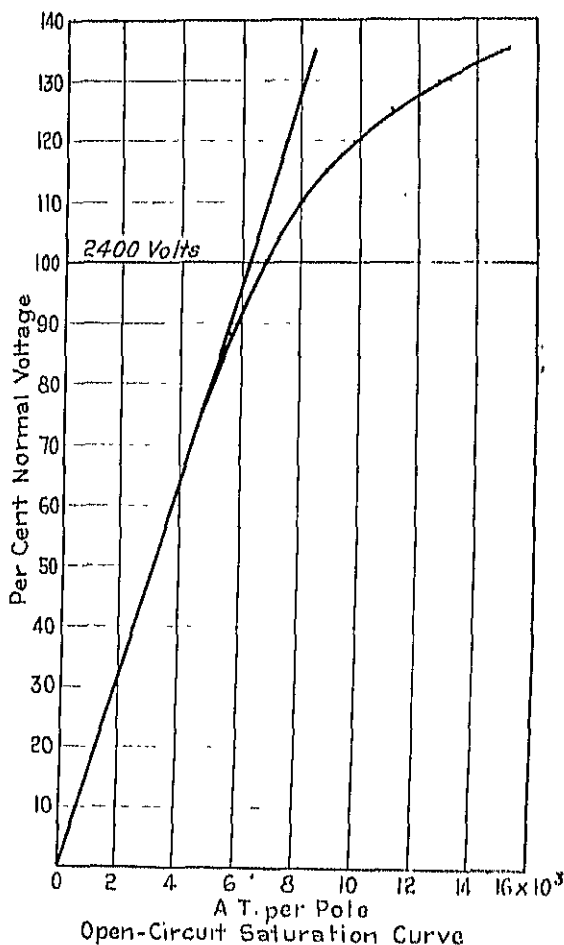


FIG. 142.

The flux density in the pole body is then,

$$B_p = \frac{4,870,000 \times 1.347}{4 \times 17.5} = 93,600 \text{ lines per sq. in.}$$

the ampere-turns per inch, $at = 31$. The length of the flux path $l_p = 7.0$ (see Fig. 139) and,

$$AT_p = l_p at_p = 7.0 \times 31 = 217 \text{ ampere-turns.}$$

The section area of the spider rim,

$$s_{vf} = \frac{\phi \lambda}{B_{vf}} = \frac{4,870,000 \times 1.347}{65,000} \\ = 101 \text{ sq. in.}$$

If the length of the spider rim parallel to the shaft is made equal to the armature length,

$$d_{vf} = \frac{101}{17.5} = 5.77 \text{ in.}$$

The length of the flux path in the field yoke (see Fig. 139),

$$l_{yf} = 4.05 \text{ in.}$$

The ampere-turns per inch for open hearth rolled steel, $at = 6$, and

$$AT_{yf} = 4.05 \times 6.0 = 24 \text{ ampere-turns.}$$

The calculations for the open-circuit saturation curve are given in Table XVII. The data in the table are plotted in Fig. 142.

TABLE XVII

Path	Length	90 % E			100 % E			115 % E			125 % E		
		B	at	AT	B	at	AT	B	at	AT	B	at	AT
Air gap.				5050	15.8		6280			7210			7,850
Teeth	2.88	90.8	16.0	46	101.0	69.0	109	116.0	342.0	990	126.0	856.0	2,470
Armature yoke . .	5.31	50.5	2.1	11	56.0	2.5	11	64.5	3.2	17	70.0	3.9	21
Pole	7.00	81.0	13.5	95	93.0	31.0	217	107.8	100.0	700	117.0	266.0	1,862
Field yoke. . . .	1.05	58.5	5.0	20	65.0	6.0	24	71.7	9.0	36	81.2	11.5	47
Total				5822			6731			8953			12,250

CHAPTER XIII

ARMATURE REACTIONS IN SYNCHRONOUS MACHINES

WHEN an alternator is carrying load, the armature current produces an alternating current field, which may be divided into two parts. One part passes through the magnetic circuit, and its effect is called armature reaction. The other part, called armature leakage field, does not pass through the magnetic circuit. Its effect is called armature leakage reactance.

Armature Leakage Reactance.—The number of interlinkages between the armature leakage flux per unit of current, times the rate of change of the flux, is called the leakage reactance of the armature. The following method of calculating the armature leakage reactance was presented by P. L. Alger¹ before the American Institute of Electrical Engineers.

For convenience in calculating the reactance, the armature leakage flux is divided into four parts:

(1) The slot leakage flux, Fig. 143, which has its path through the slot and through the iron of the teeth and below the teeth.

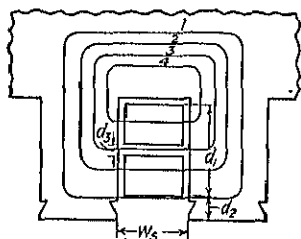


Fig. 143.

(2) The end-connection leakage flux, which encircles the armature coils at the end-connections.

(3) The zig zag leakage flux, which has its path in the air gap.

(4) The belt leakage flux, which has its path in the air gap.

The slot reactance in ohms per phase, due to the slot leakage flux, is equal to the permeance of the path across a unit length of the slot, times the length of the slot, times the number of slots in series per phase, times the number of conductors in series per slot squared, times the rate of change of flux, times 10^{-8} ohms.

The slot leakage flux path, Fig. 143, is partly through air and partly

¹ "The Calculation of the Armature Reactance of Synchronous Machines," by P. L. Alger, A.I.E.E. Trans., Vol. 47, April, 1928, p. 493.

through them. The reluctance of the part of the path in the teeth and yoke is negligible compared to the reluctance of the part in air; therefore the length of the path of the slot leakage flux is taken equal to the slot width. The permeance of the path for flux (1), Fig. 143, interlinking all the conductors per slot is

$$0.4\pi \frac{d_2}{w_s}$$

For a pitch winding, for which the currents in the two coil sides per slot are identical in magnitude and phase, the linkages per ampere produced by the flux in paths 2 and 4 are

$$0.4\pi \frac{d_1 + d_3}{3w_s}$$

because, with uniform current distribution over the height d_1 , the flux density distribution is linear and the linkage distribution is parabolic; and the average height of a parabola is one-third its maximum height. The flux through path 3 links one-half the total current. The linkages due to it are therefore one-fourth as much as they would be if this flux linked all of the current. The linkages due to the flux of path 3 are

$$0.4\pi \frac{d_3}{4w_s}$$

The total permeance for the slot per unit length is

$$0.4\pi \left(\frac{d_1}{3w_s} + \frac{d_2}{w_s} + \frac{d_3}{12w_s} \right).$$

For fractional pitch windings, the currents in the two coil sides in some of the slots are not in phase, and the expression for the slot permeance must be corrected to take this into account. This is done as explained in the paper referred to above; thus the final expression for the slot reactance per phase,

$$\begin{aligned} X_s &= \frac{0.8\pi^2}{10^8} \mu \frac{S_s}{m} \left(\frac{mN}{S_s} \right)^2 \left[K_s \left(\frac{d_1}{3w_s} + \frac{d_2}{w_s} \right) \right] \\ &= \frac{0.79 f l m N^2}{10^7 S_s} \left[K_s \left(\frac{d_1}{3w_s} + \frac{d_2}{w_s} \right) \right] \text{ ohms.} \end{aligned}$$

For dimensions in inches, the constant 0.79 must be changed to 2.0.

The third factor in the expression for the permeance is generally so small that it can be neglected. The factor K_s is shown in Fig. 144, plotted against per cent pitch.

the end-connection leakage reactance,

$$X_e = \frac{0.79 flmN^2}{10^7 S_s} \left[\frac{0.30(3P - 1)DS_s}{p^2 l} \right].$$

The zig zag leakage reactance,

$$X_z = \frac{5}{8} \left(\frac{p}{S_s} \right)^2 X_{ad}$$

The belt leakage reactance,

$$X_b = 0$$

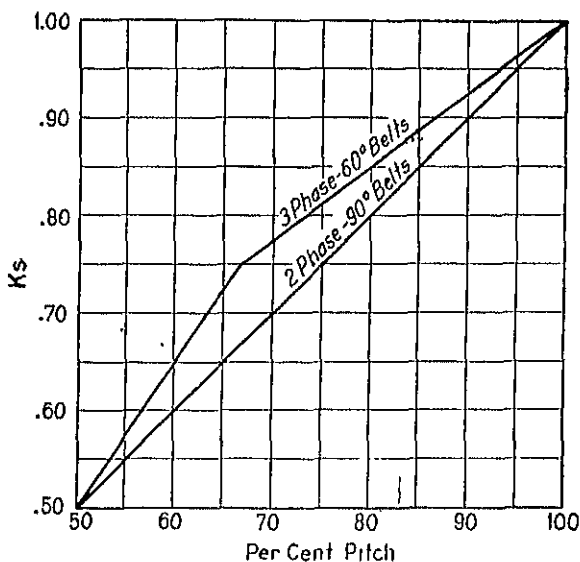


FIG. 141.

for a machine with squirrel-cage winding in the pole faces and integral number of slots per pole per phase,

$$X_b = \frac{3}{4} X_{ad} K_b$$

for salient-pole synchronous machines without squirrel-cage winding in the pole faces and with integral number of slots per pole per phase, and

$$X_b = \frac{5}{8} \left(\frac{p}{S_s} \right)^2 X_{ad}$$

for salient-pole synchronous machines with fractional number of slots per pole per phase. The belt leakage constant, K_b , is shown in Fig. 145.

with fractional number of slots per pole per phase with dimensions in inches,

$$X_l = \frac{2 \ 0flmN^2}{10^7 S_s}$$

$$\left[K_s \left(\frac{d_1}{3w_s} + \frac{d_2}{w_s} \right) + \frac{0.3(3P-1)DS_s}{p^2 l} + \frac{0.53Df_c^2 f_w^2}{S_s \delta} \right] \text{ ohms. } (148)$$

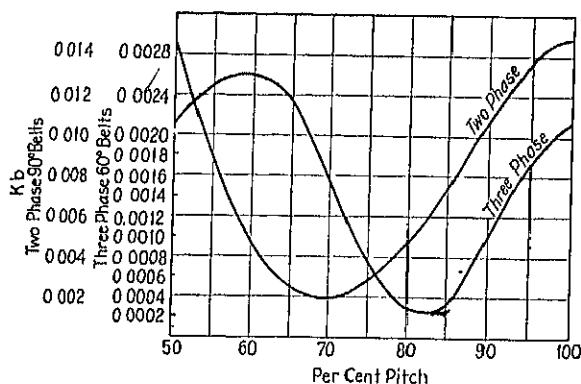


FIG. 145.—Belt leakage constants.

For machines with integral number of slots per pole and with squirrel-cage winding in the pole faces,

$$X_l = \frac{2 \ 0flmN^2}{10^7 S_s}$$

$$\left[K_s \left(\frac{d_1}{3w_s} + \frac{d_2}{w_s} \right) + \frac{0.3(3P-1)DS_s}{p^2 l} + \frac{0.266Df_c^2 f_w^2}{S_s \delta} \right] \text{ ohms. } (149)$$

For machines with integral slots per pole but without squirrel-cage winding in the pole faces,

$$X_l = \frac{2 \ 0flmN^2}{10^7 S_s}$$

$$\left[K_s \left(\frac{d_1}{3w_s} + \frac{d_2}{w_s} \right) + \frac{0.3(3P-1)DS_s}{p^2 l} + \frac{0.266Df_c^2 f_w^2}{S_s \delta} + \frac{0.319Df_c^2 f_w^2 S_s K_b}{p^2 \delta} \right] \text{ ohms. } (150)$$

The per cent reactance drop due to full-load current equals

$$\frac{X_l I}{E} \times 100.$$

with two-layer windings and with the coils in 60° belts.

The standstill reactance of a synchronous motor with open field winding can be calculated by adding to the formulas given above the squirrel-cage reactance.

The squirrel-cage reactance of a salient-pole, synchronous motor is

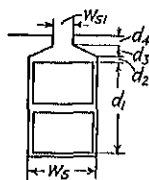


FIG. 146.

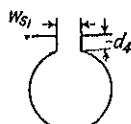


FIG. 147.

rather difficult to calculate accurately, because of the unequal distribution of the current between the bars of each pole. It is divided into slot, end-connection, and zigzag leakage reactance.

The slot reactance is calculated by assuming the bars uniformly distributed, as in the case of a squirrel-cage induction motor.

The equivalent rotor slot reactance (see Fig. 146),

$$X_{sr} = \frac{2.0flmN^2}{10^7 S_s} \frac{f_c^2 f_w^2 S_s}{S_r} \left(\frac{d_1}{3w_s} + \frac{d_2}{w_s} + \frac{2d_3}{w_s + w_{s1}} + \frac{d_1}{w_{s1}} \right) \text{ ohms.} \quad (151)$$

If round bars are used in the squirrel-cage, as shown in Fig. 147, then the rotor slot reactance,

$$X_{sr} = \frac{2.0flmN^2}{10^7 S_s} \frac{f_c^2 f_w^2 S_s}{S_r} \left(0.62 + \frac{d_1}{w_{s1}} \right) \text{ ohms.} \quad (152)$$

The end-connection reactance for the squirrel-cage winding is generally small and will be taken equal to zero.

The rotor zigzag leakage reactance,

$$X_{zr} = \frac{5}{6} X_m \left(\frac{p}{S_r} \right)^2 \text{ ohms.}$$

The magnetizing reactance of a synchronous machine,

$$X_m = \frac{2.0flmN^2}{10^7 S_s} \left(\frac{0.319 f_c^2 f_w^2 D S_s}{p^2 \delta} \right) \text{ ohms.} \quad (153)$$

Then,

$$X_{zr} = \frac{2.0flmN^2}{10^7 S_s} \left(\frac{0.266 f_c^2 f_w^2 D S_s}{S_r^2 \delta} \right) \text{ ohms.} \quad (154)$$

The standstill reactance of a synchronous motor with open field winding is then equal to the sum of the stator reactance, as calculated by formulas 148, 149, or 150, plus the rotor slot and zigzag reactances given by formulas 151 and 154.

Synchronous motors are generally started with the field winding short-circuited through a resistance, to limit the voltage induced in the field winding during starting. The standstill reactance of a synchronous motor with short-circuited field winding is equal to the standstill reactance with open field winding plus the field reactance. The total field reactance can be calculated as explained by R. H. Park and B. L. Robertson in their recent paper,² "The Reactances of Synchronous Machines."

The squirrel-cage winding of self-starting synchronous motors is active only during the starting period and must be designed to give the

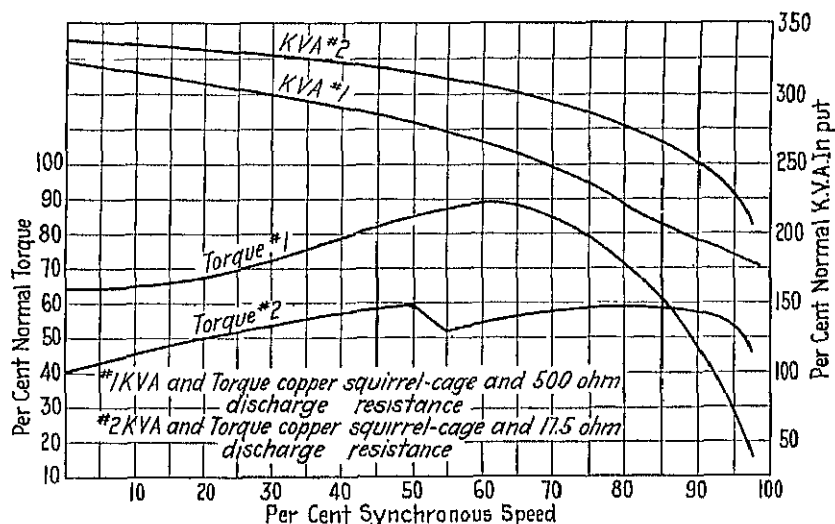


FIG. 148.—Speed-torque and speed Kva curves for 50-hp., 180-r.p.m. synchronous motor.

required starting and pull-in torque. Synchronous motors will generally pull into synchronism when the field excitation is applied, if the speed is approximately 95 per cent of synchronous speed. The torque the motor produces at this speed is called the pull-in torque. The speed-torque curve for a 50-hp, 180-r.p.m., 2300-volt, 60-cycle motor is shown in Fig. 148.

The maximum torque of the squirrel-cage winding will occur at starting or 100 per cent slip, if the equivalent resistance of the squirrel-cage winding is equal to the total reactance. The maximum torque will occur at 50 per cent of synchronous speed, if the equivalent resistance of the squirrel-cage is equal to 50 per cent of the total reactance.

² A.I.E.E. Trans, Vol. 47, April, 1928, Appendix F, p. 531.

for high starting torque, the resistance of the squirrel-cage winding must therefore be high, and for high pull-in torque low. The equivalent resistance of the squirrel-cage winding of a synchronous motor is calculated by the method explained for squirrel-cage induction motors, page 306.

$$R_r = \frac{f_e^2 f_w^2 N^2 m r}{10^6} \left(\frac{l_b}{s_b N_b} + \frac{0.64 D_{er}}{p^2 S_{er}} \right) \text{ ohms.} \quad (155)$$

When a high starting torque is required, the squirrel-cage resistance must be approximately 50

per cent of the total reactance and for high pull-in torque approximately 25 per cent of the total reactance. To obtain both a high starting and a high pull-in torque with a low starting current, the double-squirrel-cage winding³ has often been used. Figure 149 shows a pole punching with round bars for a double-squirrel-cage winding.

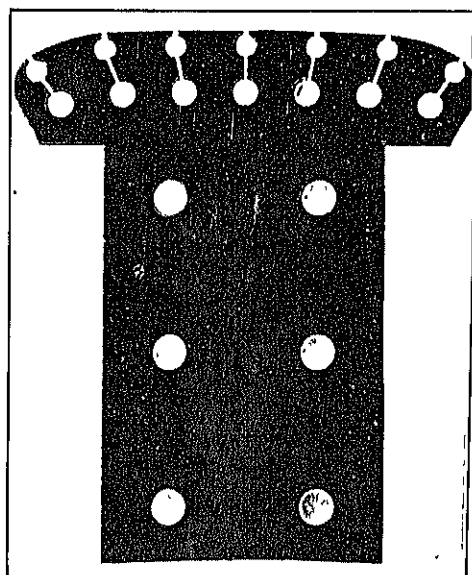


FIG. 149.—Pole punching for synchronous motor with double-squirrel-cage starting winding.

Armature Reaction.—The current flowing in the armature winding produces an alternating current field, which passes through the magnetic circuit. The action of this armature field upon the magnetic circuit is called armature reaction.

When the armature current is 90° out of phase with the induced voltage, the maximum ampere-turns of armature reaction,

$$AT_a = \frac{0.45 m N I_f f_w}{p} \quad (156)$$

The equivalent field ampere-turns per pole are found by multiplying AT_a by the ratio of the fundamental of the flux wave produced by a

³ "General Characteristics of Electric Ship Propulsion Equipments," by E. F. W. Alexanderson, *General Electric Review*, Vol. 22, April, 1919, p. 230; "The Development of Low Starting Current Induction Motors," by P. L. Alger, *General Electric Review*, Vol. 28, July, 1925, p. 499; "Starting Performance of Synchronous Motors," by H. V. Putman, *A.I.E.E. Trans.*, Vol. 46, 1927, p. 39.

sinusoidally distributed armature m.m.f., when its axis coincides with the pole center, to the fundamental of the flux wave produced by the field winding. R. W. Wieseman⁴ has derived coefficients by flux plotting for the calculation of the fundamental sine wave of flux produced in a salient-pole machine by the field winding and by a sinusoidally distributed armature m.m.f. The ratio of the fundamental of the air gap flux wave produced by a sinusoidally distributed armature m.m.f. to the fundamental of the flux wave produced by the concentrated field winding is called the armature reaction factor, K_a . Dr. Arnold⁵ gives the following formula by which the armature reaction factor can be calculated:

$$K_a = \frac{\pi f_a + \sin \pi f_a}{4 \sin f_a \frac{\pi}{2}} \quad (157)$$

The air gap flux distribution factor, f_a , is found from the flux plot as explained in Chapter X.

The equivalent field ampere-turns per pole of armature reaction for salient-pole synchronous machines,

$$\text{AT}_{af} = \frac{0.45 K_a m N I_f f_w}{p} \quad (158)$$

Short-Circuit Characteristic.—The short-circuit characteristic shows the relation between the field ampere-turns or field current and the armature current when the generator is driven at normal speed with the armature terminals short-circuited. For the short-circuit condition, the armature current is practically 90° out of phase with the voltage, and the armature magnetomotive force has a demagnetizing action upon the field. The voltage induced in the armature when short-circuited is equal to the impedance voltage, IZ_a . The field ampere-turns required to generate this voltage with the short-circuited armature are found from the open-circuit saturation curve, OB , Fig. 150. The armature, when short-circuited, has a demagnetizing action upon the field and BC , Fig. 150, is equal to the equivalent field ampere-turns per pole of armature reaction. If CD equals the armature current, I , then D is one point on the short-circuit characteristic, which is a straight line for normal values of load current. OC equals the field ampere-

⁴ "Graphical Determination of Magnetic Fields," A.I.E.E. Journal, Vol. 46, 1927, pp. 430 to 437.

⁵ "Die Wechselstromtechnik," Vol. 4, p. 31, Julius Springer, Berlin. See also "Principles of Alternating Current Machinery," by R. R. Lawrence, Vol. 2, 2nd ed., p. 107, McGraw-Hill Book Co., N. Y.

turns per pole required to circulate the current, I , in the short-circuited armature winding.

In Fig. 150, OF equals the field ampere-turns required to generate normal terminal voltage at no-load. The ratio of OF to OC is called the

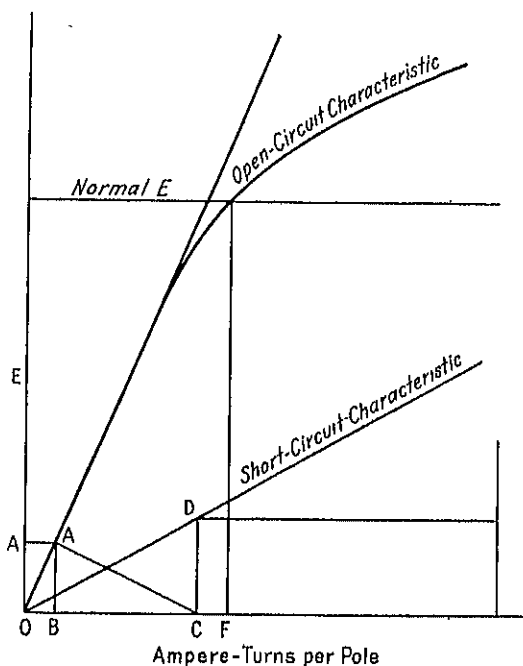


FIG. 150.

short-circuit ratio. This ratio is an important factor in the design of synchronous machines; it may be called the ratio of the field strength to the armature strength. A low short-circuit ratio means a small air gap, poor regulation, a small amount of field copper, and, in general, an inexpensive field winding. On the other hand, a large short-circuit ratio means a large air gap, good regulation, a large amount of field copper, and a more expensive field winding. A generator with low short-circuit ratio will require a large change in field excitation for small load changes.

The field current necessary

for synchronous generators for full-load and unity power factor is generally 1.90 times the no-load field current when the short-circuit ratio is 0.65, and only 1.20 times the no-load field current when the short-circuit ratio is 1.40. For full-load and 80 per cent power factor, the field current necessary is generally 2.5 times the no-load field current when the short-circuit ratio is 0.65 and 1.60 times the no-load field current when the short-circuit ratio is 1.40. The short-circuit ratio determines the stability characteristics of generators to be operated with high-voltage transmission lines. For most hydro-electric generators, the short-circuit ratio will be close to unity. In general, synchronous generators will have a short-circuit ratio from 0.60 to 1.40.

The stability and pull-out characteristics of synchronous motors depend also upon the short-circuit ratio. When this ratio is large, the motor will have a high pull-out torque and, conversely, when small the pull-out torque will be low. Synchronous motors for direct connection

to refrigerating compressors must be designed with a short-circuit ratio that will permit a suitable flywheel.⁶

Excitation for Any Load and Power Factor.—In Fig. 151 the ordinate axis represents the armature current. The power factor circle is drawn with per cent power factor as ordinates and per cent reactive factor as abscissas. The vector OA shows the terminal voltage for a generator at 80 per cent lagging power factor. The induced voltage, OC , is found by adding to the terminal voltage the armature resistance drop, AB , for a current of I amperes, in phase with the current and the armature reactance drop, BC , for a current of I amperes, 90° out of phase with the armature current. θ_1 is the phase angle between the induced voltage and armature current. From the open-circuit saturation curve, Fig. 152, the field excitation for the induced voltage is OD . The phase angle between the induced voltage and armature current is some value between zero and 90° ; therefore, the armature m.m.f. will have both a demagnetizing and a cross-magnetizing action upon the field. In Fig.

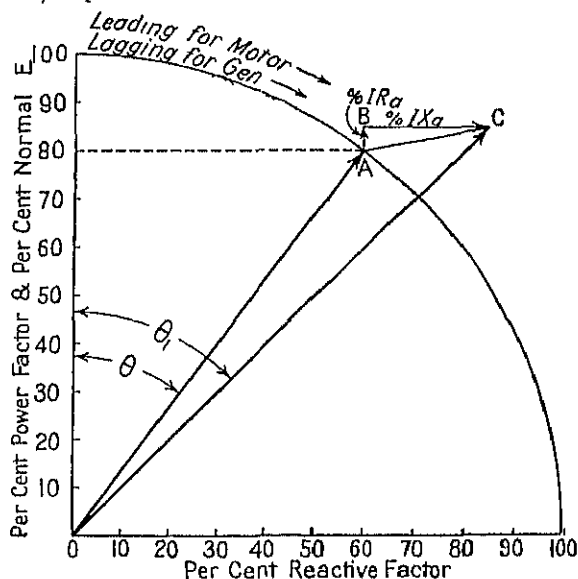


FIG. 151.

152, $DF = AT$, the equivalent field ampere-turns per pole of arma-

⁶ "Synchronizing Power in Synchronous Machines," by H. V. Putman, A.I.E.E. Trans., Vol. 45, 1926, p. 1116; "Synchronous Machines," by R. E. Doherty and C. A. Nickle, A.I.E.E. Trans., Vol. 46, 1927, p. 1; "Starting Performance of Synchronous Motors," by H. V. Putman, A.I.E.E. Trans., Vol. 46, 1927, p. 39; "The Flywheel Problem in Compressors Direct Connected to Synchronous Motors," by A. R. Stevenson, Jr., Refrigerating Engineer, Vol. 11, 1924, p. 1923; "Flywheel Requirements for Unbalanced Air and Ammonia Compressors," by C. W. Cutler, Refrigerating Engineer, Vol. 12, 1925, p. 75; "Synchronous Motors," by W. T. Berkshire, General Electric Review, Vol. 23, Feb. 1920, p. 112; "Variation of Alternator Excitation with Load," by F. D. Newbury, The Electric Journal, Vol. 15, p. 253; "Stability Characteristics of Alternators," by O. E. Shirley, A.I.E.E. Trans., Vol. 45, 1926, p. 1108.

excitation required for a current of I amperes at zero per cent power factor. $DG = AT_{af} \sin \theta_1$, $GF = AT_{af} \cos \theta_1$, and $OF = OF'$ are the field ampere-

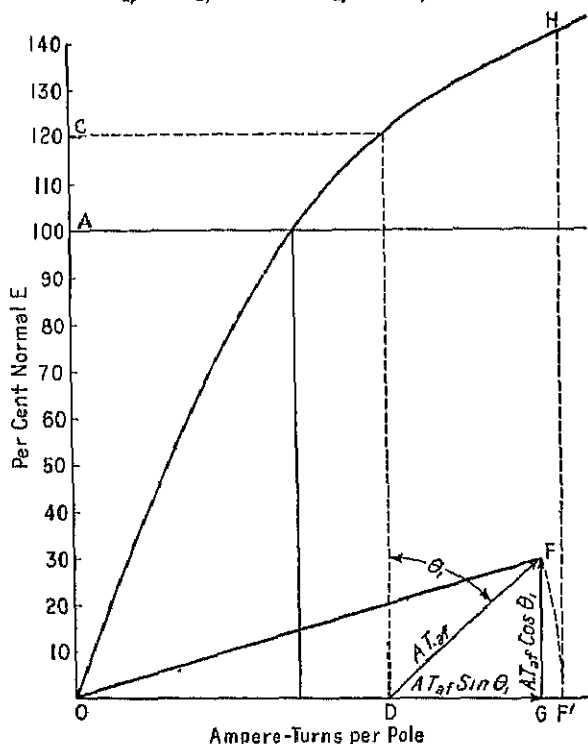


FIG. 152.

turns per pole required for an armature current of I amperes at 80 per cent lagging power factor.

The regulation of constant potential alternators is defined by the standards of the A.I.E.E. as the rise in voltage (when the rated load at specified power factor is reduced to zero) expressed in per cent of rated voltage. In Fig. 152 the per cent regulation for full-load at 80 per cent power factor

$$= \frac{F'H - OA}{OA}$$

This method of construction can also

be used to determine the excitation required for a synchronous motor for any load and power factor. The construction is the same as shown in Fig. 151, with the exception that the resistance drop is subtracted from the terminal voltage and not added as in the case of a generator. (See sample synchronous motor design.)

Field Winding Design.—It is apparent from Figs. 151 and 152 that the field excitation required for a generator for a given load and voltage increases with decreasing lagging power factor. Modern synchronous generators are rated in Kva at 80 per cent lagging power factor. The field winding must therefore be designed for the excitation required for rated load at 80 per cent lagging power factor. The section area of the conductor for the field winding,

$$s_f = \frac{ATP_f L_f p \times 0.826}{E_f \times 10^6} \text{ sq. in.} \quad (159)$$

the field winding. The standard exciter voltages are 125 volts for medium- and small-capacity machines and 250 volts for large-capacity machines. The field winding should be designed for a voltage E_f , from 15 to 20 per cent less than the exciter voltage to allow for the drop in voltage between generator field and exciter and to allow for variations in the reluctance of the magnetic circuit.

The wire-wound field coil is generally used for machines with a small number of poles. Figure 153 is a sketch of a pole with wire-wound field coil and shows how the coils are wound and insulated. The coils are generally wound in steps, because of the large clearance between adjacent poles at the pole shoe. The weighted mean-turn for the coil shown in Fig. 153 is calculated as follows:

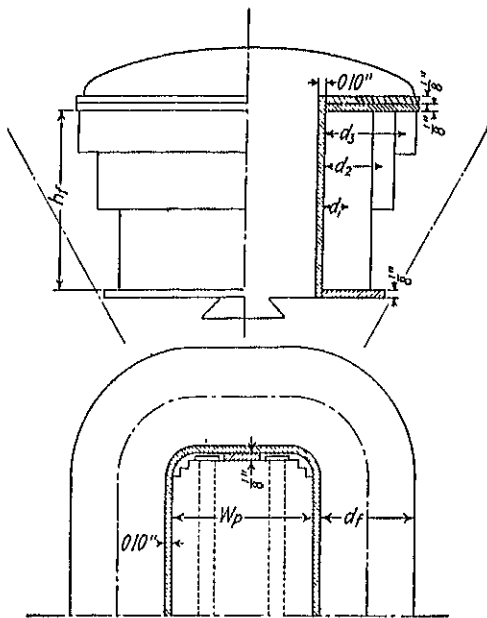


FIG. 153.—Wire-wound field pole.

$$L_{f1} = 2l_1 + 2(w_p - 0.25) + \pi(0.45 + 2d_1)$$

$$L_{f2} = 2l_1 + 2(w_p - 0.25) + \pi(0.45 + 2d_2)$$

$$L_{f3} = 2l_1 + 2(w_p - 0.25) + \pi(0.45 + 2d_3)$$

$$L_f = \frac{L_{f1}t_{f1} + L_{f2}t_{f2} + L_{f3}t_{f3}}{t_f} \text{ in.} \quad (160)$$

For machines with large number of poles, the field coils are generally wound with bare strap copper wound on edge, with paper insulation, 0.005 in. thick, between turns. The method of winding the coils is shown in Fig. 154. For very large-capacity machines with wide pole body, the coils are wound as shown in Fig. 155. The length of the mean-turn for the type of coil shown in Fig. 154,

$$L_f = 2(l_1 - 1.0) + \pi(w_p + 0.20 + d_f) \text{ in.} \quad (161)$$

required ampere-turns without an excessive temperature rise field current can be estimated by as the current density; then

$$i_f = s_f A_f \text{ amperes.}$$

For revolving field type synchronous machines,

$$A_f = 1500 \text{ to } 2500 \text{ amperes per sq.}$$

For wire-wound field coils with a large number of turns of fine wire with deep wire the lower values of A_f apply. In general may be taken equal to 2000 amperes per sq. in. for the first approximation.

The turns per pole,

$$t_f = \frac{ATP_f}{i_f}$$

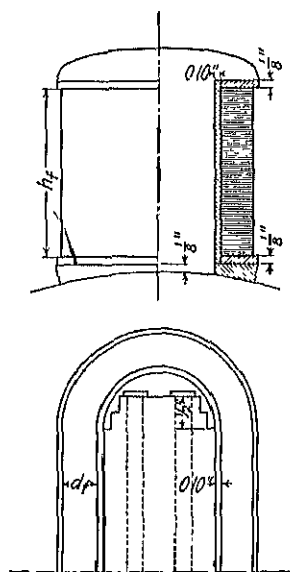


FIG. 154.—Ribbon-copper wound field pole.

The correct value for the number of turns will depend upon the temperature rise which in turn, depends upon the losses and the cooling surface of the field coils. A high temperature rise indicates too few turns and a high current density, whereas a low temperature rise indicates too large a number of turns and an uneconomical use of field copper.

An approximate check of the temperature rise of the field winding

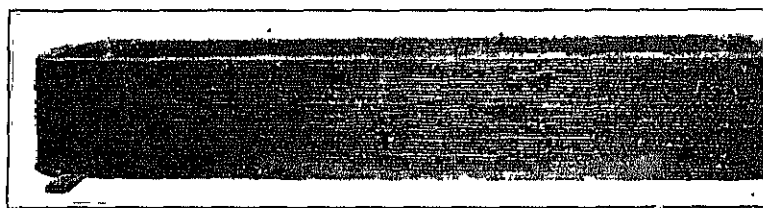


FIG. 155.—Ribbon-copper field coil for 65,000-Kva, 107-r.p.m., 28-pole generator.

can be obtained from the cooling surface per watt loss. The cooling surface for the field winding (see Figs. 153 and 154),

$$S_f = 2(d_f + h_f)L_f p \text{ sq. in.} \quad (1)$$

$$\frac{S_f}{W_f} = \frac{2(d_f + h_f)L_f p}{i_f^2 R_f} \text{ sq. in. per watt.} \quad (164)$$

For revolving-field, synchronous generators with wire-wound field coils, the surface per watt should generally be larger than 1.0 for the maximum condition of load for the field winding, full-load 80 per cent power factor. For bare strap-copper field coils, the surface per watt loss should generally be larger than 0.75.

The resistance of the field winding at 75° C.,

$$R_f = \frac{L_f l_f p \times 0.826}{s_f \times 10^6} \text{ ohms.}$$

The copper loss,

$$W_f = i_f^2 R_f \text{ watts.}$$

The exciter capacity,

$$W_o = \frac{E_o^2}{R_f \times 10^3} \text{ kilowatts.} \quad (165)$$

The weight of copper in the field winding,

$$G_f = L_f l_f p s_f \times 0.321 \text{ lb.}$$

Sample Design: Field Winding Design.—The data required for the calculation of the leakage reactance are as follows:

$$\begin{array}{lll} f = 60, & K_s = 0.88, & D = 100 \text{ in.,} \\ l = 17.5 \text{ in.,} & d_1 = 2.55 \text{ in.,} & p = 32, \\ m = 3, & d_2 = 0.25 \text{ in.,} & f_o = 0.975, \\ N = 224, & w_s = 0.456 \text{ in.,} & f_w = 0.956, \\ S = 336, & P = 0.857, & \delta = 0.406. \end{array}$$

Formula 148 must be used, because the armature winding has a fractional number of slots per pole per phase.

$$\begin{aligned} K_s \left(\frac{d_1}{3w_s} + \frac{d_2}{w_s} \right) &= 0.88 \left(\frac{2.55}{3 \times 0.456} + \frac{0.25}{0.456} \right) = 2.13 \\ \frac{0.3(3P - 1)DS_s}{p^2 l} &= \frac{0.30(3 \times 0.857 - 1)100 \times 336}{32^2 \times 17.5} = 0.882 \\ \frac{0.53Df_o^2 f_w^2}{S_s \delta} &= \frac{0.53 \times 100 \times 0.975^2 \times 0.956^2}{336 \times 0.406} = 0.337 \\ X_l &= \frac{2.0flmN^2}{10^7 S_s} (2.13 + 0.882 + 0.337) \\ &= \frac{2.0 \times 60 \times 17.5 \times 3 \times 224^2}{10^7 \times 336} (2.13 + 0.882 + 0.337) = 0.315 \text{ ohm.} \end{aligned}$$

the per cent reactance drop due to full-load current,

$$\frac{IX_l \times 100}{E} = \frac{0.315 \times 600 \times 100}{1390} = 13.6 \text{ per cent.}$$

The resistance of the armature winding is given on page 205. The per cent resistance drop due to full-load current,

$$\frac{IR_a \times 100}{E} = \frac{0.0247 \times 100 \times 600}{1390} = 1.07 \text{ per cent.}$$

The per cent impedance drop,

$$\frac{IZ_a \times 100}{E} = \sqrt{13.6^2 + 1.07^2} = 13.65 \text{ per cent.}$$

The equivalent field ampere-turns per pole of armature reaction for full-load current,

$$\begin{aligned} \text{AT}_{af} &= \frac{0.45 K_a m N I_f c f_w}{p} \\ &= \frac{0.45 \times 0.852 \times 3 \times 224 \times 600 \times 0.975 \times 0.956}{32} \\ &= 4500 \text{ ampere-turns.} \end{aligned}$$

The short-circuit characteristic is shown in Fig. 156 and is determined as explained on page 223. The short-circuit ratio,

$$\frac{\text{ATP}_0}{\text{ATP}_s} = \frac{6730}{5370} = 1.25.$$

This value lies within the limits given on page 224 and will be satisfactory unless stability requirements necessitate a lower value. The short-circuit ratio can be reduced by decreasing the length of the air gap, thereby reducing the number of ampere-turns required to generate normal voltage at no-load.

The ampere-turns per pole required on the field winding for full-load at 80 per cent lagging power factor are found graphically, as explained on page 225. The construction for the sample design is shown in Fig. 156 for unity and 80 per cent lagging power factor. For unity power factor full-load,

$$\text{ATP}_{100} = 8800 \text{ ampere-turns}$$

$$ATP_{80} = 11,400 \text{ ampere-turns.}$$

These values can also be calculated as explained in Appendix C of the paper by R. E. Doherty and O. E. Shirley.⁷

The regulation at 80 per cent power factor (see Fig. 156)

$$= 123.0 - 100 = 23.0 \text{ per cent}$$

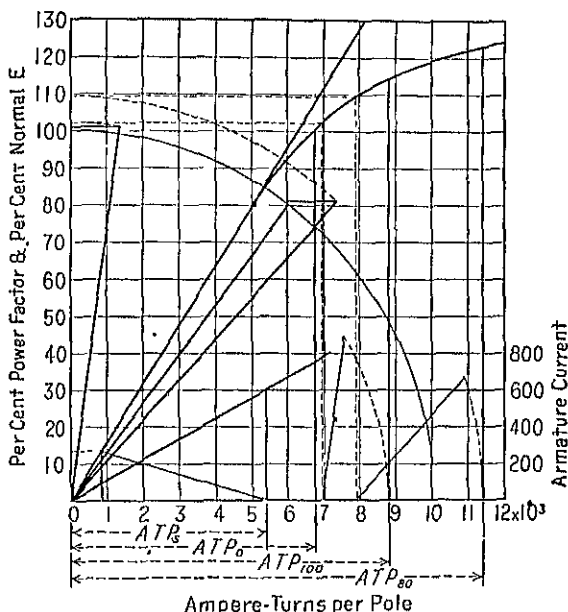


FIG. 156.—Open-circuit and short-circuit characteristics.

and at 100 per cent power factor

$$= 114.3 - 100 = 14.3 \text{ per cent.}$$

The length of the mean-turn for the field winding must first be estimated. The bare strap-copper field winding, shown in Fig. 154, will be used for this design. The length of the mean-turn for a copper strap 1.25 in. wide,

$$\begin{aligned} L_f &= 2(l_1 - 1.0) + \pi(w_p + 0.20 + d_f) \\ &= 2(17.5 - 1.0) + \pi(4.0 + 0.20 + 1.25) \\ &= 50.1 \text{ in.} \end{aligned}$$

⁷ "Reactance of Synchronous Machines and Its Applications," A.I.E.E. Trans., Vol. 37, Part 2, 1918, p. 1293.

the section-area of the conductor,

$$s_f = \frac{ATP_{80} L_f p \times 0.826}{E_f \times 10^6}$$

$$= \frac{11,400 \times 50.1 \times 32 \times 0.826}{110 \times 10^6} = 0.137 \text{ sq. in.}$$

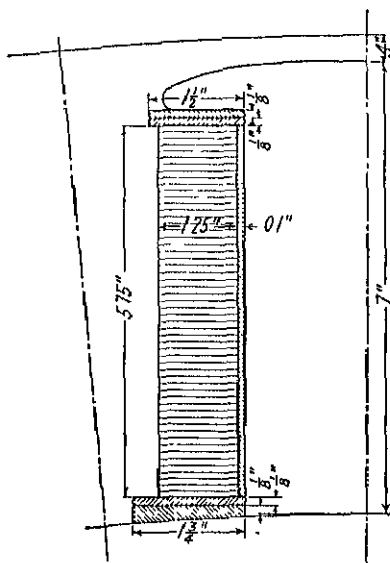


Fig. 157.

From the sketch, Fig. 157, the space available for the field winding,

$$h_f = 5.75 \text{ in.}$$

A conductor 0.109 in. \times 1.25 in., area 0.134 sq. in. is selected from the copper table. The insulation between turns consists of paper 0.005 in. thick. If 0.005 in. is allowed for buckling of the conductor in the process of winding, then the total space occupied by one turn = 0.005 + 0.005 + 0.109 = 0.119 in. The number of turns that can be wound on each pole,

$$t_f = \frac{5.75}{0.119} = 48.$$

The field current for full-load and 80 per cent lagging power factor,

$$i_{f80} = \frac{ATP_{80}}{t_f} = \frac{11,400}{48} = 238 \text{ amperes,}$$

and the current density,

$$A_f = \frac{238}{0.134} = 1775 \text{ amperes per sq. in.}$$

The resistance at 75° C.,

$$R_f = \frac{L_f t_f p \times 0.826}{s_f \times 10^6}$$

$$= \frac{50.1 \times 48 \times 32 \times 0.826}{0.134 \times 10^6} = 0.474 \text{ ohm}$$

and the copper loss for a field current of 238 amperes,

$$W_f = 238^2 \times 0.474 = 26,900 \text{ watts.}$$

The radiating surface,

$$\begin{aligned} S_f &= 2(d_f + h_f)L_f p \\ &= 2(1.25 + 5.75)50.1 \times 32 = 22,500 \text{ sq. in.} \end{aligned}$$

and the surface per watt loss,

$$\frac{S_f}{W_f} = \frac{22,500}{26,900} = 0.837 \text{ sq. in. per watt.}$$

The voltage drop in the field winding for the full-load 80 per cent lagging power factor field current,

$$E_f = 238 \times 0.474 = 113 \text{ volts.}$$

The maximum field current for 120 volts across the field winding, allowing 5 volts drop in exciter leads and brushes, is

$$i_{f \max.} = \frac{120}{0.474} = 253 \text{ amperes.}$$

The exciter capacity,

$$\begin{aligned} W_e &= \frac{E_o^2}{R_f \times 10^3} = \frac{125^2}{0.474 \times 10^3} \\ &= 33 \text{ kilowatts.} \end{aligned}$$

The weight of the field copper,

$$\begin{aligned} G_f &= L_f i_f p s_f \times 0.321 \\ &= 50.1 \times 48 \times 32 \times 0.134 \times 0.321 \\ &= 3310 \text{ lb.} \end{aligned}$$

CHAPTER XIV

LOSSES, EFFICIENCY, AND TEMPERATURE RISE

The losses in synchronous machines are:

- (1) Copper losses in armature and field winding.
- (2) Field rheostat losses.
- (3) Core losses.
- (4) Mechanical losses; bearing friction, and windage.
- (5) Stray load-losses.

Armature Copper Losses.—The method of calculating the armature resistance is given on page 200. The armature copper loss,

$$W_a = I^2 R_a m \text{ watts.} \quad (166)$$

The A.I.E.E. Standards specify that the copper losses are to be calculated for a temperature of 75° C. for all loads; therefore, R_a must be the armature resistance per phase at 75° C. The armature current varies directly with the load for a given power factor; therefore the copper loss will vary as the square of the load.

Field Copper Losses.—The resistance of the field winding is calculated as shown on page 229, and the field current for any load and power factor is determined as explained on page 225. The loss in the field winding at 75° C.,

$$W_f = i_f^2 R_f \text{ watts.}$$

A field rheostat is generally connected in series with the field winding of synchronous generators. Unity power factor synchronous motors are often operated without a field rheostat; the field winding of the motor is then designed to give the required field current when normal exciter voltage is applied. When a field rheostat is used, the rheostat losses must be included when calculating the efficiency. The total losses in the field winding, field copper plus rheostat losses,

$$W_f + W_r = i_f E_a \text{ watts.} \quad (167)$$

Core Losses.—The losses in the armature core consist of the hysteresis and eddy current losses in the teeth and yoke and the

face and surface of the armature teeth due to the flux pulsations in the air gap produced by the armature slots, losses due to punching and bending strains in the laminations, losses due to imperfect insulation between laminations caused by burrs or slot filing, and losses in the end-frames due to stray fluxes.

The method of calculating core losses for direct-current generators and motors can also be used for synchronous machines. The curves in the Appendix give the loss per pound per cycle due to the fundamental frequency flux for various grades of sheet steel. These curves were obtained from tests of samples in accordance with the standards of the American Society for Testing Materials.

The armature cores of small and medium size machines are generally built up of an open-hearth electric sheet steel with very little or no silicon and in thickness from 0.014 to 0.019 in. For machines with large armature cores, the core losses can be materially reduced by using a sheet steel alloyed with silicon. The following quotation from a recent A.I.E.E. paper¹ bears this out:

"To illustrate the reduction in core loss that results from the use of these higher grade steels, if the loss in non-silicon steel is represented by 100, the loss with 2 per cent silicon steel will be 70, and 45 with 4 per cent silicon steel. The use of 4 per cent silicon steel improves the efficiency slightly more than 1 per cent of full load, and 2½ per cent at half load, as compared with the efficiency of machines using non-silicon steel. When this steel is used, the core loss is reduced from 50 per cent of the total loss to 30 per cent of the total loss."

The additional losses are difficult to calculate and vary over a wide range for machines of the same type. The total core losses for synchronous machines are generally from 1.8 to 3.0 times the sum of the losses in the teeth and yoke due to the fundamental frequency flux. The multiplying factor should be determined from tests of machines of similar design. When such data are not available 2 to 2.5 may be used.

Friction and Windage Losses.—The loss due to bearing friction can be calculated² when the dimensions of the bearing, the peripheral speed of the shaft at the bearing, the load on the bearing, and the coefficient of friction are known. The windage losses are very difficult to calculate and depend largely upon the type of construction. The combined friction and windage loss is therefore generally taken from tests of machines of the same construction. When such data are not

¹ "Recent Improvements in Turbine Generators," by S. L. Henderson and C. R. Soderberg, A.I.E.E. Trans., Vol. 47, No. 2, p. 549.

² See footnote, page 118.

the friction and windage loss may be estimated with the help of the curves, Figs. 158 and 159.

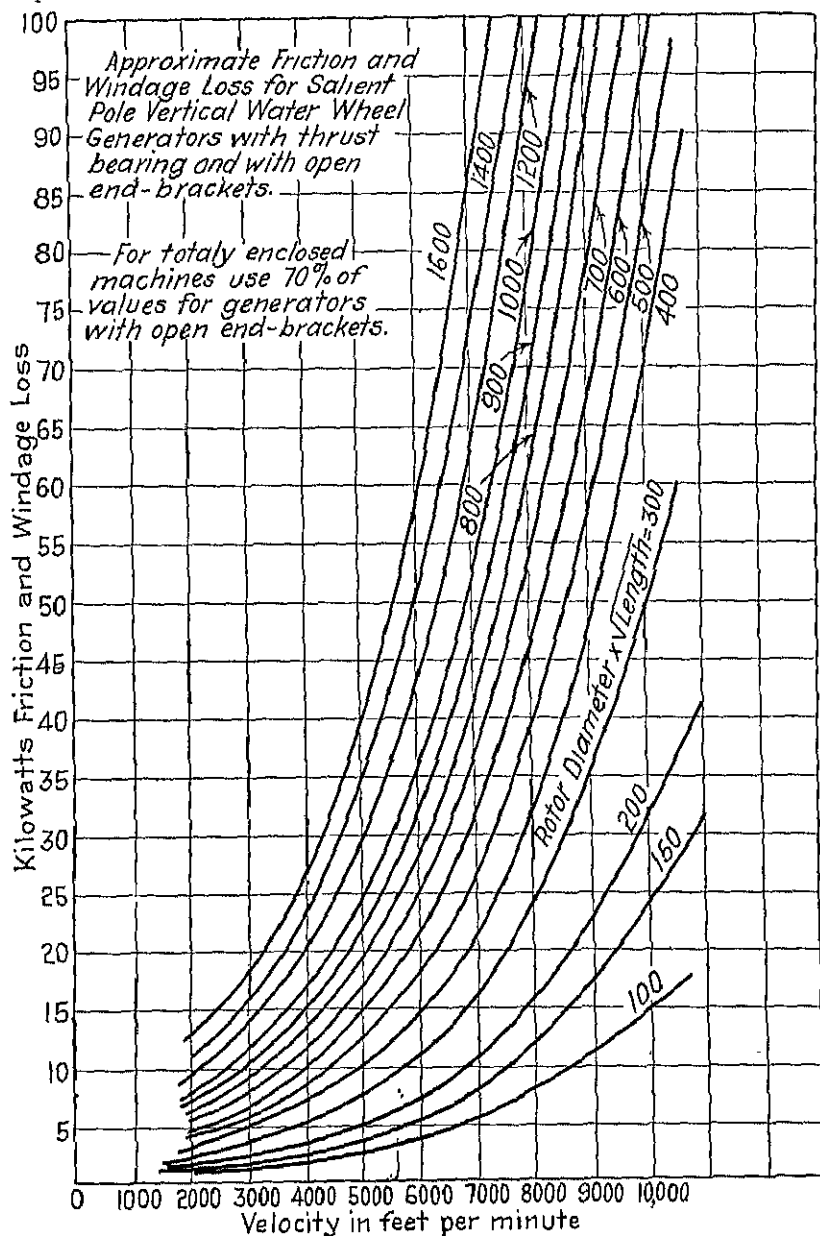


FIG. 158.

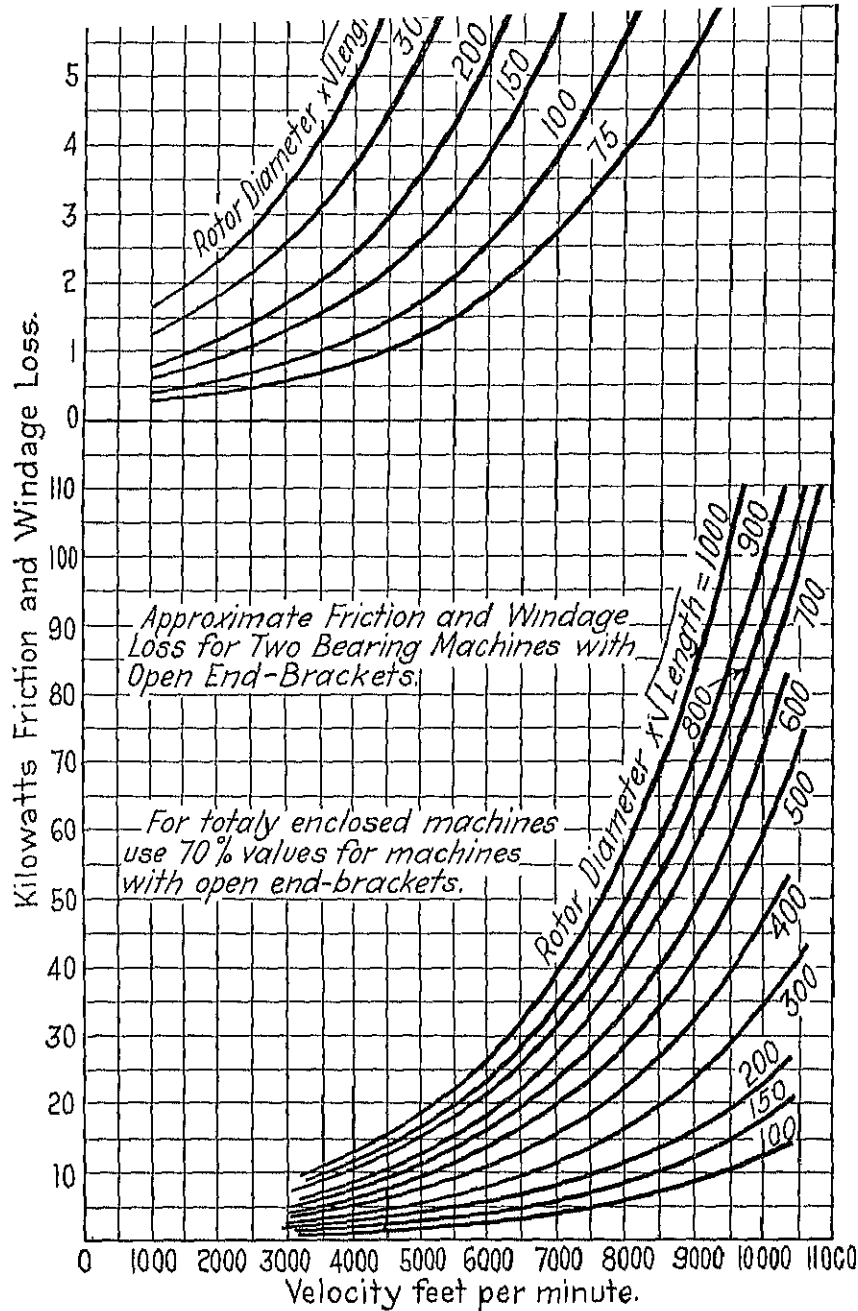


FIG. 159.

bearing surfaces have been found to occur on large-capacity machines, caused by currents flowing between shaft and bearing. The designer of large-capacity generators and motors must take the proper precautions to limit to a negligible value the current between shaft and bearing. Careful studies have been made to determine the origin and method of preventing shaft currents. The results of these investigations have been published in various technical journals.³

Stray Load-Losses.—The Standards of the A.I.E.E. define the stray load-losses as follows: "These include iron losses and eddy current losses in the copper, due to fluxes varying with the load and also saturation."

For large machines, the eddy current losses in the copper are large because of the large conductor sections and deep slots. For these reasons, most large-capacity machines are now being built with transposed⁴ conductors in the armature coils. Large conductor sections must therefore be avoided in armature windings and the conductors built up of a number of small wires in parallel.

It is difficult to calculate the stray load-losses accurately; they must therefore be assumed based on test values from machines of similar design. From the short-circuit test specified in the A.I.E.E. Standards, the effective alternating-current armature resistance can be found by dividing the total loss on short-circuit, after deducting the friction and windage loss, by the current squared. If this resistance is used to calculate the armature copper loss, the result will be I^2R plus stray load-losses. Dr. Arnold⁵ states that the effective alternating-current resistance is generally from 1.5 to 2.5 times the resistance measured by direct current in single-phase machines and 1.3 to 2.0 in polyphase machines.

Efficiency.—The efficiency of a motor or generator is the ratio of the output to the output plus all the losses. It is generally expressed as a percentage as follows:

$$\text{eff.} = \frac{\text{Kva Output} \times \text{PF} \times 100}{(\text{Kva Output} \times \text{PF}) + W_a + W_f + W_r + W_{sl} + W_{fw} + W_c} \text{ per cent.}$$

For engine-type generators and motors to be direct connected to steam or internal-combustion engines, or air or ammonia compressors, the electrical manufacturer does not furnish the bearings, and the

³ See footnote, page 154.

⁴ "Reduction of Armature Copper Losses," by J. H. Summers, A.I.E.E. Journal, Vol. 46, May, 1927, p. 451; "Transposed Armature Coils in Alternating Current Generators," by S. L. Henderson, Electric Journal, Vol. 23, July, 1926, p. 348.

⁵ "Die Wechselstromtechnik," Vol. 4, p. 54, Julius Springer, Berlin.

friction and windage losses are not included when calculating the efficiency.

When specifying the efficiency of electric machines, it is important to specify by what method the efficiency is to be determined, because marked variations⁶ in efficiency are obtained by various methods.

The curves in Fig. 160 show the approximate full-load efficiency and exciter capacity for high-speed, unity power factor, synchronous motors, for voltages including 2200 volts. The approximate full-load efficiencies for unity power factor, 50°-rated, engine-type synchronous motors is shown in Fig. 161. The approximate efficiency of standard,

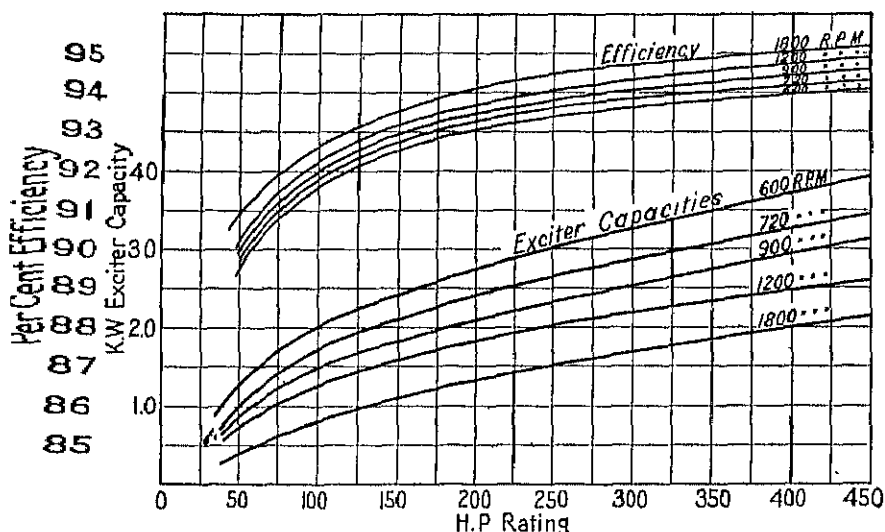


FIG. 160.—Approximate full-load efficiencies and exciter capacities for 60-cycle, unity power factor, synchronous motors.

50°-rated, synchronous generators is shown in Fig. 162 for full-load at 1.00 per cent power factor. The exciter capacities required are shown in Fig. 163.

Temperature Rise.—The losses in the armature copper and core and in the field winding are converted into heat, which increases the temperature of the machine above that of the surrounding air. The value of the final temperature depends upon the heat capacity of the various insulating materials used and upon the rate at which heat is conducted through the material to the cooling medium. The final

⁶ "A Comparison of the Efficiency of Synchronous Machines as Determined by Various Methods," by P. L. Alger, General Electric Review, Vol. 29, Nov., 1926, p. 765-774.

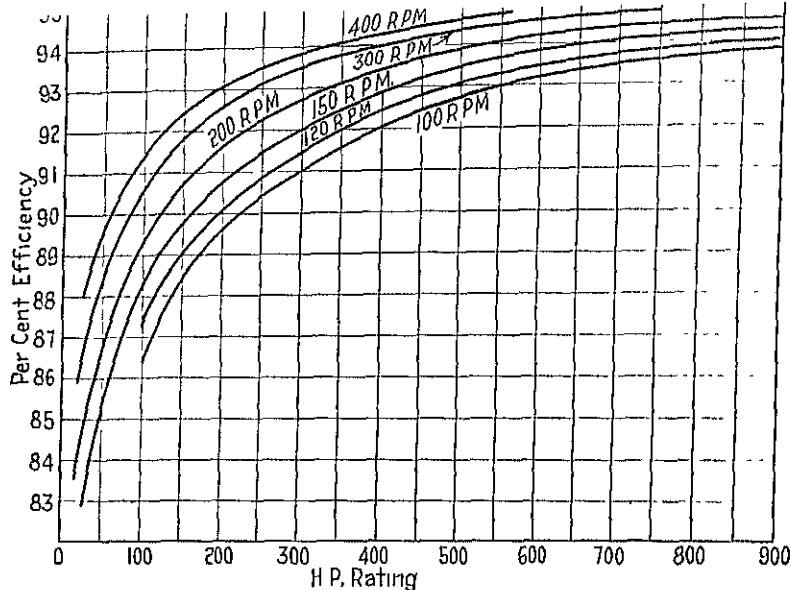


FIG. 161.—Approximate full-load efficiencies for engine-type synchronous motors 60 cycles, unity power factor.

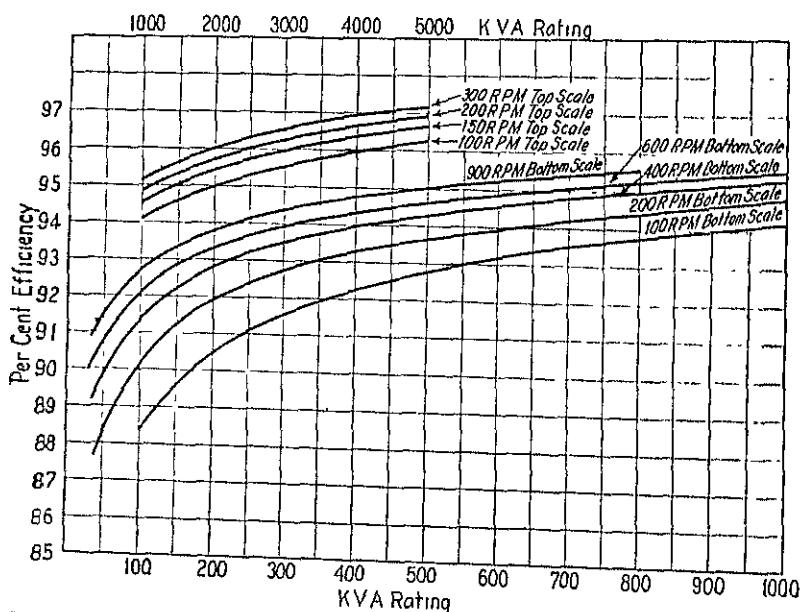


FIG. 162.—Approximate full-load, unity power factor efficiencies of 60-cycle, salient-pole synchronous generators.

equal to the rate at which the heat is dissipated. Tests on various kinds of insulating materials have shown that for each material there is a safe continuous operating temperature which can not be exceeded without impairing the life of the material. The maximum continuous operating temperature specified by the American Institute of Electrical Engineers for synchronous machines are given in Tables XVIII and XIX.

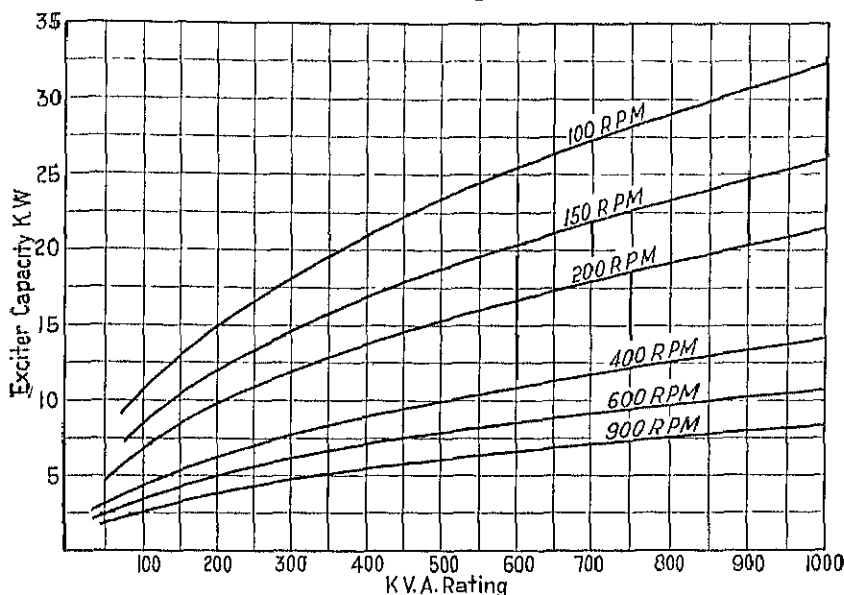


FIG. 163.—Approximate exciter capacities for 60-cycle, 80 per cent power factor, salient-pole generators.

The temperature rise of each of the various parts of steam turbine generators, above the temperature of the cooling medium, shall not exceed the values given in Table XVIII and for salient-pole motors and generators, the values given in Table XIX. The temperatures shall be determined by the methods specified in the tables.

The various kinds of insulating materials included in the different classes referred to in the tables are given on page 122, Chapter VII.

The output that can be obtained from a given frame may or may not be limited by the safe operating temperature. For salient-pole synchronous machines of the revolving-field type, satisfactory ventilation of the armature winding can generally be obtained; and operating characteristics, efficiency, regulation, etc., may be the limiting factors rather than temperature. The designer must, however, make ample

LIMITING TEMPERATURE RISES FOR STEAM TURBINE
DRIVEN ALTERNATORS

Item	Description of Part	Method of Temperature Determination Required	Limiting Temperature Rise in Degrees Centigrade	
			Class A Insulation	Class B Insulation
1	Insulated armature windings on stators of machines of 750 Kva and below.	Thermometer	50	70
2	Insulated armature windings with 2 coil sides per slot on stators of machines above 750 Kva.	Embedded detector	60	80
3	Insulated field windings.	Resistance	...	90
4	Collector rings (The class of insulation refers to insulation affected by the heat from the collector rings, which insulation is employed in the construction of the collector rings or is adjacent thereto).	Thermometer	65	85
5	Cores and mechanical parts in contact with or adjacent to insulation.	Thermometer	50	70
6	Miscellaneous parts (such as brushholders, brushes, pole tips, etc.), other than those whose temperatures affect the temperature of the insulating material, may attain such temperatures as will not be injurious.			

* A.I.E.E. Standards No. 7, July, 1925, pp. 8 and 9.

provisions for ventilation in large-capacity machines to avoid local hot spots. The radiating surfaces are usually quite large for slow-speed machines, and the problems of temperature control are generally less difficult than for high-speed machines. The field windings⁷ of high-speed machines are particularly difficult to ventilate properly.

⁷ "Recent Improvements in Turbine Generators," by S. L. Henderson and C. R. Soderberg, A.I.E.E. Trans., Vol. 47, No. 2, p. 549. "The Multiple Path Radial Ventilation of Large Turbo-Alternators," by M. D. Ross, Electric Journal, Vol. 21,

LIMITING TEMPERATURE RISES FOR SYNCHRONOUS MACHINES OTHER
THAN STEAM TURBINE DRIVEN ALTERNATORS

Item	Description of Part	Method of Temperature Determi- nation Required	Limiting Temperature Rise in Degrees Centigrade	
			Class A Insulation	Class B Insulation
1	Insulated armature windings with 2 coil sides per slot on stators of machines of 1500 Kva and below	Thermometer	50	70
2	Insulated armature windings with 2 coil sides per slot on stators of machines above 1500 Kva.	Embedded detector	60	80
3	Insulated field windings	Resistance	60	80
4	Collector rings (The class of insulation refers to insulation affected by the heat from the collector rings, which insulation is employed in the construction of the collector rings or is adjacent thereto).	Thermometer	65	85
5	Cores and mechanical parts in contact with or adjacent to Class A or B insulation.	Thermometer	50	70
6	Amortisseur windings may attain such temperature as will not occasion mechanical injury to the machine.			
7	Miscellaneous parts (such as brushholders, brushes, pole tips, etc.) other than those whose temperatures affect the temperature of the insulating material may attain such temperatures as will not be injurious.			

* A.I.E.E. Standards No 7, July, 1925, pp. 8 and 9.

Dec., 1924, p. 540. "Temperatures in Large Alternating Generators," by W. J. Foster, General Electric Review, Vol. 23, July, 1920, p. 560; General Electric Review, Vol. 23, Feb., 1920, pp. 99-108 and 147-152. See also references, page 123.

the perimeter of the core section, plus one surface for each duct (see Fig. 164),

$$S_a = \frac{\pi}{4}(D_0^2 - D^2)(2 + n_d) + \pi l(D + D_0). \quad (168)$$

The losses that must be dissipated by this surface are the core loss and

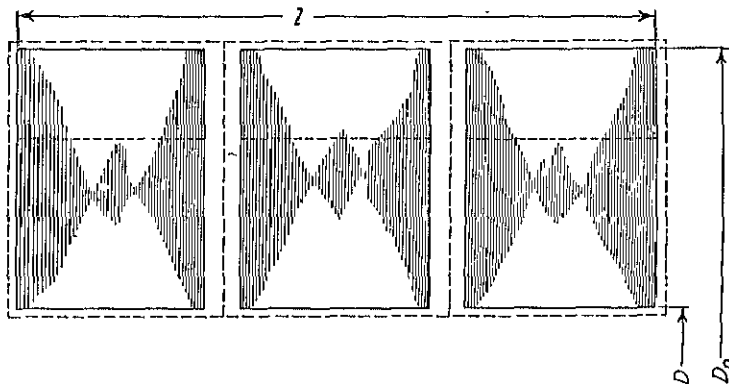


FIG. 164.—Section of armature core showing radiating surfaces.

the armature copper loss for that part of the armature coil embedded in the slots.

The radiating surface per watt loss,

$$\frac{S_a}{W} = \frac{\frac{\pi}{4}(D_0^2 - D^2)(2 + n_d) + \pi l(D_0 + D)}{W_c + W_a \frac{l}{L_a}}. \quad (169)$$

For a temperature rise not to exceed 50° C., the radiating surface per watt for the armature should generally be greater than 0.70.

The method of calculating the radiating surface for the field winding and the safe values for the surface per watt loss have been given on page 229.

Sample Design: Losses, Efficiency, and Temperature Rise.—The armature resistance is given on page 205. The copper loss at full-load,

$$\begin{aligned} W_a &= I^2 R_a m = 600^2 \times 0.0247 \times 3 \\ &= 26,700 \text{ watts.} \end{aligned}$$

ATP₁₀₀ = 8800, and the field current (see Fig. 156),

$$i_f = \frac{8800}{48} = 183 \text{ amperes.}$$

The field copper loss plus rheostat loss for full-load at unity power factor,

$$W_f + W_r = 183 \times 125 = 22,900 \text{ watts.}$$

The average armature tooth width,

$$w_{ta} = \frac{\pi(D + d_s)}{S} - w_s = \frac{\pi(100 + 2.88)}{336} - 0.456 \\ = 0.505 \text{ in.}$$

The weight of the armature teeth,

$$G_{at} = w_{ta}(l - n_a w_a)k_1 S d_s \times 0.278 \\ = 0.505(17.5 - 5 \times \frac{1}{2})0.93 \times 336 \times 2.88 \times 0.278 \\ = 1890 \text{ lb.}$$

The weight of the armature yoke,

$$G_{ay} = \frac{\pi}{4}[D_0^2 - (D + 2d_s)^2](l - n_a w_a)k_1 \times 0.278 \\ = \frac{\pi}{4}[112^2 - (100 + 2 \times 2.88)^2](17.5 - 5 \times \frac{1}{2})0.93 \times 0.278 \\ = 4260 \text{ lb.}$$

From the iron loss curve in the Appendix for 2.5 to 3.0 per cent silicon steel, the loss per pound per cycle for the tooth density, $B_{ta} = 101$ kilo-lines per sq. in., is equal to 0.0417 watt. The loss in the armature teeth due to the fundamental frequency flux,

$$W_{at} = 0.0417 \times 1890 \times 60 = 4730 \text{ watts.}$$

The loss per pound per cycle for the yoke density, $B_{ya} = 56$ kilo-lines per sq. in., equals 0.0116 watt, and the loss in the yoke due to the fundamental frequency flux,

$$W_{ay} = 0.0116 \times 4260 \times 60 = 2950 \text{ watts.}$$

The total core loss,

$$W_c = (4730 + 2950)2.0 = 15,360 \text{ watts.}$$

The friction and windage losses are taken equal to 15,000 watts, from

... 100, for vertical waterwheel generators with open end-brackets.

The stray load-losses are estimated at 30 per cent of the armature I^2R losses. The efficiencies and losses for unity power factor for various loads are given in Table XX.

TABLE XX
LOSSES AND EFFICIENCIES

	Load				
	$\frac{1}{4}$	$\frac{1}{2}$	$\frac{3}{4}$	$\frac{4}{5}$	$\frac{5}{6}$
Armature I^2R plus stray load-losses	2 17	8 68	19 60	34 70	54 20
Field losses	18 85	20 30	21 60	22 90	21 20
Core losses	15 36	15 36	15 36	15 36	15 36
Friction and windage losses	15 00	15 00	15 00	15 00	15 00
Total losses	51 38	59 34	71 56	87 96	108 76
Output	625 00	1250 00	1875 00	2500 00	3125 00
Output and losses	676 38	1309 34	1916 56	2587 96	3233 76
Efficiency, per cent.	92 10	95 50	98 30	98 60	96 60

The radiating surface of the armature,

$$\begin{aligned}
 S_a &= \frac{\pi}{4}(D_0^2 - D^2)(2 + n_d) + \pi l(D + D_0) \\
 &= \frac{\pi}{4}(112^2 - 100^2)(2 + 5) + \pi 17.5(100 + 112) \\
 &= 25,650 \text{ sq. in.}
 \end{aligned}$$

The radiating surface per watt loss for full-load,

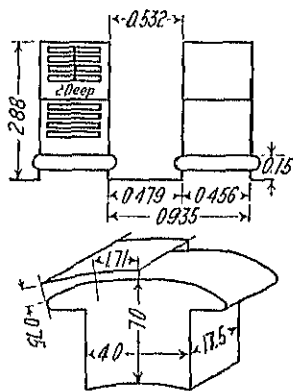
$$\frac{S_a}{W} = \frac{25,650}{15,360 + 34,700 \times \frac{17.50}{34.68}} = 0.78.$$

The radiating surface and surface per watt loss for the field winding are given on page 233.

GENERATOR-MOTOR

Hp .. Kva 2500 Volts 2400 Phase 3 Amperes 600 Cycles 60 Poles 32
R p.m., 225 kva / r p.m., 11.1 Output constant, 1.01×10^4

ARMATURE	
Sheet steel	0 011-2 5% S ₁
Outside diameter	112 0
Gap diameter	100 0
Total length	17 5
Ducts, number and size	5-1
Gross length	15 0
Effective length	14 0
Slots per pole per phase	34
Total number of slots	336
Type of winding	2 layer star
Conducts per phase	2
Coil throw	Slots 1 and 10
Per cent pitch	85 7
Conductors	
Per slot	4
Dimensions	0 119 X 0 276-1
Area	1 X 0 0325
In series per phase	221
Total	1326
Current density	2310
Length, one-half mean-turn	31 68
Resistance per phase, 25° C	0 0207
Resistance per phase, 75° C	0 0217
Resistance drop, volts	11 8
Resistance drop, per cent	1 07
Reactance drop, volts	180 0
Reactance drop, per cent	13 6
Impedance drop, volts	
Impedance drop, per cent	13 65
Armature reaction, AT per pole	5280
Armature reaction, factor	0 852
Armature reaction, on fld. AT	4500
Square inches per watt	0 78
Ampere conductors, total	303,000
Ampere conductors, per inch	1,250
Short circuit ratio	1 25
	$\frac{I^2 R}{Kva} \dots 1 58 \times 10^4$
ATP ₁₀₀	81 00
ATP ₈₀	11,100
Regulation, 80% PF	23 0%
Regulation, 100% PF	14 3%



FIELD	
Total air gap length	2 X 0 108
Rotor diameter	90 188
Peripheral speed	5840
Pole pitch	0 82
Pole arc	0 75
Material spider	Rolled steel
Dumper bars per pole	
Size of bar	
Material of bar	
Section end-ring	
Material end-ring	
Air gap coefficient	1 08
Effective length of gap	0 139
Leakage constant	1 35
$f_a, 0 066, f_b, 1 11, f_w, 0 950, C, 0 725, f_c, 0 975$	
Total flux, 231,000 K L	Flux per pole, 1870 K L.

	Sec- tion	Den- sity	Length	Amp Turns
Air gap	5100	45 8	1 08 X 0 108	6280
Teeth	2320	101 0	2 88	191
Armature yoke	87	56 0	5 31	14
Poles	70	93 6	7 09	217
Field yoke	101	65 0	4 05	24
Total ampere turns per pole				6731

Size of conductor	0 100 X 1 25
Turns per pole	48
Ampere no load	140 Maximum, 253
Length of mean-turn	50 1
Resistance, 25° C	0 398
Resistance, 75° C	0 471
IR no-load	55 8 Maximum, 120
IR no-load	7820 Maximum, 30,100
Square inch per watt maximum I	0 71
Kva	2500
Power factor	80%
Ampere	238 0
IR 75° C	113 0
IR 75° C	26,900
Square inch per watt	0 837
Exciter voltage	125 0
Exciter capacity	33 0

FULL-LOAD LOSSES, 100% P F.

Friction and windage	15,000
Core	15,360
Stray load	8,000
Armature copper	26,700
Field copper and rheostat	22,000
Total losses	87,000
Flywheel effect WPR ²	563,000 lb.-ft ²

WEIGHTS

Armature copper	1940 0
Field copper	3310 0
Armature teeth	1800 0
Armature yoke	4260 0
Field poles	4300 0

Remarks: Vertical Water-wheel Type

Designed by: J. H. Kuhlmann

Date:

CHAPTER XV

SAMPLE DESIGN OF SYNCHRONOUS MOTOR

To design a synchronous motor, calculate the Kva input and proceed as for a generator. The input,

$$Kva = \frac{hp \times 0.746}{\text{eff.} \times PF}$$

Design of 200-Hp Synchronous Motor.—The motor to be designed is to have the following rating: 200 hp, 440 volts, 3-phase, 60 cycles, 900 r.p.m. It is to be a self-starting synchronous motor for direct connection to a centrifugal pump and is to operate at 100 per cent power factor at full-load without field rheostat. The temperature rise for continuous full-load operation must not exceed 50° C., and the full-load efficiency must not be less than 93.3 per cent.

The input,

$$Kva = \frac{hp \times 0.746}{\text{eff.} \times PF} = \frac{200 \times 0.746}{0.933 \times 1.00} = 160.$$

The number of poles,

$$p = \frac{f \times 2 \times 60}{n} = \frac{60 \times 2 \times 60}{900} = 8.$$

$$\frac{Kva}{n} = \frac{160}{900} = 0.178.$$

The output constant from Fig. 105,

$$C = 2.70 \times 10^4$$

For $l/\tau = 1.0$,

$$D = \sqrt[3]{\frac{Kva p C}{\pi l / \tau n}} = \sqrt[3]{\frac{160 \times 8 \times 2.70 \times 10^4}{\pi \times 1 \times 900}} = 23.0 \text{ in.}$$

$$l = \frac{Kva C}{D^2 n} = \frac{160 \times 2.70 \times 10^4}{23.0^2 \times 900} = 9.06 \text{ in.}$$

For other values of l/τ the dimensions are:

l/τ	D	l	τ
1.0	23.0	9.06	9.04
0.9	23.8	8.50	9.33
0.8	21.8	7.80	9.73
0.7	25.0	7.15	10.17

The following dimensions are selected:

$$D = 25.0 \text{ in.}, \quad l = 7.50 \text{ in.}$$

The pole pitch,

$$\tau = \frac{\pi D}{p} = \frac{3.14 \times 25}{8} = 9.81 \text{ in.}$$

For 70 per cent pole embrace the pole arc,

$$B = 0.70 \times 9.81 = 6.875 \text{ in.}$$

The method of shaping the pole shoe suggested by R. W. Wiesman¹ will be used.

From the curves Fig. 107, the minimum air gap length should be,

$$\delta = 0.188 \text{ in.}$$

$$\frac{\delta_m}{\delta} = 1.75, \quad \frac{\delta}{\tau} = 0.0192, \quad \frac{B}{\tau} = 0.70.$$

The shape of the pole shoe is shown in Fig. 165, and the air gap flux distribution curve is shown in Fig. 166. The calculations for the fundamental, third, fifth, and seventh harmonic are given in Table XXI.

$$B_1 = \frac{598.00}{6} = 99.7 \quad B_3 = \frac{-25.61}{6} = -4.27$$

$$B_5 = \frac{-31.16}{6} = -5.19 \quad B_7 = \frac{-10.15}{6} = -1.69$$

The average ordinate for the flux wave,

$$\begin{aligned} B_a &= \frac{2}{\pi} (99.7 - \frac{1}{3} \times 4.27 - \frac{1}{5} \times 5.19 - \frac{1}{7} \times 1.69) \\ &= 61.8 \end{aligned}$$

¹ See Reference, page 172.

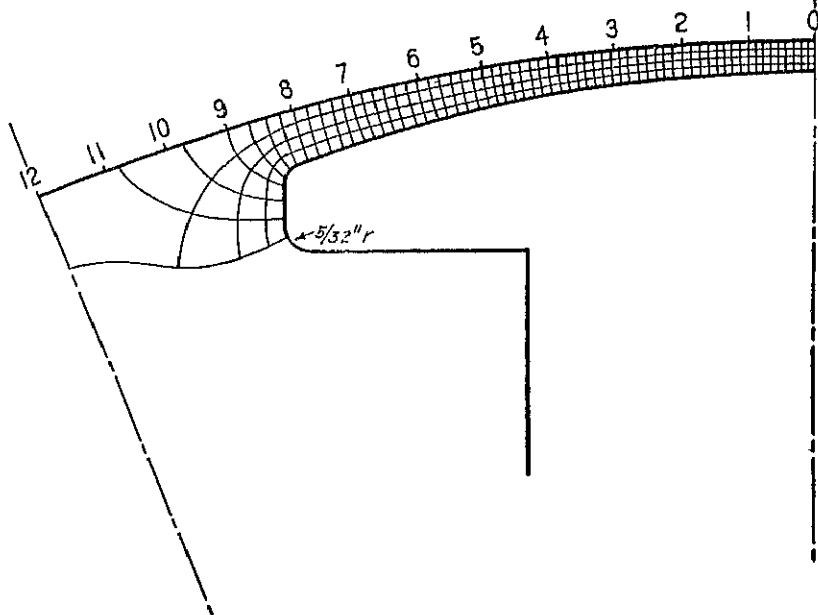


FIG. 165.—Flux plot.

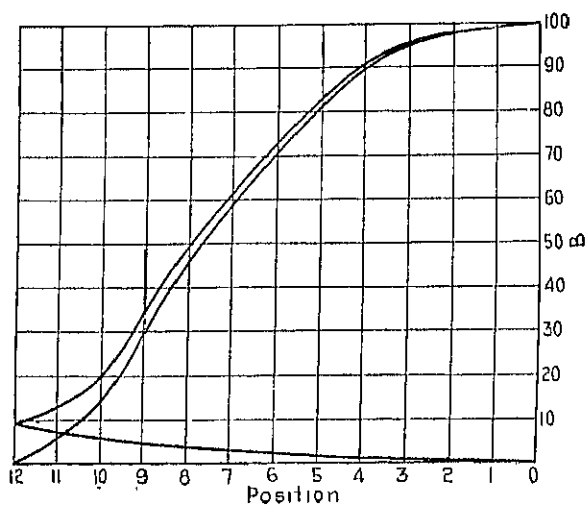


FIG. 166.—Air gap flux-distribution curve.

TABLE XXI

B_z	$\sin x$	$\sin 3x$	$\sin 5x$	$\sin 7x$	$B_x \times \sin x$	$B_x \times \sin 3x$	$B_x \times \sin 5x$	$B_x \times \sin 7x$
$B_{x11} = 5.0$	0.130	0.383	0.609	0.793	0.77	2.26	3.59	4.68
$B_{x10} = 14.2$	0.259	0.707	0.906	0.906	3.68	10.03	13.72	13.72
$B_{x9} = 30.0$	0.383	0.921	0.921	0.383	11.50	27.70	27.70	11.50
$B_{x8} = 45.7$	0.500	1.000	0.500	-0.500	22.85	45.70	22.85	-22.85
$B_{x7} = 59.0$	0.609	0.921	-0.130	-0.991	35.05	51.50	-7.07	-58.50
$B_{x6} = 70.8$	0.707	0.707	-0.707	-0.707	50.10	50.10	-50.10	-50.10
$B_{x5} = 81.5$	0.793	0.383	-0.991	0.130	61.70	31.20	-80.80	10.60
$B_{x4} = 90.0$	0.866	0.000	-0.866	0.866	78.00	00.00	-78.00	78.00
$B_{x3} = 95.0$	0.921	-0.383	-0.383	0.921	87.75	-36.10	-36.10	87.75
$B_{x2} = 97.8$	0.966	-0.707	0.259	0.259	91.50	-69.20	25.35	25.35
$B_{x1} = 99.1$	0.991	-0.921	0.793	-0.609	98.20	-91.50	78.60	-60.30
$B_{x0} = 100.0$	0.500	-0.500	0.500	-0.500	50.00	-50.00	50.00	-50.00
					598.00	-25.61	-31.16	-10.15

and the root-mean-square ordinate,

$$B_e = \sqrt{\frac{1}{2}(99.7^2 + 4.27^2 + 5.19^2 + 1.69^2)} \\ = 70.6.$$

The flux distribution factor,

$$f_d = \frac{B_a}{B_m} = \frac{61.8}{100} = 0.618.$$

The form factor,

$$f_b = \frac{B_e}{B_a} = \frac{70.6}{61.8} = 1.14.$$

The air gap density is assumed equal to 43,000 lines per sq. in.

$$\phi_t = \pi D l B_g = \pi \times 25 \times 7.50 \times 43,000 \\ = 25,400 \text{ kilo-lines.}$$

The winding constant,

$$C_w = f_d f_b f_w = 0.618 \times 1.14 \times 0.956 \\ = 0.675.$$

The number of conductors in series per phase are, for a star-connected winding with pitch coils,

$$N = \frac{E \times 60 \times 10^8}{n\phi_t f_c C_w} = \frac{254 \times 60 \times 10^8}{900 \times 25,400 \times 10^3 \times 1.0 \times 0.675} = 99.$$

For one circuit per phase, the total number of conductors = $99 \times 3 = 297$. The number of armature slots will be 72 for 3 slots per pole per phase and 84 for $3\frac{1}{2}$ slots per pole per phase. The corresponding values for the tooth pitch at the armature surface,

$$t_1 = \frac{\pi \times 25}{72} = 1.09 \text{ in.}, \quad t_1 = \frac{\pi \times 25}{84} = 0.935 \text{ in.}$$

The winding with 84 slots is selected. The conductors per slot will be 3.54 if the chord factor is 1.0. The number of conductors per slot must be an even integer; therefore 4 conductors per slot are used and the coils chorded $66\frac{2}{3}$ per cent of pitch. The coil throw will then be slot 1 and 8 and the chord factor,

$$f_c = \sin \frac{7}{10.5} 90 = 0.866.$$

The final value of the total flux,

$$\begin{aligned} \phi_t &= \frac{254 \times 60 \times 10^8}{112 \times 900 \times 0.866 \times 0.675} \\ &= 25,900 \text{ kilo-lines.} \end{aligned}$$

The armature current per phase,

$$\begin{aligned} I &= \frac{K_{VA} \times 10^3}{E \times 3} = \frac{160 \times 10^3}{254 \times 3} \\ &= 210 \text{ amperes.} \end{aligned}$$

The current density in the armature copper should be approximately 3400 amperes per sq. in., from the curves of Fig. 134. The section area of the armature conductor,

$$\begin{aligned} s_a &= \frac{I}{aA_a} = \frac{210}{1 \times 3400} \\ &= 0.0618 \text{ sq. in.} \end{aligned}$$

From the copper table a d.c.c., copper ribbon conductor is selected which has following dimensions: 0.129×0.258 in. bare, $0.149 \times$

0.276 in. insulated, area 0.0325 sq. in. Two conductors are wound in parallel and arranged in the slot as shown in Fig. 167. The slot dimensions are:

$$\text{Width} = (1 \times 0.276) + 0.15 = 0.426 \text{ in.}$$

$$\text{Depth} = (8 \times 0.149) + 0.42 = 1.61 \text{ in.}$$

The current density for this conductor,

$$A_a = \frac{210}{2 \times 0.0325} = 3230 \text{ amperes per sq. in.}$$

The length of the half-mean-turn of the armature coil is calculated as follows (see Fig. 136):

$$\sin \alpha = \frac{d}{t_1} = \frac{0.426 + 0.15}{0.935} = 0.616$$

$$\alpha = 38^\circ \text{ and } \cos \alpha = 0.788.$$

The per cent pitch for the armature coils,

$$P = \frac{7}{10.5} = 0.667$$

$$L_a = \frac{\pi(D + d_s)}{p \cos \alpha} P + 2b + d_s + l$$

$$= \frac{\pi(25 + 1.61)}{8 \times 0.788} 0.667 + 2.0 + 1.61 + 7.50$$

$$= 19.96 \text{ in.}$$

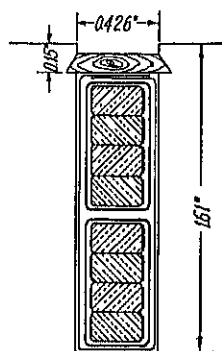


FIG. 167.

The resistance per phase of the armature winding at 75°C. ,

$$R_a = \frac{L_a N r}{a s_a \times 10^6} = \frac{19.96 \times 112 \times 0.826}{1 \times 0.065 \times 10^6}$$

$$= 0.0285 \text{ ohm per phase.}$$

The bare weight of the armature copper,

$$G_a = L_a N a m s_a 0.321 = 19.96 \times 112 \times 1 \times 3 \times 0.065 \times 0.321$$

$$= 140 \text{ lb.}$$

The approximate insulated weight = 145 lb.

Two ventilating ducts, each $\frac{1}{2}$ in. wide, are used in the armature.

The length of the gap section is taken equal to the total armature length and the air gap density,

$$B_g = \frac{\phi_t}{\pi D l} = \frac{25,900 \times 10^3}{3.14 \times 25 \times 7.5} \\ = 44.0 \text{ kilo-lines.}$$

The air gap coefficient,

$$k = \frac{t_1}{w_{t1} + (\delta \times y)} = \frac{0.935}{0.509 + (0.188 \times 1.53)} \\ = 1.174.$$

The air gap ampere-turns per pole,

$$\text{AT}_g = \frac{B_g \delta k}{3.2} = \frac{44,000 \times 0.188 \times 1.174}{3.2} \\ = 3030.0 \text{ ampere-turns.}$$

The maximum tooth density,

$$B_{t1} = \frac{\phi_t}{w_{t1}(l - n_d w_d) k_1 S} = \frac{25,900 \times 10^3}{0.509(7.5 - 2 \times 0.5) 0.93 \times 84} \\ = 100.2 \text{ kilo-lines.}$$

The width of the armature tooth at a section $\frac{1}{3}$ tooth length from the minimum width,

$$w_{t2} = \frac{\pi(D + \frac{2}{3}d_s)}{S} - w_s = \frac{\pi(25 + \frac{2}{3} \times 1.61)}{84} - 0.426 \\ = 0.55 \text{ in.}$$

$$B_{t2} = \frac{\phi_t}{w_{t2}(l - n_d w_d) k_1 S} = \frac{25,900 \times 10^3}{0.550(7.5 - 2 \times 0.5) 0.93 \times 84} \\ = 92.8 \text{ kilo-lines.}$$

From the standard saturation curve for 1 per cent silicon steel, $at_t = 20.8$ ampere-turns per inch.

$$\text{AT}_t = at_t l_t = 20.8 \times 1.61 \\ = 34 \text{ ampere-turns.}$$

The flux per pole,

$$\phi = \frac{\phi_t f_d}{p} = \frac{25,900 \times 10^3 \times 0.618}{8} \\ = 2010 \times 10^3 \text{ kilo-lines.}$$

if the max density in the armature yoke is taken equal to 55,000 lines per sq. in., then

$$d_{ya} = \frac{\phi}{(l - n_d w_d) k_1 B_{ya}} = \frac{2010 \times 10^3}{(7.5 - 2 \times 0.5) 0.93 \times 55,000} \\ = 6.04 \text{ in.}$$

The outside diameter of the armature core,

$$D_o = D + 2d_s + d_{ya} = 25 + 2 \times 1.61 + 6.04 \\ = 34.26 \text{ in.}$$

Make the outside diameter 34.25 in. and the armature yoke density, $B_{ya} = 55$ kilo-lines.

The length of the flux path,

$$l_{ya} = \frac{\pi(D + 2d_s + \frac{1}{2}d_{ya})}{2p} = \frac{\pi(25 + 2 \times 1.61 + \frac{1}{2} \times 6.03)}{2 \times 8} \\ = 6.13 \text{ in.}$$

$$at_{ya} = 3.0 \text{ ampere-turns per in.}$$

$$AT_{ya} = at_{ya} l_{ya} = 3.0 \times 6.13 = 18.0 \text{ ampere-turns.}$$

From the curves, Fig. 140, the leakage constant will be approximately 1.14. The section area of the pole body,

$$s_p = \frac{\phi \lambda}{B_p} = \frac{2010 \times 10^3 \times 1.14}{85,000} \\ = 27.0 \text{ sq. in.,}$$

if the flux density, B_p , is assumed equal to 85,000 lines per sq. in. The length of the pole parallel to the shaft is equal to the armature length, and

$$w_p = \frac{27.0}{7.5} = 3.6 \text{ in.; use 3.5 in.}$$

The radial length of the pole is estimated at 5.0 in. (see page 210). The leakage flux is calculated as shown below for machines with a small number of poles for which the sides of the poles cannot be assumed to

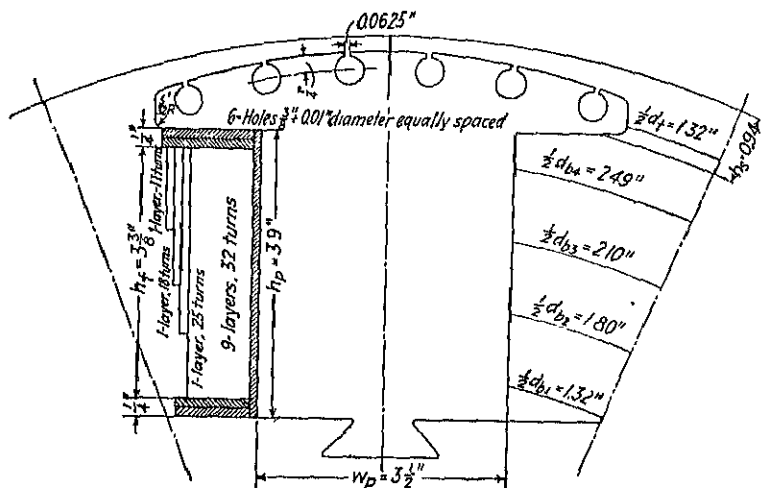


FIG. 168.

$$\begin{aligned} l &= 7.5, & h_s &= 0.94, & d_i &= 2.64, & B &= 0.875, \\ h_p &= 3.90, & d_{b1} &= 2.64, & d_{b2} &= 3.60, & d_{b3} &= 4.2, \\ d_{b4} &= 4.98, & w_p &= 3.50, & X &= 3030 + 34 + 18 = 3082. \end{aligned}$$

$$(1) \quad 13 \frac{h_s}{d_i} = 13 \frac{7.5 \times 0.94}{2.64} = 34.8$$

$$(2) \quad 19 h_s \log \left(1 + \frac{\pi B}{2 d_i} \right) = 19 \times 0.94 \log \left(1 + \frac{\pi \times 0.875}{2 \times 2.64} \right) = 12.7$$

$$(3) \quad 0.4 h_p l \left(\frac{1}{d_{b1}} + \frac{3}{d_{b2}} + \frac{5}{d_{b3}} + \frac{7}{d_{b4}} \right) = 0.4 \times 3.9 \times 7.5$$

$$\left(\frac{1}{2.64} + \frac{3}{3.60} + \frac{5}{4.2} + \frac{7}{4.98} \right) = 44.60$$

$$\begin{aligned} (4) \quad & 0.58 h_p \left[\log \left(1 + \frac{\pi w_p}{2 d_{b1}} \right) + 3 \log \left(1 + \frac{\pi w_p}{2 d_{b2}} \right) \right. \\ & \left. + 5 \log \left(1 + \frac{\pi w_p}{2 d_{b3}} \right) + 7 \log \left(1 + \frac{\pi w_p}{2 d_{b4}} \right) \right] \\ & = 0.58 \times 3.9 \left[\log \left(1 + \frac{\pi \times 3.5}{2 \times 2.64} \right) + 3 \log \left(1 + \frac{\pi \times 3.5}{2 \times 3.6} \right) \right. \\ & \left. + 5 \log \left(1 + \frac{\pi \times 3.5}{2 \times 4.2} \right) + 7 \log \left(1 + \frac{\pi \times 3.5}{2 \times 4.98} \right) \right] = 13.1 \end{aligned}$$

² "Field Leakage in Synchronous Machines," by Theo. Schou, Electrical Review, Vol. 77, Aug. 21, 1920, p. 281.

$$= 325,000 \text{ lines.}$$

$$\lambda = \frac{\phi_l}{\phi} + 1 = \frac{325,000}{2,010,000} + 1 = 1.162.$$

The flux density in the pole body will then be,

$$B_p = \frac{2010 \times 10^3 \times 1.162}{3.5 \times 7.5} = 89.0 \text{ kilo-lines per sq. in.}$$

The length of the flux path in the pole is equal to the radial length of the pole, which has been estimated at 5.0 in. The ampere-turns per pole,

$$AT_p = at_p l_p = 20 \times 5.0 = 100 \text{ ampere-turns.}$$

The field spider is punched from sheet steel and the poles are assembled as shown in Fig. 103. If the shaft diameter is taken equal to 6.0 in., two times the radial depth of the spider

$$= 25.0 - 2 \times 0.188 - 2 \times 5.0 - 6.0 = 8.624 \text{ in.}$$

The flux density,

$$B_{yf} = \frac{2010 \times 10^3 \times 1.162}{8.624 \times 7.5} = 36.2 \text{ kilo-lines per sq. in.}$$

The length of the flux path,

$$l_{yf} = \frac{(25 - 2 \times 0.188 - 2 \times 5.0)\pi}{2 \times 8} = 2.87 \text{ in.}$$

From the standard saturation curve for open-hearth sheet steel for field poles, $at_{yf} = 2.5$ ampere-turns per in.

$$AT_{yf} = at_{yf} l_{yf} = 2.5 \times 2.87 = 7.0 \text{ ampere-turns.}$$

The calculations for the open-circuit saturation curve are given in Table XXII, and the curve is shown in Fig. 169.

The armature leakage reactance is calculated by formula 148 for a fractional slot winding. The data required are:

$$\begin{aligned} f &= 60, & N &= 112, & d_2 &= 0.23, & D &= 25, & f_w &= 0.956, \\ l &= 7.5, & S_s &= 84, & w_s &= 0.426, & p &= 8, & \delta &= 0.188, \\ m &= 3, & d_1 &= 1.32, & P &= 0.667, & f_c &= 0.866, & K_s &= 0.75. \end{aligned}$$

$$X_l = \frac{2.0 f l m N^2}{S_s \times 10^7}$$

$$\left[K_s \left(\frac{d_1}{3w_s} + \frac{d_2}{w_s} \right) + \frac{0.3(3P-1)DS_s}{p^2 l} + \frac{0.53 D f_c^2 f_w^2}{S_s \delta} \right]$$

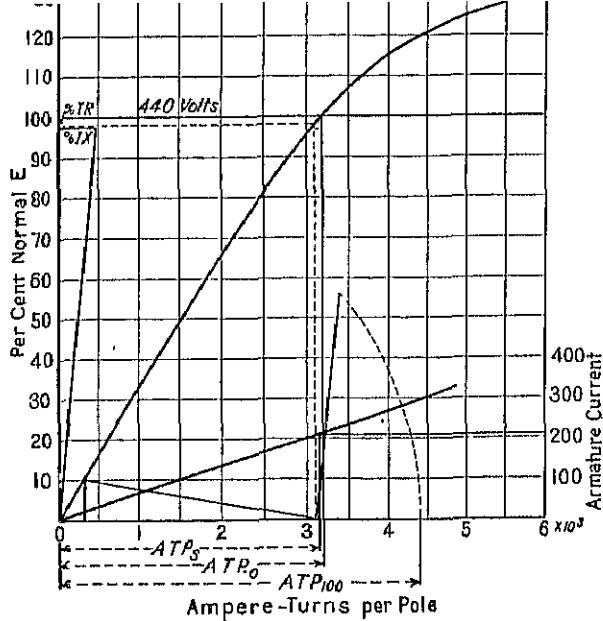


FIG. 169.

TABLE XXII

Path	Length	90 Per Cent E			100 Per Cent E			115 Per Cent E			125 Per Cent E		
		B	nt	AT	B	nt	AT	B	nt	AT	B	nt	AT
Air gap	2730	3030	3480	3800
Teeth	1 61	83 6	10.2	17 02.8	20 8	31	107 0	79 0	127	110.0	225 0	36	36
Armature yoke	0 13	49 5	2.0	10 55 0	3 0	18	63 2	4 0	35	68 0	5 0	31	31
Pole	5 0	80 0	10 7	54 80 0	20 0	100	102 5	67.0	335	111 5	105.0	82	82
Field yoke	2 87	32 0	2.5	7 30 2	2 5	7	11 7	2 8	8	45.4	3 0	1	1
Total	2824	3180	3085	6027

$$K_s \left(\frac{d_1}{3w_s} + \frac{d_2}{w_s} \right) = 0.75 \left(\frac{1.32}{3 \times 0.426} + \frac{0.23}{0.426} \right) = 1.18$$

$$\frac{0.3(3P - 1)DS_s}{p^2 l} = \frac{0.3(3 \times 0.667 - 1)25 \times 84}{8^2 \times 7.5} = 1.31$$

$$\frac{0.53 D f_c^2 f_w^2}{S_s \delta} = \frac{0.53 \times 25 \times 0.866^2 \times 0.956^2}{84 \times 0.188} = 0.575$$

$$X_l = \frac{1.18 + 1.31 + 0.575}{84 \times 10^7}$$

$$= 0.123 \text{ ohm per phase.}$$

The per cent reactance drop due to full-load current,

$$\frac{IX_l}{E} 100 = \frac{210 \times 0.123}{254} 100 = 10.2 \text{ per cent.}$$

The resistance of the armature winding is given above and the per cent resistance drop due to full-load current,

$$\frac{IR_a}{E} 100 = \frac{210 \times 0.0285}{254} 100 = 2.35 \text{ per cent.}$$

The per cent impedance drop

$$= \sqrt{2.35^2 + 10.2^2} = 10.45 \text{ per cent.}$$

The equivalent field ampere-turns per pole of armature reaction for full-load current,

$$\begin{aligned} \text{AT}_{af} &= \frac{0.45 K_a m N I_f f_{so}}{p} \\ &= \frac{0.45 \times 0.86 \times 3 \times 112 \times 210 \times 0.866 \times 0.956}{8} \\ &= 2830 \text{ ampere-turns.} \end{aligned}$$

The short-circuit characteristic is shown in Fig. 169 and the short-circuit ratio,

$$\frac{\text{ATP}_0}{\text{ATP}_s} = \frac{3189}{3140} = 1.015.$$

The field ampere-turns per pole for full-load at unity power factor are found graphically as shown in Fig. 169,

$$\text{ATP}_{100} = 4400.$$

The field winding for this machine will be of the wire-wound type. The average depth of the coil is estimated at 1.0 in. (see Fig. 168), and the approximate mean length of turn,

$$\begin{aligned} L_f &= 2 \times 7.5 + 2(3.5 - 0.25) + \pi(0.45 + 1.0) \\ &= 26.05 \text{ in.} \end{aligned}$$

$$s_f = \frac{ATP_{100} L_{fp} \times 0.826}{E_f \times 10^9} = \frac{4400 \times 26.05 \times 8 \times 0.826}{120 \times 10^9} \\ = 0.00631 \text{ sq. in.}$$

A number 11 round conductor is selected. The dimensions are: bare diameter 0.091 in., insulated diameter 0.101 in., area 0.00650 sq. in. For a current density of 2000 amperes per sq. in., the field current,

$$i_f = s_f A_f = 0.0065 \times 2000 \\ = 13.0 \text{ amperes}$$

and the turns per pole,

$$t_f = \frac{ATP_{100}}{i_f} = \frac{4400}{13.0} = 339.$$

From the sketch, Fig. 168, the height of the winding space,

$$h_f = 3.375 \text{ in. The number of turns per layer} = \frac{3.375}{0.101} = 33.4.$$

In winding the field coils, the space of one turn is required in passing one layer to the next; therefore 32 turns per layer are used. At the center of the pole, the depth of the field coil can be approximately 0.45 in. which will permit 9 layers. The remainder of the turns are wound in Fig. 168, making a total of 342 turns. The total length of mean-turn,

$$L_{f1} = 2l_1 - 0.25 + \pi(0.45 + 2d_1) \\ = 2 \times 7.5 - 0.25 + \pi(0.45 + 2 \times 0.455) = 25.77 \text{ in.} \\ L_{f2} = 2l_2 - 0.25 + \pi(0.45 + 2d_2) \\ = 2 \times 7.5 - 0.25 + \pi(0.45 + 2 \times 0.96) = 28.95 \text{ in.}$$

$$L_{f3} = 2l_3 + 2(w_p - 0.25) + \pi(0.45 + 2d_3) \\ = 2 \times 7.5 + 2(3.5 - 0.25) + \pi(0.45 + 2 \times 1.06) = 29.58 \text{ in.}$$

$$L_{f4} = 2l_4 + 2(w_p - 0.25) + \pi(0.45 + 2d_4) \\ = 2 \times 7.5 + 2(3.5 - 0.25) + \pi(0.45 + 2 \times 1.16) = 30.20 \text{ in.}$$

$$L_f = \frac{L_{f1}t_{f1} + L_{f2}t_{f2} + L_{f3}t_{f3} + L_{f4}t_{f4}}{t_f} \\ = \frac{25.77 \times 288 + 28.95 \times 25 + 29.58 \times 18 + 30.20 \times 11}{342} \\ = 26.3 \text{ in.}$$

$$R_f = \frac{L_f l_f p \times 0.826}{s_f \times 10^6} = \frac{26.3 \times 342 \times 8 \times 0.826}{0.0065 \times 10^6} \\ = 9.14 \text{ ohms.}$$

If 5 volts drop is allowed for the exciter loads and brush contacts, the field current,

$$i_f = \frac{120}{9.14} = 13.12 \text{ amperes}$$

and the field copper loss,

$$W_f = i_f^2 R_f = 13.12^2 \times 9.14 = 1570 \text{ watts.}$$

The radiating surface,

$$S_f = 2(d_f + h_f)L_f p = 2(1.2 + 3.38)26.3 \times 8 \\ = 1925 \text{ sq. in.}$$

The surface per watt loss,

$$\frac{S_f}{W_f} = \frac{1925}{1570} = 1.23.$$

The exciter capacity required,

$$W_e = \frac{E_e^2}{R_f \times 10^3} = \frac{125^2}{9.14 \times 10^3} = 1.71 \text{ kilo-watts.}$$

The weight of field copper,

$$G_f = L_f l_f p s_f \times 0.321 \\ = 26.3 \times 342 \times 8 \times 0.0065 \times 0.321 \\ = 150 \text{ lb.}$$

The following is an approximate design of the squirrel-cage winding. The number of bars per pole must always be so selected that the bar pitch will not be equal to the armature slot pitch. If it is, the motor will have "dead points," that is, for certain rotor positions no torque will be produced. The bar pitch should be approximately 15 per cent

larger or smaller than the armature tooth pitch. If the number of bars is fixed, the size of the bar and the material will determine the resistance of the squirrel-cage winding. For this design, six $\frac{3}{8}$ -in. diameter round copper bars are used in each pole and are placed in the pole shoe as shown in Fig. 168. The end-ring section (see page 296),

$$s_{er} = \frac{0.32s_b N_b}{p} = \frac{0.32 \times 0.111 \times 48}{8} \\ = 0.213 \text{ sq. in.}$$

A rolled-copper end-ring is used, $\frac{5}{16}$ in. \times $\frac{3}{4}$ in., 0.234 sq. in. area, and is welded to the bars.

The equivalent rotor resistance,

$$R_r = \frac{f_c^2 f_w^2 N^2 m r}{10^6} \left[\frac{l_b}{s_b N_b} + \frac{0.64 D_{er}}{p^2 s_{er}} \right] \\ = \frac{0.866^2 \times 0.956^2 \times 112^2 \times 3 \times 0.826}{10^6} \left[\frac{11.0}{0.111 \times 48} + \frac{0.64 \times 24}{8^2 \times 0.234} \right] \\ = 0.0655 \text{ ohm per phase.}$$

A synchronous motor for direct connection to a centrifugal pump must have a high pull-in torque with only moderate starting torque. The squirrel-cage resistance should, therefore, be approximately 25 per cent of the total reactance.

The rotor slot reactance is calculated by formula 152.

$$X_{sr} = \frac{2.0 \times 60 \times 112^2 \times 7.5 \times 3}{84 \times 10^7} \\ \left(\frac{0.866^2 \times 0.956^2 \times 84}{48} \right) \left(0.62 + \frac{0.0625}{0.0625} \right) \\ = 0.078 \text{ ohm.}$$

The rotor zigzag leakage reactance,

$$X_{zr} = \frac{2.0 \times 60 \times 112^2 \times 7.5 \times 3}{84 \times 10^7} \\ \left(\frac{0.266 \times 0.866^2 \times 0.956^2 \times 25 \times 84}{48^2 \times 0.188} \right) \\ = 0.0357 \text{ ohm.}$$

The stator reactance has been calculated above and is equal to

... the phase. The total synchronous reactance of the synchronous motor with open-field winding

$$= 0.123 + 0.078 + 0.0357$$

$$= 0.237 \text{ ohm per phase.}$$

In these calculations, the transient reactance of the short-circuited field winding was omitted. For high starting torque, the field winding should be short-circuited through a very high resistance and for high pull-in torque it should be short-circuited on itself. The field winding produces a negative torque when the slip is high, above 50 per cent, and a positive torque when the slip is low, below 50 per cent. The student who wishes to make further calculations as to the value of the torque at any slip will find much useful information in the references given on page 222.

The armature copper loss for full-load,

$$\begin{aligned} W_a &= R_a I^2 m = 0.0285 \times 210^2 \times 3 \\ &= 3770 \text{ watts.} \end{aligned}$$

The field current for full-load at 100 per cent power factor = 13.12 amperes. With 125 volts applied at the collector rings,

$$\begin{aligned} W_f &= i_f E_o = 13.12 \times 125 \\ &= 1640 \text{ watts.} \end{aligned}$$

The weight of the armature teeth,

$$\begin{aligned} G_a &= 0.509 (7.5 - 2 \times 0.5) 0.93 \times 84 \times 1.61 \times 0.278 \\ &= 129 \text{ lb.} \end{aligned}$$

The weight of the armature yoke,

$$\begin{aligned} G_{cy} &= \frac{\pi}{4} [34.25^2 - (25 + 3.22)^2] (7.5 - 2 \times 0.5) 0.93 \times 0.278 \\ &= 493 \text{ lb.} \end{aligned}$$

The loss per pound per cycle in the armature teeth, due to the fundamental frequency flux for the density, $B_t = 92.8$ kilo-lines = 0.0580 watts for 1 per cent silicon steel. The loss in the teeth,

$$W_{at} = 0.058 \times 60 \times 129 = 449 \text{ watts.}$$

The loss per pound per cycle in the armature yoke, due to the funda-

magnet frequency flux = 0.017 watts for 1 per cent silicon steel. The loss in the yoke, $W_{cy} = 0.017 \times 60 \times 493 = 503$ watts. The total core loss,

$$W_c = (449 + 503)2.2 = 2100 \text{ watts.}$$

The friction and windage losses are taken from the curves in Fig. 159 and are equal to 1200 watts.

The stray load-losses will be estimated at 25 per cent of the armature I^2R loss.

The efficiency calculations in Table XXIII are for unity power factor at all loads.

TABLE XXIII

Losses	$\frac{1}{2}$	$\frac{2}{3}$	$\frac{3}{4}$	$\frac{4}{5}$	$\frac{5}{6}$
Armature I^2R plus stray load. . . .	294	1,180	2,650	4,710	7,860
Field losses.	1,200	1,400	1,515	1,640	1,740
Core losses.	2,100	2,100	2,100	2,100	2,100
Friction and windage.	1,200	1,200	1,200	1,200	1,200
Total losses.	4,884	5,880	7,465	9,650	12,400
Output.	37,800	74,600	112,000	149,000	186,500
Output and losses.	42,184	80,480	119,465	158,650	198,900
Efficiency, per cent.	88.5	92.7	93.7	94.0	93.70

The effective radiating surface of the armature,

$$\begin{aligned}
 S_a &= \frac{\pi}{4}(D_0^2 - D^2)(2 + n_a) + \pi l(D + D_0) \\
 &= \frac{\pi}{4}(34.25^2 - 25^2)(2 + 2) + \pi \times 7.5(34.25 + 25) \\
 &= 3120 \text{ sq. in.}
 \end{aligned}$$

The radiating surface per watt loss,

$$\frac{S_a}{W} = \frac{3120}{2100 + 4710 \frac{7.5}{19.96}} = 0.806 \text{ sq. in. per watt.}$$

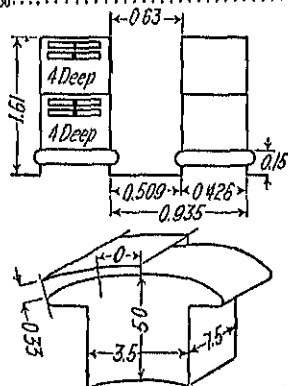
The radiating surface per watt loss for the field winding has been calculated on page 261.

GENERATOR - MOTOR

Hp 200 Kva 150 Volts 440 Phase 3 Amperes 209 Cycles 60 Poles 8
 R.p.m. 900 Kva/r.p.m. 0.177 Output constant 2.66×10^4

ARMATURE

Sheet steel 0.017-1% Si
 Outside diameter 31.25
 Gap diameter 25.0
 Total length 7.6
 Ducts, number and size 2-1
 Gross length 6.6
 Effective length 0.05
 Slots per pole per phase 34
 Total number of slots 81
 Type of winding Star
 Circuits per phase One
 Coil throw Slots 1 and 8
 Per cent pitch 66 2/3
 Conductors:
 Per slot 4
 Dimensions 0.140×0.270
 Area 2×0.0325
 In series per phase 112
 Total 336
 Current density 3230
 Length, one-half mean-turn 19.98
 Resistance per phase, 25° C. 0.021
 Resistance per phase, 75° C. 0.0285
 Resistance drop, volts 5.95
 Resistance drop, per cent 2.35
 Resistance drop, volts 25.9
 Resistance drop, per cent 10.2
 Impedance drop, volts
 Impedance drop, per cent 10.45
 Armature reaction, AT per pole 3200
 Armature reaction, factor K_a 0.86
 Armature reaction, eq. fld. AT 2830
 Square inches per watt 0.806
 Ampere conductors, total 60,800
 Ampere conductors, per inch 771
 Short circuit ratio 1.015
 $\frac{D^2 L}{K_v}$ 2.88×10^4
 AT/100 4100



FIELD

Total air gap length 2×0.188
 Rotor diameter 24.024
 Peripheral speed 5800
 Pole pitch 9.81
 Pole arc 6.875
 Material spider Sheet steel
 Damper bars per pole 6
 Size of bar 1/2 diam.
 Material of bar Copper
 Section end-ring $\frac{1}{4} \times 1 = 0.234$
 Material end-ring Copper
 Air gap coefficient 1.174
 Effective length of gap 0.22
 Leakage constant 1.162
 $f_d, 0.618, f_b, 1.14, f_w, 0.956, C_w, 0.675, f_c, 0.886$
 Total flux, 25,900 K L. Flux per pole, 2010 K L.

	Sec- tion	Den- sity	Length	Amp. Turns
Air gap . . .	589.0	44.0	1.174×0.188	3080
Teeth . . .	279.0	92.8	1.01	34
Armature yoke . . .	36.6	55.0	0.13	18
Poles . . .	26.2	80.0	5.00	100
Field yoke . . .	64.6	36.2	2.87	7
Total ampere turns per pole . . .				3180

Size of conductor No. 11 rd.
 Turns per pole 342
 Amperes no load 9.32 Maximum, 13.12
 Length of mean-turn 26.3
 Resistance, 25° C. 7.67
 Resistance, 75° C. 9.14
 IR no-load 71.5 Maximum, 120
 IR no-load 697. Maximum, 1570
 Square inch per watt maximum I 1.23
 Kva 159
 Power factor 100%
 Amperes 12.00
 IR 75° C. 118.0
 IR 75° C. 1520
 Square inch per watt 1.26
 Exciter voltage 125
 Exciter capacity 1.71

FULL-LOAD LOSSES, 100% P.F.

Friction and windage 1200.0
 Core 2100.0
 Stray load 940.0
 Armature copper 3770.0
 Field copper and rheo. 1640.0
 Total losses 9636.0
 Flywheel effect WR^2

WEIGHTS

Armature copper 140.0
 Field copper 150.0
 Armature teeth 120.0
 Armature yoke 493.0
 Field poles 314.0

Remarks: * 0 layers—32 turns

1 layer—25 turns

1 layer—18 turns

1 layer—11 turns

Designed by: J. H. Kuhlmann

Date:

III — INDUCTION MOTORS

CHAPTER XVI

CONSTRUCTION

POLYPHASE motors are built in sizes from $\frac{1}{2}$ hp to very large sizes, several thousand horse-power. There are two types of polyphase induction motors in general use: (1) the polyphase squirrel-cage motor,

and (2) the polyphase wound-rotor, or slip-ring motor.

The types of construction generally employed are shown in Figs. 170, 171, and 172.

Stator.—The construction of the stator or field of the induction motor is generally the same as the armature of synchronous machines. For small

machines, the same stator is often used for either a synchronous machine or an induction motor.

The stator laminations are punched from electric sheet steel with from 1 to 3.0 per cent silicon. The thickness of the sheet is usually from 0.014 in., for machines for which low core loss is important, to 0.019 in. For small-diameter machines, the stator laminations are often punched in one piece. For the larger diameters, segmental punchings are always used. Figure 173 shows a one-piece stator punching with partially closed slots and two segmental punchings, one with open slots and one with partially closed slots. The punchings are assembled in the stator frame as shown in Figs. 170, 171, and 172. When the length of the stator core exceeds 4 or 5 in., it must be divided into sections by radial ventilating ducts to insure proper ventilation of

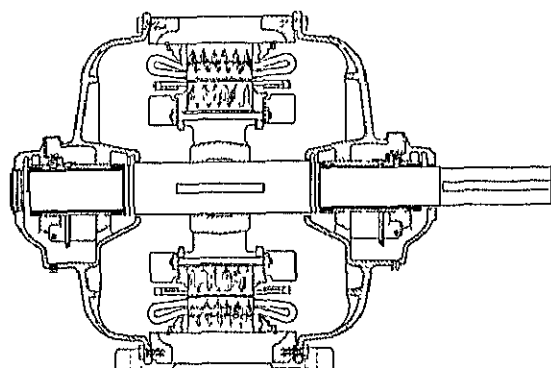


Fig. 170.—Cross-section of squirrel-cage induction motor.

sized machines and $\frac{1}{2}$ in. for large machines. The distance between centers of ducts should not exceed 3 in. A ventilating duct is generally provided at each end of the stator by the tooth supports. An assembled stator core with part of the stator coils in place is shown in Fig. 174.

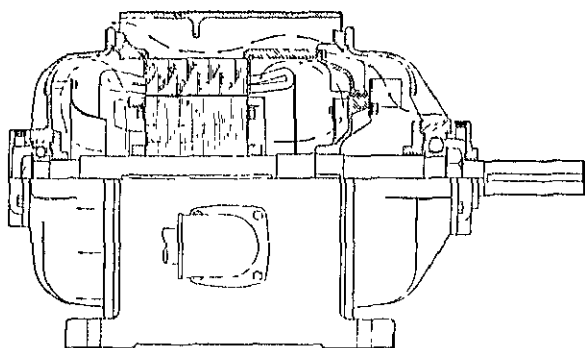


FIG. 171.—Sectional assembly of totally enclosed squirrel-cage motor with ball bearings.

For small-diameter motors partly

closed stator slots are used and the teeth, instead of the slots, have parallel sides. Figure 175 shows one punching for a 1-hp, 3-phase, 4-pole, 1800-r.p.m. motor.

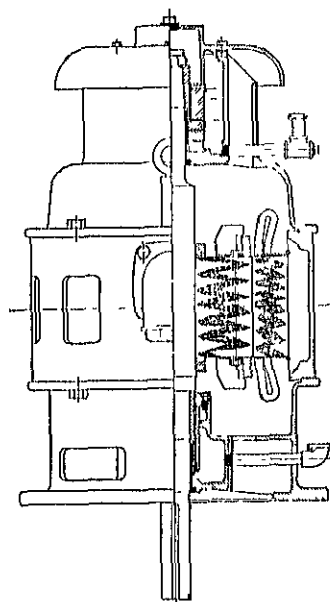


FIG. 172.—Cross-section of vertical squirrel-cage motor.

The stator frames for very large motors are as a rule built up of welded rolled steel plate just as the armature frames of synchronous machines (see Fig. 176).

Rotor.—The rotor is built of sheet steel laminations, generally punched from the same material as that used for the stator. For small motors, the rotor punchings are punched in one piece and assembled on the shaft. Figure 177 shows one rotor punching for a 1-hp, 4-pole, squirrel-cage motor. One-piece punchings are used for medium diameters; for large diameters segmental punchings must be used. These are assembled on a spider and clamped between two end-plates by through-bolts, as shown in Fig. 178.

When ventilating ducts are required in the stator, an equal number of ducts of the same size are used in the rotor. For squirrel-cage rotors, the slots are generally shallow and the tooth supports and venti-

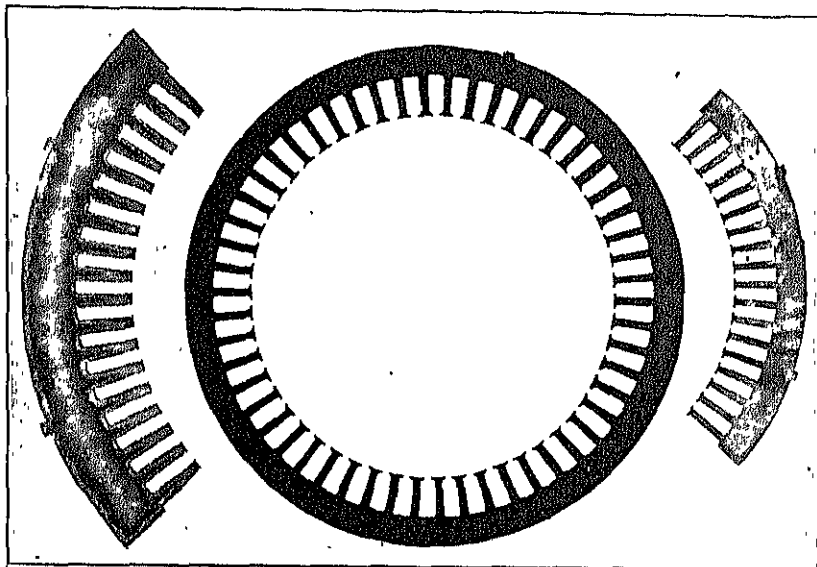


FIG. 173.—Induction motor stator punchings.

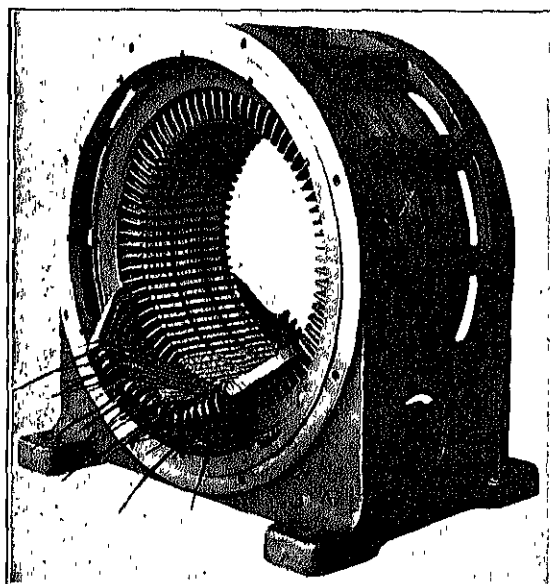


FIG. 174.—Partially wound stator with open slots.

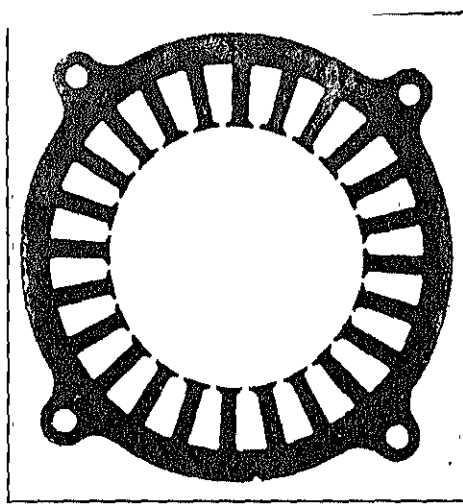


FIG. 175.—Stator punching for 1-hp, 1800-r.p.m., three-phase, 60-cycle motor.

Outside diameter $7\frac{1}{2}$ in.
 Inside diameter $4\frac{1}{2}$ in.
 Slot opening 0.11 in.

Slot width $\begin{cases} \text{top } 0.35 \text{ in.} \\ \text{bottom } 0.50 \text{ in.} \end{cases}$
 Slot depth 1.0 in.

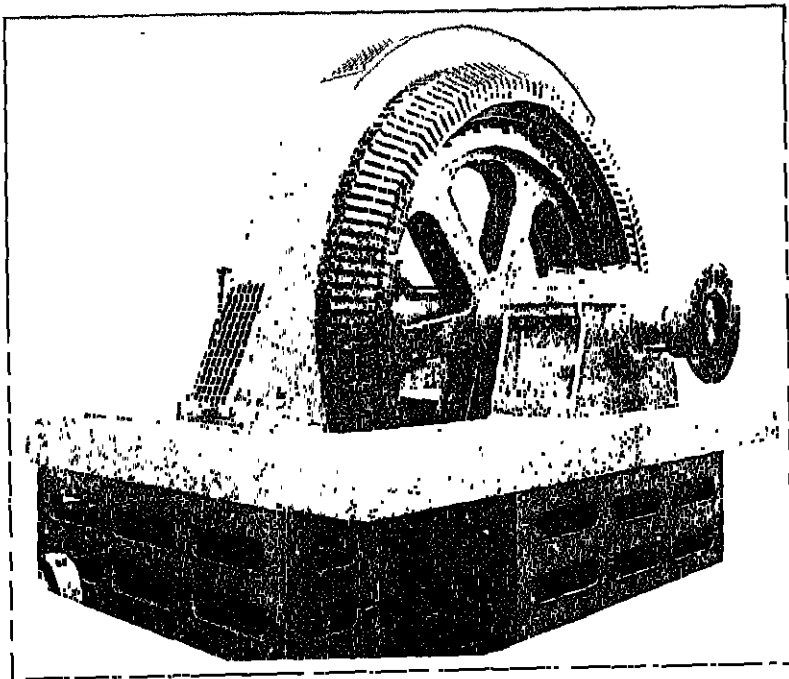


FIG. 176.—1500-hp, 36-pole, 200-r.p.m., 6600-volt mill type induction motor with welded rolled-steel stator frame.

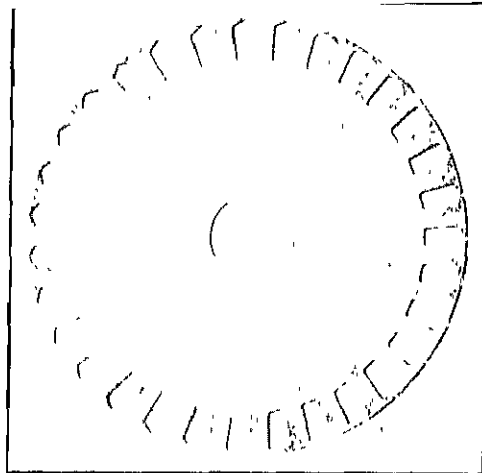


FIG. 177.—Rotor punching for 1-hp, 1800-r.p.m., three-phase, 60-cycle motor.

Outside diameter 4.22 in.

Shaft diameter $1\frac{1}{2}$ in.

Slot width $\left\{ \begin{array}{l} \text{top } 0.22 \text{ in.} \\ \text{bottom } 0.16 \text{ in.} \end{array} \right.$

Slot depth 0.41 in.

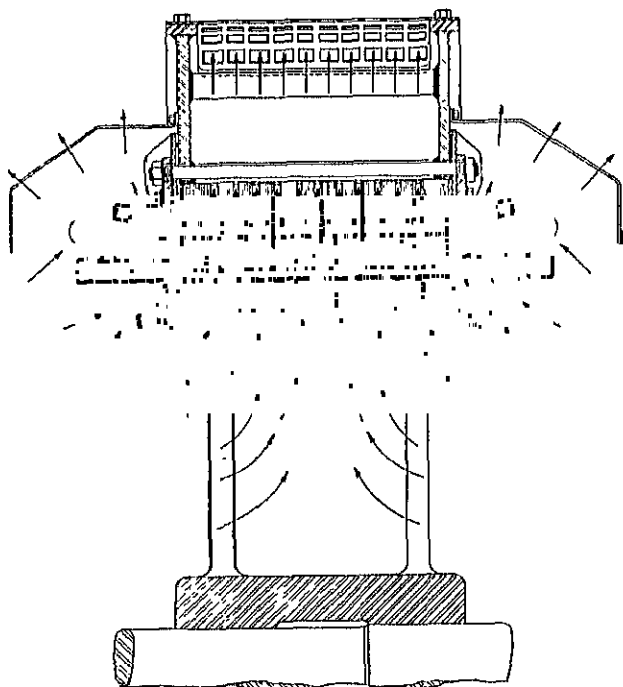


FIG. 178.—Sectional view of stator and rotor.

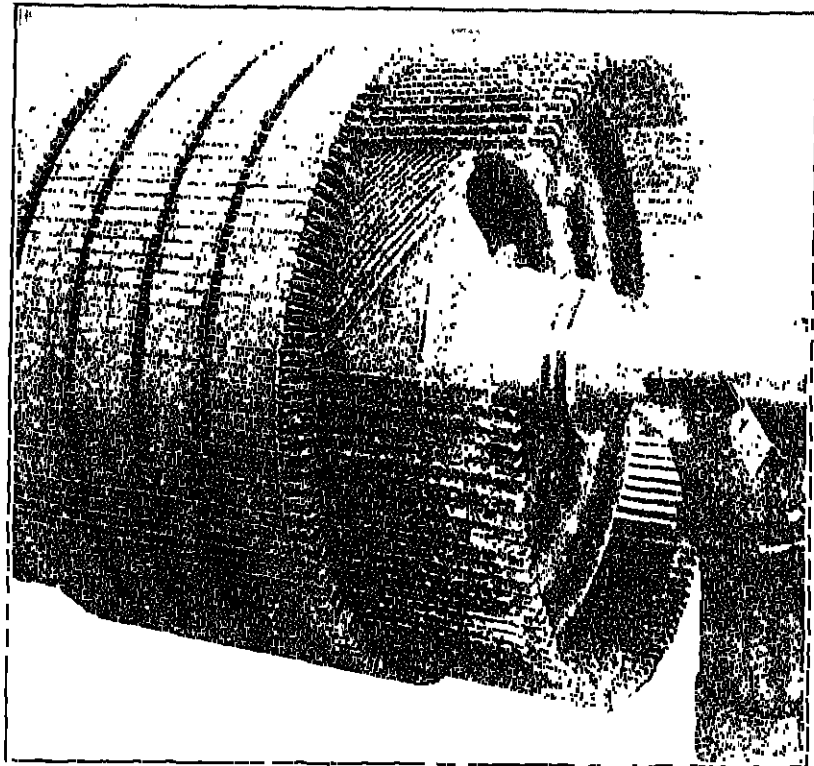


FIG. 170.—Partially wound slip-ring rotor.

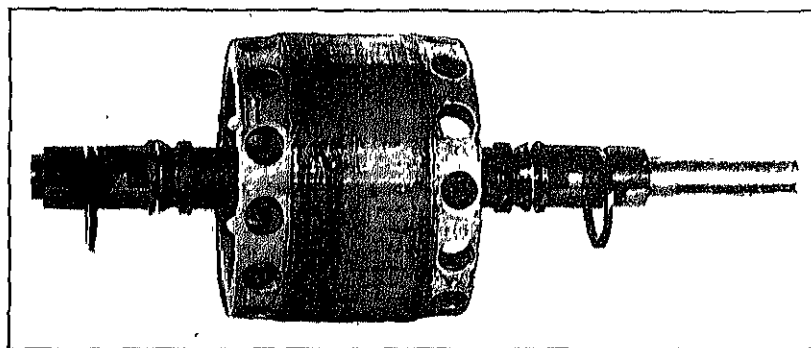


FIG. 180.—Complete rotor with cast squirrel-cage winding.

winding ducts at each end of the armature core are often omitted. For the slip-ring motor, insulated windings must be used in the rotor, which require deep slots and tooth supports at each end of the rotor core, similar to those used for the stator. A sectional view of stator and rotor for a large-capacity, wound-rotor motor is shown in Fig. 178, and a partially wound slip-ring rotor is shown in Fig. 179.

The squirrel-cage winding is generally built up of rectangular or round copper bars joined at each end by a copper end-ring. A cast squirrel-cage winding is used by several manufacturers. The metal used is aluminum and is cast into the assembled rotor core. With this method of construction, it is possible to use a large number of rotor slots on small-diameter rotors without excessive tooth densities, because teeth with parallel sides can be used with trapezoid-shaped slots. The rotor punching shown in Fig. 177 is for a cast squirrel-cage rotor. A complete rotor with cast squirrel-cage winding is shown in Fig. 180.

CHAPTER XVII

THE STATOR

THE design of the stator of an induction motor is carried out in the same way as the armature design of a synchronous motor or generator. The voltage induced in the stator winding,

$$E = \frac{\phi_t n N f_c C_w}{60 \times 10^8} \text{ volts per phase.} \quad (170)$$

This formula is explained on page 166.

A sine wave flux distribution is generally assumed for the induction motor, because the distributed stator winding produces an air gap flux wave which is very nearly sinusoidal. The form factor and flux-distribution factor have been explained on page 172. They are equal to 1.11 and 0.637 respectively for a sine wave. The winding-distribution factor has been carefully explained on page 184. It may be taken equal to 0.956 for 3-phase windings and 0.91 for 2-phase windings (see Fig. 122). The winding constant,

$$C_w = f_b f_d f_w = 1.11 \times 0.637 \times 0.956 = 0.677 \text{ for 3-phase}$$

$$C_w = f_b f_d f_w = 1.11 \times 0.637 \times 0.91 = 0.643 \text{ for 2-phase.}$$

The voltage induced in a coil is proportional to the sine of the half-angle which the coil spans. The sine of the half-angle spanned by the coil is called the chord factor.

$$f_c = \sin (P \times 90^\circ).$$

For a given voltage the total flux,

$$\phi_t = \frac{E \times 60 \times 10^8}{n N f_c C_w} \text{ lines.}$$

The terminal voltage per phase may generally be used instead of the induced voltage per phase, because the resistance drop of the stator winding is small.

of an induction motor,

$$\text{hp} = \frac{E I_m \times \text{eff.} \times \text{PF}}{746} \text{ horsepower}$$

$$E = \frac{\phi_t n N f_c C_w}{60 \times 10^8} \text{ volts, approximately.}$$

The total flux, $\phi_t = \pi D l_g B_g$ and the total ampere-conductors on the stator, $I_m N f_c = \pi D Q$. Substituting into the output equation above,

$$\begin{aligned} \text{hp} &= \frac{\pi D l_g B_g \pi D Q n C_w \times \text{eff.} \times \text{PF}}{4.55 \times 10^{11}} \\ &= \frac{D^2 l_g n B_g Q C_w \times \text{eff.} \times \text{PF}}{4.55 \times 10^{11}} \\ \frac{D^2 l_g n}{\text{hp}} &= \frac{4.55 \times 10^{11}}{B_g Q C_w \times \text{eff.} \times \text{PF}} \end{aligned} \quad (171)$$

Air Gap Density.—In an induction motor the magnetizing current or the current required to maintain the flux in the magnetic circuit is drawn from the alternating current lines to which the motor is connected. This magnetizing current lags the voltage by 90° and must be small if reasonable operating characteristics are to be obtained. For air gap lengths as short as practicable, the reluctance of the air gap is greater than that of the remainder of the magnetic circuit. To avoid excessive magnetizing currents moderate densities are therefore required. The density in the stator teeth is directly proportional to that in the air gap. High tooth densities produce high core losses and increase the magnetizing current. The flux density in the air gap of induction motors generally lies between the limits 25,000 and 45,000 lines per sq. in. The high values are for large-capacity, high-speed motors. For general purpose motors, air gap densities from 30,000 to 40,000 lines per sq. in. are most satisfactory.

Ampere-Conductors.—The value of the ampere-conductors per inch of stator gap circumference depends upon the size of the motor, the voltage of the stator winding, the type of ventilation, and the permissible leakage reactance. Average values of Q for open type, 40° C.-rated motors for voltages up to 2500 volts are given by the curve in Fig. 181.

Efficiency and Power Factor.—The operating characteristics shown in Table XXIV are for normal polyphase, 60-cycle, constant-speed, 40° , squirrel-cage motors for voltages up to 600 volts, and those in Table XXV are for normal polyphase, 60-cycle, constant-speed, 40° , slip-ring motors for voltages up to 600 volts.

1 per cent lower and the full-load power factor approximately 2 per cent lower than the values given in Tables XXIV and XXV.

It is apparent from equation 171 that a series of constants can be

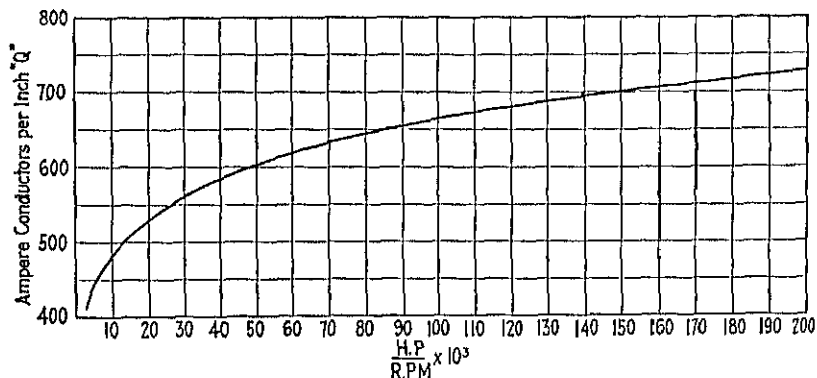


FIG. 181.—Ampere conductors per inch of stator gap circumference for polyphase induction motors.

derived for various ratings and speeds which can be used to calculate the stator diameter and length. The length, l_m , in equation 171 is the length of the stator core minus the ventilating ducts. It is generally }

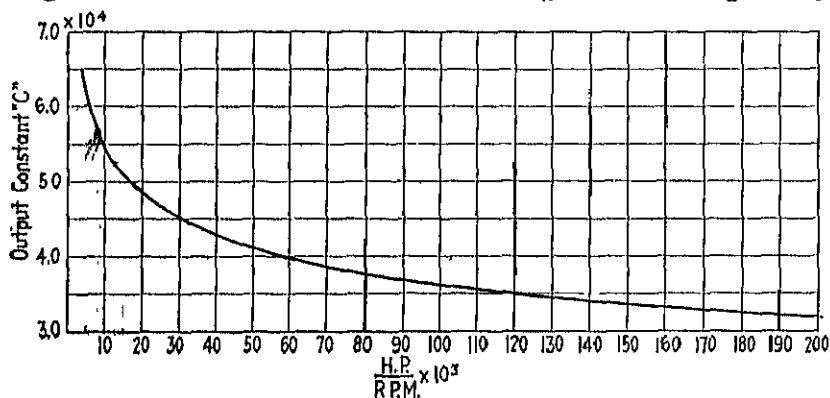


FIG. 182.—Output constants for 60 cycle, constant speed, polyphase, induction motors for voltages up to 600 volts.

convenient to calculate the total stator length instead of the length of the air gap section. For this purpose, equation 171 is written as follows:

$$\frac{D^2 l_m}{hp} = C. \quad (172)$$

The output constants given in Fig. 182 are taken from a line of tested

OPERATING CHARACTERISTICS OF 3-PHASE, 60-CYCLE, CONSTANT-SPEED HORIZONTAL MOTORS

Hp	Speed, R.p.m.		Eff, Full-Load	PF, Full-Load	Current in Amperes, 220 Volts		Torque in Pounds at 1-Ft. Radius		
	Syn.	Full-Load			Full-Load	Locked Rotor	Full-Load at Full-Load Speed (Approximate)	Starting (With Full Voltage)	Maximum Running
1/2	1200	1100	73	65	2.07	8.1	2.38	3.0	4.9
	900	835	69	49	2.0	8	3.13	4.7	6.2
1	1800	1735	80	70	2.33	14	2.27	4.2	6.2
	1200	1100	76	72	2.69	11.5	3.67	5.9	7
	900	855	75	59	3.33	14	4.00	6.0	11
1	3600	3400	82	87	2.75	20	1.5	2.8	3.5
	1800	1710	82	80	3.00	19	3.07	5.8	8.7
	1200	1130	79	75	3.31	15.5	4.61	7.7	9.4
	900	855	77	70	3.61	17	6.15	10	14
1 1/2	3600	3500	82	80	4.17	30	2.3	4.2	5.4
	1800	1735	85	85	4.07	30	4.53	8.8	13.5
	1200	1150	81	77	4.72	25	6.84	11.3	14.2
	900	865	79	68	5.48	26	9.11	15	25
2	3600	3510	82	86	5.56	46	3.1	6.2	7.9
	1800	1740	85	86	5.37	40	6.03	11.2	18
	1200	1155	84	82	5.70	36	9.10	15	19
	900	860	81	70	6.93	35	12.25	19	39
3	3600	3510	85	88	7.87	52	4.5	8.4	11.5
	1800	1730	86	88	7.76	50	9.11	16.9	25
	1200	1160	85	83	8.35	52	13.5	22.5	29
	900	860	82	73	9.85	47	18.3	28	44
5	3600	3460	86	90	12.67	86	7.6	14.1	20
	1800	1740	87	89	12.7	86	15.1	28	45
	1200	1150	86	86	13.25	86	22.8	37.7	48
	900	865	85	77	14.0	84	30.3	47	70
7 1/2	3600	3475	86	89	19.2	140	11.4	22.5	29
	1800	1740	88	90	18.6	120	22.6	42	62
	1200	1165	88	87	19.25	130	33.8	56	75
	900	865	86	77	22.2	126	45	70	95
10	3600	3510	87	92	24.5	187	15	29	39
	1800	1740	89	91	24.2	175	30.2	56	82
	1200	1160	88	88	25.3	170	45.2	74.8	96
	900	865	87	81	27.8	170	60	90	130
15	3600	3510	88	91	36.7	282	22.5	45	60
	1800	1755	90	91	36	282	44.8	83.2	147
	1200	1165	89	86	38.4	300	67	105	180
	900	875	88	83	40	290	90	160	250

Hp	Speed, R p.m.		Eff, Full-Load	PF, Full-Load	Current in Amperes, 220 Volts		Torque in Pounds at 1-Ft Radius		
	Syn	Full-Load			Full-Load	Locked Rotor	Full-Load at Full-Load Speed (Approximate)	Starting (With Full Voltage)	Maximum Running
20	3600	3500	88	91	49	450	30	50	85
	1800	1760	89.5	88	50	100	59	100	160
	1200	1170	89.5	88	50	430	80	150	300
	900	865	89.5	84	52	310	121	165	250
	720	680	88	83	55	280	151	185	200
	600	560	81.5	78	59.1	250	187	215	350
25	3600	3550	91	91	59.2	575	40	65	110
	1800	1755	90.5	90	60	410	75	112	220
	1200	1165	89.5	87	63	500	112	200	350
	900	865	89.5	81	65	110	152	190	300
	720	690	88	82	68	350	190	280	475
	600	575	88	80	70	350	228	375	580
30	1800	1755	91	91.5	71	510	90	135	230
	1200	1165	89.5	87	76	690	135	235	400
	900	860	89	86	77	500	183	300	440
	720	685	87	85	80	350	230	280	475
	600	570	87	82	82	350	270	375	580
40	1800	1735	89	92	96	630	121	250	360
	1200	1150	89.5	91	96	610	183	325	450
	900	855	89	88	100	690	245	350	500
	720	685	88.5	87	102	490	307	470	680
	600	570	88	83	107	510	309	490	800
50	1800	1740	89.5	92	119	780	150	215	440
	1200	1155	90	91	120	770	227	400	625
	900	870	89.5	88	121	900	303	510	850
	720	685	89	88	125	690	382	525	800
	600	570	87.5	83	135	620	460	550	875
60	1800	1740	90	93	110	900	181	290	600
	1200	1165	91	89	115	1230	260	525	800
	900	870	90	89	147	1070	362	650	1000
	720	700	90.5	85	153	970	450	675	1200
	600	575	89.5	82	160	840	547	675	1200
75	1800	1760	91.5	92	170	1820	223	445	800
	1200	1150	89.5	91	180	1100	342	475	840
	900	875	90	89	184	1200	452	900	1400
	720	695	90	88	186	990	560	785	1500
	600	580	89.5	83	198	950	678	780	1475
100	1800	1755	90.5	94	230	1460	299	450	800
	1200	1170	91.5	91	236	1650	418	600	1300
	900	875	90.5	90	240	1800	600	875	1600
	720	695	91	89.5	248	1360	755	910	1850
	600	575	90.5	85	256	1360	914	1200	2000

Hp	Speed, R p m		Eff., Full- Load	PF, Full- Load	Current in Amperes, 220 Volts		Torque in Pounds at 1-Ft. Radius		
	Syn	Full- Load			Full- Load	Locked Rotor	Full-Load at Full-Load Speed (Approximate)	Starting (With Full Voltage)	Maximum Running
125	1800	1755	90 5	93 5	200	1900	371	100	1,000
	1200	1175	91 0	91 5	294	2000	558	715	1,000
	900	875	91	89	302	2000	750	1100	2,200
	720	650	89 5	89	308	1320	967	1100	1,900
	600	580	91	84	320	1900	1,133	1700	3,000
150	1800	1700	91	93	*173	*1145	110	190	1,300
	1200	1170	93	92	172	1150	073	770	1,900
	900	870	90 5	91	178	1125	901	1500	2,100
	720	695	91 5	89	180	1025	1,132	1500	3,000
	600	575	90	88	185	930	1,367	1700	3,100
200	1800	1750	92	93	229	1530	600	600	1,550
	1200	1175	93 5	92	228	1510	893	845	2,100
	900	870	91 0	91	231	1500	1,205	1000	3,250
	720	700	91	89	212	2150	1,500	2050	5,000
	600	580	91 0	89	213	1400	1,810	2500	4,500
	450	430	90 5	82	265	1200	2,110	2500	5,200
	360	345	90 5	82	264	1375	3,010	1000	7,500
250	600	580	91 5	88	305	1800	2,200	2800	6,200
	450	430	91	85	317	1500	3,060	3000	6,100
	360	340	90 5	80	338	1650	3,750	2850	9,300
300	600	580	92	89	359	2100	2,710	3500	7,500
	450	430	91	85 5	380	2100	3,060	3200	8,500
	360	340	91	78	413	2100	4,520	3000	11,000
400	600	585	92	90 5	470	3000	3,000	4200	10,000
	450	437	92	85 5	500	2800	4,830	3500	12,000
	360	340	91 5	81 5	526	2300	0,000	3800	11,000
450	300	292	92	77	625	3100	8,100	5100	18,000
500	600	585	92	91	590	4700	4,500	5000	12,000
	450	437	92 5	87	602	3400	6,000	4700	16,000
	360	349	91 5	81 5	658	2750	7,500	4500	18,000
600	450	437	92 5	87	722	3850	7,200	5500	18,500
	360	350	93	86	735	4100	9,000	6800	21,000
	300	290	92	70	810	3200	10,850	5800	25,000
750	450	440	93	88 5	895	7000	8,950	8000	26,500
	360	352	92	84	955	4100	11,400	6000	23,000

These values for 440 volts.

OPERATING CHARACTERISTICS OF 3-PHASE, 60-CYCLE, CONSTANT-SPEED HORIZONTAL MOTORS

Hp	Speed, R p m.		Eff Full- Load	PF, Full- Load	Full-Load Current in Amperes, 220 Volts		Torque in Pound at 1-ft Radius	
	Syn	Full- Load			Stator	Rotor per Lead	Full-Load at Full-Load Speed (Approximate)	Maximum Running
1/2	900	825	70	50	3 50	8 3	4 78	0 7
1	1200	1100	73	70	3 81	10	4 78	0 2
	900	815	71	60	3 81	10	6 21	16 4
1 1/2	900	815	74	65	6 13	11 5	9 32	27 7
2	1800	1700	78	82	6 11	17 2	6 18	11
	1200	1115	77	72	7 06	18	9 43	10
	900	850	76	67	7 7	18	12 35	31 3
3	1800	1600	81	83	8 76	21 1	0 32	19
	1200	1110	80	78	9 41	20	13 84	28
	900	855	80	68	10 8	22	18 1	40 7
5	1800	1700	81	80	13 6	30 5	15 16	33
	1200	1140	82	81	14 8	27 3	22 05	46
	900	855	83	72	16 4	30	30 7	62
7 1/2	1800	1700	85	87	19 0	28	23 2	47
	1200	1115	85	83	20 0	27 0	31 4	72
	900	870	86	64	26 8	29 2	45	90
10	1800	1725	88	86	25 0	28	30 5	90
	1200	1145	85	81	27 4	30	45 0	91
	900	810	83	78	30	53 5	62	150
15	1800	1700	87 0	86.5	43	57	40 3	110
	1200	1125	85	83	11 0	60 5	70	160
	900	810	81 5	79	44	61	94	200
20	1800	1720	87 0	87 0	52	61	61 1	150
	1200	1115	86 5	85	53	62 5	91	220
	900	835	85	81	57	101	126	220
25	1800	1720	86 0	87.5	61	66	76 3	195
	1200	1130	86	85	67	97	116	300
	900	810	80	82	70	103	158	225
30	1800	1710	86	88	78	69 5	90	300
	1200	1115	87	85 5	79	93	137	350
	900	850	86	83	82	132	185	375
40	1800	1735	87 5	88 5	101	79	121	360
	1200	1110	87	88	102	138	184	460
	900	850	86 5	85	106	111	245	500
50	1800	1720	87.5	91	123	98.5	152	360
	1200	1150	88	90	124	133	228	575
	900	860	87 5	86	130	133.5	305	750
	720	695	87 5	84	142	102	378	850
	600	570	87	80	141	140	400	925
60	1800	1720	88	91	148	147	183	500
	1200	1160	88 5	87	152	130	271	800
	900	860	88	87	163	130	367	900
	720	690	88.5	83	160	122	455	1200
	600	575	88	81	165	134	545	1125

Hp	Speed, R p m		Eff Full- Load	PF, Full- Load	Full-Load Current in Amperes, 220 Volts		Torque in Pound at 1-Ft Radius	
	Syn	Full- Load			Stator	Rotor per Lead	Full-Load at Full-Load Speed (Approximate)	Maximum Running
75	1800	1745	89	01 5	182	125	220	575
	1200	1160	90	85	181	96	340	950
	900	870	89	87	180	127	455	1,250
	720	690	88 5	86	183	120 5	670	1,300
	600	575	89	82	200	131	685	1,500
100	1800	1745	90	92	236	103	300	750
	1200	1165	91	89	242	127	460	1,250
	900	870	89 5	88	248	130	605	1,400
	720	695	90	86	251	132	755	1,600
	600	585	90 5	85	254	132	905	2,200
125	1800	1750	90	93	216	106	375	950
	1200	1175	91 5	90	161	121	558	1,250
	900	880	90 5	88	164	129	745	2,200
	720	700	90	86	153	185	952	1,900
	600	585	91	82 5	103	122	1,120	3,000
150	1800	1750	91	92	175	109	450	1,150
	1200	1170	92 5	90	176	115	673	1,800
	900	875	90 5	90	181	147	900	2,400
	720	705	91 5	88	182	163	1,126	3,000
	600	580	90 5	88	185	191	1,350	3,200
200	1800	1755	92	92	231	177	598	1,300
	1200	1170	93	90	234	146	807	2,300
	900	875	91	90	231	103	1,200	2,700
	600	585	91 5	88	214	195	1,705	4,000
	150	435	91	84	267	182	2,110	5,500
250	360	345	90	88	269	160	3,040	6,000
	600	585	91 5	89	300	190	2,245	6,000
	450	435	91 5	85	314	199	3,015	6,500
	360	340	91	77 5	338	190	3,760	8,500
	600	585	92 5	88	302	195	2,690	7,000
300	450	440	92	81	380	357	3,570	8,500
	360	352	91	76	417	362	4,470	11,000
	600	585	92	88	485	400	3,570	8,750
	450	440	92 5	85	500	355	4,770	13,000
	360	352	93	81	520	380	5,070	14,000
450	300	293	92 5	76	630	367	8,100	18,000
	600	588	92 5	88	620	395	4,470	11,000
	450	442	93	85	620	382	5,050	16,000
	360	352	92 5	80 5	668	402	7,450	18,000
	600	442	93 5	80	733	402	7,100	17,500
600	360	353	93	85	745	402	8,080	22,000
	300	292	92 5	79	805	397	10,740	27,500
	450	442	93 5	87	907	450	8,900	22,000
	360	353	93	85	932	515	11,100	26,000
	1000	360	94	85	1225	613	14,770	37,000

*These values for 440 volts.

motors and are for constant-speed, squirrel-cage motors for voltages up to 600 volts. For higher voltages and for wound rotor motors, these constants should be increased approximately 10 per cent.

by equation 172 with the help of the output constants of Fig. 182. The diameter and length must be so selected that satisfactory operating characteristics can be obtained with minimum cost.

The operating characteristics of induction motors vary with the ratio of the length of the stator core to the pole pitch at the gap circumference. For best power factor l/τ should be equal to from 1.0 to 1.25, and for best efficiency, about 1.5. For minimum cost l/τ should be equal to from 1.5 to 2.0. The power factor of induction motors varies with the pole pitch, that is, a motor with large pole pitch and small number of poles will have a higher power factor than a motor with small pole pitch. For motors with large pole pitch the diameter and length are selected to give minimum cost, and for motors with small pole pitch the diameter and length are proportioned to give good power factor at reasonable cost. A value of l/τ equal to 1.0 can not always be used for small motors, below approximately 15 hp, because the resulting small diameter will necessitate too small a number of stator slots. In general, the ratio of stator core length to pole pitch,

$$\frac{l}{\tau} = 0.60 \text{ to } 2.0.$$

The pole pitch,

$$\tau = \frac{\pi D}{p}$$

and

$$l = \frac{\pi D}{p} (0.60 \text{ to } 2.0).$$

Substituting into the output equation,

$$D = \sqrt[3]{\frac{pC \text{ hp}}{\pi(0.60 \text{ to } 2.0)n}}. \quad (173)$$

$$l = \frac{\text{hp } C}{D^2 n}. \quad (174)$$

The safe peripheral speed may be the determining factor in the choice of the dimensions. Standard constructions can generally be used for peripheral speeds up to 8000 ft. per min. Peripheral speeds of 15,000 ft. per min. are possible with special rotor construction and increased cost.

Windings.—The windings used for the stator or field of induction motors are the same as the armature windings of synchronous machines.

XI. Concentric-coil windings are generally used for the stators of single-phase¹ motors. Sometimes concentric-coil windings² are used for polyphase motors, but they have been replaced by the double-layer winding by most manufacturers because of the saving in cost of manufacture.

General purpose induction motors are built for both 2-phase and 3-phase and for a variety of voltages. To keep the cost of manufacture as low as possible, the number of stator slots should be so chosen for each frame that the maximum number of combinations of poles, phases, and voltages is possible. For integral number of slots per pole per phase, the slots per pole will be an integer, and the total number of slots will be satisfactory for both 2-phase and 3-phase when the number of slots per pole is a multiple of both 2 and 3. Standard induction motors are generally designed with stator windings for 220 or 440 volts. This can be done by using a 1-circuit winding for 440 volts and a 2-circuit winding for 220 volts or, if a 2-circuit winding is required for 440 volts, then a 4-circuit winding must be used for 220 volts.

Fractional slot windings may be used also for induction motors. For these windings, the denominator of the fraction must not be a multiple of the number of phases for which the winding is intended. For example: A winding with $2\frac{1}{2}$ slots per pole per phase is satisfactory for a 3-phase winding but not for a 2-phase winding. Similarly $2\frac{1}{3}$ slots per pole per phase is satisfactory for 2-phase but not for 3-phase. The use of $3\frac{1}{2}$ slots per pole per phase, however, is satisfactory for both 2-phase and 3-phase. The number of parallel circuits are very much limited with fractional slot windings because these windings do not repeat every pole as the windings with integral slots per pole and phase do. For these reasons, standard induction motors are generally designed with the number of stator slots equal to a multiple of the number of poles, times the number of phases.

Chorded windings are also used for induction motors. The advantages of chording discussed in Chapter XI apply also to induction motors. A complete discussion of the advantages of fractional pitch windings for induction motors has been given by D. F. Alexander.³

¹ "Winding and Connecting of Small Single Phase Motors," by C. A. M. Weber, *Electric Journal*, Vol. 21, Aug., 1924, p. 377.

² "The Automatic-Start Polyphase Induction Motor," and Discussion by J. L. Hamilton, A. I. E. E. Journal, Vol. 41, Oct., 1922, pp. 772-795; "Connecting Induction Motors," by A. M. Dudley, pp. 37-40, McGraw-Hill Book Co., New York.

³ "Fractional Pitch Windings for Induction Motors," *Electric Journal*, Vol. 25, Feb., 1928, p. 77.

must be an even integer for double-layer windings, because one-half of the conductors per slot belong to the coil side in the top of the slot and the other half to the coil side in the bottom of the slot. The number of conductors in series per phase can be determined by formula 170,

$$N = \frac{E \times 60 \times 10^8}{n\phi_t f_c C_w}.$$

The flux density in the air gap may generally be taken equal to 35,000 lines per sq. in. for the preliminary calculations. Then the total flux,

$$\phi_t = \pi D l_g B_g \text{ lines.}$$

The total stator conductors = Nam .

The number of stator slots must, therefore, be selected to meet the requirements of the number of poles and phases with an even number of conductors per slot of such value that a satisfactory air gap density can be obtained with chord factor between the limits 0.707 and 1.0. It is generally not desirable to chord induction motor windings more than $\frac{2}{3}$ of pitch. For two-pole motors, however, a chord factor as low as 0.707 may be necessary.

For motors with open stator slots, the slot openings have an appreciable effect on the air gap reluctance. The stator and rotor slots should be so proportioned that the minimum variations in air gap reluctance will result when the rotor slots move by the stator slots. The effect of variations in air gap reluctance is to produce pulsations in the air gap flux, which produce additional core losses and noise. These effects of the stator slots can generally be kept small by using a large number of narrow slots. The larger the number of slots for a given diameter, the smaller will be the tooth pitch. The minimum tooth pitch,

$$t_{1s} = \frac{\pi D}{S_s}.$$

The width of the stator slots is generally one-half or slightly less than one-half of the tooth pitch on the gap circumference. If the tooth pitch is small, the width of the teeth is also small, and difficulties in construction often arise; that is, it becomes difficult to support the stator teeth at the ventilating ducts and at the ends of the stator core without obstructing the ventilation. Figure 183 shows a part of a stator lamination with ventilating duct spacers and minimum tooth

pitch equal to 0.100 in. The cost of manufacture is just higher for motors with a large number of slots, because there are more coils to wind, insulate, and place into the slots. In general, it will be desirable to choose the number of stator slots to give a minimum tooth pitch equal to or greater than 0.60 in.

The current per phase in the stator winding,

$$I = \frac{\text{hp} \times 746}{Em_s \times \text{eff.} \times \text{PF}} \quad (175)$$

The section area of the stator conductor,

$$s_s = \frac{I}{a\Delta_s} \quad (176)$$

The copper losses in any winding vary directly with I^2 . The temperature rise depends upon the losses for a given type of construction. The stator current density must be so chosen that a satisfactory efficiency can be obtained without excessive temperature rise. For the stator windings of standard induction motors, the current density should generally not exceed 2500 amperes per sq. in.

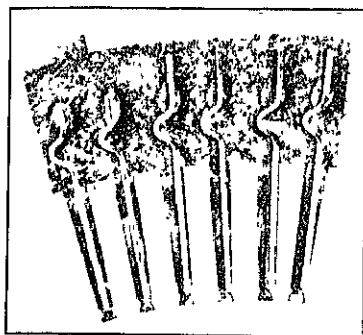


FIG. 183.—Portion of stator lamination with duct spacer.

The conductors per slot must be arranged in the slots to occupy the minimum amount of space, with the proper insulation between turns and between core and coils. Open-type stator slots are generally used for induction motors larger than approximately 15 hp, and the conductors are generally d.c.c. square wire or d.c.c. copper ribbon. For all polyphase motors, the windings are designed to have more than one turn per coil and the turns should, whenever possible, be so arranged that there is only one turn per layer, as shown in Fig. 130*A* and *B*. Large conductor sections are built up of two or more small wires in parallel, to prevent excessive eddy current losses⁴ (see Fig. 130*B*). For windings requiring many turns per coil, it is not always possible to use only one turn per layer; for such cases the coils should be wound as shown in Fig. 132*A* and *B*. For small motors, less than approximately 15 hp, partially closed stator slots are as a rule required because of the

⁴ See references, page 198.

as shown in Fig. 184, and the shape of the slots is as shown in Fig. 175. For this type of slot, the coils are random-wound of round d.c.c. wire with insulated diameter less than $\frac{1}{8}$ in.

The size of the stator slot depends upon the number of conductors per slot, the size of the conductors, and upon the insulation thickness required. The insulation on the conductors is the standard double cotton covering of insulated wires impregnated with insulating varnish. The insulation between the core and coils is built up of varnished cambric, cotton tape, insulating varnish, and paper. The following is an insulation specification for induction motor stator windings with open slots for voltages up to 600 volts.

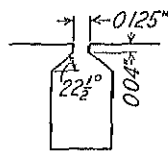


FIG. 184.

INSULATION SPECIFICATION—550 VOLTS—OPEN SLOTS— TWO COIL SIDES PER SLOT

Coils

1. After coils are wound on shuttle and pulled out to shape, care must be taken to form the ends properly before dipping in varnish so that no pounding or hammering will be necessary when assembling coils in slots.

2. Dry untaped coils thoroughly in oven and while hot dip in flexible black baking varnish, and allow coils to remain in varnish bath for one-half hour or until cool. After removing coils from varnish, drain thoroughly and bake at 100° C. (212° F.) from 8 to 10 hours or until dry.

3. Wrap the straight part of coils with two thicknesses of 0.007-in. black varnished cambric lapping so as to give three thicknesses on one side. Brush inner side of this varnished cambric wrapper with varnish so as to moisten it and allow a good tight fit.

4. Tape the ends of coils with one thickness of 0.007-in. black varnished cambric tape cut on the bias, half-lapped.

5. Tape coils all over with 0.007-in. linen finished tape, half-lapped, and give two dippings, in flexible black baking varnish, and bake after each dip at 100° C. (212° F.) for 8 to 10 hours or until dry.

Slots

1. In slots place U-shaped tube of 0.010-in. red rope overlapping under wedge.
2. Between coils in slot place a 0.010-in. red rope strip as separator.

Wedges

1. Seal slots with wedges $\frac{1}{8}$ -in. thick cut from sheet Bakelite-Dilco.

Connections

1. Tape all series leads and stub-connections with two tapings of 0.007-in. black varnished cambric tape, half-lapped and bound with friction tape.

2. Tape all pole connections with three half-lapped 0.007-in. black varnished cambric tapes.

1. When rings for supporting coils are used, insulate them with two half-lapped, 0.007-in. black varnished cambric tape and one half-lapped, dry linen-finished tape.
2. After coils are in place and all connections made, finish by spraying thoroughly with air drying varnish.

Insulation Allowance: Depth = 0.35 in.
Width = 0.12 in.

The insulation allowances given in the specification above are the total insulation thickness plus clearance over the insulated conductors. The allowance in the depth of the slot includes the thickness of the wedge, which may generally be taken equal to 0.12 in. For stator windings for voltages from 600 to 2500 volts with open slots, the insulation allowances are: Width of slot, 0.16 in.; Depth of slot, 0.45 in.

For open-type slots the insulation is wrapped on the coil with a 0.010-in. paper slot lining to protect the coil while it is placed into the slot. For partially closed slots, the insulation is placed into the slots, because the narrow slot opening makes it necessary to place the conductors into the slot one by one. The insulation allowances for the width of the slot may be taken the same as given above for open slots. For the depth of the slot, the allowance for the wedge must be corrected for partially closed slots (see Fig. 184).

The width of the stator slot is generally approximately 50 per cent of the minimum stator tooth pitch and should seldom if ever exceed 60 per cent of the minimum tooth pitch. To avoid a high leakage reactance and consequent poor operating characteristics, the stator slot should generally not be deeper than 6 times the slot width.

Stator Tooth and Yoke Densities.—For a given total flux, the dimensions of the slots determine the tooth density. For high tooth densities, the losses in the teeth are high, and a large number of ampere-turns are required to send the flux through the teeth. The maximum value of the stator tooth density for the minimum section,

$$B_{ts_1} = \frac{\phi_t}{w_{ts_1}(l - n_a w_a) k_1 S_s} \quad (177)$$

The width of the tooth for the minimum section,

$$w_{ts_1} = l_{1s} - w_{ss} \quad (178)$$

The maximum value of the stator tooth density for the minimum section should generally not exceed,

$$B_{ts_1} = 100,000 \text{ lines per sq. in. for 60 cycles}$$

$$B_{ts_1} = 120,000 \text{ lines per sq. in. for 25 cycles.}$$

the flux density in the yoke. The iron losses in the yoke and the ampere-turns required to send the flux through the yoke determine the density. The flux density should not exceed,

$$B_{ys} = 95,000 \text{ lines per sq. in. for 60 cycles}$$

$$B_{ys} = 110,000 \text{ lines per sq. in. for 25 cycles.}$$

Generally B_{ys} is equal to from 50,000 to 85,000 lines per sq. in. for 60 cycles and 60,000 to 100,000 lines per sq. in. for 25 cycles.

The flux per pole,

$$\phi = \frac{\phi_t f_d}{p}.$$

The depth of the iron below the slots for both sides of the diameter,

$$d_{ys} = \frac{\phi}{B_{ys}(l - n a w_d) k_1}. \quad (179)$$

The outside diameter of the stator laminations,

$$D_0 = D + 2d_{ss} + d_{ys}. \quad (180)$$

Sample Design: *Design of Stator for a 15-Hp, 3-Phase, 60-Cycle, 1200-R.p.m., 220-Volt, Squirrel-Cage General Purpose Motor.*—The full-load efficiency and power factor are to be not less than 89.0 per cent and 86.0 per cent, respectively. The motor must have a starting torque not less than 150 per cent of full-load torque for normal voltage and a maximum running torque not less than 250 per cent of full-load torque. The temperature rise of no part of the motor should exceed 40° C. for continuous full-load operation.

The number of poles,

$$p = \frac{f \times 2 \times 60}{n} = \frac{60 \times 2 \times 60}{1200} = 6$$

$$\frac{\text{hp}}{n} \times 10^3 = \frac{15}{1200} \times 10^3 = 12.5.$$

From the curve in Fig. 182, the output constant,

$$C = 5.25 \times 10^4.$$

For the ratio, $l/\tau = 1.0$

$$\begin{aligned} D &= \sqrt[3]{\frac{C \text{ hp } p}{n \pi l/\tau}} = \sqrt[3]{\frac{5.25 \times 10^4 \times 15 \times 6}{1200 \times \pi \times 1}} \\ &= 10.77 \text{ in.} \end{aligned}$$

$$l = \frac{l}{D^2 n} = \frac{10.77^2 \times 1200}{5.65 \text{ in.}}$$

The following table shows the values of D and l for several values of l/τ .

l/τ	D	l	τ
1.20	10.12	6.40	5.29
1.00	10.77	5.65	5.64
0.90	11.15	5.28	5.84
0.80	11.60	4.88	6.08
0.70	12.10	4.40	6.33

The following dimensions are selected:

$$D = 11.00 \text{ in.}, \quad l = 5.50 \text{ in.}, \quad \tau = 5.75 \text{ in.}, \quad l/\tau = 0.957.$$

For the diameter and length selected, it will not be necessary to use radial ventilating ducts in the stator core. The length of the air gap section will then equal the total length of the stator core,

$$l_g = l = 5.5 \text{ in.}$$

A flux density of 35,000 lines per sq. in. is assumed for the air gap, and

$$\begin{aligned} \phi_i &= \pi D l_g B_g = \pi \times 11 \times 5.5 \times 35,000 \\ &= 6650 \text{ kilo-lines.} \end{aligned}$$

If the star-connected winding is chosen, the phase voltage,

$$E = \frac{220}{1.73} = 127 \text{ volts.}$$

For a chord factor $f_c = 1.0$ the conductors in series per phase,

$$\begin{aligned} N &= \frac{E \times 60 \times 10^8}{n \phi_i C_w f_c} = \frac{127 \times 60 \times 10^8}{1200 \times 6,650 \times 10^3 \times 0.677 \times 1} \\ &= 141. \end{aligned}$$

It will be desirable to use two parallel circuits per phase; the winding can then be reconnected to one circuit per phase for 440 volts. For two parallel circuits, the total number of conductors $= 2 \times 3 \times 141 = 846$.

$$S_s = 3 \times 3 \times 6 = 54;$$

and the minimum tooth pitch,

$$t_{1s} = \frac{\pi D}{S_s} = \frac{\pi \times 11}{54} = 0.64 \text{ in.}$$

The number of conductors per slot,

$$= \frac{846}{54} = 15.7.$$

The stator winding will then have 16 conductors per slot, 8 turns per coil, and two parallel circuits per phase. A coil throw, slot 1 to 9 or 88.9 per cent of pitch, is chosen, and the chord factor,

$$f_c = \sin (P \times 90) = \sin (0.889 \times 90) = 0.985.$$

The conductors in series per phase,

$$N = \frac{16 \times 54}{2 \times 3} = 144$$

and the total flux,

$$\begin{aligned} \phi_t &= \frac{E \times 60 \times 10^8}{nNC_s f_c} = \frac{127 \times 60 \times 10^8}{1200 \times 144 \times 0.677 \times 0.985} \\ &= 6610 \text{ kilo-lines.} \end{aligned}$$

The final value of the air gap density,

$$\begin{aligned} B_g &= \frac{\phi_t}{\pi D l_g} = \frac{6610 \times 10^3}{\pi \times 11.0 \times 5.5} \\ &= 34.8 \text{ kilo-lines.} \end{aligned}$$

The stator current per phase,

$$I = \frac{\text{hp } 746}{E m_s \times \text{eff.} \times \text{PF}} = \frac{15 \times 746}{127 \times 3 \times 0.89 \times 0.86} = 38.4 \text{ amperes.}$$

For a current density of 2300 amperes per sq. in.,

$$s_s = \frac{I}{a A_s} = \frac{38.4}{2 \times 2300} = 0.00835 \text{ sq. in.}$$

The conductor selected from the copper table has the following dimensions: 0.045×0.190 in. bare, 0.060×0.201 in. insulated,

0.00805 sq. in. area. The arrangement of the conductors in the slot is as shown in Fig. 185, and the slot dimensions are:

$$\text{Width } 0.201 + 0.12 = 0.321 \text{ in.}$$

$$\text{Depth } 0.060 \times 16 + 0.35 = 1.31 \text{ in.}$$

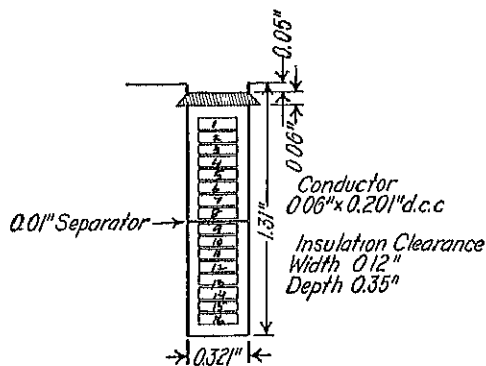


FIG. 185.

The current density in the stator conductors,

$$A_s = \frac{38.4}{2 \times 0.00805} = 2390 \text{ amperes per sq. in.}$$

The minimum stator tooth pitch is given above and the minimum tooth width,

$$w_{ts1} = t_{1s} - w_{ss} = 0.64 - 0.321 = 0.319 \text{ in.}$$

The maximum density in the stator tooth,

$$B_{ts1} = \frac{\phi_t}{w_{ts1}(l - n_{atwa})0.92S_s} = \frac{6610 \times 10^3}{0.319(5.5 - 0)0.92 \times 54} = 75.8 \text{ kilo-lines.}$$

The flux per pole,

$$\phi = \frac{\phi_t f_a}{p} = \frac{6610 \times 10^3 \times 0.637}{6} = 701 \text{ kilo-lines.}$$

For a flux density of 65 kilo-lines per sq. in. in the stator yoke,

$$d_{ys} = \frac{\phi}{B_{ys}(l - n_{atwa})0.92} = \frac{701 \times 10^3}{65,000(5.5 - 0)0.92} = 2.13 \text{ in.}$$

The outside diameter of the stator,

$$D_o = D + 2d_{ss} + d_{ys} = 11.0 + (2 \times 1.31) + 2.13 = 15.75 \text{ in.}$$

CHAPTER XVIII

THE ROTOR

Air Gap Length.—The ampere-turns required to send the flux through the air gap are directly proportional to the density and the length of the gap. Even with low air gap densities and short air gap lengths, the gap ampere-turns are larger than the ampere-turns for the remainder of the magnetic circuit. The air gap density and length, therefore, determine the magnetizing current. To obtain good operating characteristics, the magnetizing current should be as small as possible and the length of the air gap should be as small as mechanical construction will permit. The approximate minimum air gap length can be determined by the following empirical formula,

$$\delta = 0.125 - \frac{10.17}{D + 92} \quad (181)$$

The rotor diameter,

$$D_r = D - 2\delta.$$

Rotor Windings.—Squirrel-cage windings are built up of bar conductors short-circuited at each end by end-rings. The bars are either round or rectangular in shape and are of either copper, brass, or aluminum. The end-ring is generally of the same material as that used for the bars and may have any convenient shape. Various methods¹ have been used to join the end-ring to the bars. Because of the large temperature changes from no-load to full-load, the best possible connection between bars and end-ring is necessary to avoid high contact resistance at the joints. The cast squirrel-cage winding, shown in Fig. 180, is very desirable in this respect, because there are no joints. For large motors the end-ring is generally brazed or welded to the bars, and the methods of construction shown in Fig. 186 are generally used.

For wound-rotor motors, 3-phase, double-layer windings are used on the rotor, which are modified wave windings.² They may be con-

¹ "Connecting Induction Motors," by A. M. Dudley, p. 58, McGraw-Hill Book Co., New York.

² "Connecting Induction Motors," by A. M. Dudley, pp. 69-75, McGraw-Hill Book Co., New York.

ings can be laid out to determine the proper coil sequence by the method explained in Chapter XI for armature windings of synchronous machines. Figure 187 shows the winding diagram for a 3-phase, 6-pole, 1-circuit, star-connected, modified wave winding with 54 slots and 4 conductors per slot. In this figure, all of the coils are shown for one phase. For the other two phases only the beginning and ending coils are shown. A 3-phase, 8-pole, 1-circuit, delta-connected rotor winding with 96 slots and two conductors per slot is shown in Fig. 188.

Number and Size of Rotor Slots.—For squirrel-cage motors the number of rotor slots must be selected to avoid dead-points or positions

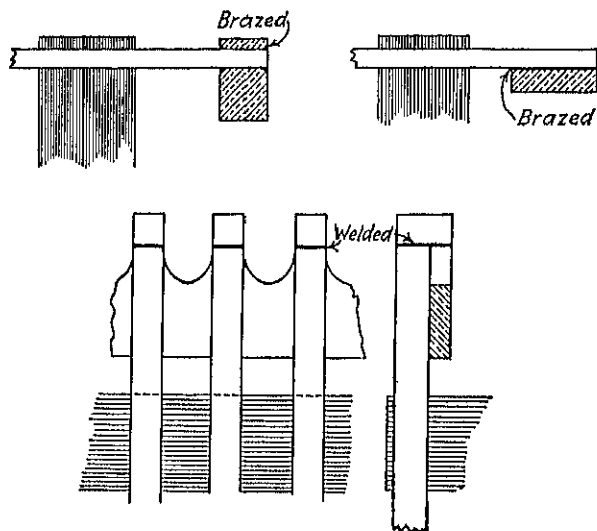


FIG. 188.

of no torque at starting. To avoid excessive starting currents, squirrel-cage motors are started with reduced voltage. The main flux is therefore small at starting, whereas the leakage flux is large because of the high starting current. The zigzag leakage flux is a maximum when the rotor slot opening is opposite the center of a stator tooth and a minimum when it is opposite the center of a stator slot. The locking torque is produced by the zigzag leakage flux. In order that it shall be as small as possible, the number of rotor slots should be so chosen that a minimum number of rotor slot openings will be opposite the center of a stator tooth for any rotor position. The number of rotor slots must therefore never be equal to the number of stator slots, but must be either larger or smaller. Satisfactory results can generally

1.30 per cent or from 70 per cent to 85 per cent of the number of stator slots. For squirrel-cage motors it is generally desirable to make the number of rotor slots 80 per cent or 120 per cent of the number of stator slots. To have the minimum number of rotor slot openings opposite the center of a stator tooth for any position of the rotor, the

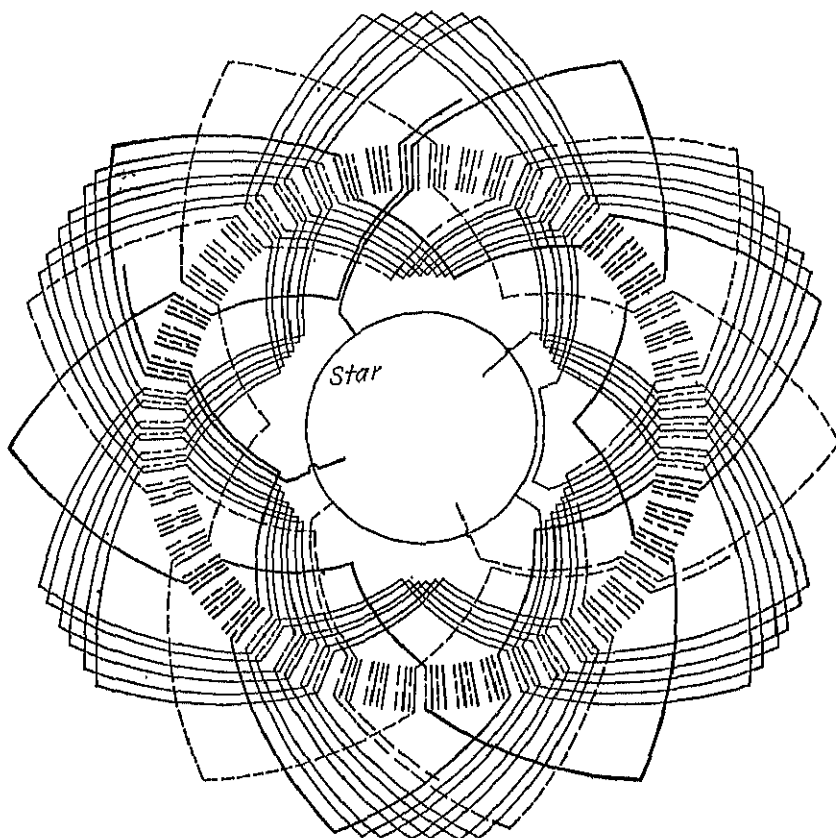


FIG. 187.—Rotor winding diagram—three-phase, 6 poles, 54 slots, 4 conductors per slot, one circuit star.

number of stator and rotor slots must be prime to each other. For small motors, diagonal rotor slots are often used to reduce the locking torque and magnetic noises, because it is not always possible to use the most desirable proportions of stator and rotor slots for small diameters.

The rotor windings for wound-rotor motors are 3-phase windings,

and the number of rotor slots must be integral, windings with an integral number of slots per pole per phase are used for the rotor. Fractional slot windings may also be used, but for most cases only those will be satisfactory for which the number of slots is a multiple of the number of phases times the number of pairs of poles. Wound-rotor motors are started with normal voltage applied to the

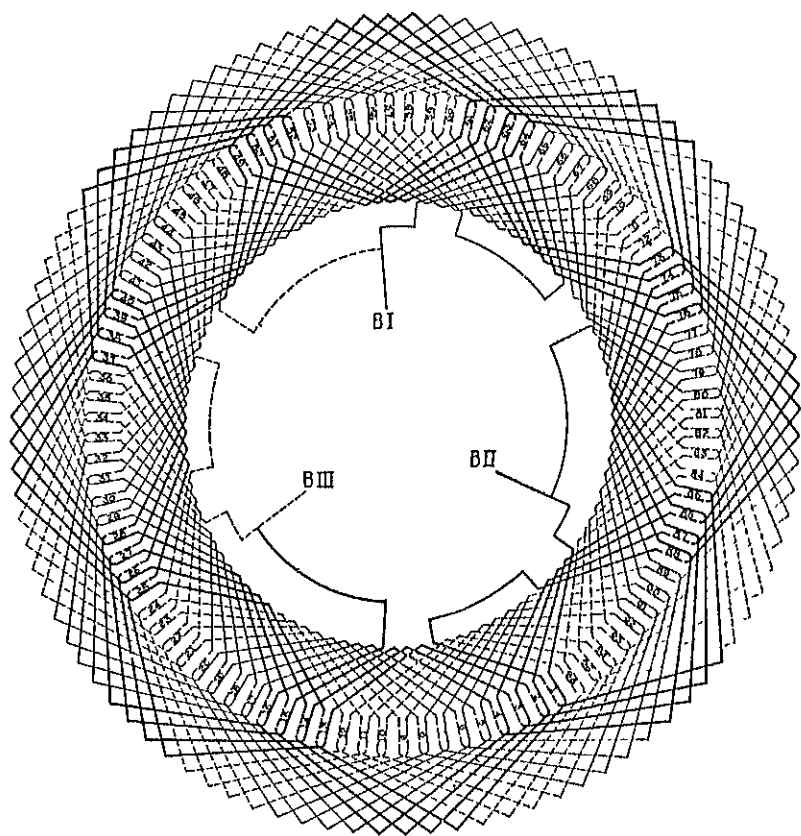


FIG. 188.—Rotor winding diagram—three-phase, 8 poles, 96 slots, two conductors per slot, one circuit delta.

stator winding and enough resistance in the rotor circuit to give full-load torque with full-load current. The main field is therefore of normal strength during the starting period. Since the zigzag leakage flux is only a small per cent of the main flux for normal voltage, the effect of dead points is very small for wound-rotor motors. To avoid magnetic noises and excessive flux pulsations in the air gap, however, the ratio of

the stator slots to the rotor slots should, whenever possible, lie within the limits given above.

If the total rotor ampere-turns are assumed to be 10 per cent less than the total stator ampere-turns, the ratio of the total copper section of the rotor to the total stator copper section,

$$\frac{S_{cr}}{S_{cs}} = 0.90 \frac{A_s}{A_r}. \quad (182)$$

For squirrel-cage windings, the current density may be higher than for the stator winding because the mean length of turn is shorter and the ventilation is better. For a current density of 2500 amperes per sq. in. in the stator winding and 4000 amperes per sq. in. in the bars of the squirrel-cage winding, the ratio of the total rotor copper section to the total stator copper section,

$$\frac{S_{cr}}{S_{cs}} = 0.9 \frac{2500}{4000} = 0.562.$$

The total rotor copper section should never be less than 50.0 per cent of the total stator copper section. It is generally from 60 to 80 per cent for squirrel-cage windings.

For wound-rotor windings, the length of the mean-turn is approximately equal to the length of the mean-turn of the stator coils.

Consequently, to avoid excessive rotor copper losses,

the rotor current density can not be made much higher than the stator current density. The total rotor copper section is therefore generally from 80 to 95 per cent of the total stator copper section.

The distribution of the current in the bars and end-rings of a squirrel-cage winding³ is shown in Fig. 189. It is apparent from Fig. 189 that

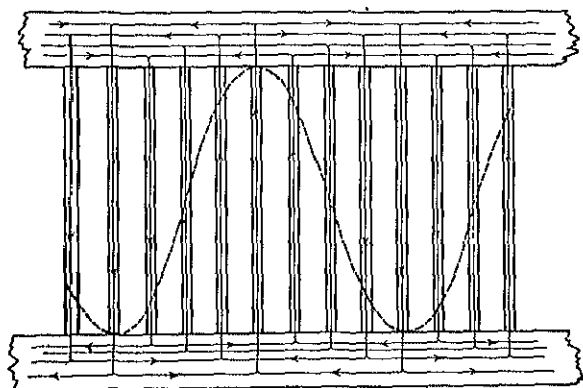


FIG. 189.—Section of squirrel-cage winding showing distribution of current.

³ "Turns and Phases in Squirrel-Cage Windings," Bulletin 5, Engineering Experiment Station, University of Minnesota.

the current in each bar divides in the end-ring, one-half returning through a bar a pole pitch to the right and the other half through a bar a pole pitch to the left. If the maximum value of the current in each bar is I_m and if the current is maximum in all the bars at the same time, then the maximum value of the current in the end-ring

$$= \frac{I_m}{2} \times \frac{N_b}{p}.$$

The current is not maximum in all the bars per pole at the same instant, but varies according to the sine law; hence, the maximum value of the current in the end-ring

$$= \frac{I_m}{2} \times \frac{N_b}{p} \times \frac{2}{\pi}$$

and the effective value of the current in the end-ring

$$= \frac{I_m}{2} \times \frac{N_b}{p} \times \frac{2}{\pi} \times \frac{\sqrt{2}}{2}.$$

The effective value of the current in each bar, $I_b = I_m/\sqrt{2}$ and the end-ring current

$$= \frac{0.32 I_b N_b}{p}, \quad (183)$$

The section area of each end-ring,

$$s_{er} = \frac{0.32 I_b N_b}{p A_{er}} \quad (184)$$

and the total bar section,

$$S_{er} = \frac{I_b N_b}{A_r}, \quad (185)$$

By combining these two equations and simplifying, the section area of each end-ring in terms of the total rotor copper section,

$$s_{er} = \frac{0.32 S_{er}}{p} \frac{A_r}{A_{er}}. \quad (186)$$

The ventilation is generally better for the end-rings than for the bars, and the current density can be made equal to the current density in the bars or slightly higher.

The rotor slots are always of the partially closed type as shown in Figs. 190 and 191. The rectangular-shaped bar and slot is generally preferred, because the higher reactance of the lower part of the bar during the starting period forces the current to the top of the bar, thereby increasing slightly the resistance of the rotor winding. Deep rotor slots, however, increase the leakage reactance and lead to small tooth widths and high density at the root of the teeth. Rotor slot depths equal to 4 times the width are used for squirrel-cage windings, but more often the depth of the slot is from 1.5 to 2.0 times the width. The section area of each bar,

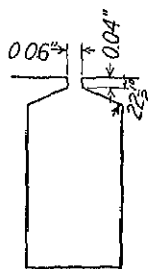


FIG. 190.

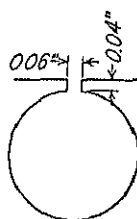


FIG. 191.

$$s_b = \frac{S_{cr}}{N_b} \quad (187)$$

No insulation is used between the bars and the rotor core. A small clearance, about 0.005 in., must, however, be allowed between the bar and the core.

For low-starting-current, high-torque squirrel-cage motors, the double squirrel-cage rotor⁴ is often used. At starting the reactance of the lower winding is high and only the high-resistance winding near the surface is active. After the motor has reached full speed, the reactance of the lower winding is small and it will carry the largest portion of the rotor current.

The number of rotor conductors for a wound-rotor motor depends upon the voltage between slip rings when the rotor is stationary, with the rings open, and normal voltage applied to the stator winding. For general purpose motors, the rotor voltage between slip rings will generally not exceed about 400 volts. For large motors, higher rotor voltages are necessary to avoid large conductor sections. The rotor voltage,

$$E_r = \frac{N_r f_r f_{wr}}{N_f f_w} k_2 E. \quad (188)$$

⁴ "The Development of Low Starting Current Induction Motors," by P. L. Alger, General Electric Review, Vol. 28, July, 1925, pp. 499 to 508.

For star-connected rotor windings, $k_2 = 1.70$, and for delta-connected rotor windings, $k_2 = 1.00$.

Rectangular bar conductors are used for the rotor winding. When the rectangular type of slot shown in Fig. 190 is used, the coils are only partly formed before placing into the slots as shown in Fig. 179, Chapter XVI. For the type of slot shown in Fig. 191, the coils are insulated and formed before they are placed into the slots.

The insulation thickness required depends upon the rotor voltage. A slot lining consisting of 0.010-in. horn fiber is placed into the slot and the remaining insulation is placed on the coils. The single thickness of insulation on the coils is generally 0.025 in. for voltages up to 600 and 0.035 in. for voltages up to 2500. The coil insulation is built up of varnished cambric, cotton tape, and insulating varnish. The allowance for the wedge for closing the slot is generally as shown in Figs. 190 and 191.

The area of each conductor,

$$s_r = \frac{S_{cr}}{N_r m a} \quad (189)$$

Rotor Tooth and Yoke Densities.—The maximum density for the rotor teeth,

$$B_{tr_2} = \frac{\phi_t}{w_{tr_2}(l - na wa)k_1 S_r}$$

The minimum tooth width,

$$w_{tr_2} = \frac{(D_r - 2l_{sr})\pi}{S_r} - w_{sr} \quad (190)$$

For constant-speed induction motors, the frequency of the flux reversals in the rotor are very small, per cent slip times the stator frequency. The core losses in the rotor iron will therefore be small even if the densities are high. The maximum density in the rotor teeth can generally be only slightly higher than the maximum stator tooth density, because of the ampere-turns required to send the flux through the teeth.

The rotor yoke density is generally equal to or only slightly higher than the stator yoke density and can be calculated as explained for the stator yoke (see page 287).

Sample Design: Design of Squirrel-Cage Rotor.—The length of the air gap,

$$\begin{aligned} \delta &= 0.125 - \frac{10.17}{D + 92} = 0.125 - \frac{10.17}{11.0 + 92} \\ &= 0.0262 \text{ in.; use } 0.026 \text{ in.} \end{aligned}$$

The rotor diameter,

$$D_r = D - 2\delta = 11.0 - 0.052 = 10.948 \text{ in.}$$

The number of rotor slots (see page 292),

$$S_r = 1.20 \times 54 = 64.8; \text{ use } 65.$$

The total stator copper section,

$$\begin{aligned} S_{cs} &= Nm_{as_s} = 1.41 \times 3 \times 2 \times 0.00805 \\ &= 6.96 \text{ sq. in.} \end{aligned}$$

If the rotor copper section is taken equal to 65 per cent of the total stator copper section (see page 295), then

$$S_{cr} = 0.65 \times 6.96 = 4.52 \text{ sq. in.,}$$

and the area of each bar,

$$s_b = \frac{4.52}{65} = 0.0696 \text{ sq. in.}$$

The rotor tooth pitch at the gap,

$$t_{lr} = \frac{\pi D_r}{S_r} = \frac{\pi \times 10.948}{65} = 0.529 \text{ in.}$$

To avoid a very narrow tooth width at the bottom of the slot, it is generally necessary to make the rotor slot width less than half of t_{lr} . Copper bars, 0.200×0.350 in., 0.0700-sq. in. area, will be used for the squirrel-cage winding. The slot dimensions are (see Fig. 192),

Width 0.205 in., Depth 0.43 in.

If the current density in the end-ring is equal to the current density in the bars, the end-ring section (see page 296),

$$s_{er} = \frac{0.32 \times 4.54}{6} \times 1 = 0.242 \text{ sq. in.}$$

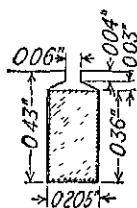


FIG. 192.

A copper end-ring, 0.25×0.875 in., or 0.219 sq. in. in area, will be used and will be brazed to the inside of the bars (see Fig. 186).

The minimum rotor tooth width,

$$\begin{aligned} w_{r2} &= \frac{\pi(D_r - 2d_{sr})}{S_r} - w_{sr} = \frac{\pi(10.948 - 2 \times 0.43)}{65} - 0.205 \\ &= 0.282 \text{ in.} \end{aligned}$$

the maximum density in the rotor teeth,

$$B_{tr_2} = \frac{\phi_t}{w_{tr_2}(l - n_a w_a)k_1 S_r} = \frac{6610 \times 10^3}{0.282(5.50 - 0)0.92 \times 65} \\ = 71.3 \text{ kilo-lines.}$$

For a flux density of 70,000 lines per sq. in. in the rotor yoke,

$$d_{yr} = \frac{\phi}{B_{yr}(l - n_a w_a)k_1} = \frac{701 \times 10^3}{70,000(5.5 - 0)0.92} \\ = 1.98 \text{ in.}$$

and the inside diameter of the rotor core,

$$D_i = D_r - 2d_{sr} - d_{yr} = 10.948 - 2 \times 0.43 - 1.98 \\ = 8.108 \text{ in.; make this 8.0 in.}$$

Then

$$d_{yr} = 2.088 \text{ in.}$$

and

$$B_{yr} = \frac{701 \times 10^3}{2.088(5.5 - 0)0.92} = 66.4 \text{ kilo-lines per sq. in.}$$

CHAPTER XIX

MOTOR CHARACTERISTICS

The Magnetizing Current.—Figure 193 shows the magnetic circuit for a 4-pole motor. The flux set up by the stator ampere-turns passes through the air gap into the rotor and through the rotor teeth into the rotor yoke. There the flux of each pole divides, one-half returning through the rotor teeth, air gap, stator teeth, and yoke of each of the adjacent poles.

Air Gap Ampere-Turns.—The ampere-turns per pole required on the stator to send the flux through the air gap,

$$\Delta T_g = B_g \delta k_s k_r \times 0.313. \quad (191)$$

The slot openings of both stator and rotor increase the reluctance of the air gap. Their effect may be taken into account by assuming that the air gap section is reduced a given amount, thereby increasing the density, or by assuming that the slot openings are equivalent to an increased length of air gap. F. W. Carter¹ derived an equation by which the air gap coefficient can be calculated. A similar equation is given by Dr. Arnold.² R. W. Wieseman³ obtained air gap coefficients by plotting graphically the flux distribution around a tooth. His results check very well with those obtained by the formulas given by Dr. Arnold and F. W. Carter. The air gap coefficient for the stator slot openings, assuming a smooth rotor without slots,

$$k_s = \frac{l_s}{w_{ts} + (\delta y)}. \quad (192)$$

Similarly, the air gap coefficient for the rotor slot openings, assuming a smooth stator without slots,

$$k_r = \frac{l_r}{w_{tr} + (\delta y)}. \quad (193)$$

¹ *Electrical World*, Vol. 38, p. 884, 1901.

² "Die Wechselstromtechnik," by Dr. Arnold, Vol. 4, pp. 78 and 79.

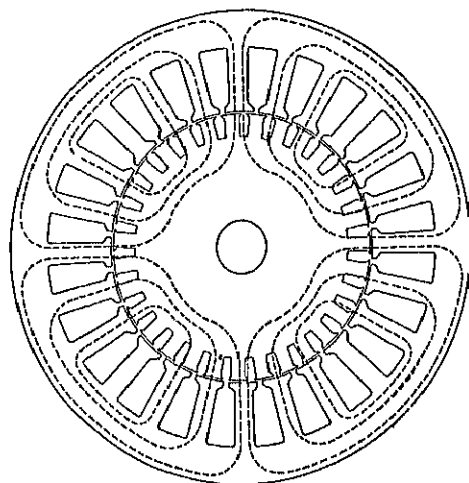
³ "Graphical Determination of Magnetic Fields," by R. W. Wieseman, A.I.E.E. Journal, Vol. 46, May, 1927, p. 431.

The value for y in equations 192 and 193 is taken from the curve in Fig. 53.

For most induction motors, the rotor slot opening is very small. The air gap coefficient for the rotor slots, k_r , can generally be taken equal to unity. The expression for the air gap ampere-turns per pole can then be written as follows:

$$AT_g = B_g \delta k_s \times 0.313. \quad (194)$$

Ampere-Turns Stator and Rotor Teeth.—For tapered stator and rotor teeth, the density varies along the length of the tooth.



Various methods have been proposed for calculating the ampere-turns required to send the flux through tapered teeth. Satisfactory results are generally obtained by calculating the ampere-turns for the density at a section $\frac{1}{3}$ tooth length from the minimum section. From the standard saturation curve for the grade of sheet steel used, the ampere-turns per inch are found for this density, and

$$AT_{ts} = at_{ts} l_{ts}.$$

FIG. 193.—Magnetic circuit—1 hp, 1800 r.p.m., 4 pole, three-phase motor (for dimensions see Figs. 175 and 177).

For the rotor teeth,

$$AT_{tr} = at_{tr} l_{tr}.$$

The length of the flux path in the teeth is equal to the depth of the slot.

Ampere-Turns Stator and Rotor Yoke.—The method of calculating the flux density in the yoke for the stator and rotor has been given above. The ampere-turns per inch for this density are determined from the proper saturation curve in the Appendix. The length of the flux path in the yokes may be taken equal to one-half the pole pitch on the mean diameter of the yoke. For the stator,

$$l_{ys} = \frac{(D + 2d_{ss} + \frac{1}{2}d_{rs})\pi}{2p} \quad (195)$$

and for the rotor,

$$l_{vr} = \frac{(D_r - 2d_{sr} - \frac{1}{2}d_{vr})\pi}{2p}. \quad (196)$$

The ampere-turns per pole for the stator yoke,

$$AT_{ys} = at_{ys}l_{ys}$$

and for the rotor yoke,

$$AT_{yr} = at_{yr}l_{yr}.$$

The total ampere-turns per pole required to send the flux through the magnetic circuit,

$$ATP = AT_g + AT_{ts} + AT_{tr} + AT_{ys} + AT_{yr}.$$

The effective value of the magnetizing current⁴ per phase,

$$I_m = \frac{2.22pATP}{m_s N f_w f_c}. \quad (197)$$

The per cent magnetizing current = $\frac{I_m}{I} 100$.

Dr. Arnold⁵ has shown that the per cent magnetizing current must be equal to the per cent reactance drop and must be equal to or less than 23 per cent if the power factor is to be equal to 90 per cent and be maximum at full-load. For small motors, it is not possible to meet these requirements without excessive cost. Tables XXIV and XXV give usual values of full-load power factor for motors of various capacities and speeds.

No-Load Current.—The no-load current of an induction motor is made up of two components: one, the magnetizing current, which is 90° out of phase with the voltage; two, the watt component of the no-load current, which is in phase with the voltage. The in-phase component of the no-load current is the current required by the no-load losses. These consist of core losses, friction and windage losses, and armature copper losses due to the no-load current.

Core Losses.—The losses⁶ in the cores of induction motors consist of the hysteresis and eddy current losses in the teeth and yokes due to the fundamental frequency flux plus additional losses. The additional losses comprise surface losses in the teeth due to variations in the air

⁴ "Wechselstromtechnik," Vol. 5-1, Julius Springer, Berlin.

⁵ "Wechselstromtechnik," Vol. 5-1, p. 336, Julius Springer, Berlin.

⁶ "Induction Motor Core Losses," by P. L. Alger and R. Eksergian, A.I.E.E. Journal, Vol. 39, Oct., 1920, pp. 906-20.

gap density, tooth pulsation losses due to variations in the tooth density, losses due to slot filing, losses due to non-uniform flux distribution, and losses in the end-plates and end-brackets. In the stator core, the frequency of the flux reversals is equal to line frequency; in the rotor it is equal to line frequency times the per cent slip. For wound-rotor motors operating at reduced speed, the rotor core losses must be included when calculating the operating characteristics. The loss in the stator teeth due to the fundamental frequency flux is equal to the loss per pound per cycle for the stator tooth density, times the frequency of the flux reversals, times the weight of the iron in the teeth. The loss per pound per cycle for various flux densities and for several grades of sheet steel is given by the curves in the Appendix. These curves are obtained from tests on samples in accordance with the American Society for Testing Materials. The loss in the stator yoke due to the fundamental frequency flux is calculated as explained for the teeth.

The additional losses are difficult to calculate. The surface losses in the teeth and the tooth pulsation losses can be calculated by the method proposed by T. Spooner⁷ and I. F. Kinard. The total core losses for induction motors are generally 1.5 to 2.5 times the sum of the stator tooth and yoke losses due to the fundamental frequency flux. The multiplying factor should be obtained from tests of motors of similar design. When such data are not available 1.75 to 2.2 may be used.

Friction and Windage Losses.—The bearing friction losses can be calculated when the bearing dimensions are known. The windage losses depend upon the type of construction and are very difficult to calculate. The combined friction and windage losses should be determined from tests of machines of similar design and construction. These losses are generally equal to from 3.5 per cent of the Kw output for 5-hp, 1800-r.p.m. motors to 1.0 per cent for 200- to 300-hp, 450-r.p.m. motors.

No-Load Stator Copper Loss.—The length of the half mean-turn of the stator coils is calculated as explained for the armature coils of synchronous machines, page 198. The coil extension and the clearance between coils at the end-connections are generally smaller than those used for the armature windings of synchronous machines. Table XXVI gives suitable values for induction motor stator and rotor windings.

⁷ "Tooth Pulsation in Rotating Machines," by T. Spooner, Trans. A.I.E.E., Vol. 43, 1924, p. 252; "Surface Iron Losses with Reference to Laminated Materials," by T. Spooner and I. F. Kinard, A.I.E.E. Trans., Vol. 43, 1924, p. 262; "No-Load Induction Motor Core Losses," by T. Spooner and C. W. Kincaid, presented at winter convention A.I.E.E., Jan. 28 to Feb. 1, 1929.

Voltage	$2b$	s
0 to 500	1.5 in.	0.10 in.
500 to 2500	2.0 in.	0.18 in.
2500 to 4500	2.5 in.	0.18 in.

The length of the half mean-turn of a stator coil,

$$L_s = \frac{\pi(D + d_{ss})}{\cos \alpha p} P + 2b + d_{ss} + l \text{ in.} \quad (198)$$

$$\sin \alpha = \frac{w_{ss} + s}{t_{ls}}.$$

The length of the half mean-turn of a rotor coil for wound-rotor type motors,

$$L_r = \frac{\pi(D_r - d_{rr})}{\cos \alpha p} P + 2b + d_{rr} + l \text{ in.} \quad (199)$$

$$\sin \alpha = \frac{w_{rr} + s}{t_{lr}}.$$

The resistance per phase of the stator winding,

$$R_s = \frac{L_s N_r}{as_s \times 10^9} \text{ ohms.} \quad (200)$$

The resistance of the rotor winding for a wound-rotor motor in terms of the stator winding,

$$R_r = \frac{f_w^2 f_c^2 N^2}{f_{wr}^2 f_{cr}^2 N_r^2} \frac{L_r N_r r}{as_r \times 10^9} \text{ ohms per phase} \quad (201)$$

or

$$R_r = \frac{f_w^2 f_c^2}{f_{wr}^2 f_{cr}^2} \frac{L_r}{L_s} \frac{S_{cs}}{S_{cr}} R_s \text{ ohms per phase.} \quad (201a)$$

For a temperature of 25° C., $r = 0.692$ and for 75° C., $r = 0.826$. The stator copper losses due to the no-load current are approximately,

$$W_{sc_0} = I_m^2 m R_s \text{ watts.} \quad (202)$$

The in-phase component of the no-load current,

$$I_w = \frac{W_o + W_{fw} + W_{sc_0}}{m E} \text{ amperes} \quad (203)$$

and the no-load current,

$$I_0 = \sqrt{I_m^2 + I_w^2} \text{ amperes.} \quad (204)$$

The power factor of the motor at no-load,

$$\text{PF}_0 = \frac{I_w}{I_0}. \quad (205)$$

Short-Circuit Current.—The current that an induction motor will draw from the line when the rotor is blocked depends upon the applied voltage and the total impedance of the motor at standstill. The total impedance comprises the stator and rotor resistance and the stator and rotor leakage reactance.

Rotor Resistance.—The method of calculating the resistance of the rotor winding for wound-rotor motors has been given above. Figure 189 shows the distribution of the current in a squirrel-cage winding. The total resistance of the squirrel-cage bars

$$= \frac{l_b N_b r}{10^6 s_b} \text{ ohms}$$

and the total resistance of the two end rings

$$= \frac{2\pi D_{er} r}{10^6 s_{er}} \text{ ohms.}$$

The total resistance of the squirrel-cage winding is equal to the total copper loss divided by the current squared, and is

$$\begin{aligned} &= \frac{l_b N_b r}{10^6 s_b} + \frac{N_b^2}{\pi^2 p^2} \frac{2\pi D_{er} r}{10^6 s_{er}} \\ &= N_b^2 \left(\frac{l_b r}{10^6 s_b N_b} + \frac{0.64 D_{er} r}{10^6 s_{er} p^2} \right) \text{ ohms.} \end{aligned}$$

The rotor resistance must be expressed in terms of the stator winding before it can be added to the stator resistance to give the total resistance of the motor. At standstill, the induction motor is simply a polyphase transformer; the equivalent resistance of the rotor is therefore equal to the total rotor resistance times the square of the ratio of the effective stator turns to the effective rotor turns. The number of phases in a squirrel-cage winding is equal to the number of bars per pole = N_b/p , and the number of turns in series per phase is equal to the number of

per pole = $p/2$. The total resistance of a squirrel-cage winding in terms of the stator winding is then,

$$= \left(\frac{N/2 f_c f_w m}{p/2 N_b/p} \right)^2 \frac{r}{10^6} N_b^2 \left(\frac{l_b}{s_b N_b} + \frac{0.64 D_{er}}{p^2 s_{er}} \right) \\ = \left(\frac{N^2 f_c^2 f_w^2 m^2 r}{10^6} \right) \left(\frac{l_b}{s_b N_b} + \frac{0.64 D_{er}}{p^2 s_{er}} \right).$$

The equivalent rotor resistance per phase,

$$R_r = \frac{N^2 f_c^2 f_w^2 m r}{10^6} \left(\frac{l_b}{s_b N_b} + \frac{0.64 D_{er}}{p^2 s_{er}} \right) \text{ ohms.} \quad (206)$$

In this formula, $r \times 10^{-6}$ is the resistance of copper per square inch section, 1 in. long; $r = 0.826$ for 75°C. and 0.692 for 25°C. If a material other than copper is used for the squirrel-cage winding the corresponding value of r must be used. Standard brass has a resistance about 4 times, and aluminum about 2 times that of copper.

Leakage Reactance.—The leakage reactance of induction motors is divided into four parts: the slot, zigzag, belt, and end-connection leakages.

For open-stator slots,⁸ Fig. 194, the slot leakage reactance,

$$X_{ss} = \frac{2.0 f l_p m N^2}{10^7 S_s} \left[K_s \left(\frac{d_{1s}}{3 w_{ss}} + \frac{d_{2s}}{w_{ss}} \right) \right] \text{ ohms.}$$

For partly closed stator slots,⁹ Fig. 195, the slot reactance,

$$X_{ss} = \frac{2.0 f l_p m N^2}{10^7 S_s} \left[K_s \left(\frac{d_{1s}}{3 w_{ss}} + \frac{d_{2s}}{w_{ss}} + \frac{2 d_{3s}}{w_{ss} + w_{ss1}} + \frac{d_{4s}}{w_{ss1}} \right) \right] \text{ ohms.}$$

For rectangular rotor slots, Fig. 196, the rotor slot reactance, in terms of the stator,

$$X_{sr} = \frac{2.0 f l_p m N^2 f_c^2 f_w^2 S_s}{10^7 S_s f_{cr}^2 f_{wr}^2 S_r} \\ \left[K_r \left(\frac{d_{1r}}{3 w_{sr}} + \frac{d_{2r}}{w_{sr}} + \frac{2 d_{3r}}{w_{sr} + w_{sr1}} + \frac{d_{4r}}{w_{sr1}} \right) \right] \text{ ohms.}$$

For round rotor slots,⁹ Fig. 197, the rotor slot reactance in terms of the stator,

$$X_{sr} = \frac{2.0 f l_p m N^2 f_c^2 f_w^2 S_s}{10^7 S_s f_{cr}^2 f_{wr}^2 S_r} \left[K_r \left(0.62 + \frac{d_{4r}}{w_{sr1}} \right) \right] \text{ ohms.}$$

⁸ "The Calculation of the Armature Reactance of Synchronous Machines," by P. L. Alger, A.I.E.E. Trans., Vol. 47, April, 1928, p. 493.

⁹ "Self-Starting Synchronous Motors," by C. J. Fehleimer, A.I.E.E. Trans., Vol. 31, Part 1, pp. 575-580.

$$X_{sz} = \frac{5}{6} X_m \left(\frac{p}{S_s} \right)^2 \text{ ohms}$$

and the rotor zigzag leakage reactance,

$$X_{rz} = \frac{5}{6} X_m \left(\frac{p}{S_r} \right)^2 \text{ ohms.}$$

The magnetizing reactance of an induction motor in ohms per phase is approximately equal to the terminal voltage per phase, divided by the magnetizing current per phase corresponding to the air gap ampere-turns. The total stator and rotor zigzag leakage reactance,

$$X_s = \frac{E}{1.2 I_{mg}} \left[\left(\frac{p}{S_s} \right)^2 + \left(\frac{p}{S_r} \right)^2 \right] \text{ ohms.}$$

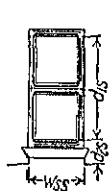


FIG. 194.

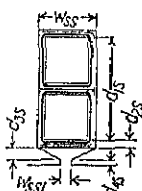


FIG. 195.

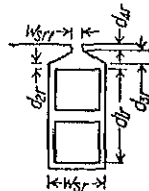


FIG. 196.

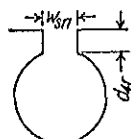


FIG. 197.

The belt leakage reactance is equal to zero for motors with squirrel-cage rotor windings and integral number of slots per pole. For wound-rotor motors, the total belt leakage reactance for stator and rotor,

$$X_b = \frac{E}{I_{mg}} (K_{bs} + K_{br}).$$

The belt leakage constants, K_{bs} and K_{br} , vary with the per cent pitch of the respective windings. They are shown in Fig. 145. They have been derived by P. L. Alger in his A.I.E.E. paper referred to above.

The end-connection leakage reactance is less for induction motors than for synchronous machines because of the mutual linkages between stator and rotor end flux. The total end-connection ¹⁰ leakage reactance for stator and rotor,

$$X_e = \frac{2.0 f l_g m N^2 0.40 S_s P \sqrt{\tau}}{10^7 S_s p l_g}.$$

¹⁰ "Reactance in Synchronous Machines and Its Applications," by R. E. Doherty and O. E. Shirley, A.I.E.E. Trans., Vol. 37, part 2, 1918, p. 1224.

THE TOTAL LEAKAGE reactance of stator plus rotor in terms of the stator winding in ohms per phase,

$$X_i = X_{sd} + X_{sr} + X_e + X_b + X_c. \quad (207)$$

$$\text{The per cent reactance drop} = \frac{IX}{E} 100.$$

For a maximum output equal to 2.0 times rated output, the reactance drop must be less than 25 per cent. For squirrel-cage motors, the starting torque for rated voltage should generally not be less than 1.5 times full-load torque. To meet this requirement without an excessive slip at full-load, the reactance drop should not exceed 17 per cent.

The impedance at standstill,

$$Z = \sqrt{X_l^2 + (R_s + R_f)^2} \text{ ohms per phase}$$

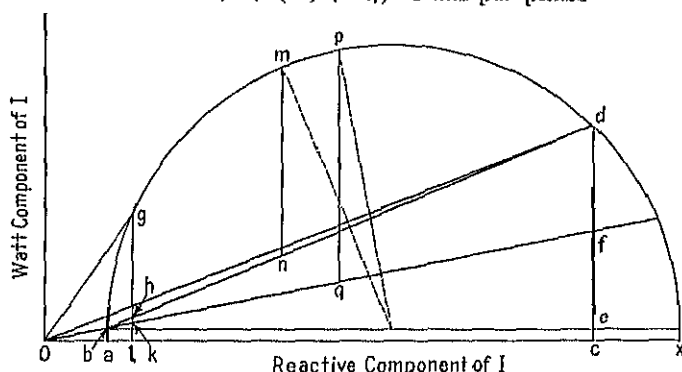


FIG. 198.—Circle diagram.

and the short-circuit current,

$$I_s = \frac{E}{Z} \text{ amperes per phase.}$$

The power factor at standstill,

$$\text{PF}_s = \frac{R_s + R_r}{Z}.$$

The operating characteristics are determined graphically by the circle-diagram, which is constructed as follows:¹¹ On the horizontal axis, Ox , Fig. 198, lay off Oa equal to the magnetizing current. From the point a lay off ab , the watt component of the no-load current, at

¹¹ "Methods of Testing Electrical Apparatus," *Electric Journal*, Vol. 24, Sept., 1927, p. 406.

right angles to the horizontal axis. Through the point *c* draw a horizontal line parallel to the *x*-axis; this is called the constant-loss line

Lay off, on the horizontal axis, *Oc* equal to the reactive component of the short-circuit current. From *c* lay off *cd*, the watt component of the short-circuit current, perpendicular to the *x*-axis. Through points *b* and *d* draw a semicircle with center on the constant-loss line

The vertical line *de* represents the total copper loss corresponding to the short-circuit current. The stator copper loss per phase for current equals $I_s^2 R_s$ and is represented by

$$ef = I_s^2 R_s / E.$$

The stator current corresponding to the rated horsepower, Fig. 198, equals $\text{hp } 746 / E \times 3$.

$$\text{The full-load current} = Og.$$

$$\text{The full-load efficiency} = \frac{gh}{gl}.$$

$$\text{The full-load power factor} = \frac{gl}{Og}.$$

$$\text{The slip at full-load} = \frac{hk}{gk}.$$

$$\text{The full-load speed} = n(1 - \text{slip}).$$

$$\text{The full-load torque} = \frac{\text{hp} \times 5250}{\text{full-load speed}} \text{ lb. at 1-ft. radius}$$

$$\text{The starting torque} = \frac{dfmE \times 5250}{746n} \text{ lb. at 1-ft. radius}$$

$$\text{The maximum horsepower output} = \frac{mnEm}{746}.$$

$$\text{The maximum torque} = \frac{pqEm \times 5250}{746n}.$$

To obtain accurate results at full-load and part loads, the circle diagram must be drawn to a large scale, which is often inconvenient. For this reason analytical methods¹² have been devised to calculate the operating characteristics.

¹² "Theoretical Elements of Electrical Engineering," by C. P. Steinmetz, McGraw-Hill Book Co., New York; General Electric Review, Vol. 22, April 1919, p. 230; Electric Journal, Vol. 24, Nov., 1927, pp. 569-573.

Rheostat Data.—Wound-rotor motors are started by inserting a resistance into the rotor circuit, which is generally star-connected and of such value to give full-load torque at starting. The voltage across the slip-rings at stand-still, with normal voltage applied to the stator, is calculated by formula 188 and is,

$$E_r = \frac{N_r f_{cr} f_w}{N_s f_w} k_2 E \text{ volts.}$$

At synchronous speed, the rate of change of the primary flux through the rotor coils is the same as that produced by the alternations of the primary flux at standstill. The counter e.m.f. at synchronous speed is therefore equal to E_r . The counter e.m.f. varies directly with the speed; for any load it is then equal to $E_r(1 - \text{slip})$. The motor output in watts is equal to the counter voltage, times the rotor current. Neglecting the phase displacement between rotor voltage and current, which is negligible for normal speeds, the rotor current per phase for 3-phase rotor windings,

$$I_r = \frac{\text{hp } 746 k_2}{E_r(1 - \text{slip}) 3} \text{ amperes.} \quad (208)$$

For a star-connected rotor winding, $k_2 = 1.73$; and for delta-connected rotor winding, $k_2 = 1.0$. This formula does not take into account all of the factors affecting the rotor current, but it is sufficiently accurate for design calculations.

The rheostat resistance per phase when star-connected for full-load starting torque,

$$R_{rh} = \frac{E_r(1 - \text{slip})}{I_r k_3} \text{ ohms.} \quad (209)$$

For star-connected rotor winding, $k_3 = 1.73$; and for delta-connected rotor winding, $k_3 = 3.0$.

Sample Design: Operating Characteristics.—The ratio of stator slot opening to air gap length

$$= \frac{0.321}{0.026} = 12.35.$$

From the curve in Fig. 53, $y = 3.58$ and the air gap coefficient for the stator slots,

$$k_s = \frac{t_{1s}}{w_{1s1} + (\delta y)} = \frac{0.64}{0.319 + (0.026 \times 3.58)} = 1.55.$$

The permeability in the air gap is given on page 289. The air gap ampere-turns per pole,

$$\begin{aligned} AT_g &= B_g \delta k_s \times 0.313 = 34,800 \times 0.026 \times 1.55 \times 0.313 \\ &= 439 \text{ ampere-turns.} \end{aligned}$$

The stator tooth width at a point $\frac{1}{3}$ tooth length from the minimum width,

$$\begin{aligned} w_{ts} &= \frac{\pi(D + \frac{2}{3}d_{ss})}{S_s} - w_{ss} = \frac{\pi(11.0 + \frac{2}{3} \times 1.31)}{54} - 0.321 \\ &= 0.370 \text{ in.} \end{aligned}$$

and the flux density,

$$\begin{aligned} B_{ts} &= \frac{\phi_t}{w_{ts}(l - n_a w_a) k_1 S_s} = \frac{6610 \times 10^3}{0.370(5.5 - 0)0.92 \times 54} \\ &= 65.5 \text{ kilo-lines per sq. in.} \end{aligned}$$

From the standard saturation curve for 1 per cent silicon steel, $at_{ts} = 4.4$ ampere-turns per in., and the ampere-turns per pole for the stator teeth,

$$AT_{ts} = 4.4 \times 1.31 = 6.0 \text{ ampere-turns.}$$

The rotor tooth width at a point $\frac{1}{3}$ tooth length from the minimum width,

$$\begin{aligned} w_{tr} &= \frac{\pi(D_r - 1\frac{1}{3}d_{sr})}{S_r} - w_{sr} = \frac{\pi(10.948 - 1\frac{1}{3} \times 0.43)}{65} - 0.205 \\ &= 0.297 \text{ in.} \end{aligned}$$

and

$$\begin{aligned} B_{tr} &= \frac{\phi_t}{w_{tr}(l - n_a w_a) k_1 S_r} = \frac{6610 \times 10^3}{0.297(5.5 - 0)0.92 \times 65} \\ &= 67.6 \text{ kilo-lines per sq. in.} \end{aligned}$$

$$AT_{tr} = 4.7 \times 0.43 = 2.0 \text{ ampere-turns.}$$

The length of the flux path in the stator yoke,

$$\begin{aligned} l_{ys} &= \frac{\pi(D + 2d_{ss} + \frac{1}{2}d_{ys})}{2p} = \frac{\pi(11.0 + 2 \times 1.31 + \frac{1}{2} \times 2.13)}{2 \times 6} \\ &= 3.84 \text{ in.} \end{aligned}$$

For the flux density in the stator yoke (see page 290), $at_{ys} = 4.3$ ampere-turns per in., and the ampere-turns per pole,

$$AT_{ys} = 4.3 \times 3.84 = 17.0.$$

the length of the max path in the rotor yoke,

$$l_{yr} = \frac{\pi(D_r - 2d_{sr} - \frac{1}{2}d_{yr})}{2p} = \frac{\pi(10.948 - 2 \times 0.43 - \frac{1}{2} \times 2.088)}{2 \times 6}$$

$$= 2.36 \text{ in.}$$

$$AT_{yr} = 4.5 \times 2.36 = 11.0 \text{ ampere-turns.}$$

The total ampere-turns per pole,

$$ATP = 439 + 6.0 + 2.0 + 17.0 + 11.0 = 475.$$

The magnetizing current per phase,

$$I_m = \frac{2.22 ATP \times p}{m_s N f_c f_w} = \frac{2.22 \times 475 \times 6}{3 \times 144 \times 0.956 \times 0.985}$$

$$= 15.5 \text{ amperes} = 40.3 \text{ per cent.}$$

The average width of a stator tooth

$$= \frac{\pi(D + d_{ss})}{S_s} - w_{ss} = \frac{\pi(11.0 + 1.31)}{54} - 0.321 = 0.395 \text{ in.}$$

and the weight of the iron in the teeth,

$$G_{ct} = 0.395 \times 5.5 \times 0.92 \times 54 \times 1.31 \times 0.278$$

$$= 39.3 \text{ lb.}$$

The loss per pound per cycle for the stator tooth density,

$$B_{ts} = 65.5 \text{ kilo-lines per sq. in.,}$$

is equal to 0.023 watts for 1 per cent silicon steel, 0.017 in. thick. The loss in the stator teeth due to the fundamental frequency flux,

$$W_{ct} = 0.023 \times 60 \times 39.3 = 54.2 \text{ watts.}$$

The weight of the iron in the stator yoke,

$$G_{cy} = \frac{\pi}{4} [D_0^2 - (D + 2d_{ss})^2] l_y \times 0.92 \times 0.278$$

$$= \frac{\pi}{4} [15.75^2 - (11.0 + 2 \times 1.31)^2] 5.5 \times 0.92 \times 0.278$$

$$= 69.0 \text{ lb.}$$

The loss per pound per cycle for the stator yoke density,

$$B_{ys} = 65 \text{ kilo-lines per sq. in.,}$$

mental frequency flux,

$$\begin{aligned}W_{cy} &= 0.0226 \times 60 \times 69.0 \\&= 93.6 \text{ watts.}\end{aligned}$$

The total core loss (see page 303).

$$W_c = (54.2 + 93.6)2.0 = 296 \text{ watts.}$$

The friction and windage losses are estimated at 2.5 per cent of the output in watts, 280 watts.

The length of the half mean-turn of a stator coil (see page 305),

$$\begin{aligned}L_s &= \frac{\pi(11.0 + 1.31)}{0.753 \times 6} 0.889 + 1.5 + 1.31 + 5.5 \\&= 15.91 \text{ in.}\end{aligned}$$

The resistance per phase of the stator winding at 75° C.,

$$R_s = \frac{L_s N r}{as \times 10^6} = \frac{15.91 \times 144 \times 0.826}{2 \times 0.00805 \times 10^6} = 0.1180 \text{ ohm.}$$

The loss in the stator winding due to the magnetizing current

$$= 15.5^2 \times 3 \times 0.118 = 85.0 \text{ watts.}$$

The watt component of the no-load current,

$$I_w = \frac{296 + 280 + 85.0}{3 \times 127} = 1.73 \text{ amperes.}$$

The no-load current,

$$\begin{aligned}I_0 &= \sqrt{I_m^2 + I_w^2} = \sqrt{15.5^2 + 1.73^2} \\&= 15.6 \text{ amperes.}\end{aligned}$$

The no-load power factor,

$$\text{PF}_0 = \frac{I_w}{I_0} = \frac{1.73}{15.6} = 11.1 \text{ per cent.}$$

The average reluctance is calculated as explained on page 307.
The following data are required:

$$\begin{aligned}
 f &= 60, \\
 l_g &= 5.5, & w_{ss} &= 0.321, & d_{1r} &= 0.35, & K_r &= 1, \\
 m &= 3, & P &= 0.889, & d_{2r} &= 0, & f_{cr} &= 1, \\
 N &= 144, & K_s &= 0.92, & d_{3r} &= 0.03, & f_{wr} &= 1, \\
 S_s &= 54, & f_c &= 0.985, & d_{4r} &= 0.04, & D &= 11.0, \\
 d_{1s} &= 1.065, & f_w &= 0.956, & w_{sr} &= 0.205, & p &= 6, \\
 d_{2s} &= 0.183, & S_r &= 65, & w_{sr1} &= 0.06, & \tau &= 5.75.
 \end{aligned}$$

The stator slot factor,

$$F_{ss} = K_s \left(\frac{d_{1s}}{3w_{ss}} + \frac{d_{2s}}{w_{ss}} \right) = 0.92 \left(\frac{1.065}{3 \times 0.321} + \frac{0.183}{0.321} \right) = 1.54.$$

The rotor slot factor,

$$\begin{aligned}
 F_{sr} &= \frac{f_c^2 f_w^2 S_s}{S_r} K_r \left(\frac{d_{1r}}{3w_{sr}} + \frac{d_{2r}}{w_{sr}} + \frac{2d_{3r}}{w_{sr} + w_{sr1}} + \frac{d_{4r}}{w_{sr1}} \right) \\
 &= \frac{0.985^2 \times 0.956^2 \times 54}{65} \cdot 1 \\
 &\quad \left(\frac{0.35}{3 \times 0.205} + \frac{0}{0.205} + \frac{2 \times 0.03}{0.205 + 0.06} + \frac{0.04}{0.06} \right) \\
 &= 1.07.
 \end{aligned}$$

The stator and rotor end-connection leakage factor,

$$F_e = \frac{0.40 S_s P \sqrt{\tau}}{p l_g} = \frac{0.40 \times 54 \times 0.889 \sqrt{5.75}}{6 \times 5.5} = 1.39.$$

The magnetizing current per phase due to the air gap ampere-turns,

$$\begin{aligned}
 I_{m0} &= \frac{2.22 \text{ AT}_g p}{m N f_c f_w} = \frac{2.22 \times 439 \times 6}{3 \times 144 \times 0.985 \times 0.956} \\
 &= 14.4 \text{ amperes.}
 \end{aligned}$$

The stator and rotor zigzag leakage reactance,

$$\begin{aligned}
 X_z &= \frac{l_g^2}{1.2 I_{m0}} \left[\left(\frac{p}{S_s} \right)^2 + \left(\frac{p}{S_r} \right)^2 \right] \\
 &= \frac{127}{1.2 \times 14.4} \left[\left(\frac{6}{54} \right)^2 + \left(\frac{6}{65} \right)^2 \right] = 0.154 \text{ ohm per phase.}
 \end{aligned}$$

stator winding,

$$\begin{aligned} X_l &= \frac{2.0 f l_g m N^2}{10^7 S_s} (F_{ss} + F_{sr} + F_e) + X_s \\ &= \frac{2.0 \times 60 \times 5.5 \times 3 \times 144^2}{10^7 \times 54} (1.54 + 1.07 + 1.39) + 0.154 \\ &= 0.458 \text{ ohm per phase} = 13.9 \text{ per cent.} \end{aligned}$$

The length of the bars in the squirrel-cage winding is 8.0 in. (see Fig. 199). The rotor resistance in terms of the stator winding at 75° C.,

$$\begin{aligned} R_r &= \frac{f_c^2 f_w^2 N^2 m r}{10^6} \left[\frac{l_b}{s_b N_b} + \frac{0.61 D_{er}}{p^2 s_{er}} \right] \\ &= \frac{0.985^2 \times 0.956^2 \times 144^2 \times 3 \times 0.826}{10^6} \\ &\quad \left[\frac{8.0}{0.070 \times 65} + \frac{0.64 \times 9.84}{6^2 \times 0.219} \right] \\ &= 0.117 \text{ ohm per phase.} \end{aligned}$$

The impedance of the motor at standstill,

$$\begin{aligned} Z &= \sqrt{X_l^2 + (R_s + R_r)^2} = \sqrt{0.458^2 + (0.118 + 0.117)^2} \\ &= 0.514 \text{ ohm per phase.} \end{aligned}$$

The short-circuit current per phase,

$$I_s = \frac{E}{Z} = \frac{127}{0.514} = 247 \text{ amperes.}$$

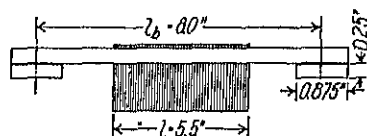


Fig. 199.

The power factor at standstill,

$$\text{PF}_s = \frac{R_s + R_r}{Z} = \frac{0.235}{0.514} = 45.7 \text{ per cent.}$$

The circle diagram for the 15-hp sample motor design is shown in Fig. 200 and is constructed as explained on page 309. The operating characteristics are:

Full-load current,

$$I = Oq = 38.3 \text{ amperes.}$$

Full-load power-factor,

$$\text{PF} = \frac{gl}{Oq} = \frac{33.0}{38.3} = 86.2 \text{ per cent.}$$

Full-load efficiency,

$$\text{eff.} = \frac{gh}{gl} = \frac{29.4}{33.0} = 89.0 \text{ per cent.}$$

Slip at full-load

$$= \frac{hk}{gk} = \frac{1.00}{30.3} = 3.3 \text{ per cent.}$$

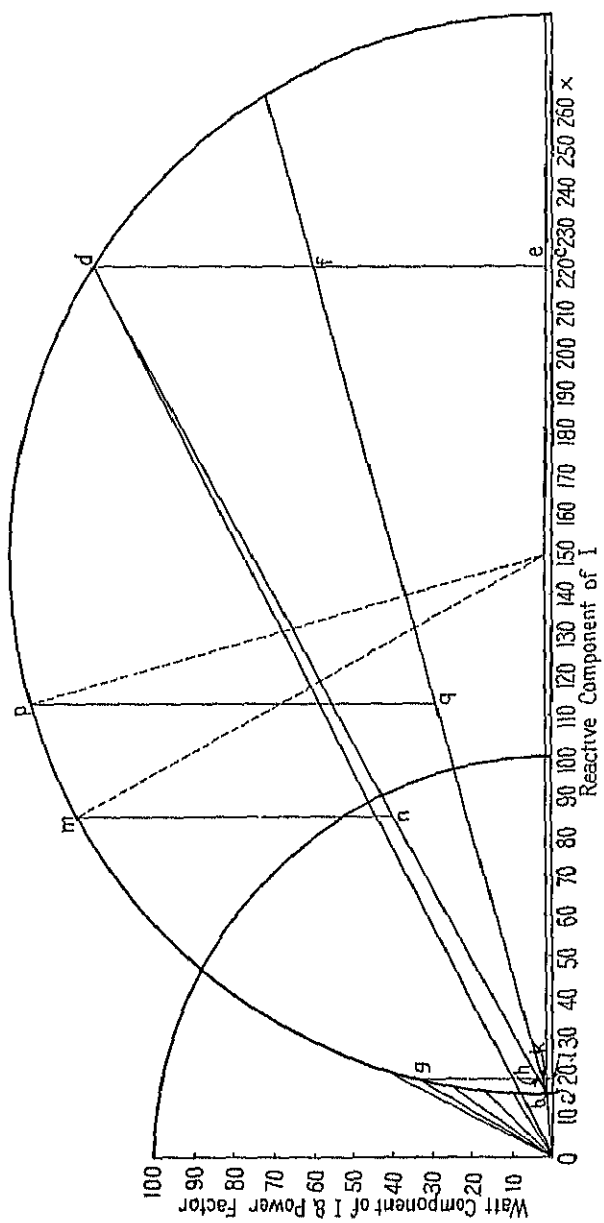


FIG. 200.—Circle diagram for 15 h.p., 1200 r.p.m., squirrel-cage motor.

Full-load torque

$$\begin{aligned}
 &= 1200(1.00 - 0.033) \\
 &= 1161 \text{ r.p.m.} \\
 &= \frac{\text{hp} \times 5250}{n} = \frac{15 \times 5250}{1161} \\
 &= 67.9 \text{ lb. at 1-ft. radius.}
 \end{aligned}$$

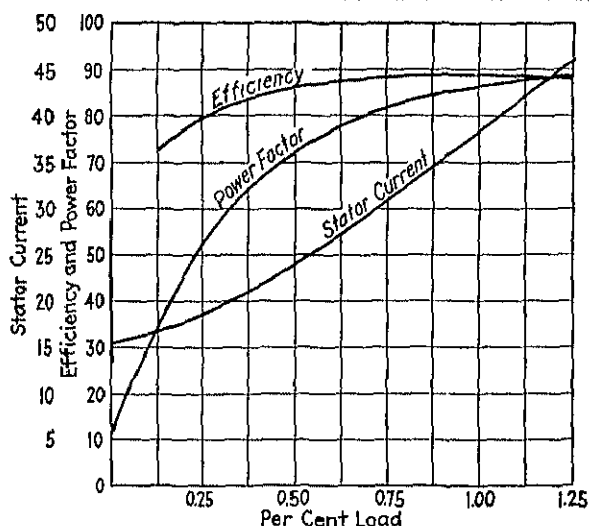


FIG. 201.—Performance curves for 15 h.p., 1200 r.p.m., three-phase, squirrel-cage motor.

Starting torque for normal voltage = $\frac{df mE \times 5250}{746n}$

$$\begin{aligned}
 &= \frac{55.3 \times 3 \times 127 \times 5250}{746 \times 1200} \\
 &= 123.6 \text{ lb. at 1-ft. radius} \\
 &= 182 \text{ per cent of full-load torque.}
 \end{aligned}$$

Maximum torque

$$\begin{aligned}
 &= \frac{pq mE \times 5250}{746n} \\
 &= \frac{101.7 \times 3 \times 127 \times 5250}{746 \times 1200} \\
 &= 227.0 \text{ lb. at 1-ft. radius} \\
 &= 334 \text{ per cent of full-load torque.}
 \end{aligned}$$

The maximum horsepower output = $\frac{mn Em}{746} = \frac{79.6 \times 127 \times 3}{746}$

$$= 40.6 \text{ hp.}$$

The performance curves for this motor are shown in Fig. 201.

INDUCTION MOTOR DESIGN SHEET

Hp. 15 S. R.p m, 1200 Cycles, 60 Poles, 6 Phases, 3 Volts, 220 Amps Line, 38.3
 Amperes per Phase, 38.3 Volts per Phase, 127 Apparent Efficiency, 67.6

STATOR

Sheet steel	0.017—1% Si
Outside diameter	15.75
Gap diameter	11.00
Total length	5.5
Ducts, number and size	None
Gross iron length	5.5
Effective length	5.06
Slots:	
Number, 3 X 3 X 6	54
Depth	1.31
Width	0.321
Opening	0.321
Minimum tooth width	0.310
Conductors:	
Per slot	10
Size	D.C.C. 0.080 X 0.201
Area	0.00803
Total section	6.96
In series per phase	144
Ampere per square inch	239.0
Conductors arranged in slot	1 X 16
Insulation allowance:	
Depth	0.35
Width	0.12
Circuits per phase	2
Connections	Star
Coil throw	Slots 1 and 9
Per cent pitch	88.0
Length half mean-turn	15.91
Resistance per phase, 75° C.	0.118
Copper weight	35.0

ROTOR

Sheet steel	0.017—1% Si
Gap diameter	10.948
Inside diameter	8.0
Total length	5.5
Ducts, number and size	None
Effective length	5.00
Slots:	
Number	65
Depth	0.43
Width	0.205
Opening	0.06
Minimum tooth width	0.282
Total flux, 6610 kilo-lines	ϕ_m , 0.085
Flux per pole	701 kilo-lines

CONDUCTORS.

Per slot	Squirrel-cage
Size, bare	0.20 X 0.35
Material	Copper
Section total	4.65
In series per phase	
Insulation allowance:	
Depth	
Width	
Circuits per phase	
Connections	
Coil throw	
Per cent pitch	
End ring:	
Section	0.25 X 0.875 = 0.210
Material	Copper
Length half mean-turn	
Resistance per phase, 75° C.	0.117
Conductor weight	17.35
Length of bar	8.0

STATOR AND ROTOR

Total resistance per phase	0.235—7.08%
Total reactance per phase	0.458—13.94%
Total impedance per phase	0.514—15.55%
Short-circuit power factor	45.7%
Short-circuit current	247
Friction and windage loss	280
No-load stator I^2R	85
Magnetizing current	15.5—40.3%
Watt component of I_0	1.73
No-load current	15.6—40.6%
No-load power factor	11.1%
Full-load current	38.3
Full-load slip	3.30%
Full-load speed	1161
Full-load torque	67.9
Starting torque	123.6
Maximum torque	227.0
Maximum output	40.6

	$\frac{1}{2}$	$\frac{1}{4}$	$\frac{1}{8}$	$\frac{1}{16}$
Efficiency			89.0	
Power factor			80.2	

	Section	Density	Length	Ampere Turns	Weight	Core Loss
Stator teeth	101.0	65.5	1.31	6.0	39.3	54.2
Stator yoke	10.78	65.0	3.84	17	69.0	93.0
Rotor teeth	97.00	67.6	0.43	2		147.8
Rotor yoke	10.60	66.4	2.36	11		X 2.0
Air gap	190.00	34.8	1.55 X 0.026	430		295.6
Total ampere-turns per pole				475		

Rheostat Data

Open-circuit volts across rings	
Ampere per phase	
Starting resistance per phase	
$\frac{hp \times 10^3}{n} = 12.5$	

$\frac{D^2 L n}{hp} = 5.32 \times 10^4$
Pole pitch = 5.75
Total length = 0.957
Pole pitch

Designed by J. H. Kuhlmann

Date: July 10, 1928.

CHAPTER XX

SAMPLE DESIGN OF WOUND-ROTOR INDUCTION MOTOR

Design of Wound-Round Motor.—The complete calculations for a heavy duty 400-hp, 2000-volt, 3-phase, 60-cycle, 14-pole, wound-rotor induction motor will be given. The full-load efficiency and power factor should not be less than 92.0 per cent and 84 per cent respectively, and the maximum torque should not be less than 250 per cent of full-load torque. The temperature rise of no part of the motor should exceed 40° C. for continuous full-load operation.

STATOR

The synchronous speed,

$$n = \frac{f \times 2 \times 60}{p} = \frac{60 \times 2 \times 60}{14} = 514 \text{ r.p.m.}$$

$$\frac{\text{hp}}{n} \times 10^3 = \frac{400}{514} \times 10^3 = 777.0.$$

From the curve in Fig. 182, the output constant, $C = 2.7 \times 10^4$. This must be increased 20 per cent for this motor (see page 280). Therefore,

$$C = 2.7 \times 10^4 \times 1.20 = 3.24 \times 10^4.$$

For the ratio, $l/\tau = 1.0$,

$$D = \sqrt[3]{\frac{C \text{ hp} \times p}{n\pi l/\tau}} = \sqrt[3]{\frac{3.24 \times 10^4 \times 400 \times 14}{514 \times \pi \times 1.0}}$$

$$= 48.2 \text{ in.}$$

$$l = \frac{C \text{ hp}}{D^2 n} = \frac{3.24 \times 10^4 \times 400}{48.2^2 \times 514}$$

$$= 10.9 \text{ in.}$$

The diameter and length for several values of l/τ are given in the following table:

TABLE XXVII

l/τ	D	l	τ
1.50	42.1	14.2	9.45
1.25	41.8	12.6	10.05
1.00	48.2	10.9	10.80
0.90	50.0	10.1	11.20

The following dimensions are selected:

$$D = 45.125 \text{ in.}, \quad l = 12.5 \text{ in.}, \quad \tau = 10.12 \text{ in.}, \quad l/\tau = 1.235.$$

To ventilate the stator core properly, four ventilating ducts will be required (see page 267). The length of the air gap section,

$$l_g = l - n_{gwa} = 12.5 - 4 \times 0.25 = 11.5 \text{ in.}$$

For an air gap density equal to 32,000 lines per sq. in. the total flux,

$$\begin{aligned} \phi_t &= \pi D l_g B_g = \pi \times 45.125 \times 11.50 \times 32,000 \\ &= 52,100 \text{ kilo-lines.} \end{aligned}$$

If a star-connected stator winding is used, the phase voltage,

$$E = \frac{2000}{1.73} = 1157 \text{ volts.}$$

For a chord factor, $f_c = 1.0$ the conductors in series per phase,

$$\begin{aligned} N &= \frac{E \times 60 \times 10^8}{n \phi_t C_w f_c} = \frac{1157 \times 60 \times 10^8}{514 \times 52,100 \times 10^3 \times 0.677 \times 1.00} \\ &= 383. \end{aligned}$$

With 6 slots per pole per phase, the total number of stator slots,

$$S_s = 6 \times 3 \times 14 = 252$$

and the minimum tooth pitch,

$$l_{1s} = \frac{\pi \times 45.125}{252} = 0.563 \text{ in.}$$

The total number of conductors = $2 \times 3 \times 383 = 2300$ for a 2-circuit winding. It will be desirable to use a 2-circuit winding to avoid a large

with one circuit. The conductors per slot,

$$= \frac{2300}{252} = 9.1.$$

The stator winding will then have 10 conductors per slot, 5 turns coil, and two parallel circuits per phase, with a coil throw slot 17 or 88.9 per cent of pitch. The chord factor,

$$f_c = \sin(P \times 90) = \sin(0.889 \times 90) = 0.985.$$

The conductors in series per phase,

$$N = \frac{10 \times 252}{2 \times 3} = 420$$

and the total flux,

$$\phi_t = \frac{E \times 60 \times 10^8}{nNC_v f_c} = \frac{1157 \times 60 \times 10^8}{514 \times 420 \times 0.677 \times 0.985} = 48,100 \text{ kilo-lines.}$$

The flux density in the air gap,

$$B_g = \frac{\phi_t}{\pi D_l g} = \frac{48,100 \times 10^3}{\pi \times 45.125 \times 11.5} = 29.5 \text{ kilo-lines per sq. in.}$$

From the table on page 280 the efficiency and power factor at full load are estimated at 92 per cent and 84 per cent respectively. The full-load stator current per phase,

$$I = \frac{\text{hp } 746}{E_m \times \text{eff.} \times \text{PF}} = \frac{400 \times 746}{1157 \times 3 \times 0.92 \times 0.84} = 111.0 \text{ amperes.}$$

A current density of 2500 amperes per sq. in. is assumed. The stator conductor section,

$$s_s = \frac{I}{aA_s} = \frac{111}{2 \times 2500} = 0.0222 \text{ sq. in.}$$

The conductor selected from the copper table has the following dimensions: 0.102×0.204 in. bare; 0.118×0.218 in. insulated; 0.020

202. With the type of wedge used, the allowance for insulation, clearance, and wedge given on page 286 must be increased to 0.50 in. The slot dimensions are:

$$\text{Width} \quad 0.218 + 0.16 = 0.378; 0.375 \text{ is used.}$$

$$\text{Depth } 0.118 \times 10 + 0.50 = 1.68; 1.70 \text{ is used.}$$

The current density for the conductor selected for the stator winding,

$$A_s = \frac{111.0}{2 \times 0.0203} = 2740 \text{ amperes per sq. in.}$$

The minimum stator tooth pitch has been given and the minimum tooth width,

$$w_{ts1} = t_{1s} - w_{ss} = 0.188 \text{ in.}$$

The maximum flux density in the stator teeth,

$$\begin{aligned} B_{ts1} &= \frac{\phi_t}{w_{ts1}(l - n_a w_a) 0.92 S_s} \\ &= \frac{48,100 \times 10^3}{0.188(12.5 - 4 \times 0.25) 0.92 \times 252} \\ &= 96 \text{ kilo-lines per sq. in.} \end{aligned}$$

The flux per pole,

$$\begin{aligned} \phi &= \frac{\phi_t l_a}{p} = \frac{48,100 \times 10^3 \times 0.637}{14} \\ &= 2190 \text{ kilo-lines.} \end{aligned}$$

If a flux density of 80,000 lines per sq. in. is assumed for the stator yoke, then

$$\begin{aligned} d_{ys} &= \frac{\phi}{B_{ys}(l - n_a w_a) 0.92} = \frac{2190 \times 10^3}{80,000(12.5 - 4 \times 0.25) 0.92} \\ &= 2.59 \text{ in.} \end{aligned}$$

The outside diameter of the stator,

$$\begin{aligned} D_o &= D + 2d_{ys} + d_{ys} = 45.125 + 2 \times 1.70 + 2.59 \\ &= 51.115 \text{ in.; use } 51.0 \text{ in.} \end{aligned}$$

and

$$d_{ys} = 2.475 \text{ in.}$$

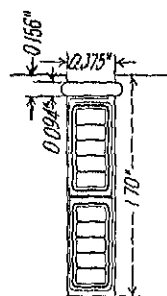


FIG. 202.

$$B_{vs} = \frac{2190 \times 10^3}{2.475(12.5 - 4 \times 0.25)0.92} = 83.6 \text{ kilo-lines per sq. in.}$$

ROTOR

The length of the air gap,

$$\delta = 0.125 - \frac{10.17}{.15 \ 125 + 92} = 0.051 \text{ in.}$$

Since this motor is intended for heavy duty, it must be of rugged construction to withstand the shocks of heavy service. A large air gap length is therefore desirable. The flux density in the air gap as calculated is rather low. A large air gap length can be used without an excessive magnetizing current. The length of the air gap is therefore made

$$= 0.0625 \text{ in.}$$

The rotor diameter,

$$\begin{aligned} D_r &= 45.125 - 2 \times 0.0625 \\ &= 45.00 \text{ in.} \end{aligned}$$

The number of rotor slots should be approximately 20 per cent more than the number of stator slots and must permit a balanced 3-phase winding (see page 294). For this design, 4.5 slots per pole per phase will be used or 189 slots, with a coil throw, slot 1 and 14—96.2 per cent of pitch. The chord factor, $f_c = \sin(0.962 \times 90) = 0.998$. In this winding, the coils per phase are in alternate groups of 4 and 5 each.

If 600 volts is assumed for the voltage between slip rings when the rotor is stationary with normal voltage applied to the stator winding, then the rotor conductors in series per phase for a star-connected winding,

$$\begin{aligned} N_r &= \frac{E_r N f_c f_w}{E k_2 f_{cr} f_{wr}} = \frac{600 \times 420 \times 0.985 \times 0.956}{1157 \times 1.73 \times 0.998 \times 0.956} \\ &= 124. \end{aligned}$$

With 1 circuit per phase, the total number of rotor conductors

$$= 1 \times 3 \times 124 = 372.$$

per slot. The rotor voltage,

$$E_r = \frac{126 \times 0.998 \times 0.956}{420 \times 0.985 \times 0.956} 1157 \times 1.73 = 608 \text{ volts.}$$

The current density for the stator winding is rather high. To avoid high copper losses and consequent low efficiency the total rotor copper section will be taken equal to the total stator copper section.

$$S_{cs} = S_{cr} = 420 \times 3 \times 2 \times 0.0203 = 51.1 \text{ sq. in.}$$

The section area of each rotor conductor,

$$s_r = \frac{51.1}{2 \times 189} = 0.136 \text{ sq. in.}$$

Two bare strap copper conductors in parallel are used for the rotor winding, each having the following dimensions: 0.141×0.50 in. — 0.0686 sq. in. area. The type of rotor slot used and the arrangement of the conductors in the slot is shown in Fig. 203. The bare coils are insulated with cotton tape and insulating varnish. The insulation between core and coils, 0.015 in. single thickness, is placed into the slots. The width of the slot = $2 \times (0.141 + 0.015) + (0.015 \times 2) + 0.02 = 0.422$ in.; use 0.425 in. A clearance of 0.020 in. is allowed for staggering of the laminations. In the depth of the slot, a separator, 0.020 in., is placed between the coil sides in top and bottom of the slot. The allowance for the wedge = 0.194 in. (see Fig. 203). The depth of the slot = $2(0.50 + 0.015) + 0.020 + 0.015 + 0.020 + 0.194 = 1.309$ in.; use 1.31 in.

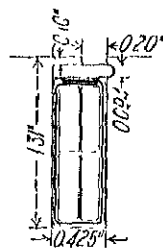


FIG. 203.

The minimum rotor tooth width,

$$w_{tr2} = \frac{\pi(D_1 - 2d_{ar})}{S_r} - w_{ar} = \frac{\pi(15.0 - 2 \times 1.31)}{189} - 0.425 = 0.281 \text{ in.}$$

The maximum rotor tooth density,

$$\begin{aligned} B_{tr2} &= \frac{\phi_t}{w_{tr2}(l - n_{at}w_a)0.92S_r} \\ &= \frac{48,100 \times 10^3}{0.281(12.5 - 4 \times 0.25) \times 0.92 \times 189} \\ &= 85.6 \text{ kilo-lines per sq. in.} \end{aligned}$$

yoke, then

$$d_{yr} = \frac{\phi}{B_{yr}(l - n_d w_d) 0.92} = \frac{2190 \times 10^3}{70,000(12.5 - 4 \times 0.25) 0.92} = 2.96 \text{ in.}$$

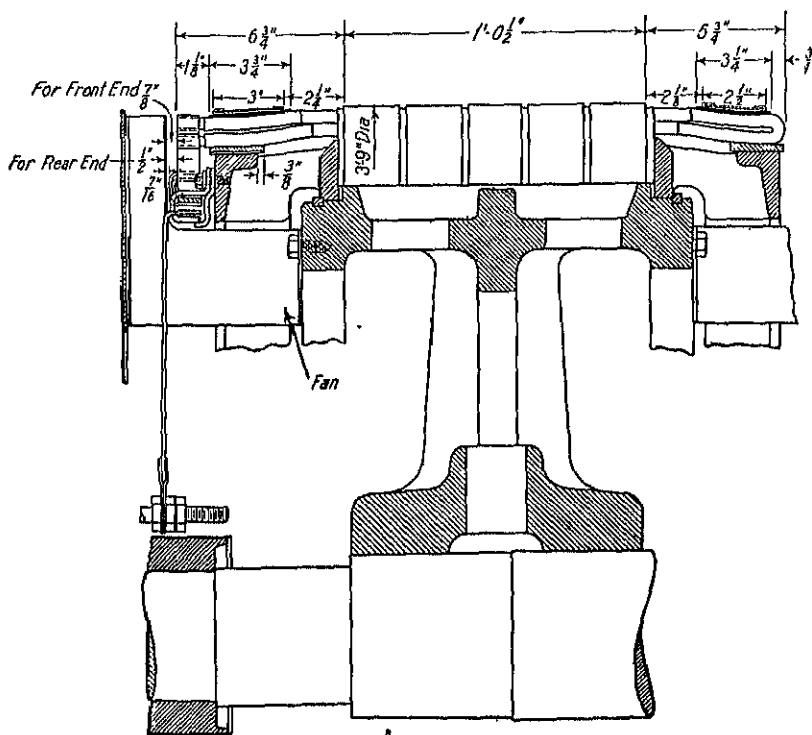


FIG. 204.

The inside diameter of the rotor,

$$D_i = D_r - 2d_{sr} - d_{yr} = 45.0 - 2.62 - 2.96 = 39.42 \text{ in., use } 39.25 \text{ in.}$$

and

$$B_{yr} = \frac{2190 \times 10^3}{3.13(12.5 - 4 \times 0.25) 0.92} = 66.1 \text{ kilo-lines per sq. in.}$$

A sectional drawing of the assembled rotor is shown in Fig. 204.

The ratio of stator slot opening to air gap length

$$= \frac{0.375}{0.0625} = 6.0.$$

From the curve, Fig. 53, $y = 2.60$. The air gap coefficient for the stator slots,

$$k_s = \frac{l_{1s}}{w_{1s1} + (y\delta)} = \frac{0.563}{0.188 + (2.6 \times 0.0625)} = 1.61.$$

The rotor slot opening = 0.20 in. The air gap coefficient for the rotor slots,

$$k_r = \frac{l_{1r}}{w_{1r1} + (y\delta)} = \frac{0.749}{0.549 + (1.90 \times 0.0625)} = 1.12.$$

The flux density in the air gap is given on page 322. The ampere-turns per pole for the air gap,

$$\begin{aligned} AT_g &= B_g \delta k_s k_r \times 0.313 = 29,500 \times 0.0625 \times 1.61 \times 1.12 \times 0.313 \\ &= 1040 \text{ ampere-turns.} \end{aligned}$$

The stator tooth width at a section $\frac{2}{3}$ tooth length from the minimum section,

$$\begin{aligned} w_{1s2} &= \frac{\pi(D + \frac{2}{3}d_{s2})}{S_s} - w_{ss} = \frac{\pi(45.125 + \frac{2}{3} \times 1.70)}{252} - 0.375 \\ &= 0.201 \text{ in.} \end{aligned}$$

The tooth density,

$$B_{1s2} = \frac{48,100 \times 10^3}{0.201(12.5 - 4 \times 0.25)0.92 \times 252} = 89.8 \text{ kilo-lines per sq. in.}$$

From the standard saturation curve for 1 per cent silicon steel,

$$at_{1s} = 15.4 \text{ ampere-turns per inch.}$$

The ampere-turns per pole for the stator teeth,

$$AT_{1s} = 15.4 \times 1.70 = 26.$$

The rotor tooth width at a section $\frac{1}{3}$ tooth length from the minimum section,

$$\begin{aligned} w_{1r2} &= \frac{\pi(D_r - \frac{1}{3}d_{r2})}{S_r} - w_{sr} = \frac{\pi(45.0 - \frac{1}{3} \times 1.31)}{189} - 0.425 \\ &= 0.295 \text{ in.} \end{aligned}$$

$$B_{r_2} = \frac{48,100 \times 10^3}{0.295(12.5 - 4 \times 0.25)0.92 \times 189} = 81.5 \text{ kilo-lines per sq}$$

The ampere-turns per inch for this density, $at_r = 9.10$ for 1 per cent silicon steel. The ampere-turns per pole for the rotor teeth,

$$AT_{tr} = 9.10 \times 1.31 = 12.0.$$

The length of the flux path in the stator yoke,

$$l_{vs} = \frac{\pi(D + 2d_s + \frac{1}{2}d_{ys})}{2p} = \frac{\pi(45.125 + 2 \times 1.70 + \frac{1}{2} \times 2)}{2 \times 14} \\ = 5.58 \text{ in.}$$

For the rotor yoke,

$$l_{vr} = \frac{\pi(D_r - 2d_{sr} - \frac{1}{2}d_{yr})}{2p} = \frac{\pi(45.0 - 2 \times 1.31 - \frac{1}{2} \times 3.18)}{2 \times 14} \\ = 4.58 \text{ in.}$$

The flux density in the stator yoke is given on page 324, and

$$at_{vs} = 10.2 \text{ ampere-turns per inch.}$$

Then,

$$AT_{vs} = 10.2 \times 5.58 = 57 \text{ ampere-turns.}$$

For the flux density in the rotor yoke (see page 326),

$$at_{vr} = 4.5 \text{ ampere-turns per inch, and}$$

$$AT_{vr} = 4.5 \times 4.58 = 21.0 \text{ ampere-turns.}$$

The total ampere-turns per pole,

$$ATP = 1040 + 26 + 12 + 57 + 21 = 1156.$$

The magnetizing current per phase,

$$I_m = \frac{2.22 \times ATP \times p}{m_s N f_c f_w} = \frac{2.22 \times 1156 \times 14}{3 \times 420 \times 0.985 \times 0.956} \\ = 30.3 \text{ amperes} = 27.3 \text{ per cent.}$$

The average width of a stator tooth,

$$= \frac{\pi(D + d_{ss})}{S_s} - w_{ss} = \frac{\pi(45.125 + 1.70)}{252} - 0.375 = 0.21 \text{ in.}$$

$$G_{st} = 0.21 \times 11.5 \times 0.92 \times 252 \times 1.70 \times 0.278 \\ = 264 \text{ lb.}$$

The loss per pound per cycle for the stator tooth density, $B_{ts} = 89.8$ kilo-lines per sq. in., is equal to 0.0483 watt for 1 per cent silicon steel, 0.017 in. thick. The loss in the stator teeth due to the fundamental frequency flux,

$$W_{st} = 0.0483 \times 60 \times 264 = 765 \text{ watts.}$$

The weight of the iron in the stator yoke,

$$G_{sy} = \frac{\pi}{4} [D_0^2 - (D + 2d_{ss})^2] l_y \times 0.92 \times 0.278 \\ = \frac{\pi}{4} [51.0^2 - \{45.125 + (2 \times 1.7)\}^2] 11.5 \times 0.92 \times 0.278 \\ = 576 \text{ lb.}$$

The loss per pound per cycle for the stator yoke density, $B_{ys} = 83.6$ kilo-lines per sq. in., is equal to 0.0393 watt for 1 per cent silicon steel, 0.017 in. thick. The loss in the stator yoke, due to the fundamental frequency flux,

$$W_{sy} = 0.0393 \times 60 \times 576 = 1360 \text{ watts.}$$

The total core loss (see page 303),

$$W_c = (765 + 1360) 2.0 = 4250 \text{ watts.}$$

The friction and windage losses are estimated at 0.85 per cent of the output in watts, 2540 watts.

The clearance between the stator coils at the end-connections is taken equal to 0.12 in. instead of 0.18 in., as given in the table, page 305. The length of the half-mean-turn of a stator coil (see page 305),

$$L_s = \frac{\pi(45.125 + 1.70)}{0.478 \times 14} 0.889 + 2.0 + 1.70 + 12.5 \\ = 35.7 \text{ in.}$$

The resistance per phase of the stator winding at 75° C.,

$$R_s = \frac{L_s N r}{as_s 10^9} = \frac{35.7 \times 420 \times 0.826}{2 \times 0.0203 \times 10^9} = 0.305 \text{ ohm.}^1$$

$$= 30.3^2 \times 0.305 \times 3 = 840 \text{ watts}$$

and the watt component of the no-load current,

$$I_w = \frac{4250 + 2540 + 840}{3 \times 1157} = 2.20 \text{ amperes.}$$

The no-load current,

$$I_0 = \sqrt{I_m^2 + I_w^2} = \sqrt{30.3^2 + 2.20^2} \\ = 30.4 \text{ amperes.}$$

The no-load power factor,

$$\text{PF}_0 = \frac{I_w}{I_0} = \frac{2.20}{30.4} = 7.24 \text{ per cent.}$$

The reactance is calculated by the formulas given on page 10. The following data are required:

$$\begin{array}{llll} f = 60, & w_{ss} = 0.375, & d_{2r} = 0.114, & f_{wr} = 0.95 \\ l_g = 11.5, & P = 0.889, & d_{3r} = 0, & D = 45.1 \\ m_s = 3, & K_s = 0.92, & d_{4r} = 0.10, & p = 14, \\ N = 420, & f_c = 0.985, & w_{sr} = 0.425, & \tau = 10.1 \\ S_s = 252, & f_w = 0.956, & w_{sr1} = 0.20, & K_{b1} = 0.00 \\ d_{1s} = 1.34, & S_r = 189, & K_r = 0.96, & K_{br} = 0.00 \\ d_{2s} = 0.255, & d_{1r} = 1.05, & f_{er} = 0.998, & \end{array}$$

The stator slot factor,

$$\Gamma_{ss} = K_s \left(\frac{d_{1s}}{w_{ss} \times 3} + \frac{d_{2s}}{w_{ss}} \right) = 0.92 \left(\frac{1.34}{3 \times 0.375} + \frac{0.255}{0.375} \right) = 1.72.$$

The rotor slot factor,

$$\Gamma_{sr} = \frac{f_c^2 f_w^2 S_s}{f_{er}^2 f_{wr}^2 S_r} K_r \left(\frac{d_{1r}}{3w_{sr}} + \frac{d_{2r}}{w_{sr}} + \frac{d_{4r}}{w_{sr1}} \right) \\ = \frac{0.985^2 \times 0.956^2 \times 252}{0.998^2 \times 0.956^2 \times 189} 0.96 \\ \left(\frac{1.05}{3 \times 0.425} + \frac{0.114}{0.425} + \frac{0.10}{0.20} \right) = 1.97.$$

The end-connection leakage factor,

$$F_e = \frac{0.40 S_s P \sqrt{\tau}}{p l_g} = \frac{0.40 \times 252 \times 0.889 \sqrt{10.12}}{14 \times 11.5} = 1.77.$$

$$I_{m0} = \frac{2.22 \times 1040 \times 14}{3 \times 420 \times 0.985 \times 0.956} = 27.2 \text{ amperes.}$$

The stator and rotor zigzag leakage reactance,

$$\begin{aligned} X_z &= \frac{E}{1.2 I_{m0}} \left[\left(\frac{p}{S_s} \right)^2 + \left(\frac{p}{S_r} \right)^2 \right] \\ &= \frac{1157}{1.2 \times 27.2} \left[\left(\frac{14}{252} \right)^2 + \left(\frac{14}{189} \right)^2 \right] = 0.304 \text{ ohm.} \end{aligned}$$

The stator and rotor belt leakage reactance,

$$X_b = \frac{E}{I_{m0}} (K_{bs} + K_{br}) = \frac{1157}{27.2} (0.0009 + 0.00185) = 0.117 \text{ ohm.}$$

$$\begin{aligned} X_l &= \frac{2.0 f l_r m_s N^2}{10^7 S_s} (F_{ss} + F_{sr} + F_e) + X_z + X_b \\ &= \frac{2.0 \times 60 \times 11.5 \times 3 \times 420^2}{10^7 \times 252} (1.72 + 1.97 + 1.77) \\ &\quad + 0.304 + 0.117 \\ &= 2.0 \text{ ohms per phase} = 19.2 \text{ per cent.} \end{aligned}$$

The length of the half mean-turn of a rotor coil (see page 305),

$$\begin{aligned} L_r &= \frac{\pi(15.0 - 1.31)}{0.711 \times 14} 0.963 + 2.0 + 1.31 + 12.5 \\ &= 29.11 \text{ in.} \end{aligned}$$

For the equivalent rotor resistance per phase (see page 305),

$$\begin{aligned} R_r &= \frac{f_w^2 f_c^2}{f_{wr}^2 f_{cr}^2} \times \frac{L_r}{L_s} \times \frac{S_{cs}}{S_{cr}} R_s \\ &= \frac{0.956^2 \times 0.985^2}{0.956^2 \times 0.998^2} \times \frac{29.11}{35.7} \times \frac{51.1}{51.6} 0.305 = 0.24 \text{ ohm.} \end{aligned}$$

The impedance at standstill, with no external resistance in the rotor circuit,

$$\begin{aligned} Z &= \sqrt{X_l^2 + (R_s + R_r)^2} = \sqrt{2.0^2 + (0.305 + 0.24)^2} \\ &= 2.07 \text{ ohms per phase.} \end{aligned}$$

The stator current per phase at standstill, with normal voltage applied to stator and short-circuited rotor,

$$I_s = \frac{1157}{2.07} = 558 \text{ amperes.}$$

$$\text{PF}_s = \frac{R_s + R_r}{Z} = \frac{0.545}{2.07} = 26.4 \text{ per cent.}$$

The circle diagram is shown in Fig. 205. The operating characteristics are:

$$\text{Full-load current, } I = Og = 105.5 \text{ amperes.}$$

$$\text{Full-load power factor, PF} = \frac{gl}{Og} = \frac{93.0}{105.5} = 88.0 \text{ per cent.}$$

$$\text{Full-load efficiency, eff.} = \frac{gh}{gl} = \frac{86.0}{93.0} = 92.5 \text{ per cent.}$$

$$\text{Slip at full-load} = \frac{hk}{gk} = \frac{2.0}{88.0} = 2.28 \text{ per cent.}$$

$$\begin{aligned} \text{Full-load speed} &= n(1.0 - \text{slip}) = 514(1.0 - 0.0228) \\ &= 502 \text{ r.p.m.} \end{aligned}$$

$$\begin{aligned} \text{Full-load torque} &= \frac{\text{hp} \times 5250}{\text{Full-load speed}} = \frac{400 \times 5250}{502} = 417 \\ &\text{at 1-ft. radius.} \end{aligned}$$

$$\begin{aligned} \text{Maximum torque} &= \frac{pq \text{ mE} \times 5250}{746n} = \frac{232 \times 3 \times 1157}{746 \times 514} \\ &= 11,000 \text{ lb. at 1-ft. radius.} \end{aligned}$$

$$\text{Maximum hp} = \frac{mn \text{ mE}}{746} = \frac{206 \times 3 \times 1157}{746} = 958.$$

RHEOSTAT DATA

The rotor voltage at standstill has been calculated on page 100.
The rotor current per phase for full-load,

$$I_r = \frac{\text{hp } 746k_2}{E_r(1 - \text{slip})3} = \frac{400 \times 746 \times 1.73}{608(1 - 0.0228)3} = 290 \text{ amperes}$$

The rheostat resistance for full-load starting torque,

$$R_{rh} = \frac{E_r(1 - \text{slip})}{I_r k_3} = \frac{608(1 - 0.0228)}{290 \times 1.73} = 1.19 \text{ ohms.}$$

STATOR	
Sheet steel	0 017—1% Si
Outside diameter	51 0
Gap diameter	45 125
Total length	12 50
Ducts, number and size	1—4
Gross iron length	11 50
Effective length	10 60
Slots:	
Number, 3×6×14	252
Depth	1 70
Width	0 375
Opening	0 375
Minimum tooth width	0 188
Conductors:	
Per slot	10
Size	D C C 0 118×0 218
Area	0 0203
Total section	51 1
In series per phase	420
Ampere per square inch	27 10
Conductors arranged in slot	1×10
Insulation allowance:	
Depth	0 50
Width	0 10
Circuits per phase	2
Connections	Star
Coil throw	Slots 1 and 17
Per cent pitch	88 3
Length half mean-turn	35 7
Resistance per phase, 75° C.	0 305
Copper weight	585 0

ROTOR	
Sheet steel	0 017—1% Si
Gap diameter	45 0
Inside diameter	30 25
Total length	12 50
Ducts, number and size	4—4
Effective length	10 60
Slots:	
Number	180
Depth	1 31
Width	0 425
Opening	0 20
Minimum tooth width	0 281
Total flux, 48,100 kilo-lines	ϕ_w , 0 985

CONDUCTORS:	
Per slot	2
Size, bare	2—0 141×0 50—0 0880
Material	Copper
Section total	51 0
In series per phase	120
Insulation allowance:	
Depth	0 270
Width	0 110
Circuits per phase	One
Connections	Star
Coil throw	Slots 1 and 14
Per cent pitch	90 2
End ring:	
Section	
Material	
Length half mean-turn	29 11
Resistance per phase, 75° C.	0 24
Conductor weight	481 0

STATOR AND ROTOR	
Total resistance per phase	0 515—4 98%
Total reactance per phase	2 0—18 25%
Total impedance per phase	2 07—18 0%
Short-circuit power factor	28 4%
Short-circuit current	658
Friction and windage loss	2 540
No-load stator I^2R	8 10
Magnetizing current	30 3—27 3%
Watt component of I_m	2 2
No-load current	30 4—27 4%
No-load power factor	7 24%
Full-load current	105 5
Full-load slip	2 28%
Full-load speed	502 0
Full-load torque	4180
Starting torque	
Maximum torque	11,000
Maximum output	0 58

	1	2	3	4	5
Efficiency				92 5	
Power factor				88 0	

	Section	Density	Length	Ampere-Turns	Weight	Core Loss
Stator teeth	536 00	89 80	1 70	26	204	765
Stator yoke	28 20	83 60	5 58	57	612	1360
Rotor teeth	590 00	81 50	1 31	12		2125
Rotor yoke	33 20	66 10	4 58	21		× 2 0
Air gap	1030 0	20 50	1 01×1 12×0 0625	1010		4250
Total ampere-turns per pole				1150		

Rheostat Data	
Open-circuit volts across rings	608
Ampere per phase	200
Starting resistance per phase	1 19
$\phi_r = 0 998$	
$\frac{hp \times 10^3}{n} = 777$	

$\frac{D^2 l n}{hp} = 3.27 \times 10^4$	
Pole pitch = 10.12	
$\frac{\text{Total length}}{\text{Pole pitch}} = 1.235$	

Designed by J H Kuhlmann

Date: Aug. 7, 1928.

IV—TRANSFORMERS

CHAPTER XXI

CONSTRUCTION

THE transformer is a device for "stepping up" or "down" the voltage or current in an alternating current circuit. The essential parts are: a magnetic circuit, built up of sheet steel; and an electric circuit, consisting of one or more windings. Transformers may be divided into three classes: (1) Instrument transformers, (2) Constant-current transformers, (3) Constant-potential transformers. In the following pages, only the design and construction of constant-potential transformers, such as used to transform power from a high voltage and small current to a lower voltage and large current, or vice versa, will be discussed.

Constant potential transformers are used for light and power service and are generally divided into two groups: (1) distribution transformers, (2) power transformers.

Distribution transformers include sizes 200 Kva and smaller which are used to step down the voltage from the distribution voltage to a standard service voltage, or from the transmission voltage to the distribution voltage. They are built for voltages up to and including 66,000 volts, either single-phase or 3-phase. Standard sizes, voltage ratings, and taps for single-phase and 3-phase distribution transformers for the various system voltages have been adopted by the National Electric Manufacturers Association.¹

Power transformers include those sizes larger than 200 Kva which are used to step up the voltage to the transmission voltage at the generating station, or to step down the voltage at the substation. They also include those transformers in sizes larger than 200 Kva which are used to step down the voltage from either a transmission or a distribution voltage to a standard service voltage. They may be either single-phase or 3-phase and have been built for 220,000 volts star. The

¹ "Handbook of Transformer Standards," 5th ed., National Electric Manufacturers' Association, 420 Lexington Avenue, New York.

sizes, voltage ratings, and taps.

Core.—The magnetic circuit of all transformers is built up of sheet-steel laminations. For 60-cycle transformers, a 4 to 4.5 per cent silicon sheet steel 0.014 in. thick is used; for low frequencies, 2 to 2.5 per cent silicon steel sheet up to 0.019 in. thick is often used. Silicon steel is used because of its non-aging properties and low

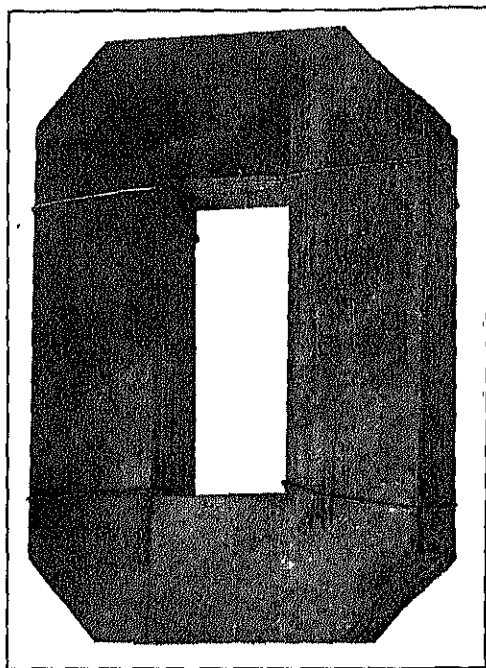


FIG. 206.—Core for small capacity rectangular core type distribution trans

For more complete information on the properties of electric sheet steel, the reader is referred to the splendid book by Thomas Spangenberg, "Properties and Testing of Magnetic Materials."² After the laminations are cut or punched to the proper size, they are carefully annealed to remove all punching or shearing strains, which increase the hysteresis loss. When the laminations have been annealed, a thin coating of insulating varnish is applied in the same manner as described for armature laminations of direct current machines, page 3. For small distrib

² "Properties and Testing of Magnetic Materials," McGraw-Hill Book Co., New York, N. Y.

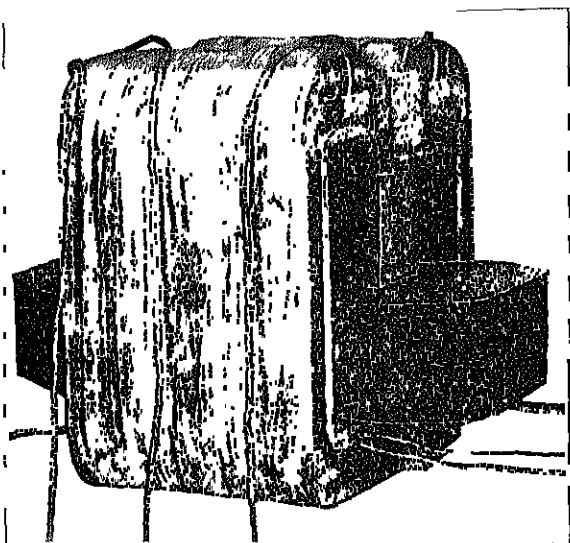


FIG. 207.—Partially assembled core and coils of a rectangular core type distribution transformer.

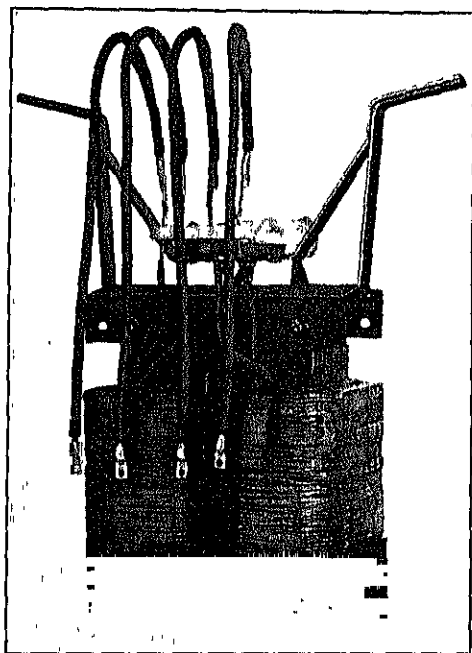


FIG. 208.—Rectangular core type transformer removed from tank.

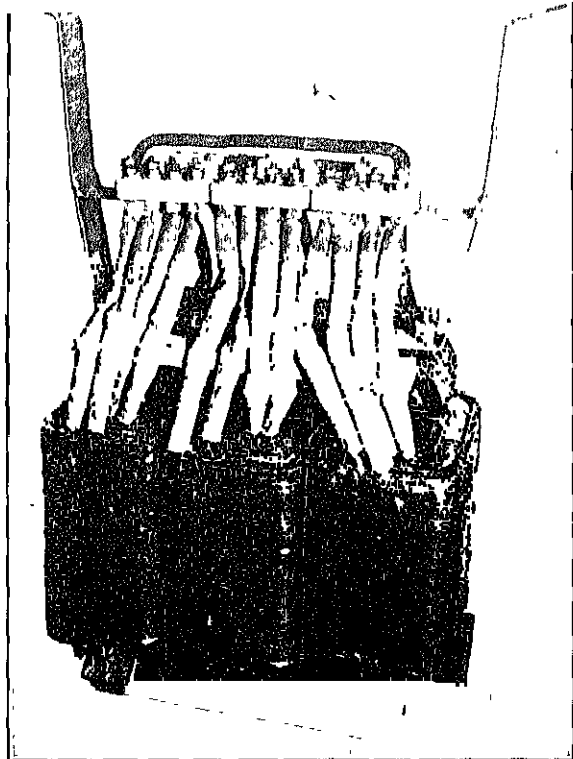


FIG. 200.—Three-phase core type distribution transformer removed from ta

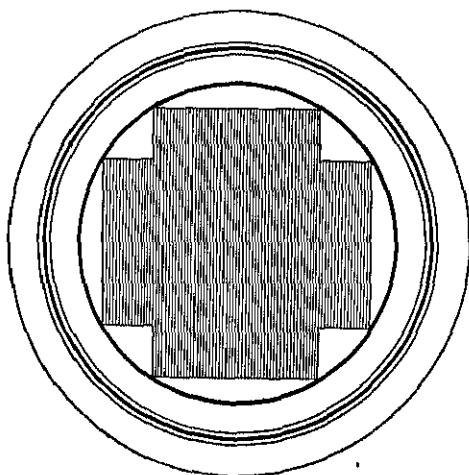


FIG. 210.—Section of cruciform shaped core with circular coils.

ing cooling is generally not necessary, as the heavy scale always present on silicon steel offers sufficient insulation.

There are three types of construction in common use: core type, shell type, and distributed core type.

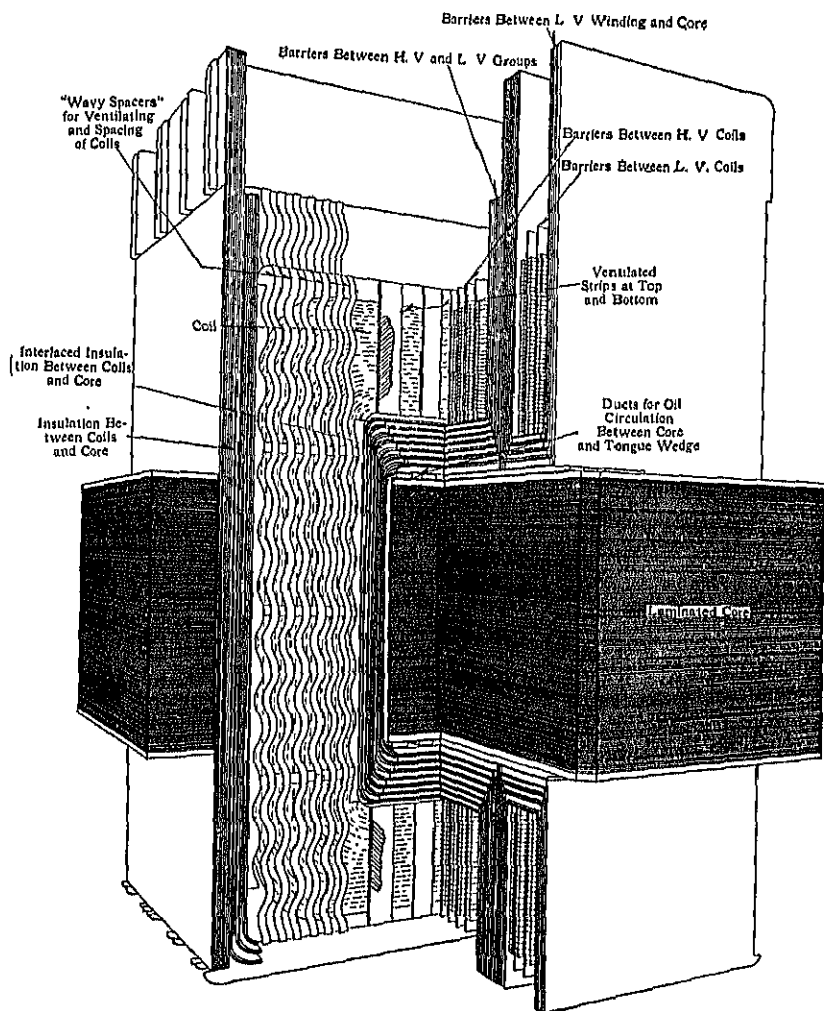


FIG. 211.—Sectional drawing of shell type transformer.

Core Type.—Figure 206 shows the core for a small core-type distribution transformer. The laminations are L-shaped and are assembled through the coils which are wound on a form, as shown in Fig. 207. Figure 208 shows a completely assembled, 15-Kva, 6900-volt, rect-

completely assembled, 3-phase rectangular core type distribution transformer is shown in Fig. 209. For high voltages, 22,000 volt higher, the cruciform-shaped core section with circular coils shown in Fig. 210, is used.

Shell Type.—The shell type of construction is generally best

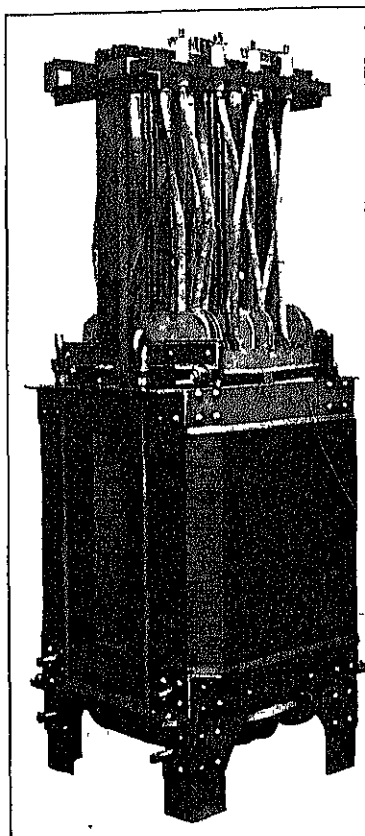


FIG. 212.—Complete shell type transformer removed from tank.

for transformers for relatively low voltage or for relatively large capacity, which have a good power factor in the winding. A section drawing³ of a shell type transformer is shown in Fig. 211. The windings are built up of "cake" type coils, as shown in Fig. 211. A completely assembled type transformer is shown in Fig. 212.

Distributed Core Type.—The distributed core type construction is built with 2-part, 3-part, and 4-part distributed core. The 3-part distributed core type is used for small-capacity distribution transformers for moderate voltages. The 2-part distributed core type is used for distribution transformers and power transformers. For small capacity and moderate voltage 3 and 4-part distributed-core transformers, the core is assembled as shown in Fig. 213, and the windings are wound directly on the core. For the larger capacities and high voltages, the coils are form-wound and assembled on the core, as shown in Fig. 214.

Tank.—Transformers are cooled by either one of the following methods:

(1) *Natural-air-cooled*, for which the natural circulation of the surrounding air is relied upon to carry away the heat generated by

³ "The Modern Manufacture of Large Power Transformers," by L. H. Electric Journal, Vol. 24, April, 1927, pp. 146 to 151.

constant-current transformers, and auto-transformers used to supply reduced voltage for starting alternating-current motors.

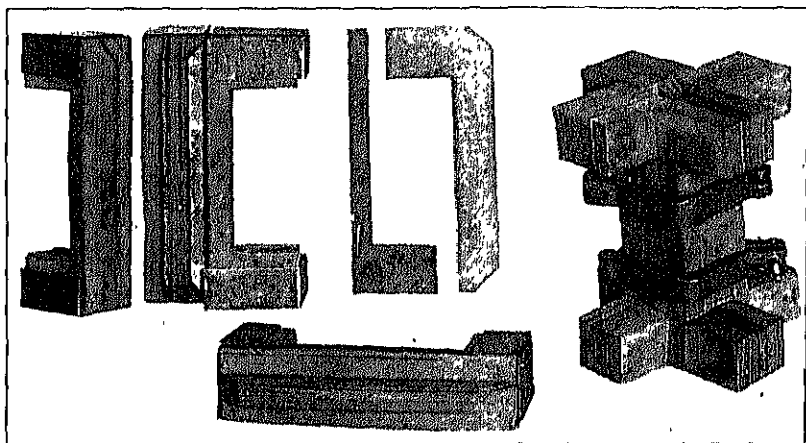


FIG. 213.—Shape of punching and method of assembling core of small four-part distributed core type transformer.

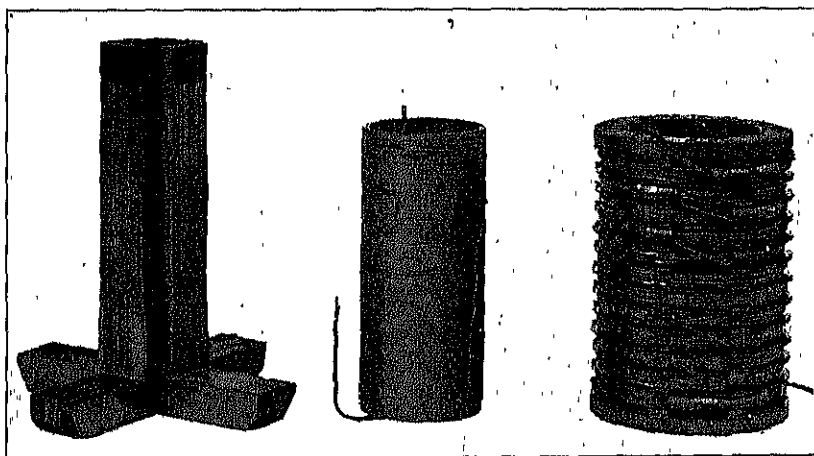


FIG. 214.—Method of assembling core and coils of large capacity four-part distributed core type transformer.

(2) *Natural-oil-cooled*, which method is used for all distribution and for power transformers. The transformer is immersed in a transformer oil which carries the heat to the walls of the containing tank.

(3) *Oil and Water Cooled*.—For this method the transformer is

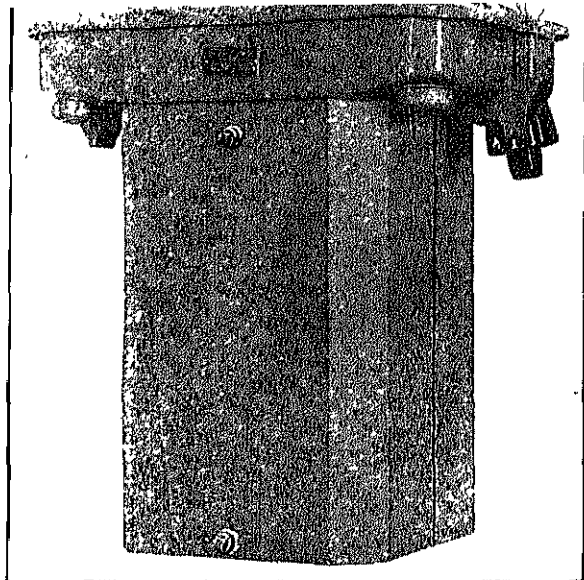


FIG. 215.—Welded sheet steel tank for transformer shown in Fig. 203.

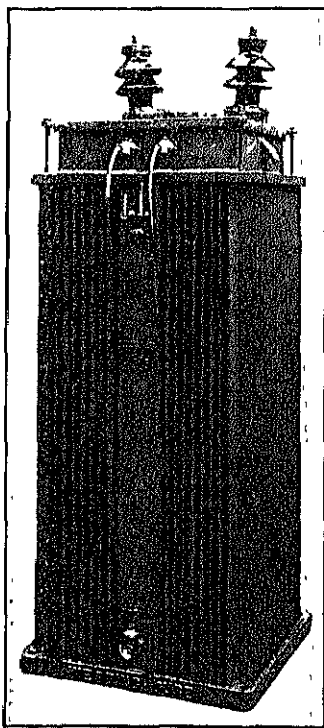


FIG. 216.—Complete transformer with corrugated sheet steel tank.

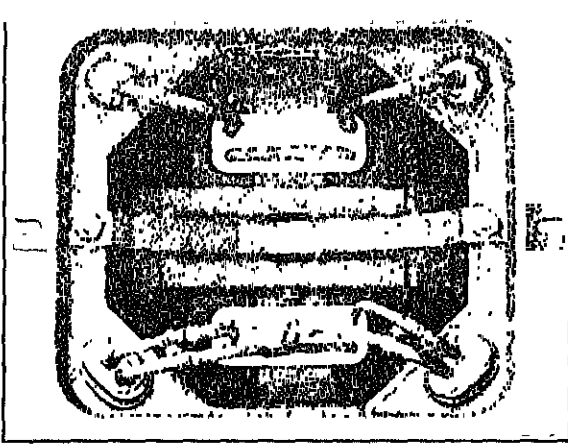


FIG. 217.—Top view of transformer and tank with cover removed.

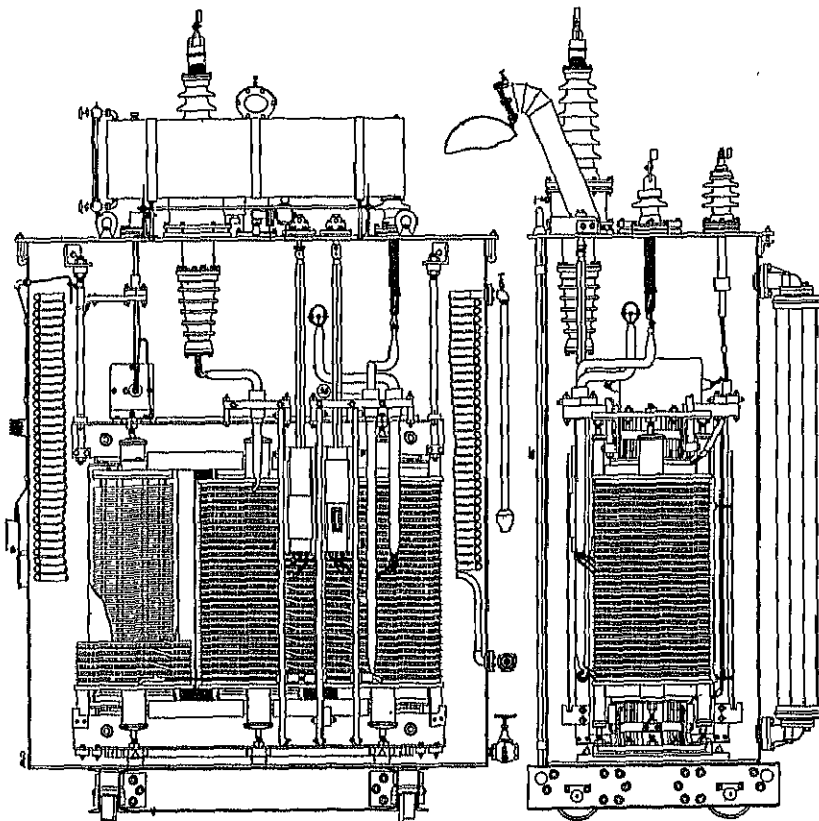


FIG. 218.—Sectional assembly drawing of three-phase transformer oil and water cooled.

coils of pipe placed near the top of the tank under the surface of the oil.

(4) *Cooled by Forced Circulation of the Oil.*—For this method the oil is drawn from the tank, passed through cooling coils on the outside of the tank, and returned to the bottom of the tank.

(5) *Cooled by Air Blast,* for which a continuous stream of cool air is forced through the core and windings.

For small distribution transformers, a plain cast-iron tank has often been used. The welded-sheet-steel tank is, however, used almost exclusively for modern transformers. Figure 215 shows a welded-sheet-steel transformer tank which is for the 15 Kva, 6900-volt, core-type transformer shown in Fig. 208. For the larger-capacity distribution transformers, it is difficult to obtain sufficient radiating surface with plain sheet steel tanks to dissipate the heat without excessive temperature rise. To increase the radiating surface, cooling vanes are welded to the tank or corrugated sheet steel tanks are used as shown in Fig. 216. Figure 217 is a top view of a tank with cover removed and shows how the transformer is secured in the tank and how the leads are brought out of the tank.

For oil and water-cooled transformers, plain sheet steel tanks are generally used. A sectional drawing of a 3-phase, oil and water-cooled transformer is shown in Fig. 218. It shows the position of the transformer and cooling coils in the tank.

CHAPTER XXII

CORE AND WINDINGS

TRANSFORMERS may be designed for minimum cost without regard to the losses, or for minimum total losses.

There is a lower limit to the cost for which a given transformer can be designed, because the copper density cannot be worked above a certain value because of heating; also, the core density is fixed by saturation of the magnetic circuit. The lowest-cost transformer will generally be the one for which the cost of iron and cost of copper are approximately equal.

With the densities fixed in core and copper, the minimum total loss transformer is the one for which the core loss is approximately equal to the copper loss at full-load. Such a transformer will have maximum efficiency at full-load.

Transformers intended for lighting load—distribution transformers—should have the core loss as small as possible, because they operate at light-load the greater part of the day and at full-load only a few hours. For such transformers the ratio of the core loss to the copper loss,

$$\frac{W_c}{W_k} = 0.30 \text{ to } 0.70.$$

Large power transformers are generally designed with the core loss approximately equal to the copper loss at full-load.

The loss per pound for the core can be found from the loss curves in the Appendix for various grades of sheet steel. The copper loss for 75° C. is calculated by formula 139a.

$$W_k = A^2 G_k \times 2.58 \times 10^{-6} \text{ watts.}$$

The loss per pound,

$$w_k = \frac{W_k}{G_k} = A^2 \times 2.58 \times 10^{-6} \text{ watts.}$$

When the flux density in the core and the current density in the copper have been determined, the loss per pound in core and copper can readily be calculated.

The magnetizing current of a transformer is the current drawn from the line to maintain the flux in the magnetic circuit. In order that this current shall be as small as possible, the flux density in the core must be below the saturation point of the grade of sheet steel used. Silicon steel has a high permeability at low values of induction, but at high values of induction the permeability decreases rapidly (see standard saturation curve in Appendix). For distribution transformers, the flux density in the core is generally,

$$B = 55,000 \text{ to } 75,000 \text{ lines per sq. in.}$$

Distributed-core-type transformers are usually designed with densities of 75,000 to 90,000 lines per sq. in. in the center leg and 40,000 to 55,000 lines per sq. in. in the remainder of the magnetic circuit. In this way the length of the mean-turn of the windings can be reduced without sacrifice in core loss, because the central core is only a small part of the entire magnetic circuit. When neither core loss nor magnetizing current but only first cost is important, slightly higher values for B can be used. For large power transformers, the flux densities in the core should generally not exceed 90,000 lines per sq. in.

The current density in the copper is limited by the efficiency and the allowable temperature rise. For distribution and small power transformers, self-oil-cooled,

$$A = 700 \text{ to } 1500 \text{ amperes per sq. in.}$$

The low values apply to the small capacities up to about 50 Kva. For large power transformers, self-oil-cooled,

$$A = 1400 \text{ to } 1900 \text{ amperes per sq. in.}$$

The ratio of core loss to copper loss,

$$\frac{W_c}{W_k} = \frac{w_c \times G_c}{w_k \times G_k} \quad (210)$$

When the densities in the core and copper are fixed, the loss per pound for core and copper can readily be determined. The ratio of weights for a given ratio of losses can easily be calculated by equation 210. The ratio of core weight to copper weight generally lies between the limits 1.5 and 3.0 for distribution transformers. For small-capacity, single-phase, core-type transformers, the ratio of weights is often less than 1.50. For high-voltage power transformers, it may be twice the values given above.

when the total flux is known. The curve in Fig. 219 gives average values of ϕ_t for distributed-core-type transformers. The reader must not conclude that distributed-core-type transformers are to be designed with values of total flux as given by this curve. These data are given merely to guide the beginner. Satisfactory designs can be obtained with values of ϕ_t either larger or smaller than those given by the curve. For the core type of construction, the best design is generally obtained with a smaller total flux than that used for the distributed-core-type transformer. For single-phase, core-type transformers, multiply the

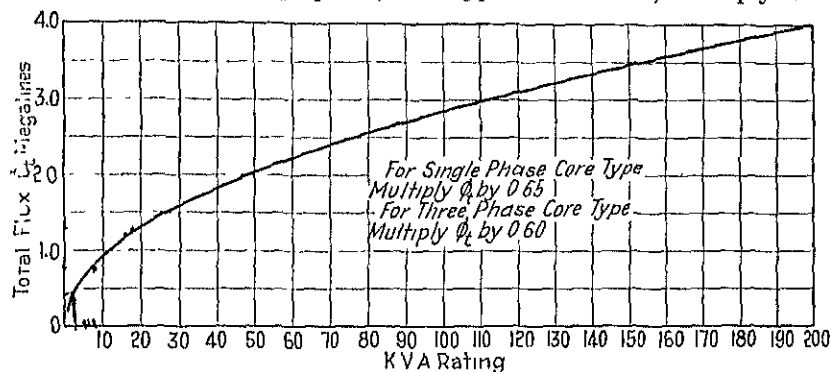


FIG. 219.—Total flux for four-part distributed core type transformer.

values of ϕ_t in Fig. 219 by 0.65 and for 3-phase core type by 0.60. The section area of the core,

$$A_c = \frac{\phi_t}{B}$$

Dr. Arnold¹ has developed the following output equation by which the section area of the core can be calculated when the output constant is known. For a single-phase transformer the output,

$$Kva = EI \cdot 10^{-3}.$$

The induced voltage,

$$E = 4.44fBA_c \cdot 10^{-8} \text{ volts}$$

and

$$I = As_c.$$

¹ "Dio Wechselstromtechnik," by E. Arnold, Vol. II, 2nd ed., p. 310, Julius Springer, Berlin; see also "The Essentials of Transformer Practice," by Emerson G. Reed, 2nd ed., p. 62, D. Van Nostrand Co., New York.

$$Kva = 4.44fBA_oA_s 10^{-11}. \quad (211)$$

The weight of the core,

$$G_c = A_c l_c g_o \text{ lb.}$$

and the weight of the copper, Φ

$$G_k = 2ts_c l_k g_k \text{ lb.,}$$

if the weights of the high voltage and that of the low voltage winding are assumed to be equal.

The ratio of the core weight to the copper weight,

$$\frac{G_c}{G_k} = \frac{A_c l_c g_o}{2ts_c l_k g_k}.$$

If the ratio of the mean length of the magnetic circuit to the mean-turn of the winding is assumed to be constant, which is approximately true for a given type of transformer, then

$$\frac{G_c}{G_k} = C_1 \frac{A_c}{ts_o}$$

and

$$ts_o = \frac{G_k}{G_c} A_o C_1.$$

Substituting this expression into equation 211, the core section,

$$A_o = C \sqrt{\frac{Kva \frac{G_o}{G_k} 10^{11}}{BAf}}. \quad (212)$$

The output constants for the various types of construction are given below:

Type of Transformer	C
Distributed core type.....	0.55 to 0.65
Single-phase core type.....	0.40 to 0.55✓
Three-phase core type.....	0.30 to 0.50
Single-phase shell type.....	0.80 to 1.0

The shape of the core section is rectangular, square, or cruciform. For core-type distribution and small power transformers for moderate

and low voltages, the rectangular-shaped core section shown in Fig. 220 is generally used. The dimensions of the section can be calculated as follows: The long side of the core section is generally from 1.4 to 2.0 times the short side. The notches on the corners of the section shown in Fig. 220 are often omitted on transformers below 25-Kva capacity. For small core sections,

$$A_o = abk_1$$

$$b = (1.4 \text{ to } 2.0)a.$$

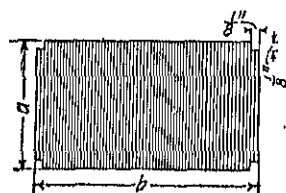


FIG. 220.

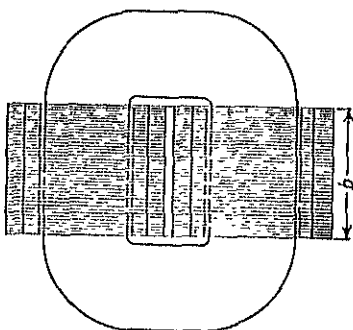
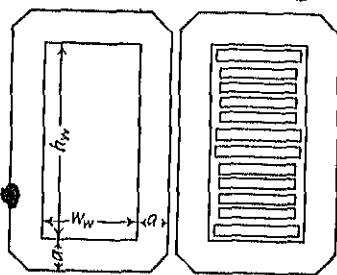


FIG. 221.

Therefore

$$a = \sqrt{\frac{A_c}{(1.4 \text{ to } 2.0)k_1}}. \quad (213)$$

When the corners are notched, as shown in Fig. 220,

$$a = \sqrt{\frac{A_o + 0.004k_1}{(1.4 \text{ to } 2.0)k_1}}. \quad (214)$$

For shell-type transformers (see Fig. 221), the ratio $b/2a$ generally lies between the limits 2 and 3. When there are no ventilating ducts in the core,

$$b = \frac{A_o}{2ak_1}$$

$$2a = \sqrt{\frac{A_o}{(2 \text{ to } 3)k_1}}. \quad (215)$$

When circular coils are required for high voltage distribution and large power transformers, the cruciform-shaped core shown in Fig. 222 is used. The dimensions of the section to give the maximum area of

for the section shown in Fig. 222 equals

$$\frac{A_c}{k_1} = 2ab + (2b - 2a) 2a = 4(2ab - a^2)$$

Then
$$a = \frac{D}{2} \sin \alpha; \quad b = \frac{D}{2} \cos \alpha.$$

$$\frac{A_c}{k_1} = 4 \left(2 \frac{D}{2} \sin \alpha \frac{D}{2} \cos \alpha - \frac{D^2}{4} \sin^2 \alpha \right) = D^2 (2 \sin \alpha \cos \alpha - \sin^2 \alpha).$$

The value of the angle α that will give the maximum core section can be found by differentiating the above equation with respect to α and equating the resultant expression to zero,

$$\frac{d \frac{A_c}{k_1}}{d\alpha} = D^2 (2 \cos 2\alpha - 2 \sin \alpha \cos \alpha) = 0$$

$$\tan 2\alpha = 2; \quad \alpha = 31.75^\circ.$$

Therefore

$$a = 0.263D; \quad b = 0.425D.$$

The gross section area of the core is, then

$$\frac{A_c}{k_1} = 2a2b + (2b - 2a)2a = 0.618D^2.$$

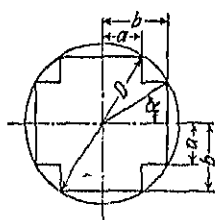


FIG. 222.

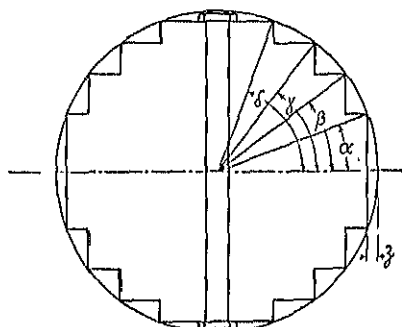


FIG. 223.—Four-step circular core section.

The ratio of the net area of the core to the area of the circumscribed circle is called the core space factor, f_{cs} . The lamination factor, k_1 , can be taken equal to 0.90 for 0.014-in. silicon sheet steel. Then,

$$f_{cs} = \frac{0.618D^2 \times 0.90}{\pi/4 D^2} = 0.70. \quad (216)$$

For large core areas, a section, such as that shown in Fig. 223, with three or more steps is often used. Such cores are expensive to build but

ter for a given core area. Circular coils are preferred for large power transformers because of their superior mechanical characteristics.² A transformer coil, under the magnetic stresses produced by excessive leakage flux due to short-circuit, tends to assume a circular form. On circular coils, these forces are radial and there is no tendency for the coil to change its shape; on rectangular coils the forces are perpendicular to the conductor and tend to give the coil a circular form.

The values of the various angles for 2-, 3-, 4-, and 5-step cores, to give the maximum area for a given diameter, have been calculated by W. B. Garrett³ and are given in the following table.

The dimension z , Fig. 223, must be large enough to allow for end plates, nuts, etc. The space so required generally varies from 15 per cent of the core diameter in large cores to 25 per cent in small cores, which corresponds to an angle for the most remote step of from 57° to 48° , respectively. Table XXVIII gives the various angles for 2-, 3-, 4-, and 5-step cores in terms of the angle for the most remote step, which is called the fixed angle.

TABLE XXVIII

Angle	2-Step	3-Step	3-Step (1 Duct) *	4-Step	4-Step (1 Duct) *	5-Step (1 Duct) *	5-Step (3 Ducts) †
ϵ	Fixed	Fixed
δ	Fixed	Fixed	0.833 ϵ	0.850 ϵ
γ	Fixed	Fixed	0.785 δ	0.785 δ	0.667 ϵ	0.702 ϵ
β	Fixed	0.712 γ	0.714 γ	0.563 δ	0.570 δ	0.491 ϵ	0.511 ϵ
α	0.553 β	0.400 γ	0.414 γ	0.321 δ	0.337 δ	0.291 ϵ	0.299 ϵ

* Width of duct = 0.030 D .

† Width of duct = 0.015 D .

With the section area of the core determined and the flux density, B , fixed, the total flux,

$$\phi_t = BA_c. \quad (217)$$

The number of turns for the high-voltage winding,

$$i_h = \frac{E_h \times 10^8}{4.44 f \phi_t}$$

² "Circular-Coil High-Voltage Power Transformers," by Clinton Jones, General Electric Review, Vol. 24, May, 1921, pp. 399-401; "Fundamental Principles of Present-Day Transformer Design," by W. M. McCahey and J. F. Peters, Electrical World, Vol. 69, Jan. 20, 1917, pp. 129-132.

³ "An Investigation into the Sectional Proportions of the Cores of Circular Core Type Transformers," by W. B. Garrett, World Power, Vol. 6, Dec. 1926, pp. 292-298.

$$t_l = \frac{E_l}{E_h} t_h.$$

The voltage per turn

$$= \frac{E_h}{t_h}.$$

The current in the high-voltage winding,

$$I_h = \frac{\text{Kva} \cdot 10^3}{E_h} \text{ amperes}$$

and in the low-voltage winding,

$$I_l = \frac{t_h}{t_l} I_h \text{ amperes.}$$

The section area of the conductor for the high-voltage winding,

$$s_{ch} = \frac{I_h}{A} \text{ sq. in.}$$

and for the low-voltage winding,

$$s_{cl} = \frac{I_l}{A} \text{ sq. in.}$$

To obtain the desired ratio of core loss to copper loss, it is necessary to determine the core dimensions that will give the previously fixed ratio of core weight to copper weight. The ratio of the height of the window opening to the width will generally lie between the following limits:

$$h_w/w_w = 2.0 \text{ to } 4.0.$$

✓ The copper space factor, that is, the ratio of the net copper area in the window to the area of the window, varies with the capacity of the transformer and with the voltage of the windings. The curves in Fig. 224 give average values for f_s for the various types of transformers.

For single-phase transformers, the area of the window,

$$h_w w_w = \frac{s_{ch} t_h + s_{cl} t_l}{f_s} = \frac{2(s_{ch} t_h)}{f_s} \text{ sq. in.}$$

and for 3-phase core type transformers,

$$h_w w_w = \frac{2(s_{chh} + s_{cti})}{f_s} = \frac{4(s_{chh})}{f_s} \text{ sq. in.}$$

From the expression for the ratio of the dimensions,

$$w_w = \frac{h_w}{2.0 \text{ to } 4.0} \text{ in.}$$

Therefore

$$h_w = \sqrt{\frac{(2.0 \text{ to } 4.0) 2 s_{chh}}{f_s}} \text{ in. for single-phase} \quad (218)$$

and

$$h_w = \sqrt{\frac{(2.0 \text{ to } 4.0) 4 s_{chh}}{f_s}} \text{ in. for 3-phase.} \quad (219)$$

Before proceeding with the design of the windings, it will be desirable to check the approximate core and copper weight, to determine whether the desired ratio of weight can be obtained with the core dimensions selected. (See sample designs, Chapter XXIV.)

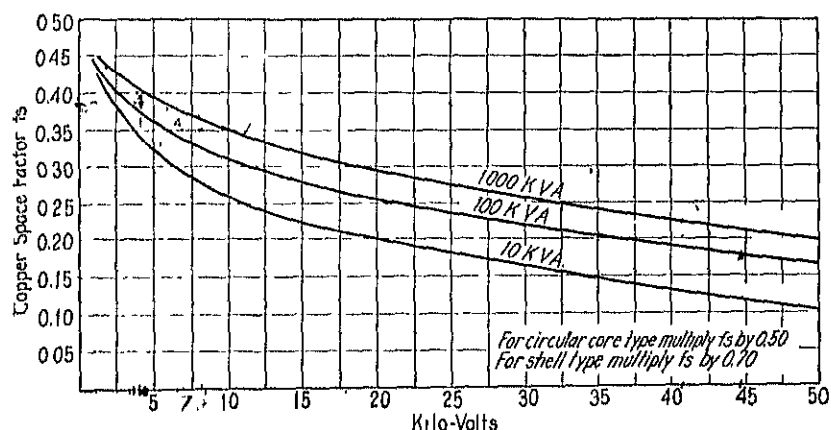


FIG. 224.—Approximate copper space factors.

Design of Windings.—The windings of transformers must be designed to give the best possible electrical characteristics with the proper mechanical strength to withstand the stresses due to short-circuits and with proper ventilation to avoid excessive temperature rise and "hot spots." The approximate electrical characteristics of single-phase distribution transformers for 2300, 4600, and 6900 volts are given in Tables XXIX and XXX. Similar data are given in Table XXXI for 3-phase, 4600-volt, star-connected, distribution transformers.

TABLE XXXA

ELECTRICAL CHARACTERISTICS OF SELF-OIL-COOLED DISTRIBUTION TRANSFORMERS
SINGLE-PHASE, 60 CYCLES, 2300 AND 4600 TO 115 AND 230 VOLTS

Kva	Losses		Efficiency, Full-Load	Regulation		Per Cent		
	Core	Copper		100% PF	80% PF	IR	IX	IZ
1.5	25	54	95.0	3.61	3.57	3.60	1.15	3.78
3.0	32	85	96.2	2.88	3.25	2.83	1.65	3.27
5.0	46	128	96.6	2.58	3.16	2.56	1.85	3.16
7.5	58	176	96.9	2.39	3.00	2.34	1.89	3.02
10.0	73	226	97.1	2.28	2.77	2.26	1.60	2.77
15.0	96	320	97.3	2.10	3.21	2.13	2.51	3.30
25.0	133	490	97.5	1.98	3.20	1.96	2.72	3.35
37.5	172	570	97.6	1.98	3.25	1.95	2.82	3.43
50.0	210	780	98.0	1.08	3.15	1.56	3.16	3.53
75.0	330	1200	98.0	1.65	3.15	1.60	3.11	3.50
100.0	450	1400	98.1	1.50	3.20	1.46	3.38	3.68
150.0	695	1900	98.3	1.32	3.30	1.27	3.80	4.00
200.0	920	2400	98.3	1.27	3.37	1.20	4.02	4.20

TABLE XXX

ELECTRICAL CHARACTERISTICS OF SELF-OIL-COOLED DISTRIBUTION TRANSFORMERS
SINGLE-PHASE, 60 CYCLES, 6900 TO 115 AND 230 VOLTS

Kva	Losses		Efficiency, Full-Load	Regulation		Per Cent		
	Core	Copper		100% PF	80% PF	IR	IX	IZ
1.5	28	42	95.5	3.00	5.00	2.80	4.60	5.40
3.0	38	85	96.0	3.00	5.00	2.83	4.57	5.37
5.0	49	140	96.3	2.95	5.00	2.80	4.60	5.40
7.5	71	175	96.8	2.45	4.90	2.34	5.05	5.56
10.0	81	220	97.0	2.35	4.85	2.20	5.15	5.60
15.0	106	320	97.2	2.30	4.70	2.13	5.00	5.44
25.0	158	464	97.5	2.05	5.10	1.86	7.02	7.25
37.5	208	595	97.9	1.80	5.00	1.59	6.21	6.41
50.0	280	785	97.9	1.75	4.90	1.57	6.06	6.25
75.0	394	1030	98.1	1.55	4.70	1.38	6.00	6.15
100.0	600	1230	98.2	1.40	4.30	1.23	5.54	5.68
150.0	900	2010	98.1	1.50	4.35	1.34	5.47	5.64
200.0	1100	2650	98.1	1.50	4.40	1.33	5.57	5.72

TABLE XXXI

ELECTRICAL CHARACTERISTICS OF SELF-OIL-COOLED DISTRIBUTION TRANSFORMERS
THREE-PHASE, 60 CYCLES, 4600 TO 230 AND 460 VOLTS

Kva	Losses		Efficiency, Full-Load	Regulation		Per Cent		
	Core	Copper		100% PF	80% PF	IR	IX	IZ
5.0	74	148	95.8	3.00	4.01	2.96	2.73	4.03
7.5	84	203	96.5	2.75	3.85	2.71	2.80	3.89
10.0	96	250	96.6	2.56	3.70	2.50	2.84	3.78
15.0	122	340	97.0	2.30	3.70	2.26	3.15	3.88
25.0	176	510	97.3	2.00	3.65	2.04	3.37	3.94
37.5	227	750	97.4	2.00	3.78	2.00	3.04	4.15
50.0	277	940	97.6	1.95	3.87	1.88	3.95	4.37
75.0	352	1310	97.8	1.81	3.75	1.75	3.92	4.30
100.0	476	1530	98.0	1.60	3.60	1.53	3.97	4.26
150.0	620	2140	98.1	1.51	3.60	1.43	4.10	4.34
200.0	892	2720	98.2	1.48	3.65	1.36	4.27	4.49

The A.I.E.E. Standards⁴ specify that the temperature rise of transformer windings shall not exceed 55° C. for class A insulation, and 75° C. for class B insulation. The temperature is to be determined by the resistance method and checked by thermometer. The types of materials included in class A and class B insulations are given on page 122.

In winding and assembling the coils of a transformer, either of two polarities, subtractive or additive, may be produced. Figure 225 shows an elementary diagram of a loaded transformer.⁵ The direction of the voltage induced in the primary winding at a particular instant is shown by E_p . The flow of current in the primary winding is from the terminal at which the impressed primary voltage is positive to the terminal at which it is negative and is opposed by the induced primary voltage E_p . The load component of the primary current sets up a magnetomotive force which tends to produce a flux in the core in the direction indicated by m.m.f._p. Since the direction of current flow in the secondary must produce a magnetomotive force to oppose m.m.f._p, it must flow in the direction shown in the diagram, producing a flux tendency in the direction indicated by m.m.f._s. The flow of current

⁴ A.I.E.E. Standards No. 13, Transformers, Induction Regulators and Reactors, p. 8.

⁵ "Notes on Transformer Polarity and Connections," Part I, by John Anchincloss, General Electrical Review, Vol. 20, Nov., 1926, p. 783.

through the load connected across the secondary terminals E_s ; therefore, from left to right, that is, the left-hand terminal of the secondary winding is positive and the right-hand one is negative. The secondary voltage, E_s , has the direction shown in Fig. 225. It will be observed that E_p and E_s have the same direction. Adjacent primary and secondary terminals, therefore, have the same polarity, the left-hand primary and secondary terminals at the instant chosen being positive, and the right terminals negative.

The polarity of the transformer just described is called subtractive. If two adjacent primary and secondary terminals are connected, as shown in Fig. 225b, and voltage applied, say, to the primary winding, the voltage measured by a voltmeter connected across the other adjacent terminals will be the difference between the primary and secondary voltages; hence, the term subtractive polarity.

If the secondary winding in Fig. 225a were wound on the core in the

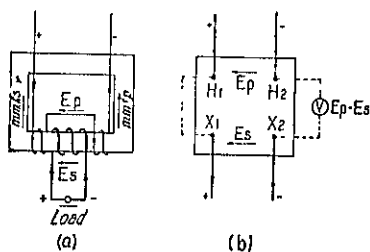


FIG. 225.

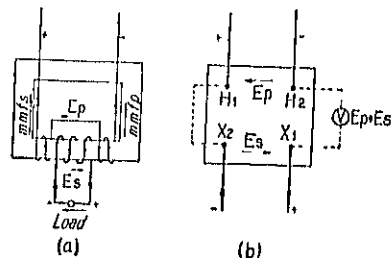


FIG. 226.

opposite direction, as shown in Fig. 226a, the secondary current would have to flow in a direction opposite to that shown in Fig. 225a. Therefore, at the instant when the left-hand primary terminal is positive, the left-hand secondary terminal is negative, and the current flow in the external circuits is in the opposite direction, as are also the voltages E_p and E_s in the internal circuits of the transformer. The polarity for the transformer shown in Fig. 226 is called additive for the reason that, if two adjacent primary and secondary terminals are connected, and voltage is applied to either the high or low voltage winding, the voltage measured by a voltmeter connected across the other adjacent terminals will be the sum of the primary and secondary voltages.

The windings of transformers may be arranged concentrically with reference to one another, or they may be arranged in groups of high voltage and low voltage coils stacked alternately one upon the other. The former is known as the concentric type of winding and the latter as the interleaved type.

in cylindrical form or in rectangular tubular form and generally have only one layer. Two-layer, low-voltage coils are, however, not uncommon and more layers may be used if proper ventilating ducts are provided. The high-voltage coils for moderate voltages, 6900 volts and below, are generally wound with several layers and are placed on the outside of the low-voltage coil. To avoid hot spots in the coils, the depth of winding must be kept small. This is done by winding the coils in sections and separating them by ventilating ducts. Figure 227 shows the coil group for a rectangular core type transformer with a

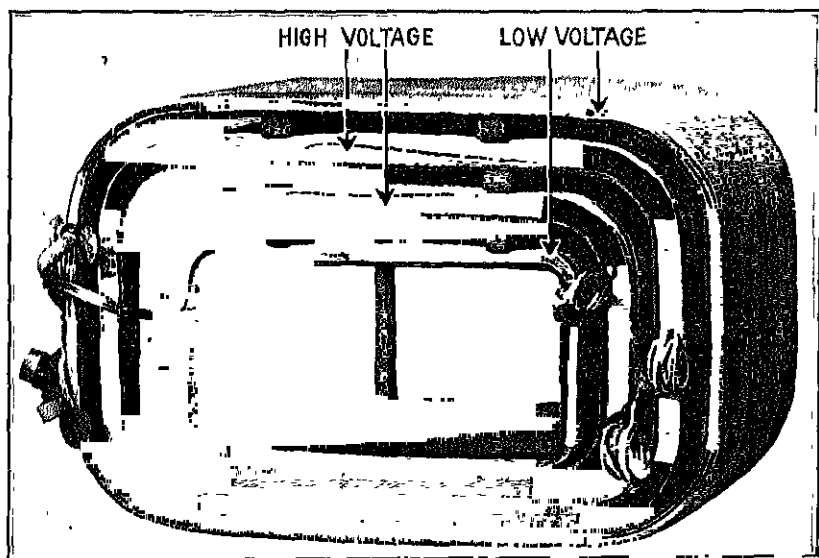


FIG. 227.—Concentric wound coil with two-section low voltage and high voltage coils.

two-section, high-voltage winding placed between the two coils of the low-voltage winding. For high-voltage, concentric-coil-type windings, the coils are generally wound and arranged as shown in Fig. 228.

The interleaved type of winding is shown in Fig. 229. It consists of thin circular or rectangular shaped coils arranged in high-voltage and low-voltage groups and stacked alternately one upon the other.

The conductors are either round, square, or rectangular in section and are double-cotton-covered or insulated with a treated paper held in place by bands of cotton thread. To avoid large eddy-current losses, large conductor sections must be built up of several small conductors in parallel. When the parallel conductors are wound on top

of one another in a radial direction, the inside conductors will have a higher reactance than the outside one. Consequently, the current is not equally distributed among the group of parallel conductors. Uniform distribution of the current can be obtained by transposing the conductors, as shown in Fig. 230.

The insulating materials used for transformer windings must have high dielectric strength and good mechanical strength and must not be soluble in hot transformer oil. The materials generally employed are:

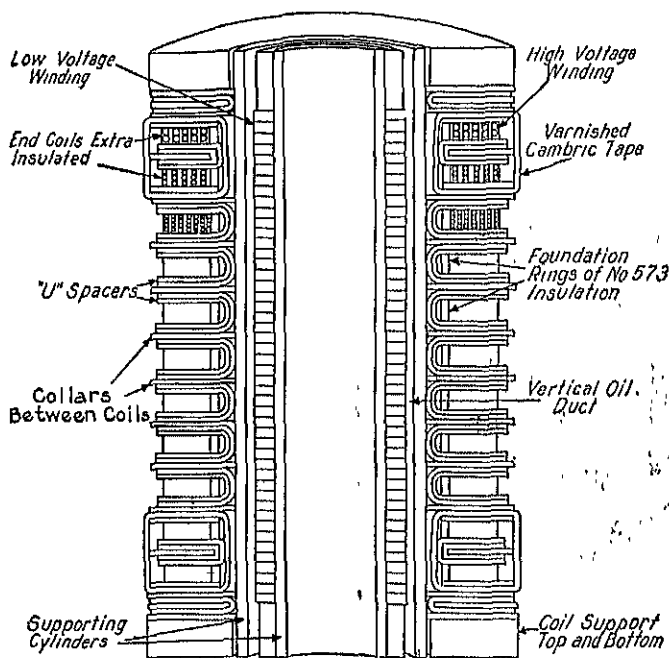


FIG. 228.—Section of concentric type winding with disc type high-voltage coils.

Cotton tape, empire cloth, paper in various forms, insulating varnish, and insulating oils.

Double-cotton-covered conductors, or their equivalent, can generally be used when the voltage per turn does not exceed 25 volts. For layer-wound coils, the maximum voltage between the turns of two layers should not exceed approximately 300 volts. Figure 231 shows four layers of a coil with six turns per layer. It is apparent that the maximum voltage per layer at *b* and *c* is equal to two times the voltage per turn, times the number of turns per layer. Coils with high layer voltage require heavy insulation between layers, which leads to a low

space factor and low heat conductivity. Paper and empire cloth are generally used for the layer insulation. The thickness depends upon the size of the conductor and the voltage stress between layers. For large conductors, the tension required to wind the coils is greater than for small ones; therefore the layer insulation must have greater mechani-

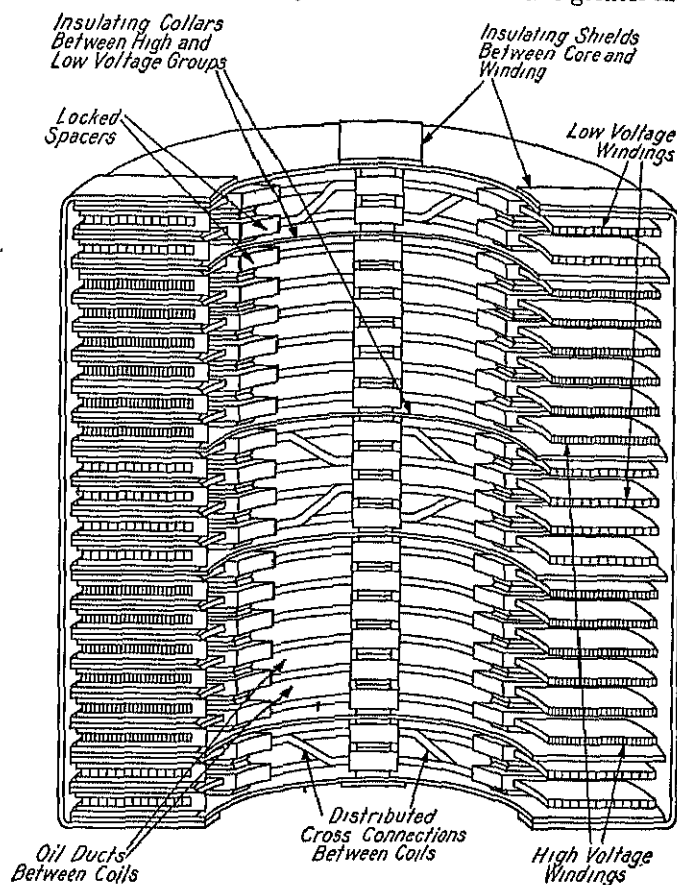


FIG. 220.—Section of interleaved type of winding with disc type high voltage and low voltage coils.

cal strength. For conductors of 0.040-sq. in. area and smaller the thickness⁶ of the insulation between layers may be taken equal to 0.005 in. for each 20 to 30 volts.

⁶ Much useful information on the insulation of transformer windings is given by A. P. M. Fleming and R. Johnson in "Insulation and Design of Electrical Windings," pp. 155 to 176, Longmans, Green & Co., London.

For section-wound coils with only one turn per layer, such as the coils used for the interleaved type of winding arrangement, the voltage per turn may be 70 to 80 volts, because additional insulation can readily be wound between turns.

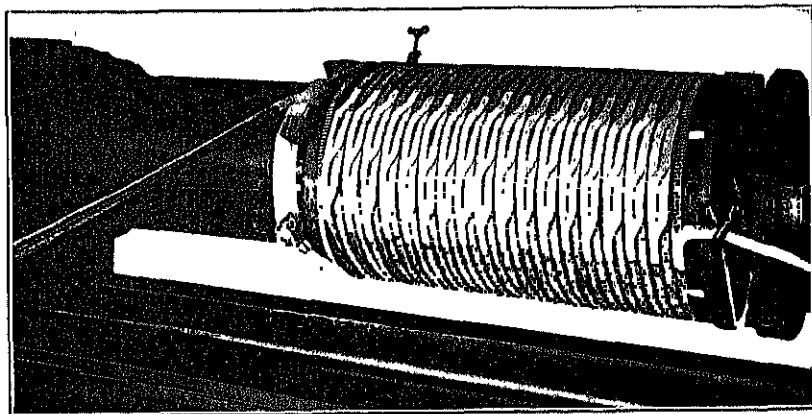


FIG. 230.—Partially wound low voltage coil with three transposed conductors.

For transformers for 7500 volts and higher, the end turns must be specially insulated because abrupt changes in potential may raise the voltage between the conductors near the terminals to many times the normal value.⁷ The percentage of end turns that must be specially insulated varies from 2.5 per cent for 7500 to 15,000 volts to approximately 15 per cent for 220,000 volts. Messrs. Fleming and Johnson recommend 2.5 per cent for 10,000-volt windings and an additional $\frac{1}{2}$ per cent for every 10,000 volts. Figure 232 shows the end-turn insulation for a 132,000-volt, concentric-type winding.

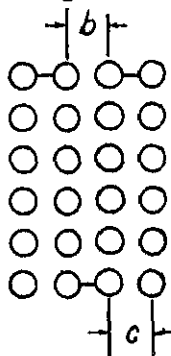


FIG. 231.

The insulation between core and windings and between high-voltage and low-voltage windings of concentric-coil-type transformers generally consists of molded cylinders or rectangular tubes. These tubes have high dielectric and mechanical strength and are

⁷ "Protection of Internal Insulation of a Static Transformer against High Frequency Strains," by W. S. Moody, Trans. A.I.E.E., Vol. 26, Part 2, p. 1173; "Choke-Coils Versus Extra Insulation on the End Windings of Transformers," by S. M. Kintner, Trans. A.I.E.E., Vol. 26, Part 2, p. 1169; "Transformers: Some Theoretical and Practical Considerations," by A. P. M. Fleming and K. M. Faye-Hansen, Journal I.E.E. Br. Vol. 42, 1908-09, p. 373.

not affected by insulating oils. The dielectric strength of the insulation between the various parts of the winding must be high enough to meet

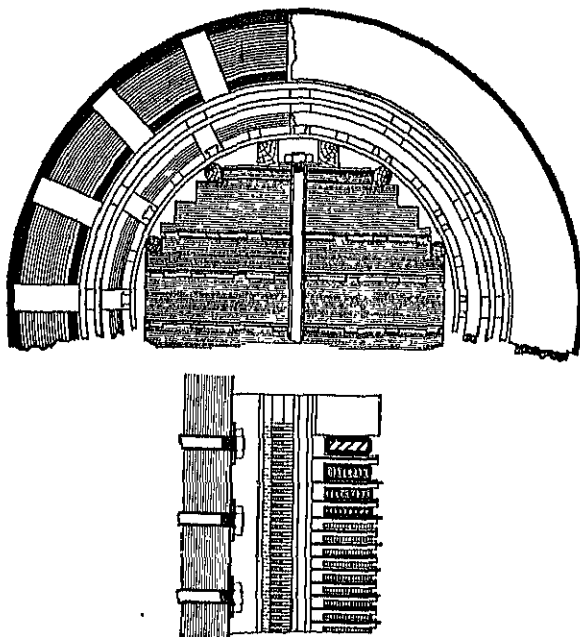


FIG. 232.—Concentric type winding and insulation—132,000 volt transformer.

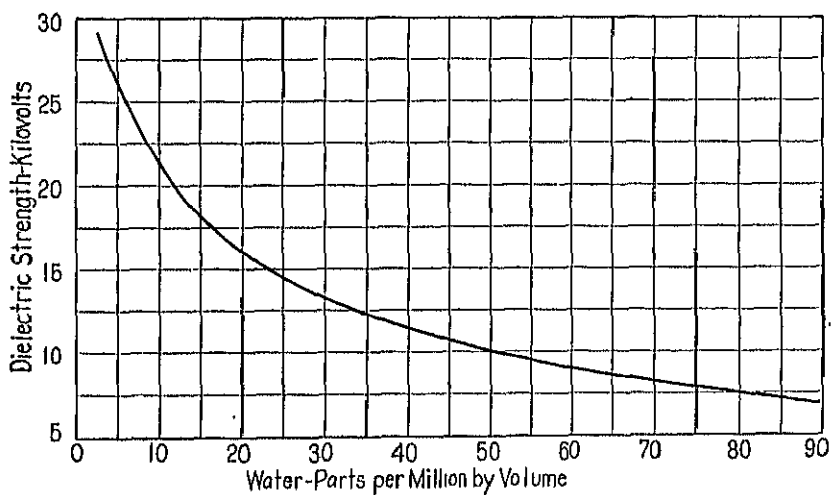


FIG. 233.—Dielectric strength of insulating oil.

the requirements of service with a reasonable factor of safety. The insulation test made on transformers is usually in accordance with the standardization rules of the American Institute of Electrical Engineers. For standard transformers, the standard test voltage⁸ to be applied between windings and between windings and ground is as follows:

Transformers and other induction apparatus shall have each winding tested by applying to the winding under test an alternating voltage, for one minute, of twice the rated voltage of the circuit to which the winding under test is connected, plus 1000 volts. For windings rated below 550 volts, the test voltage to be applied between high-voltage and low-voltage winding and core is 4000 volts, and for windings rated 550 volts to 4500 volts, the test voltage is 10,000 volts. For low-voltage windings, rated 1500 volts and below, the test voltage between winding and core is 4000 volts, and for 1500 to 4500-volt windings, 10,000 volts.

The thickness of the insulation between high-voltage and low-voltage coils and between low-voltage and core will depend upon the voltage of the windings and upon the mechanical strength required for winding and assembling the coils. The dielectric strength of molded insulating tubes $\frac{1}{4}$ in. thick is 100 kilovolts. More complete information on the insulation thickness required for transformer windings is given by Messrs. Fleming and Johnson.⁹ In addition to the insulating barriers, ducts are used between low-voltage winding and core, and between high- and low-voltage winding. The width of the ducts is generally $\frac{1}{4}$ in. in small capacity transformers and $\frac{1}{16}$ to $\frac{1}{2}$ in. in large capacity, high voltage, power transformers. These ducts are used primarily for cooling purposes, but for oil immersed transformers they also have a marked insulation value. Insulating oils, such as used for transformers, have a high dielectric strength when clean and free from moisture. Figure 233 shows the relation between the amount of water in insulating oil and the dielectric strength.¹⁰ The transformer standards of the Electric Power Club specify that insulating oil used for transformers must meet the following requirements:

"Transformer oils shall be capable of withstanding at commercial frequencies, 22,000 volts between 1-in. disc-terminals spaced 0.10 in. apart."

For voltages above 6900 volts, the insulation between windings and between windings and core is generally arranged as shown in Fig. 234 (see also Figs. 227 and 232).

⁸ For complete statement of dielectric test, see A.I.E.E. Standards No. 13, Aug., 1925, p. 14.

⁹ "Insulation and Design of Electrical Windings," pp. 155-175, Longmans, Green & Co., London; "Herkolite Insulating Materials in Transformers," General Electric Review, Vol. 29, Feb., 1926, pp. 102-108.

¹⁰ "Electric Insulating Oil," by Dean Harvey, Electric Journal, Vol. 25, Feb. and March, 1928.

the thickness of the insulating collars at each end of the windings varies from $\frac{1}{4}$ in. for windings below 500 volts to 6 in. for 70,000-volt

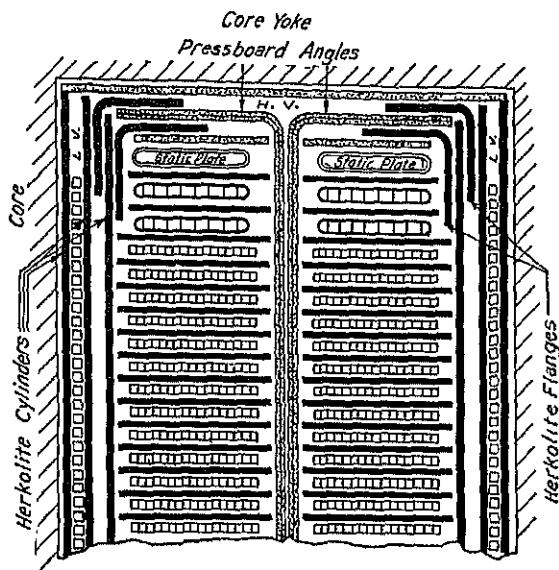


FIG. 234.—Sketch showing section through window of a high voltage concentric disc type transformer.

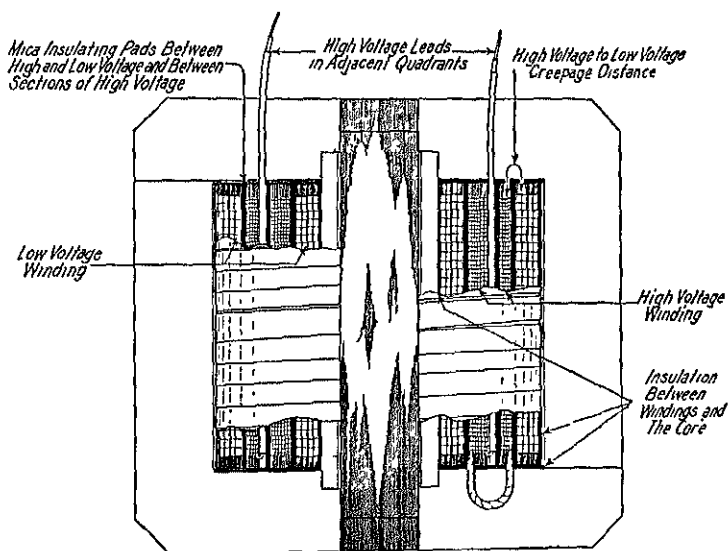


FIG. 235.—Section of moderate voltage four-part distributed core type transformer.

windings. Large-capacity, high-voltage power transformers must have rigid supports at the ends of the coils to prevent distortion produced by the short-circuit forces.

For voltages below 6900 volts, the insulation between core and coils, and between high-voltage and low-voltage winding, is generally a mica pad. Figure 235 is a sectional drawing of a moderate-voltage, distributed-core-type transformer and shows the usual method of arranging and insulating the windings. No ducts are used between high-voltage and low-voltage coils, but one duct is used in the high-voltage coil. To avoid hot spots and to insure uniform temperature, the thickness of the coils from outside to duct, between ducts, or from duct to core should generally not exceed 1.0 in.

Interleaved-type windings are usually insulated as shown in Figs. 211 and 229. Pressboard collars are generally used to insulate the windings from one another. The insulation between core and coils is either molded insulation or pressboard. Ducts are provided between winding and between individual coils. The duct spacers are built up of pressboard, or are of treated wood.

After the coils are wound, they are thoroughly dried and impregnated by the vacuum process or treated with insulating varnish, the method used depending upon the type and size of coil. Small transformers are generally treated by the vacuum process after the core and coils are assembled. The insulating varnish and impregnating compound fill all the crevices of the coils and cement the turns firmly together. The insulation is thereby greatly strengthened, the heat conductivity of the coils increased, and the winding made moisture proof.

CHAPTER XXIII

OPERATING CHARACTERISTICS

Resistance.—The length of the mean-turn of the windings can easily be calculated from a sketch of the coils (see the sample designs in Chapter XXIV).

The weight of the copper in the low-voltage coil is,

$$G_l = L_{ltscl} \times 0.321 \text{ lb.} \quad (220)$$

and in the high-voltage coil,

$$G_h = L_{htsch} \times 0.321 \text{ lb.} \quad (221)$$

The copper loss for the two windings, at 75° C., are calculated by formula 139a (see page 345).

The resistance of each winding at 75° C.,

$$R_l = \frac{W_l}{I_l^2} \text{ ohms, and } R_h = \frac{W_h}{I_h^2} \text{ ohms.}$$

The total resistance of the transformer in terms of the high voltage winding,

$$R_t = R_h + R_l \frac{t_h^2}{t_l^2} = \frac{W_l + W_h}{I_h^2} \text{ ohms.}$$

The per cent resistance drop,

$$P_r = \frac{I_h R_t}{E_h} 100.$$

Leakage Reactance.—The leakage reactance can be calculated only approximately because certain assumptions must be made as to the length and area of the flux path. Formulas for calculating the reactance of transformers have been developed by various authors.¹ The

¹ "Die Wechselstromtechnik," by Dr. Arnold, Vol. 2, pp. 22-29, Julius Springer, Berlin; "Die Transformatoren," by Dr. Milan Vidmar, pp. 93-114, Julius Springer, Berlin; "Principles of Alternating Current Machinery," by R. R. Lawrence, pp. 180-191, McGraw-Hill Book Co., New York; "The Essentials of Transformer Practice," by E. G. Reed, pp. 115-123, D. Van Nostrand Co., New York.

leakage flux path for a core-type transformer with concentric winding and with the low-voltage coil on the inside and high-voltage winding outside is shown in Fig. 236. The total reactance, high voltage plus low voltage in terms of high voltage, for one leg of a transformer, with windings arranged as shown in Fig. 236,

$$X_l = \frac{21.5ft_h'^2}{h \times 10^8} \left(\frac{d_h + d_l}{3} + d \right) \frac{L_h + L_l}{2} \text{ ohms.}$$

The per cent reactance drop,

$$P_x = \frac{X_l I_h}{E_h} 100 = \frac{21.5ft_h'^2 I_h}{h E_h \times 10^6} \left(\frac{d_h + d_l}{3} + d \right) \frac{L_h + L_l}{2}. \quad (222)$$

Here t_h' = the turns per leg of the high-voltage winding.

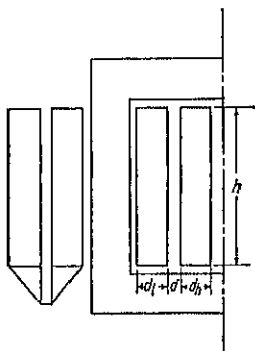


FIG. 236.

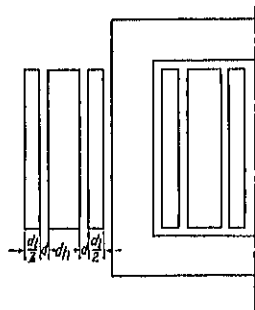


FIG. 237.

When the windings on the two legs are connected in series, the per cent reactance calculated by formula 222 must be multiplied by 2.0, and when connected in parallel it must be multiplied by 0.50. Formula 222 shows that the per cent reactance drop varies directly with the number of turns, the thickness of the coils, the spaces between windings, the average mean-length of turn, and inversely with the length of the coils.

A lower reactance drop can be obtained, for a given number of turns and core length, by arranging the windings as shown in Fig. 237. The per cent reactance for this arrangement,

$$P_x = \frac{10.8ft_h'^2 I_h}{h E_h \times 10^6} \left(\frac{d_h + d_l}{6} + d \right) L_h, \quad (223)$$

per cent impedance drop for the interleaved type of windings arranged as shown in Fig. 238 is,

$$P_z = \frac{11.0 f l_h'^2 I_h x_{hl}}{w_w E_h \times 10^8} \left(\frac{x_h d_{xh} + x_l d_{xl}}{6} + d \right) L_h k_4. \quad (224)$$

The constant

$$k_4 = 1 - \frac{x_h d_{xh} + x_l d_{xl} + 2d}{2\pi w_w}, \quad (225)$$

where x_h and x_l are the number of high-voltage and low-voltage coils per group respectively, l_h' is the number of high-voltage turns per group, and x_{hl} is the number of "high-low" groups.

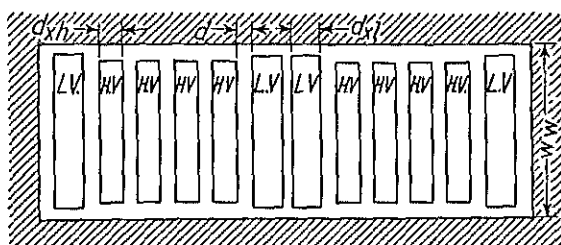


FIG. 238.

This formula does not take into account the leakage flux that passes through the space between the coils of high-voltage and low-voltage groups, which is generally small.²

The per cent impedance drop,

$$P_z = \sqrt{P_x^2 + P_r^2}.$$

The sustained short-circuit current for normal primary voltage,

$$I_s = \frac{E_h}{Z} = \frac{I \times 100}{P_z} \text{ amperes.} \quad (226)$$

The mechanical forces³ on the windings, set up electromagnetically, vary as the square of the current. On short-circuit, these forces may be large enough to distort the coils and destroy the insulation. The windings of large capacity transformers must therefore be carefully braced to withstand the shocks due to short-circuits.

² "Beitrag zur Berechnung der Streuspannung von Transformatorenwicklungen," by R. Kuechler, E. T. Z., Vol. 45, 1924, pp. 273 and 274.

³ "Die Wechselstromtechnik," by Dr. Arnold, Vol. II, p. 185, Julius Springer, Berlin; "Mechanical Stresses in Transformers," by J. F. Peters, Electric Journal, Vol. 12, Dec., 1916, p. 555.

veniently calculated by the formulas given in the Standards of the A.I.E.E., which are explained in various textbooks. For unity-power-factor load,

$$\text{Per cent regulation} = P_r + \frac{P_x^2}{200} \text{ approximately.}$$

For inductive loads of power factor $\cos \theta$ and reactive factor $\sin \theta$,

$$\text{Per cent regulation} = \cos \theta P_r + \sin \theta P_x + \frac{(\cos \theta P_x - \sin \theta P_r)^2}{200}$$

approximately.

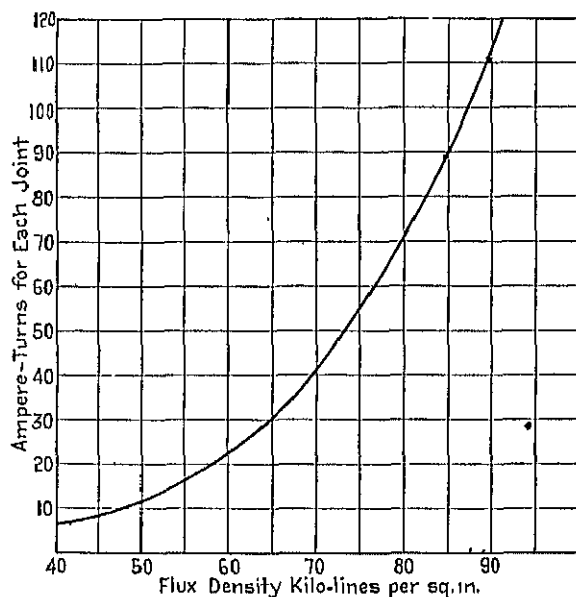


FIG. 239.—Ampere-turns per joint.

Exciting Current.—The current that a transformer draws from the line at no-load may be thought of as consisting of two components: (1) the magnetizing current, I_m , which is 90° out of phase with the impressed voltage, and (2) the core-loss current, I_w , which is in phase with the impressed voltage. The curve in Fig. 239 shows the ampere-turns for each joint in the magnetic circuit of a transformer. The method of calculating the magnetizing current and the core-loss current is explained in the sample problems in Chapter XXIV. The exciting current,

$$I_0 = \sqrt{I_m^2 + I_w^2} \text{ amperes.}$$

Efficiency.—The losses in a transformer are no-load losses and load losses. The no-load losses include core losses, I^2R losses in the windings due to the exciting current, and dielectric losses. Of the no-load losses, only the core losses are calculated because the remaining losses are generally so small that they may be disregarded. The curves in the Appendix give the loss per pound of transformer steel for various densities. In the finished transformer core, these losses are generally from 10 to 15 per cent larger, due to bending and shearing strains, imperfect insulation between sheets, etc.

The load losses include I^2R losses in the windings and stray losses due to stray fluxes in the windings, core clamps, etc. The I^2R losses for the windings are calculated by formula 139a. The stray losses are difficult to predetermine accurately. Dr. Arnold⁴ states that they are generally equal to from 5 to 25 per cent of the total copper losses.

$$\text{The efficiency} = \frac{\text{Kva output} \times \text{PF}}{\text{Kva output} \times \text{PF} + \text{Kw losses}}$$

Temperature Rise.—The Standardization Rules of the A.I.E.E. specify that the limiting temperature rise of transformer windings insulated with cotton, silk, paper, and similar organic materials, when impregnated or immersed in oil, shall not exceed 55° C. The temperature is to be determined by resistance and checked by thermometer. The temperature rise can be predetermined approximately by calculating the exposed surface of the core and ducts and of the coils and ducts. Practice has shown that the ducts are only half as effective as the outside surfaces; therefore only half of the duct surface is used in calculating the effective radiating surface. For a temperature rise not to exceed 55° C. the radiating surface in square-inches-per-watt loss should be equal to 4.5 to 5.5 for natural-air-cooled transformers, from 2.0 to 3.0 for natural-oil-cooled transformers, and from 1.0 to 1.75 for oil-and-water-cooled transformers. The method of calculating the total radiating surface is illustrated by the sample problems in Chapter XXIV.

Design of Tank.—The heat generated by the losses is radiated by the exposed surfaces of the transformer to the cooling medium. When the transformer is immersed in oil, the heat is transmitted by the oil to the tank walls and thence to the surrounding air. Figure 240 shows the results of a test on a small distribution transformer operating at full-load in still air. The temperatures for the various parts of the tank are the values obtained after the temperature has become constant.

⁴ "Die Wechselstromtechnik," Vol. 2, p. 360, Julius Springer, Berlin.

from 1.15 to 1.50 times the average temperature and depends upon the depth of oil above the transformer and upon the circulation. The dimensions of the tank are generally so proportioned that the amount of oil required will be as small as possible. The depth of oil above the transformer should never be less than 2 in.

The difference between the temperature of the transformer windings and the average oil temperature is usually from 15° C. to 20° C. This

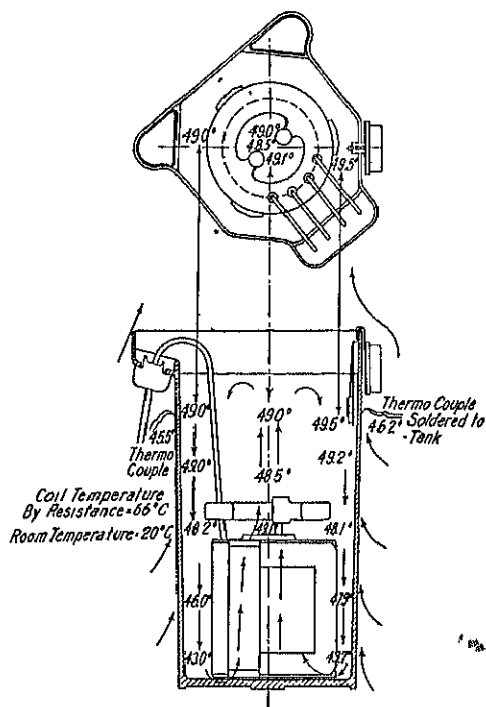


FIG. 240.—Oil temperature in various parts of transformer tank when operating at full load in still air.

difference depends upon the insulation on the coils, the thickness of the coils, etc. For a temperature rise of 55° C. for the windings, the average rise of the oil will then be from 35° C. to 40° C.

Plain sheet-steel tanks such as shown in Fig. 215 are generally used for moderate-voltage distribution transformers of 25-Kva capacity and smaller. For a transformer temperature rise not to exceed 55° C., the square inch wetted tank surface (not including top or bottom) per watt loss should be from 4 to 5.5.

For large-capacity and high-voltage distribution transformers and for power transformers, tanks with corrugated sides or with cooling tubes are used. The square

inch wetted tank surface required for each watt will depend upon the type of tank used. For plain steel tanks with cooling tubes, the wetted square inch tank surface for each watt loss should be from 5 to 6. For corrugated sheet-steel tanks,⁵ S/IV is generally equal to from 6.0 to 9.0 sq. in. per watt loss and depends upon the pitch and depth of the corrugations.

⁵ "Dissipation of Heat from Self-Cooled Oil-Filled Transformer Tanks," by J. J. Frank and H. O. Stephens, A.I.E.E. Trans., Vol. 30, Part I, 1911, pp. 447-456.

the heating and cooling curves for self-oil-cooled transformers can be predetermined with satisfactory accuracy when the specific heat of the various materials used in their construction is known. These curves are necessary to determine the average temperature rise of a transformer used for intermittent duty.

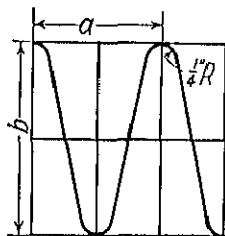


FIG. 241.

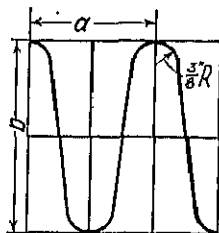


FIG. 242.

Generally, only a small clearance is allowed between the transformer and the walls of the tank (see Figs. 217 and 218). The depth of the oil is then equal to the wetted area of the walls, divided by the perimeter of the tank. The approximate length of the corrugated surface per inch length of center line is given in Table XXXII for several types of corrugated tank walls.

TABLE XXXII

FIGURE 241			FIGURE 242		
<i>a</i>	<i>b</i>	Mean Length of Corrugation per Inch of Center Line	<i>a</i>	<i>b</i>	Mean Length of Corrugation per Inch of Center Line
1½ in.	4 in.	5.75 in.	2.00 in.	4.0 in.	4.45 in.
1½ in.	4 in.	5.00 in.	2.25 in.	4.0 in.	4.05 in.
1½ in.	3 in.	4.50 in.	2.50 in.	4.0 in.	3.66 in.
1½ in.	3 in.	3.86 in.	3.00 in.	4.0 in.	3.42 in.
1½ in.	2 in.	3.75 in.	2.00 in.	3.0 in.	3.51 in.
1½ in.	2 in.	3.17 in.	2.25 in.	3.0 in.	3.12 in.
1½ in.	2 in.	2.73 in.			

The volume of oil required is equal to the volume of the tank, minus the volume of the transformer.

“Essentials of Transformer Practice,” by Emerson G. Reed, 2nd ed., p. 136, D. Van Nostrand Co., New York; and “Cooling of Transformer Windings after Shut-Down,” by V. M. Montsinger, General Electric Review, Vol. 22, Dec., 1919, pp. 1056 to 1066.

CHAPTER XXIV

SAMPLE TRANSFORMER DESIGNS

Design No. 1: *Design of a 400-Kva, Single-Phase, Core-Type Power Transformer.*—The complete rating of the transformer is as follows: 400 Kva, single phase, 60 cycles, 42,000 volts primary to 2400 volts secondary. The transformer is to be of the self-oil-cooled type and must carry its rated load continuously with a temperature rise not to exceed 55° C. The full-load 100 per cent power factor efficiency must not be less than 98.0 per cent and the ratio of losses should be approximately 1.0.

For a ratio of losses equal to 1.0, the flux density in the core can be chosen equal to 90,000 lines per sq. in. From the iron loss curves in the Appendix for 0.014-in., 4.0 per cent silicon steel, the loss per pound for this density, $w_c = 0.029 \times 1.12 \times 60 = 1.94$ watts, if the additional losses are taken equal to 12.0 per cent of the fundamental frequency loss (see page 369).

For an average current density, $A = 1500$ amperes per sq. in., the copper loss per pound (formula 139a),

$$w_k = 2.58A^2 \times 10^{-6} = 2.58 \times 1500^2 \times 10^{-6} = 5.8 \text{ watts.}$$

The ratio of core weight to copper weight,

$$\frac{G_c}{G_k} = \frac{w_k}{w_c} \times \frac{W_c}{W_k} = \frac{5.8}{1.94} \times 1 = 2.99.$$

The output constant is taken equal to 0.45 (see page 348) and the net section area of the core,

$$\begin{aligned} A_c &= C \sqrt{\frac{\text{Kva} \frac{G_c}{G_k} 10^{11}}{BAf}} = 0.45 \sqrt{\frac{400 \times 2.99 \times 10^{11}}{90,000 \times 1500 \times 60}} \\ &= 54.5 \text{ sq. in.} \end{aligned}$$

The cruciform-shaped core section shown in Fig. 222 will be used for this transformer. The diameter of the core,

$$D = \sqrt{\frac{A_c \times 4}{\pi f_{cs}}} = \sqrt{\frac{51.5 \times 4}{3.14 \times 0.70}} = 9.95; \text{ use } 10.0 \text{ in.}$$

The calculations for the core space factor, f_{cs} , are given on page 350.

The dimensions of the core section (see Fig. 243) are:

$$2a = 0.526D = 0.526 \times 10.0 = 5.26; \text{ use } 5.25 \text{ in.}$$

$$2b = 0.85D = 0.85 \times 10 = 8.5 \text{ in.} \checkmark$$

The total flux for a density of 90,000 lines per sq. in.,

$$\phi = A_c B = 54.5 \times 90,000 = 4900 \text{ kilo-lines.}$$

The number of turns for high-voltage and low-voltage windings,

$$t_h = \frac{E_h \times 10^8}{4.44 f \phi_t} = \frac{42,000 \times 10^8}{4.44 \times 60 \times 4900 \times 10^3} = 3220.$$

$$t_l = \frac{E_l}{E_h} \times t_h = \frac{2400}{42,000} \times 3220 = 184.$$

The full-load current in the two windings,

$$I_h = \frac{KVA \times 10^3}{E_h} = \frac{400 \times 10^3}{42,000} = 9.52 \text{ amperes}$$

$$I_l = \frac{t_h}{t_l} I_h = \frac{3220}{184} 9.52 = 166.5 \text{ amperes.}$$

For the average current density assumed above, the section area of the conductors for the high-voltage and low-voltage windings,

$$s_{ch} = \frac{I_h}{A} = \frac{9.52}{1500} = 0.00635 \text{ sq. in.}$$

$$s_{cl} = \frac{I_l}{A} = \frac{166.5}{1500} = 0.111 \text{ sq. in.}$$

The area of the window opening,

$$\begin{aligned} h_w w_w &= \frac{2s_{ch} t_h}{f_s} = \frac{2 \times 0.00635 \times 3220}{0.105} \\ &= 389.0 \text{ sq. in.} \end{aligned}$$

The copper space factor, f_s , is taken from the curves of Fig. 224.

For a ratio of window height to window width equal to 3, the dimensions of the window are:

$$h_w = \sqrt{3 \times 389} = 34.2 \text{ in.}; \text{ use } 35.0 \text{ in.}$$

$$w_w = \frac{34.2}{3} = 11.4 \text{ in.}; \text{ use } 11.0 \text{ in.}$$

It is desirable at this point to calculate the approximate core and copper weight, to determine whether the core dimensions selected above give approximately the ratio of core weight to copper weight desired.

The flux density in the yoke will be made equal to the flux density in the core legs. The height of the yoke section

$$= \frac{54.5}{0.90 \times 8.5} = 7.125 \text{ in.}$$

The length of the yoke,

$$l_y = w_w + (2 \times 2b) = 11.0 + (2 \times 8.5) = 28.0 \text{ in.}$$

The total weight of the core,

$$\begin{aligned} G_c &= [2l_y A_c + (2h_w A_c)] 0.272 \\ &= [2 \times 28.0 \times 54.5 + (2 \times 35 \times 54.5)] 0.272 = 1870 \text{ lb.} \end{aligned}$$

The clearance, β , between the two coils in the window opening should be approximately 1.25 in. The length of the average mean-turn for the windings,

$$L_{av} = \left(D + \frac{w_w - \beta}{2} \right) \pi = \left(10.0 + \frac{11.0 - 1.25}{2} \right) \pi = 46.7 \text{ in.}$$

The approximate total copper weight,

$$\begin{aligned} G_k &= 2l_{hsc} I_{L_{av}} \times 0.321 \\ &= 2 \times 3220 \times 0.00635 \times 46.70 \times 0.321 = 613.0 \text{ lb.} \end{aligned}$$

The ratio of core weight to copper weight,

$$\frac{G_c}{G_k} = \frac{1870.0}{613.0} = 3.05.$$

The dimensions of the window are, then,

$$h_w = 35.0 \text{ in.}, \quad w_w = 11.0 \text{ in.}$$

Low-Voltage Winding.—The section area of the low-voltage conductor, $s_{cl} = 0.111$ sq. in. Two conductors, each 0.204×0.258 -in. bare, 0.227×0.280 -in. insulated, 0.0507 sq. in. area, are wound in parallel.

A helical-wound coil with transposed conductors as shown in Fig. 230 is used for the low-voltage winding.

The number of turns per core leg

$$= \frac{184}{2} = 92.$$

The conductor is wound flat, with the two parallel wires on top of each other. The space occupied by the winding in the direction of the window height

$$= 0.28 \times 92 = 25.8 \text{ in.}$$

For a window 35 in. high, there will be a clearance of 4.6 in. at each end of the winding, which is required for insulation and supporting collars.

The insulation between the low-voltage winding and core consists of $\frac{1}{16}$ -in. fuller-board channels placed over the corners of the core, $\frac{3}{16}$ -in. pressed paper cylinder, and a $\frac{1}{4}$ -in. duct as shown in Fig. 243.

High-Voltage Winding.—Disc type coils will be used for the high-voltage winding. The following conductor is selected from the copper table:

Bare.....	0.025 × 0.258 in.
Insulated.....	0.043 × 0.270 in.
Area.....	0.00632 sq. in. ~

The number of turns per core

$$= \frac{3220}{2} = 1610.$$

Extra insulation is required on the end-turns of high-voltage transformers (see page 360). Therefore the number of turns in the coils should be so proportioned that the end coils will have a smaller number of turns, to provide space for the extra insulation. Approximately 4.5 per cent of the high-voltage turns on each end of the winding should have extra insulation. Coils with two turns per layer, half of the turns wound backward to avoid cross-over, will be used. Fuller-board 0.020

coils and number of turns per layer are as follows:

Number of Coils per Core Leg	Turns per Section	Turns per Coil	Total Turns
24	30	60	1440
1	28	56	56
1	25	50	50
1	20	40	40
1	10 and 14	24	24
Turns per core leg.....	1610

The coils are insulated from each other by $\frac{5}{16}$ -in. oil ducts; between the end coils wider ducts are used, as shown in Fig. 243.

The width of each coil in the direction of the window height

$$= 2 \times 0.27 + 0.020 = 0.560 \text{ in.}$$

The four end coils have extra insulation and therefore require more space. If 10 per cent is allowed for the space required for the extra insulation, the width of each of the four end coils

$$= 0.560 \times 1.10 = 0.616 \text{ in.}$$

The total space occupied by the coils in the direction of the window height

$$= 24 \times 0.560 + 4 \times 0.616 = 15.91 \text{ in.}$$

The total duct space between the coils (see Fig. 243)

$$= 24 \times \frac{5}{16} + 2 \times \frac{3}{8} + \frac{6}{16} = 8.81 \text{ in.}$$

The high-voltage winding therefore occupies 24.72 in. in the direction of the window height. With a window opening 35 in. high, there is a space of 5.23 in. at each end of the winding, which is required for insulation and supporting collars.

The insulation between the high-voltage and low-voltage winding consists of a $\frac{1}{2}$ -in. duct, plus a pressed paper insulating cylinder $\frac{5}{16}$ -in. thick, plus $\frac{1}{2}$ -in. duct. The total thickness of the windings

$$= 0.75 + 0.50 + 2 \times 0.227 + 0.50 + 0.3125 + 0.50 +$$

$$30(0.043 + 0.015) = 4.76 \text{ in.}$$

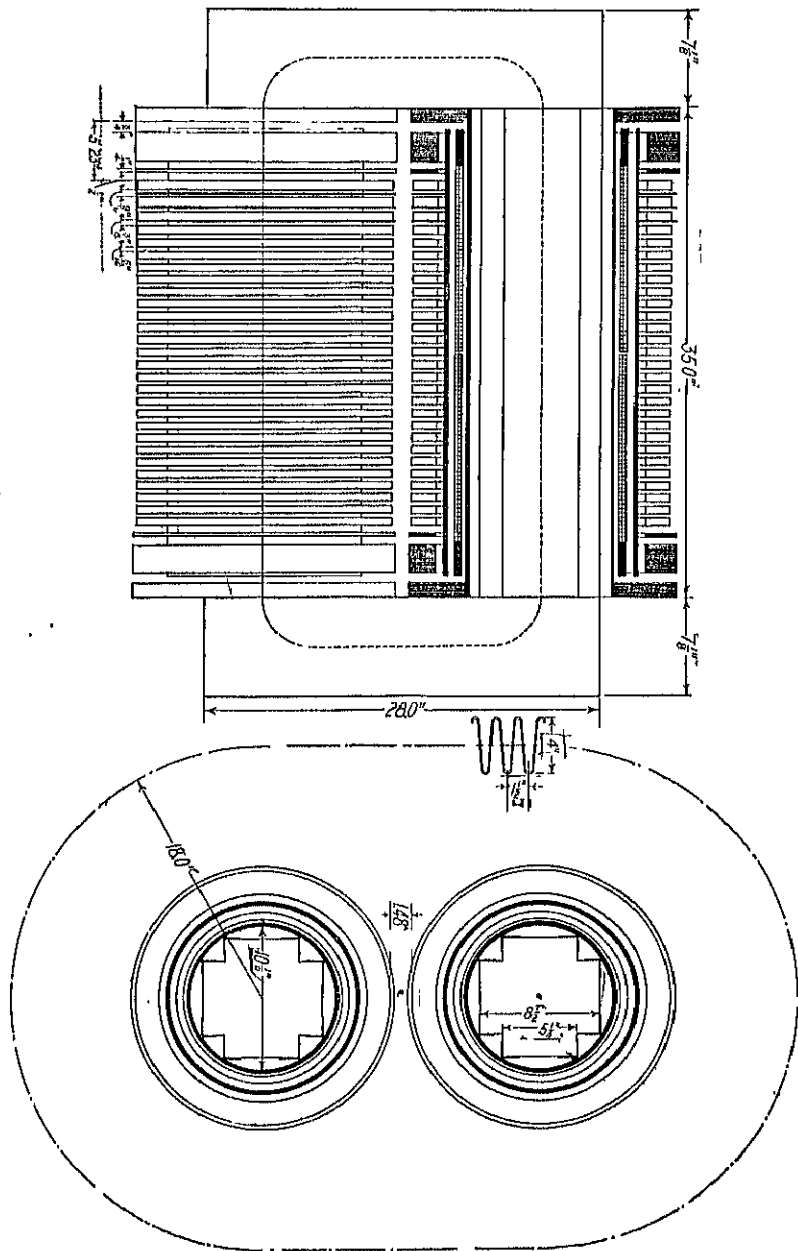


FIG. 243.

The clearance between the coils in the window opening

$$\approx 11.0 - 2 \times 4.76 = 1.48 \text{ in.}$$

The total flux,

$$\phi_t = \frac{E_h \times 10^8}{4.44 f l_h} = \frac{42,000 \times 10^8}{4.44 \times 60 \times 3220} = 4900.0 \text{ kilo-lines.}$$

The flux density in the core,

$$B = \frac{4900 \times 10^3}{54.5} = 90,000 \text{ lines per sq. in.}$$

The dimensions of the core have not been changed; therefore the total core weight is the same as given.

The current density in the low-voltage winding,

$$A_l = \frac{166.5}{2 \times 0.0507} = 1640 \text{ amperes per sq. in.}$$

and in the high-voltage winding,

$$A_h = \frac{9.52}{0.00632} = 1503 \text{ amperes per sq. in.}$$

The length of the mean-turn for the low-voltage winding,

$$L_l = \pi[10.0 + (0.50 \times 2) + (2 \times 0.227)] = 36.0 \text{ in.}$$

and for the high-voltage winding,

$$\begin{aligned} L_h &= \pi[10.0 + (2 \times 0.50) + 2(2 \times 0.227) + (2 \times 1.3125) \\ &\quad + 30(0.043 + 0.015)] \\ &= 51.1 \text{ in.} \end{aligned}$$

The copper weight for each of the windings,

$$\begin{aligned} G_l &= t_{sc_l} L_l \times 0.321 \\ &= 184 \times 2 \times 0.0507 \times 36.0 \times 0.321 = 216.0 \text{ lb.} \end{aligned}$$

$$\begin{aligned} G_h &= t_{sc_h} L_h \times 0.321 \\ &= 3220 \times 0.00632 \times 51.1 \times 0.321 = 334.0 \text{ lb.} \end{aligned}$$

The total copper weight,

$$G_k = 216 + 334 = 550.0 \text{ lb.}$$

The ratio of core weight to copper weight,

$$\frac{G_o}{G_k} = \frac{1870}{550} = 3.40.$$

This value of the ratio of weights is higher than the one calculated above because of the high current density chosen for the low-voltage winding.

The output constant,

$$C = \frac{A_c}{\sqrt{\frac{\text{Kva } G_r/G_k \times 10^{11}}{BAf}}} = \frac{54.5}{\sqrt{\frac{400 \times 3.40 \times 10^{11}}{90,000 \times 1572 \times 60}}} = 0.43.$$

The copper space factor,

$$\begin{aligned} f_s &= \frac{s_{cht_h} + s_{clt_l}}{h_w w_w} = \frac{0.00632 \times 3220 + 0.1014 \times 184}{35.0 \times 11.0} \\ &= 0.1015. \end{aligned}$$

From the loss curve for 0.014 in., 4.0 per cent silicon steel, the loss per pound for a density of 90 kilo-lines per sq. in.,

$$w_o = 0.029 \times 1.12 \times 60 = 1.94 \text{ watts.}$$

The total core loss,

$$W_o = w_o G_k = 1.94 \times 1870 = 3630 \text{ watts.}$$

The I^2R loss in each of the windings at 75°C. ,

$$\begin{aligned} W_l &= 2.58 A_l^2 G_l \times 10^{-6} \\ &= 2.58 \times 1640^2 \times 216 \times 10^{-6} = 1490 \text{ watts} \end{aligned}$$

$$\begin{aligned} W_h &= 2.58 A_h^2 G_h \times 10^{-6} \\ &= 2.58 \times 1503^2 \times 334 \times 10^{-6} = 1940 \text{ watts.} \end{aligned}$$

The ratio of losses,

$$\frac{W_o}{W_k} = \frac{3630}{3430} = 1.06.$$

The resistance of the low-voltage and high-voltage windings at 75°C. ,

$$R_l = \frac{W_l}{I_l^2} = \frac{1490}{160.5^2} = 0.0537 \text{ ohm}$$

$$R_h = \frac{W_h}{I_h^2} = \frac{1940}{9.52^2} = 21.4 \text{ ohms.}$$

The total resistance in terms of the high-voltage winding,

$$R_t = \frac{1490 + 1940}{9.52^2} = 37.90 \text{ ohms.}$$

The per cent resistance drop,

$$P_r = \frac{I_h R_t}{E_h} 100 = \frac{9.52 \times 37.90}{42,000} 100 = 0.858 \text{ per cent.}$$

Formula 222 gives the per cent reactance drop for one core leg of a core type transformer with concentric type winding. For our problem, the windings on the two core legs are connected in series; therefore, formula 222 must be multiplied by 2.

$$\begin{aligned} P_x &= 2 \frac{21.5 f l_h'^2 I_h}{h_w E_h \times 10^6} \left(\frac{d_h + d_l}{3} + d \right) \frac{I_h + I_l}{2} \\ &= 2 \frac{21.5 \times 60 \times 1610^2 \times 9.52}{24.72 \times 42,000 \times 10^6} \left(\frac{1.74 + 0.454}{3} + 1.313 \right) \checkmark \\ &\quad \frac{51.1 + 36.0}{2} = 5.45 \text{ per cent.} \end{aligned}$$

The per cent impedance drop,

$$P_z = \sqrt{P_x^2 + P_r^2} = \sqrt{5.45^2 + 0.858^2} = 5.52 \text{ per cent.}$$

The sustained short-circuit current for normal primary voltage,

$$I_s = \frac{I \times 100}{P_z} = \frac{9.52 \times 100}{5.52} = 172.5 \text{ amperes.}$$

To calculate the mechanical stresses on the windings due to the short-circuit current, see references on page 367.

The per cent regulation for 100 per cent power factor load

$$= P_r + \frac{P_x^2}{200} = 0.858 + \frac{5.45^2}{200} = 1.007 \text{ per cent}$$

and for 80 per cent power factor load, per cent regulation

$$\begin{aligned} &= \cos \theta P_r + \sin \theta P_x + \frac{(\cos \theta P_x - \sin \theta P_r)^2}{200} \\ &= 0.80 \times 0.858 + 0.60 \times 5.45 \\ &\quad + \frac{(0.80 \times 5.45 - 0.60 \times 0.858)^2}{200} \\ &= 4.03 \text{ per cent.} \end{aligned}$$

The mean length of the flux path is shown by the dotted line in Fig. 243 and is

$$= (35.0 + 7.125)2 + (11.0 + 8.5)2 = 123.25 \text{ in.}$$

From the standard magnetization curve for 4.0 per cent silicon steel,

the ampere-turns per inch for a density of 90 kilo-lines, $at = 29.5$.
The total ampere-turns necessary to maintain the flux in the iron part of the magnetic circuit

$$= at \times 123.25 = 29.5 \times 123.25 = 3640.$$

The ampere-turns for each joint for a density of 90.0 kilo-lines = 113.0 (see Fig. 239). With 4 joints in the magnetic circuit, the ampere-turns

$$= 4 \times 113.0 = 452.$$

The magnetizing current,

$$I_m = \frac{AT}{\sqrt{2} l_h} = \frac{4092}{\sqrt{2} \times 3220} = 0.90 \text{ amperes.}$$

The in-phase component of the no-load current,

$$I_w = \frac{W_o}{E_h} = \frac{3630}{42,000} = 0.0865 \text{ amperes.}$$

The exciting current,

$$I_o = \sqrt{I_m^2 + I_w^2} = \sqrt{0.90^2 + 0.0865^2} = 0.904 \text{ amperes.}$$

The stray load-losses will be estimated equal to 10 per cent of the total I^2R losses (see page 369). The efficiencies and losses for various loads at 100 per cent and 80 per cent lagging power factor are as follows:

	$\frac{1}{4}$	$\frac{2}{4}$	$\frac{3}{4}$	$\frac{4}{4}$	$\frac{5}{4}$
I^2R + stray load-losses	236.5	946	2,134	3,773	5,918
Core losses	3,030.0	3,030	3,030	3,030	3,030
Total losses	3,866.5	4,576	5,764	7,403	9,548
Output	100,000.0	200,000	300,000	400,000	500,000
Input	103,866.5	204,576	305,764	407,403	509,548
Efficiency 100% PF	96.30	97.70	98.20	98.20	98.20
Efficiency 80% PF	95.40	97.20	97.70	97.70	97.70

The total radiating surface of the transformer winding and core is calculated as follows:

$$\text{Core legs: } (4 \times 5.25 + 4 \times 3.25) 2 \times 35 = 2,380 \text{ sq. in.}$$

$$\text{Yokes: } (4 \times 7.125 \times 28 + 8.5 \times 28.0 \times 2 + 7.125 \times 8.5 \times 4) = 1,516 \text{ sq. in.}$$

$$\text{Low-voltage winding: } (2 \times 36.0 \times 25.8 \times 2) = 3,720 \text{ sq. in.}$$

High-voltage winding: $2(0.56 + 1.74) 51.1 \times 28 \times 2 = 13,200$ sq. in.
 Total radiating surface $= 20,816$ sq. in.
 and the surface per watt loss,

$$\frac{S}{W} = \frac{20,816}{7403} = 2.81.$$

For a corrugated sheet-steel tank, the surface per watt loss should be approximately 7.5 (see page 370). The total wetted tank surface,

$$S_t = (W_o + W_k)S/W = 7403 \times 7.5 = 55,500 \text{ sq. in.}$$

Figure 243 shows the shape of the tank section and the position of the transformer in the tank. The length of the surface of the corrugations for each inch of length of the center line equals 5.75 in. The clearance between the outside of the coils and the inside of the tank is 7.0 in. and the length of the center line of the corrugated tank wall

$$= 2(11.0 + 8.5) + \pi \times 36.0 = 152.0 \text{ in.}$$

The depth of the hot oil

$$= \frac{55,500}{152.0 \times 5.75} = 63.5 \text{ in.}$$

The volume of oil required is equal to the volume of the tank minus the volume of the transformer. The volume of the transformer can be calculated approximately from the weight of the active materials. The insulation, core clamps, coil supports, etc., occupy only a small per cent of the space required for the active material. The volume of the tank

$$= \left(\frac{\pi}{4} \times 36.0^2 + 36 \times 19.5 \right) 63.5 = 109,000 \text{ cu. in.}$$

The approximate volume of the transformer

$$= \frac{1870}{0.272} + \frac{550}{0.321} = 8595 \text{ cu. in.}$$

The volume of oil required is therefore equal to 100,405 cu. in. The number of cubic inches in a gallon is 231; therefore 435 gallons of oil are required, or 1.09 gallons per Kva. One gallon of transformer oil weighs approximately 7.0 lb.; the total weight of the oil is then,

$$7.0 \times 435 = 3050.0 \text{ lb.}$$

In the assembly drawing of the transformer, Fig. 243, the core clamps, coil supports, etc., have been omitted.

Kva, 400	Phase, Single	Cycles, 60	Volts {	IV, 42,000	Phase Volts {	IV, . . .
	Line Amperes {	IV, 9 52		LV, 2,400		LV, . . .
		LV, 166.5			Phase Amperes {	IV, . .
	Type, Circular Core					LV, . .
			Type of Cooling, Self Oil			

Per cent				
Resistance				0.85
Reactance				5.45
Impedance				5.52
Power factor		80		100
Regulation		4.03		1.007
Losses				
Total core				3630.0
Stray load				343.0
Total copper				3130.0
Per cent.				
Load	25	50	75	100
Efficiency	96.3	97.7	98.2	98.2
Square inches per watt				2.81
Ratio of losses				1.06
Ratio of weights				3.10

Type of tank, corrugated sheet steel, 1½ X 4 0	
Square inches per watt	7 5
Total wetted surface	55,500
Depth of oil	63 5
Gallons of oil	135 0
Weight of oil	3050 0
Cooling coils.	
Size	
Length	
Surface	
Water, gallons per minute	

HIGH VOLTAGE	LOW VOLTAGE
Disc coils	Helical
0.013 X 0.27 d.c.c.	0.227 X 0.28 d.c.c.
0.00632	0.0507
None	2
1503	1640
3220	184
56	2
28	1
*	02
†	02
2-sections	1
Series	Series
0.56 X 1.74	0.451 X 25.8
1-1/2; 2-1/2; 1-1/2	
0.015	
D. + 1/16 P.B. + 1/4 D.	1/16 P.B. + 1/16 P.B. + 1/4 D.
13.05	
783	
51.1	36.0
334.0	216.0
1940.0	1400.0
21.4	0.0537
5.3	

Remarks:	* 2½ coils, 60 turns	1 2½ coils, 30 turns per section
	1 coil, 50 turns	1 coil, 28 turns per section
	1 coil, 50 turns	1 coil, 25 turns per section
	1 coil, 40 turns	1 coil, 20 turns per section
*	1 coil, 24 turns	1 coil, 10 and 14 turns per section

Date:

Design No. 2: *Design of a 1000-Kva, Three-Phase, Core-Type Power Transformer.*—The complete rating of the transformer is as follows: 1000 Kva, three-phase, 60 cycles, 7960 volts primary to 575 volts secondary, with delta-connected primary and secondary windings. The transformer is to be of the self-oil-cooled type and must carry its rated load continuously with a temperature rise not to exceed 50° C. The full-load, 100 per cent power factor efficiency must not be less than 98.2 per cent and the ratio of the core loss to copper loss should be approximately 0.90.

For a ratio of losses equal to 1.0, the flux density in the core can be taken equal to 90,000 lines per sq. in. For this density the core loss per pound for 2.5 per cent silicon steel, 0.014 in. thick,

$$w_c = 0.032 \times 1.12 \times 60 = 2.15 \text{ watts,}$$

if the additional losses are taken equal to 12.0 per cent of the fundamental frequency loss (see page 369).

For an average current density, $A = 1550$ amperes per sq. in, the copper loss per pound,

$$w_k = 2.58A^2 \times 10^{-6} = 2.58 \times 1550^2 \times 10^{-6} = 6.18 \text{ watts.}$$

The ratio of core weight to copper weight,

$$\frac{G_c}{G_k} = \frac{w_k}{w_c} \frac{W_c}{W_k} = \frac{6.18}{2.15} 0.90 = 2.58.$$

With an output constant equal to 0.36 (see page 348) the net core section area,

$$\begin{aligned} A_c &= C \sqrt{\frac{Kva \ G_c/G_k \times 10^{11}}{BAf}} = 0.36 \sqrt{\frac{1000 \times 2.58 \times 10^{11}}{90,000 \times 1550 \times 60}} \\ &= 63.2 \text{ sq. in.} \end{aligned}$$

The cruciform core section shown in Fig. 222 is chosen. The diameter of the core (see page 350),

$$D = \sqrt{\frac{A_c \times 4}{\pi f_{cs}}} = \sqrt{\frac{63.2 \times 4}{3.14 \times 0.70}} = 10.70 \text{ in.}$$

Make this 10.75 in. and the dimensions of the core section (see Fig. 244) are:

$$2a = 0.526 \times D = 0.526 \times 10.75 = 5.65; \text{ use } 5\frac{5}{8} \text{ in.}$$

$$2b = 0.85D = 0.85 \times 10.75 = 9.13; \text{ use } 9\frac{1}{8} \text{ in.}$$

With these dimensions, the net section of the core,

$$A_c = [5\frac{5}{8} \times 9\frac{1}{8} + 5\frac{5}{8}(9\frac{1}{8} - 5\frac{5}{8})] 0.90 = 63.9 \text{ sq. in.}$$

With a density of 90,000 lines per sq. in., the total flux,

$$\phi_t = A_c B = 63.9 \times 90,000 = 5750 \text{ kilo-lines.}$$

The number of turns per phase for the high-voltage and low-voltage windings,

$$t_h = \frac{E_h \times 10^8}{4.44 f \phi_t} = \frac{7960 \times 10^8}{4.44 \times 60 \times 5750 \times 10^3} = 520; \text{ use } 512.$$

$$t_l = \frac{E_l}{E_h} t_h = \frac{575}{7960} 520 = 37.6; \text{ use } 37.0.$$

Using 37.0 turns per phase on the low-voltage winding, the number of high voltage turns per phase will be equal to 512.

The voltage per turn

$$= \frac{7960}{512} = 15.5 \text{ volts.}$$

The full-load current per phase for the high-voltage winding,

$$I_h = \frac{Kva \times 10^3}{3 E_h} = \frac{1000 \times 10^3}{3 \times 7960} = 41.8 \text{ amperes}$$

and for the low-voltage winding,

$$I_l = \frac{Kva \times 10^3}{3 E_l} = \frac{1000 \times 10^3}{3 \times 575} = 580.0 \text{ amperes.}$$

For the average current density assumed above, the section area of the conductor for the high-voltage winding,

$$s_{ch} = \frac{I_h}{A} = \frac{41.8}{1550} = 0.027 \text{ sq. in.}$$

The area of the window opening,

$$h_w w_w = \frac{4 s_{ch} t_h}{f_s} = \frac{4 \times 0.027 \times 512}{0.18} = 308.0 \text{ sq. in.}$$

The copper space factor, f_s , is taken from the curves (Fig. 224).

If window height equal to three times the width is chosen, the dimensions of the window are,

$$h_w = \sqrt{3 \times 308.0} = 30.4 \text{ in.}; \text{ use } 30.5 \text{ in.}$$

$$w_w = \frac{308.0}{30.5} = 10.10 \text{ in.}; \text{ use } 10\frac{1}{8} \text{ in.}$$

With the flux density in the yoke equal to the flux density in the core legs, the height of the yoke

$$= \frac{63.9}{9.125 \times 0.90} = 7.75 \text{ in.}$$

The length of the yoke,

$$\begin{aligned} l_y &= 2w_w + 3 \times 2b = 2 \times 10.125 + 3 \times 9.125 \\ &= 47.625 \text{ in.} \end{aligned}$$

The total core weight,

$$\begin{aligned} G_c &= (2l_y A_c + 3h_w A_c) 0.272 \\ &= (2 \times 47.625 \times 63.9 + 3 \times 30.5 \times 63.9) 0.272 = 3250 \text{ lb.} \end{aligned}$$

With a clearance, β , between adjacent coils in the window opening equal to 1.0 in., the length of the average mean-turn for the windings,

$$L_{av} = \left(D + \frac{w_w - \beta}{2} \right) \pi = \left(10.75 + \frac{10.125 - 1.0}{2} \right) \pi = 48.0 \text{ in.}$$

The approximate total copper weight,

$$\begin{aligned} G_k &= 2 \times 3t_k s_{ch} L_{av} \times 0.321 \\ &= 2 \times 3 \times 512 \times 0.027 \times 48.0 \times 0.321 = 1280 \text{ lb.} \end{aligned}$$

The ratio of active material weight is then,

$$\frac{G_c}{G_k} = \frac{3250}{1280} = 2.54.$$

This is approximately the same as the value previously determined.

DESIGN OF WINDINGS

Low-Voltage Winding.—The low-voltage winding is placed close to the core and, consequently, has a shorter mean-turn than the high-

voltage coil. A higher current density can therefore be used without excessive copper loss. With a current density equal to 1700 amperes per sq. in., the conductor section,

$$s_{cl} = \frac{580.0}{1700} = 0.341 \text{ sq. in.}$$

Five parallel conductors are used, each 0.182×0.365 in. bare, 0.206×0.386 in. insulated, and of 0.0645 sq. in. area. With this conductor, the current density in the low-voltage winding,

$$A_l = \frac{580.0}{5 \times 0.0645} = 1800 \text{ amperes per sq. in.}$$

A helical-wound coil with transposed conductors such as shown in Fig. 230 is used. The five parallel conductors are wound on top of one another with a 0.25-in. duct between turns. The height of the low-voltage coil

$$= 37 \times 0.386 + 36 \times 0.25 = 23.30 \text{ in.}$$

and the thickness of the coil,

$$d_l = 5 \times 0.206 = 1.03 \text{ in.}$$

The insulation between the low-voltage winding and core consists of a pressed paper cylinder $\frac{1}{8}$ in. thick and a $\frac{1}{4}$ -in. duct, as shown in Fig. 244.

High-Voltage Winding.—The high-voltage winding is wound over the low voltage coil and therefore has a large mean-turn. To avoid excessive copper loss, the current density should be less than for the low-voltage coil. With 1200 amperes per sq. in., the section area of the conductor,

$$s_{oh} = \frac{41.8}{1200} = 0.0348 \text{ sq. in.}$$

A conductor 0.129×0.258 in. bare, 0.149×0.276 in. insulated, 0.0325 sq. in. area is selected and,

$$A_h = \frac{41.8}{0.0325} = 1280 \text{ amperes per sq. in.}$$

Disc type coils with two turns per layer are chosen for the high-voltage winding. One-half of the turns of each coil are wound backward to avoid cross-overs. The two sections of each coil are insulated

from each other by fuller-board 0.013 in. thick. The number of coils per core leg and number of turns per coil are as follows:

Number of Coils per Core Leg	Turns per Section	Turns per Coil	Total Turns
27	9	18	486
1	8	16	16
1	5	10	10
Turns per core leg.	512

The coils are insulated from each other by $\frac{1}{4}$ -in. ducts. Between the end coils, a wider duct is used as shown in Fig. 244. The width of the high-voltage coils

$$= 2 \times 0.276 + 0.013 = 0.565 \text{ in.}$$

If 10 per cent is allowed for the space required by the extra insulation on the end coils, then the width of the two end coils

$$= 0.565 \times 1.10 = 0.620 \text{ in.}$$

The total space required for the high-voltage coils in the direction of the window height

$$= 27 \times 0.565 + 2 \times 0.62 = 16.49 \text{ in.}$$

There are twenty-seven $\frac{1}{4}$ -in. ducts and one $\frac{3}{16}$ -in. duct between the coils. The total height of the winding is then

$$= 16.49 + 7.31 = 23.80 \text{ in.}$$

A clearance of 2.5 in. at each end of the winding for insulating and supporting collars is satisfactory for a 7960-volt transformer winding. The window height is therefore reduced to 29.0 in. and the total clearance at both ends of the winding

$$= 29.0 - 23.80 = 5.20 \text{ in.}$$

With the insulation between turns 0.013 in. thick, the thickness of the high-voltage coils

$$= 0.149 \times 9 + 8 \times 0.013 = 1.45 \text{ in.}$$

The insulation between high-voltage and low-voltage windings consists of a $\frac{3}{8}$ -in. duct, plus $\frac{3}{16}$ -in. pressed paper insulating cylinder,

plus a $\frac{1}{2}$ -in. duct. The total depth of the windings per core leg is then

$$= 0.813 + 0.375 + 1.03 + 1.063 + 1.45 = 4.731 \text{ in.}$$

With a window width equal to 10.125 in., the clearance between adjacent coils in the window opening

$$= 10.125 - 2 \times 4.731 = 0.663 \text{ in.}$$

This clearance should preferably be about 1.0 in. for a transformer of

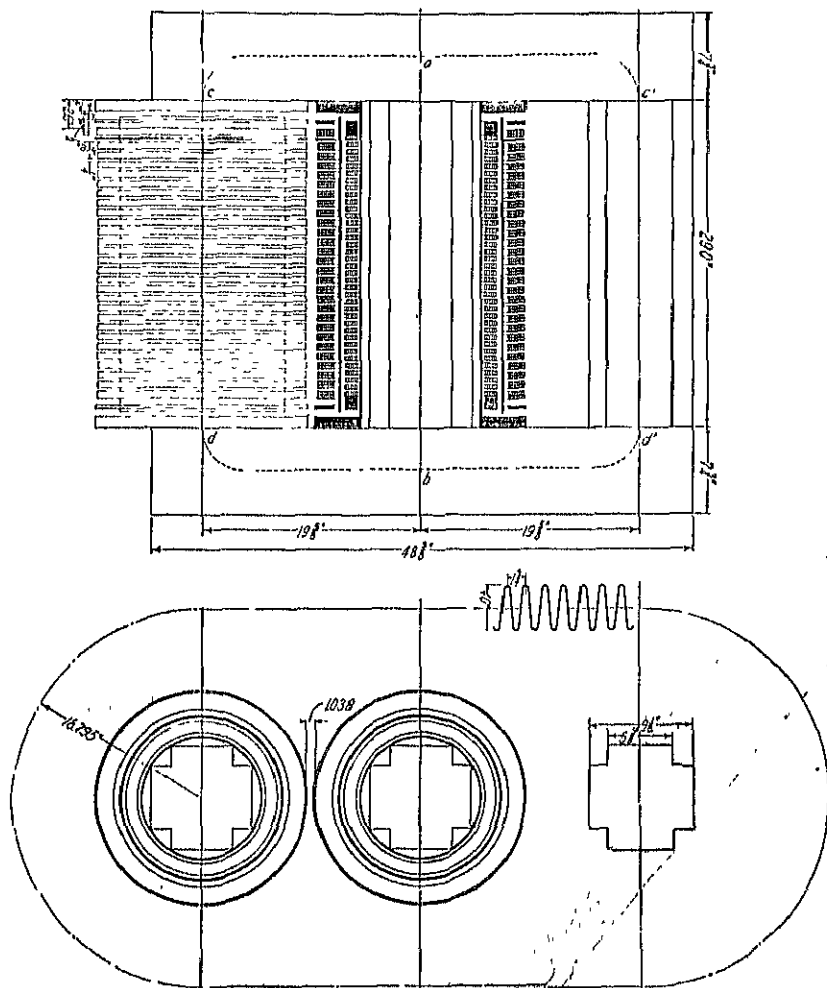


FIG. 244.

clearance between coils equals 1.038 in.

The dimensions of the window are then,

$$h_w = 29.0 \text{ in.}, \quad w_w = 10.5 \text{ in.}$$

The total flux,

$$\phi_t = \frac{E_h \times 10^8}{4.44 f l_h} = \frac{7960 \times 10^8}{4.44 \times 60 \times 512} = 5830 \text{ kilo-lines.}$$

The flux density in the core,

$$B = \frac{5830 \times 10^3}{63.9} = 91.3 \text{ kilo-lines.}$$

Since the dimensions of the window have been changed from the values first determined, it will be necessary to recalculate the weight of the core. The length of the yoke,

$$l_y = 2 \times 10.5 + 3 \times 9.125 = 48.375 \text{ in.}$$

and

$$G_c = (2 \times 48.375 \times 63.9 + 3 \times 29.0 \times 63.9) 0.272 = 3190 \text{ lb.}$$

The length of the mean-turn for the low-voltage winding,

$$L_l = \pi[10.75 + (2 \times 0.375) + 1.03] = 39.40 \text{ in.}$$

and for the high-voltage winding,

$$\begin{aligned} L_h &= \pi[10.75 + (2 \times 0.375) + (2 \times 1.03) + (2 \times 1\frac{1}{16}) + 1.45] \\ &= 53.9 \text{ in.} \end{aligned}$$

The weight of the copper in each winding,

$$\begin{aligned} G_l &= 3 t_{sl} L_l \times 0.321 \\ &= 3 \times 37 \times 0.3225 \times 39.40 \times 0.321 = 452.0 \text{ lb.} \end{aligned}$$

$$\begin{aligned} G_h &= 3 t_{sh} L_h \times 0.321 \\ &= 3 \times 512 \times 0.0325 \times 53.9 \times 0.321 = 863.0 \text{ lb.} \end{aligned}$$

The total copper weight,

$$G_k = 452 + 863 = 1315 \text{ lb.}$$

The final value for the ratio of the weights of the active material is therefore,

$$\frac{G_c}{G_k} = \frac{3190}{1315} = 2.43,$$

which is slightly lower than the value previously determined, because of the changes made in the core dimensions.

The design constant for this transformer is then,

$$C = \frac{A_e}{\sqrt{\frac{K_{va} G_c / G_k \times 10^{11}}{BAf}}} = \frac{63.9}{\sqrt{\frac{1000 \times 2.43 \times 10^{11}}{91,300 \times 1540 \times 60}}} \\ = 0.376$$

The copper space factor,

$$f_s = \frac{2(s_{ch}t_h + s_{cl}t_l)}{h_w w_{lv}} = \frac{2(0.0325 \times 512 + 0.3225 \times 37)}{29.0 \times 10.5} \\ = 0.188.$$

From the loss curve for 0.014 in. - 2.5 per cent silicon sheet steel, the loss per pound for a flux density of 91.3 kilo-lines per sq. in.,

$$w_c = 0.033 \times 1.12 \times 60 = 2.22 \text{ watts.}$$

The total core loss,

$$W_c = w_c G_c = 2.22 \times 3190 = 7060 \text{ watts.}$$

The I^2R loss in each winding at 75° C.,

$$W_t = 2.58 A_t^2 G_t \times 10^{-6} \\ = 2.58 \times 1800^2 \times 452 \times 10^{-6} = 3760 \text{ watts.}$$

$$W_h = 2.58 A_h^2 G_h \times 10^{-6} \\ = 2.58 \times 1280^2 \times 863 \times 10^{-6} = 3630 \text{ watts.}$$

The total copper loss, $W_k = 3760 + 3630 = 7390$.

The ratio of losses,

$$\frac{W_c}{W_k} = \frac{7060}{7390} = 0.956.$$

The resistance per phase of the windings at 75° C.,

$$R_t = \frac{W_t}{3 I_t^2} = \frac{3760}{3 \times 580^2} = 0.00373 \text{ ohm per phase}$$

$$R_h = \frac{W_h}{3 I_h^2} = \frac{3630}{3 \times 41.8^2} = 0.691 \text{ ohm per phase.}$$

The total resistance in terms of the high voltage winding,

$$R_t = \frac{3760 + 3630}{3 \times 41.8^2} = 1.405 \text{ ohms per phase.}$$

The per cent resistance drop,

$$P_r = \frac{I_h R_t}{E_h} 100 = \frac{41.8 \times 1.405}{7960} 100 = 0.738 \text{ per cent.}$$

Formula 222 must be used to calculate the per cent reactance. It gives the reactance drop per phase for three-phase transformers,

$$\begin{aligned} P_x &= \frac{21.5 f l_h^2 I_h}{h E_h 10^6} \left(\frac{d_h + d_l}{3} + d \right) \frac{I_h + I_l}{2} \\ &= \frac{21.5 \times 60 \times 512^2 \times 41.8}{23.80 \times 7960 \times 10^6} \left(\frac{1.45 + 1.03}{3} + 1.003 \right) \\ &\quad \frac{53.9 + 39.4}{2} \\ &= 6.60 \text{ per cent.} \end{aligned}$$

The per cent regulation for 100 per cent power factor

$$= P_r + \frac{P_x^2}{200} = 0.738 + \frac{6.6^2}{200} = 0.956 \text{ per cent,}$$

and for 80 per cent power factor load

$$\begin{aligned} &= \cos \theta P_r + \sin \theta P_x + \frac{(\cos \theta P_x - \sin \theta P_r)^2}{200} \\ &= 0.80 \times 0.738 + 0.60 \times 6.6 + \frac{(0.80 \times 6.6 - 0.60 \times 0.738)^2}{200} \\ &= 4.69 \text{ per cent.} \end{aligned}$$

An approximate method is used to calculate the magnetizing current for a three-phase transformer. The mean length of the magnetic circuit (see Fig. 244) is divided into three parts—the length, ab , from the center of the top yoke through the center core leg to the center of the bottom yoke and the length $acdb$ and $ac'd'b$ through the yokes and the outside core legs. The mean length of the path, ab

$$= 29.0 + 7.75 = 36.75 \text{ in.,}$$

and of the paths $acdb$ and $ac'd'b$

$$= 2(10.5 + 9.125) + 7.75 + 29 = 76.0 \text{ in.}$$

The magnetizing current for the path ab ,

$$I_m = \frac{36.75 \times 17 + (119 \times 2)}{\sqrt{2} \times 512} = 1.19 \text{ amperes}$$

and for paths $acdb$ and $ac'd'b$,

$$I_m = \frac{76.0 \times 17 + (119 \times 2)}{\sqrt{2} \times 512} = 2.10 \text{ amperes.}$$

The core loss current,

$$I_w = \frac{W_o}{E_{k3}} = \frac{7060}{7960 \times 3} = 0.295 \text{ ampere.}$$

The no-load current for each of the paths

$$= \sqrt{1.19^2 + 0.29^2} = 1.22 \text{ amperes}$$

$$= \sqrt{2.10^2 + 0.29^2} = 2.12 \text{ amperes}$$

and the no-load current for the transformer,

$$I_0 = \frac{2 \times 2.12 + 1.22}{3} = 1.82 \text{ amperes}$$

$$= \frac{1.82}{41.8} 100 = 4.35 \text{ per cent.}$$

The stray load-losses are estimated at 10 per cent of the total I^2R losses (see page 369). The efficiency and losses for various loads at 100 per cent power factor are as follows:

	1	2	3	4	5
I^2R + stray load-losses.....	508	2,035	4,576	8,129	12,760
Core losses.....	7,060	7,060	7,060	7,060	7,060
Total losses.....	7,568	9,095	11,636	15,189	19,820
Output.....	250,000	500,000	750,000	1,000,000	1,250,000
Input.....	257,568	509,095	761,636	1,015,189	1,269,820
Efficiency.....	97.0	98.2	98.4	98.50	98.50

The total radiating surface of the core and windings is calculated as follows:

$$\text{Core legs: } (4 \times 5.625 + 4 \times 3.5) 3 \times 29 = 3,180 \text{ sq. in.}$$

$$+ (4 \times 7.75 \times 9.125) = 2,666 \text{ sq. in.}$$

Low-voltage coils: $(2 \times 39.4 \times 23.3 \times 3)$

$$+ (39.4 \times 1.03 \times 6) = 5,754 \text{ sq. in.}$$

High-voltage coils $2(0.565 + 1.45) 53.9 \times 29 \times 3 = 18,900 \text{ sq. in.}$

The total radiating surface $= 30,500 \text{ sq. in.,}$

and the surface per watt,

$$\frac{S}{W} = \frac{30,500}{15,189} = 2.01.$$

With a corrugated sheet-steel tank, the surface per watt loss should be from 6.0 to 9.0 (see page 370). If 7.5 is used, the total tank surface,

$$S_t = (W_c + W_k)7.5 = 15,189 \times 7.5 = 114,000 \text{ sq. in.}$$

The shape of the tank section and the position of the transformer in the tank are shown in Fig. 244. A corrugated tank wall with a pitch of 1.75 in., depth of 4.0 in., and a mean length of 5.0 in. is selected. With a clearance of 5.5 in. between the outside of the coils and the inside of the tank, the perimeter of the tank on the center line of the corrugated tank wall

$$= 4(10.50 + 9.125) + \pi \times 33.59 = 184.0 \text{ in.}$$

The depth of the hot oil

$$= \frac{114,000}{184.0 \times 5.0} = 124.0 \text{ in.}$$

The volume of the tank

$$= \left[2(10.5 + 9.125)33.59 + \frac{\pi}{4} 33.59^2 \right] 124.0$$

$$= 274,000 \text{ cu. in.}$$

The volume of the active materials

$$= \frac{3190}{0.272} + \frac{1315}{0.321} = 15,820 \text{ cu. in.}$$

The volume of oil required $= 274,000 - 15,820 = 258,180 \text{ cu. in.}$ This value is slightly high because the volume of the insulating material, core clamps, coil supports, leads, etc., has not been included in calculating the volume of the transformer.

TRANSFORMER DESIGN SHEET

Kva 1000	Phase, 3	Cycles, 60	Volts { HV, 7,980 LV, 575	Phase Volts { HV, 7,980 LV, 575
Line Amperes { HV, 72.6 LV, 1005.0		Phase Amperes { HV, 41.8 LV, 580.0		
Type, Circular Core			Type of Cooling, Self Oil	

CORE

Sheet steel 0 014-3.0% Si
Output constant 0 376
Core leg Center Outside
Area 63.0
Diameter 10.75
Dimensions $2a = 5\frac{1}{2}; 2b = 9\frac{1}{2}$
Density 91,300
Weight 1510
Core factor 0.70
Yoke:
Area 63.0
Dimensions 7.75 x 9.125
Density 91,300
Weight 1680
Copper space factor, f_c 0.188
Window dimensions 10.5 x 20.0
Lamination factor k_1 0.90

CORE AND WINDINGS

Mean length of flux path 36.75 & 56.375
Total ampere-turns 883.0 & 1190.0
Magnetizing current 1.10 & 1.65
Core loss current 0.295
Exciting current:
Amperes 1.82
Per cent 4.35

Per cent.

Resistance 0.738
Reactance 6.60
Impedance 6.64
Power factor 80 100
Regulation 4.69 0.956
Losses.
Total core 7080.0
Stray load 739.0
Total copper 7390.0
Per cent:
Load 25 50 75 100
Efficiency 97.0 98.2 98.4 98.5
Square inches per watt 2.01
Ratio of losses 0.96
Ratio of weights 2.43

TANK

Type of tank, corrugated sheet steel, 1.75 x 4.0
Square inches per watt 7.5
Total wetted surface 114,000
Depth of oil 124.0
Gallons of oil 1120.0
Weight of oil 7810.0
Cooling coils:
Size
Length
Surface
Water, gallons per minute

WINDINGS	HIGH VOLTAGE	LOW VOLTAGE
Type of winding	Disc coils	Helical
Connections	Delta	Delta
Conductor:		
Dimensions	0 110 x 0 276 d.c.c.	0.208 x 0 386 d.c.c.
Section	0 0325	0.0645
Number in parallel	None	5
Current Density	1280	1800
Turns per phase	512	37
Coils:		
Total number	77	3
Per core leg	29	1
Turns:		
Per coil	*	37
Per layer	†	37
Number of layers	2-sections	1
Coil:		
Connections	Series	
Dimensions	0 565 x 1 45	1 03 x 23 3
Ducts, number and size	27- $\frac{1}{4}$ & 1- $\frac{1}{4}$	0 25 Between turns
Insulation:		
Layer	0.013	
Core and coils	$\frac{1}{2}$ D. + $\frac{1}{4}$ P.B. + $\frac{1}{2}$ D.	$\frac{1}{2}$ P.B. + $\frac{1}{2}$ D.
HV and LV	15.5	
Voltage per turn	279.0	
Maximum voltage between layers	53.9	39.4
Length of mean-turn		
Copper:		
Weight	863.0	452
Loss	3630.0	3760.0
Resistance, 75° C.	0.691	0.00373
Per cent end turns with extra insulation	5.08	

Remarks: *27 coils, 18 turns † 27 coils, 9 turns per section

1 coil, 16 turns 1 coil, 8 turns per section

1 coil, 10 turns 1 coil, 5 turns per section

Designed by: J. H. Kuhlmann

Date:

The number of gallons of oil required

$$= \frac{258,180}{231} = 1120.0.$$

The total weight of the oil

$$= 7.0 \times 1120.0 = 7840.0 \text{ lb.}$$

The core clamps, coil, and lead supports are not shown in the assembly drawing of the transformer, Fig. 244.

Design No. 3: *Design of 10-Kva, Single-Phase, Four-Part Distributed-Core-Type Distribution Transformer.*—The complete rating is as follows: 10 Kva, single phase, 60 cycles, 2300 volts primary to 115 and 230 volts secondary. The transformer is to be of the self-oil-cooled type and must carry its rated load continuously with a temperature rise not to exceed 55° C. The efficiency and regulation at full-load and 100 per cent power factor should be approximately 97.5 per cent and 1.95 per cent respectively. The ratio of the core loss to the full-load copper loss should be approximately 0.40. The transformer must also be suitable for operation at 2400 and 2200 volts.

For the method of punching the laminations and assembling the core of this type of transformer see Fig. 213. The weight of the core is proportioned approximately as follows: Center leg 22.0 per cent, yokes 49.0 per cent, and outside legs 30.0 per cent of the total weight. The flux densities in the yokes and outside legs are generally 51.0 and 67.0 per cent respectively of the density in the center leg. If the flux density in the center leg is assumed equal to 75,000 lines per sq. in., then the density in the yokes and outside legs should be approximately 40,500 and 50,200 lines per sq. in. respectively.

From the curve Fig. 219, the total flux for a 10-Kva transformer,

$$\phi_t = 900 \text{ kilo-lines.}$$

The section area of the center leg for the assumed density of 75 kilo-lines per sq. in.,

$$A_c = \frac{\phi_t}{B} = \frac{900 \times 10^3}{75 \times 10^3} = 12.0 \text{ sq. in.}$$

The center core section is square and the dimensions

$$= \sqrt{\frac{12.0}{0.90}} = 3.65; \text{ use } 3.68 \text{ in.}$$

The core punchings are L-shaped and are assembled as shown in

Fig. 245. The dimensions for the section of the outside legs are fixed by the center leg dimensions (see Fig. 245) and are

$$= 1.84 \times 2.76 \text{ in.}$$

The flux density in the yoke has been assumed equal to 40,500 lines per sq. in. The section area is then

$$= \frac{900,000}{4 \times 40,500} = 5.55 \text{ sq. in.}$$

The height of the yoke section is then

$$= \frac{5.55}{2.76 \times 0.90} = 2.24; \text{ use } 2.25 \text{ in.}$$

The number of turns for the high and low voltage winding,

$$t_h = \frac{E_h \times 10^8}{4.44 f \phi_t} = \frac{2400 \times 10^8}{4.44 \times 60 \times 900 \times 10^3} = 1000.$$

$$t_l = \frac{E_l}{E_h} t_h = \frac{240}{2400} 1000 = 100.$$

The flux densities assumed above are for the highest voltage at which the transformer is to operate; therefore 2400 volts is used for the calculation of the number of turns in the winding.

To calculate the maximum current in the windings, the lowest voltage at which the transformer is to operate must be used. The full-load current in the windings,

$$I_h = \frac{10 \times 10^3}{2200} = 4.55 \text{ amperes}$$

and

$$I_l = \frac{t_h}{t_l} I_h = \frac{1000}{100} 4.55 = 45.5 \text{ amperes.}$$

A current density of 1000 amperes per sq. in. is assumed. The section area of the conductor for high-voltage and low-voltage winding,

$$s_{ch} = \frac{I_h}{A} = \frac{4.55}{1000} = 0.00455 \text{ sq. in.}$$

$$s_{cl} = \frac{I_l}{A} = \frac{45.5}{1000} = 0.0455 \text{ sq. in.}$$

$$h_w w_w = \frac{2l_h s_{ch}}{f_s} = \frac{2 \times 1000 \times 0.00455}{0.40}$$

$$= 22.8 \text{ sq. in.}$$

The copper space factor, f_s , is taken from the curves of Fig. 224.

The ratio of window height to width may be taken equal to 3. The dimensions of the window,

$$h_w = \sqrt{3 \times 22.8} = 8.28; \text{ use } 8.25 \text{ in.}$$

$$w_w = \frac{22.8}{8.25} = 2.76; \text{ use } 2.75 \text{ in.}$$

The mean length of the center and outside leg can be taken equal to the window height. The respective weights are then,

$$\text{Center leg} = 8.25 \times 12.2 \times 0.272 = 27.4 \text{ lb.}$$

$$5 \times \text{Outside legs} = 8.25 \times 4.57 \times 4 \times 0.272 = 41.0 \text{ lb.}$$

The mean length of the yoke is estimated at 10.75 in. (see Fig. 245) and the weight,

$$\text{Yokes} = 10.75 \times 5.59 \times 4 \times 0.272 = 65.4 \text{ lb.}$$

The total core weight,

$$G_c = 133.8 \text{ lb.}$$

The mean length of turn for the windings,

$$L_{av} = 4 \times 3.68 + \pi(2.75 - 0.25) = 22.56 \text{ in.}$$

The approximate copper weight,

$$G_t = 22.56 \times 1000 \times 0.00455 \times 2 \times 0.321 = 65.8 \text{ lb.}$$

The ratio of core weight to copper weight is then,

$$\frac{G_c}{G_t} = \frac{133.8}{65.8} = 2.03.$$

The losses should now be calculated to determine whether the selected core dimensions will give approximately 0.40 for the ratio of

losses. The additional core losses will be assumed equal to 12 per cent of the fundamental frequency losses.

	Density, Kilo-lines per Square Inch	Loss per Pound, Watts	Weight, Pounds	Total Loss, Watts
Center legs	73.8	1.015	27.4	27.8
Outside legs	49.2	0.518	41.0	21.2
Yokes	40.2	0.396	65.4	25.9
Total core loss				74.9

The approximate total copper loss,

$$W_k = 2.58 A^2 G_k \times 10^{-6}$$

$$= 2.58 \times 1000^2 \times 65.8 \times 10^{-6} = 169.0 \text{ watts.}$$

The ratio of loss is then,

$$\frac{W_c}{W_k} = \frac{74.9}{169.0} = 0.443.$$

DESIGN OF WINDINGS

Low-Voltage Winding.—The conductor chosen for the low-voltage winding has the following dimensions: 0.162×0.258 in. bare, 0.184×0.278 in. insulated, 0.0410 sq. in. area. The secondary winding must be so arranged that 115 and 230 volts can be obtained at rated capacity. To accomplish this, the low-voltage coil is divided into two equal sections, which are connected in parallel for 115 volts and in series for 230 volts. The total number of low-voltage turns,

$$t_l = 100.$$

The low-voltage coils will, therefore, be wound with two layers of 25 turns each and one of the coils will be placed on the inside of the high-voltage coil and the other on the outside (see Fig. 245).

For layer-wound coils, the space of one turn must be allowed for the start of the winding. The total height of the coils is then

$$= 0.278 \times 26 = 7.22 \text{ in.}$$

With a window height equal to 8.25 in., the space for insulation at each end of the winding equals 0.515 in., which is larger than necessary.

The window can not be changed until the space required by the high-voltage winding has been determined.

The voltage per turn

$$= \frac{240}{100} = 2.40 \text{ volts}$$

and the maximum voltage between layers

$$= 2 \times 25 \times 2.4 = 120 \text{ volts.}$$

Paper insulation 0.021 in. thick will be used between layers of the low-voltage coils.

The depth of each low-voltage coil is then

$$= 2 \times 0.181 + 0.021 = 0.392 \text{ in.}$$

The insulation between the core and winding consists of a paper channel 0.10 in. thick.

High-Voltage Winding.—A No. 13 sq. d.c.c. copper conductor is selected from the copper table. The dimensions of the conductor are: 0.072×0.072 in. bare, 0.083×0.083 in. insulated, 0.00465 sq. in. area. The high-voltage coil is divided into two sections by a $\frac{1}{4}$ -in. duct through which the high-voltage leads are brought out. The total number of turns,

$$t_h = 1000.$$

Use 12 layers: 11 of 84 turns each, and one of 76 turns.

The height of the high-voltage coil is then

$$= 0.083 \times 85 = 7.06 \text{ in.}$$

The maximum voltage between layers

$$= 2.40 \times 2 \times 84 = 403.2 \text{ volts.}$$

Two layers of treated paper insulation, each 0.012 in. thick, are used between layers. The depth of the coil plus the duct is then

$$= (12 \times 0.083) + (11 \times 0.024) + 0.25 = 1.51 \text{ in.}$$

The insulation between the yokes and the ends of the coils consists of a mica pad $\frac{1}{8}$ in. thick plus press-board space blocks $\frac{1}{8}$ in. thick for the low-voltage coils, and plus press-board space blocks 0.22 in. thick for the high-voltage coils (see Fig. 245). The height of the coils plus insulation is then:

$$\text{Low-voltage, } 7.22 + 2(0.125 + 0.125) = 7.72 \text{ in.}$$

$$\text{High-voltage, } 7.06 + 2(0.125 + 0.22) = 7.75 \text{ in.}$$

The window height is therefore reduced from 8.25 in. to 7.75 in.
 The insulation between the high-voltage and low-voltage windings consists of a mica pad 0.15 in. thick. The total depth of the winding

$$= 0.10 + 0.392 + 0.15 + 1.51 + 0.15 + 0.392 = 2.694 \text{ in.}$$

With a window 2.75 in. wide, the clearance between the outside core leg and the winding is 0.056 in., which is too small. The window is therefore made 2.875 in. wide and the clearance = 0.181 in.

OPERATING CHARACTERISTICS

The operating characteristics will be calculated for the normal voltage rating, that is, 2300 volts to 230/115 volts.

The total flux,

$$\phi_t = \frac{E_h \times 10^8}{4.44 f l_h} = \frac{2300 \times 10^8}{4.44 \times 60 \times 1000} = 863 \text{ kilo-lines.}$$

The dimensions, flux densities, weights, and losses for the various parts of the magnetic circuit are as follows:

	Section Area, Square Inches	Flux Density, Kilo-lines	Weight, Pounds	Loss per Pound, Watts	Total Loss, Watts
Center leg.....	12.2	70.7	25.7	0.025	23.8
Outside leg.....	4.57	47.2	38.6	0.470	18.1
Yokes.....	5.59	38.6	67.0	0.376	25.2
Total core loss.....					67.1

The additional losses have been estimated at 12 per cent of the fundamental frequency loss.

The secondary winding is symmetrical about the primary winding. The length of the mean-turn of the high-voltage coil is therefore also the average mean-turn for the low-voltage winding,

$$L_h = 4 \times 3.68 + \pi(2 \times 0.10 + 2 \times 0.392 + 2 \times 0.15 + 1.51) \\ = 23.46 \text{ in.}$$

The copper weight for the two windings,

$$G_i = 23.46 \times 100 \times 0.041 \times 0.321 = 30.9 \text{ lb.}$$

$$G_h = 23.46 \times 1000 \times 0.00465 \times 0.321 = 35.0 \text{ lb.}$$

The ratio of core weight to copper weight,

$$\frac{G_c}{G_k} = \frac{131.3}{65.9} = 1.99.$$

The copper space factor,

$$f_s = \frac{s_{ct}t_h + s_{ct}t_l}{h_w w_w} = \frac{0.00465 \times 1000 + 0.041 \times 100}{7.75 \times 2.875} = 0.393.$$

The full-load current in the windings for the normal voltage rating,

$$I_l = 43.5 \text{ amperes, and } I_h = 4.35 \text{ amperes.}$$

The current densities,

$$A_l = \frac{43.5}{0.041} = 1060 \text{ amperes per sq. in.}$$

$$A_h = \frac{4.35}{0.00465} = 935 \text{ amperes per sq. in.}$$

The I^2R losses at 75°C. ,

$$W_l = 2.58 A_l^2 G_l 10^{-6} = 2.58 \times 1060^2 \times 30.9 \times 10^{-6} = 89.2 \text{ watts.}$$

$$W_h = 2.58 \times 935^2 \times 35.0 \times 10^{-6} = 78.5 \text{ watts.}$$

The ratio of losses,

$$\frac{W_c}{W_h} = \frac{67.1}{167.7} = 0.40.$$

The resistance of the windings at 75°C. ,

$$R_l = \frac{W_l}{I_l^2} = \frac{89.2}{43.5^2} = 0.0472 \text{ ohm}$$

$$R_h = \frac{W_h}{I_h^2} = \frac{78.5}{4.35^2} = 4.14 \text{ ohms.}$$

The total resistance in terms of the high-voltage winding,

$$R_t = \frac{89.2 + 78.5}{4.35^2} = 8.86 \text{ ohms.}$$

The per cent resistance drop,

$$P_r = \frac{I_h R_t}{E_h} 100 = \frac{4.35 \times 8.86}{2300} 100 = 1.68 \text{ per cent.}$$

$$\begin{aligned}
 P_x &= \frac{10}{h} \frac{8 f l_h^2 I_h}{E_h \times 10^6} \left(\frac{d_h + d_i}{6} + d \right) L_h \\
 &= \frac{10}{7.06} \frac{8 \times 60 \times 1000^2 \times 4.35}{2300 \times 10^6} \left(\frac{1.51 + 0.784}{6} + 0.15 \right) 23.46 \\
 &= 2.17 \text{ per cent.}
 \end{aligned}$$

The per cent impedance drop,

$$P_s = \sqrt{P_r^2 + P_x^2} = \sqrt{1.68^2 + 2.17^2} = 2.74 \text{ per cent.}$$

The per cent regulation for 100 per cent power factor

$$= P_r + \frac{P_x^2}{200} = 1.68 + \frac{2.17^2}{200} = 1.70 \text{ per cent,}$$

and for 80 per cent power factor

$$\begin{aligned}
 &= \cos \theta P_r + \sin \theta P_x + \frac{(\cos \theta P_x - \sin \theta P_r)^2}{200} \\
 &= 0.80 \times 1.68 + 0.60 \times 2.17 + \frac{(0.80 \times 2.17 - 0.60 \times 1.68)^2}{200} \\
 &= 2.645 \text{ per cent.}
 \end{aligned}$$

The approximate mean length of the flux path for the various parts of the magnetic circuit and the corresponding number of ampere-turns are as follows:

	Flux Density, Kilo-lines	Mean Length, Inches	Ampere-turns per Inch	Ampere-turns
Center leg	70.7	7.75	5.5	42.0
Outside leg	47.2	7.75	2.5	19.4
Yokes	38.6	11.00	2.2	24.2
Joints	38.6	12.0
Total ampere-turns	98.2

The magnetizing current,

$$I_m = \frac{AT}{\sqrt{2} \times t_h} = \frac{98.2}{1.42 \times 1000} = 0.0692 \text{ ampere.}$$

The core loss current,

$$I_w = \frac{W_c}{E_h} = \frac{67.1}{2300} = 0.0292 \text{ ampere.}$$

The exciting current,

$$I_0 = \sqrt{I_m^2 + I_w^2} = \sqrt{0.0692^2 + 0.0292^2} = 0.075 \text{ ampere}$$

$$= \frac{0.075 \times 100}{4.35} = 1.73 \text{ per cent of the full-load current.}$$

The stray load-losses are estimated equal to 10 per cent of the total I^2R losses (see page 369). The losses and efficiencies for various loads at 100 per cent power factor are as follows:

	1	2	3	4	5
I^2R + stray load-losses.	11.53	46.09	103.62	184.47	288.20
Core losses	67.10	67.10	67.10	67.10	67.10
Total losses	78.63	113.19	170.72	251.57	355.30
Output	2500.00	5000.00	7500.00	10,000.00	12,500.00
Input	2578.63	5113.19	7670.72	10,251.57	12,855.30
Efficiency, per cent. . .	97.0	97.8	97.7	97.5	97.2

The total radiating surface of core and coils is calculated as follows:

$$\text{Outside legs: } (1.84 + 2.76)2 \times 7.75 \times 4 = 285.0 \text{ sq. in.}$$

$$\text{Yokes: } (2.25 + 2.76)2 \times 11.0 \times 4 + 2.25 \times 2.75$$

$$\times 4 \times 2 = 491.5 \text{ sq. in.}$$

$$\text{Windings: } 23.46 \times 7.00 + 31.05 \times 7.22 + 23.46$$

$$\times 2.694 \times 2 = 520.5 \text{ sq. in.}$$

$$1270.0 \text{ sq. in.}$$

The radiating surface per watt loss,

$$\frac{S}{W} = \frac{1279.0}{251.57} = 5.08 \text{ (see page 369).}$$

A plain sheet-steel tank will be used. The surface per watt loss should then be about 4.50 (see page 370). The total area of the tank walls,

$$S_t = (W_o + W_k)S/W = 251.57 \times 4.5 = 1130.0 \text{ sq. in.}$$

The tank is circular in section, as shown in Fig. 245. The over-all dimensions of the transformer are:

$$\text{Width: } 3.68 + 2 \times 2.875 + 2 \times 1.84 = 13.11 \text{ in.}$$

$$\text{Height: } 7.75 + 2 \times 2.25 = 12.25 \text{ in.}$$

Make the inside diameter of the tank 14.25 in., then the outside diameter is 14.375 in., if the thickness of the wall is $\frac{1}{8}$ in.

The depth of the hot oil

$$= \frac{1130.0}{\pi \times 14.375} = 25.0 \text{ in.}$$

The volume of the tank

$$= \frac{\pi}{4} \times 14.25^2 \times 25.0 = 3980.0 \text{ cu. in.}$$

The volume of the transformer, if calculated from the active material weights with no allowance for insulation, core clamps, etc.,

$$= \frac{131.3}{0.272} + \frac{65.9}{0.321} = 688.0 \text{ cu. in.}$$

The volume of oil required

$$= 3980.0 - 688.0 = 3292.0 \text{ cu. in.}$$

The number of gallons of oil

$$= 3292.0 \times 0.00433 = 14.30.$$

The weight of the oil

$$= 14.30 \times 7.0 = 100.0 \text{ lb.}$$

An assembly drawing of the transformer without core clamps and lead supports is shown in Fig. 245.

Design No. 4: *Design of a 500-Kva, Single-Phase, Shell-Type Power Transformer.*—The complete rating is as follows: 500 Kva, single phase, 60 cycles, 22,000 to 2300 volts. The transformer is to be of the self-oil-cooled type and must carry its rated load continuously with a temperature rise not to exceed 55° C. The efficiency and regulation at full-load and 100 per cent power factor should be approximately 98.5 per cent and 0.85 per cent respectively.

The ratio of losses for a power transformer is generally approximately equal to 1.0. For this design, the ratio will be taken equal to

0.90. The copper density for high-voltage and low-voltage windings may be estimated at 1550 amperes per sq. in. A flux density of 87,000 lines per sq. in. is satisfactory with a 4.0 per cent silicon sheet-steel 0.014 in. thick. From the loss curves in the Appendix, the loss per pound, $w_c = 0.0265 \times 1.12 \times 60 = 1.78$ watts. The additional losses have been assumed equal to 12 per cent of the fundamental frequency losses (see page 369).

The copper loss per pound at 75° C.,

$$w_k = 2.58 A^2 \times 10^{-6} = 2.58 \times 1550^2 \times 10^{-6} = 6.19 \text{ watts.}$$

The ratio of weights is then,

$$\frac{G_c}{G_k} = \frac{w_k}{w_c} \times \frac{W_c}{W_k} = \frac{6.19}{1.78} 0.90 = 3.13 \text{ (see page 346).}$$

For an output constant, $C = 0.85$ (see page 348), the net core section,

$$A_c = C \sqrt{\frac{K_{va} \times G_c / G_k \times 10^{11}}{fBA}} = 0.85 \sqrt{\frac{500 \times 3.13 \times 10^{11}}{60 \times 87,000 \times 1550}} \\ = 118.0 \text{ sq. in.}$$

For shell-type transformers, the ratio of $b/2a$ (see page 349) is generally from 2.0 to 3.0. For a ratio of $b/2a$ equal to 2.3,

$$2a = \sqrt{\frac{A_c}{0.9 \times 2.3}} = \sqrt{\frac{118.0}{0.9 \times 2.3}} = 7.54 \text{ in.; use 7.5 in.}$$

The depth of the core laminations,

$$b = \frac{A_c}{0.9 \times 2a} = \frac{118.0}{0.9 \times 7.5} = 17.50 \text{ in.}$$

The width of each lamination,

$$a = \frac{7.5}{2} = 3.75 \text{ in.}$$

The total flux,

$$\phi_t = A_c B = 118.0 \times 87,000 = 10,270 \text{ kilo-lines.}$$

The number of turns for the high-voltage and low-voltage windings,

$$t_h = \frac{E_h \times 10^8}{4.44 f \phi_t} = \frac{22,000 \times 10^8}{4.44 \times 60 \times 10,270,000} = 804$$

$$t_l = \frac{E_l}{E_h} t_h = \frac{2300}{22,000} 804 = 84.$$

The full-load current in the windings,

$$I_h = \frac{Kva \times 10^3}{E_h} = \frac{500 \times 10^3}{22,000} = 22.7 \text{ amperes}$$

$$I_l = \frac{t_h}{t_l} I_h = \frac{804}{84} 22.7 = 217.0 \text{ amperes.}$$

For the current density selected, 1550 amperes per sq. in., the section area of the conductor for high-voltage and low-voltage winding,

$$s_{sh} = \frac{22.7}{1550} = 0.01465 \text{ sq. in.}$$

$$s_{sl} = \frac{217.0}{1550} = 0.140 \text{ sq. in.}$$

The approximate copper space factor is 0.183 (see Fig. 224) and the area of the window,

$$\begin{aligned} h_w w_w &= \frac{2s_{sh} t_h}{f_s} = \frac{2 \times 0.01465 \times 804}{0.183} \\ &= 129.0 \text{ sq. in.} \end{aligned}$$

The ratio of the window dimensions is generally from 2.0 to 3.0. For a ratio 2.25,

$$h_w = \sqrt{2.25 \times 129.0} = 17.0 \text{ in.; use } 17.25 \text{ in.}$$

$$w_w = \frac{129.0}{17.0} = 7.60 \text{ in.; use } 7.5 \text{ in.}$$

The dimensions of the window are then,

$$h_w w_w = 17.25 \times 7.5 = 129.4 \text{ sq. in.}$$

The approximate core and copper weights will now be calculated to determine the ratio of weights, which should be approximately equal to the value assumed above.

The flux density in the yokes is made equal to the flux density in the center core, and the width of the laminations for the yoke is one-half of the width of the lamination in the center core (see Fig. 246).

The mean-length of the magnetic circuit,

$$\begin{aligned} L_o &= 2(h_w + w_w) + \pi a = 2(17.25 + 7.5) + 3.14 \times 3.75 \\ &= 61.30 \text{ in.} \end{aligned}$$

the weight of the core,

$$G_c = L_c A_c \times 0.272 = 61.30 \times 118.0 \times 0.272 = 1970 \text{ lb.}$$

The clearance between the two halves of the center core is 0.50 in. (see Fig. 246). The center of the coils generally coincides with the center of the window, and the insulation at each end of the coils over the center core is approximately the same for both high-voltage and low-voltage coils. With an insulation thickness at each end of the center core equal to 3.0 in. and a radius at the inside corners equal to 0.75 in., the approximate length of the mean-turn (see Fig. 246),

$$L_{av} = 2[(2 \times 3.75 + 0.50) + 17.50 + 2(3.0 - 0.75)] + \pi \times 7.5 \\ = 83.60 \text{ in.}$$

The total copper weight,

$$G_k = 2L_{av} s_{ck} \times 0.321 = 2 \times 83.6 \times 804 \times 0.01465 \times 0.321 \\ = 632 \text{ lb.}$$

The ratio of weights,

$$\frac{G_c}{G_k} = \frac{1970}{632} = 3.11.$$

The window dimensions can therefore be used as calculated above, that is,

$$h_w = 17.25 \text{ in., } w_w = 7.50 \text{ in.}$$

DESIGN OF WINDINGS

High-Voltage Winding.—The windings of shell-type transformers are generally of the interleaved type, with rectangular "pancake" type coils. A rectangular conductor with only one turn per layer is most satisfactory for such coils.

The area of the conductor for the high-voltage winding, $s_{ck} = 0.01465$. The conductor selected from the copper table has the following dimensions: 0.064×0.258 in. bare; 0.08×0.271 in. insulated d.c.c.; 0.016 sq. in. area.

In order to provide space for the additional insulation for the end-turns of the high-voltage winding, the end coils should have a smaller number of turns (see page 360).

The voltage per turn

$$= \frac{E_h}{t_h} = \frac{22,000}{804} = 27.4 \text{ volts.}$$

Fuller-board insulation 0.017 in. thick is used between turns and the coils are wound with only one layer. The number of coils and turns per coil are as follows:

Coils	Turns per Coil	Total Turns
10	62	620
2	56	112
2	36	72
		<hr/> 804

The depth of the center coils $= 0.080 \times 62 + 0.017 \times 61 = 6.0$ in. With a window 7.5 in. wide, the space at each end of the coils $= 0.75$ in., which is required for insulation (see Fig. 246). One coil with 56 turns and one with 36 turns are placed at each end of the winding. These coils are insulated with extra heavy insulation on the turns to approximately the same dimensions as the center coils.

After the coils are wound, they are thoroughly dried and dipped in insulating varnish and baked until dry. The varnish treatment is repeated until the coils have a smooth, glossy surface, which indicates that all crevices are filled with the impregnating compound. The average thickness of the high-voltage coils may be taken equal to 0.285 in.

Low-Voltage Winding.—The conductor for the low-voltage winding will be built up of 4 parallel conductors. The dimensions of each conductor are: 0.120×0.258 in. bare; 0.149×0.276 in. insulated d.c.c.; 0.0325 sq. in. area. Four low-voltage coils are used with 21 turns per coil, wound in two sections, with $10\frac{1}{2}$ turns per section. The four parallel conductors are wound flat on top of one another, with fuller-board insulation 0.034 in. thick between turns. The depth of each coil

$$= 4 \times 0.149 \times 10.5 + 0.034 \times 9.5 = 6.58 \text{ in.}$$

With a window 7.5 in. wide, the clearance at each end of the coils for insulation $= 0.46$ in., which is satisfactory for a 2300-volt winding.

The thickness of each low voltage coil

$$= 2 \times 0.276 + 0.035 = 0.587 \text{ in.}$$

Here 0.035 in. is the thickness of the insulation between the two sections of the coils.

The high-voltage and low-voltage coils are arranged in the window as shown in Fig. 246. The insulation between high-voltage and low-

plus another $\frac{3}{8}$ -in. duct. Between high-voltage coils, $\frac{1}{16}$ -in. filler-board insulation plus another $\frac{1}{4}$ -in. duct is used. The two low-voltage coils in the center of the window are separated by a $\frac{1}{2}$ -in. duct. The clearance between the low-voltage coils and yoke at each end of the window is approximately 1.0 in., as shown in Fig. 246.

The clearance between the ends of the high-voltage coils and the center core is 3.0 in. For the low-voltage winding this clearance is $2\frac{5}{8}$ in. (see Fig. 246).

OPERATING CHARACTERISTICS

The total flux,

$$\begin{aligned}\phi_t &= \frac{N_h \times 10^8}{4.44 f l_h} = \frac{22,000 \times 10^8}{4.44 \times 60 \times 801} \\ &= 10,270 \text{ kilo-lines.}\end{aligned}$$

The net section of the center core,

$$A_c = 3.75 \times 17.5 \times 0.90 \times 2 = 118.0 \text{ sq. in.}$$

and the flux density in the magnetic circuit,

$$B = \frac{\phi_t}{A_c} = \frac{10,270 \times 10^3}{118.0} = 87.0 \text{ kilo-lines.}$$

No changes have been made in the core dimensions. The total weight is therefore as given, $G_c = 1970$ lb.

The coils for both windings are wound on a form with a $\frac{3}{4}$ -in. radius at the corners. The mean-length of turn for the high-voltage coils (see Fig. 246),

$$\begin{aligned}L_h &= 2[(2 \times 3.75 + 0.50) + 17.50 + 2(3.0 - 0.75)] + \pi \times 7.5 \\ &= 83.60 \text{ in.}\end{aligned}$$

For the low-voltage coils,

$$\begin{aligned}L_l &= 2[(2 \times 3.75 + 0.50 - 0.75) + 17.50 + 2(2.625 - 0.75)] \\ &\quad + \pi(7.5 + 0.75) \\ &= 82.9 \text{ in.}\end{aligned}$$

The weight of copper in each winding,

$$\begin{aligned}G_h &= L_h l_h s_{ch} \times 0.321 = 83.6 \times 801 \times 0.016 \times 0.321 \\ &= 345 \text{ lb.}\end{aligned}$$

$$\begin{aligned}G_l &= L_l l_l s_{cl} \times 0.321 = 82.9 \times 84 \times 0.13 \times 0.321 \\ &= 290.0 \text{ lb.}\end{aligned}$$

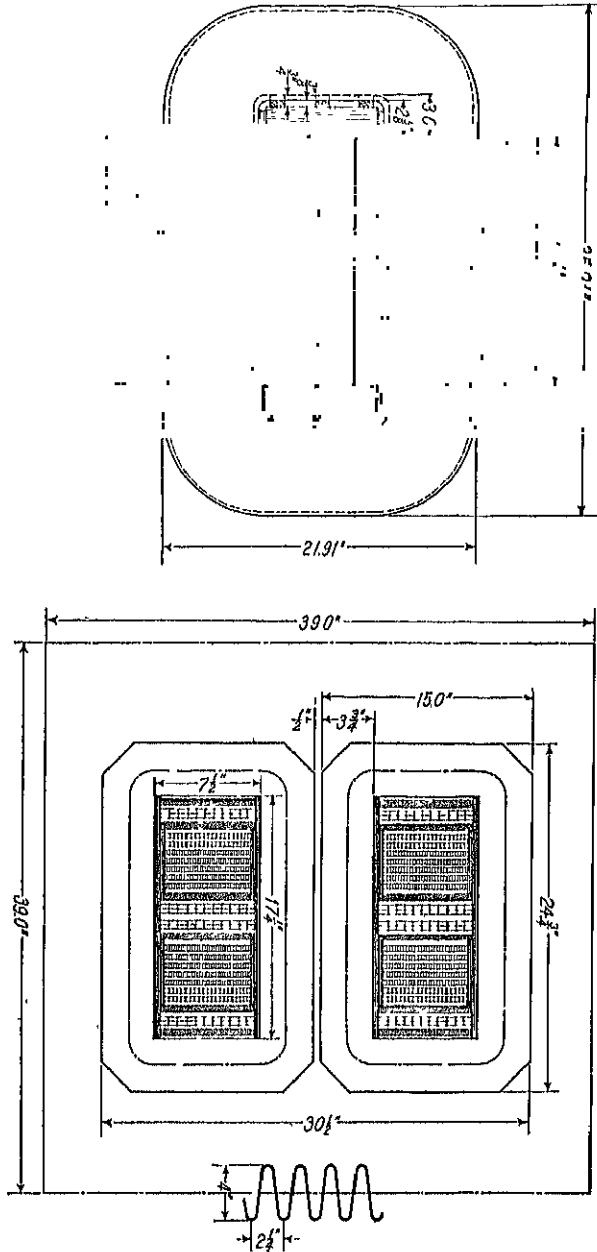


FIG. 240.

the ratio of weights,

$$\frac{G_o}{G_k} = \frac{1970}{345 + 290} = 3.10.$$

The current density in the two windings,

$$A_h = \frac{22.7}{0.016} = 1420 \text{ amperes per sq. in.}$$

$$A_l = \frac{217}{0.13} = 1670 \text{ amperes per sq. in.}$$

The output constant,

$$C = \frac{A_c}{\sqrt{\frac{K_{va} G_c / G_k \times 10^{11}}{fBA}}} = \frac{118.0}{\sqrt{\frac{500 \times 3.10 \times 10^{11}}{60 \times 87,000 \times 1545}}} = 0.852$$

The copper space factor,

$$f_s = \frac{s_{ch_h} + s_{cl_l}}{h_w w_w} = \frac{0.016 \times 804 + 0.13 \times 84}{17.25 \times 7.5} = 0.184.$$

The loss per pound per cycle for 4.0 per cent, 0.014-in., silicon sheet steel, for a flux density of 87.0 kilo-lines, is 0.0265 watt. If the additional losses are estimated to be equal to 12 per cent of the fundamental frequency losses, the total core loss,

$$W_o = 0.0265 \times 60 \times 1.12 \times 1970 = 3500 \text{ watts.}$$

The I^2R loss in each winding at 75° C.,

$$W_h = 2.58 A_h^2 G_h \times 10^{-6} = 2.58 \times 1420^2 \times 345 \times 10^{-6} = 1788 \text{ watts}$$

$$W_l = 2.58 A_l^2 G_l \times 10^{-6} = 2.58 \times 1670^2 \times 290 \times 10^{-6} = 2080 \text{ watts}$$

The ratio of losses,

$$\frac{W_o}{W_k} = \frac{3500}{1788 + 2080} = 0.904.$$

The resistance of each winding at 75° C.,

$$R_h = \frac{W_h}{I_h^2} = \frac{1788}{22.7^2} = 3.47 \text{ ohms.}$$

$$R_l = \frac{W_l}{I_l^2} = \frac{2080}{217^2} = 0.0442 \text{ ohm.}$$

The total resistance at 75° C., in terms of the high-voltage winding,

$$R_t = \frac{1788 + 2080}{22.7^2} = 7.5 \text{ ohms.}$$

The per cent resistance drop,

$$P_r = \frac{I_h R_t}{E_h} 100 = \frac{22.7 \times 7.5}{22,000} 100 = 0.775 \text{ per cent.}$$

The per cent reactance drop is calculated by formula 224,

$$\begin{aligned} P_x &= \frac{11.0 f l_h'^2 x_{hl} I_h}{h E_h \times 10^6} \left(\frac{x_h d_{xh} + x_l d_{xl}}{6} + d \right) L_h k_4 \\ &= \frac{11.0 \times 60 \times 402^2 \times 2 \times 22.7}{7.5 \times 22,000 \times 10^6} \\ &\quad \left(\frac{7 \times 0.285 + 2 \times 0.587}{6} + 1.156 \right) 83.6 \times 0.884 \\ &= 3.65 \text{ per cent.} \end{aligned}$$

The per cent impedance drop,

$$P_z = \sqrt{P_x^2 + P_r^2} = \sqrt{3.65^2 + 0.775^2} = 3.74 \text{ per cent.}$$

The sustained short-circuit current for normal primary voltage,

$$I_s = \frac{I \times 100}{P_z} = \frac{22.7 \times 100}{3.74} = 607 \text{ amperes.}$$

To calculate the mechanical stresses on the coils due to the short-circuit current, see references page 367.

The regulation for 100 per cent power factor load

$$= P_r + \frac{P_x^2}{200} = 0.775 + \frac{3.65^2}{200} = 0.842 \text{ per cent.}$$

For 80 per cent power factor load, the regulation

$$\begin{aligned} &= \cos \theta P_r + \sin \theta P_x + \frac{(\cos \theta P_x - \sin \theta P_r)^2}{200} \\ &= 0.80 \times 0.775 + 0.60 \times 3.65 + \frac{(0.80 \times 3.65 - 0.60 \times 0.775)^2}{200} \\ &= 2.84 \text{ per cent.} \end{aligned}$$

The mean length of the flux path has been calculated and is equal to 61.3 in. From the standard saturation curve for 4.0 per cent silicon

steel, the ampere-turns per inch for $B = 87.0$ kilo-lines, at =
There are 4 joints in the magnetic circuit and the ampere-turns for each joint (see Fig. 239) = 99.

The total ampere-turns,

$$AT = 22 \times 61.30 + 4 \times 99 = 1746.$$

The magnetizing current,

$$I_m = \frac{AT}{\sqrt{2} t_h} = \frac{1746}{1.42 \times 804} = 1.53 \text{ amperes.}$$

The component of the no-load current in phase with the voltage,

$$I_w = \frac{W_c}{E_h} = \frac{3500}{22,000} = 0.159 \text{ amperes.}$$

The exciting current,

$$I_0 = \sqrt{I_m^2 + I_w^2} = \sqrt{1.53^2 + 0.159^2} = 1.54 \text{ amperes}$$

$$= \frac{1.54}{22.7} 100 = 6.7 \text{ per cent of full-load current.}$$

The stray load-losses are estimated equal to 12.5 per cent of the total I^2R losses at 75°C. (see page 369). The efficiency and losses for various loads at 100 per cent power factor are as follows:

	$\frac{1}{4}$	$\frac{1}{2}$	$\frac{3}{4}$	$\frac{4}{4}$	$\frac{5}{4}$
I^2R + stray load-losses . . .	273	1,091	2,452	4,351	6,817
Core losses	3,500	3,500	3,500	3,500	3,500
Total losses	3,773	4,591	5,952	7,851	10,315
Output	125,000	250,000	375,000	500,000	625,000
Output plus losses	128,773	254,591	380,952	507,851	635,315
Efficiency	97.2	98.2	98.4	98.5	98.3

The total radiating surface of the transformer core and windings is calculated as follows:

$$\text{Core} \quad 2[2(3.75 + 17.5)61.30] = 5,210 \text{ sq. in.}$$

$$\text{H. V. Coils } (6.0 \times 83.6) (4 + 12) + (0.285 \times 83.6) 2 \times 14 = 8,686 \text{ sq. in.}$$

$$\text{L. V. Coils } 2(6.58 + 0.587) 82.9 \times 4 = 4,750 \text{ sq. in.}$$

$$\text{The total radiating surface} = 18,646 \text{ sq. in.}$$

and the surface per watt loss,

$$\frac{S}{W} = \frac{18,646}{7851} = 2.38 \text{ (see page 369).}$$

A corrugated sheet-steel tank is required for this transformer and the tank surface per watt loss should be approximately 7.5 (see page 370). The total wetted tank surface,

$$S_t = (W_o + W_i) \frac{S}{W} = 7851 \times 7.5 = 58,900 \text{ sq. in.}$$

The corrugation used for the tank will be the type shown in Fig. 242 with depth equal to 4 in., pitch equal to 2.25 in., and a mean length per inch of center line equal to 4.05 in. The tank is made square in section, with a length of center line equal to 156.0 in. (see Fig. 246). The depth of the hot oil

$$= \frac{58,900}{1560 \times 4.05} = 93.2 \text{ in.}$$

The volume of oil required is equal to the volume of the tank, minus the volume of the transformer. The volume of the active material of the transformer can readily be calculated from the weights. The tank volume

$$= 39.0 \times 39.0 \times 93.2 = 142,000 \text{ cu. in.}$$

and the volume of the active material of the transformer

$$= \frac{1970}{0.272} + \frac{635.0}{0.321} = 9230 \text{ cu. in.}$$

The total volume of oil required is then equal to 132,770 cu. in., which is slightly high because the volume of the insulating material, core clamps, coil supports, leads, etc., has not been subtracted.

The number of gallons of oil

$$= \frac{132,770}{231} = 573 = 1.15 \text{ gallons per Kva.}$$

The total weight of the oil = $7.0 \times 573 = 4010 \text{ lb.}$

Figure 212 shows a complete shell type transformer removed from the tank and shows the method of clamping the core and the coils.

TRANSFORMER DESIGN SHEET

Kva, 500	Phase, Single	Cycles, 60	Volts $\left\{ \begin{array}{l} \text{HV, 22,000} \\ \text{LV, 2,300} \end{array} \right.$	Phase Volts $\left\{ \begin{array}{l} \text{HV,} \\ \text{LV,} \end{array} \right.$
	Line Amperes $\left\{ \begin{array}{l} \text{HV, 22 7} \\ \text{LV, 217 0} \end{array} \right.$		Phase Amperes $\left\{ \begin{array}{l} \text{HV, ...} \\ \text{LV, ...} \end{array} \right.$	
	Type, Shell		Type of Cooling, Self Oil	

CORE			
Sheet steel		0.014-1% Si	
Output constant		0.85	
Core leg	Center	Outside	
Area	118 0	50 0	
Diameter			
Dimensions	(2 X 3 75) X 17.5	3 75 X 17 5	
Density	87,000	87,000	
Weight	Total core	1070 0	
Core factor			
Yoke:			
Area		50.0	
Dimensions		3.75 X 17 5	
Density		87,000	
Weight			
Copper space factor, f_c		0.181	
Window dimensions		7.5 X 17 25	
Lamination factor k_1		0.90	
CORE AND WINDINGS			
Mean length of flux path		61.30	
Total ampere-turns		17.46	
Magnetizing current		1.63	
Core loss current		0.159	
Exciting current:			
Amperes		1.51	
Per cent		0.78	
Per cent: Resistance 0.775 Reactance 3.660 Impedance 3.740 Power factor 100 Regulation 2.81 Losses: Total core 3500 0 Stray load 483.0 Total copper 3868.0 Per cent: Load 25 50 75 100 Efficiency 97.2 98.2 98.4 98.5 Square inches per watt 2.38 Ratio of losses 0.904 Ratio of weights 3.1 Short circuit current 007 0			
TANK			
Type of tank, corrugated sheet steel, 2.25 X 1.0			
Square inches per watt		7.5	
Total wetted surface		58,000	
Depth of oil		93.2	
Gallons of oil		573.0	
Weight of oil		4010 0	
Cooling coils:			
Size			
Length			
Surface			
Water, gallons per minute			

Windings	High Voltage	Low Voltage
Type of winding	Interleaved	Interleaved
Connections		
Conductor:		
Dimensions	0.08 X 0.271 d.c.c.	0.149 X 0.276 d.c.c.
Section	0.010	0.0325
Number in parallel	None	4
Current Density	11200	16700
Turns per phase	804	84
Tools:		
Total number	14	4
Per core leg	14	4
Turns:		
Per coil	*	21
Per layer	*	10.5 per section
Number of layers	1	2 sections
Coil:		
Connections	Series	Series
Dimensions	0.285 X 0.0	0.637 X 0.68
Ducts, number and size	W F.B. + 1 D.	1 D.
Insulation		
Layer	0.017	0.034
Core and coils	0.75	0.46
H.V. and L.V.	1/2 D. + 1 1/2 F.B. + 1/2 D.	
Voltage per turn	27.4	
Maximum voltage between layers		575 between sections
Length of mean-turn	83.00	82.00
Copper:		
Weight	345.0	290.0
Loss	1788.0	2080.0
Resistance, 75° C	3.47	0.0442
Per cent end turns with extra insulation	11.5	

Remarks: * 10 coils, 62 turns

2 coils, 50 turns

2 coils, 36 turns

Designed by: *J. H Kuhlmann*

Date: _____

APPENDIX

ROUND COPPER WIRE—BARE AND INSULATED

Gauge Number	Bare Diameter	S.C.C. Wire	D.C.C. Wire	Enamel C. Wire	S.C.C. Enamel C. Wire	D.C.C. Enamel C. Wire	Ash C. Wire	Area of Copper		Ohms per 1000 Ft.		Weight in Pounds per 1000 Ft.				Bar Diameter
								Circular Mils.	Square Inch	At 25° C.	At 75° C.	Bare	S.C.C.	D.C.C. and A-B. C.	Additional Weight for Enamel	
36	.0030	25 0	.000196	424	305	07550023	003
35	.0035	31.4	.000246	335	403	09450027	006
34	.0063	39 7	.000312	266	318	1200033	.006
33	.0071	50.4	.000396	210	250	1540035	.007
32	.0080	64.0	.000523	165	197	.1940036	.009
31	.0089	79.2	.000623	134	159	.2400037	.009
30	.0100	.0130	.0190	.0111	.0160	.0125	100	.000755	106	126	.302	344	.390	.0044	.011
29	.0113	.0163	.0203	.0125	.0183	.0139	125	.000919	83.4	79.2	.482	530	.553	.0060	.013
28	.0126	.0175	.0215	.0139	.0198	.0153	158	.001129	68.4	62.7	.609	662	.719	.0073	.013
27	.0142	.0190	.0230	.0155	.0203	.0245	202	.00138	52.5	49.8	.767	830	.883	.0084	.015
26	.0159	.0210	.0250	.0172	.0223	.0263	253	.00199	41.7	49.8	.971	1 04	1 11	.012	.015
25	.0179	.0230	.0270	.0193	.0253	.0293	320	.00252	33.0	31.2	1.23	1 29	1 37	.016	.020
24	.0201	.0250	.0290	.0216	.0275	.0305	404	.00317	26.2	24.7	1.54	1 62	2 03	.020	.022
23	.0226	.0275	.0315	.0242	.0303	.0333	511	.00401	20.7	19.5	1.95	2 05	2 14	.023	.025
22	.0254	.0305	.0345	.0271	.0333	.0360	645	.00507	16.4	15.5	2.46	2 26	2 35	.023	.025
21	.0285	.0335	.0375	.0302	.0363	.0393	812	.00638	13.0	12.3	3.10	2 46	2 55	.023	.025
20	.0325	.0375	.0415	.0342	.0403	.0433	1020	.00804	10.3	9.71	3.93	2 66	2 75	.023	.025
19	.0365	.0415	.0455	.0382	.0443	.0473	1230	.01002	8.14	7.58	4.85	2 86	2 95	.023	.025
18	.0405	.0455	.0495	.0422	.0483	.0513	.055	1 500	.01250	6.50	6.20	6.12	3 06	3 15	.023	.025
17	.0445	.0495	.0535	.0462	.0523	.0553	.059	2 000	.01600	4.67	4.36	7.86	3 26	3 35	.023	.025
16	.0485	.0535	.0575	.0502	.0563	.0593	.063	2 500	.02000	3.26	3.08	9.82	3 46	3 55	.023	.025
15	.0525	.0575	.0615	.0542	.0603	.0633	.067	3 250	.02555	2.43	2.23	12.7	3 66	3 75	.023	.025
14	.0565	.0615	.0655	.0582	.0643	.0673	.071	4 100	.03200	1.80	1.62	15.8	3 86	3 95	.023	.025
13	.0605	.0655	.0695	.0622	.0683	.0713	.075	5 100	.04000	1.25	1.12	19.8	4 06	4 15	.023	.025
12	.0645	.0695	.0735	.0662	.0723	.0753	.079	6 250	.05000	.814	.712	25.3	4 26	4 35	.023	.025
11	.0685	.0735	.0775	.0702	.0763	.0793	.083	7 500	.06250	.531	.450	31.5	4 46	4 55	.023	.025
10	.0725	.0775	.0815	.0742	.0803	.0833	.087	8 900	.07700	.351	.280	39.3	4 66	4 75	.023	.025
9	.0765	.0815	.0855	.0782	.0843	.0873	.091	10 500	.09300	.220	.180	49.8	4 86	4 95	.023	.025
8	.0805	.0855	.0895	.0822	.0883	.0913	.095	12 300	.01100	.145	.110	62.8	5 06	5 15	.023	.025
7	.0845	.0895	.0935	.0862	.0923	.0953	.099	14 300	.01300	.092	.075	79.4	5 26	5 35	.023	.025
6	.0885	.0935	.0975	.0902	.0963	.0993	.103	16 500	.01500	.063	.050	100	5 46	5 55	.023	.025
5	.0925	.0975	.1015	.0942	.1003	.1033	.107	19 000	.01700	.040	.030	126	5 66	5 75	.023	.025
4	.0965	.1015	.1055	.0982	.1043	.1073	.111	21 800	.01900	.026	.018	159	5 86	5 95	.023	.025
3	.1005	.1055	.1095	.1022	.1083	.1113	.115	25 000	.02100	.016	.010	201	6 06	6 15	.023	.025
2	.1045	.1095	.1135	.1062	.1123	.1153	.119	28 500	.02300	.010	.006	240	6 26	6 35	.023	.025
1	.1085	.1135	.1175	.1102	.1163	.1193	.123	32 700	.02500	.006	.003	280	6 46	6 55	.023	.025
0	.1125	.1175	.1215	.1142	.1203	.1233	.127	37 500	.02700	.003	.001	320	6 66	6 75	.023	.025
2-0	.365	133 000	.107	.0791	.0943	404	365
4-0	.460	212 000	.166	.0560	.0597	630	460

Weight: per cubic inch of copper = .321

Resistance per circular mil-foot
at 25° C.
10.35 ohms at 25° C.
12.61 ohms at 75° C.

Resistance per 1000 ft. of 1-sq-in section
at 25° C.
103900 ohm at 25° C.
109900 ohm at 75° C.

SQUARE COPPER WIRE—BARE AND INSULATED

Gauge Number	Bare Diameter	Radius of Corners	Bare	D.C.C.	Asb. C.	Area of Copper		Ohms per 1000 Ft.		Weight, Pounds per 1000 Ft.	
						Circular Mils	Square Inch	At 25° C.	At 75° C.	Bare	D.C.C. Asb. C.
13	.072	.025083	5,920	.00465	1 79	2.13	17 9	18 6
12	.081	.025092	7,670	.00603	1 38	1 64	23 2	24 0
11	.091	.025103	.107	9,860	.00775	1 07	1 28	29 8	30 8
10	.102	.025115	.119	12,600	.00987	842	1 00	38 0	39 2
9	.114	.031129	.132	15,500	.0122	682	.814	46 9	48 6
8	.129	.031145	.148	20,100	.0158	.525	.626	61 0	63 0
7	.144	.031161	.164	25,400	.0199	.417	.498	76.7	79 0
6	.162	.031181	.183	32,400	.0254	327	390	98.0	101
5	.182	.047202	.204	39,800	.0312	.266	317	120	124
4	.204	.047	.204	.225	.227	50,600	.0397	209	.249	153	157
3	.229	.063	.229	.251	.253	62,400	.0490	.169	.202	189	194
2	.258	.063	.258	.281	.283	80,400	.0632	.132	.157	243	249
1	.289	.063	.289	.313	.315	102,000	.0801	.104	.124	309	315
0	.325	.063350	130,000	.102	.0813	.0969	394	401

DOUBLE-COTTON-COVERED COPPER RIBBON

Bare Dimension			Insulated Dimension		Area of Copper		Per 1000 Feet		
Thickness	Width	Thickness	Width	Circular Mills	Square Inch	Ohms		Weight in Pounds	
						At 25° C.	At 75° C.	Bare	Insulated
.0126	.1875	.0295	.2015	2,964	.002328	3.57	4.26	9.03	9.4
.0126	.25	.0295	.2645	3,967	.003116	2.67	3.185	12.00	12.5
.016	.255	.035	.270	5,190	.00407	2.04	2.43	15.7	16.9
.020	.258	.039	.270	6,460	.00507	1.64	1.95	19.6	20.8
.025	.258	.043	.270	8,040	.00632	1.32	1.57	24.3	25.6
.025	.365	.045	.377	11,400	.00899	.954	1.10	34.7	36.4
.032	.102	.047	.112	3,880	.00304	2.73	3.25	12.3	12.3
.032	.129	.048	.139	5,190	.00391	2.13	2.54	15.1	15.8
.032	.182	.049	.193	7,140	.00560	1.48	1.77	21.6	22.6
.032	.258	.050	.270	10,500	.00804	1.03	1.23	31.0	32.3
.032	.365	.052	.377	14,600	.0115	.725	.864	44.2	46.0
.040	.102	.056	.112	4,190	.00364	2.22	2.63	13.4	13.0
.040	.129	.056	.139	5,190	.00482	1.73	2.06	18.2	18.4
.040	.182	.056	.193	7,510	.00612	1.33	1.61	25.2	26.1
.040	.204	.057	.215	9,950	.00752	1.06	1.27	30.1	31.2
.040	.258	.058	.270	12,700	.00998	.823	.993	38.5	39.8
.040	.325	.059	.337	16,100	.0127	.656	.783	50.4	50.4
.040	.365	.060	.377	18,200	.0143	.583	.695	54.9	56.7
.045	.091	.037	.101	4,660	.00366	2.37	2.71	14.1	14.7
.045	.144	.060	.155	7,700	.00605	1.37	1.64	23.3	24.2
.045	.190	.060	.201	3,990	.00805	1.03	1.23	31.0	32.2
.051	.072	.062	.083	3,990	.00314	2.65	3.16	12.1	12.7
.051	.081	.062	.092	4,580	.00360	2.31	2.76	13.9	14.6
.051	.102	.064	.113	5,940	.00467	1.78	2.12	18.0	18.7
.051	.114	.064	.125	6,720	.00528	1.57	1.88	20.3	21.1
.051	.129	.065	.140	7,690	.00604	1.37	1.64	23.3	24.1
.051	.162	.065	.173	9,840	.00773	1.08	1.28	29.8	30.6
.051	.182	.065	.194	11,100	.00875	.950	1.13	32.7	33.6
.051	.204	.066	.216	12,600	.00987	.842	1.00	38.0	39.3
.051	.258	.067	.271	16,100	.0126	.658	.785	48.6	50.1

DOUBLE-COTTON-COVERED COPPER RIBBON—Continued

Bare Dimension			Insulated Dimension		Area of Copper		Per 1000 Feet		
Thickness	Width	Thickness	Width	Thickness	Circular Mills	Square Inch	Ohms		Weight in Pounds
							At 25° C.	At 75° C.	
.051	.325	.087	.338	.087	20,400	.0160	.518	.618	61.8
.051	.365	.088	.378	.088	23,000	.0181	.459	.548	69.7
.057	.081	.088	.092	.088	5,200	.00408	2.04	2.43	71.5
.057	.091	.088	.102	.088	5,550	.00465	1.79	2.13	15.7
.057	.129	.071	.140	.071	8,630	.00682	1.22	1.45	17.9
.057	.144	.071	.155	.071	9,770	.00767	1.08	1.29	26.3
.057	.204	.072	.216	.072	14,100	.0111	.749	.893	29.6
.064	.081	.075	.082	.075	6,030	.00472	1.76	2.10	30.6
.064	.091	.075	.102	.075	6,730	.00529	1.57	1.87	18.9
.064	.102	.077	.113	.077	7,630	.00599	1.38	1.65	13.2
.064	.114	.077	.125	.077	8,610	.00676	1.23	1.47	20.4
.064	.129	.078	.140	.078	9,830	.00772	1.03	1.28	27.0
.064	.144	.078	.155	.078	11,100	.00868	.957	1.14	30.3
.064	.162	.078	.173	.078	12,500	.00983	.845	1.03	33.6
.064	.182	.078	.194	.078	14,100	.0111	.747	.892	37.0
.064	.204	.079	.216	.079	15,900	.0125	.663	.791	42.8
.064	.258	.080	.271	.080	20,300	.0160	.490	.590	48.3
.064	.323	.081	.338	.081	23,100	.0203	.410	.489	61.6
.064	.362	.081	.378	.081	26,100	.0238	.364	.434	75.1
.072	.129	.086	.140	.086	11,100	.00875	.949	1.13	80.0
.072	.144	.086	.155	.086	12,500	.00983	.845	1.01	88.1
.072	.182	.087	.194	.087	15,000	.0126	.661	.788	99.0
.072	.204	.087	.216	.087	18,000	.0162	.547	.661	114.7
.072	.258	.087	.271	.087	23,000	.0203	.460	.559	139.1
.072	.323	.088	.338	.088	29,100	.0229	.383	.453	171.1
.081	.102	.094	.114	.094	9,840	.00773	1.08	1.28	29.8
.081	.114	.094	.125	.094	11,100	.00870	.955	1.14	33.5
.081	.129	.095	.141	.095	12,600	.00991	.838	1.00	38.2
.081	.144	.095	.156	.095	14,200	.0111	.746	.890	42.5
.081	.162	.095	.173	.095	16,000	.0126	.660	.787	48.3
.081	.182	.096	.195	.096	18,100	.0142	.585	.697	56.1

.091	.129	.105	.141	14,300	.0112	741	.884	43 2	44 4
.091	.144	.105	.156	16,000	.0126	641	.788	46 7	48 1
.091	.162	.105	.175	18,100	.0143	585	.685	48 7	50 1
.091	.204	.106	.217	23,000	.0180	497	.597	52 1	54 1
.091	.258	.107	.272	29,200	.0229	401	.501	58 2	60 3
.091	.325	.108	.339	37,000	.0290	362	.432	68 2	70 3
.091	.410	.109	.424	46,900	.0368	286	.341	82 0	84 0
.102	.129	.116	.142	16,100	.0126	658	.785	48 6	50 0
.102	.162	.117	.176	20,400	.0200	520	.616	61 6	63 2
.102	.182	.118	.196	23,000	.0180	461	.550	69 5	71 2
.102	.204	.118	.218	25,800	.0203	410	.489	78 1	79 9
.102	.258	.119	.273	32,800	.0258	322	.384	99 4	102
.102	.325	.120	.340	41,300	.0326	255	.304	126	128
.114	.142	.130	.138	19,900	.0156	593	.635	61 9	63 0
.114	.162	.131	.179	22,300	.0176	471	.562	68 0	70 0
.114	.182	.132	.198	25,400	.0199	417	.497	76 8	78 9
.114	.204	.132	.220	28,600	.0224	370	.442	86 5	88 7
.114	.258	.133	.275	36,000	.0286	291	.347	110	113
.114	.325	.134	.342	46,100	.0362	229	.274	140	143
.114	.410	.135	.427	58,500	.0488	181	.216	177	181
.129	.162	.147	.179	25,600	.0201	414	.484	77 4	79 6
.129	.204	.148	.221	32,500	.0235	326	.389	98 3	101
.129	.258	.149	.276	41,300	.0315	256	.303	125	128
.129	.325	.150	.343	52,300	.0411	202	.241	158	163
.129	.410	.151	.428	66,300	.0521	160	.190	201	205
.144	.182	.163	.200	32,300	.0254	327	.390	97 8	100
.144	.204	.163	.222	36,400	.0286	291	.347	110	113
.144	.258	.165	.276	46,300	.0363	229	.273	140	143
.144	.289	.165	.307	51,900	.0408	204	.243	157	161
.144	.325	.166	.344	58,500	.0460	181	.216	177	181
.162	.204	.182	.222	41,000	.0322	258	.307	124	127
.162	.258	.184	.278	52,200	.0410	203	.242	158	162
.162	.289	.185	.345	66,000	.0518	191	.191	200	204
.162	.325	.187	.349	80,700	.0638	209	.249	153	157
.162	.389	.194	.310	94,600	.0807	164	.195	196	200
.182	.258	.206	.386	82,200	.0645	129	.154	249	254
.182	.325	.227	.380	98,600	.0860	181	.182	178	182
.182	.389	.227	.380	116,000	.0907	129	.154	249	254
.182	.410	.228	.347	132,000	.0944	164	.195	196	200
.182	.458	.238	.360	154,000	.1048	129	.154	249	254
.182	.512	.240	.360	179,900	.1128	171	.204	187	191
.204	.565	.252	.312	204,000	.1228	132	.158	242	247
.204	.612	.254	.389	232,000	.1348	109	.109	350	356

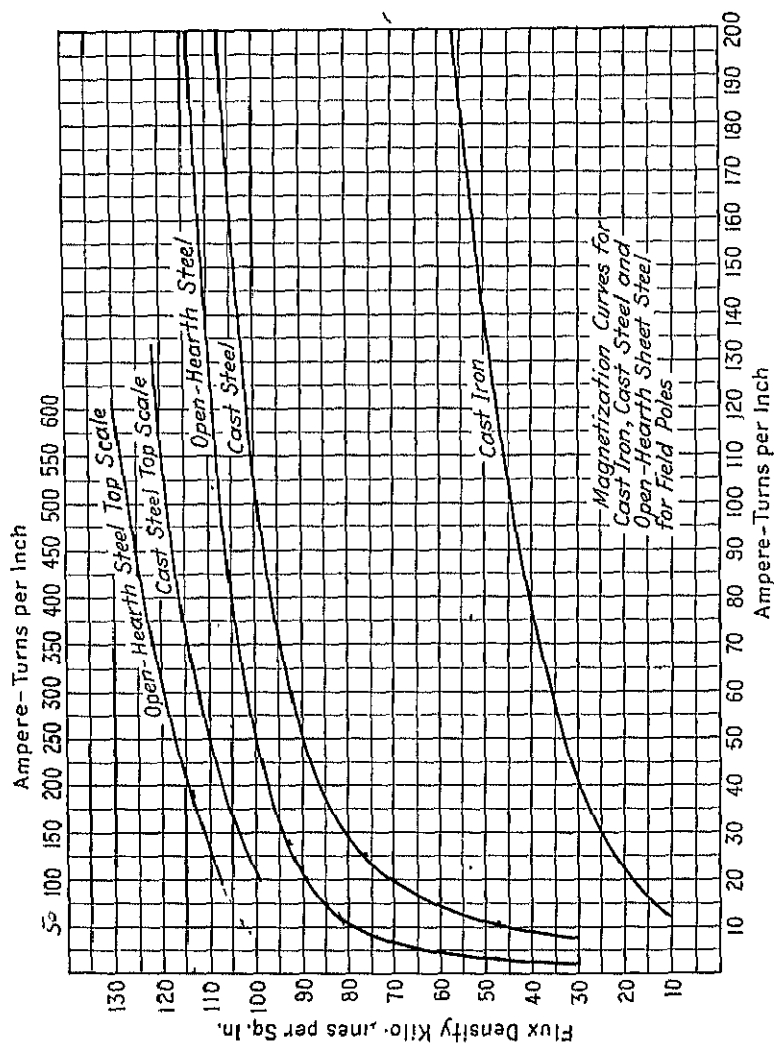
COPPER STRAPS—SOFT

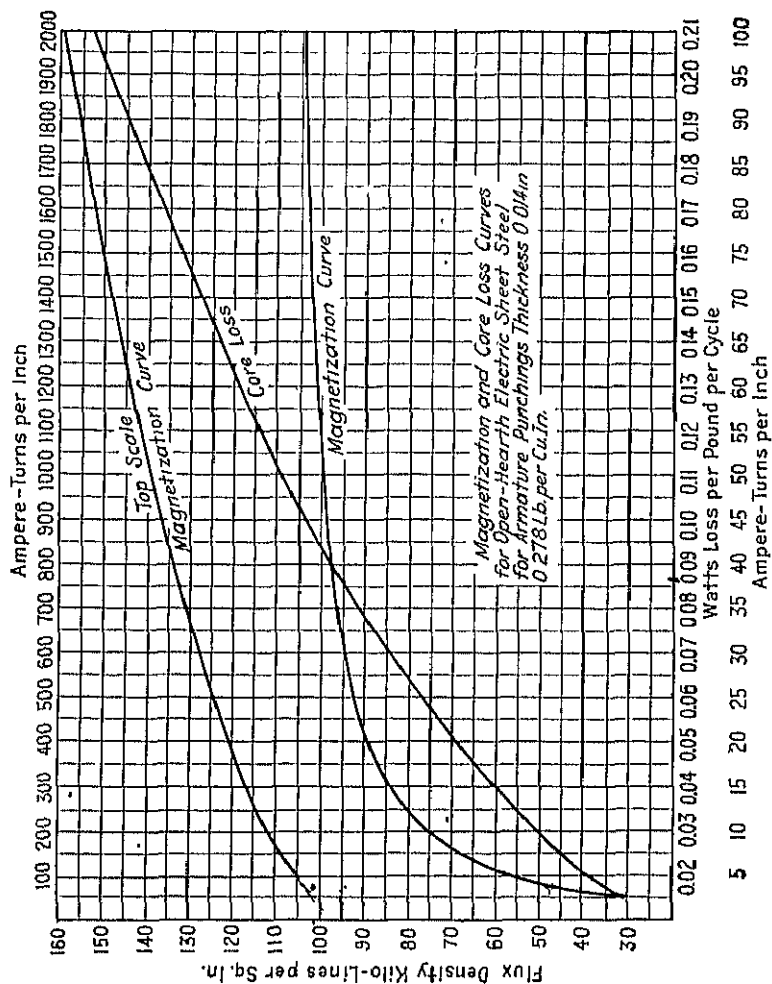
Size		Area in Square Inch	Per 1000 Ft.		
Thickness	Width		Ohms at 25° C.	Ohms at 75° C.	Weight in Pounds
.013	.325	.00419	1.98	2.37	16.1
.016	.365	.00579	1.44	1.71	22.3
.020	.365	.00721	1.15	1.37	27.8
.020	.75	.0149	.557	.664	57.5
.020	1.25	.0249	.333	.398	96.0
.025	.365	.00899	.924	1.10	34.7
.025	.5	.0124	.672	.801	47.7
.025	1.0	.0249	.334	.398	95.8
.025	1.5	.0374	.222	.265	144
.032	.365	.0115	.725	.864	44.2
.032	.5	.0158	.526	.628	60.8
.032	.625	.0198	.420	.501	76.2
.032	.75	.0238	.349	.417	91.7
.032	.875	.0278	.299	.357	107
.032	1.0	.0318	.261	.312	122
.032	1.25	.0398	.209	.249	153
.032	1.5	.0478	.174	.207	184
.032	2.0	.0638	.130	.155	246
.040	.365	.0143	.583	.695	55.0
.040	.625	.0247	.337	.402	95.0
.040	.75	.0297	.280	.334	114
.040	1.25	.0497	.167	.200	191
.040	1.5	.0597	.139	.166	230
.047	.5	.0230	.361	.430	88.7
.047	.625	.0289	.287	.343	111
.047	.75	.0348	.239	.285	134
.047	1.0	.0465	.179	.213	179
.047	1.25	.0583	.143	.170	225
.047	1.5	.0700	.119	.142	270
.047	1.75	.0818	.102	.121	315
.047	2.0	.0935	.0888	.106	360
.051	.365	.0181	.459	.548	69.7
.063	.438	.0271	.307	.366	104
.063	.5	.0307	.271	.323	118
.063	.625	.0385	.216	.257	148
.063	.75	.0464	.179	.214	179

Size		Area in Square Inches	Per 1000 Ft.		
Thickness	Width		Ohms at 25° C.	Ohms at 75° C.	Weight in Pounds
.063	.875	.0543	.153	.183	209
.063	1	.0622	.134	.159	240
.063	1.25	.0779	.107	.127	300
.063	1.5	.0937	.0887	.106	361
.063	1.75	.109	.0759	.0906	422
.063	2	.125	.0661	.0792	482
.063	2.25	.141	.0590	.0703	543
.064	2.53	.0160	.520	.620	61.6
.064	.365	.0228	.364	.434	88.0
.078	.5	.0377	.220	.263	145
.078	.625	.0475	.175	.209	183
.078	.75	.0572	.145	.173	220
.078	.875	.0670	.124	.148	258
.078	1.0	.0767	.108	.129	296
.078	1.25	.0962	.0863	.103	371
.078	1.5	.116	.0718	.0856	446
.078	2.0	.155	.0537	.0640	596
.094	.438	.0406	.204	.244	157
.094	.5	.0451	.184	.220	174
.094	.625	.0569	.146	.174	219
.094	.75	.0686	.121	.144	264
.094	.875	.0804	.103	.123	310
.094	1.0	.0921	.0902	.108	355
.094	1.25	.116	.0719	.0856	446
.094	1.5	.139	.0597	.0712	536
.094	1.75	.163	.0511	.0609	627
.094	2.0	.186	.0446	.0532	717
.109	.5	.0520	.160	.191	200
.109	.625	.0656	.127	.151	253
.109	.75	.0792	.105	.125	306
.109	.875	.0928	.0895	.107	358
.109	1	.107	.0780	.0931	411
.109	1.25	.134	.0621	.0741	515
.109	1.5	.161	.0516	.0615	621
.109	1.75	.188	.0441	.0526	725
.125	.438	.0589	.154	.184	208

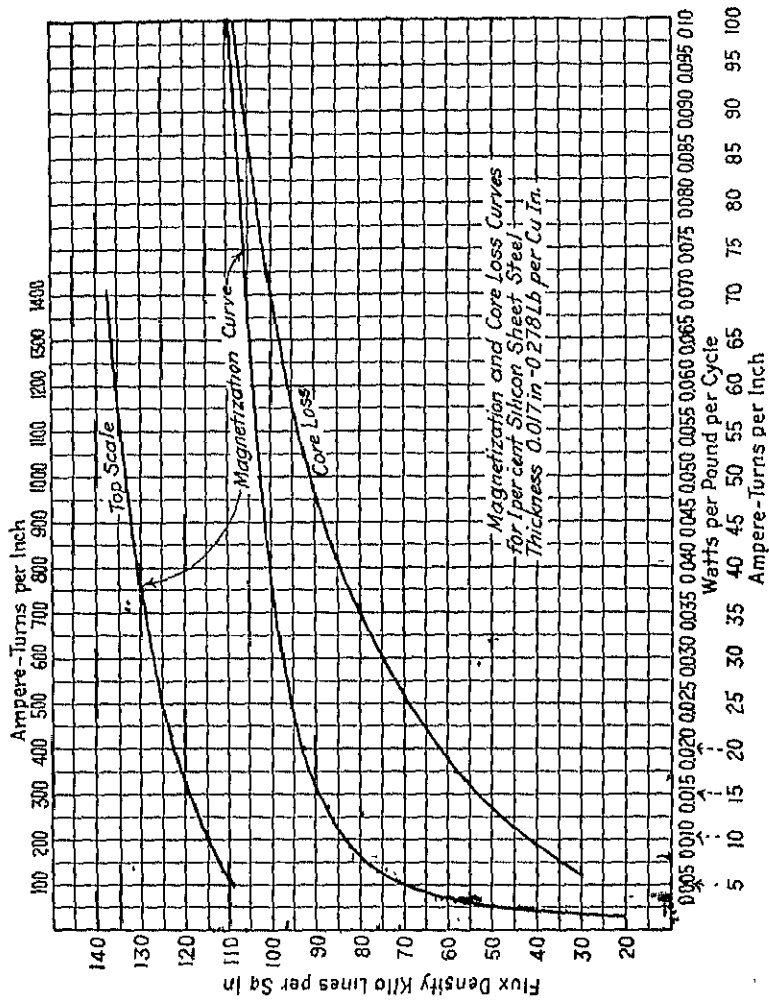
Size		Area in Square Inches	Per 1000 Ft.		
Thickness	Width		Ohms at 25° C.	Ohms at 75° C.	Weight in Pounds
.125	.5	.0592	.140	.168	228
.125	.625	.0748	.111	.133	288
.125	.75	.0904	.0919	.110	348
.125	.875	.106	.0783	.0934	409
.125	1.0	.122	.0683	.0814	469
.125	1.25	.153	.0513	.0648	589
.125	1.5	.184	.0451	.0538	710
.125	1.75	.215	.0386	.0460	830
.125	2	.247	.0337	.0402	950
.129	.258	.0325	.256	.305	125
.141	.5	.0686	.121	.144	264
.141	.875	.120	.0692	.0826	463
.144	.258	.0363	.229	.273	140
.156	.5	.0761	.109	.130	293
.156	.625	.0956	.0869	.104	269
.156	.75	.114	.0731	.0872	438
.156	.875	.133	.0624	.0744	513
.156	1.0	.153	.0514	.0649	588
.156	1.25	.192	.0434	.0517	738
.156	1.5	.231	.0360	.0430	889
.156	1.75	.270	.0308	.0367	1040
.156	2.25	.348	.0239	.0285	1340
.162	.325	.0518	.160	.191	200
.162	.365	.0583	.143	.170	225
.188	.5	.0921	.0902	.108	355
.188	.625	.116	.0718	.0857	446
.188	.875	.161	.0516	.0615	621
.188	1.0	.185	.0450	.0537	712
.188	1.25	.232	.0359	.0428	893
.188	1.5	.279	.0298	.0356	1070
.188	2	.373	.0223	.0266	1440
.188	2.5	.467	.0178	.0212	1800
.219	.438	.0940	.0883	.105	362
.219	.5	.108	.0772	.0921	415
.219	.625	.135	.0615	.0734	520

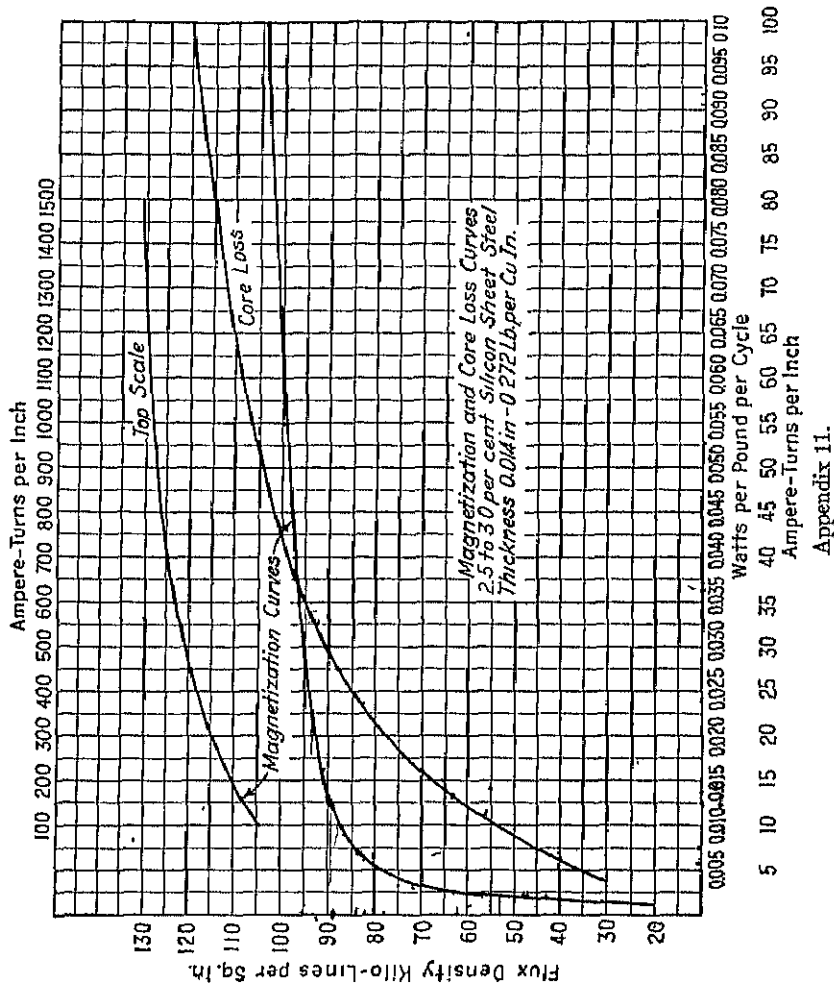
Size		Area in Square Inches	Per 1000 Ft.		
Thickness	Width		Ohms at 25° C.	Ohms at 75° C.	Weight in Pounds
.219	1	.216	.0385	.0459	831
.229	.280	.0628	.132	.168	242
.229	.365	.0802	.104	.124	309
.250	.5	.122	.0683	.0815	409
.250	.875	.211	.0393	.0469	814
.250	1	.242	.0343	.0409	934
.250	1.25	.305	.0272	.0325	1189
.250	1.5	.367	.0226	.0270	1420
.250	2	.492	.0169	.0201	1900
.250	2.5	.617	.0135	.0160	2380
.250	3	.742	.0112	.0134	2860
.250	4	.992	.00837	.00998	3830
.258	.365	.0908	.0915	.109	350
.313	.5	.153	.0513	.0647	590
.313	1.0	.305	.0272	.0324	1180
.313	1.25	.384	.0217	.0258	1480
.313	1.5	.462	.0180	.0214	1780
.313	2	.618	.0131	.0160	2380
.375	1	.367	.0226	.0270	1420
.375	1.25	.461	.0180	.0215	1780
.375	1.5	.555	.0150	.0179	2140
.375	2.0	.742	.0112	.0134	2860
.375	2.5	.930	.00893	.0107	3580
.375	3.0	1.12	.00743	.00886	4310
.375	4.0	1.49	.00557	.00661	5750

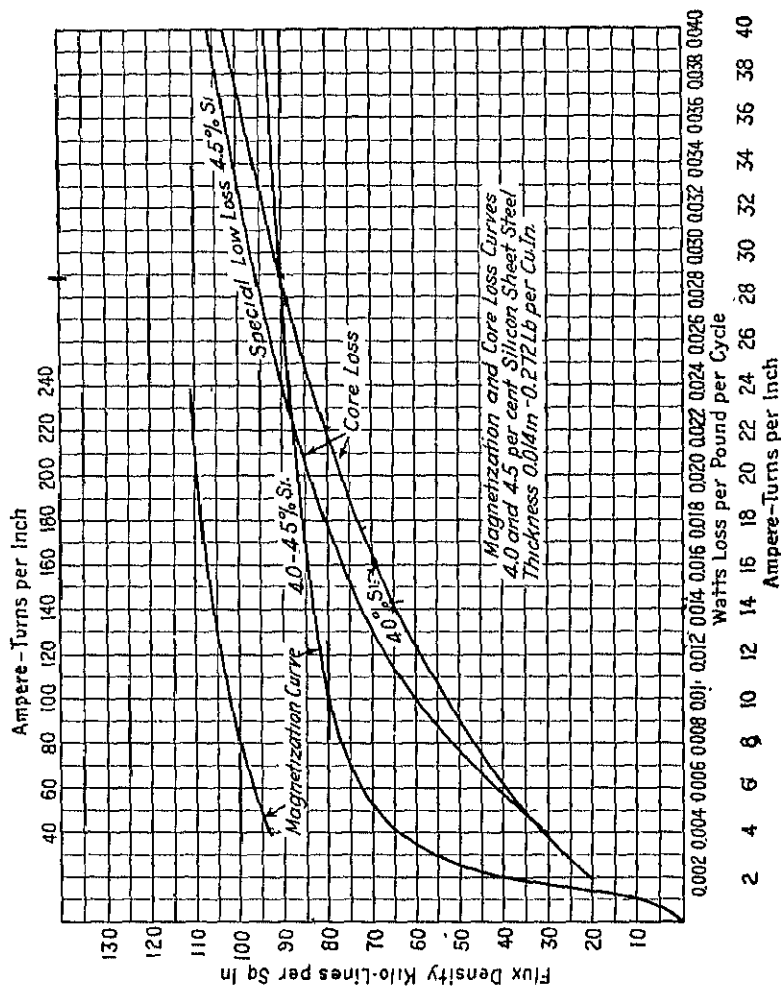




Appendix 9.







Appendix 12.

LIST OF SYMBOLS

A

- A = current density, amperes per square inch
 A = width of commutating zone for one coil in inches of armature circumference
 A_a = current density in armature conductor
 A_b = current density at brush contacts
 A_c = area of core section
 A_{er} = current density in the end-ring
 A_f = current density in field copper (shunt field for d-c. machine)
 A_h = current density in high voltage winding
 A_i = current density in commutating field copper
 A_l = current density in low voltage winding
 A_r = current density in rotor copper (bars of squirrel-cage winding)
 A_s = current density in series field copper
 A_s = current density in stator copper
 AT = ampere-turns
 AT_a = maximum ampere-turns per pole of armature reaction
 AT_{af} = equivalent field ampere-turns per pole of armature reaction
 AT_g = air gap ampere-turns per pole
 AT_{gt} = ampere-turns per pole for commutating pole air gap
 AT_p = ampere-turns per pole for field pole
 AT_{pt} = ampere-turns per pole for commutating pole
 AT_t = ampere-turns per pole for armature teeth
 AT_{tt} = ampere-turns per pole for teeth under commutating pole
 AT_{tr} = ampere-turns per pole for rotor teeth
 AT_{ts} = ampere-turns per pole for stator teeth
 AT_{ya} = ampere-turns per pole for armature yoke
 AT_{yai} = ampere-turns per commutating pole for flux in armature yoke
 AT_{yf} = ampere-turns per pole for field yoke
 AT_{yfi} = ampere-turns per commutating pole for flux in field yoke
 AT_{yr} = ampere-turns per pole for rotor yoke
 AT_{ys} = ampere-turns per pole for stator yoke
 ATP = total ampere-turns per pole
 ATP_a = armature ampere-turns per pole
 ATP_c = armature cross-magnetizing ampere-turns
 ATP_d = armature magnetizing ampere-turns
 ATP_f = ampere-turns per field pole (shunt field for d-c. machines)
 ATP_i = ampere-turns per commutating pole
 ATP_o = no-load ampere-turns per pole synchronous machines
 ATP_s = series field ampere-turns per pole
 ATP_s = ampere-turns per field pole for full-load and short circuit
 ATP_{80} = ampere-turns per field pole for full-load and 80 per cent power factor
 ATP_{100} = ampere-turns per field pole for full-load and 100 per cent power factor

a = dimension of core section (see Figs. 220, 221 and 222)
 a_x = width of tube of force at armature circumference
 at = ampere-turns per inch
 at_p = ampere-turns per inch for the pole density
 at_t = ampere-turns per inch for the tooth density
 at_{tr} = ampere-turns per inch for rotor tooth density
 at_{ts} = ampere-turns per inch for stator tooth density,
 at_{ya} = ampere-turns per inch for the armature yoke density
 at_{yf} = ampere-turns per inch for the field yoke density
 at_{yr} = ampere-turns per inch for rotor yoke density
 at_{ys} = ampere-turns per inch for stator yoke density

B

B = pole arc, inches of armature circumference
 B = flux density
 B_a = average value of air gap flux density
 B_e = effective value of air gap flux density
 B_g = flux density in main pole air gap
 B_{g1} = flux density in commutating pole air gap
 B_m = maximum value of air gap flux density
 B_p = flux density in pole
 B_t = flux density in teeth
 B_{t1} = flux density in teeth at air gap surface
 B_{t2} = flux density in teeth at minimum tooth section
 B_{t3} = flux density in teeth at point $\frac{1}{2}$ slot depth from minimum section
 B_{tr2} = flux density in rotor teeth at bottom of slot
 B_{tr3} = flux density in rotor teeth for section $\frac{1}{2}$ tooth length from minimum section
 B_{ts1} = flux density in stator teeth at air gap surface
 B_{ts2} = flux density in stator teeth for section $\frac{1}{2}$ tooth length from minimum section
 B_{ya} = flux density in armature yoke
 B_{yf} = flux density in field yoke
 B_{yr} = flux density in rotor yoke
 B_{ys} = flux density in stator yoke
 B_1 = maximum value of fundamental of flux wave
 B_3 = maximum value of third harmonic
 B_5 = maximum value of fifth harmonic
 B_7 = maximum value of seventh harmonic
 b = armature coil extension (see Figs. 50 and 136)
 b = number of commutator bars covered by brush
 b = dimension of core section (see Figs. 220, 221 and 222)
 b_s = angle of brush shift, inches of armature circumference
 b_t = brush thickness, inches
 b_x = mean width of tube of force

C

C = output constant
 C = length of straight part of armature coil end-connection (see Figs. 50 and 136)

E = induced voltage
 E = effective value of induced voltage per phase for alternating current machines
 E_a = exciter voltage
 E_f = voltage drop in field winding (shunt field d.-c. machine)
 E_h = high voltage
 E_l = low voltage
 E_r = rotor voltage between slip rings
 E_T = terminal voltage per phase for alternating current machines
 E_1 = voltage induced by armature flux (see formula 130)
 e_r = reactance voltage per coil
 e_{sa} = average voltage between adjacent commutator bars
 e_{sm} = maximum voltage between adjacent commutator bars
 e_t = voltage per turn
 eff = efficiency

F

F_c = stator and rotor end-connection leakage factor
 F_{sr} = rotor slot leakage factor
 F_{ss} = stator slot leakage factor
 f = see Figs. 50 and 136
 f = frequency cycles per second
 f_b = form factor
 f_c = chord factor
 f_{cr} = chord factor for rotor winding
 f_{cs} = core space factor
 f_d = air gap flux distribution factor
 f_s = copper space factor (see Fig. 224)
 f_w = winding distribution factor (see Fig. 122)
 f_{wr} = winding distribution factor for rotor winding

G

G_a = armature copper weight
 G_c = total core weight
 G_{ct} = weight of core in teeth
 G_{cy} = weight of core in yoke
 G_f = field copper weight (shunt field d.-c. machines)
 G_h = copper weight in high voltage winding
 G_s = copper weight in commutating field winding
 G_k = total copper weight transformers
 G_l = copper weight in low voltage winding
 G_s = copper weight in series field winding
 g = see Figs. 50 and 136
 g_c = core weight per cubic inch
 g_k = copper weight per cubic inch

H

H = magnetizing force
 h = height of winding (see Figs. 236 and 237)
 h_f = height of field coil (shunt field coil d.-c. machine)

r_p = radius of pole body (see Figs. 51 and 141)
 h_s = height of pole shoe (see Figs. 51 and 141)
 h_w = height of window opening

I

I = terminal current amperes per phase for alternating current machines
 I_a = armature current
 I_b = effective value of current in each bar
 I_h = current in high voltage winding
 I_l = current in low-voltage winding
 I_m = maximum value of current per bar
 I_m = magnetizing current per phase
 I_{mq} = magnetizing current per phase due to air gap reluctance only
 I_o = no-load current per phase (exciting current)
 I_r = rotor current per phase
 I_s = short circuit current per phase
 I_s = series field current
 I_w = watt component of the no-load current per phase
 i_a = armature current per path
 i_f = field current (shunt field d-c. machines)
 $i_{f_{max}}$ = maximum field current with rheostat all cut out and 120 volts across collector rings
 i_{fo} = no-load field current
 $i_{f_{100}}$ = field current for full-load and 100 per cent power factor
 $i_{f_{80}}$ = field current for full-load and 80 per cent power factor

K

K = number of commutator bars
 K_a = armature reaction factor
 K_b = belt leakage constant (see Fig. 145)
 K_{br} = rotor belt leakage constant (see Fig. 145)
 K_{bs} = stator belt leakage constant (see Fig. 145)
 K_r = correction factor for chorded rotor windings (see Fig. 144)
 K_s = correction factor for chorded stator windings (see Fig. 144)
 Kva = kilovolt-amperes
 Kw = kilowatt
 Kw_a = armature kilowatt output
 k = air gap coefficient
 k_r = air gap coefficient for rotor slots
 k_s = air gap coefficient for stator slots
 k_1 = stacking factor (0.90 to 0.93)
 k_2 = 1.73 for star-connected and 1.00 for delta-connected rotor winding
 k_3 = 1.73 for star-connected and 3 for delta-connected winding
 k_4 = see formula 225

L

L = coefficient of self-induction
 L = total length of conductor in winding
 L_a = length of one-half mean-turn of armature coil

L_f = length of mean-turn of field coil (shuntfield for d-c. machine)
 L_{f_1} , L_{f_2} , and L_{f_3} = length of mean-turn of sections 1, 2 and 3, respectively, of wire-wound field coil (see Fig. 153)
 L_h = length of mean-turn of high voltage coil
 L_c = length of mean-turn of commutating field coil
 L_l = length of mean-turn of low voltage coil
 L_r = length of one-half mean-turn of rotor coil
 L_s = length of mean-turn of series field coil
 $L_{s'}$ = length of one-half mean-turn of stator coil
 L' = coefficient of self and mutual induction
 L'_1 = coefficient of self and mutual induction for armature leakage flux path one
 L'_2 = coefficient of self and mutual induction for armature leakage flux path two
 L'_3 = coefficient of self and mutual induction for armature leakage flux path three
 L'_4 = coefficient of self and mutual induction for armature leakage flux path four
 l = length of armature core—stator core induction motors
 l_b = effective length of bar-squirrel-cage winding
 l_c = length of commutator
 l_c = mean length of magnetic circuit (transformers)
 l_e = horizontal length of armature coil end-connections ($b + f + g$, Fig. 50 and Fig. 136)
 l_g = length of air gap section
 l_o = gross core length ($l - n_d w_d$)
 l_p = length of flux path in pole (radial length of pole)
 l_s = length one-half armature coil end-connections $= L_a - l$
 l_t = length of flux path in teeth
 l_{tr} = length of flux path in rotor teeth
 l_{ts} = length of flux path in stator teeth
 l_u = length of yoke, transformers
 l_{yu} = length of flux path in armature yoke
 l_{yf} = length of flux path in field yoke
 l_{yr} = length of flux path in rotor yoke
 l_{ys} = length of flux path in stator yoke
 l_1 = axial length of pole shoe
 l_2 = axial length of the field yoke

M

M = coefficient of mutual induction
 m = degree of multiplicity, d-c. windings
 m = number of phases
 m = number of commutator bars per slot
 mmf = magnetomotive force
 m_r = number of phases in rotor winding
 m_s = number of phases in stator winding

N

N = total number of conductors, d-c. machines
 N = number of conductors in series per phase

N_s = number of rotor conductors in series per phase
 n = speed, revolutions per minute (synchronous speed a-c. machines)
 n_a = number of brush arms
 n_b = number of brushes per arm
 n_d = number of ventilating ducts
 n_0 = motor no-load speed
 n_s = revolutions per second
 n_1 = motor full-load speed

P

P = brush pressure pounds per square inch
 P = per cent pitch
 P_r = per cent resistance drop
 P_x = per cent reactance drop
 P_z = per cent impedance drop
 PF = power factor
 PF_0 = power factor no-load
 PF_s = power factor short-circuit
 p = number of poles

Q

Q = ampere conductors per inch of armature circumference
 Q = ampere conductors per inch of stator gap circumference

R

R = resistance
 R_a = resistance of armature winding—per phase for synchronous machines
 R_c = armature circuit resistance
 R_f = resistance of field winding (shunt field for d-c. machines)
 R_h = resistance of high voltage winding (per phase for 3-phase)
 R_i = resistance of commutating field winding
 R_l = resistance of low voltage winding (per phase for 3 phase)
 R_r = rheostat resistance
 R_r = equivalent rotor resistance per phase
 R_{rh} = rheostat resistance per phase (wound rotor induction motor)
 R_{r0} = field rheostat resistance for no-load
 R_{r1}, R_{r2} = starting box resistance for first button, second button, etc.
 R_s = resistance of series field winding
 R_s = resistance per phase of stator winding
 R_t = total resistance in terms of high voltage winding
 R_1 = resistance at temperature T_1
 R_2 = resistance at temperature T_2
 r = 0.692 for 25° C.; 0.826 for 75° C.
 r.p.m. = revolutions per minute

S

S = number of slots
 S = radiating surface
 S_a = armature radiating surface

S_c = radiating surface of commutator
 S_{cr} = total rotor copper section
 S_{cs} = total stator copper section
 S_f = radiating surface of field winding—shunt field d-c. machine
 S_t = radiating surface of commutating field winding
 S_r = number of rotor slots
 S_s = number of stator slots
 S_t = total wetted tank surface
 s = clearance between armature coils at end-connections (see Figs. 50 and 130)
 s = section area
 s_a = section area of armature conductor
 s_b = section area of bar in squirrel-cage winding
 s_c = conductor section
 s_{ch} = conductor section for high voltage winding
 s_{cl} = conductor section for low voltage winding
 s_{er} = section area of end-ring
 s_f = section area of field winding conductor (shunt field d-c. machine)
 s_{f_1} = section area of field conductor with t_{f_1} turns per pole
 s_{f_2} = section area of field conductor with t_{f_2} turns per pole
 s_g = air gap section
 s_i = section area of commutating field conductor
 s_p = section area of pole
 s_r = section area of rotor conductors (wound-rotor motor)
 s_s = section area of series field conductor
 s_s = section area of stator conductor
 s_t = section area of teeth
 s_{t_1} = section area of teeth at air gap surface
 s_{t_2} = section area of teeth at bottom of slot
 s_{t_3} = area of teeth at point $\frac{1}{2}$ slot depth from minimum section
 s_{ya} = section area of armature yoke
 s_{yf} = section area of field yoke

T

T_a = armature temperature rise
 T_c = commutator temperature rise
 T_f = shunt field winding temperature rise
 T_t = commutating field winding temperature rise
 T_1 = temperature at which R_1 is measured
 T_2 = temperature for which R_2 is calculated
 t = time of commutation of one coil
 t = number of turns
 t_a = number of turns per armature coil
 t_f = number of turns per field coil (shunt field d-c. machines)
 t_{f_1} = number of turns per field coil of conductor section s_{f_1}
 t_{f_2} = number of turns per field coil of conductor section s_{f_2}
 t_{f_1} , t_{f_2} , and t_{f_3} = number of turns per sections 1, 2 and 3 respectively, of wire-wound field coil (see Fig. 153)
 t_h = number of turns in high voltage coil
 t'_h = high voltage turns per core leg for single-phase core type transformers

t_1 = number of turns per commutating pole
 t_l = number of turns in low voltage coil
 t_s = number of turns per series field coil
 t_1 = tooth pitch at armature surface
 t_2 = minimum tooth pitch
 t_r = rotor tooth pitch at air gap surface
 t_{1s} = stator tooth pitch at air gap surface

V

v = peripheral velocity, feet per minute
 v_c = commutator peripheral speed, feet per minute

W

W_a = armature copper loss
 W_b = brush contact loss
 W_{bf} = brush friction loss
 W_c = core loss
 W_c = commutator losses
 W_{ct} = core loss in teeth due to fundamental frequency flux
 W_{cy} = core loss in yoke due to fundamental frequency flux
 W_e = exciter capacity
 W_f = copper loss in field winding (shunt field d-c. machines)
 W_{fw} = bearing friction and windage loss
 W_h = copper loss in high voltage winding
 W_i = copper loss in commutating field winding
 W_k = total copper loss
 W_l = copper loss in low voltage winding
 W_r = rheostat loss
 W_s = series field copper loss
 W_s = stray load-loss
 W_{scd} = stator copper loss due to no-load current
 W_{sl} = stray load-losses
 w = number of turns in series per phase
 w_b = width of brush
 w_c = width of commutating zone in inches of armature circumference
 w_k = core loss per pound
 w_d = width of ventilating duct
 w_i = width of commutating pole
 w_k = copper loss per pound
 w_p = width of pole body
 w_s = width of slot
 w_{sr} = width of rotor slot
 w_{sr_1} = width of rotor slot opening partly closed slot (see Fig. 190)
 w_{s_1} = width of slot opening partly closed slot (see Fig. 146)
 w_{ss} = width of stator slot
 w_{ss_1} = width of stator slot opening partly closed slot (see Fig. 195)
 w_{ta} = average tooth width

w_{tr2} = width of rotor tooth at bottom of slot
 w_{tr3} = width of rotor tooth at point $\frac{1}{2}$ tooth length from minimum width
 w_{ts1} = width of stator tooth at air gap surface
 w_{ts2} = width of stator tooth at point $\frac{1}{2}$ tooth length from minimum width
 w_{t1} = width of tooth at air gap surface
 w_{t2} = width of tooth at bottom of slot
 w_{t3} = width of tooth at point $\frac{1}{2}$ slot depth from minimum width
 w_w = width of window opening

X

$X = AT_g + AT_t + AT_{ya}$
 X_b = belt leakage reactance per phase
 X_c = end-connection leakage reactance per phase
 X_l = total leakage reactance per phase
 X_m = magnetizing reactance per phase
 X_{r2} = rotor zigzag leakage reactance per phase
 X_s = slot leakage reactance per phase
 X_{sr} = rotor slot leakage reactance per phase
 X_{ss} = stator slot leakage reactance per phase
 X_{sz} = stator zigzag leakage reactance per phase
 X_z = zigzag leakage reactance per phase
 X_{zr} = rotor zigzag leakage reactance per phase
 x = see Fig. 100
 x_l = number of low voltage coils per group
 x_h = number of high voltage coils per group
 x_{hl} = number of "high-low" groups

Y

Y_c = commutator pitch
 Y_s = coil pitch
 Y_1 = back pitch
 Y_2 = front pitch
 y = see Fig. 53

Z

Z = short-circuit impedance per phase
 Z = standstill impedance per phase
 Z_a = armature impedance per phase

GREEK SYMBOLS

α = angle (see Figs. 50 and 136)
 β = angle of brush shift in electrical degrees
 β = commutator bar pitch in inches of commutator circumference
 β_r = commutator bar pitch in inches of armature circumference
 δ = length of air gap at center of pole
 δ_s = length of air gap under commutating pole
 δ_m = length of air gap under pole tip
 δ_x = length of air gap at some point x
 θ = power factor angle

μ = permeability
 π = 3.1416
 τ = pole pitch in inches of armature circumference
 τ = pole pitch in inches of stator gap circumference
 ϕ = flux per pole
 ϕ_a = flux per commutating pole
 ϕ_l = field leakage flux per pole
 ϕ_{l1} = field leakage flux for path 1
 ϕ_{l2} = field leakage flux for path 2
 ϕ_{l3} = field leakage flux for path 3
 ϕ_{l4} = field leakage flux for path 4
 ϕ_t = hypothetical total flux
 φ = phase difference in commutation
 ψ = per cent pole embrace

3354

(65) 1.31.33 (10)

INDEX

A

- Additional losses, direct-current machines, 117, 127, 149
 - induction motors, 304, 314, 320
 - synchronous machines, 235, 245, 264
 - transformer, 360, 372, 384, 390, 408
- Advantages of compensated machine, 1
- Air blast transformer, 344
- Air gap, ampere-turns, direct-current machines, 61, 70, 136
 - induction motors, 301, 312, 327
 - synchronous machines, 207, 212, 254
 - coefficient, direct-current machines, 63, 70, 136
 - induction motors, 301, 311, 327
 - synchronous machines, 207, 211, 254
- density, average values of, direct-current machines, 16
 - induction motors, 274
 - synchronous machines, 168
- density, direct-current machines, 61, 70, 136
 - induction motors, 289, 322
 - synchronous machines, 206, 211, 254
- length, approximate minimum value of direct-current machines, 23, 75, 79
 - induction motors, 291, 298, 324
 - synchronous machines, 172, 224
- section, direct-current machines, 62, 70, 136
 - length of, synchronous machines, 206, 211, 254
 - synchronous machines, 206
- Aluminum resistance of, 307
- Ampere conductors per inch of, armature circumference, direct-current machines, 16
 - synchronous machines, 168
- stator gap circumference, induction motors, 274
- Ampere-turns, armature teeth, direct-current machines, 63, 72, 137
 - synchronous machines, 208, 212, 254
- armature yoke, direct-current machines, 65, 73, 138
 - synchronous machines, 208, 213, 255
- field pole, direct-current machines, 66, 74, 138
 - synchronous machines, 210, 215, 257
- field yoke, direct-current machines, 66, 75, 139
 - synchronous machines, 211, 215, 257
- per commutating pole, 106, 113, 145
- per inch of flux path, 61, Appendix
- per joint transformer cores, 368
- per pole, direct-current machines, 61, 69, 75, 139
 - synchronous machines, 206, 215, 258
- rotor teeth, 302, 312, 328
 - yoke, 303, 313, 328
- stator teeth, 302, 312, 327
 - yoke, 303, 312, 328
- Appendix, 419-432
- Armature, coil, construction, direct-current machines, 44
 - synchronous machines, 193
- end-connection clearances, direct-current machines, 55
 - synchronous machines, 190
- insulation, direct-current machines, 47-49
 - synchronous machines, 195, 196
- conductor section, direct-current machine, 52, 58, 134
 - synchronous machines, 196, 202, 252
- conductors, in series per phase, synchronous machines, 201, 252
- conductors, total, synchronous machines, 201, 252
- construction, direct-current machines, 3
 - synchronous machines, 154

machines, 115, 125, 148
 synchronous machines, 196, 231, 244, 268
 cross-magnetizing ampere-turns, 77, 147
 current, direct-current machines, 52
 synchronous machines, 202
 demagnetizing ampere-turns, 76
 diameter and length, direct-current machines, 19, 28, 131
 synchronous machines, 170, 178, 249
 frame, construction of, synchronous machines, 158
 laminations, thickness of, direct-current machines, 3
 synchronous machines, 154
 leakage flux paths, direct-current machines, 98
 reactance synchronous machines, 219, 229, 257
 length, direct-current machines, 19, 28, 131
 synchronous machines, 170, 178, 248
 peripheral speed, direct-current machines, 18
 synchronous machines, 170
 reaction, synchronous machines, 222
 ampere-turns, maximum value of, 222
 factor, 223, 230, 259
 slot dimensions, direct-current machines, 53, 58, 135
 synchronous machines, 198, 204, 253
 effect upon flux wave, direct-current machines, 26, 43
 synchronous machines, 192
 tooth density, average values for, synchronous machines, 208
 direct-current machines, 71, 137
 maximum values for direct-current machines, 64
 synchronous machines, 207, 212, 254
 teeth, section of, direct-current machines, 64, 71, 137
 synchronous machines, 207
 tooth support, direct-current machines, 5
 synchronous machines, 156

machines, windings, direct-current machines, classification of, 30
 synchronous machines, classification of, 179
 connections of, 190
 method of laying out, 182
 parallel circuits of, 190, 201, 252
 yoke section, direct-current machines, 65, 73, 137
 synchronous machines, 212, 255
 Arrangement of coils, transformer windings, 358
 Average temperature rise of oil, 370
 Axial length of field yoke, direct-current machines, 67, 74, 138

B

Back pitch, lap winding, 31, 57
 wave winding, 36, 134
 Bar pitch squirrel-cage winding, synchronous motors, 261
 Bar section, squirrel-cage winding, 297, 299
 Bars per pole squirrel-cage winding, synchronous motors, 261
 Bearings, direct-current machines, 12
 Belt leakage, constant synchronous machines, 219
 reactance synchronous machines, 218
 Brass, resistance of, 307
 Brush, contact, 95
 drop, 108
 loss, 110, 126, 148
 surface, 107, 111, 143
 friction loss, A. I. E. E. Standards, direct-current machines, 118, 127, 149
 thickness, 96, 107, 109, 110
 width, total per arm, 109, 111, 143
 Brushes, characteristics of, 108
 lubricating qualities of, 95
 stagger of, 95

C

Chain windings, 179
 Choice of armature winding, direct-current machines, 50, 56, 132
 Chord factor, calculation of, 180, 186
 definition of, 166
 stator winding, 273, 289, 322

motors, 282, 289, 322
Chorded windings, direct-current machines, 131
 synchronous machines, 180
Circle diagram, 309, 317, 333
Circular transformer coils, advantages of, 350
Coefficient of, mutual induction, 98
 self induction, 98
Coil pitch, 33
 armature coils, direct-current machines, 55
 synchronous machines, 190
Coil support, synchronous machines, 157
Commutating field, copper loss, 116, 126, 146
 winding, conductor section, 86, 113, 145
 design of, 85, 113, 145
 insulation of, 85, 114, 145
Commutating pole, air gap, ampere-turns, 105, 113, 145
 density, 104, 112, 145
 length, 102, 111, 143
 design of, 101
 flux, 105
 length, 102, 112, 144
Commutating pole machine, 1
 magnetic circuit, 105
 shoe bevel of, 104
 width, 101, 111, 144
Commutating zone, maximum width of, 98
Commutation, 91
 effect of mechanical condition of commutator and brushes, 95
Commutator bar, minimum thickness of, 106
 construction, 5
 diameter, 106, 110, 142
 length, 107, 111, 143
 mica thickness of, 106
 peripheral speed, 106
 pitch, lap winding, 32, 57
 wave winding, 38, 134
 segment pitch, 107, 110, 142
 minimum value of, 107
Compensated machine, 1
Compensating winding, 79

Concentric type transformer winding, 357
Conductor insulation, armature coils, direct-current machines, 47, 49
 synchronous machines, 195, 204, 252
 rotor winding, 297, 298, 325
 stator winding, 285, 289, 322
 transformer windings, 357
Conductor section, high-voltage winding, 352
 low-voltage winding, 352
 stator winding, induction motors, 284, 289, 322
 wound rotor winding, 298, 325
Conductors, in series, per phase, stator winding, 283, 288, 321
 wound rotor winding, 297, 324
 per slot, armature, direct-current machines, 57, 132
 synchronous machines, 179, 201, 252
 arrangement of, synchronous machines, 193, 204, 253
 per stator slot, 283, 289, 322
 arrangement of, 284, 290, 323
 total stator induction motors, 283, 288, 321
Constant potential transformers, 335
Construction of, belt tightener base, 13
 brush holder and brush yoke, 12
 commutating pole winding, 10
 field coil, direct-current machines, 9
 synchronous machines, 163
 field poles, direct-current machines, 9
 synchronous machines, 164
 field winding, non-salient pole machines, 159
 field yoke, direct-current machines, 11
 rotor, 267
 stator, 266
Cooling constant, armature, direct-current machines, 124, 129, 150
 field winding, direct-current machines, 125, 129, 151
Cooling curves, transformers, 371
Cooling surface, armature, direct-current machines, 123
 synchronous machines, 244, 246, 261
 field winding, synchronous machines, 228, 233, 261
 shunt field winding, 83, 91, 142

formers, 354, 355
 per pound, 345
 Copper space factor, average values of, 352
 Copper table, bare copper strap, 424-427
 double-cotton-covered ribbon, 421-423
 round wire, 419
 square wire, 420
 Copper weight, armature winding, direct-current machines, 56, 59, 135
 synchronous machines, 200, 205, 253
 commutating field winding, 86, 114, 146
 field winding, synchronous machines, 229, 233, 261
 high-voltage coil, 365
 low-voltage coil, 365
 series field winding, 85, 93
 shunt field winding, 83, 91, 142
 Core loss, average values of, transformers, 354, 355
 current, 368
 direct-current machines, 117, 126, 148
 induction motors, 303, 314, 329
 per pound, 315
 per cycle, open-hearth 0.014-in. electric sheet steel, 429
 1.0 per cent 0.017-in. silicon sheet steel, 430
 2.5 to 3.0 per cent 0.014-in. silicon sheet steel, 431
 4.0 and 4.5 per cent 0.014-in. silicon sheet steel, 432
 synchronous machines, 235, 245, 261
 Core space factor, 350
 Core type transformer, construction of, 339
 Current density, armature conductor, direct-current machines, 53, 58, 134
 synchronous machines, 198, 201, 253
 brush contacts, 107, 111, 143
 commutating field conductor, 86, 113, 145
 field winding, synchronous machines, 228, 232, 260
 in copper, of transformer, 346
 series field conductor, 85, 92
 shunt field conductor, 83, 91, 141

current density, squirrel-cage winding, 295, 299
 stator windings, induction motors, 284, 290, 323
 Current in high-voltage winding, 352
 low-voltage winding, 352
 Current per path, direct-current armature winding, 52
 per phase, induction motors, 284, 289, 322

D

Dead coil, 40
 Dead-points, squirrel-cage motors, 292
 Density, armature yoke, direct-current machines, 65, 73, 137
 synchronous machines, 208, 213, 255
 field pole, direct-current machines, 66, 73, 138
 synchronous machines, 209, 213, 255
 field yoke, direct-current machines, 67, 74
 synchronous machines, 210, 215, 257
 Depth of oil, 371
 Design of, pole shoe, direct-current machines, 21
 synchronous machines, 171
 shunt field rheostat, 86, 93
 Design sheet, direct-current generator, 130
 motor, 153
 distributed core-type transformer, 407
 shell-type transformer, 418
 single-phase core-type transformer, 383
 squirrel-cage motor, 319
 synchronous generator, 247
 synchronous motor, 265
 three-phase core-type transformer, 395
 wound rotor motor, 334
 Difference between temperature of windings and average oil temperature, 370
 Direct-current machines, classification of, 1
 Distributed core-type transformer, construction of, 340
 core design, 306
 operating characteristics, 402
 tank design, 405
 winding design, 399

winding, 295
transformers, 335
Double-layer windings, 179
squirrel-cage winding, induction
motors, 297
synchronous motors, 222
Ducts in transformer windings, 362

E

Eddy current losses in, armature coils,
synchronous machines, 198
stator copper, induction motors, 284
transformer windings, 357
Effect of, slot openings upon air gap flux,
induction motors, 283
under-cutting mica, 95
Effective value of current, in end-rings,
squirrel-cage winding, 296
per bar, squirrel-cage winding, 296
Efficiency, average values of, direct-cur-
rent generators, 120
direct-current motors, 121
slip-ring motors, 279-280
squirrel-cage motors, 276-278
synchronous machines, 239, 240, 241
transformers, 354, 355
direct-current machines, 120, 128,
150
synchronous machines, 238, 246, 264
transformer, 369
End-connection leakage reactance, syn-
chronous machines, 218
End-ring section, squirrel-cage winding,
induction motors, 290, 299
synchronous motor, 262
End turn, insulation, transformers, 360
Equalizer connection, conductor section,
41
pitch, 40
Equalizer connections, number, 41, 59
Equivalent field ampere-turns of arma-
ture reaction, 223, 230, 259
Excitation for any load and power factor,
225, 231, 258
Exciter capacity, synchronous machines,
229, 233, 261
Exciter voltage, synchronous machines,
227

Field current, synchronous machines, 228,
232, 260
Leakage, constant, synchronous ma-
chines, 209, 214, 257
factor, direct-current machines,
66, 67
flux, calculation of, direct-current
machines, 67
synchronous machines, 209, 213,
256
Field pole, punchings, thickness of, syn-
chronous machines, 164
rheostat loss, synchronous machines,
234, 245
winding, conductor section, synchro-
nous machines, 226, 232, 260
copper loss, synchronous machines,
234, 245, 263
design, synchronous machines, 226
windings, synchronous machines, 161
Flux, density in transformer core, 346
distribution curve, analysis of, 172, 251
average ordinate of, 176, 249
construction of, 22, 171
effective ordinate of, 176, 251
harmonics of, 175, 249
maximum ordinate of, 176
distribution factor, direct-current ma-
chines, 26, 132
induction motors, 273
synchronous machines, 172, 251
distribution in induction motors, 273
per pole, direct-current machines, 65,
72, 137
induction motors, 287, 290, 323
synchronous machines, 208, 212, 254
plot, construction of, direct-current
machines, 23, 133
synchronous machines, 171, 250
Forced oil-cooled transformer, 344
Forces on transformer windings, 367
Form factor, induction motors, 273
synchronous machines, 172, 251
Fractional slot, rotor windings, 294
stator windings, 282
Frequency, direct-current machines, 20,
28, 132
Friction and windage loss, direct-current
machines, 118, 128, 149

motors, 304, 314, 329
 synchronous machines, 235, 245, 264
 Frogleg winding, 42
 Front pitch, lap winding, 31, 57
 wave winding, 36, 134
 Full-load, current, induction motors, 310,
 318, 332
 efficiency, induction motors, 310, 318,
 332
 power factor, induction motors, 310,
 318, 332
 speed, direct-current motors, 147
 induction motors, 310, 318, 332

II

Heating curves of transformers, 371
 High mica, 95

I

Impedance, at standstill, induction
 motor, 309, 316, 331
 average values of transformers, 354,
 355
 Impregnation of transformer coils, 361
 Induced voltage in armature winding,
 direct-current machines, 14, 56
 synchronous machines, 166
 Induced voltage, in stator winding, in-
 duction motors, 273
 in transformer windings, 347
 Induction motors, construction of, 266
 Inside diameter, of field yoke, direct-
 current machines, 74, 137
 of rotor core, 300, 326
 Insulating collars, thickness of, 363
 Insulating materials for transformer
 windings, 358
 Insulating oil, dielectric strength of, 362
 Insulation, allowances, stator winding,
 induction motors, 286
 between core and windings, trans-
 formers, 360, 375, 387, 400, 412
 between high-voltage and low-voltage
 windings, transformers, 360,
 376, 388, 402, 412
 of armature flanges, 50
 of transformer laminations, 336
 specification, stator windings, induc-
 tion motors, 285

motors, 304, 314, 329
 synchronous machines, 235, 245, 264
 test A. I. E. E. Standards, 362
 armature windings, direct-current
 machines, 47
 synchronous machines, 196
 thickness, wound rotor coils, 208, 325
 Interleaved type of transformer winding,
 357

I.

Lamination factor, 61, 207, 350
 Lap winding, progressive, 32
 retrogressive, 32
 Layer insulation, thickness of trans-
 former windings, 359
 Leakage reactance, induction motors,
 307, 315, 330
 synchronous machines, 219, 229, 257
 transformers, 365
 Length of, bars squirrel-cage winding,
 316
 corrugated tank surface per inch of
 center line, 371
 field pole, axial, direct-current ma-
 chines, 62, 73, 138
 synchronous machines, 209, 213, 255
 field yoke, axial, direct-current ma-
 chines, 67, 74, 138
 synchronous machines, 211, 215,
 257
 flux path, armature teeth, direct-cur-
 rent machines, 65, 72, 137
 synchronous machines, 208
 armature yoke, direct-current ma-
 chines, 65, 73, 138
 synchronous machines, 209, 213,
 255
 field pole, direct-current machines,
 66, 73, 138
 synchronous machines, 210, 215,
 257
 field yoke, direct current machines,
 67, 74, 139
 synchronous machines, 211, 215,
 257
 rotor yoke, 303, 313, 328
 stator yoke, 302, 312, 328
 mean-turn, commutating field coil,
 86, 114, 146

chronous machines, 227, 231, 260
 series field coil, 85, 92
 shunt field coil, 82, 90, 140
 One-half man-turn, armature coil,
 direct-current machines, 55, 53,
 135
 synchronous machines, 199, 201,
 253
 rotor coil, 305, 331
 stator coil, 305, 314, 329
 Limiting temperature rise, salient pole
 synchronous generators and
 motors, 213
 steam-turbine-driven synchronous gen-
 erators, 242
 transformers, A. I. E. E. Standards, 369
 Load losses in transformers, 369
 Losses in, direct-current machines, 115
 synchronous machines, 231
 transformer, 369

M

Magnetic circuit, commutating-pole ma-
 chine, 105
 induction motors, 301
 non-commutating pole machine, 61
 salient pole, synchronous machine,
 206
 transformer, construction of, 336
 Magnetization curve, cast iron, 428
 cast steel, 428
 open-hearth sheet steel, for armatures,
 429
 field poles, 428
 1 per cent silicon sheet steel, 430
 2.5 to 3.0 per cent silicon sheet steel,
 431
 4.0 and 4.5 per cent silicon sheet steel,
 432
 magnetizing current, 368
 calculation of, distributed core-type
 transformer, 404
 induction motors, 303, 313, 328
 shell-type transformer, 416
 single-phase core-type transformer,
 381
 3-phase core-type transformer, 392
 induction motors, 274, 291
 magnetizing force, 61

maximum horsepower output, induc-
 tion motor, 310, 318, 332
 Maximum torque, induction motors, 310,
 318, 332
 Method of, forming direct-current arma-
 ture coils, 44, 15
 insulating armature punchings, 3
 measuring transformer temperature,
 A. I. E. E. Standards, 369
 sealing slots, direct-current machines,
 5
 Minimum cost transformer, 345
 Minimum loss transformer, 345

N

Natural-air-cooled transformer, 340
 Natural-oil-cooled transformer, 341
 Neutral zone, 98, 111, 143
 No-load current, induction motors, 300,
 314, 330
 transformer, 368
 watt component of, induction motors,
 305, 314, 330
 transformers, 368
 field form, construction of, 22, 177
 losses in transformer, 369
 power factor, induction motors, 306,
 314, 330
 Non-commutating pole machines, 1
 Number of, armature slots, direct-cur-
 rent machines, 42, 57, 132
 synchronous machines, 192, 201, 252
 brush sets for wave windings, 38
 coil sides per slot for wave windings, 39
 phases squirrel-cage windings, 306
 poles, direct-current machines, 20, 28,
 130
 induction motors, 287, 320
 rotor conductors, wound rotor winding,
 297
 slots per pole, direct-current machines,
 44
 turns, high-voltage winding, 351
 low-voltage winding, 352

O

Oil and water-cooled transformer, 341
 Open-circuit saturation curve, direct-
 current machines, 60, 139
 synchronous machines, 211, 215, 257

of, induction motors, 309, 316, 332

Output constants, direct-current machines, 18

induction motors, 275

synchronous machines, 169

transformers, 318

Output equation, direct-current machines, 14

induction motors, 274

synchronous machines, 167, 178, 248

transformer, 317

Outside diameter, armature, synchronous machines, 212, 255

field yoke, direct-current machines, 74, 139

stator core, 287, 290, 323

Over-commutation, 94

P

Per cent impedance, synchronous machines, 230, 250

transformers, 367

magnetizing current, induction motors, 303, 313, 328

Per cent pole embrace, direct-current machines, 22, 29, 132

synchronous machines, 171, 249

Per cent reactance, average value of, transformers, 354, 355

effect upon, maximum horsepower, 309

starting torque, 309

induction motors, 309, 316, 331

synchronous machines, 210, 230, 259

transformers, 366

Per cent resistance, average values of, transformers, 354, 355

synchronous machines, 230, 259

transformers, 365

Per cent slip, induction motors, 310, 318, 332

Peripheral speed, induction motors, 281

Phase difference of commutation, 97, 110, 142

Polarity of, commutating poles, 1

transformers, 355

Power factor, at standstill, 309, 316, 332

average values of, slip-ring motors, 279, 280

rel-cage motor, 276, 278

Power transformers, 335

Pull-in torque, synchronous motor, 221

R

Radial length of field pole, synchronous machines, 210, 213, 255

Radiating surface, calculation of, core-type transformers, 381, 393

distributed core-type transformer, 405

shell-type transformer, 416

per watt, transformers, 369

Rate of change of current, average value of, 99

Ratio of, air gap ampere-turns to armature ampere-turns, 79, 136

armature length to pole pitch, direct-current machines, 19

synchronous machines, 170, 178, 249

core loss to copper loss, distribution transformer, 345

power transformer, 345

core weight to copper weight of transformer, 346

field ampere-turns to armature ampere-turns, 75, 79, 139

stator length to pole pitch, induction motors, 281, 287, 320

window height to width, transformers, 352

Reactance of short-circuited field winding, synchronous motor, 221

Reactance voltage, curve, shape of, 103

fundamental equation of, 98

per coil, 100, 112, 144

Regulation average, values of, transformers, 354, 355

Regulation of, synchronous generators, 226, 231

transformer, 368

Resistance of, armature winding, direct-current machines, 56, 59, 135

commutating field winding, 86, 114, 146

field winding, synchronous machines, 229, 232, 261

high-voltage winding, 365

low-voltage winding, 365

resistance of, series field winding, 85, 92
 shunt field winding, 82, 91, 141
 squirrel-cage winding, induction motor, 306, 316
 synchronous motor, 155, 262
 total transformer windings, 365
 resistance per phase, armature winding, synchronous machines, 200, 205, 253
 stator winding, 305, 314, 329
 wound rotor winding, equivalent value of, 305, 331
 rotor, current, wound rotor motor, 311, 332
 diameter, 291, 299, 324
 end-connection, leakage reactance, synchronous motor, 220
 frequency, 298
 laminations, 267
 resistance, squirrel-cage winding, equivalent value of, 306, 316
 slots, number of, squirrel-cage motors, 292, 299
 wound rotor motors, 294, 324
 reactance synchronous motor, 220, 262
 types of, 297, 299, 325
 tooth, density, maximum value of, 298, 300, 325
 width, minimum value of, 298, 300, 325
 voltage, wound rotor motors, 297, 324
 windings, connection of, 292, 324
 induction motors, 291
 slip-ring motors, 291
 yoke density, 300, 326
 zigzag leakage reactance, synchronous motor, 220, 262

S

Sample design, armature winding, direct-current generator, 56
 synchronous generator, 201
 commutator and commutating poles, 110
 direct-current motor, 131-153
 diameter and length, direct-current generator, 27
 synchronous generator, 177
 field winding, synchronous generator, 229

Sample design, losses, efficiency, and temperature rise, direct-current generator, 125
 synchronous generator, 244
 magnetic circuit, direct-current machines, 70
 synchronous generator, 211
 operating characteristics, squirrel-cage motor, 311
 rotor, squirrel-cage motor, 298
 shunt and series field winding, direct-current generator, 89
 stator, squirrel-cage motor, 287
 synchronous motor, 248
 transformer designs, 372
 wound rotor motor, 320
 Section area of, field yoke, direct-current machines, 67, 74, 138
 pole, direct-current machines, 66, 73, 138
 transformer core, 347
 Section-wound coils, transformers, 360
 Series field, ampere-turns, 80, 92
 copper loss, 116, 126
 current, 84, 92
 winding, conductor section, 84, 92
 design, 84, 92
 Shaft currents, synchronous machines, 151, 238
 Shape of, bar squirrel-cage winding, 297, 299
 core section, circular-core-type transformer, 349
 rectangular-core-type transformers, 348
 shell-type transformer, 349
 Shell-type transformer, construction of, 340
 core design, 406
 operating characteristics, 412
 tank design, 417
 winding design, 410
 Sheet steel, quality of, transformers, 336
 thickness of, transformers, 336
 Short-circuit, characteristic, 223, 231, 258
 current curves, 95
 induction motor, 309, 316, 331
 sustained value of, 367
 ratio, 224, 230, 259
 Shunt field, ampere-turns, 80, 90, 140

current, average values of, 52
 calculation of, 82, 91, 141
 rheostat loss, 116, 126
 winding, conductor section, 82, 90, 111
 design, 81, 90, 140
 insulation of, 80, 111
 Simplex lap windings, 30
 Simplex wave winding, 34
 Single-phase core-type transformer, core
 design, 372
 operating characteristics, 378
 tank design, 382
 winding design, 375
 Silicon sheet steel, properties of, 336
 Slot leakage reactance, synchronous ma-
 chines, 217
 Slot size, squirrel-cage winding, 297, 299
 Slots per pole per phase, stator winding
 induction motors, 282, 289, 321
 Sparking at brushes, 96-98
 Spider, construction of, synchronous ma-
 chines, 164
 direct-current machines, 3
 Squirrel-cage winding, construction of,
 induction motors, 272
 design of, synchronous motor, 261
 induction motor, 291
 Stabilizing winding, 147
 Star connection, advantages of, syn-
 chronous machines, 190
 Starting resistance, direct-current motor,
 151
 Starting rheostat, wound rotor motor, 311,
 332
 Starting torque, squirrel-cage motor, 310,
 318
 synchronous motor, 221
 Straight-line commutation, 94
 Stator, coil, construction of, 281
 end-connection clearance, 305
 insulation of (see Insulation allow-
 ance)
 copper loss no-load, 305, 314, 330
 design of, 273
 diameter and length, 281, 287, 320
 frame, 267
 laminations, quality of, 266
 thickness of, 266
 length, 281, 288, 320

Stator, slot, size, 285, 290, 323
 width, 283
 slots, number of, 283, 289, 321
 tooth density, maximum value of, 286,
 290, 323
 pitch, minimum value of, 283, 289, 321
 width, minimum value of, 286, 290,
 323
 windings, 281
 yoke density, 287, 290, 323
 depth, 287, 290, 323
 Strap copper field coil, insulation of,
 synchronous machines, 227, 232
 length mean-turn of, synchronous ma-
 chines, 227, 231
 synchronous machines, 227, 232
 Stray load-losses, A. I. E. E. Standards,
 direct-current machines, 115
 synchronous machines, 238, 246, 264
 Stray loss in transformers, 369
 Surface per watt, armature, direct-current
 machines, 124, 129, 150
 synchronous machines, 244, 246, 264
 commutator, direct-current machines,
 125, 129, 151
 field winding, direct-current machines,
 124, 129, 151
 synchronous machines, 229, 233, 261
 shunt field winding, 83, 91, 142
 Synchronous machines, classification of,
 154

T

Tank surface per watt, corrugated sheet-
 steel tanks, 370
 plain sheet-steel tanks, 370
 with cooling tubes, 370
 Temperature, in various parts of trans-
 former tank, 369
 of oil at surface, 370
 rise, A. I. E. E. Standards, direct-cur-
 rent machines, 122
 armature, direct-current machines,
 123, 129, 150
 commutator, 125, 129, 151
 field winding, direct current ma-
 chines, 124, 129, 151
 synchronous machines, 239
 Thickness of coils, transformer windings,
 364

Thickness of field yoke, direct-current machines, 67, 74, 138
 synchronous machines, 211, 215, 257
 Three-phase, core-type transformer, core design, 384
 operating characteristics of, 390
 tank design, 391
 winding design, 386
 Tooth pitch, direct-current machines, 53, 71, 136
 synchronous machines, 193, 202, 252
 Torque, average values of, slip-ring motors, 279, 280
 squirrel-cage motors, 276-278
 Total ampere-turns per pole, induction motors, 303, 313, 328
 Total bar section, squirrel-cage windings, 296
 Total flux, average values of, transformers, 317
 direct-current machines, 14, 56, 132
 induction motors, 273
 synchronous machines, 166, 202, 252
 transformer, 351
 Total rotor copper section, slip-ring motors, 295, 325
 squirrel-cage windings, 295, 299
 Total standstill reactance with open field winding, synchronous motor, 221, 263
 Transformer, classification of, 335
 construction, types of, 339
 cooling of, 340
 essential parts of, 335
 tank, types of, 344
 temperature rise, A. I. E. E. Standards, 355
 windings, design of, 353
 Transposed conductors, armature coils, synchronous machines, 198
 in transformer windings, 358
 Turns, in series per phase, squirrel-cage winding, 306
 per pole, commutating field winding, 86, 113, 145
 field winding, synchronous machines, 228, 232, 260

Turns, per pole, series field winding, 81, 92
 shunt field winding, 83, 91, 141

U

Under-commutation, 94

V

Ventilated field coil, 82
 Ventilating ducts, in armature, direct-current machines, 5, 71, 136
 synchronous machines, 156, 211, 253
 in rotor core, 267
 in stator core, 267, 288, 321
 Voltage, between commutator bars, 51, 57, 131
 layers, transformer windings, 358
 drop in field winding, synchronous machines, 227, 232, 260
 formula, synchronous machines, 166
 per turn, direct-current armature winding, 46
 transformer winding, 352
 Volume of oil, 371

W

Wave winding, progressive, 37
 retrogressive, 37, 134
 Weight, stator, teeth, 313, 320
 yoke, 313, 320
 Width of commutating zone, 96, 110, 143
 Winding constant, induction motors, 273
 synchronous machines, 167, 201, 251
 Winding distribution factor, calculation of, 186
 definition of, 166
 induction motors, 273
 values of, 189
 Window area, single-phase transformer, 352
 3-phase transformer, 353
 Wire-wound field coil, length, mean-turn of, synchronous machines, 227, 260

Z

Zigzag leakage reactance, synchronous machines, 218

